NOV 8 19[illegible]

SECRET

UNCLASSIFIED

UCRL 7315

Copy No. 163A

TORY II-C

MASTER

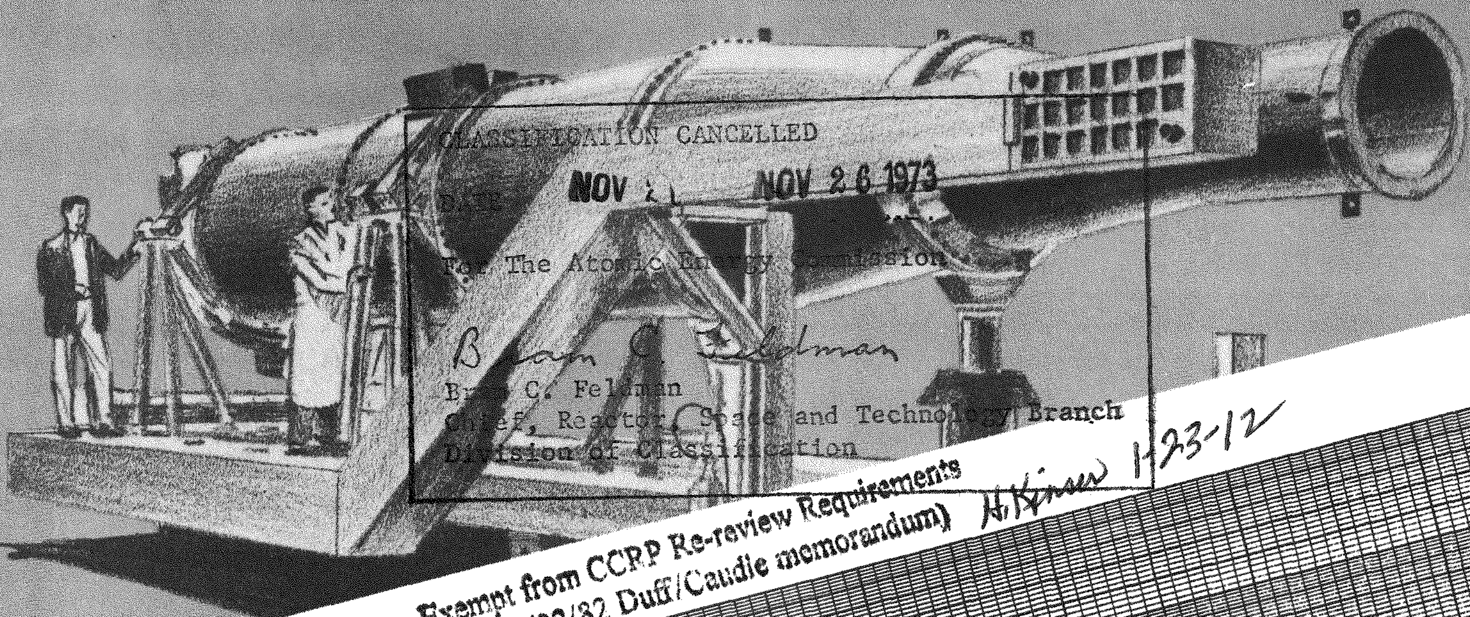

CLASSIFICATION CANCELLED

DATE NOV 26 1973

For The Atomic Energy Commission

Bryan C. Feldman
Chief, Reactor, Space and Technology Branch
Division of Classification

Exempt from CCRP Re-review Requirements
(per 7/22/82 Duff/Caudle memorandum) H.Kinner 1-23-12

GROUP 1

Excluded from automatic downgrading and declassification

data book

LAWRENCE RADIATION LABORATORY

UNIVERSITY OF CALIFORNIA

AEC RESEARCH AND DEVELOPMENT REPORT

DISTRIBUTION OF THIS DOCUMENT IS UNLIMITED

RESTRICTED DATA This document contains restricted data as defined in the Atomic Energy Act of 1954. Its transmittal or the disclosure of its contents in any manner to an unauthorized person is prohibited.

SECRET

1 7958

DISCLAIMER

DISCLAIMER

UCRL-7315
Nuclear Reactors for
Ram-Jet Propulsion, C-90
M-3679 (30th Ed.)

This document contains 365 pages,
including pp. i-xviii.
This is copy 63 of 202 Series A .

UNIVERSITY OF CALIFORNIA
Lawrence Radiation Laboratory
Livermore, California

Contract No. W-7405-eng-48

TORY II-C DATA BOOK

(Title: Unclassified)

Carl E. Walter
Parker C. Smiley

June 17, 1963

Printed in USA. Charge $7.40. Available from the U. S. Atomic Energy Commission, Division of Technical Information Extension, P. O. Box 1001, Oak Ridge, Tenn. Please direct to the same address inquiries covering the procurement of other classified AEC reports.

DISTRIBUTION

Series A

	Copy No.
LRL Livermore,	
Information Division	1 - 10
John S. Foster	11
Wallace D. Decker	12
T. C. Merkle	13
H. L. Reynolds	14
E. Goldberg	15
S. Kellman	16
V. Hampel	17
A. Lorenz	18
J. Hadley	19
J. Moyer	20
A. Cole	21
M. Mintz	22
C. Barnett	23
W. Russell	24
E. Sheridan	25
J. Day	26
H. McDonald	27
H. Rodean	28
T. Stubbs	29
W. Miller	30
W. Myers	31
C. Walter	32
E. Platt	33 - 35
W. Wells	36
J. Behne	37
P. Smiley	38
J. Morton	39
A. Rothman	40
P. Landon	41

DISTRIBUTION (Continued)

Series A

	Copy No.
J. Kane	42
J. Patterson	43
C. M. Van Atta	44
Roger E. Batzel	45
Richard P. Connell	46
Albert J. Kirschbaum	47
Robert W. Westbrook	48
W. E. Humphrey	49
William C. Grayson, Jr.	50
DASA Livermore Liaison Office,	
Norman G. Hunt	51
LRL Berkeley,	
R. K. Wakerling	52
Hayden S. Gordon	53
LRL Mercury, Nevada,	
P. Neal	54 - 57
C. M. Bacigalupi	58
USAEC Technical Library, Washington, D. C.,	
Harold Finger	59
Wright-Patterson AFB, Ohio,	
John S. McCollom	60 - 61
Lockheed Missile and Space Company, Sunnyvale,	
J. Wenzel	62
Chance-Vought Corporation, Grand Prairie, Texas,	
Austin Corbin	63
ACF – South Albuquerque Works	64
Aerojet-General Corporation (NASA)	65
Aeronautical Systems Division	66 - 71
Air Force Weapons Laboratory	72 - 73
Air University Library	74
Albuquerque Operations Office	75

DISTRIBUTION (Continued)

Series A

	Copy No.
Argonne National Laboratory	76
Army Combat Developments	77
Army Missile Command	78
ARO, Inc.	79
Atomic Energy Commission, Washington	80 - 83
Atomics International	84
Battelle Memorial Institute	85
Brookhaven National Laboratory	86
Bureau of Naval Weapons	87 - 90
Bureau of Naval Weapons (SPO)	91
Bureau of Ships	92
Canoga Park Area Office	93
Chicago Patent Group	94
Continental Army Command	95
Defense Atomic Support Agency, Sandia	96
Department of the Army	97
Deputy Chief of Naval Operations, Development	98
Director of Defense Research and Engineering (OAP)	99
duPont Company, Aiken	100
Edgerton, Germeshausen and Grier, Inc., Las Vegas	101
Edgerton, Germeshausen and Grier, Inc., Goleta	102
General Electric Company, Cincinnati	103 - 108
General Electric Company, Richland	109 - 110
Institute for Defense Analysis	111
Jet Propulsion Laboratory	112
Johns Hopkins University (APL)	113
Ling Temco Vought, Inc.	114
Los Alamos Scientific Laboratory	115 - 116
Marquardt Corporation	117 - 120
NASA Langley Research Center	121
NASA Lewis Research Center	122 - 126

DISTRIBUTION (Continued)

Series A

	Copy No.
NASA Marshall Space Flight Center	127
NASA Scientific and Technical Information Facility	128 - 130
Naval Air Development Center	131
Naval Ordnance Test Station	132
Naval Postgraduate School	133
Nevada Operations Office	134 - 135
North American Aviation, Inc., Downey	136
Oak Ridge Operations Office	137
Office of the Assistant General Council for Patents (AEC)	138
Office of the Chief of Naval Operations	139
Office of the Chief of Naval Operations (OP-03EG)	140 - 141
Phillips Petroleum Company (NRTS)	142
Pratt and Whitney Aircraft Division	143
RAND Corporation	144 - 145
San Francisco Operations Office	146
Sandia Corporation	147
School of Aerospace Medicine	148
Strategic Air Command	149
Union Carbide Nuclear Company (ORNL)	150 - 159
USAF Headquarters	160
U. S. Naval Radiological Defense Laboratory	161
Westinghouse Electric Corporation (NASA)	162
Division of Technical Information Extension	163 - 202

CONTENTS

	Page No.
Distribution	iii
Contents	vii
Introduction	xi
Symbols and Conventions	xii
General Station Arrangement	xvii-xviii
I. Performance	
A. Pluto Performance	I-1
B. Tory II-C Reactor Performance	I-3
1. Summary of Operating Conditions	I-3
2. Component Operating Conditions	I-4
Design Point Condition	I-4
Structural Design Condition	I-18
Cold Inlet Gas Condition	I-32
Hot Wall Condition	I-46
3. Performance Maps	I-60
Inlet Air Temperature 946°F	I-60
Inlet Air Temperature 1065°F	I-63
Inlet Air Temperature 600°F	I-66
4. Parameter Influence on Performance	I-69
Thrust Loss Analysis for Parameters Not Analyzed by NOMAC Code	I-69
Fueled Tube Hole Size Optimization	I-71
Exit Nozzle Throat Area Optimization	I-72
5. Analysis and Heat Transfer Data	I-73
Inlet Diffuser	I-73
Reactor	I-73
Exit Nozzle	I-75
6. Time Constants and Thermal Capacities	I-75
II. Neutronics	
A. Criticality	II-1
B. Reactivity Requirements	II-2
C. Reactor Characteristics	II-3

CONTENTS (Continued)

Page No.

D. Control Rod Worth II-4

E. Fuel Distribution II-7

F. Power Distribution II-16

G. Radiation Energy Spectra II-21

H. Nuclear Heating II-25

I. Radiation Leakage II-34

J. Radiation Dose II-42

III. Mechanical Design

A. Reactor Assembly III-1

1. Reactor III-1

2. Reactor Control System III-61

3. Reactor Safety System III-68

B. Test Vehicle III-73

1. Flat Car III-73

2. Brake System III-73

3. Right Outrigger Wheels III-75

4. Left Outrigger Wheels III-76

5. Truck Assembly III-76

6. Auxiliary Drive III-77

7. Wireway III-77

8. Nozzle Cooling Air Pipe III-77

9. Control Air Pipe III-78

10. Duct Support System III-78

11. Duct System III-78

C. Instrumentation III-82

1. Non-Nuclear III-82

2. Reactor Thermocouples III-87

3. Nuclear Instrumentation III-95

D. Test Facility III-99

1. Site 401 Description III-99

2. Test Air System III-99

3. Air Storage System III-103

4. Air Compression System III-104

CONTENTS (Continued)

		Page No.
	5. Air Heater	III-105
	6. Air Heater Furnace	III-107
	7. Test Bunker	III-107
	E. Locomotive	III-109
IV.	Environment and Analysis	
	A. Accelerations of Reactor Vehicle	IV-1
	B. Weights and CG Locations	IV-2
	C. Component Analysis	IV-4
V.	Operation	
	A. Proposed Test Plan	V-1
	B. Typical Reactor Operation Sequence	V-2
	C. Nuclear Control Modes	V-3
	D. Air Flow Rate Control	V-5
	E. Air Temperature Control	V-6
	F. Operating Limits	V-6
VI.	Material Properties	VI-1
	A. Air	VI-2
	B. Ceramics and Cermets	VI-4
	1. BeO	VI-4
	2. Fueled BeO	VI-10
	3. Carbon P 56 HT	VI-15
	4. Carbon P 303 C	VI-15
	5. Chrome 2400-30	VI-16
	C. Coatings	VI-18
	1. Alumina	VI-18
	2. Si/Cr-FeB	VI-18
	D. Cobalt Alloys	VI-20
	1. Haynes 25	VI-20
	2. Stellite 68	VI-22
	E. Columbium Alloys	VI-23
	1. D-36	VI-23
	2. D-40 (F-48)	VI-25

CONTENTS (Continued)

Page No.

F. Ferrous Alloys
1. Mild Steel VI-28
2. Stainless Steel (Type 347) VI-30
3. Stainless Steel (Type 405) VI-32
4. Stainless Steel (Type 410) VI-34
5. Nickel Chromium Steel A286 . . . . . . VI-36
6. Ultra High Strength Steel (Vascojet 1000) . . VI-38
G. Hafnium VI-40
H. Nickel Alloys
1. Nickel (Grade 200) VI-42
2. Hastelloy B VI-44
3. Hastelloy C VI-46
4. Hastelloy X VI-48
5. Hastelloy R-235 . . . . VI-50
6. René 41 . . . . VI-52
7. Inconel X VI-54
J. Platinum Alloys
1. Pt-5Ru VI-56

Appendixes:
A. List of Tory II-C Memoranda, by Number . . . A-1
B. List of Key Tory II-C Memoranda, by Subject . . B-1
C. List of Pertinent UCRL Reports C-1
D. Drawings . . . .(Separate book)
Index Ind-1

INTRODUCTION

This data book presents a tabulation of the various data which defines or describes the configuration, performance, materials, etc., of the Tory II-C Reactor Experiment. Some of this data is still subject to change.

The data book is intended to be a handy reference for all persons associated with Tory II-C. It also serves as a common source of information for separate groups involved in the Tory II-C program. Because of its necessary brevity, only data of most general interest are included. In some cases typical values only of parameters are given. For further information on a specific subject, the reader is referred to the appendixes which list pertinent Tory II-C memoranda and UCRL reports. Copies of these documents are usually available on request.

The data book has been under continual compilation and revision for almost two years by Harold Stern, James Collins, and Parker Smiley in turn. The data book is reviewed by Carl Walter and Harry Reynolds. The data book has also been reviewed in specific areas as follows:

Ethan Platt	Reactor
Eugene Goldberg	Neutronics
Charles Barnett	Operation
William Russell	Instrumentation
Michael Mintz	Heat Transfer
Joseph Behne	Test Vehicle
William Miller	Facility
Earl Sheridan	Controls

SYMBOLS AND CONVENTIONS

For the purpose of this data book the following definitions are adopted:

Reactor Assembly:	The complete reactor duct and all components contained therein, consisting of
Reactor:	The aft reactor duct and all components contained therein, and
Reactor Control System:	The forward reactor duct, including the control rods, the control actuators, their supports, and the external control packages, and
Reactor Safety System:	The safety rods, their supports and those of their actuating components mounted on the duct.
Test Vehicle:	The flatcar and all components on it except the reactor assembly and instrumentation.
Reflected Core:	All BeO components plus peripheral shims, grouped and defined as shown:

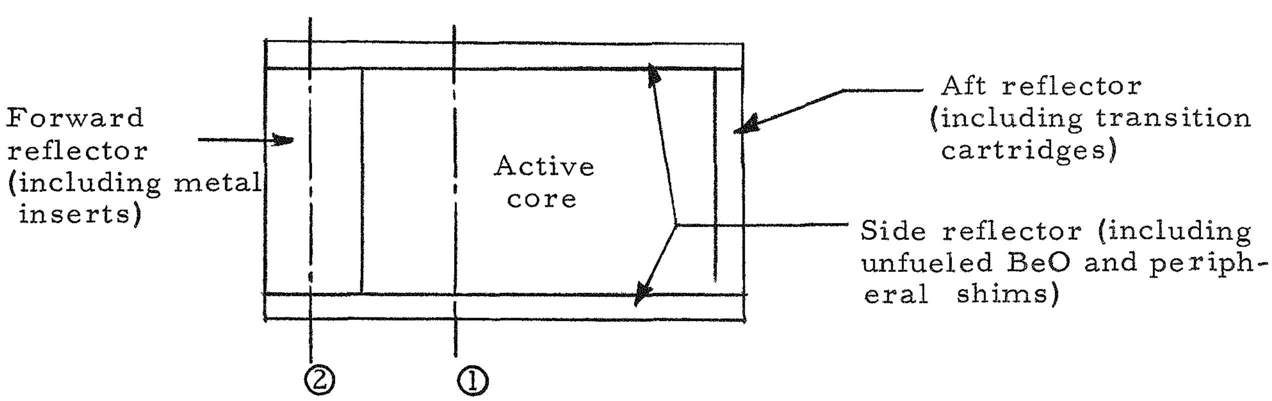

See notes below:

1. "In the region of the active core" is taken to mean in a plane normal to the axis of the reactor and between the forward and aft reflectors. Such a cross section includes the annular side reflector.

2. "In the region of the forward reflector" is taken to mean in a plane normal to the axis of the reactor and forward of the active core. Such a cross section also includes the annular side reflector (see sketch above).

Average dimensions, e. g., the active core diameter length, are shown thus . . . . 3.000 in. (av)

UNLESS OTHERWISE SPECIFIED ALL DIMENSIONS ARE NOMINAL DIMENSIONS AND ARE AT 70°F

SYMBOLS

A	Acceleration
AC	Air cool
AV	Air valve
B	Blower
BF	Ball fitting
C_f	Thrust coefficient
C_p	Specific heat at constant pressure, Btu/lb-°F
CV	Check valve
C. V.	Minimum Charpy V-notch impact strength
D	Displacement, hydraulic diameter, ft
E	Energy, strain, elastic modulus
f	Friction factor
F	Furnace
F1-F3	Fueled tubes
FM	Flowmeter
G	Mass flow rate, lb/ft^2-hr (evaluate at bulk velocity, T_b, and static pressure)
$g(\epsilon)$	Power distribution function to air $\left(\int_0^1 g(\epsilon)d\epsilon \equiv 1\right)$
$g'(\epsilon)$	Nuclear power distribution function $\left(\int_0^1 g'(\epsilon)d\epsilon \equiv 1\right)$
h	Film coefficient, Btu/hr-ft^2-°R
$\overline{h}$	Gas film property group (see definition below)
H	Heating power density, heater
HT	Heat treat
Izod	Minimum Izod-notch impact strength
k	Multiplication constant, thermal conductivity
l	Length variable, axial
L	Total length
M	Mach number, motor
MP	Melting point
(n, γ)	Radiative capture reaction
Oy	Oralloy
P	Static pressure
P°	Total pressure

SYMBOLS (Continued)

Pr	Prandtl number
PS	Pressure switch
PT	Pressure transducer
q	Heat flux, Btu/hr-ft^2
r	Radius variable
R	Regulator
Rec	Receiver
RT	Room temperature
S	Source function
SOL	Solenoid
ST	Solution treat
SSS	Side support system
T	Temperature
T°	Total temperature
T_b	Bulk air static temperature
T_b°	Bulk air stagnation temperature
T_f	Mean film static temperature
T_{tp}°	Air total temperature in trapezoid (void between tie rod and guard tubes)
T_w	Wall temperature
U1-U7	Unfueled side reflector tubes
V	Volume, valve
$\dot{w}$	Flow rate
WQ	Water quench
x	Length variable, axial
XJ	Expansion joint
α	Instantaneous coefficient of linear thermal expansion
$\bar{\alpha}$	Mean coefficient of linear thermal expansion
β	Delayed neutron fraction
γ	Worth of delayed neutrons, specific heat ratio
Γ	Porosity (flow area divided by total area)
ϵ	Elongation, normalized distance
λ	Decay constant of delayed neutron precursor group
μ	Dynamic viscosity, lb/hr-ft

SYMBOLS (Continued)

μ_a	Energy absorption coefficient (gamma ray)
ν	Number of neutrons per fission, Poisson's ratio
σ	Microscopic cross section, stress, psi
σ_u	Ultimate tensile strength
σ_y	Yield tensile strength
ϕ	Flux

Subscripts

amb	Ambient
c	Core
eff	Effective
f	Dynamic
i	Internal
w	Wall
x	Axial coordinate
y	Transverse coordinate
z	Vertical coordinate
γ	Gamma radiation
1	Inlet
2	Outlet

SECRET

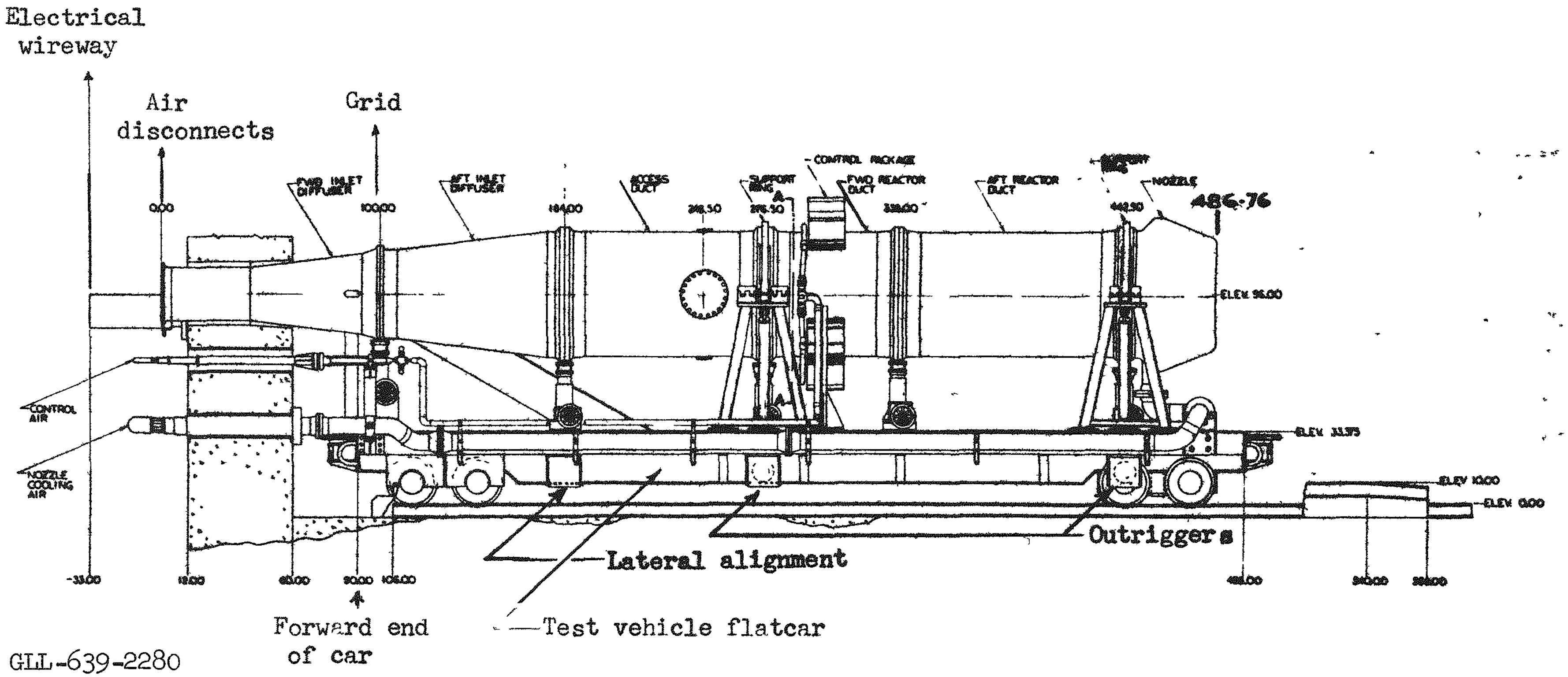

GLL-639-2280

General Station Arrangement.
(See p. III-5 for Reactor Dimensions)

SECRET

CHAPTER I - PERFORMANCE

A. PLUTO PERFORMANCE

1. Diffuser Design Point Condition

Missile Mach no.	2.8
Missile altitude	1000 ft
Ambient temperature (hot day)	100°F
Diffuser angle of attack	0°
Diffuser pressure recovery ratio	0.80
Bleed fraction	0.04
Momentum recovery of bleed	0.80
Supersonic spillage	0
Diffuser operation	Critical
Missile diameter	57 in.
Nozzle throat area	750 in^2
Nozzle exhaust pressure	Ambient
Nozzle velocity coefficient	0.98
Nozzle divergence factor	1.00
Net thrust	34,718 lb
Thrust coefficient	0.174

2. Reactor Structural Design Condition

Missile Mach no.	3.0
Missile altitude	1000 ft
Ambient temperature (hot day)	100°F
Diffuser operation	Supercritical
Net thrust	28,911 lb
Thrust coefficient	0.126

3. Off Design Performance

Thrust vs Mach no.	See p. I-2
Thrust coefficient vs Mach no.	See p. I-2

Note: "Information in this chapter has been slightly modified and presented in UCRL-7933."

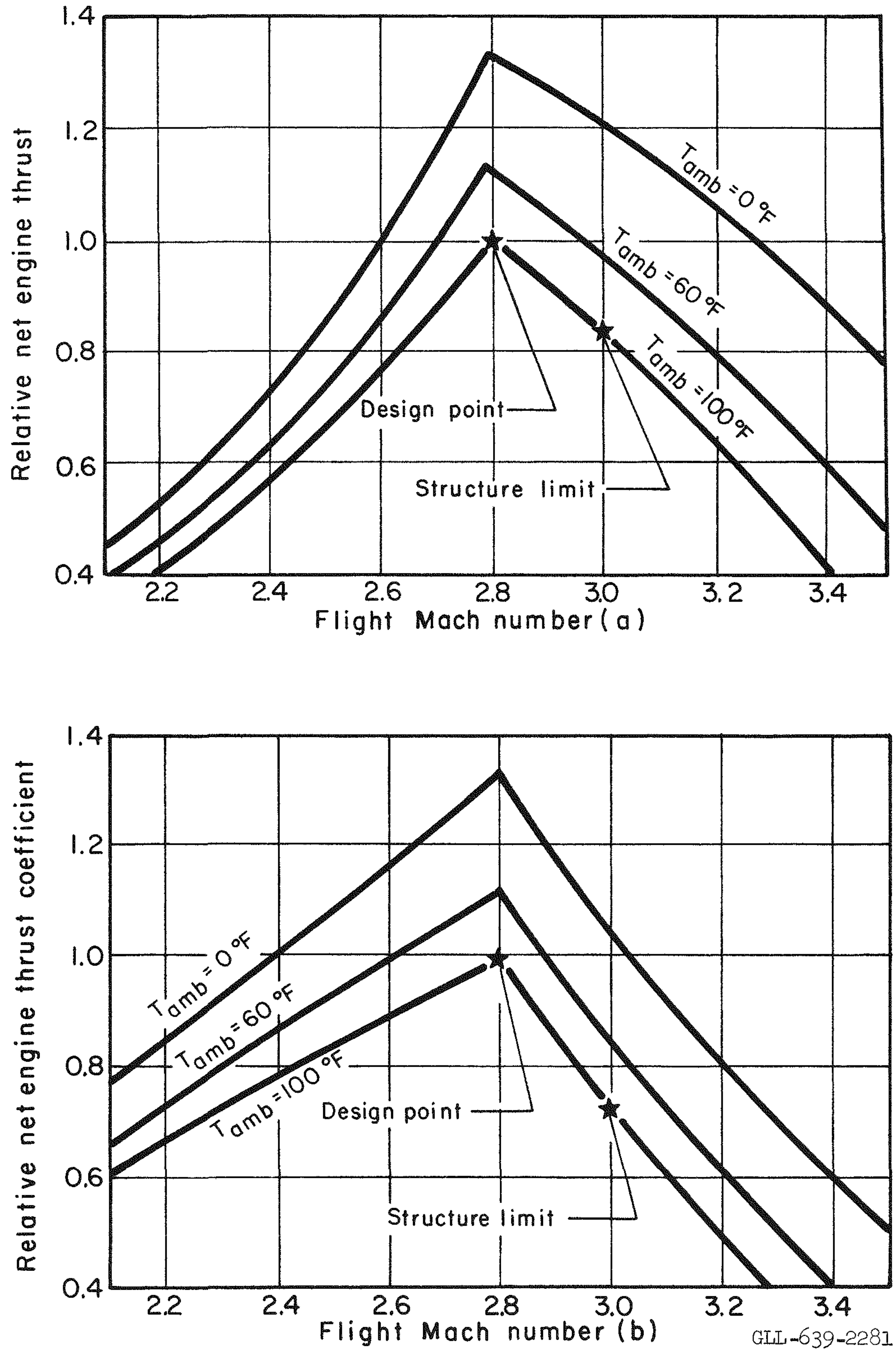

Relative net engine thrust (a) and relative net engine thrust coefficient (b) vs flight Mach number (altitude = 1000 ft, $T_{W_{max}}$ = 2500°F).

B. TORY II-C REACTOR PERFORMANCE

1. Summary of Operating Conditions, with Performance Parameters

	Condition			
	Diffuser design point	Reactor structural design	Cold inlet gas	Hot wall off-design
Flight Mach no.	2.8	3.0	2.8	2.8
Ambient temperature (°F)	100	100	-44	100
Altitude (ft)	1,000	1,000	1,000	1,000
Reactor inlet total temp (°F)	946	1,063	600	946
Reactor inlet total pressure (psia)	316	342	313	316
Reactor thermal power (MW)	491	489.	594	583
Reactor flow rate (lb/sec)	1,697	1,814	1,771	1,627
Flow distribution (%):				
Fueled tubes	77.35	77.84	75.55	76.64
Guard tubes (active core)	1.42	1.41	1.47	1.43
Side reflector tubes	1.83	1.81	1.90	1.85
Peripheral shims	1.47	1.45	1.54	1.49
Tie rods	4.09	3.98	4.46	4.24
Control rods*	1.92	1.87	2.11	2.00
Spare control tie rods	0.82	0.80	0.89	0.85
Side support structure	11.10	10.83	12.09	11.50
Net thrust (lb)	34,718	28,911	52,109	42,362
Peak fueled tube wall temp (°F)	2,500	2,500	2,500	2,850
Max fueled tube thermal stress (psi)	16,187	16,149	19,619	21,731
Max fueled tube material power density (MW/ft^3)	27.57	27.47	33.38	32.77
Normal fueled tube exit Mach no.	0.421	0.422	0.418	0.421
Reactor total pressure drop (psi)	101.9	111.9	96.4	101.3
Total reactor axial thrust loading (lb)	254,000	279,000	241,000	253,000
Fueled tube exit total temp (°F)	2,160	2,181	2,073	2,446
Reactor mixed mean total temp (°F)	1,936	1,979	1,777	2,161
Reactor exit total pressure (psi)	218	235	220	218
Reactor exit static pressure (psi)	213	230	215	214
Nozzle inlet Mach no.	0.175	0.175	0.175	0.175

* At 5-hour nominal operating position.

2. Component Operating Characteristics

Summary of Component Operating Characteristics for Diffuser Design Point Condition

Component	Peak wall temp (°F)	Exit gas temp (°F)	Single-element flow rate (lb/sec)	Total pressure drop (psi)	Peak material power density (MW/ft^3)
Fueled tubes (average)	2500	2160	0.06246	82.9	27.57
Tie rod } Center position	1448	1128	0.6893	65.7	8.62
Guard tubes } Center position	2087	1947	0.01812	114.1	2.50
Control rod (17.2 in. insertion)	1374	1034	2.431	71.6	20.8
Control tie rod	1243	1034	2.431	71.6	8.89
Guard tubes	1970	1889	0.02031	113.9	2.97
Spare control tie rod	1059	967	3.474	42	8.89
Side reflector (BeO)					
Inner radius	2080	1970	0.007920 (average)	122.0 (average)	1.07
Outer radius	1530	1520			0.624
Peripheral shim					
Inner radius	1580	1535	0.01918 (average)	119 (average)	2.21
Outer radius	1488	1451			1.92
Side support structure					
Spring	1199	1120	153.2(total)	101.7	1.17
Rail	1219	1120	153.2(total)	101.7	0.914
Duct	1308	1120	153.2(total)	101.7	0.647

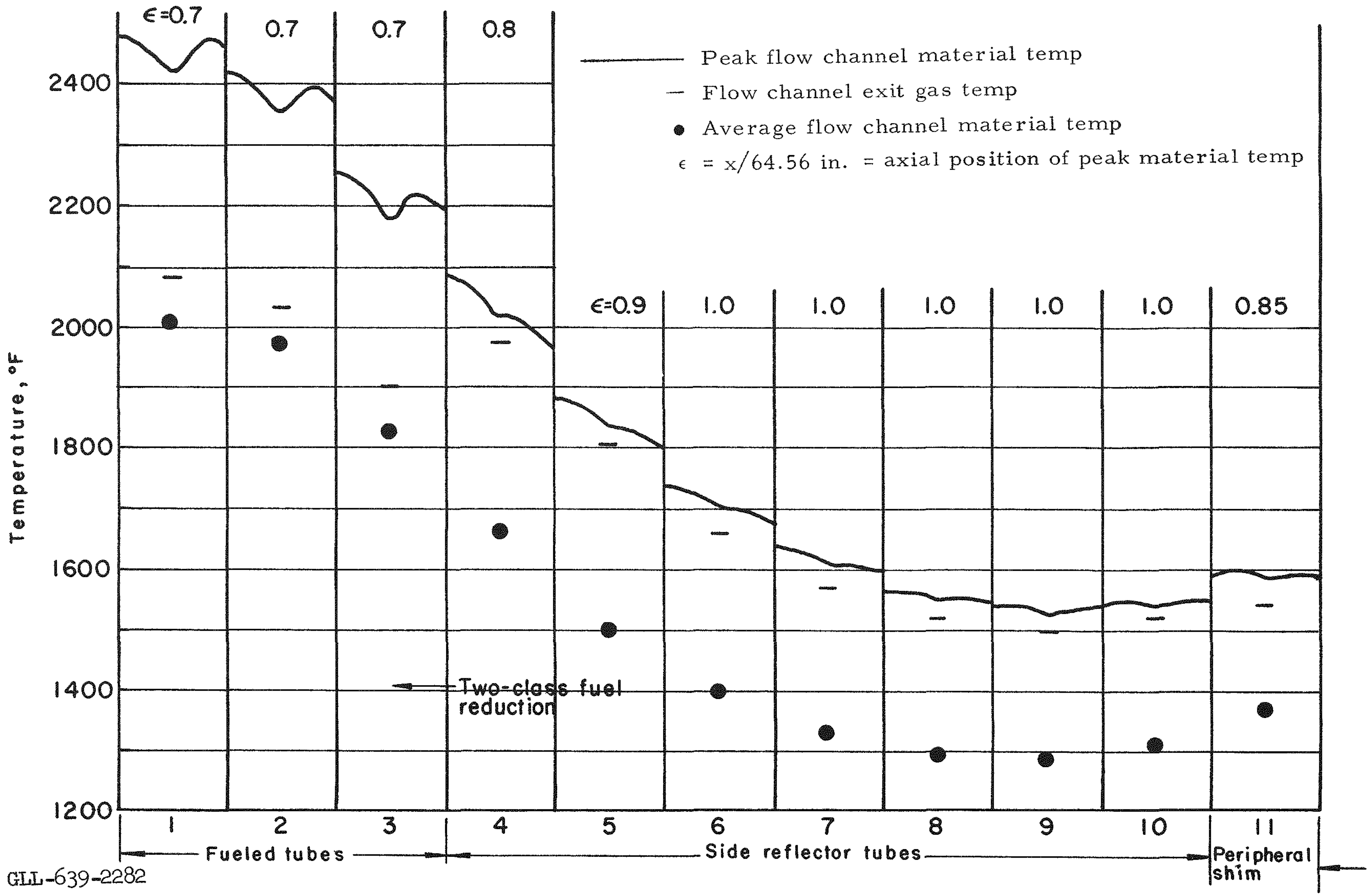

Analysis of peripheral region radial temperature, at diffuser design point condition.

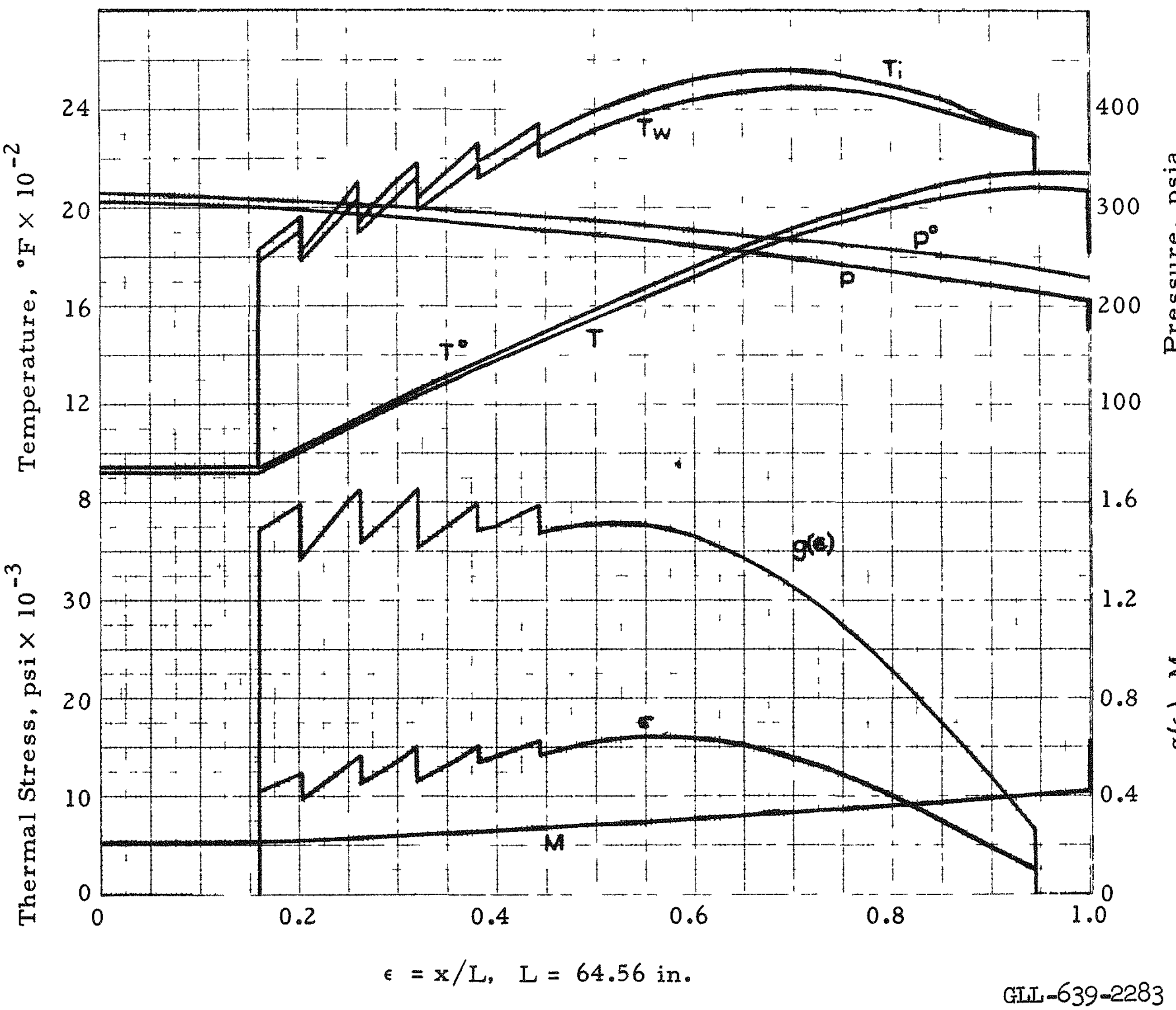

Flow channel diam:	0.227 in.	Exit Mach number:	0.421
Porosity:	0.5297	Peak wall temp:	2500°F
Inlet total temp:	946°F	Power to air:	22.377 kW
Exit total temp:	2160°F	Average material power density:	16.670 MW/ft^3
Inlet total pressure:	316.4 psia	Flow rate:	0.062456 lb/sec
Exit total pressure:	233.5 psia	All dimensions at:	60°F

Average fueled tube, diffuser design point condition.

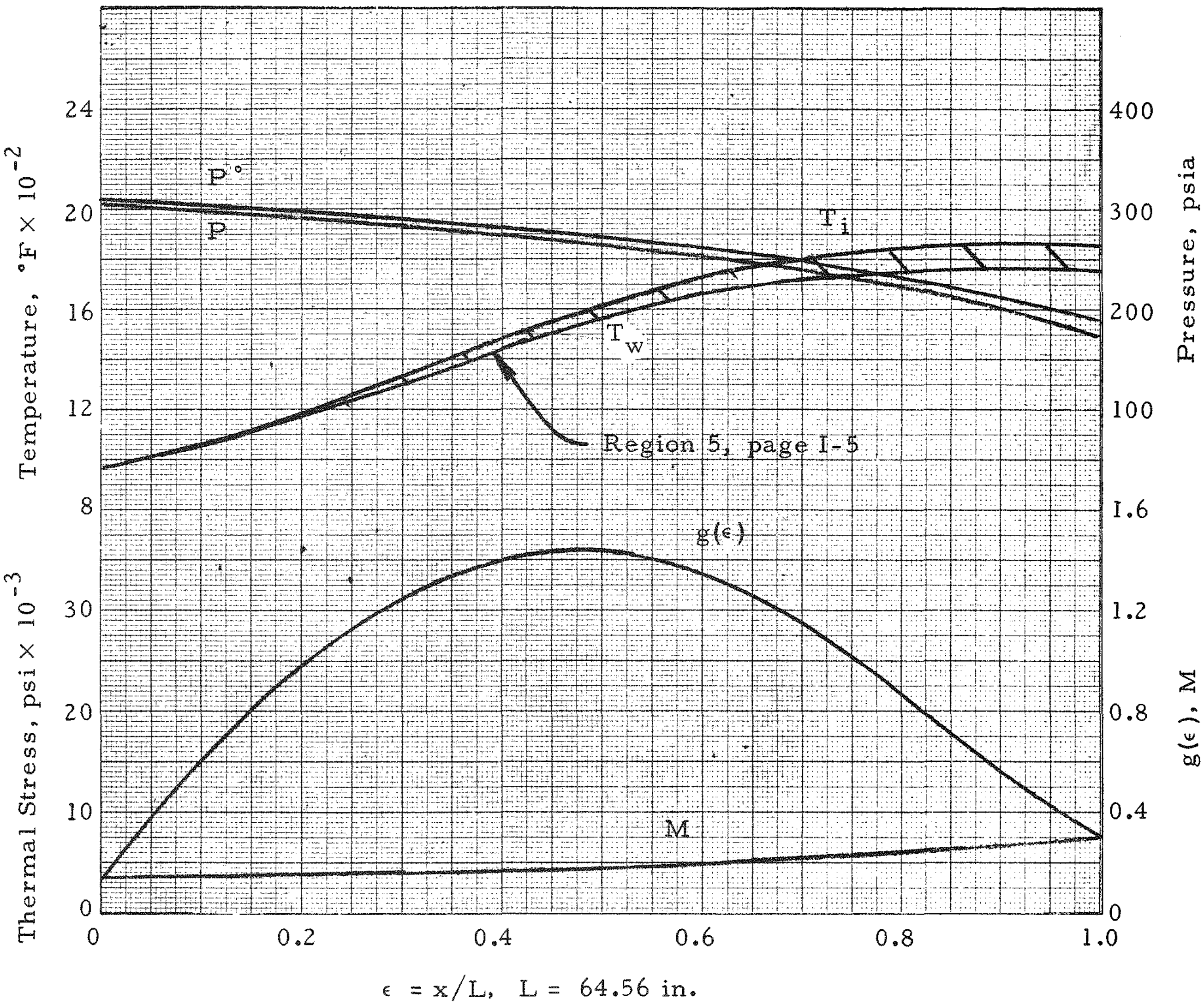

Flow channel diam:	0.093 in.	Exit Mach number:	0.324 av
Porosity:	0.0895	Peak wall temp:	2080°F (Region 4, page I-5)
Inlet total temp:	946°F	Power to air:	1.47 kW av
Exit total temp:	1646°F av	Average material power density:	0.569 MW/ft^3 av
Inlet total pressure:	316 psia	Flow rate:	0.00792 lb/sec av
Exit total pressure:	194 psia av	All dimensions at:	60°F

Side reflector tube, diffuser design point condition.

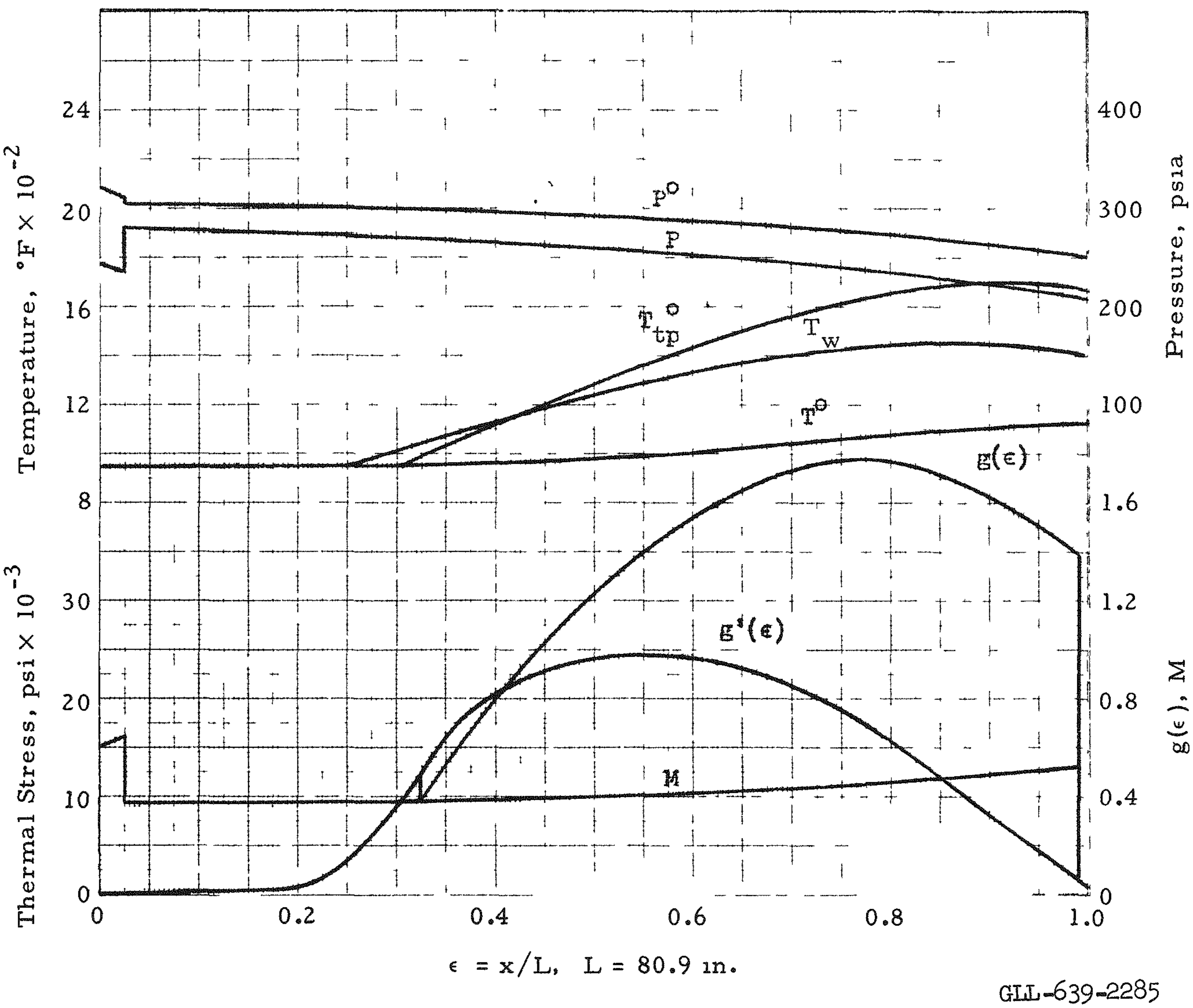

Flow channel diam:	0.576 in.	Exit Mach number:	0.506
Porosity:	0.7391	Peak wall temp:	1448°F
Inlet total temp:	946°F	Power to air:	35.1 kW
Exit total temp:	1128°F	Average material power density:	5.73 MW/ft^3
Inlet total pressure:	316.4 psia	Flow rate:	0.6893 lb/sec
Exit total pressure:	250.7 psia	All dimensions at:	60°F

Tie rod (central), diffuser design point condition.

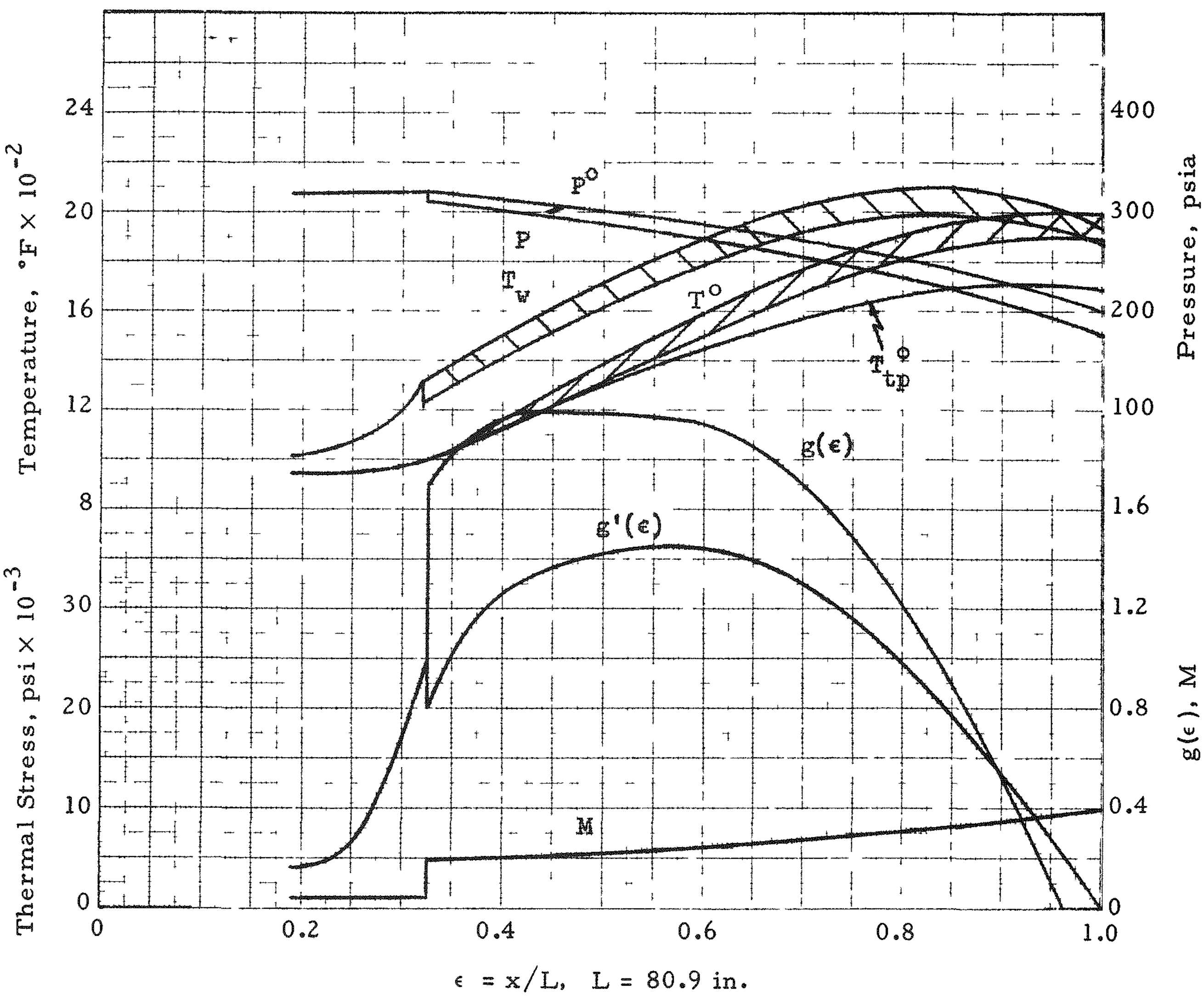

GLL-639-2286

Flow channel diam:	0.130 in.	Exit Mach number:	0.410
Porosity:	0.1761	Peak wall temp:	2087°F
Inlet total temp:	946°F	Power to air:	5.081 kW
Exit total temp:	1947°F	Average material power density:	1.66 MW/ft^3
Inlet total pressure:	316.4 psia	Flow rate:	0.01812 lb/sec
Exit total pressure:	202.3 psia	All dimensions at:	60°F

Guard tube (central), diffuser design point condition.

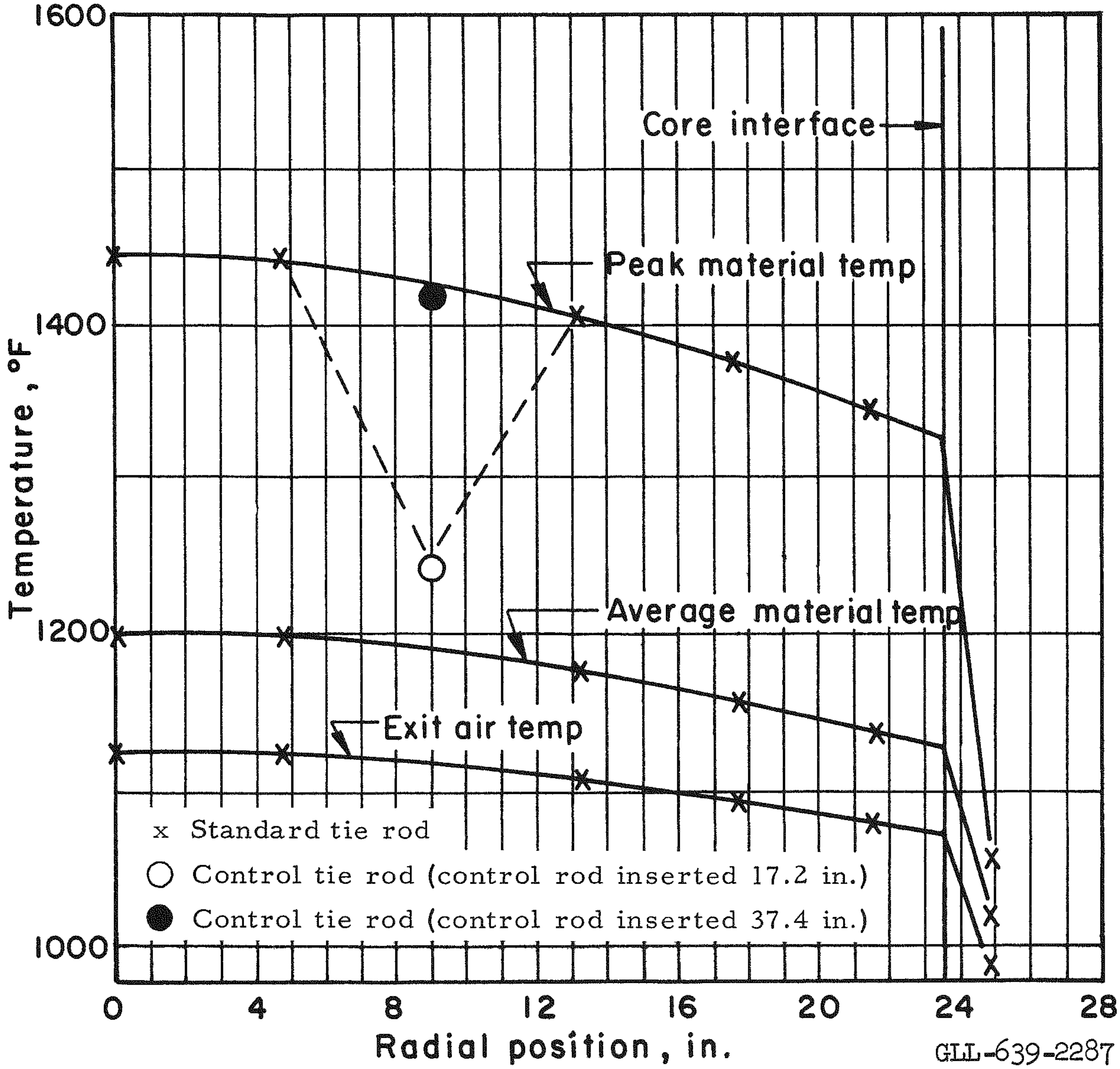

Nominal radial profile of tie rod temperatures, diffuser design point condition.

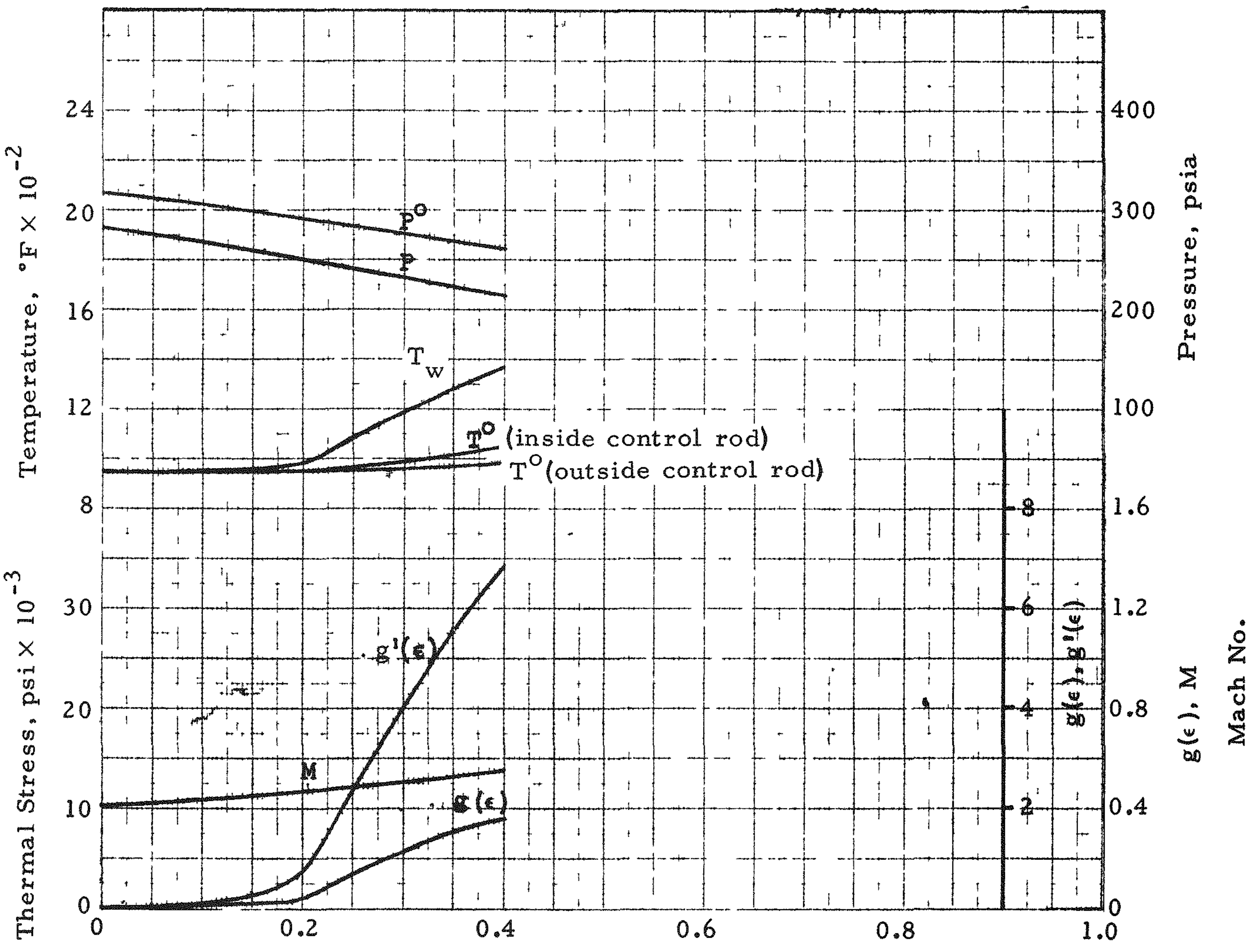

GLL-639-2288

		Exit Mach number:	0.5499
		Peak wall temp:	1374°F
Inlet total temp:	946°F	Power to air:	6.36 kW
Exit total temp:	1048°F	Average material power density:	6.582 MW/ft^3
Inlet total pressure:	316.4 psia	Flow rate:*	0.2222 lb/sec
Exit total pressure:	260.7 psia	All dimensions at:	60°F

*Inside control rod.

Control rod (inserted 17.2 in.), diffuser design point condition.

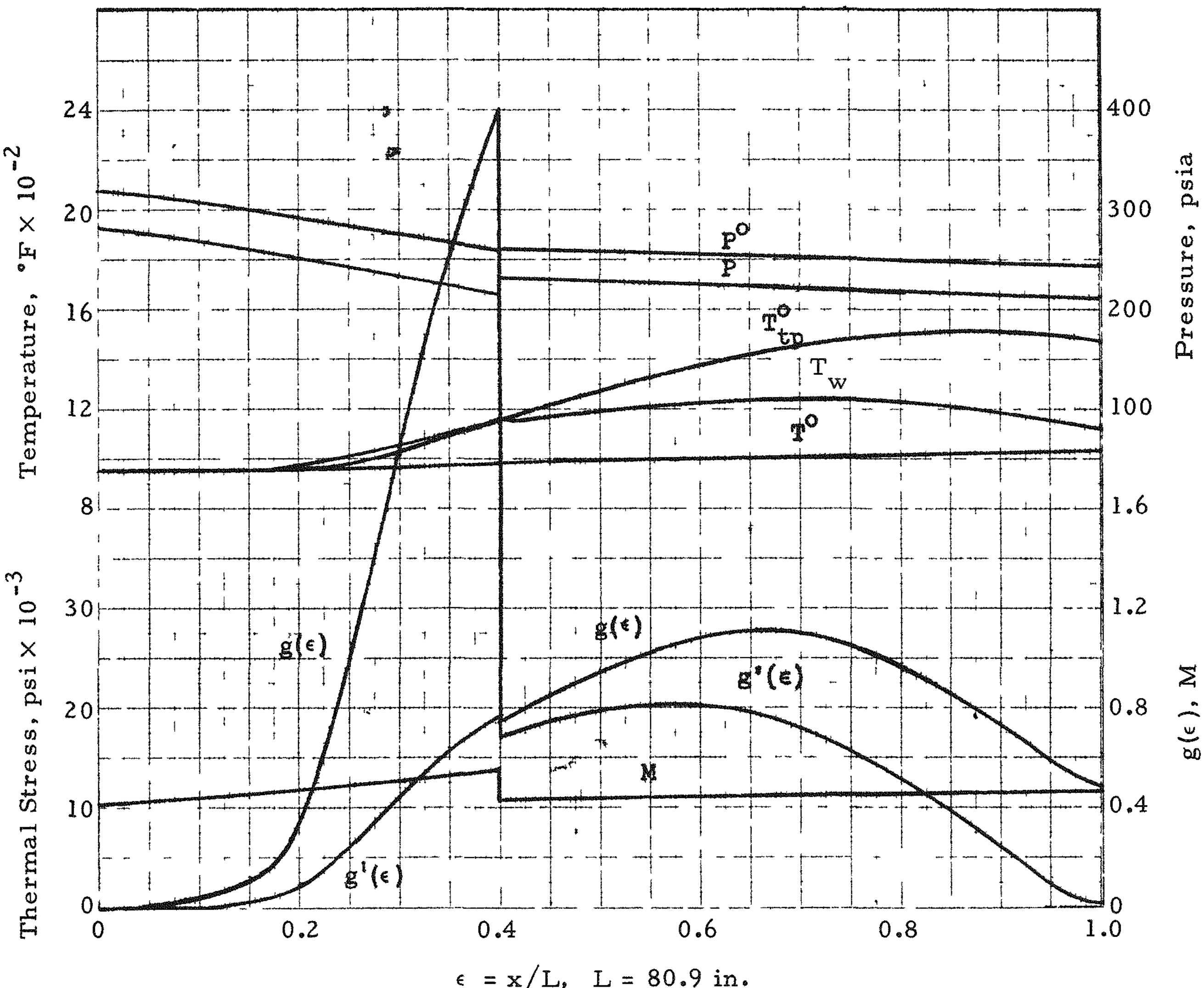

GLL-639-2289

Flow channel diam:	1.162 in.	Exit Mach number:	0.4693
Porosity:*	0.7478	Peak wall temp:	1243°F
Inlet total temp:	946°F	Power to air:	57.218 kW
Exit total temp:	1034°F	Average material power density:	4.814 MW/ft^3
Inlet total pressure:	316.4 psia	Flow rate:	2.2085 lb/sec
Exit total pressure:	244.8 psia	All dimensions at:	60°F

*Control rod inserted.

Control tie rod (control rod inserted 17.2 in.), diffuser design point condition.

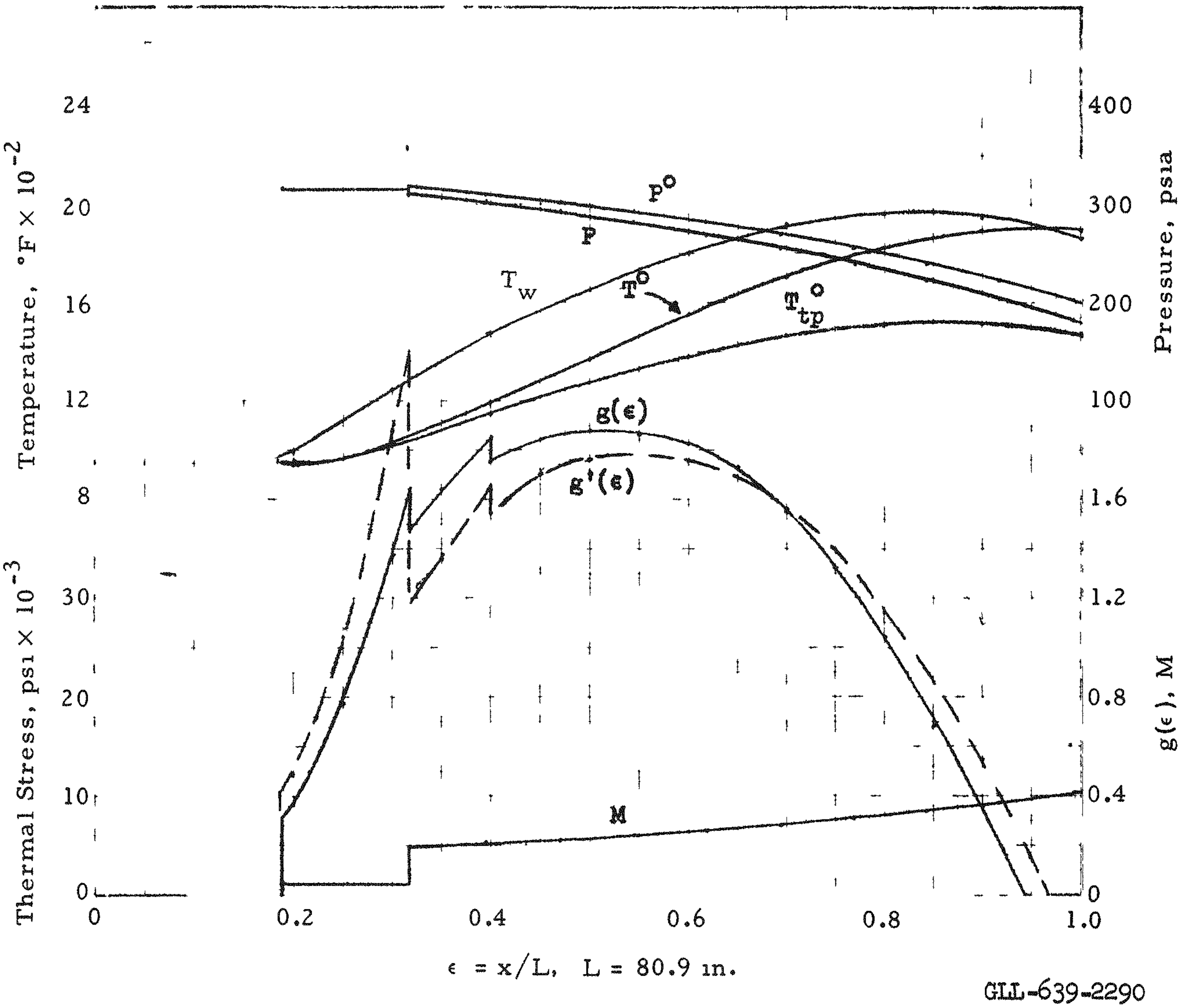

Flow channel diam:	0.130 in.	Exit Mach number:	0.4118
Porosity:	0.1761	Peak wall temp:	1970°F
Inlet total temp:	946°F	Power to air:	5.057 kW
Exit total temp:	1889°F	Average material power density:	2.291 MW/ft^3
Inlet total pressure:	316.4 psia	Flow rate:	0.01835 lb/sec
Exit total pressure:	202.5 psia	All dimensions at:	60°F

Guard tube (control tie rod, control rod inserted 17.2 in.), diffuser design point condition.

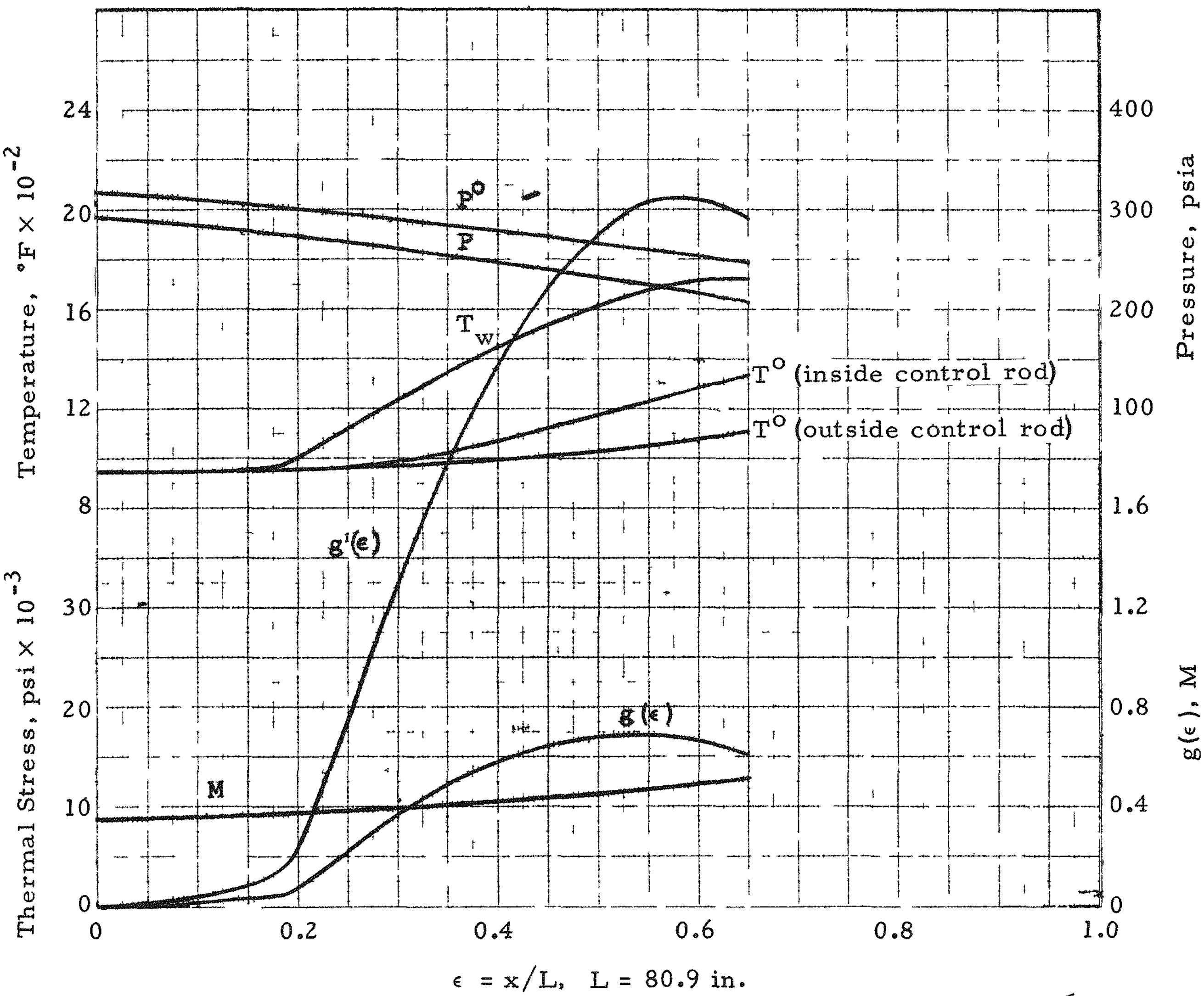

GLL-639-2291

		Exit Mach number:	0.5170
		Peak wall temp:	1723°F
Inlet total temp:	946°F	Power to air:	20.48 kW
Exit total temp:	1342°F	Average material power density:	14.235 MW/ft^3
Inlet total pressure:	316.4 psia	Flow rate: *	0.1820 lb/sec
Exit total pressure:	246 psia	All dimensions at:	60°F

*Inside control rod.

Control rod (inserted 37.4 in.), diffuser design point condition.

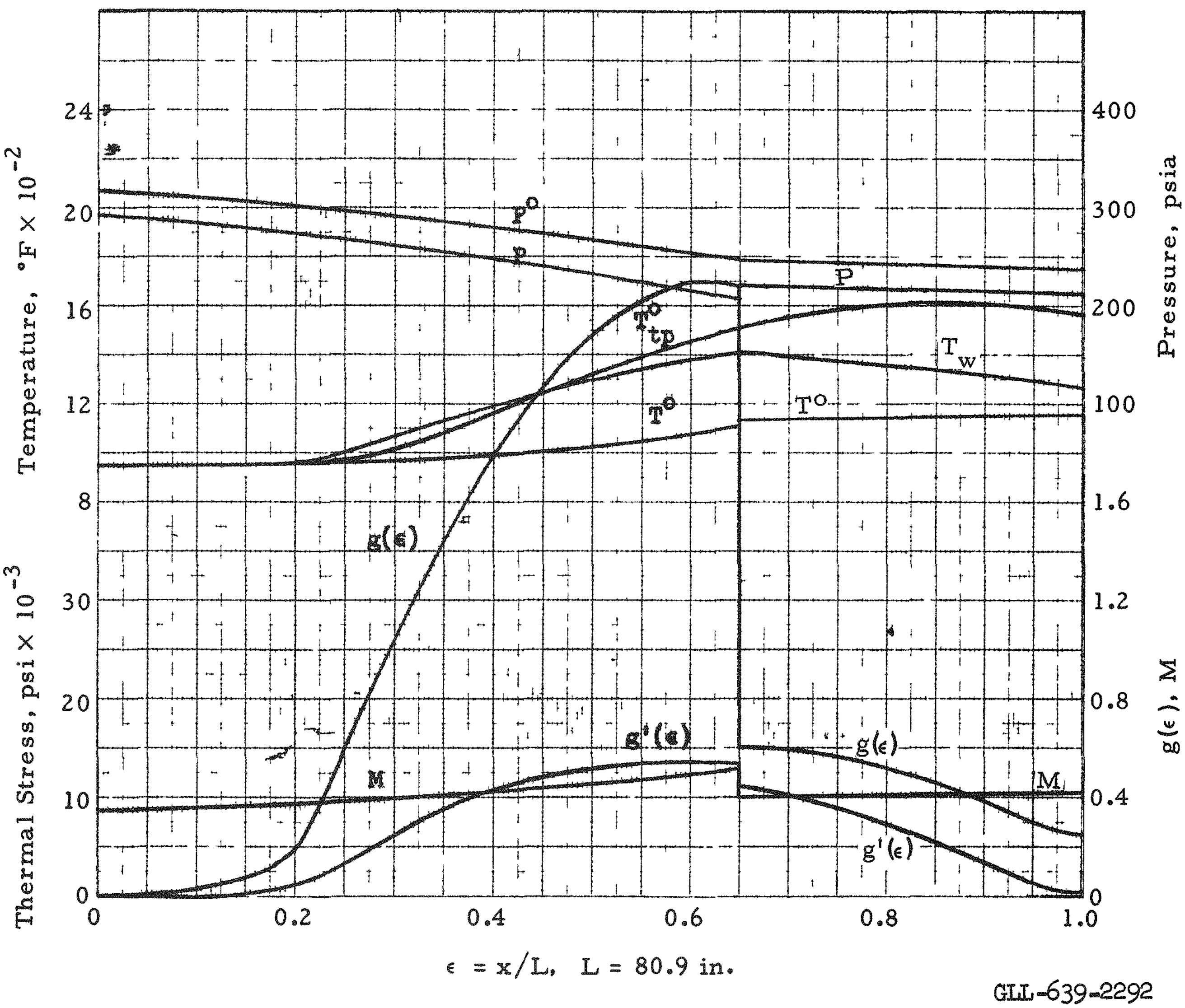

Flow channel diam:	1.162 in.	Exit Mach number:	0.4234
Porosity: *	0.7478	Peak wall temp:	1412°F
Inlet total temp:	946°F	Power to air:	102.363 kW
Exit total temp:	1156°F	Average material power density:	5.196 MW/ft^3
Inlet total pressure:	316.4 psia	Flow rate:	1.813 lb/sec
Exit total pressure:	238.2 psia	All dimensions at:	60°F

*Control rod inserted.

Control tie rod (control rod inserted 37.4 in.), diffuser design point condition.

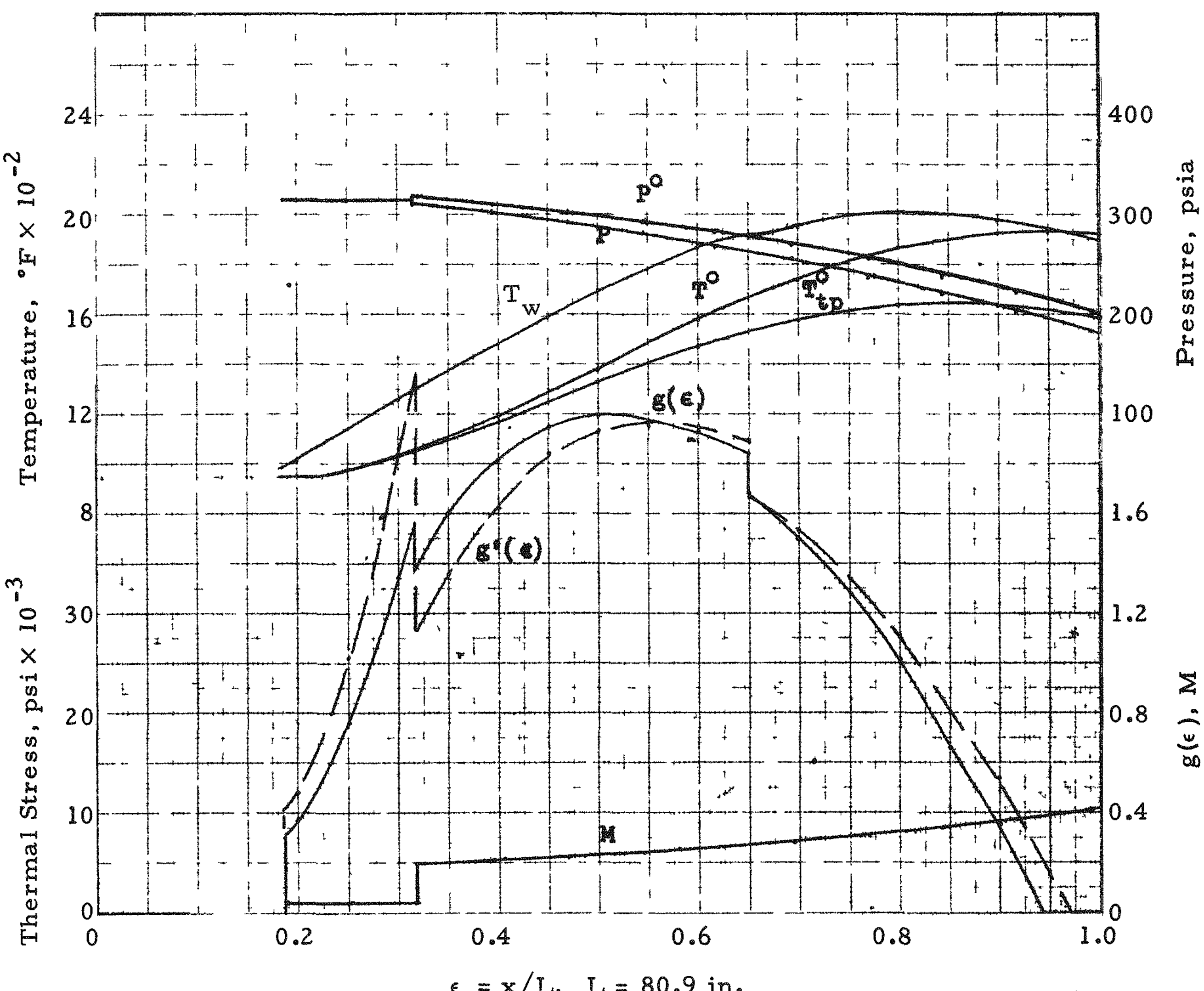

GLL-639-2293

Flow channel diam:	0.130 in.	Exit Mach number:	0.4119
Porosity:	0.1761	Peak wall temp:	2008°F
Inlet total temp:	946°F	Power to air:	5.225 kW
Exit total temp:	1927°F	Average material power density:	2.467 MW/ft^3
Inlet total pressure:	316.4 psia	Flow rate:	0.01818 lb/sec
Exit total pressure:	202.5 psia	All dimensions at:	60°F

Guard tube (control tie rod, control rod inserted 37.4 in.), diffuser design point condition.

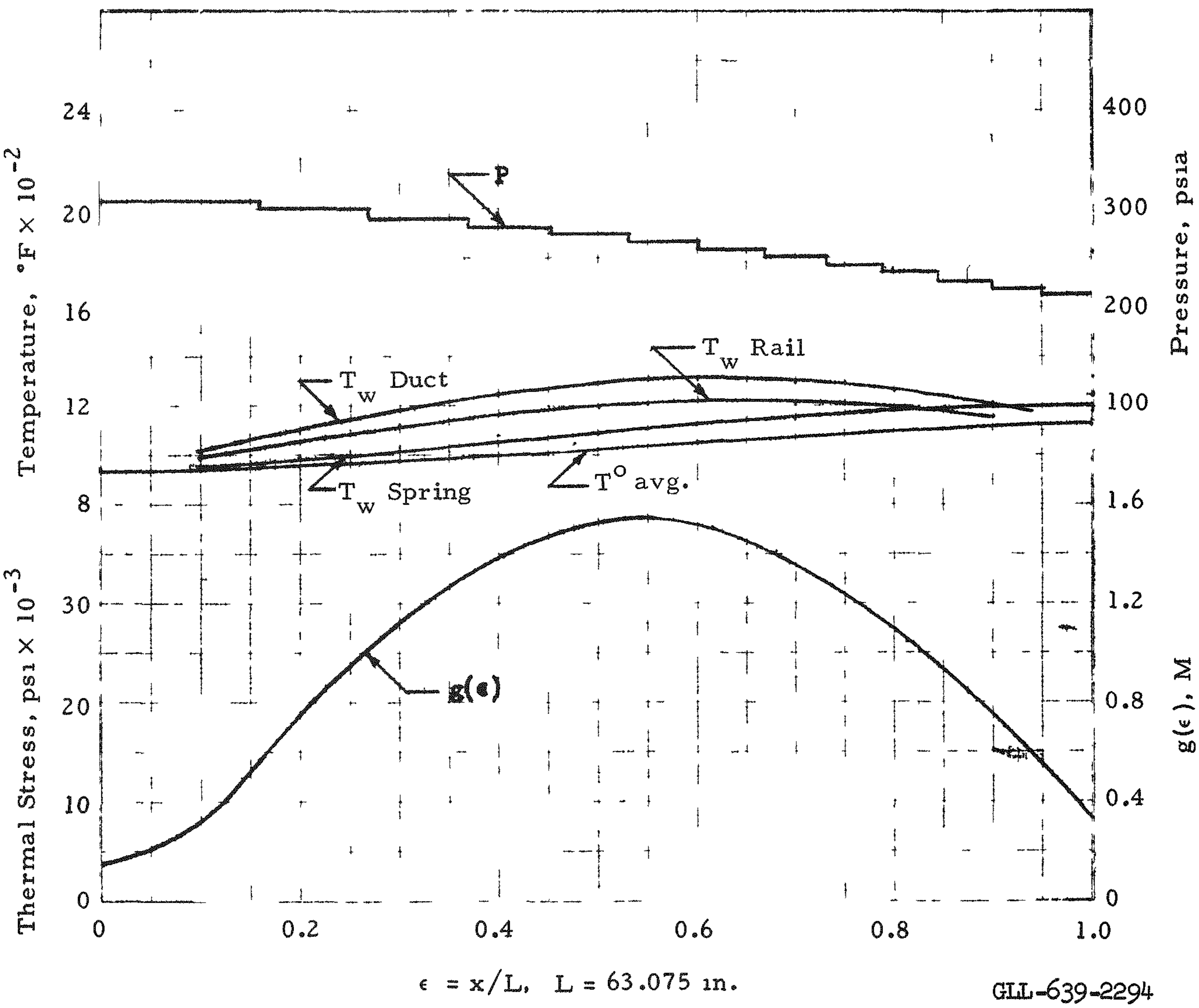

Exit Mach number:	0.21
Peak wall temp: Duct, 1308°F	Rail, 1219°F Spring, 1199°F
Power to air:*	7.30 MW
Average material power density:	768.60 kW/ft^3
Flow rate:	153.21 lb/sec
All dimensions at:	60°F

Inlet total temp:	946°F
Exit total temp:	1120°F
Inlet total pressure:	316.4 psia
Exit total pressure:	214.7 psia

*Includes 53% of heat generated in peripheral shim.

Side support structure, diffuser design point condition.

Summary of Component Operating Characteristics for Reactor Structural Design Condition

Component	Peak wall temp (°F)	Exit gas temp (°F)	Single-element flow rate (lb/sec)	Total pressure drop (psi)	Peak material power density (MW/ft^3)
Fueled tubes (average)	2500	2181	0.06719	90.4	27.46
Tie rod } Center position	1522	1230	0.7224	66.9	8.64
Guard tubes } Center position	2112	1984	0.01947	123.9	2.49
Control rod (17.2 in. insertion)	1466	1147	2.533	78.1	20.7
Control tie rod	1342	1147	2.533	78.1	8.86
Guard tube	2002	1929	0.01972	123.8	2.96
Spare control tie rod	1171	1084	3.615	46.4	8.86
Side reflector (BeO)					
Inner radius	2120	2010	0.008384 (average)	132.9 (average)	1.07
Outer radius	1630	1590			6.22
Peripheral shim					
Inner radius	1670	1620	0.02027 (average)	126.0 (average)	2.20
Outer radius	1569	1534			1.91
Side support structure					
Spring	1299	1205	183.0(total)	110.9	1.17
Rail	1275	1205	183.0(total)	110.9	0.910
Duct	1354	1205	183.0(total)	110.9	0.644

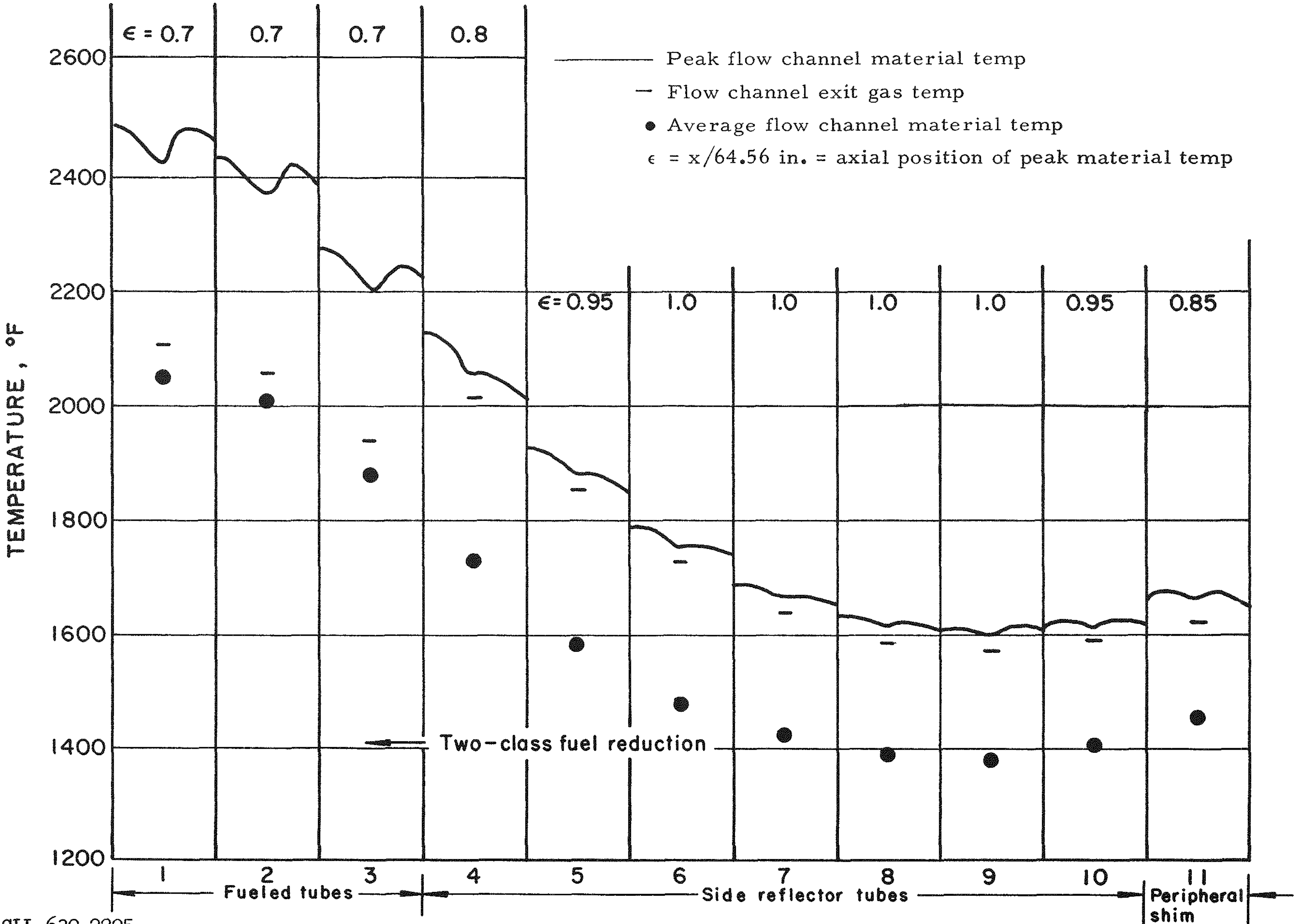

GLL-639-2295

Analysis of side reflector region radial temperature, at reactor structural design condition.

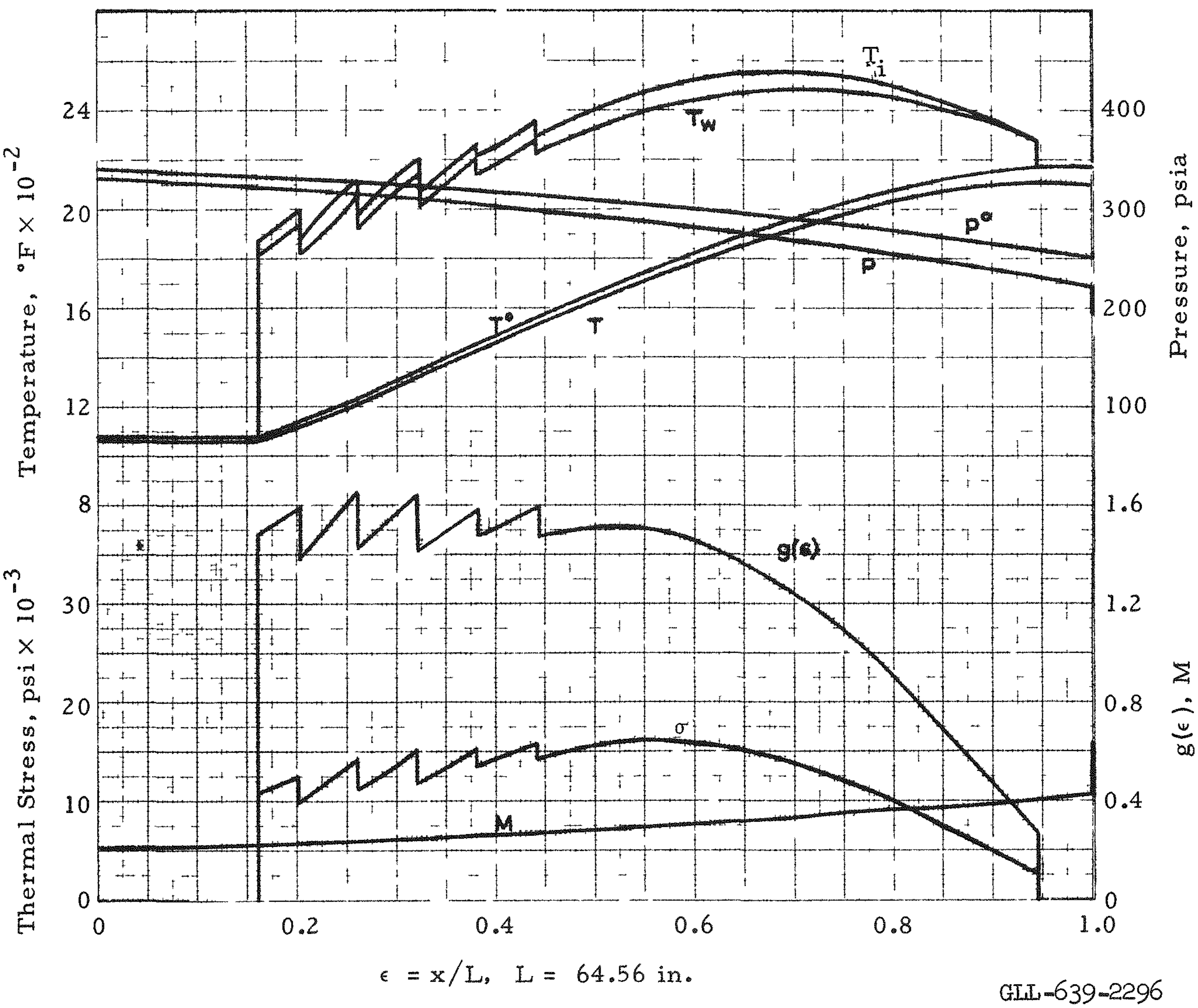

Flow channel diam:	0 227 in.	Exit Mach number:	0.422
Porosity:	0.5297	Peak wall temp:	2500°F
Inlet total temp:	1065°F	Power to air:	22.289 kW
Exit total temp:	2181°F	Average material power density:	16.605 MW/ft^3
Inlet total pressure:	342.3 psia	Flow rate:	0.067191 lb/sec
Exit total pressure:	251.9 psia	All dimensions at:	60°F

Average fueled tube, reactor structural design condition.

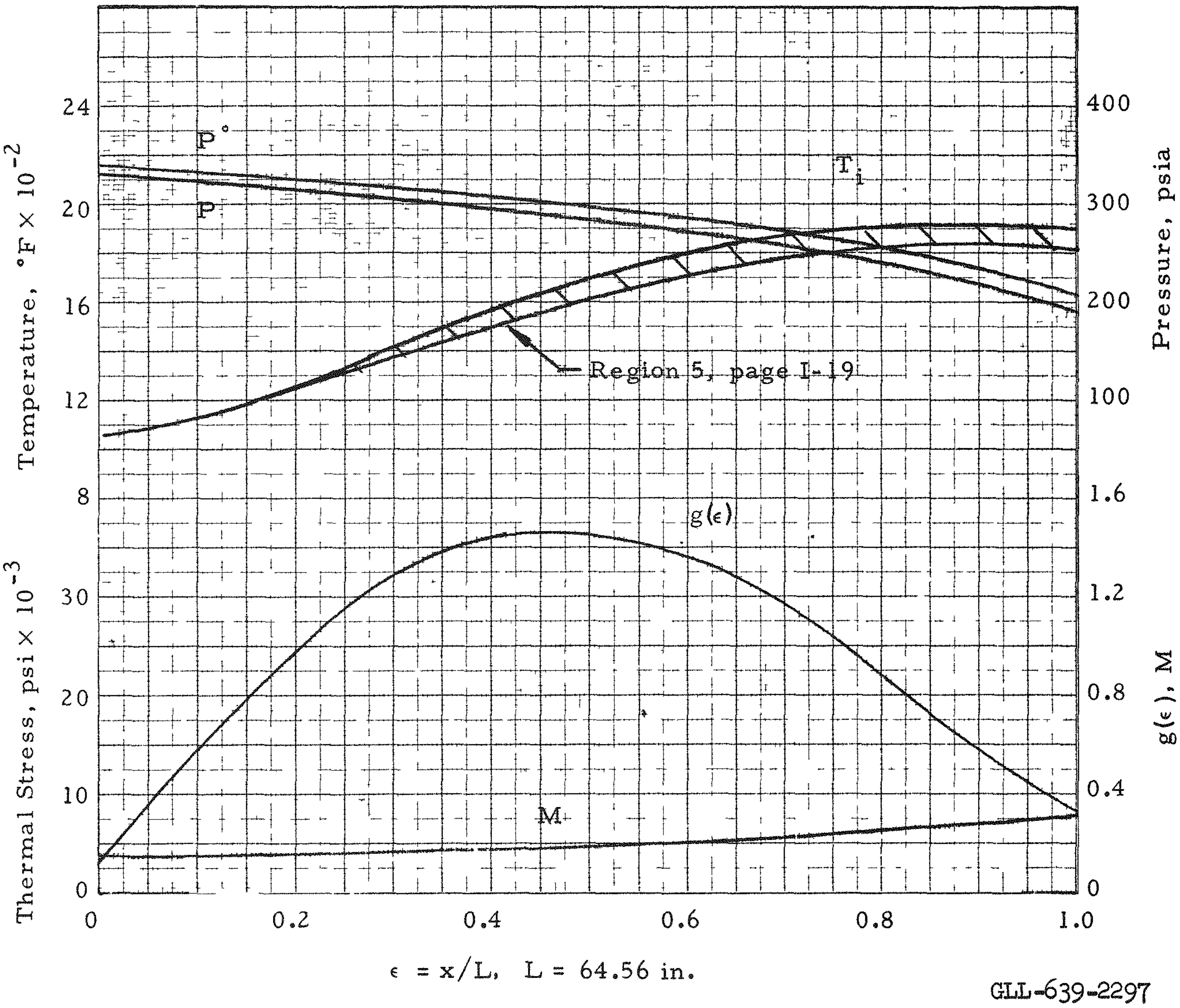

Flow channel diam:	0.093 in.	Exit Mach number:	0.324
Porosity:	0.0895	Peak wall temp:	2182°F (region 4, page I-19)
Inlet total temp:	1065°F	Power to air:	1.463 kW av
Exit total temp:	1710°F av	Average material power density:	0.567 MW/ft^3 av
Inlet total pressure:	342.3 psia	Flow rate:	0.008384 lb/sec av
Exit total pressure:	209.4 psia av	All dimensions at:	60°F

Side reflector tube, reactor structural design condition.

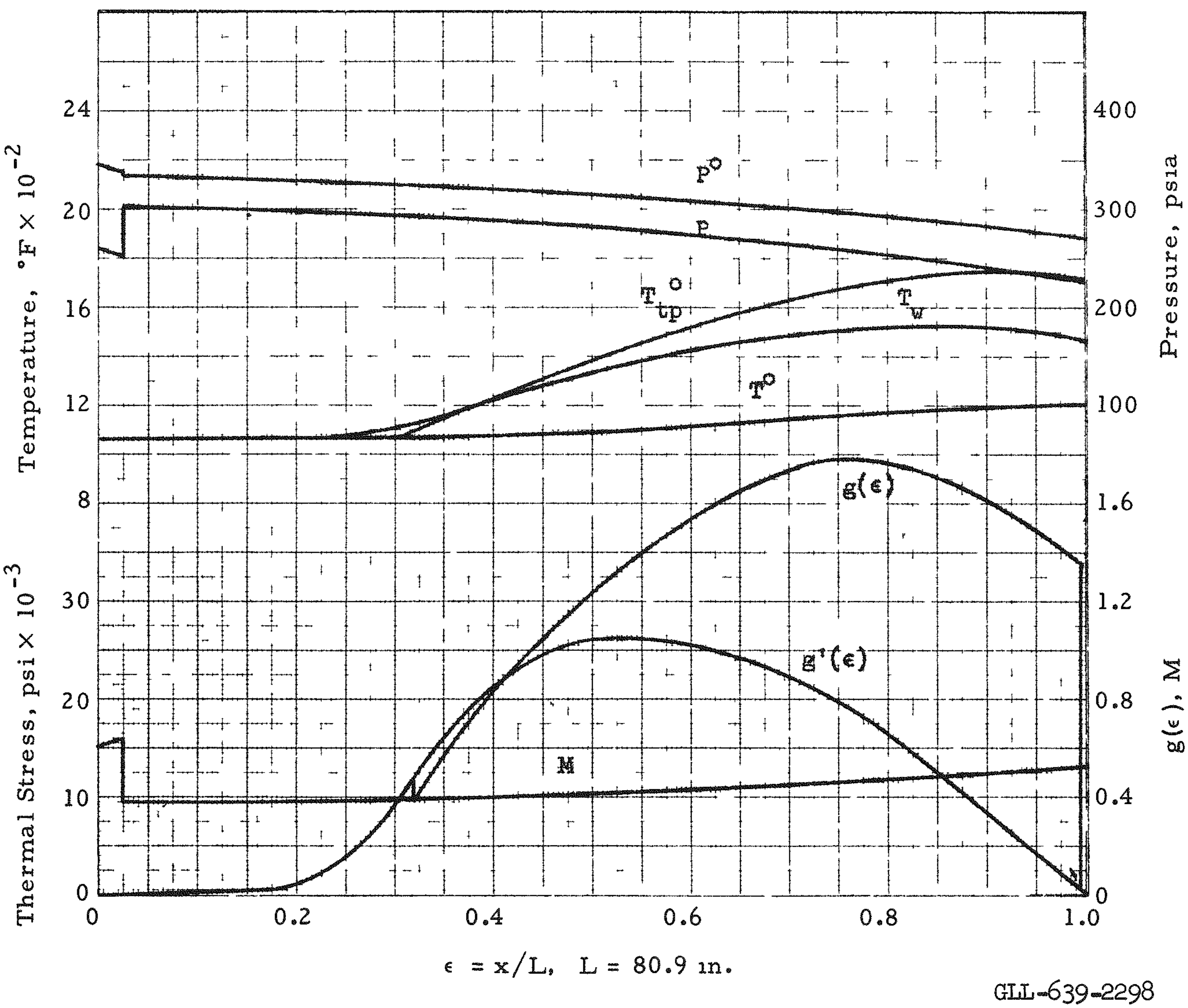

Flow channel diam:	0.576 in.	Exit Mach number:	0.536
Porosity:	0 7391	Peak wall temp:	1522°F
Inlet total temp:	1065°F	Power to air:	34.1 kW
Exit total temp:	1230°F	Average material power density:	5.72 MW/ft^3
Inlet total pressure:	342.3 psia	Flow rate:	0.7224 lb/sec
Exit total pressure:	275.4 psia	All dimensions at:	60°F

Tie rod (central), reactor structural design condition.

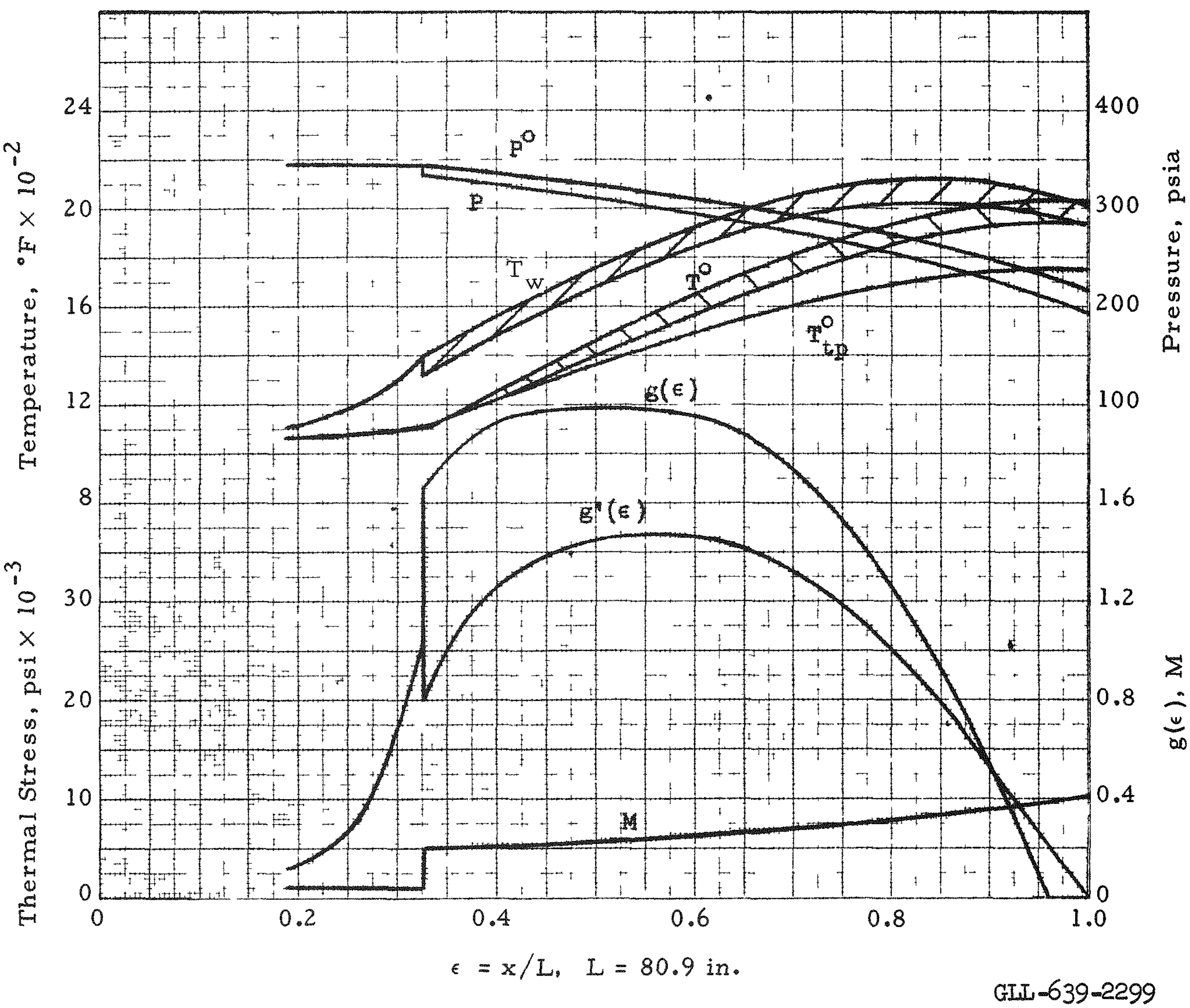

Flow channel diam:	0.130 in.	Exit Mach number:	0.412
Porosity:	0.1761	Peak wall temp:	2112°F
Inlet total temp:	1065°F	Power to air:	5.05 kW
Exit total temp:	1984°F	Average material power density:	1.65 MW/ft^3
Inlet total pressure:	342.3 psia	Flow rate:	0.01947 lb/sec
Exit total pressure:	218.4 psia	All dimensions at:	60°F

Guard tube (central), reactor structural design condition.

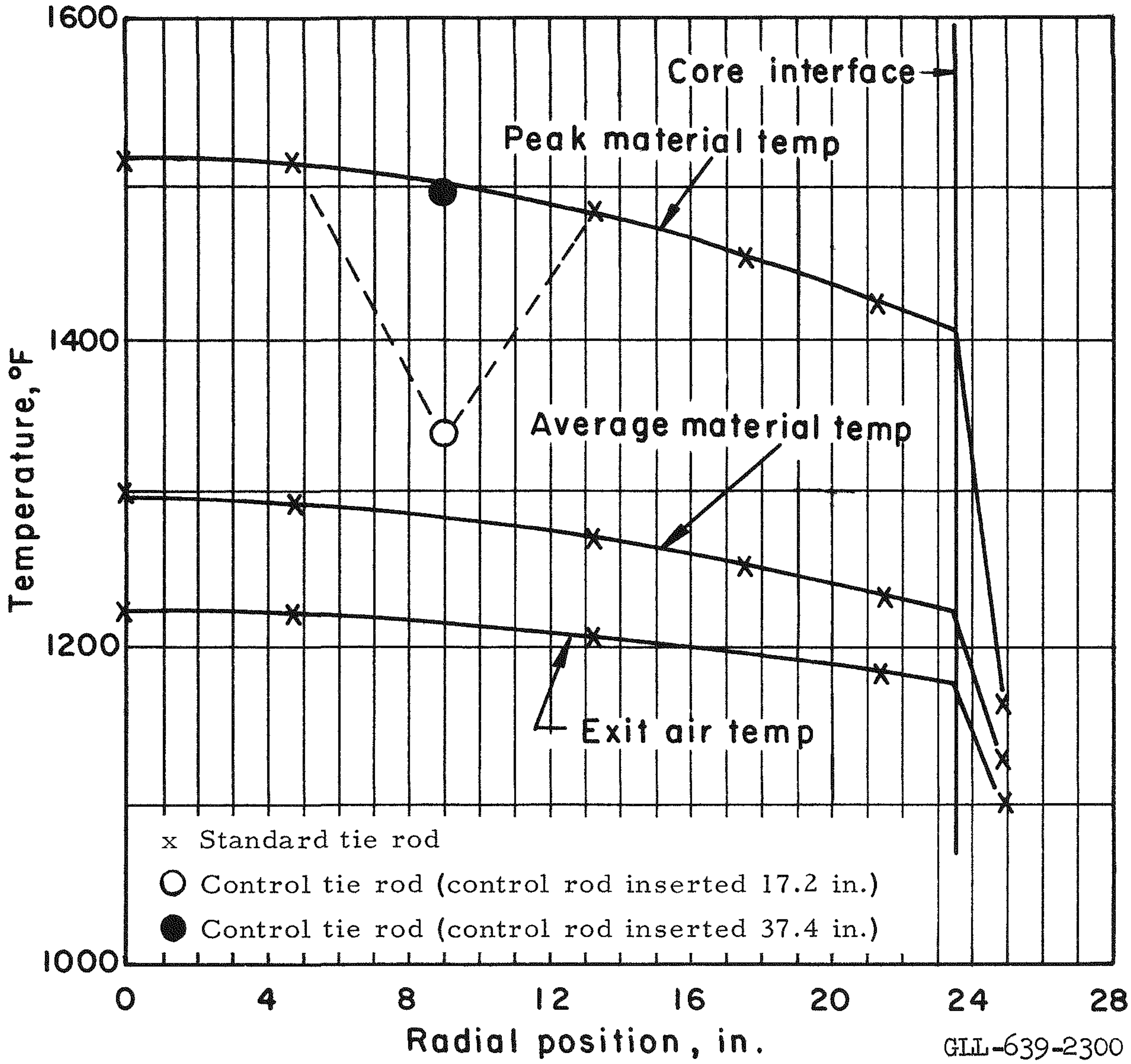

Nominal radial profile of tie rod temperatures, reactor structural design condition.

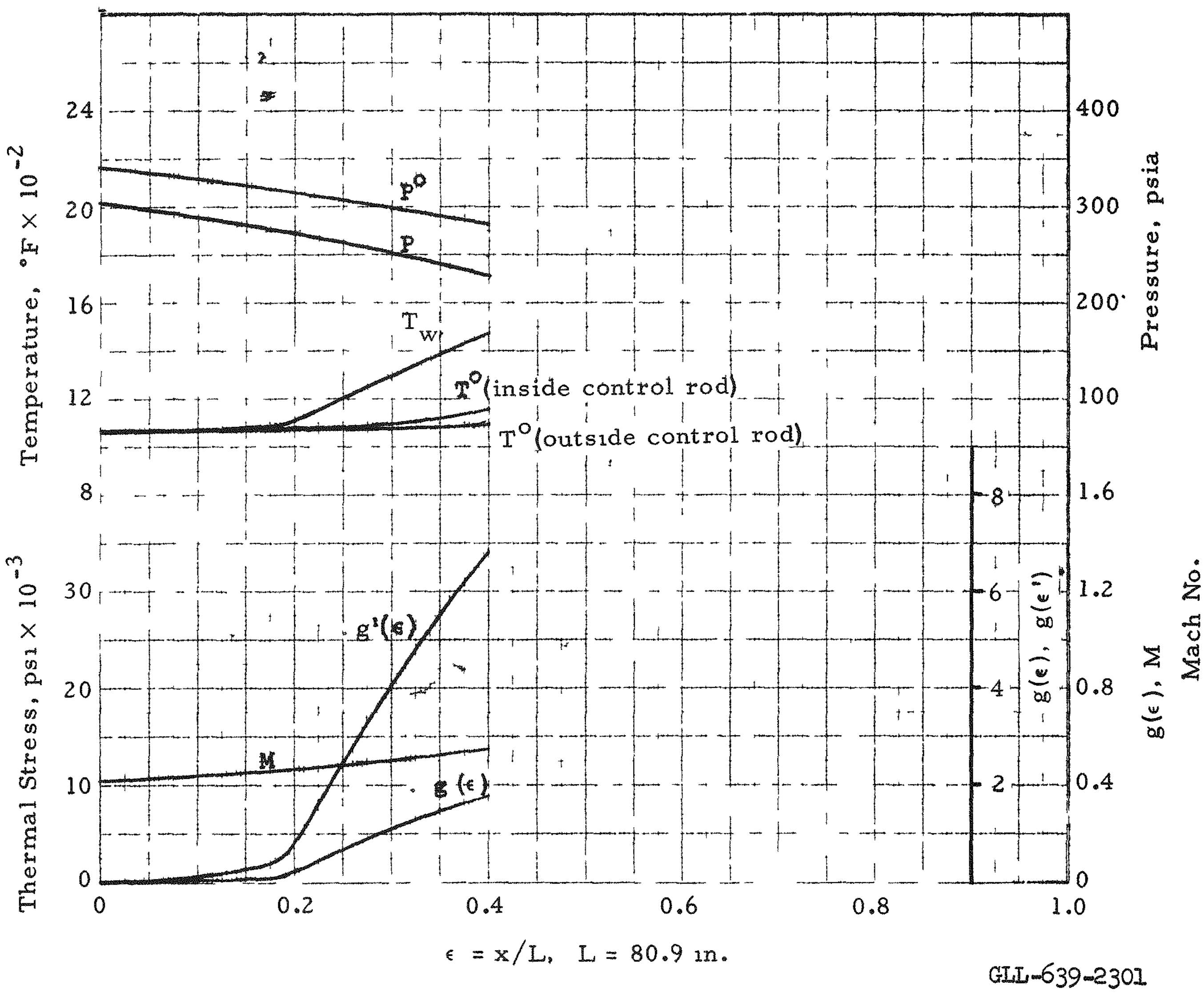

		Exit Mach number:	0.5545
		Peak wall temp:	1466°F
Inlet total temp:	1065°F	Power to air:	6.31 kW
Exit total temp:	1160°F	Average material power density:	6.554 MW/ft^3
Inlet total pressure:	342.3 psia	Flow rate:*	0.2316 lb/sec
Exit total pressure:	281.1 psia	All dimensions at:	60°F

*Inside control rod.

Control rod (inserted 17.2 in.), reactor structural design condition.

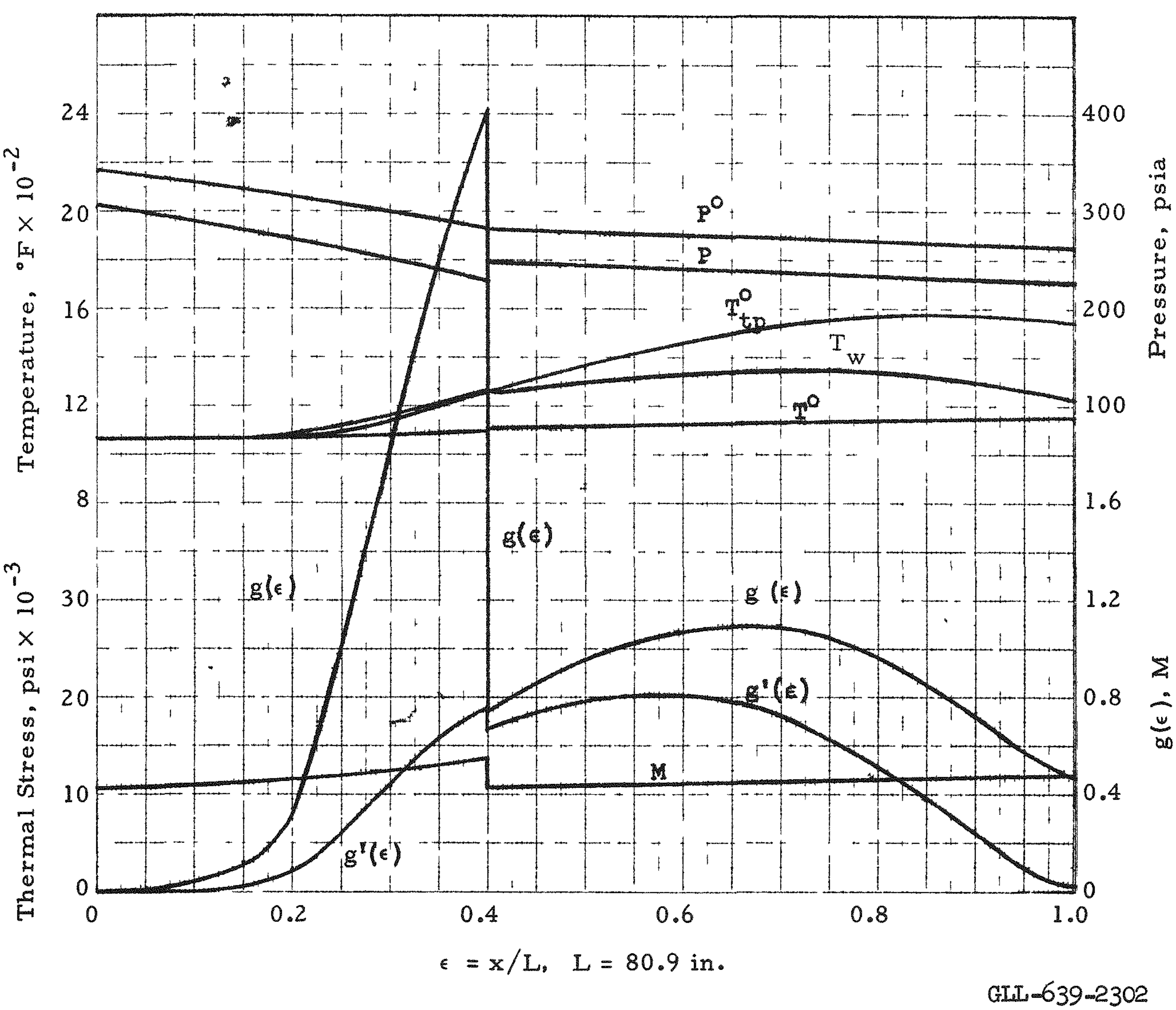

Flow channel diam:	1.162 in.	Exit Mach number:	0.4716
Porosity:*	0.7478	Peak wall temp:	1342°F
Inlet total temp:	1065°F	Power to air:	56.812 kW
Exit total temp:	1147°F	Average material power density:	4.793 MW/ft^3
Inlet total pressure:	342.3 psia	Flow rate:	2.3017 lb/sec
Exit total pressure:	264.2 psia	All dimensions at:	60°F

*Control rod inserted.

Control tie rod (control rod inserted 17.2 in.), reactor structural design condition.

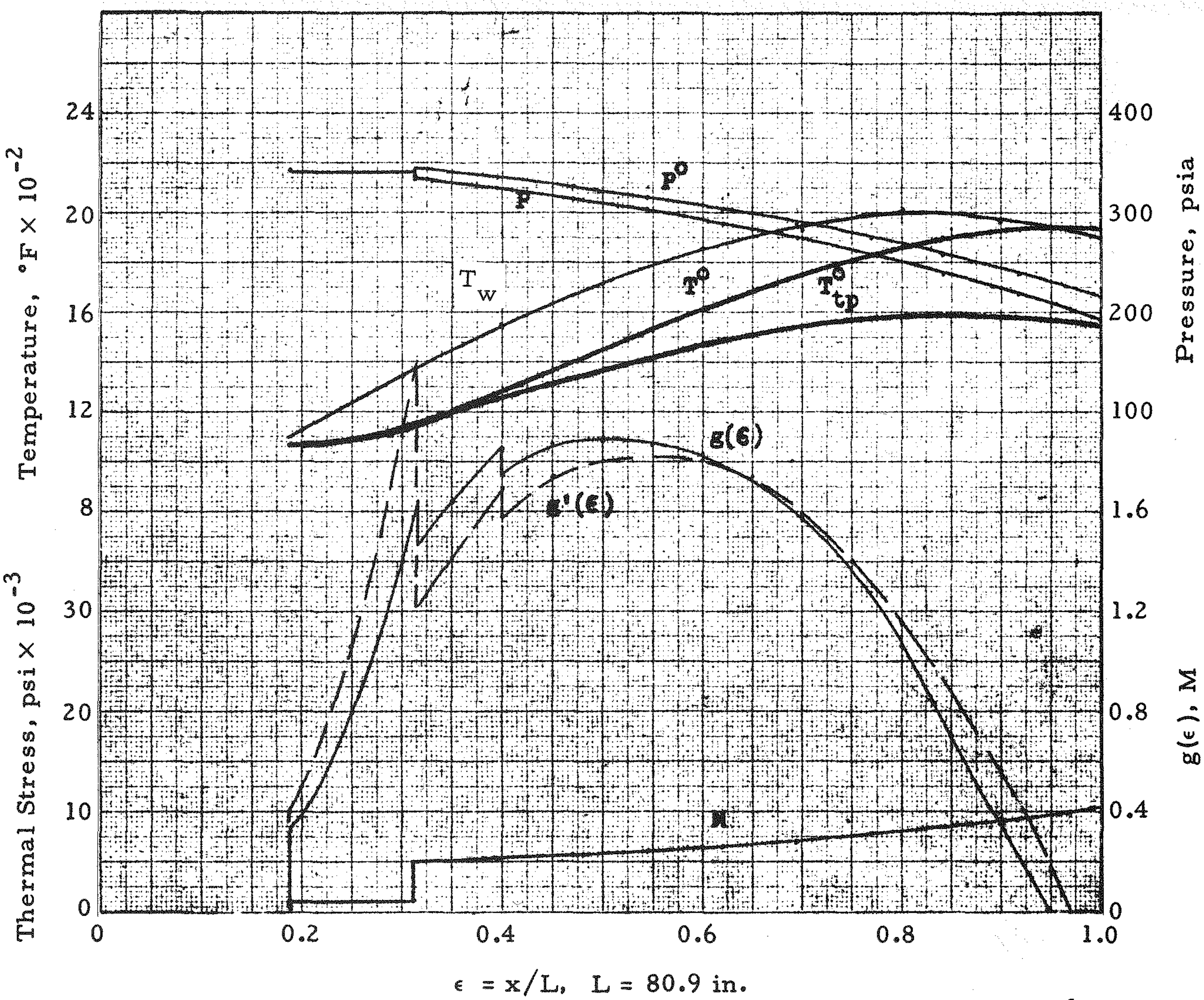

GLL-639-2303

Flow channel diam:	0.130 in.	Exit Mach number:	0.4139
Porosity:	0.1761	Peak wall temp:	2002°F
Inlet total temp:	1065°F	Power to air:	5.013 kW
Exit total temp:	1929°F	Average material power density:	2.281 MW/ft^3
Inlet total pressure:	342.3 psia	Flow rate:	0.01972 lb/sec
Exit total pressure:	218.5 psia	All dimensions at:	60°F

Guard tube (control tie rod, control rod inserted 17.2 in.), reactor structural design condition.

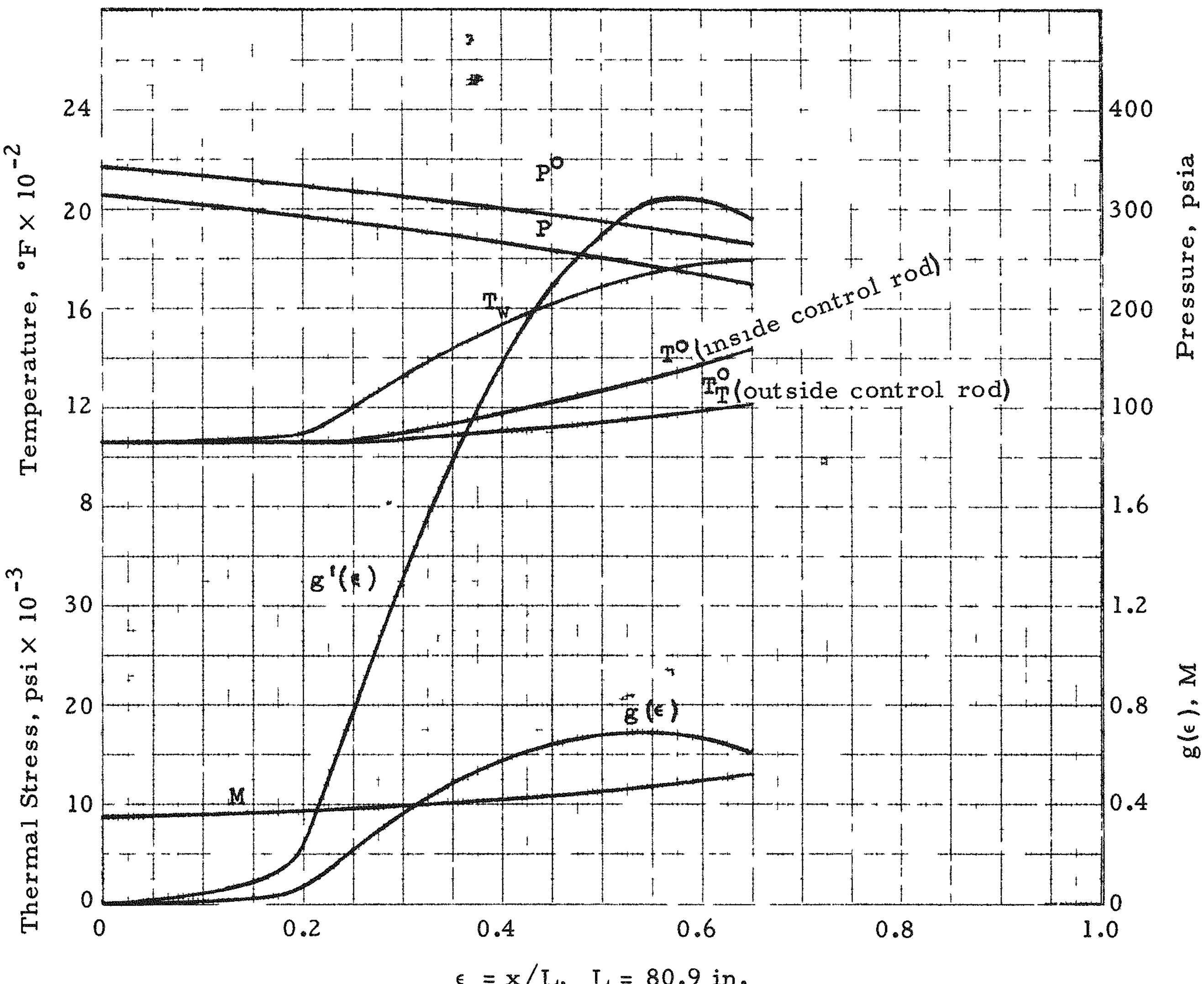

		Exit Mach number:	0.5187
		Peak wall temp:	1792°F
Inlet total temp:	1065°F	Power to air:	20.33 kW
Exit total temp:	1435°F	Average material power density:	14.171 MW/ft^3
Inlet total pressure:	342.3 psia	Flow rate:	0.1910 lb/sec
Exit total pressure:	265.3 psia	All dimensions at:	60°F

Control rod (inserted 37.4 in.), reactor structural design condition.

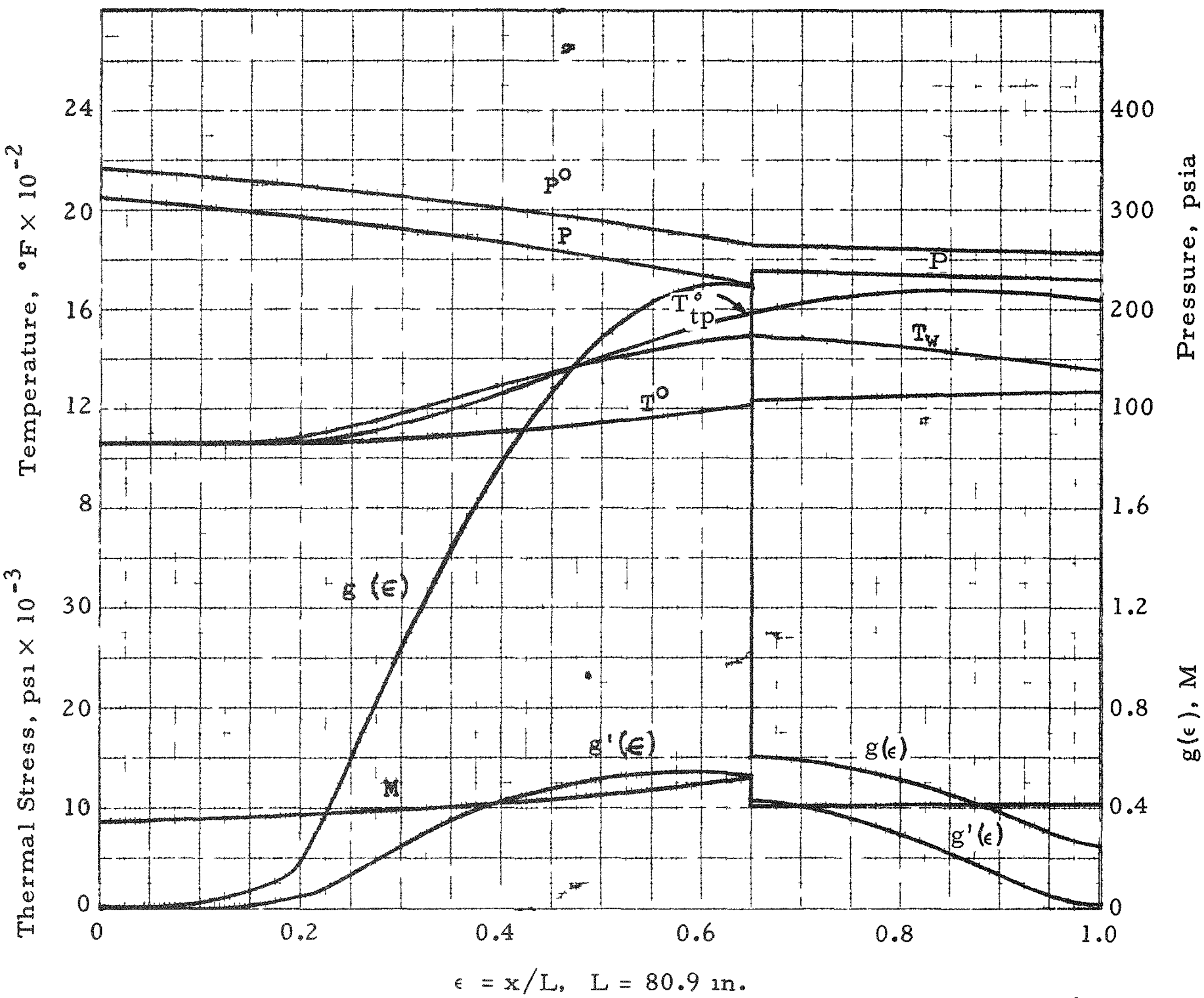

GLL-639-2305

Flow channel diam:	1.162	Exit Mach number:	0.4243
Porosity:*	0.7478	Peak wall temp:	1500°F
Inlet total temp:	1065°F	Power to air:	101.877 kW
Exit total temp:	1263°F	Average material power density:	5.174 MW/ft^3
Inlet total pressure:	342.3 psia	Flow rate:	1.897 lb/sec
Exit total pressure:	256.9 psia	All dimensions at:	60°F

*Control rod inserted.

Control rod tie rod (control rod inserted 37.4 in.), reactor structural design condition

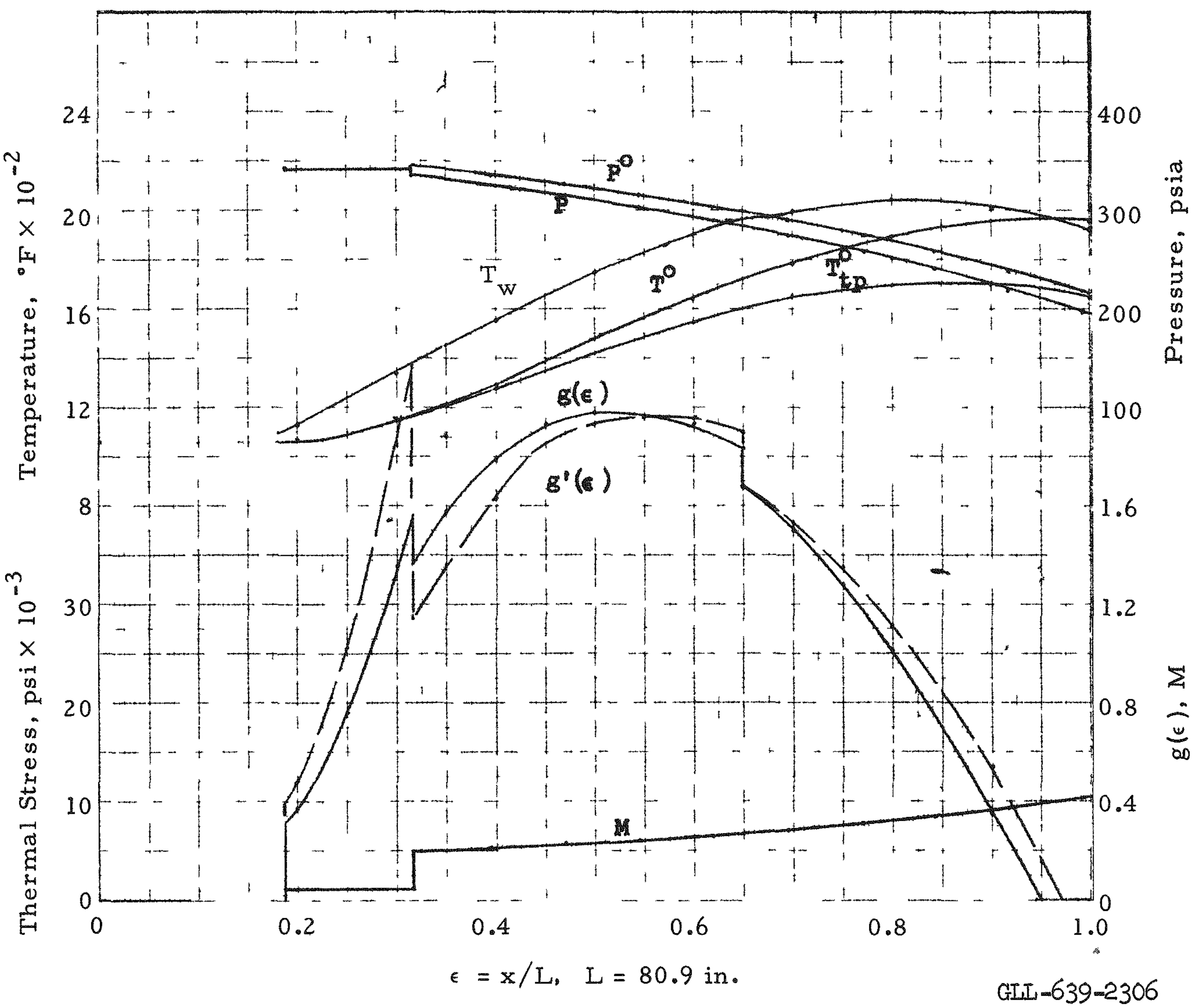

Flow channel diam:	0.130	Exit Mach number:	0.4141
Porosity:	0.1761	Peak wall temp:	2038°F
Inlet total temp:	1065°F	Power to air:	5.189 kW
Exit total temp:	1963°F	Average material power density:	2.457 MW/ft^3
Inlet total pressure:	342.3 psia	Flow rate:	0.01956 lb/sec
Exit total pressure:	218.5 psia	All dimensions at:	60°F

Guard tube (control tie rod, control rod inserted 37.4 in.), reactor structural design condition.

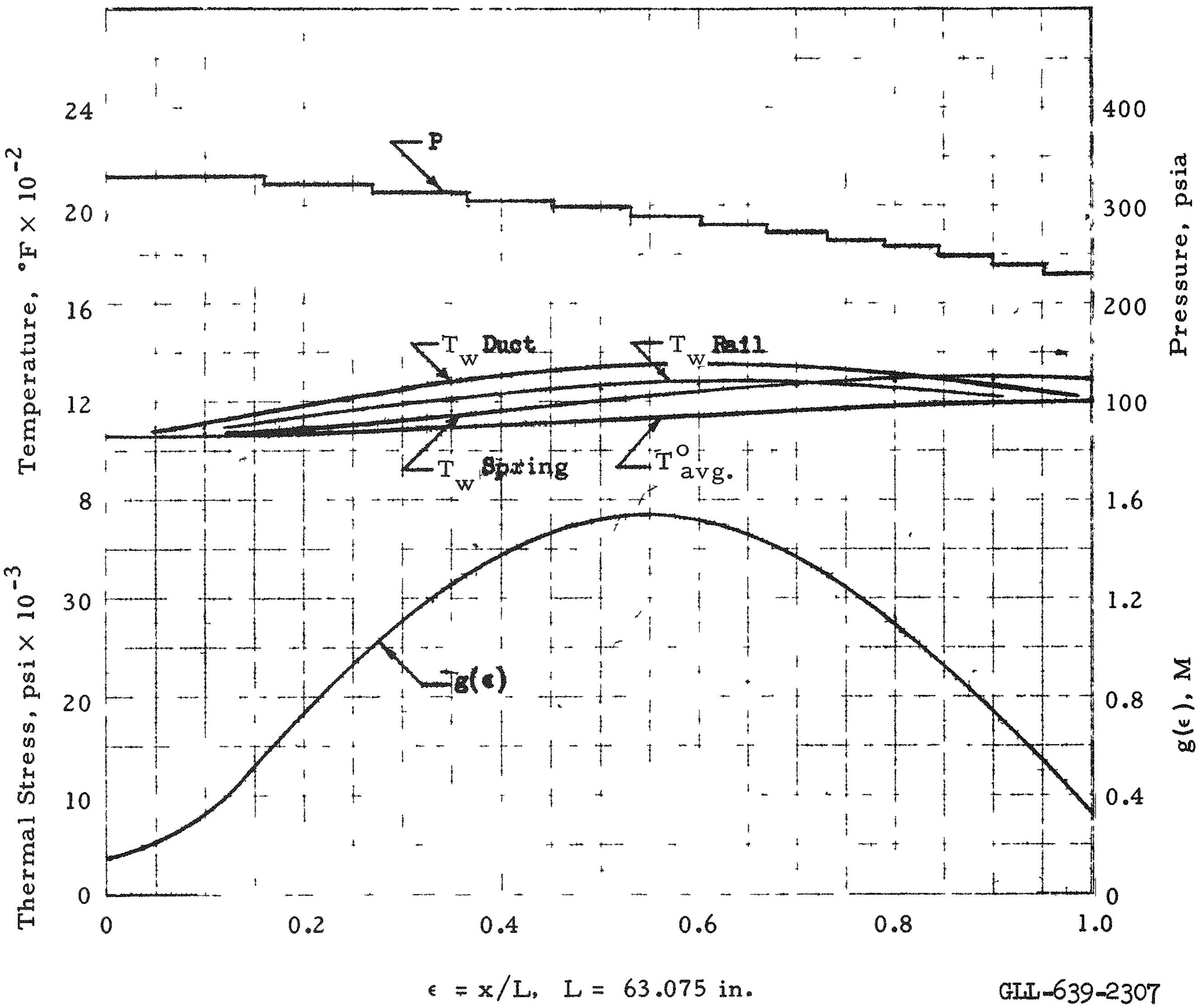

Inlet total temp:	1063°F
Exit total temp:	1205°F
Inlet total pressure:	342.3 psia
Exit total pressure:	231.4 psia

*Includes 53% of heat generated in peripheral shim.

Exit Mach number:	0.24
Peak wall temp:	Duct, 1354°F, Rail, 1275°F, Spring, 1299°F
Power to air:*	7.30428MW
Average material power density:	765.60 kW/ft^3
Flow rate:	182.97 lb/sec
All dimensions at:	60°F

Side support structure, reactor structural design condition.

Summary of Component Operating Characteristics for Cold Inlet Gas Condition

Component	Peak wall temp (°F)	Exit gas temp (°F)	Single-element flow rate (lb/sec)	Total pressure drop (psi)	Peak material power density (MW/ft^3)
Fueled tubes (average)	2500	2073	0.06367	77.5	33.39
Tie rod (Center position)	1198	804	0.7960	51.4	10.50
Guard tubes (Center position)	2011	1846	0.01815	108.6	3.03
Control rod (17.2 in. insertion)	1113	696	2.776	66.4	25.19
Control tie rod	939	696	2.776	66.4	10.77
Guard tube	1862	1761	0.01879	108.5	3.60
Spare control tie rod	735	624	3.954	39.2	10.77
Side reflector (BeO)					
Inner radius	1960	1825	0.008618 (average)	116.0 (average)	1.30
Outer radius	1280	1250			0.756
Peripheral shim					
Inner radius	1350	1280	0.02095 (average)	109.7 (average)	2.68
Outer radius	1226	1180			2.33
Side support structure					
Spring	884	824	146.7(total)	96.4	1.42
Rail	980	824	146.7(total)	96.4	1.11
Duct	1100	824	146.7(total)	96.4	0.784

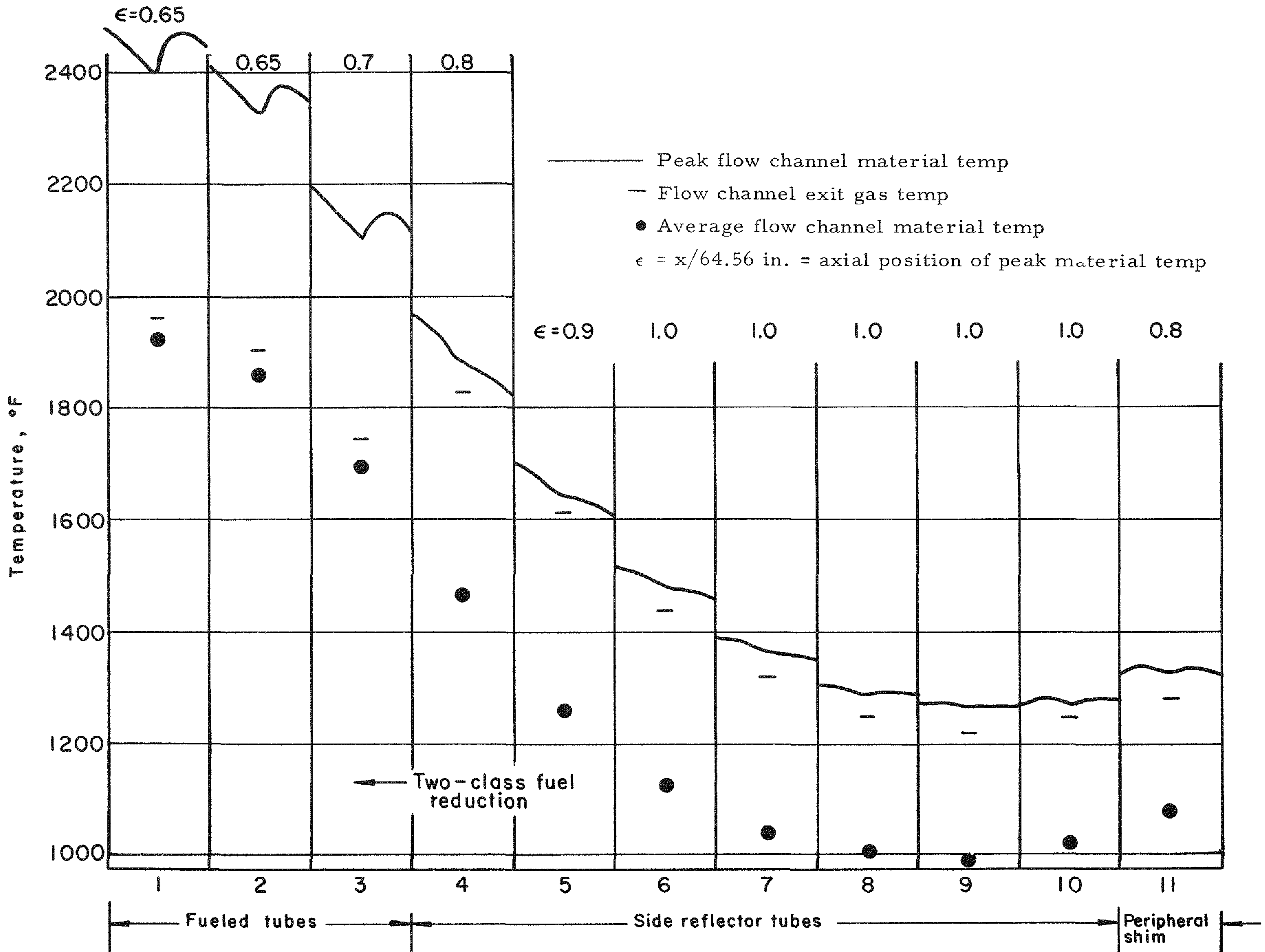

GLL-639-2308

Analysis of side reflector region radial temperature, at cold inlet gas condition.

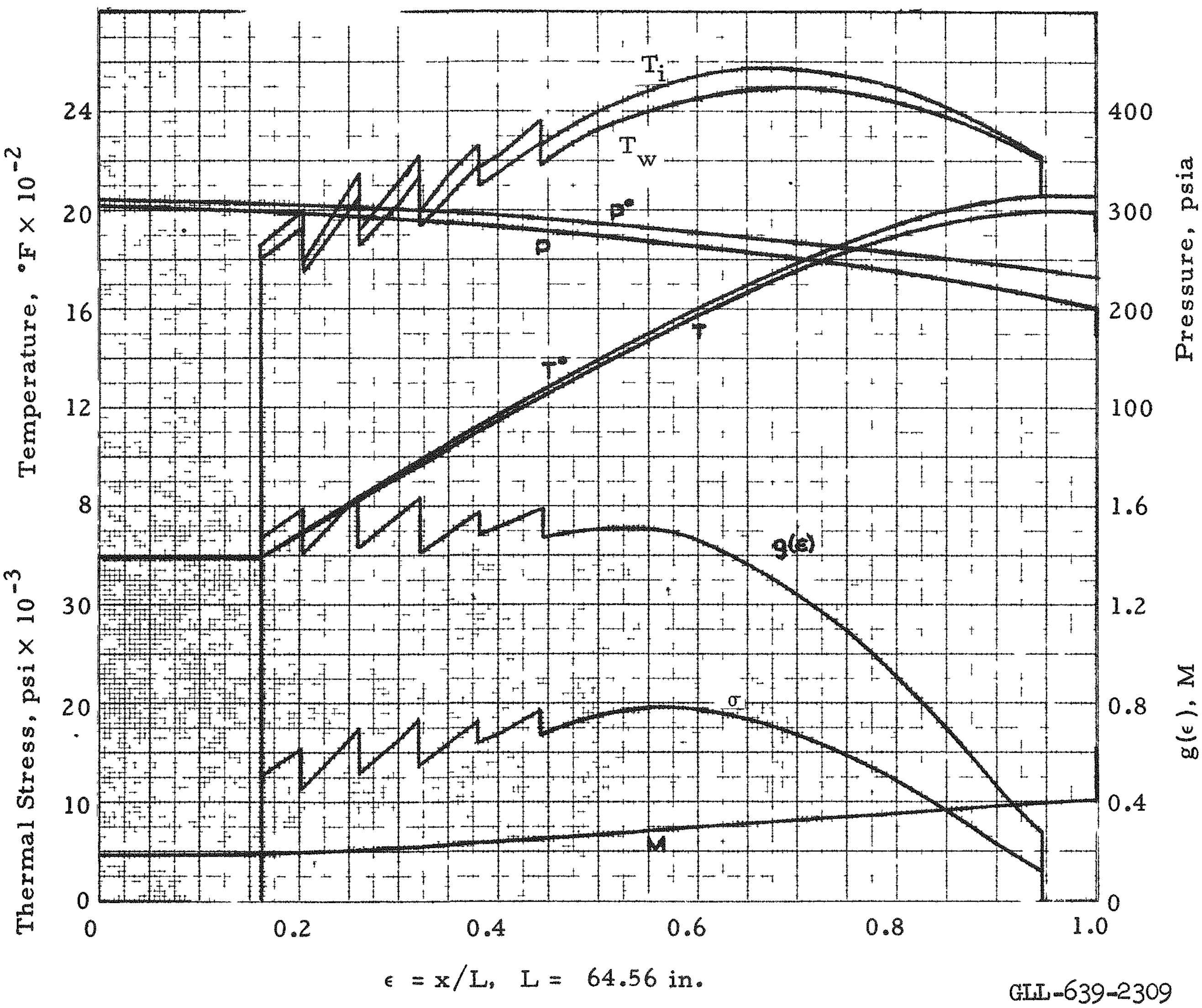

Flow channel diam:	0.227 in.	Exit Mach number:	0.418
Porosity:	0.5297	Peak wall temp:	2500°F
Inlet total temp:	600°F	Power to air:	27.091 kW
Exit total temp:	2073°F	Average material power density:	20.181 MW/ft^3
Inlet total pressure:	312.9 psia	Flow rate:	0.063673 lb/sec
Exit total pressure:	235.4 psia	All dimensions at:	60°F

Average fueled tube, cold inlet gas condition.

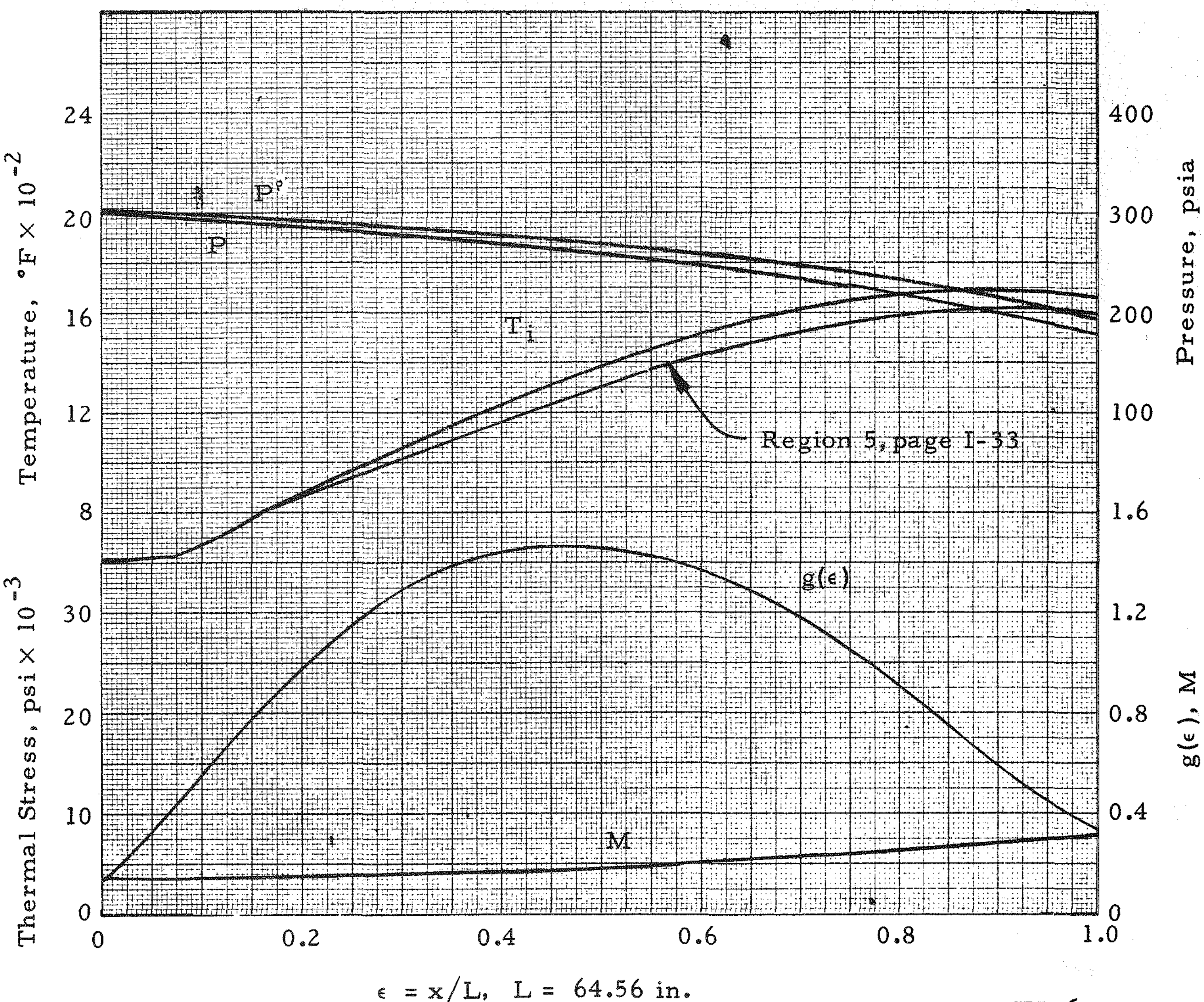

GLL-639-2310

Flow channel diam:	0.093 in.	Exit Mach number:	0.325
Porosity:	0.0895	Peak wall temp: 1961°F(region 4, page I-33)	
Inlet total temp:	600°F	Power to air:	1.78 kW av
Exit total temp:	1416°F av	Average material power density:	0.689 MW/ft^3 av
Inlet total pressure:	312.9 psia	Flow rate:	0.008618 lb/sec
Exit total pressure:	196.9 psia av	All dimensions at:	60°F

Side reflector tube, cold inlet gas condition.

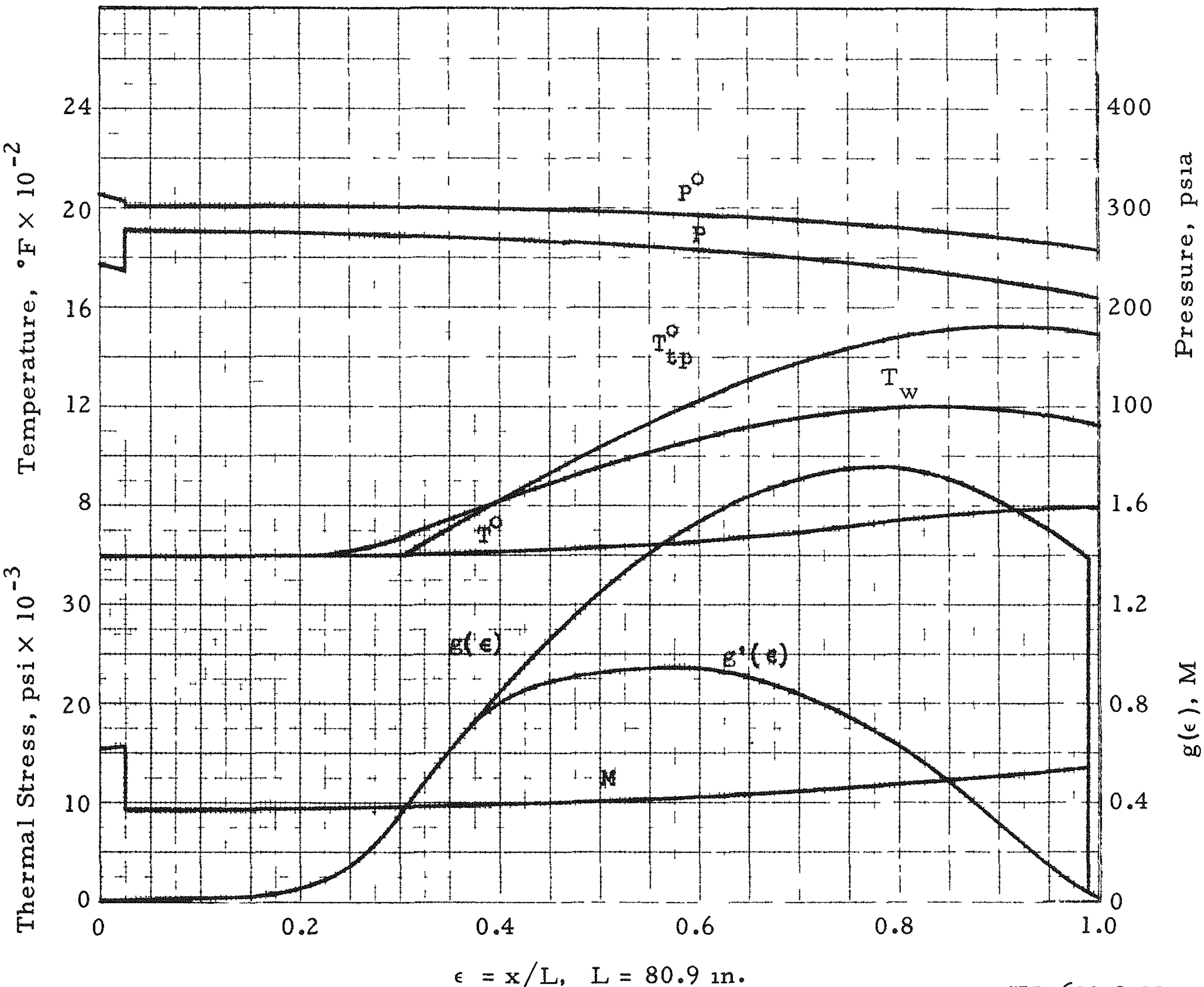

GLL-639-2311

Flow channel diam:	0.576 in.	Exit Mach number:	0.534
Porosity:	0.7391	Peak wall temp:	1198°F
Inlet total temp:	600°F	Power to air:	43.9 kW
Exit total temp:	804°F	Average material power density:	6.94 MW/ft^3
Inlet total pressure:	312.9 psia	Flow rate:	0.7960 lb/sec
Exit total pressure:	261.5 psia	All dimensions at:	60°F

Tie rod (central), cold inlet gas condition.

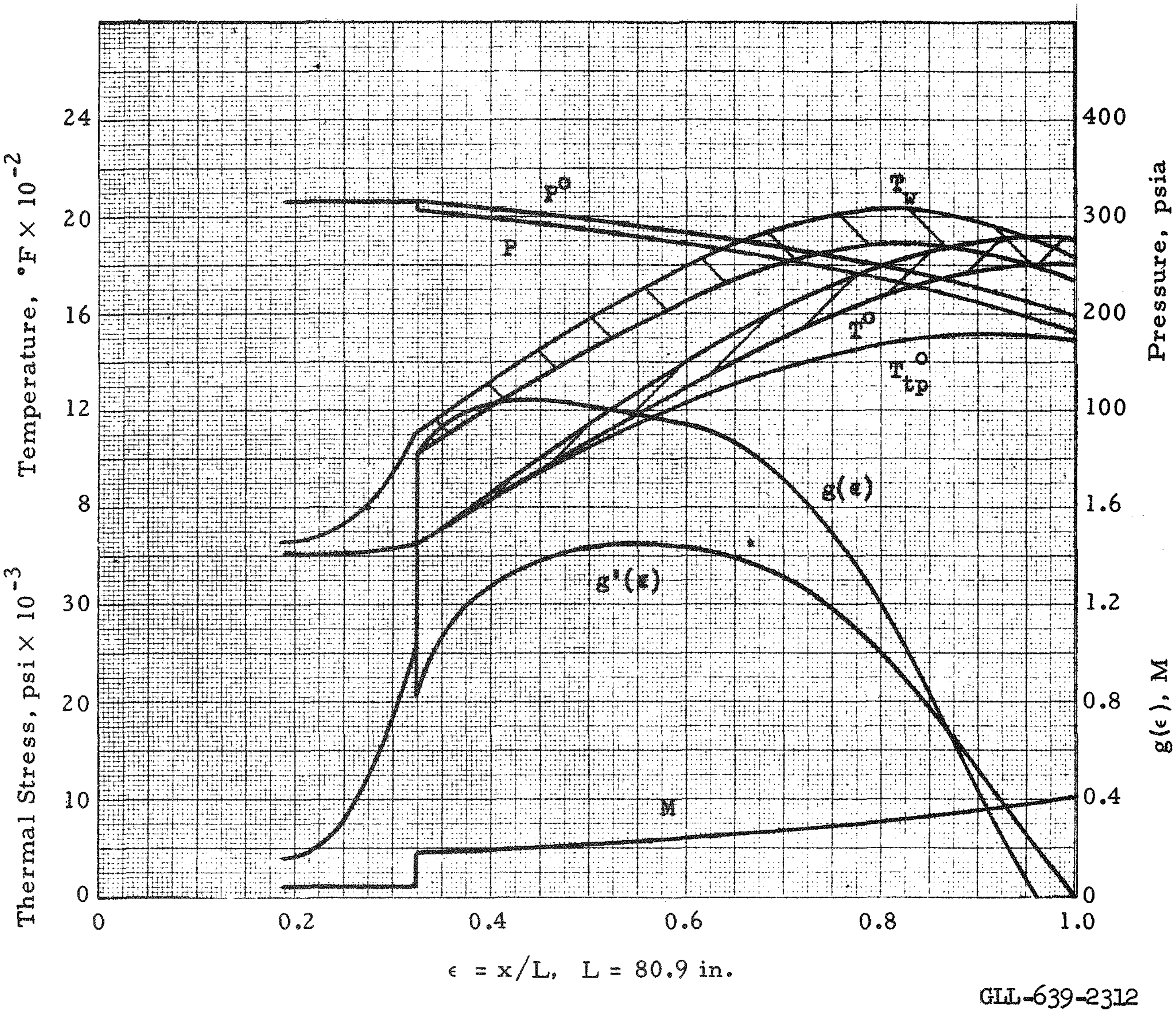

Flow channel diam:	0.130 in.	Exit Mach number:	0.405
Porosity:	0.1761	Peak wall temp:	2011°F
Inlet total temp:	600°F	Power to air:	5.95 kW
Exit total temp:	1846°F	Average material power density:	2.01 MW/ft^3
Inlet total pressure:	312.9 psia	Flow rate:	0.01815 lb/sec
Exit total pressure:	204.3 psia	All dimensions at:	60°F

Guard tube (central), cold inlet gas condition.

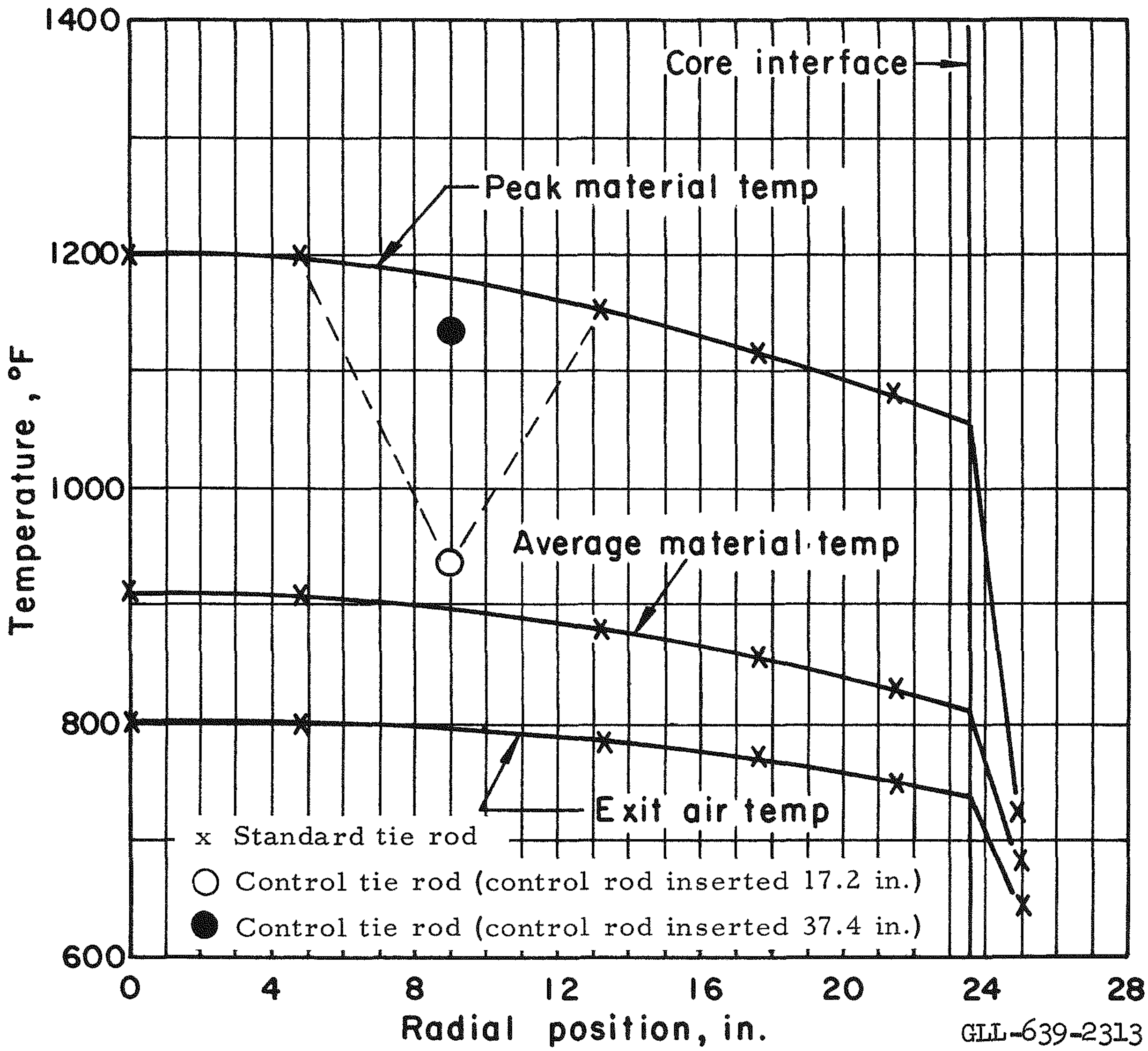

Nominal radial profile of tie rod temperatures, cold inlet gas conditions.

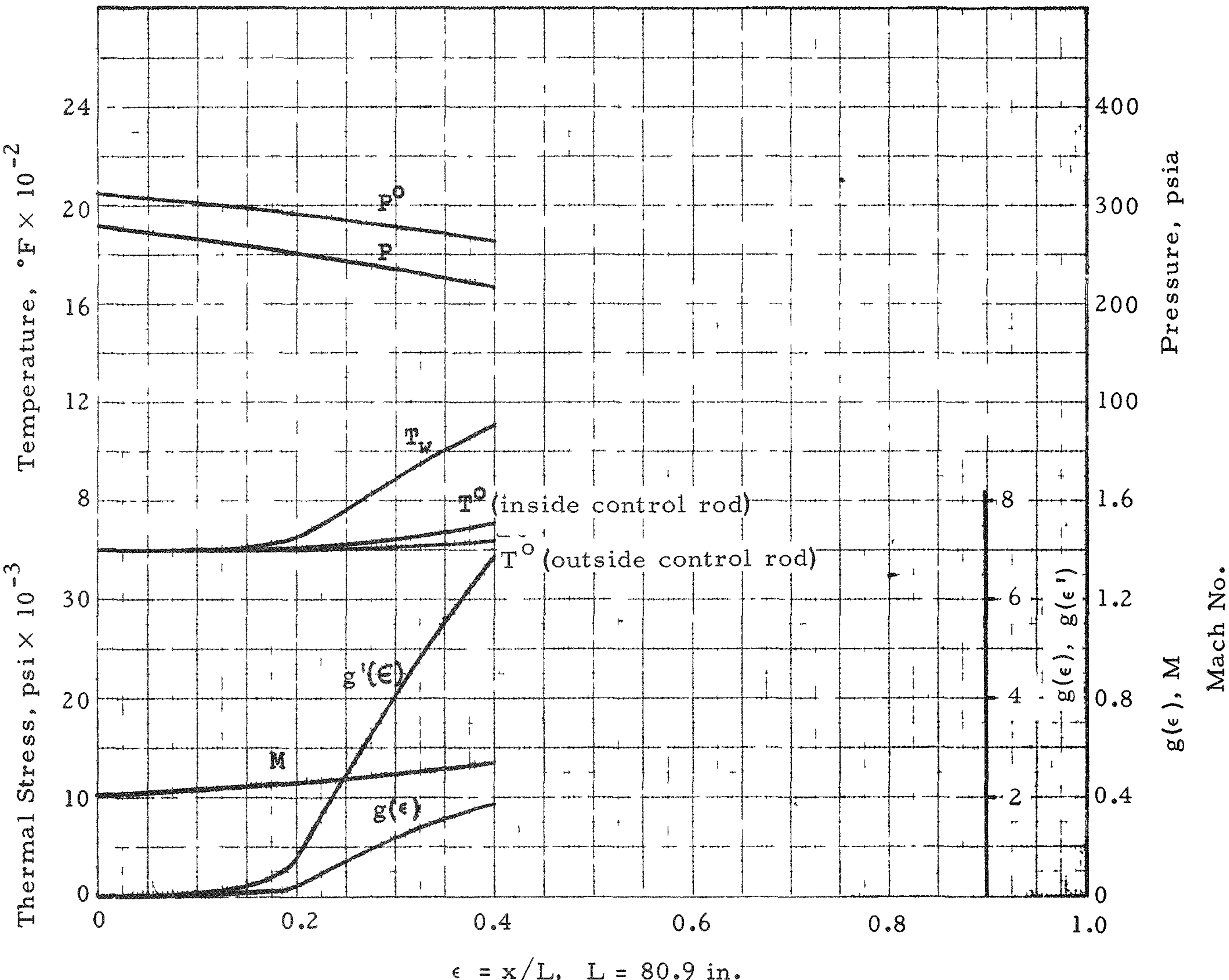

GLL-639-2314

Exit Mach number:	0.5389
Peak wall temp:	1113°F
Power to air:	7.827 kW
Average material power density:	7.969 MW/ft^3
Flow rate:	0.2538 lb/sec
All dimensions at:	60°F

Inlet total temp:	600°F
Exit total temp:	714°F
Inlet total pressure:	312.9 psia
Exit total pressure:	261.8 psia

Inside control rod.

Control rod (inserted 17.2 in.), cold inlet gas condition.

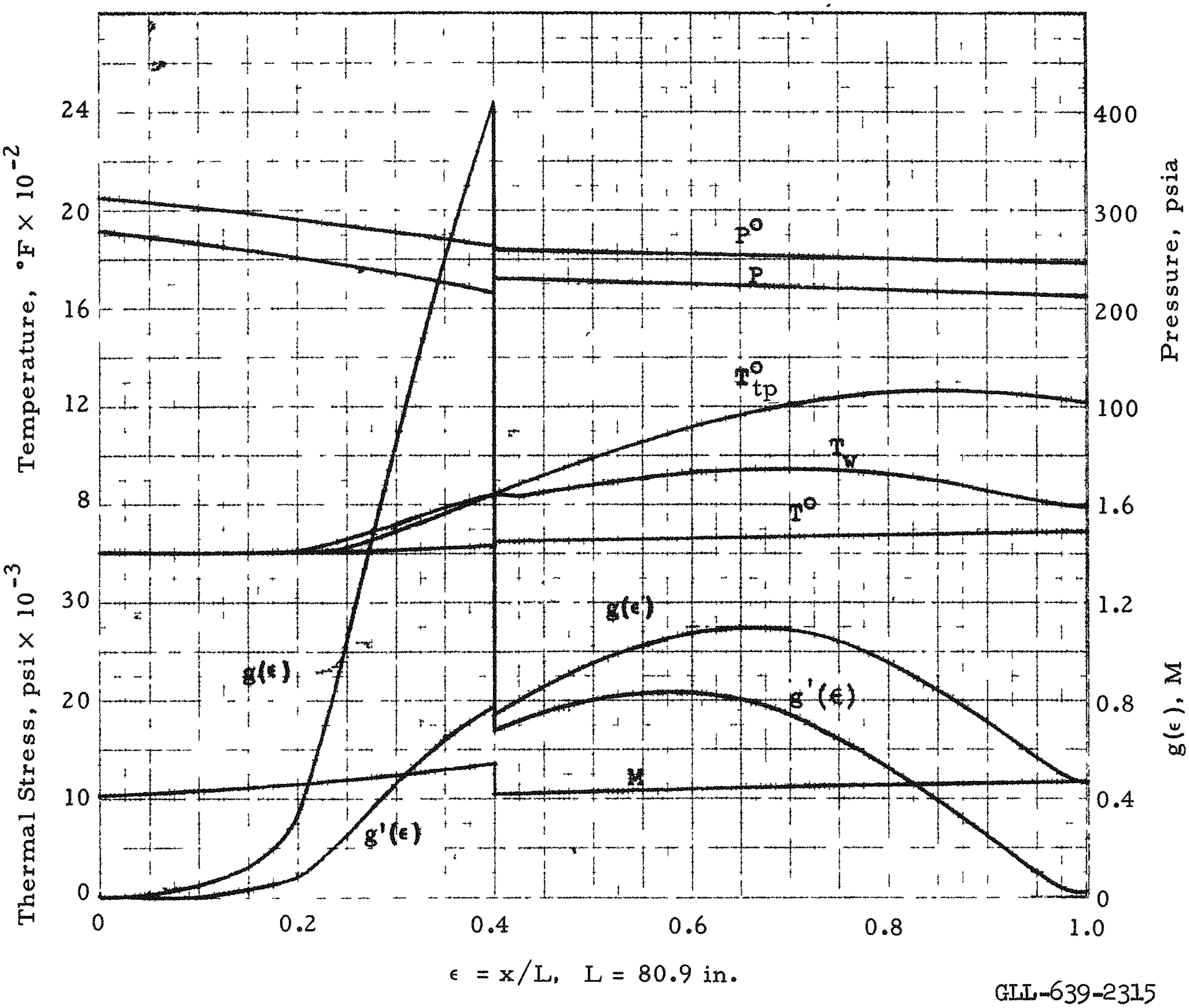

Flow channel diam:	1.162 in.	Exit Mach number:	0.4627
Porosity: *	0.7478	Peak wall temp:	939°F
Inlet total temp:	600°F	Power to air:	68.094 kW
Exit total temp:	696°F	Average material power density:	5.828 MW/ft^3
Inlet total pressure:	312.9 psia	Flow rate:	2.522 lb/sec
Exit total pressure:	246.5 psia	All dimensions at:	60°F

* Control rod inserted.

Control tie rod (control rod inserted 17.2 in.), cold inlet gas condition.

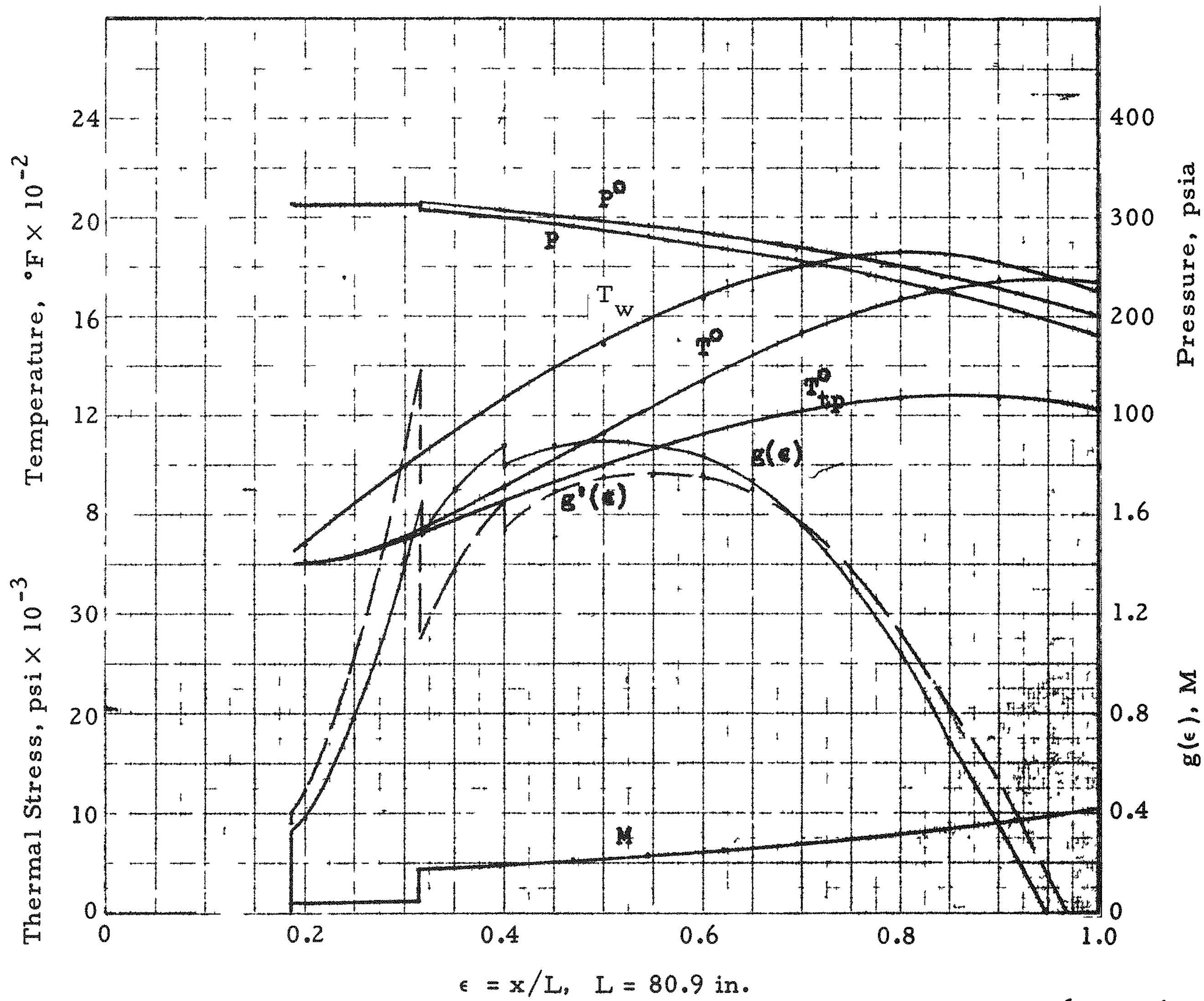

GLL-639-2316

Flow channel diam:	0.130 in.	Exit Mach number:	0.4065
Porosity:	0.1761	Peak wall temp:	1862°F
Inlet total temp:	600°F	Power to air:	6.229 kW
Exit total temp:	1761°F	Average material power density:	2.774 MW/ft^3
Inlet total pressure:	312.9 psia	Flow rate:	0.01879 lb/sec
Exit total pressure:	204.4 psia	All dimensions at:	60°F

Guard tube (control tie rod, control rod inserted 17.2 in.), cold inlet gas condition.

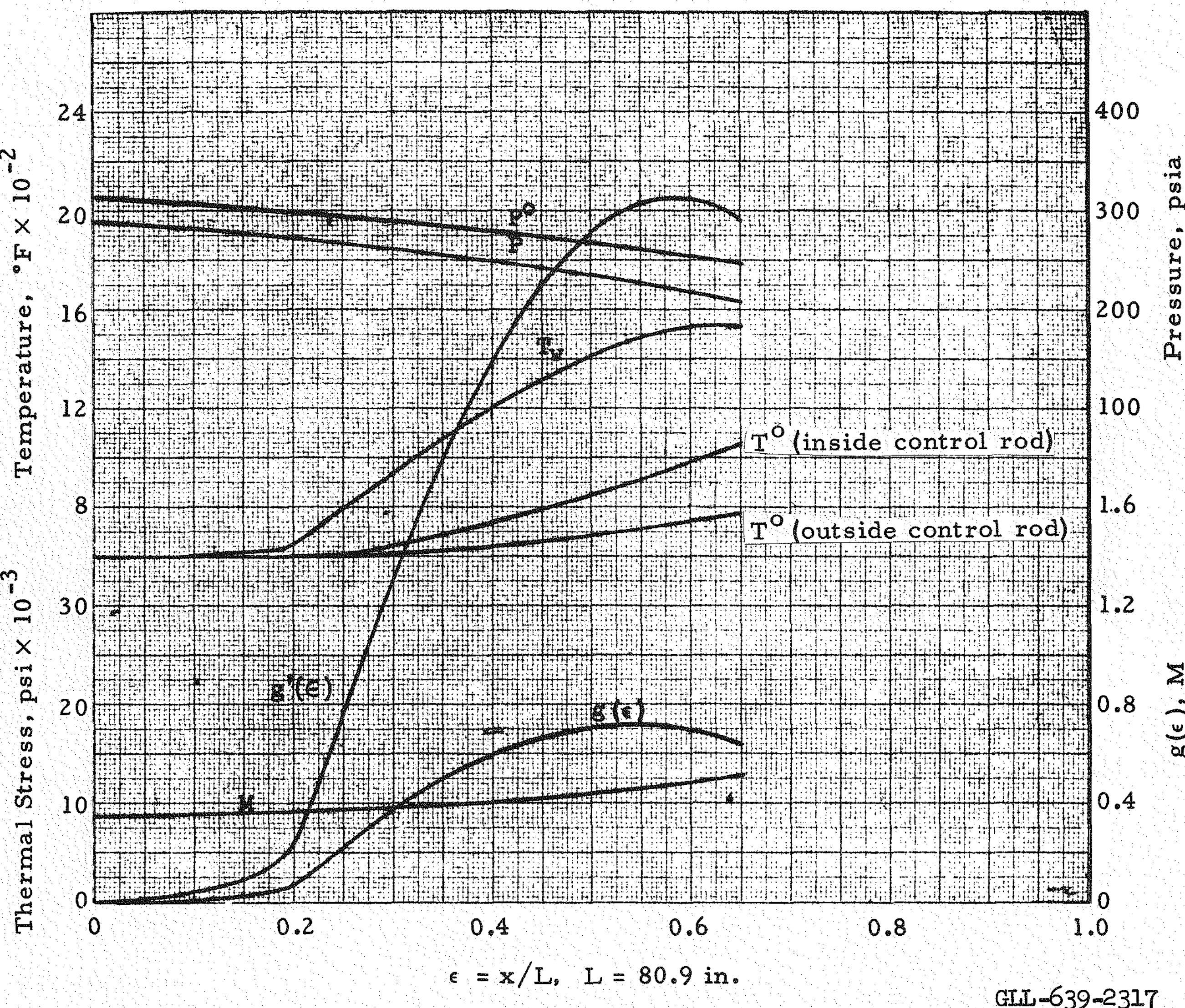

		Exit Mach number:	0.5107
		Peak wall temp:	1534°F
Inlet total temp:	600°F	Power to air:	25.694 kW
Exit total temp:	1057°F	Average material power density:	17.231 MW/ft^3
Inlet total pressure:	312.9 psia	Flow rate:	0.2040 lb/sec
Exit total pressure:	247.7 psia	All dimensions at:	60°F

Control rod (inserted 37.4 in.), cold inlet gas condition.

γ

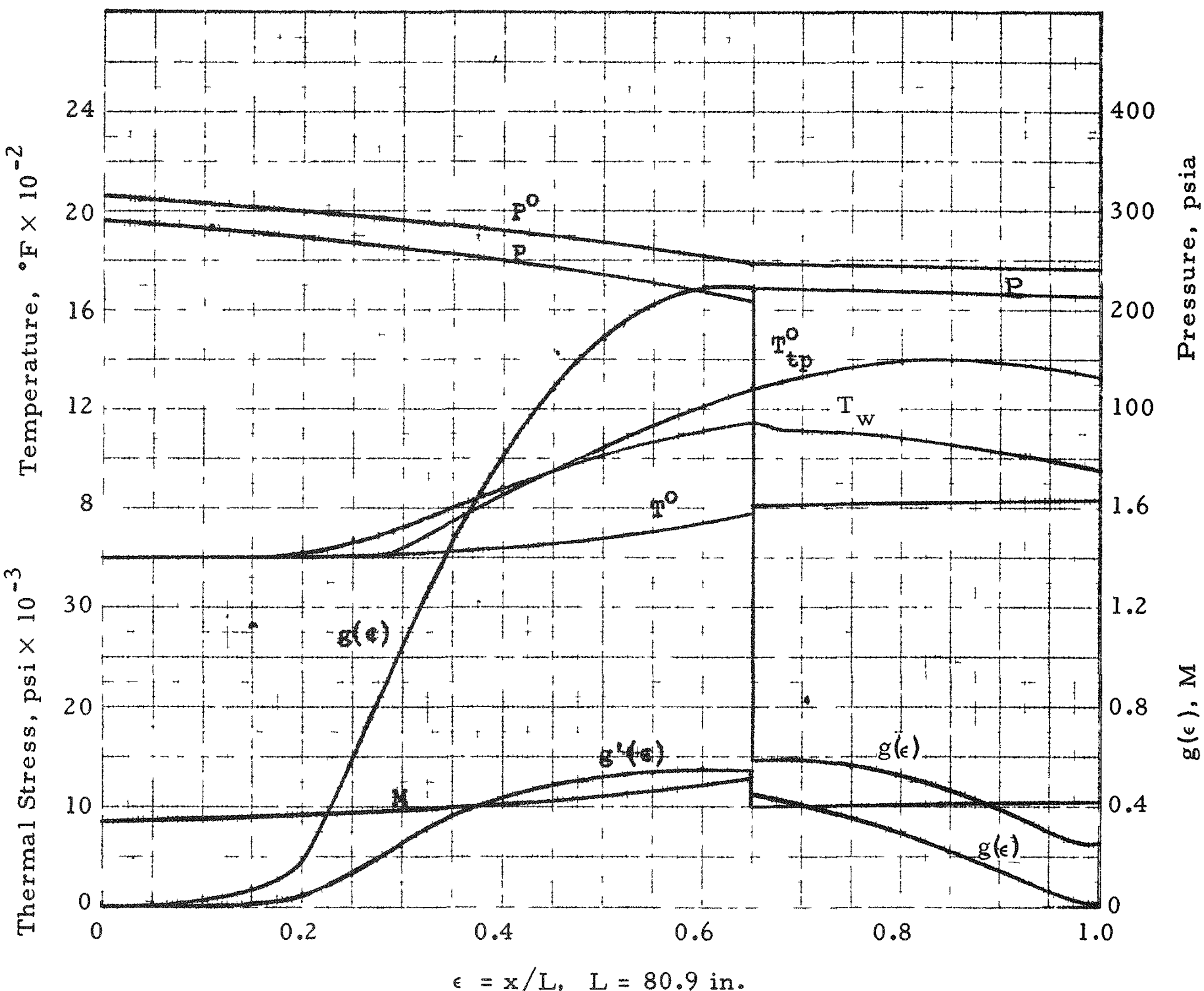

GLL-639-2318

Flow channel diam:	1.162 in.	Exit Mach number:	0.4197
Porosity:*	0.7478	Peak wall temp:	1133°F
Inlet total temp:	600°F	Power to air:	122.356 kW
Exit total temp:	834°F	Average material power density:	6.291 MW/ft^3
Inlet total pressure:	312.9 psia	Flow rate:	2.031 lb/sec
Exit total pressure:	240.4 psia	All dimensions at:	60°F

*Control rod inserted.

Control tie rod (control rod inserted 37.4 in.), cold inlet gas condition.

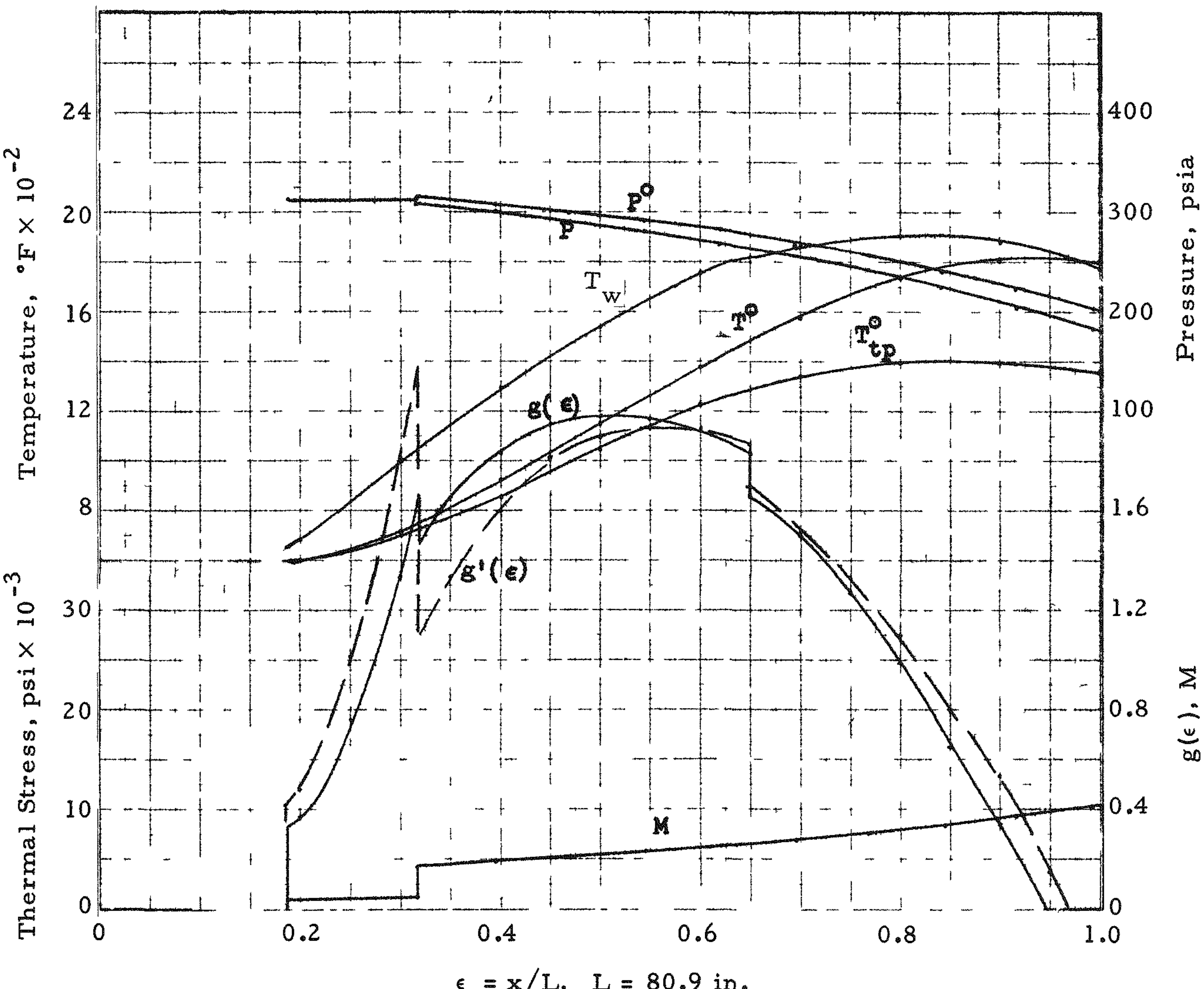

GLL-639-2319

Flow channel diam:	0.130 in.	Exit Mach number:	0.4064
Porosity:	0.1761	Peak wall temp:	1905°F
Inlet total temp:	600°F	Power to air:	6.416 kW
Exit total temp:	1806°F	Average material power density:	2.987 MW/ft^3
Inlet total pressure:	312.9 psia	Flow rate:	0.01855 lb/sec
Exit total pressure:	204.4 psia	All dimensions at:	60°F

Guard tube (control tie rod, control rod inserted 37.4 in.), cold inlet gas condition.

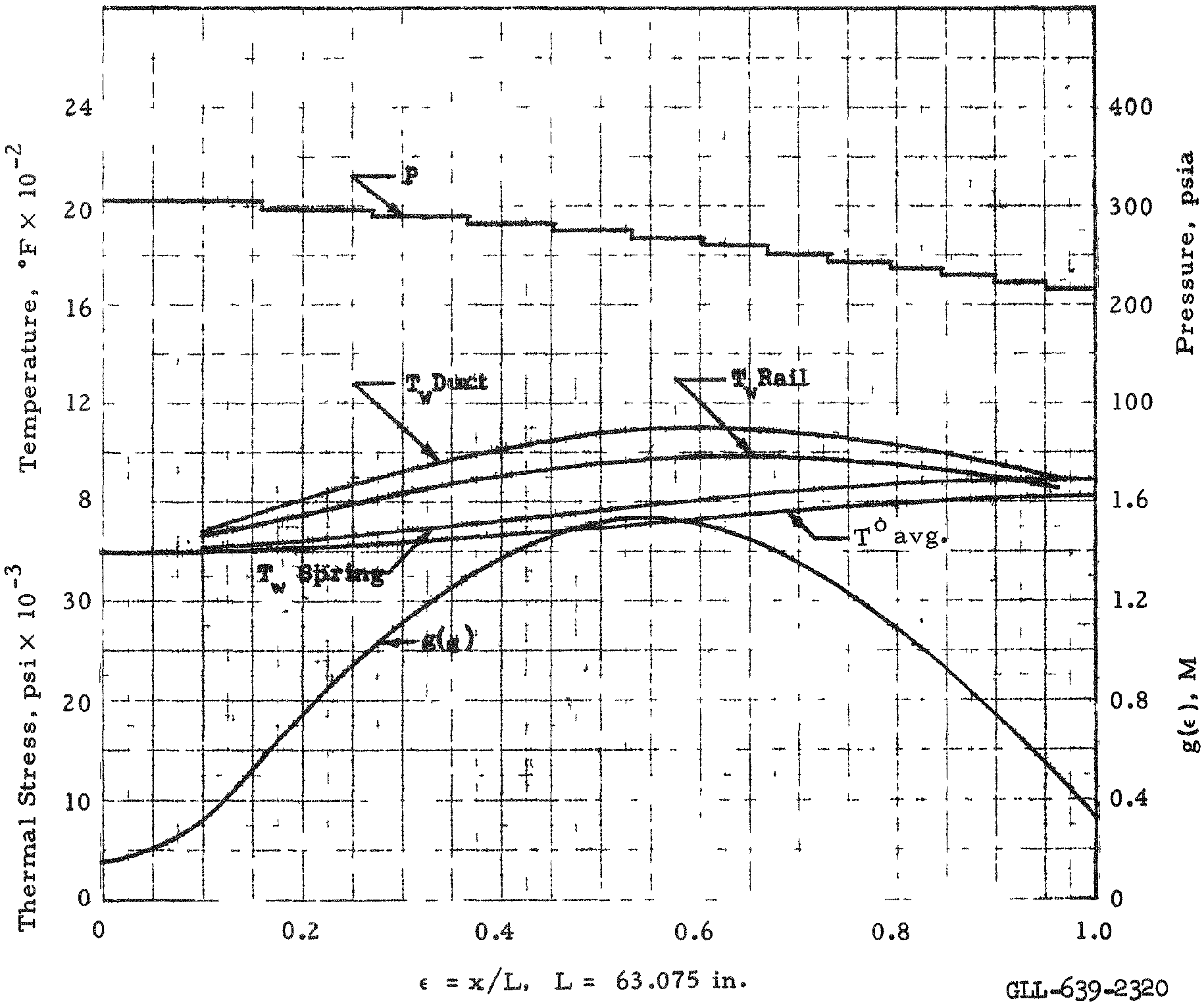

Exit Mach number:	0.16
Peak wall temp:	Duct, 1100°F; Rail, 980°F; Spring, 884°F
Power to air:*	8.79 MW
Average material power density:	930.55 kW/ft^3
Flow rate:	146.67 lb/sec
All dimensions at:	60°F

Inlet total temp:	600°F
Exit total temp:	824°F
Inlet total pressure:	312.9 psia
Exit total pressure:	216.5 psia

*Includes 53% of heat generated in peripheral shim.

Side support structure, cold inlet gas condition.

Summary of Component Operating Characteristics for Hot-Wall Off-Design Condition

Component	Peak wall temp (°F)	Exit gas temp (°F)	Single-element flow rate (lb/sec)	Total pressure drop (psi)	Peak material power density (MW/ft^3)
Fueled tubes (average)	2850	2446	0.05933	82.3	32.78
Tie rod (Center position)	1565	1169	0.6794	60.9	10.31
Guard tubes (Center position)	2362	2188	0.01721	113.4	2.97
Control rod (17.2 in. insertion)	1461	1054	2.419	70.9	24.73
Control tie rod	1309	1054	2.419	70.9	10.57
Guard tube	2200	2105	0.01747	113.4	3.53
Spare control tie rod	1083	971	3.463	42.2	10.57
Side reflector (BeO)					
Inner radius	2370	2210	0.007698 (average)	121.3 (average)	1.27
Outer radius	1660	1645			0.742
Peripheral shim					
Inner radius	1725	1661	0.01869 (average)	115.0 (average)	2.63
Outer radius	1602	1558			2.28
Side support structure					
Spring	1255	1191	129.6(total)	101.7	1.39
Rail	1363	1191	129.6(total)	101.7	11.09
Duct	1439	1191	129.6(total)	101.7	0.769

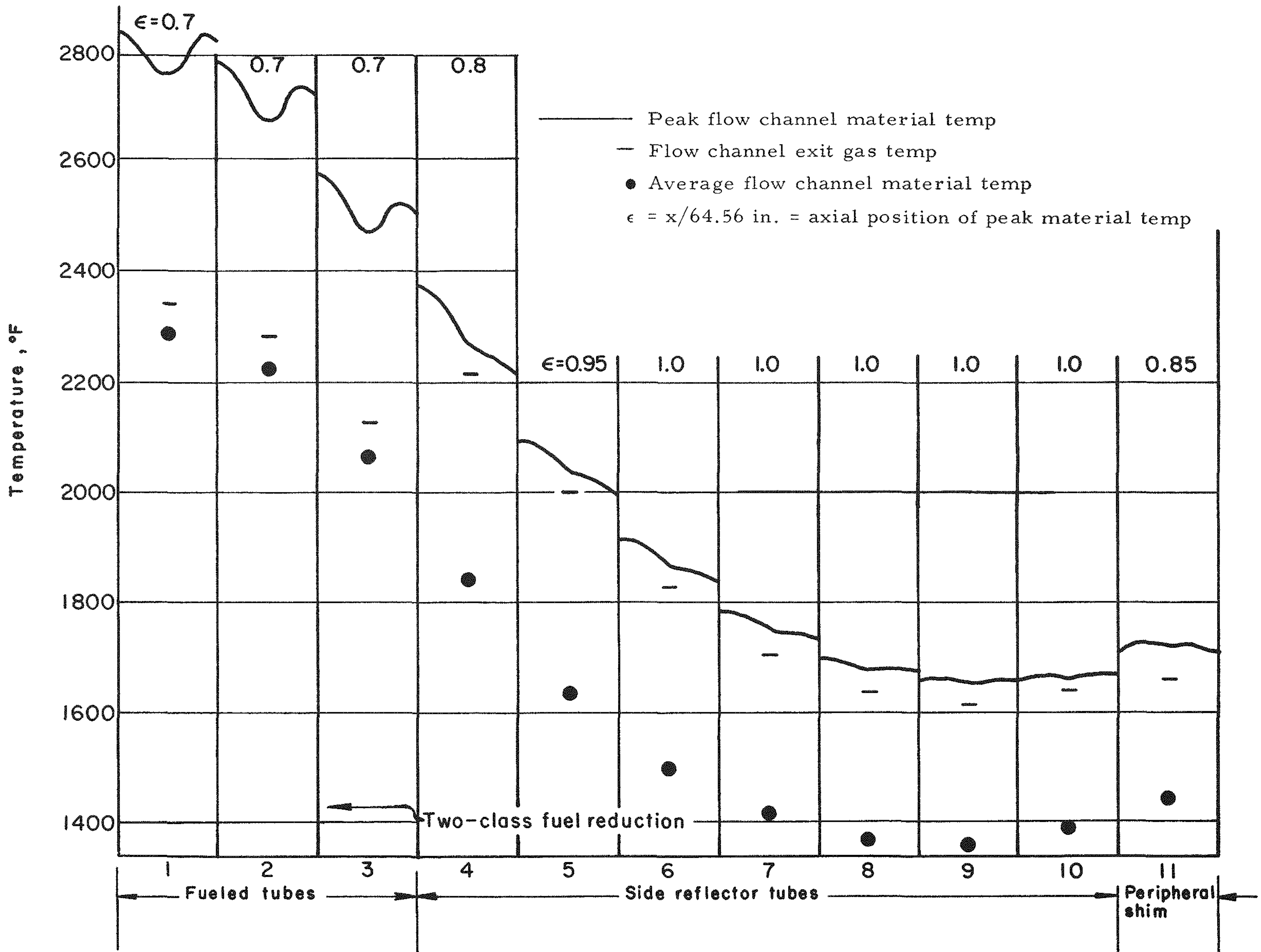

GLL-639-2321

Analysis of side reflector region radial temperature, at hot-wall off-design condition.

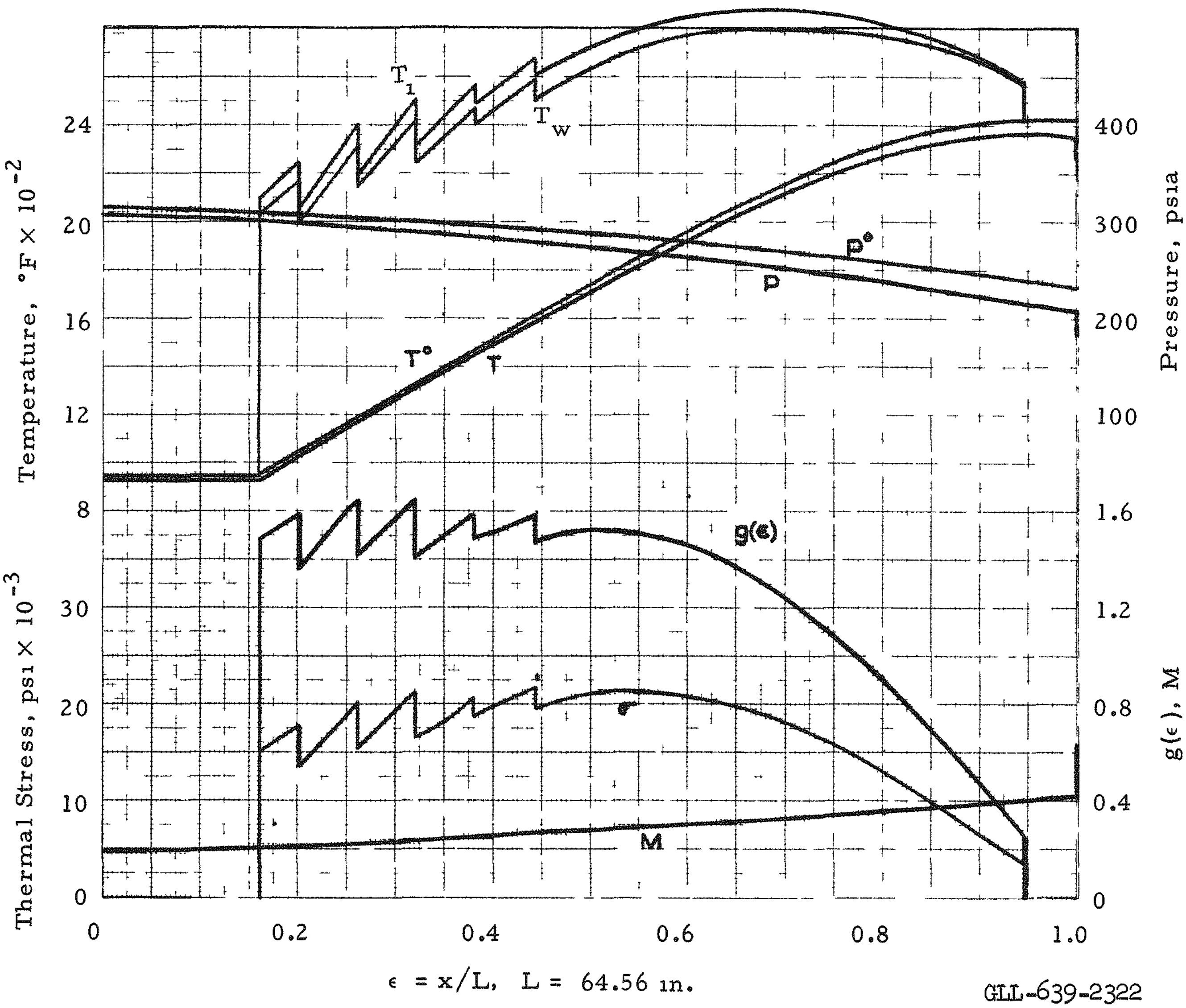

Flow channel diam:	0.227 in.	Exit Mach number:	0.421
Porosity:	0 5297	Peak wall temp:	2850°F
Inlet total temp:	946°F	Power to air:	26.599 kW
Exit total temp:	2446°F	Average material power density:	19.815 MW/ft^3
Inlet total pressure:	316.4 psia	Flow rate:	0.059334 lb/sec
Exit total pressure:	234.1 psia	All dimensions at:	60°F

Average fueled tube, hot-wall off-design condition.

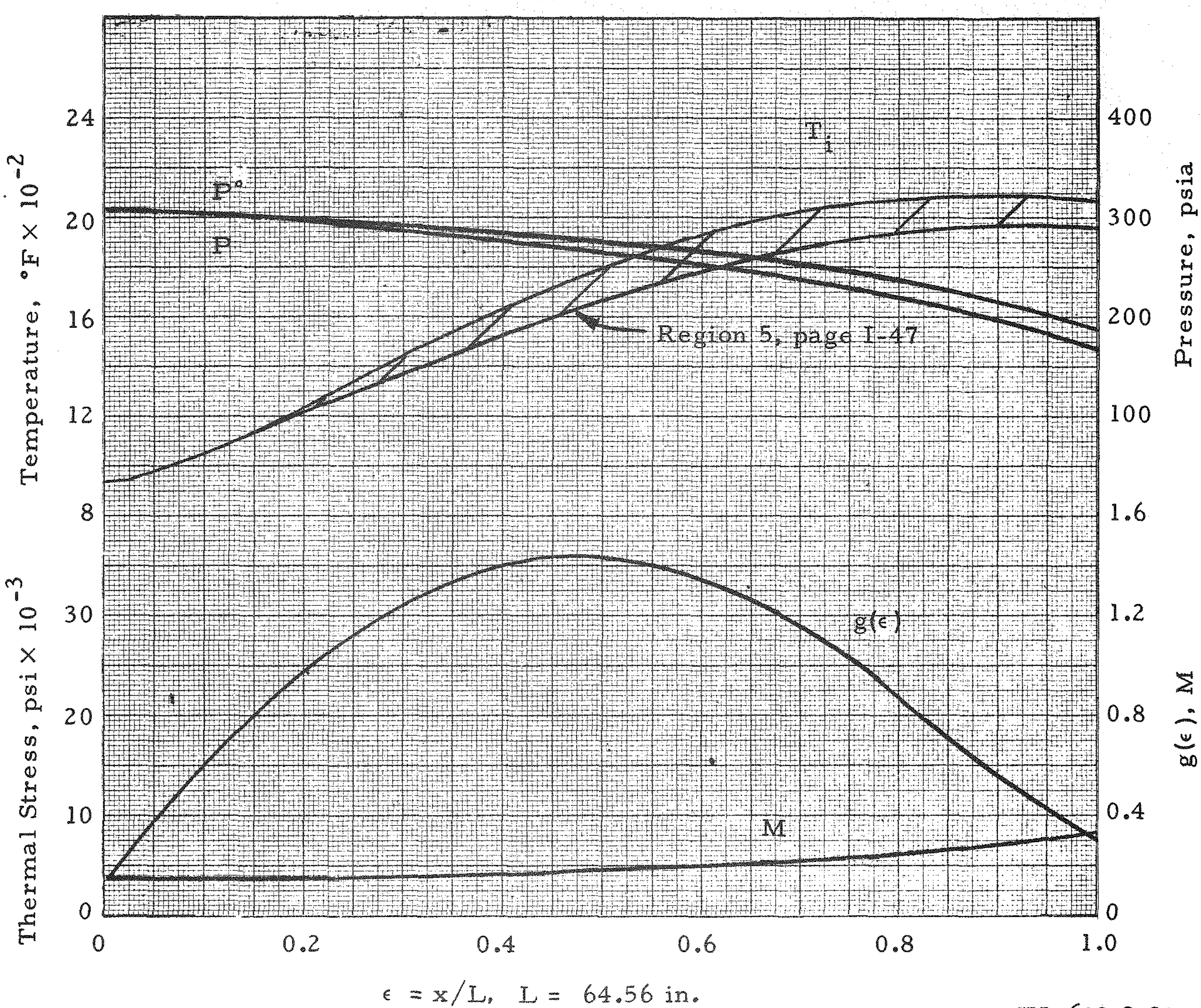

GLL-639-2323

Flow channel diam:	0.093 in.	Exit Mach number:	0.325
Porosity:	0.0895	Peak wall temp: 2362°F	(Region 4, page I-47)
Inlet total temp:	946°F	Power to air:	1.75 kW av
Exit total temp:	1804°F av	Average material power density:	0.677 MW/ft^3
Inlet total pressure:	316.4 psia	Flow rate:	0.007698 lb/sec av
Exit total pressure:	195.1 psia av	All dimensions at:	60°F

Side reflector tube, hot-wall off-design condition.

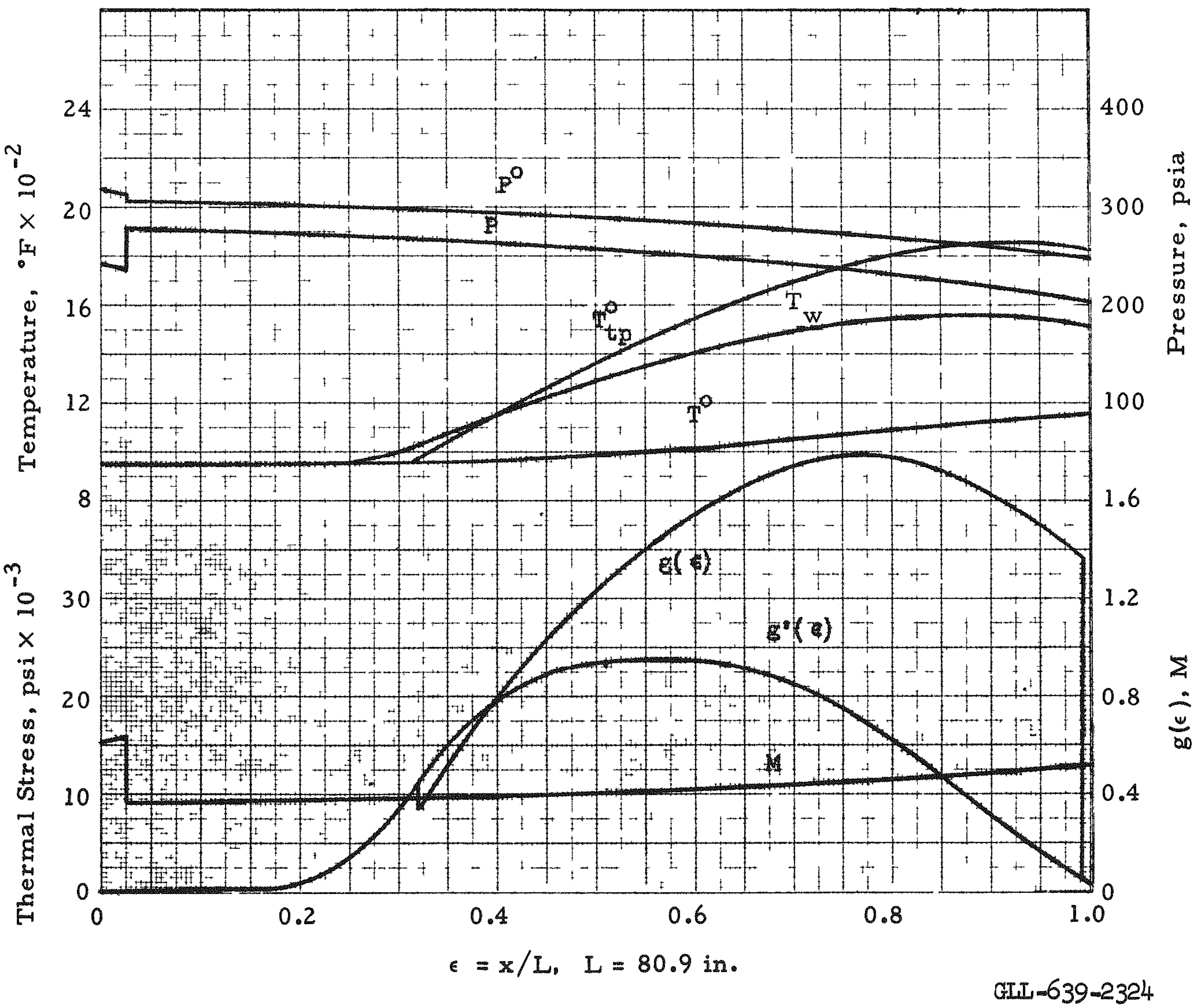

Flow channel diam:	0.576 in.	Exit Mach number:	0.532
Porosity:	0.7391	Peak wall temp:	1565°F
Inlet total temp:	946°F	Power to air:	42.8 kW
Exit total temp:	1169°F	Average material power density:	6.80 MW/ft^3
Inlet total pressure:	316.4 psia	Flow rate:	0.6794 lb/sec
Exit total pressure:	255.5 psia	All dimensions at:	60°F

Tie rod (central), hot-wall off-design condition.

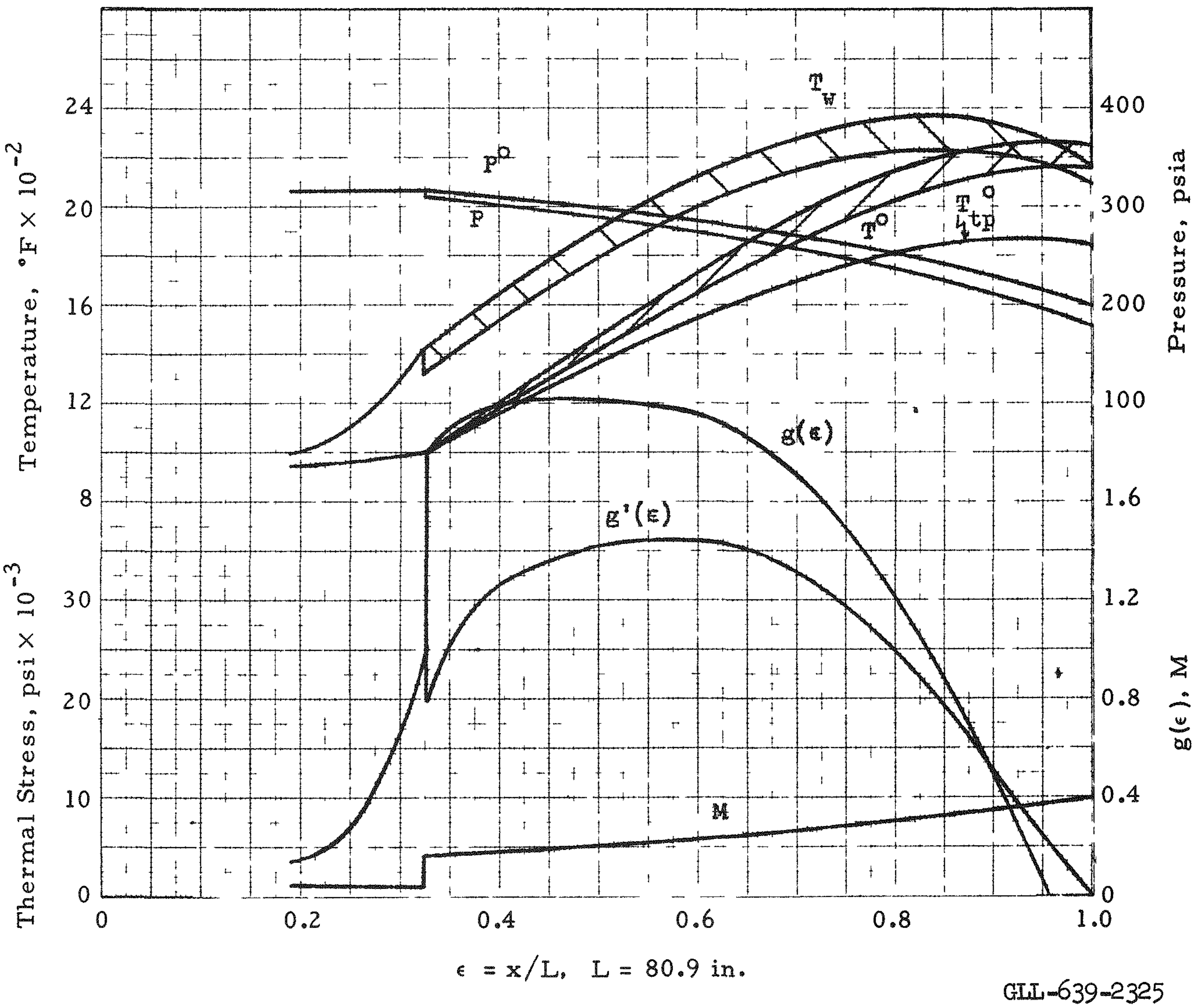

Flow channel diam:	0.130 in.	Exit Mach number:	0.408
Porosity:	0.1761	Peak wall temp:	2362°F
Inlet total temp:	946°F	Power to air:	6.07 kW
Exit total temp:	2188°F	Average material power density:	1.97 MW/ft^3
Inlet total pressure:	316.4 psia	Flow rate:	0.01721 lb/sec
Exit total pressure:	203 psia	All dimensions at:	60°F

Guard tube (central), hot-wall off-design condition.

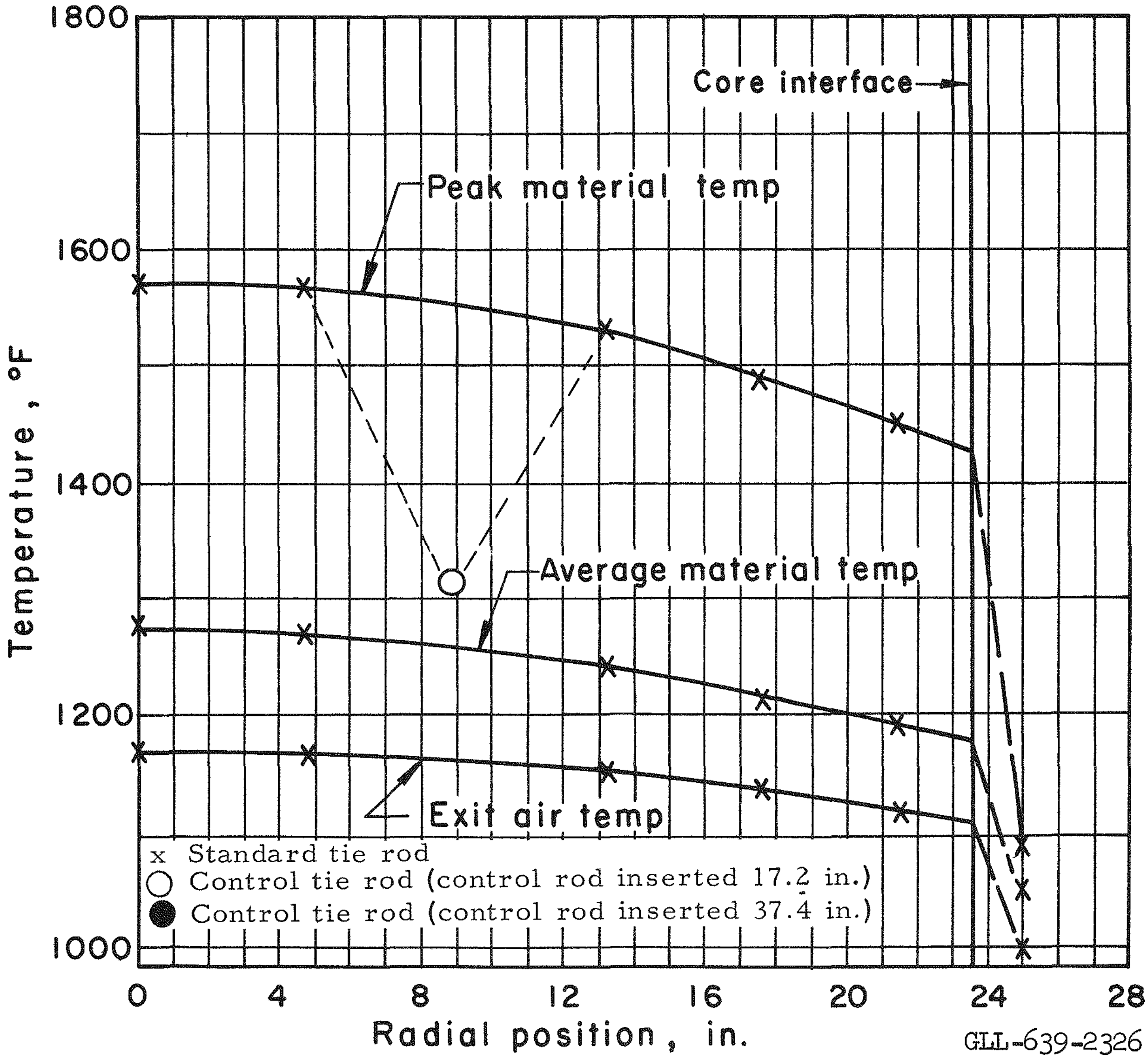

Nominal radial profile of tie rod temperatures, hot-wall off-design condition.

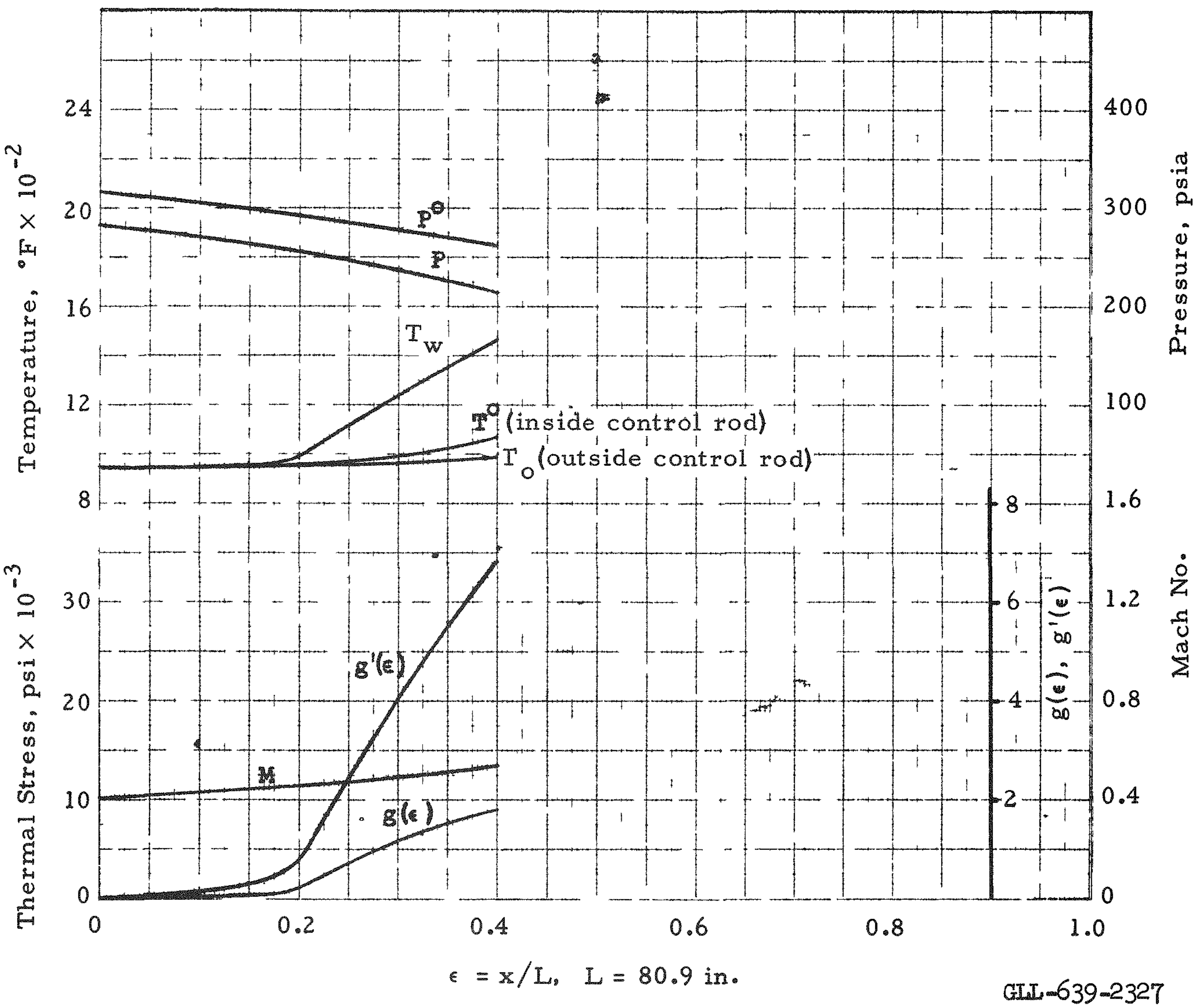

		Exit Mach number:	0.5455
		Peak wall temp:	1461°F
Inlet total temp:	946°F	Power to air:	7.556 kW
Exit total temp:	1068°F	Average material power density:	7.808 MW/ft^3
Inlet total pressure:	316.4 psia	Flow rate:*	0.2212 lb/sec
Exit total pressure:	261.3 psia	All dimensions at:	60°F

*Inside control rod.

Control rod (inserted 17.2 in.), hot-wall off-design condition.

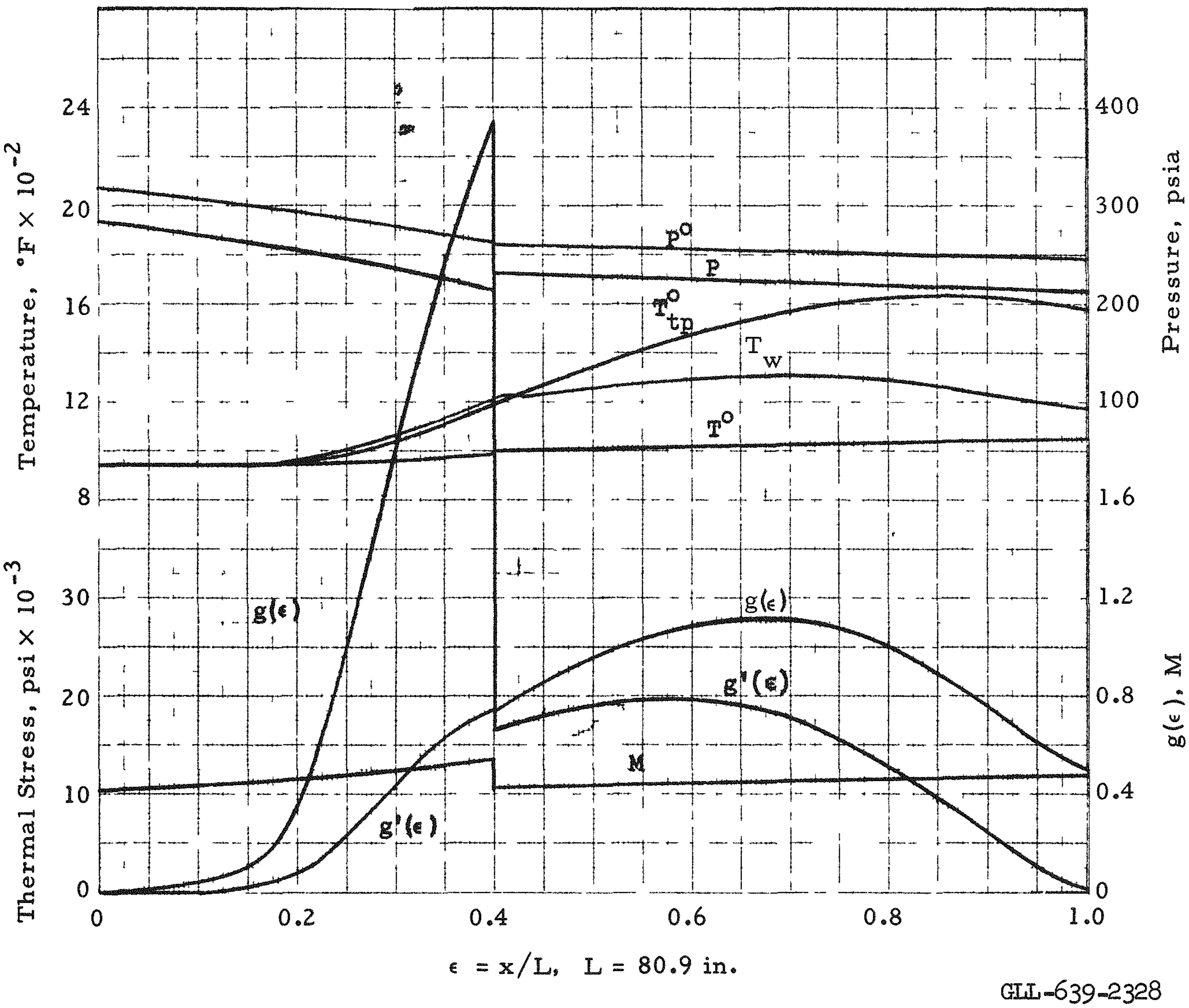

Flow channel diam:	1.162 in.	Exit Mach number:	0.4684
Porosity: *	0.7478	Peak wall temp:	1309°F
Inlet total temp:	946°F	Power to air:	69.477 kW
Exit total temp:	1054°F	Average material power density:	5.71 MW/ft^3
Inlet total pressure:	316.4 psia	Flow rate:	2.1981 lb/sec
Exit total pressure:	245.5 psia	All dimensions at:	60°F

* Control rod inserted.

Control tie rod (control rod inserted 17.2 in.), hot-wall off-design condition.

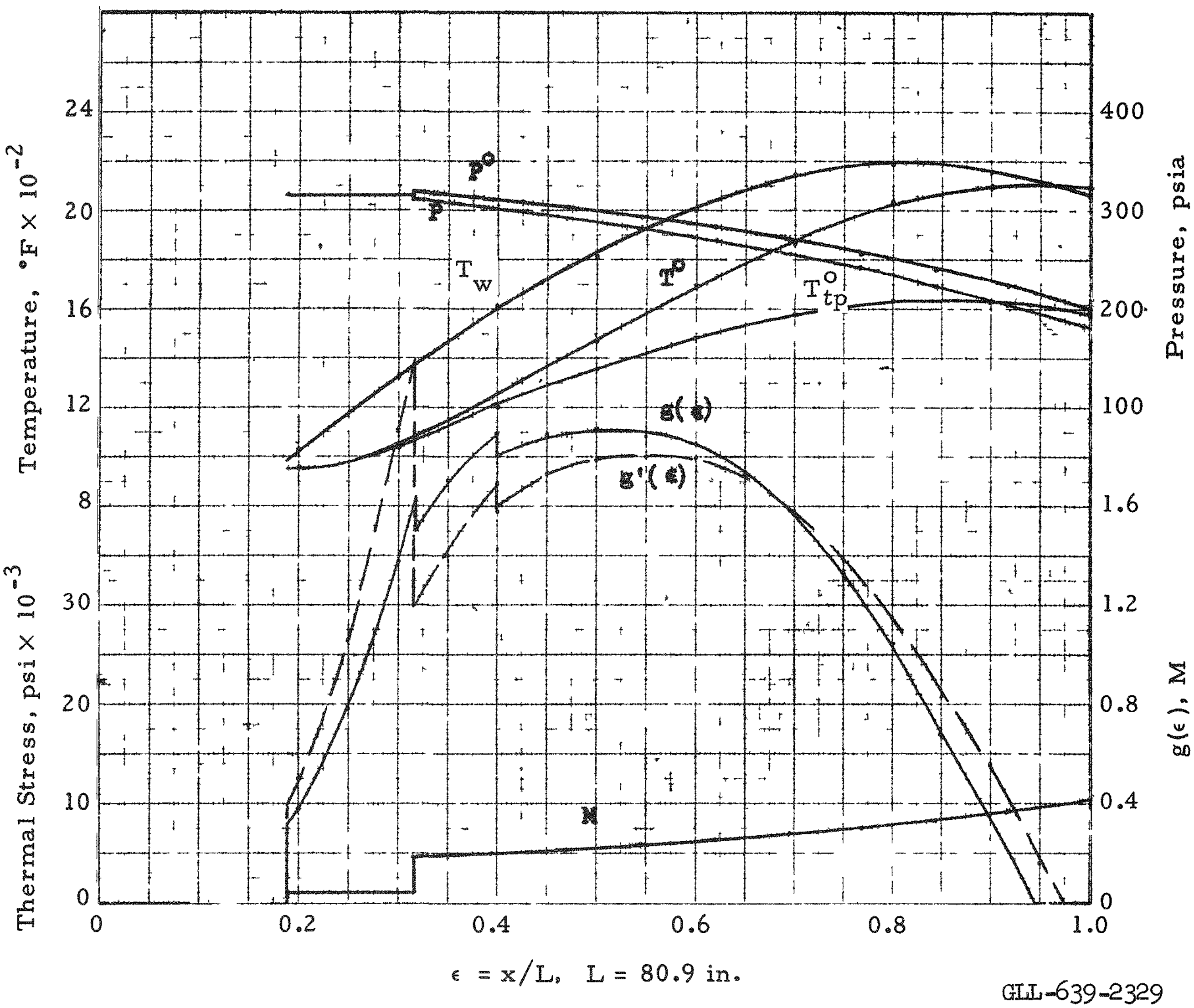

Flow channel diam:	0.130 in.	Exit Mach number:	0.4101
Porosity:	0.1761	Peak wall temp:	2200°F
Inlet total temp:	946°F	Power to air:	5.988 kW
Exit total temp:	2105°F	Average material power density:	2.718 MW/ft^3
Inlet total pressure:	316.4 psia	Flow rate:	0.1747 lb/sec
Exit total pressure:	203 psia	All dimensions at:	60°F

Guard tube (control tie rod, control rod inserted 17.2 in.), hot-wall off-design condition.

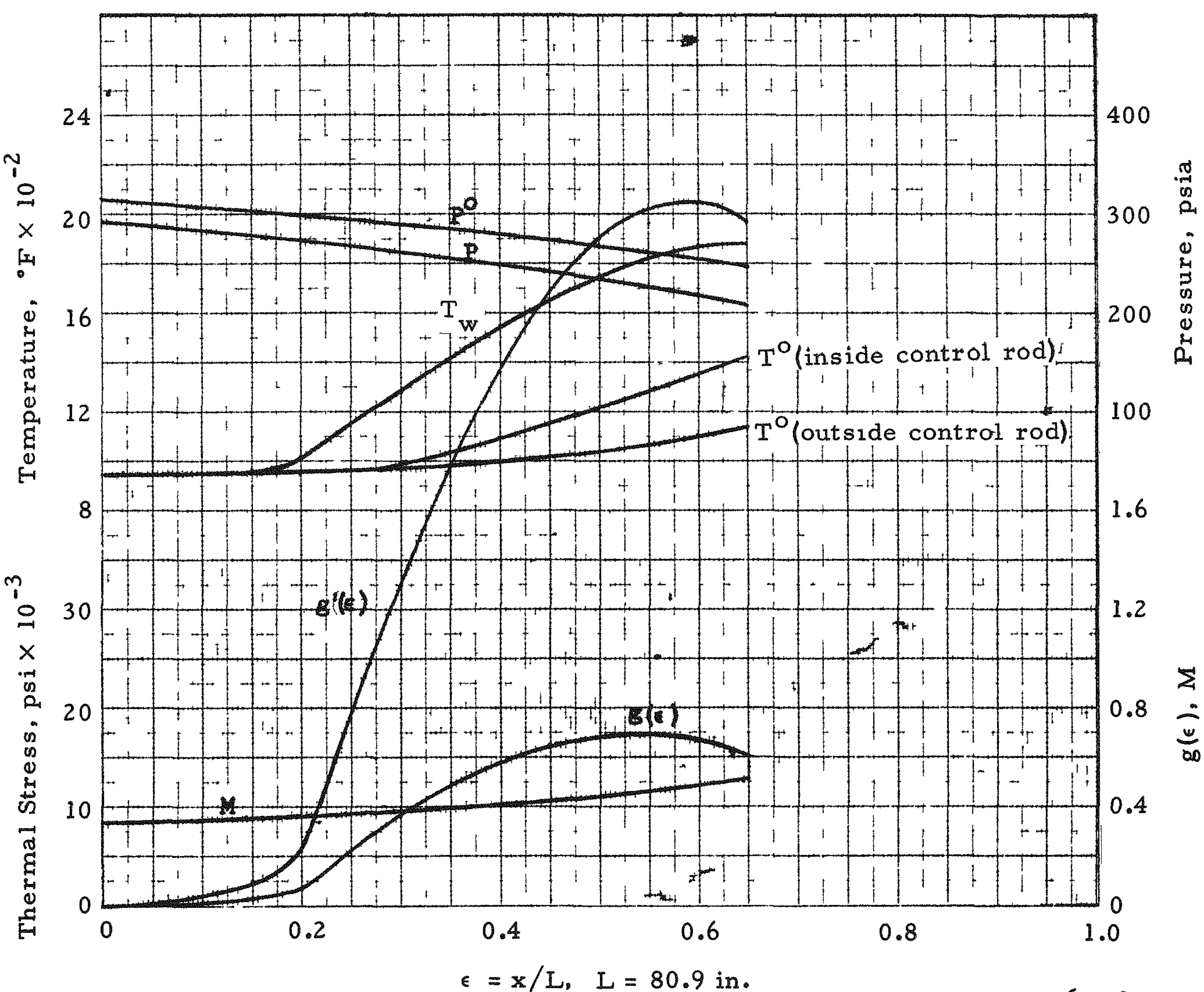

		Exit Mach number:	0.5153
		Peak wall temp:	1880°F
Inlet total temp:	946°F	Power to air:	24.456 kW
Exit total temp:	1423°F	Average material power density:	16.883 MW/ft^3
Inlet total pressure:	316.4 psia	Flow rate: *	0.180 lb/sec
Exit total pressure:	246.8 psia	All dimensions at:	60°F

* Inside control rod.

Control rod (inserted 37.4 in.), hot-wall off-design condition.

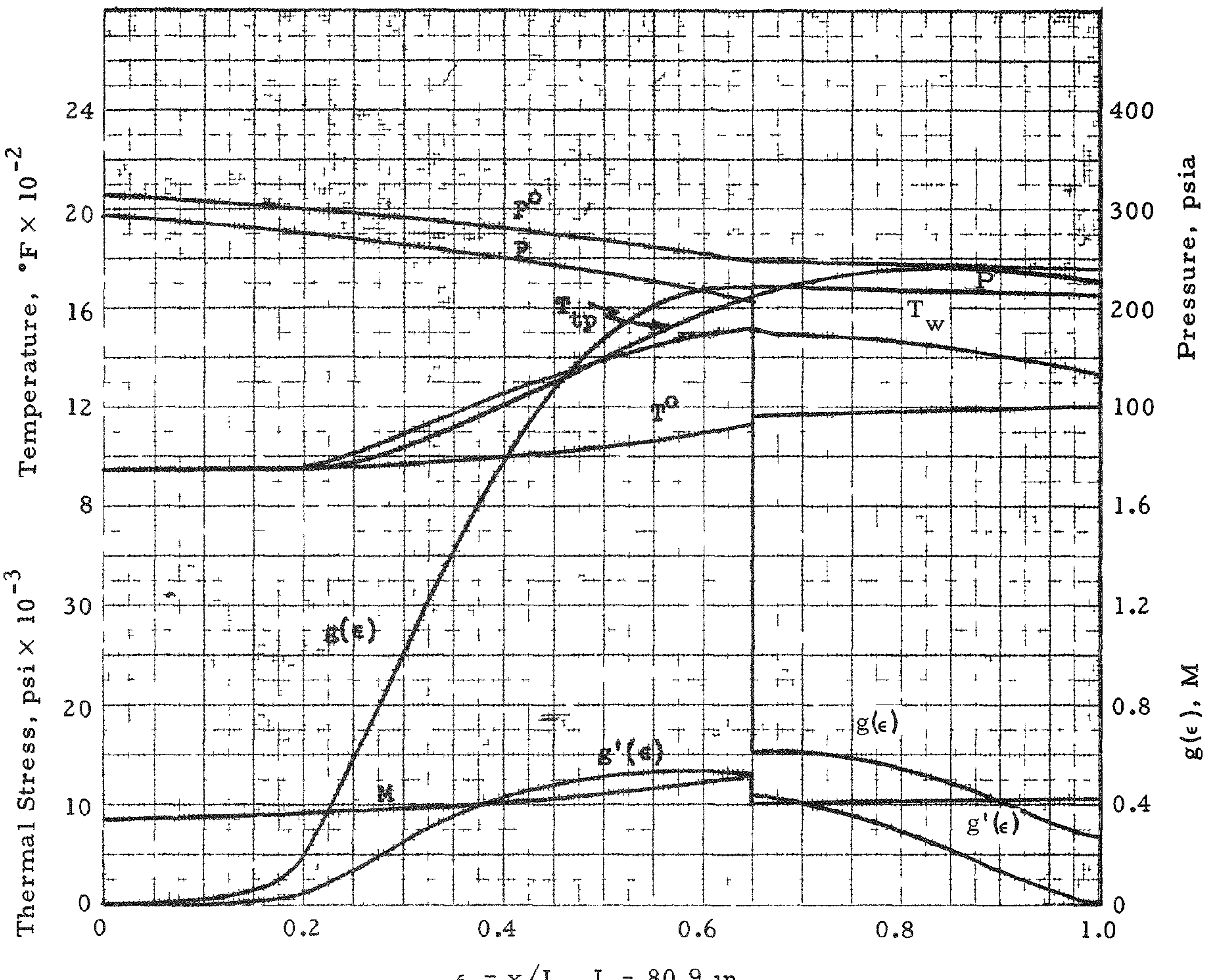

GLL-639-2331

Flow channel diam:	1.162 in.	Exit Mach number:	0.4234
Porosity:*	0.7478	Peak wall temp:	1524°F
Inlet total temp:	946°F	Power to air:	123.029 kW
Exit total temp:	1201°F	Average material power density:	6.164 MW/ft^3
Inlet total pressure:	316.4 psia	Flow rate:	1.790 lb/sec
Exit total pressure:	238.9 psia	All dimensions at:	60°F

* Control rod inserted.

Control rod tie rod (control rod inserted 37.4 in.), hot-wall off-design condition.

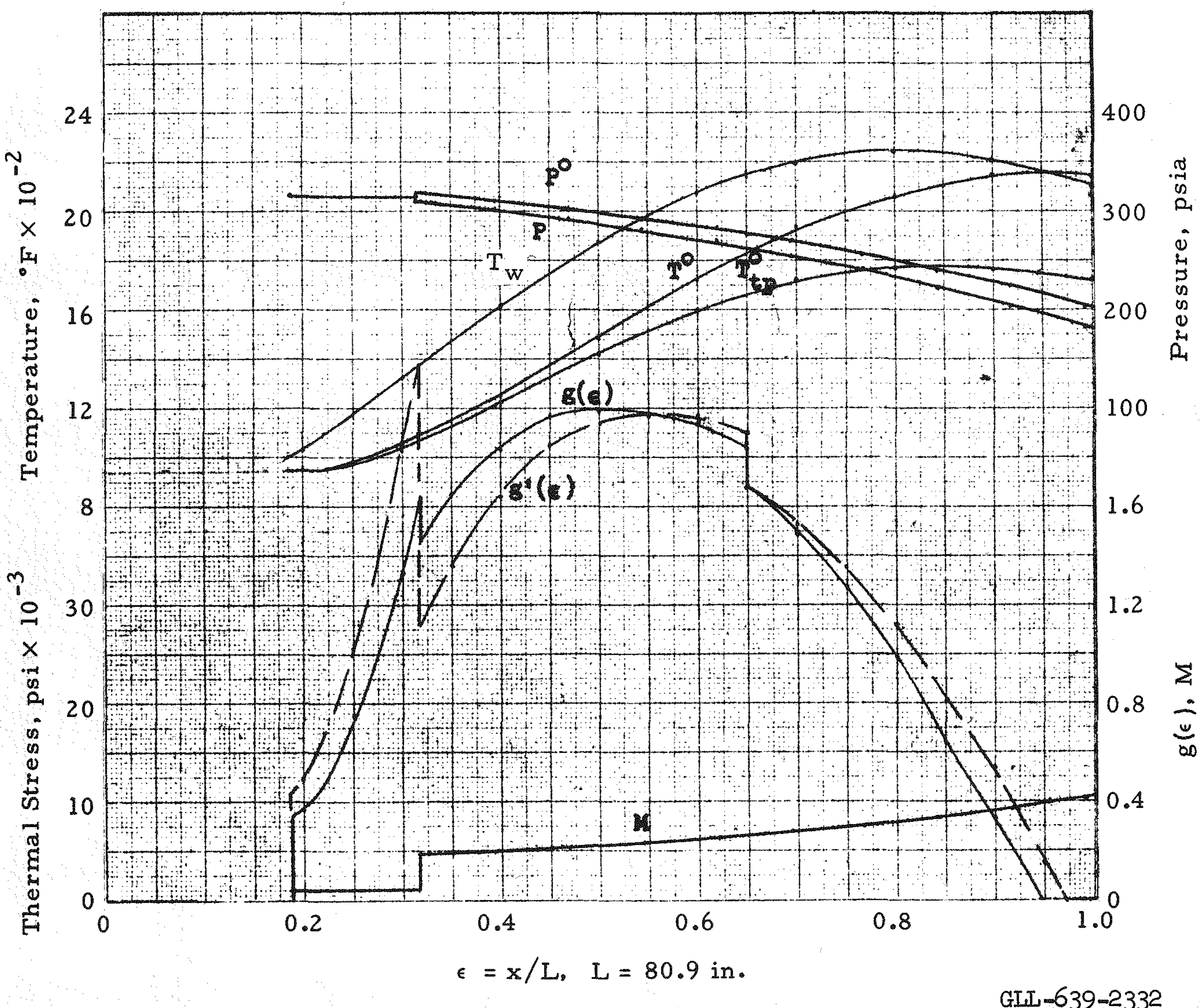

Flow channel diam:	0.130 in.	Exit Mach number:	0.4100
Porosity:	0.1761	Peak wall temp:	2247°F
Inlet total temp:	946°F	Power to air:	6.173 kW
Exit total temp:	2152°F	Average material power density:	2.927 MW/ft^3
Inlet total pressure:	316.4 psia	Flow rate:	0.01727 lb/sec
Exit total pressure:	203 psia	All dimensions at:	60°F

Guard tube (control tie rod, control rod inserted 37.4 in.), hot-wall off-design condition.

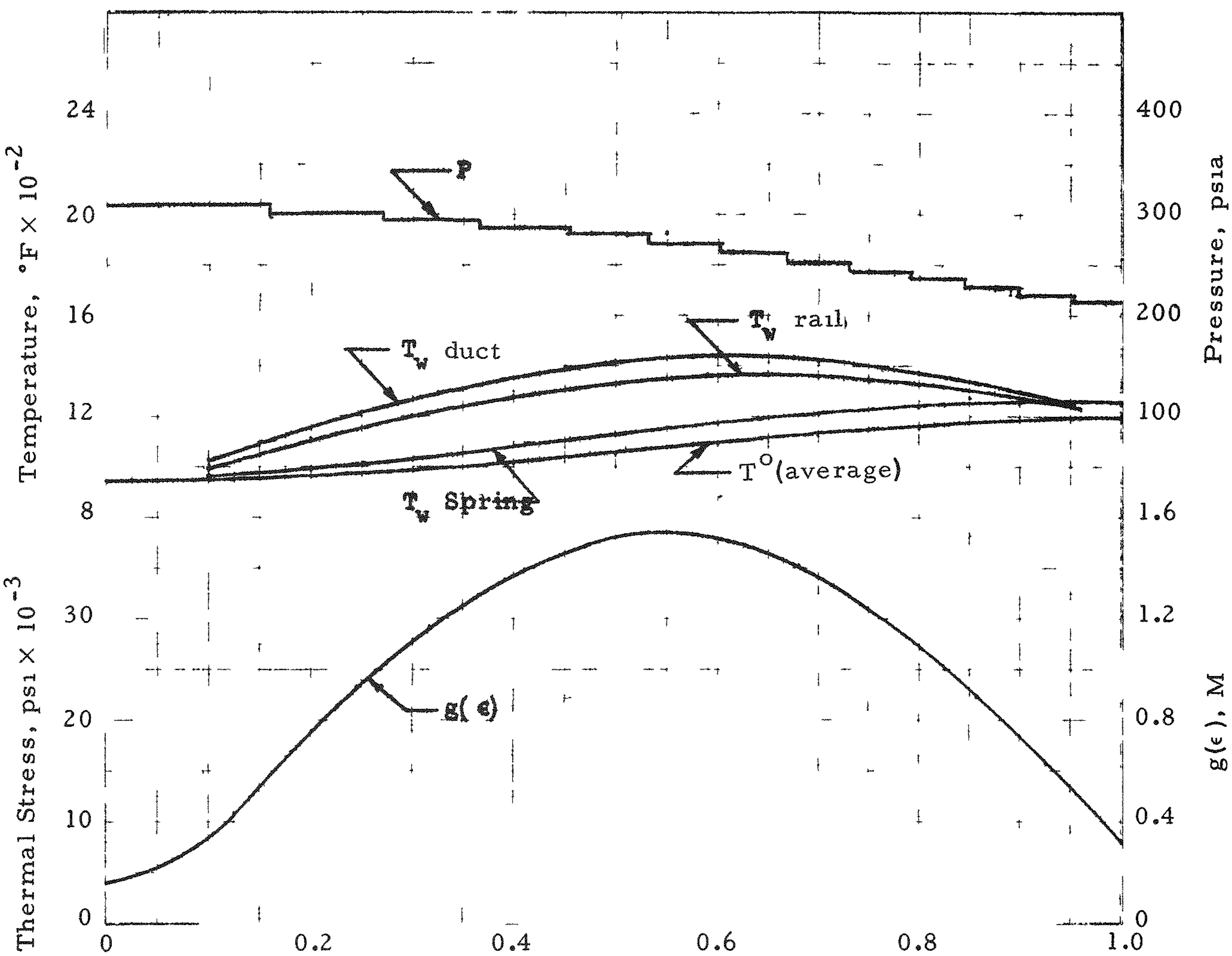

$\epsilon = x/L$, L = 63.075 in.

GLL-639-2333

Inlet total temp:	946°F
Exit total temp:	1191°F
Inlet total pressure:	316 4 psia
Exit total pressure:	214.7 psia

*Includes 53% of heat generated in peripheral shim.

Exit Mach number:	0.18
Peak wall temp:	Duct, 1439°F; Rail, 1363°F; Spring, 1255°F
Power to air: *	8.73 kW
Average material power density:	913.63 MW/ft^3
Flow rate:	129.6 lb/sec
All dimensions at:	60°F

Side support structure, hot-wall off-design condition.

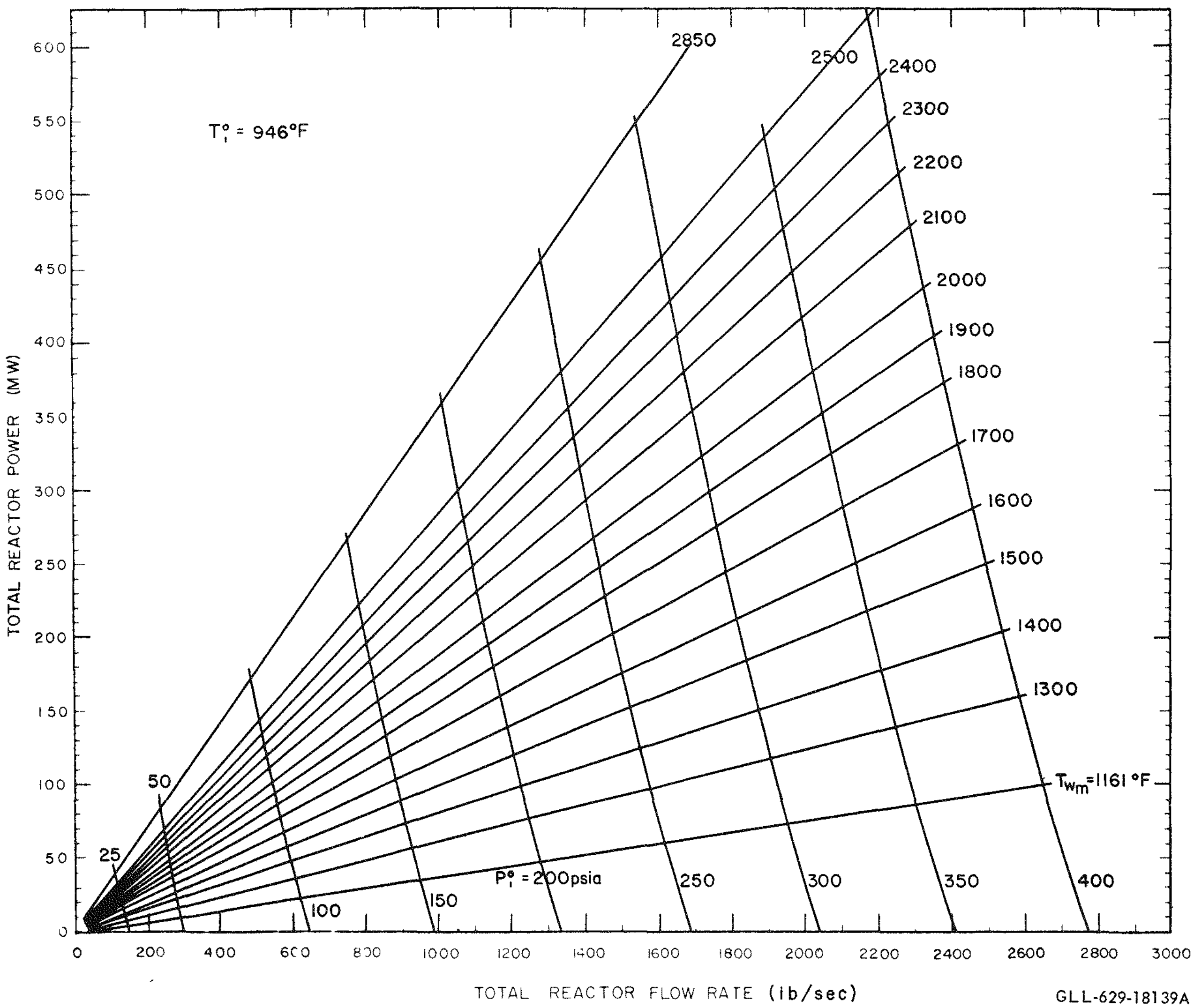

Performance map — lines of constant P_1° and T_w. (T_w = fueled tube peak wall temperature.)

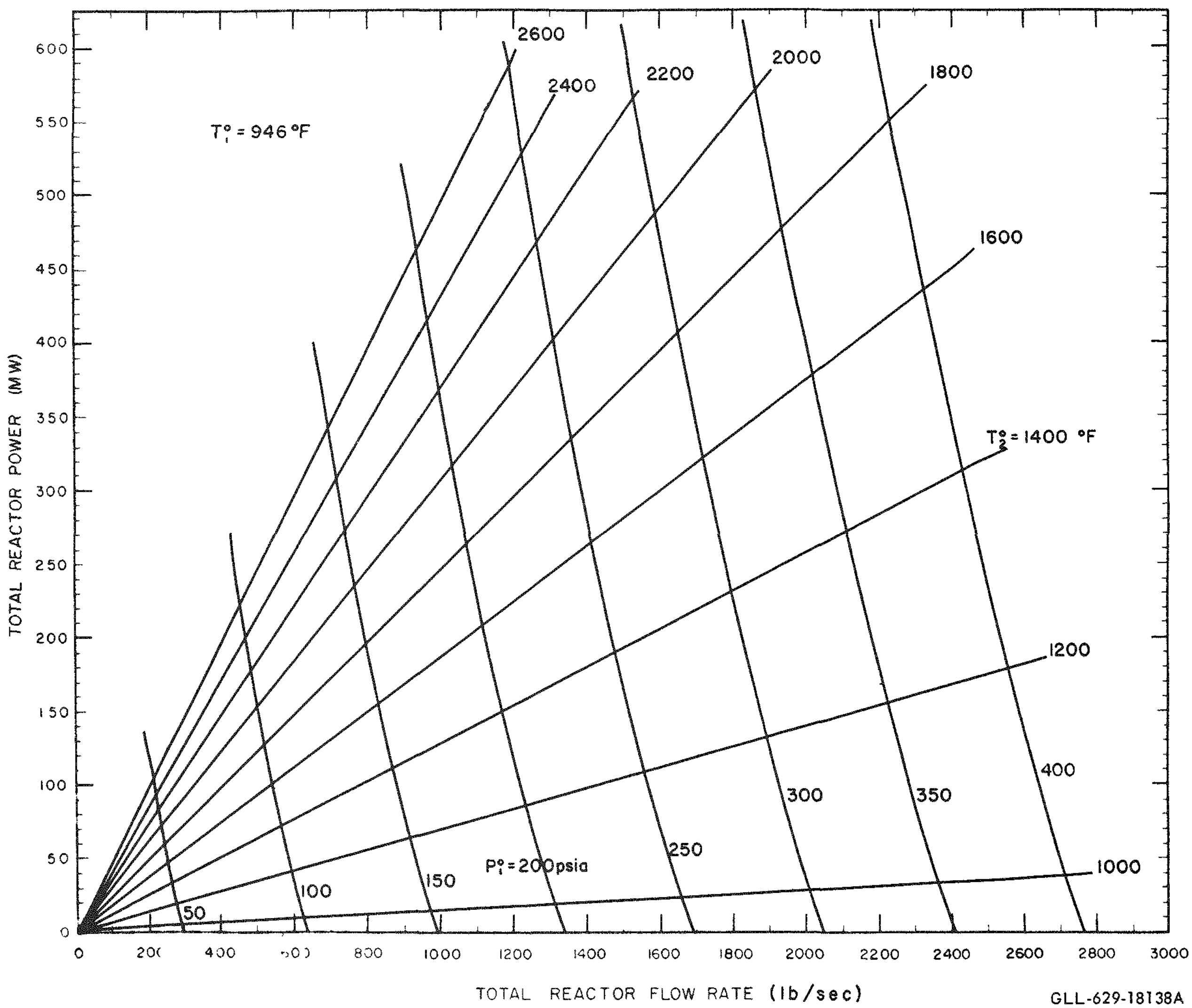

Performance map - lines of constant P_1° and T_2°.

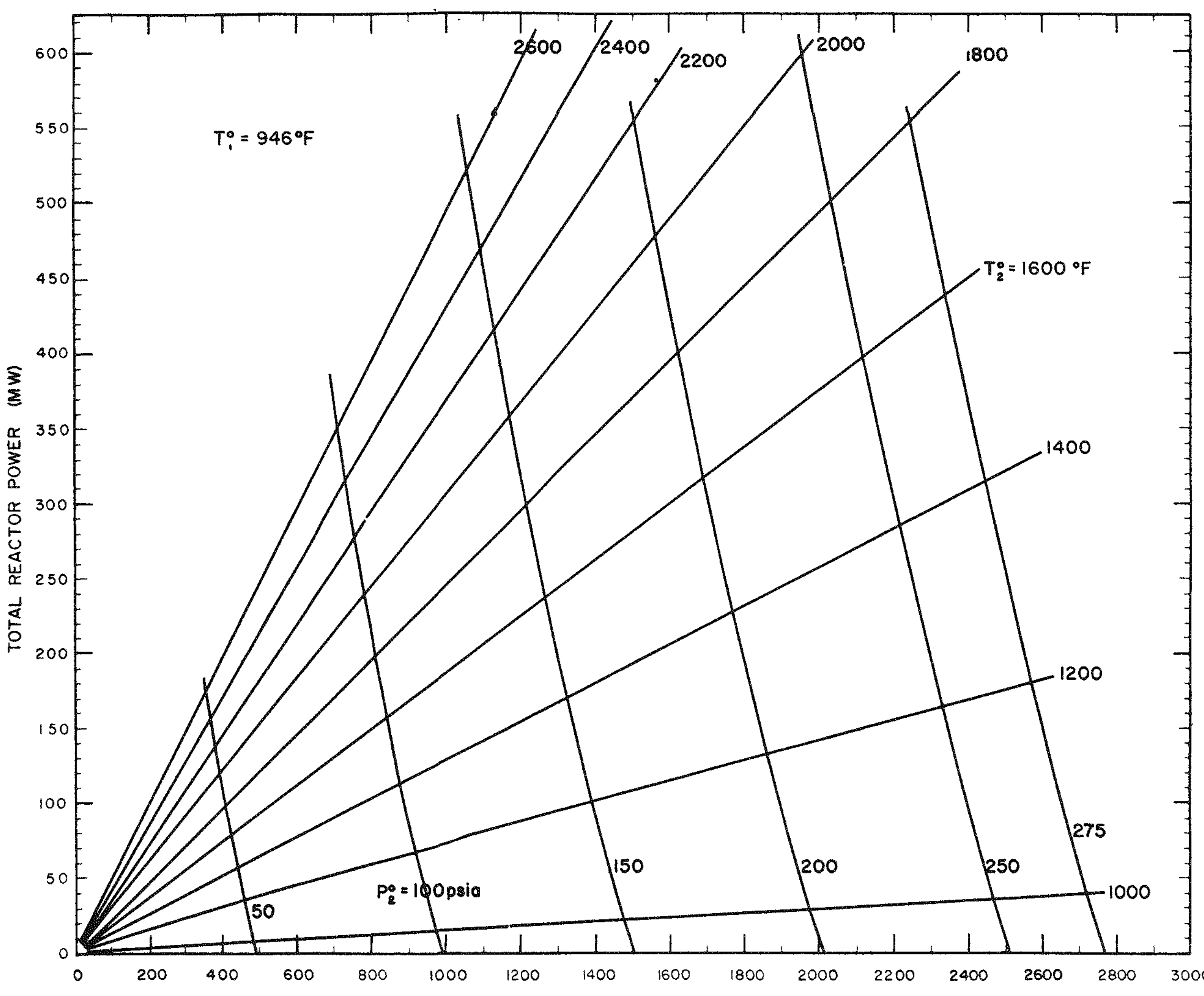

Performance map - lines of constant P_2° and T_2°.

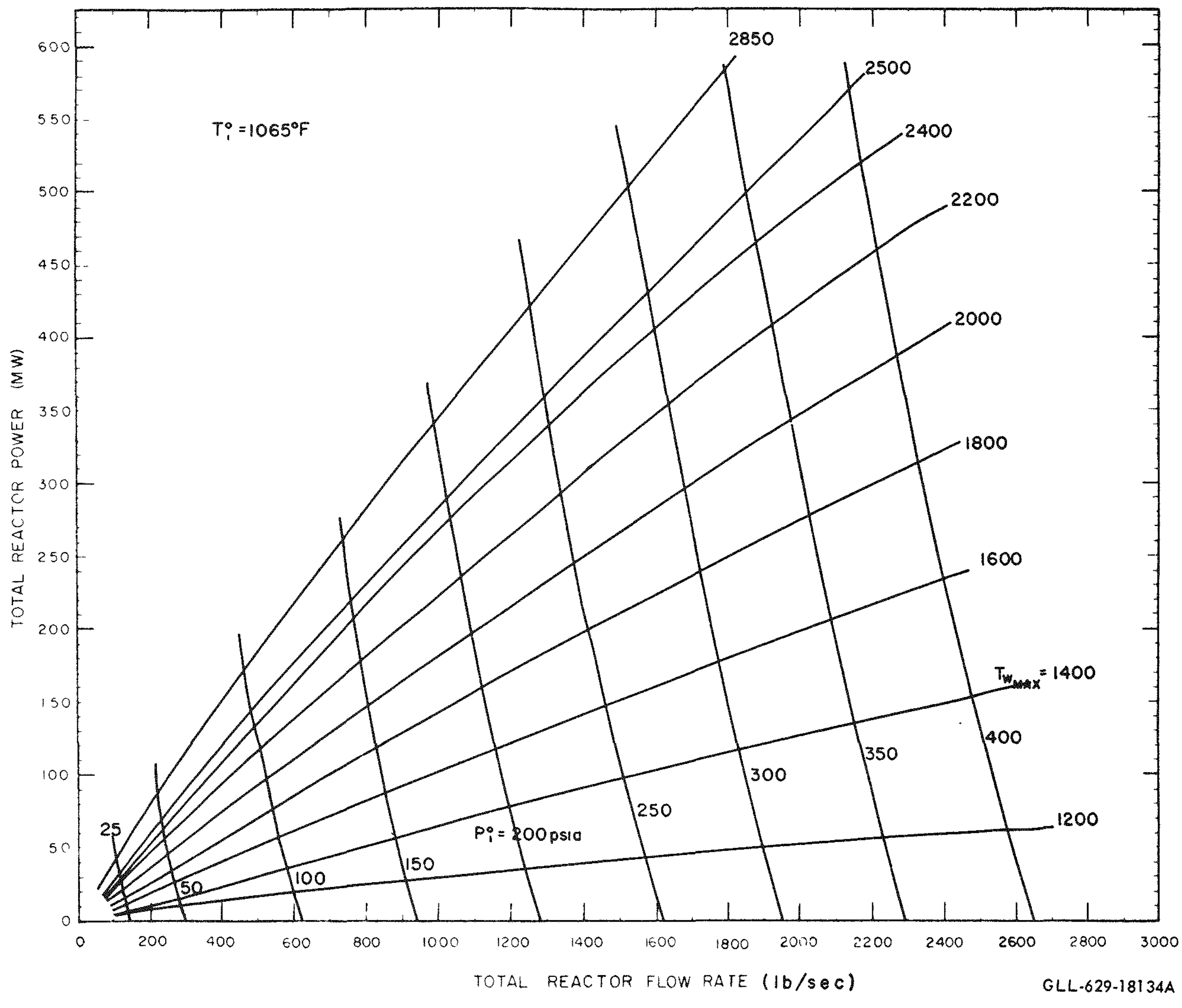

Performance map - lines of constant P_1° and T_W (T_W = fueled tube peak wall temperature).

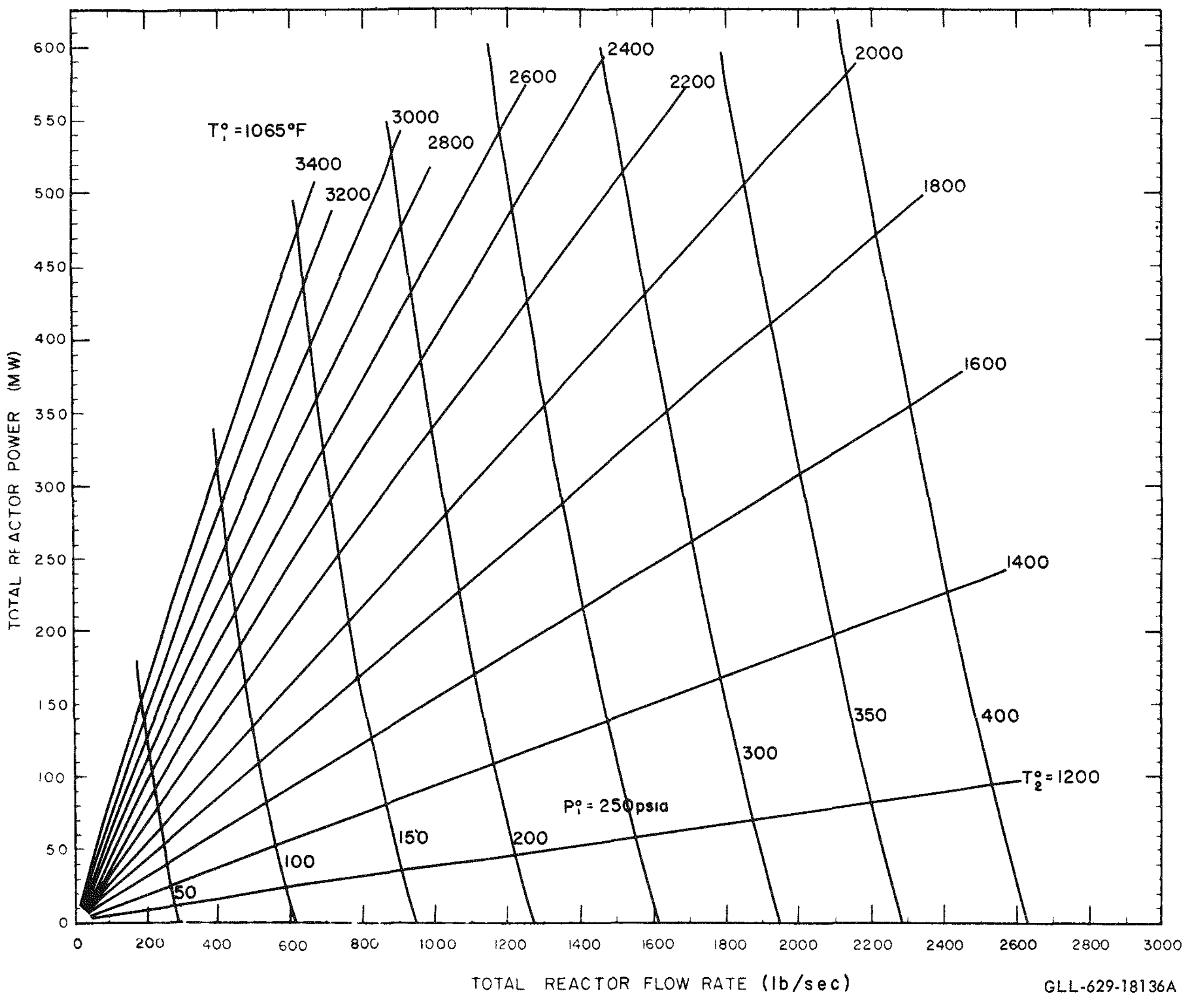

Performance map – lines of constant P_1° and T_2°.

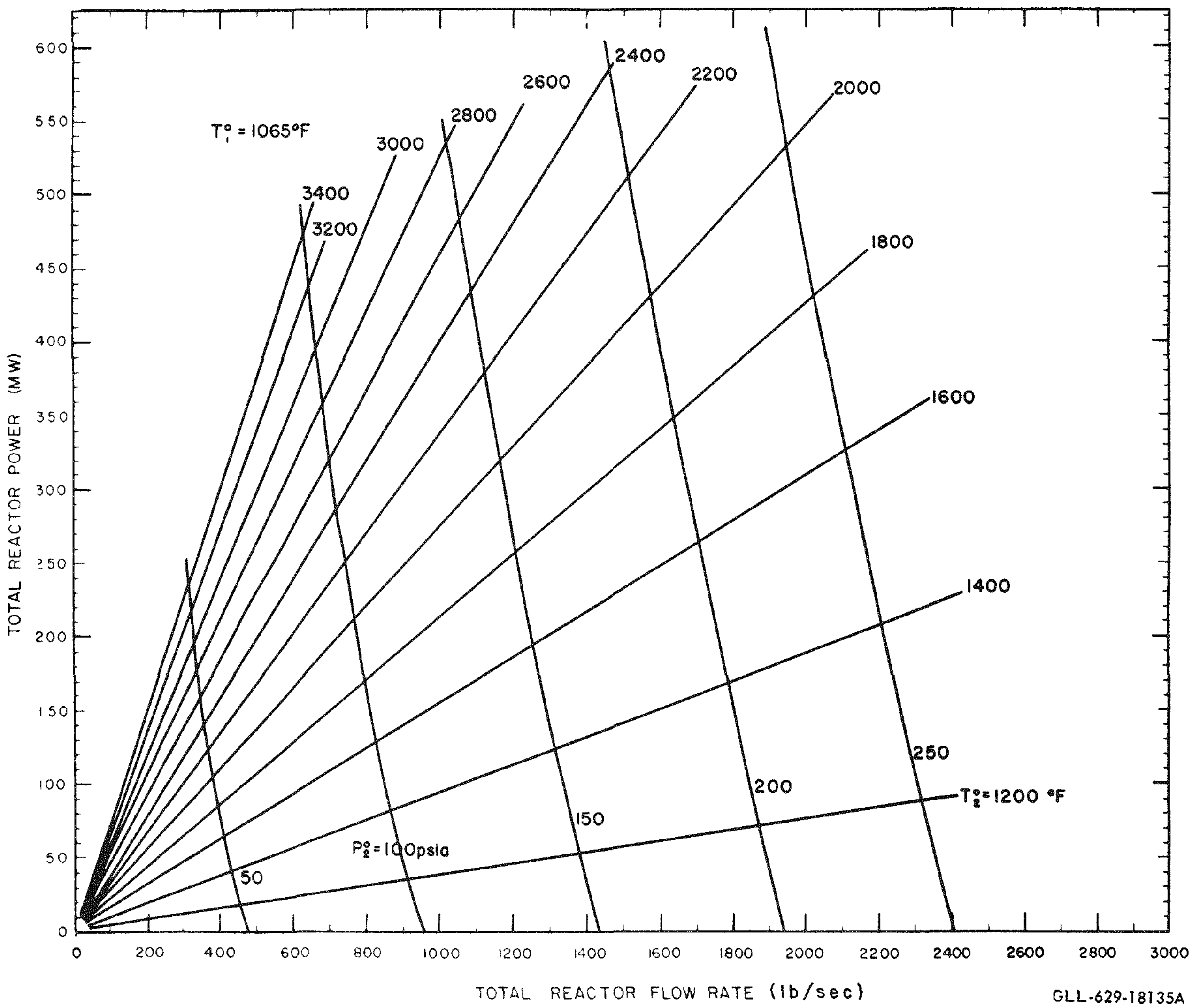

Performance map - lines of constant P_2° and T_2°.

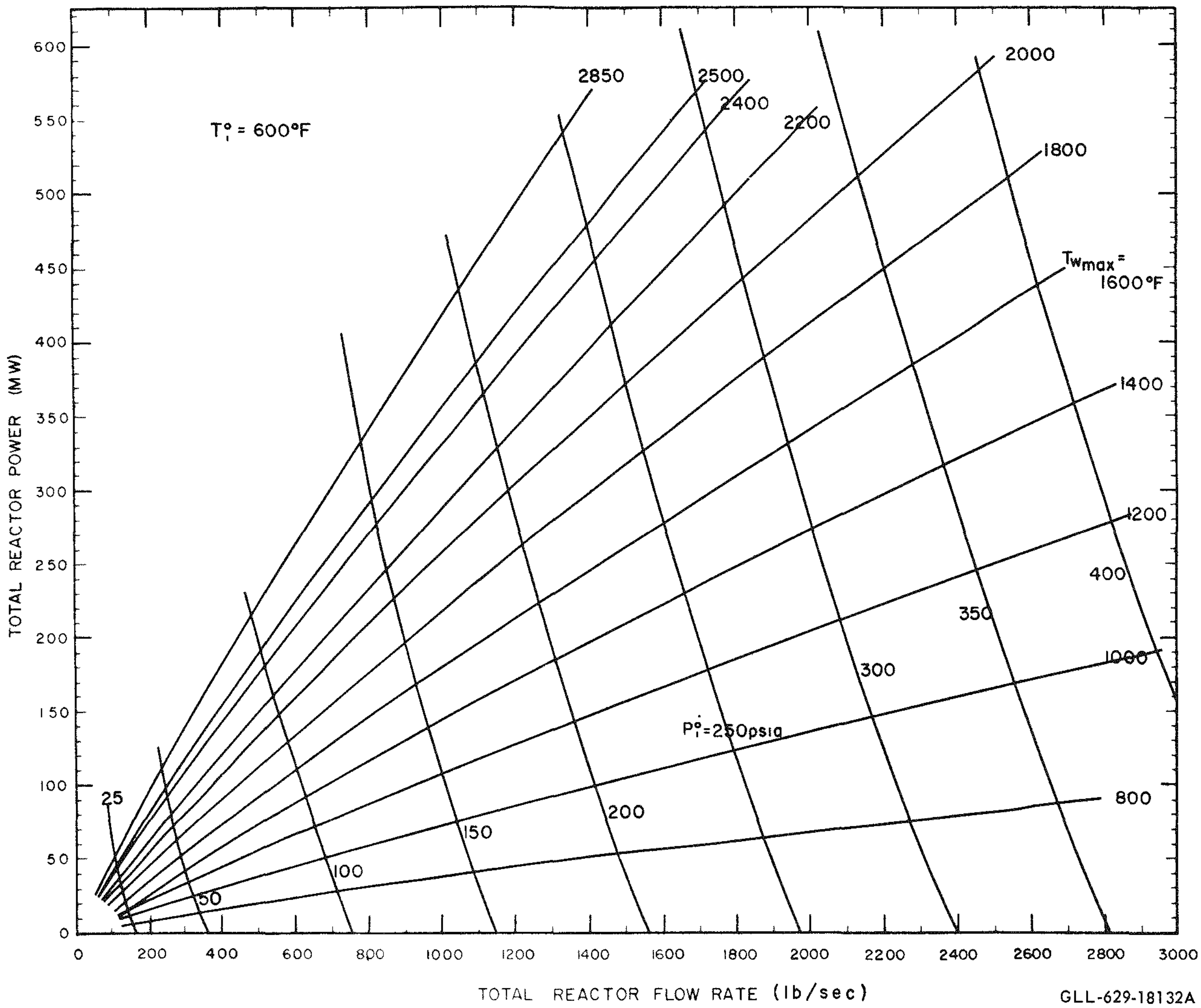

Performance map - lines of constant P_1° and T_w (T_w = fueled tube peak wall temperature).

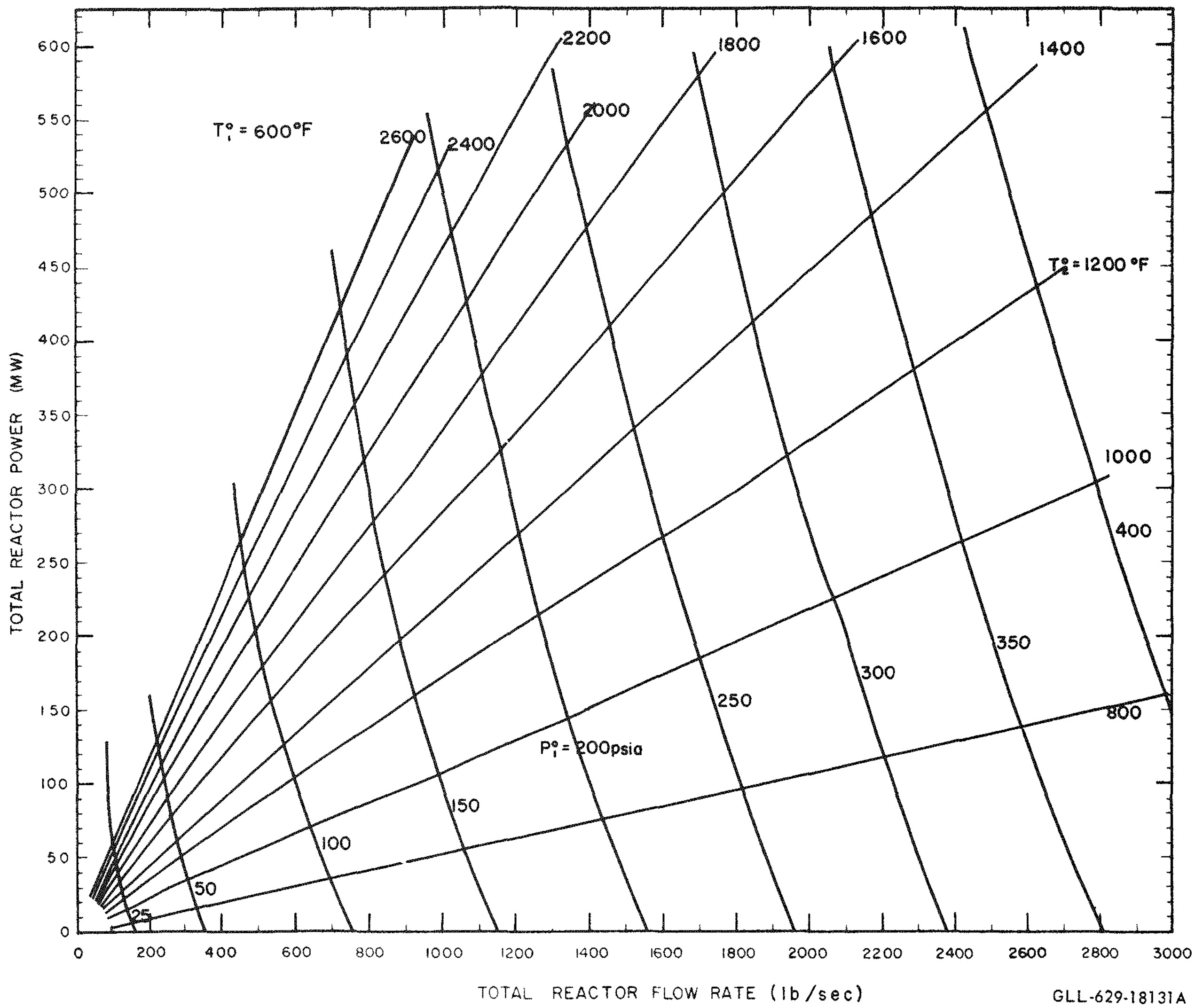

Performance map - lines of constant P_1° and T_2°.

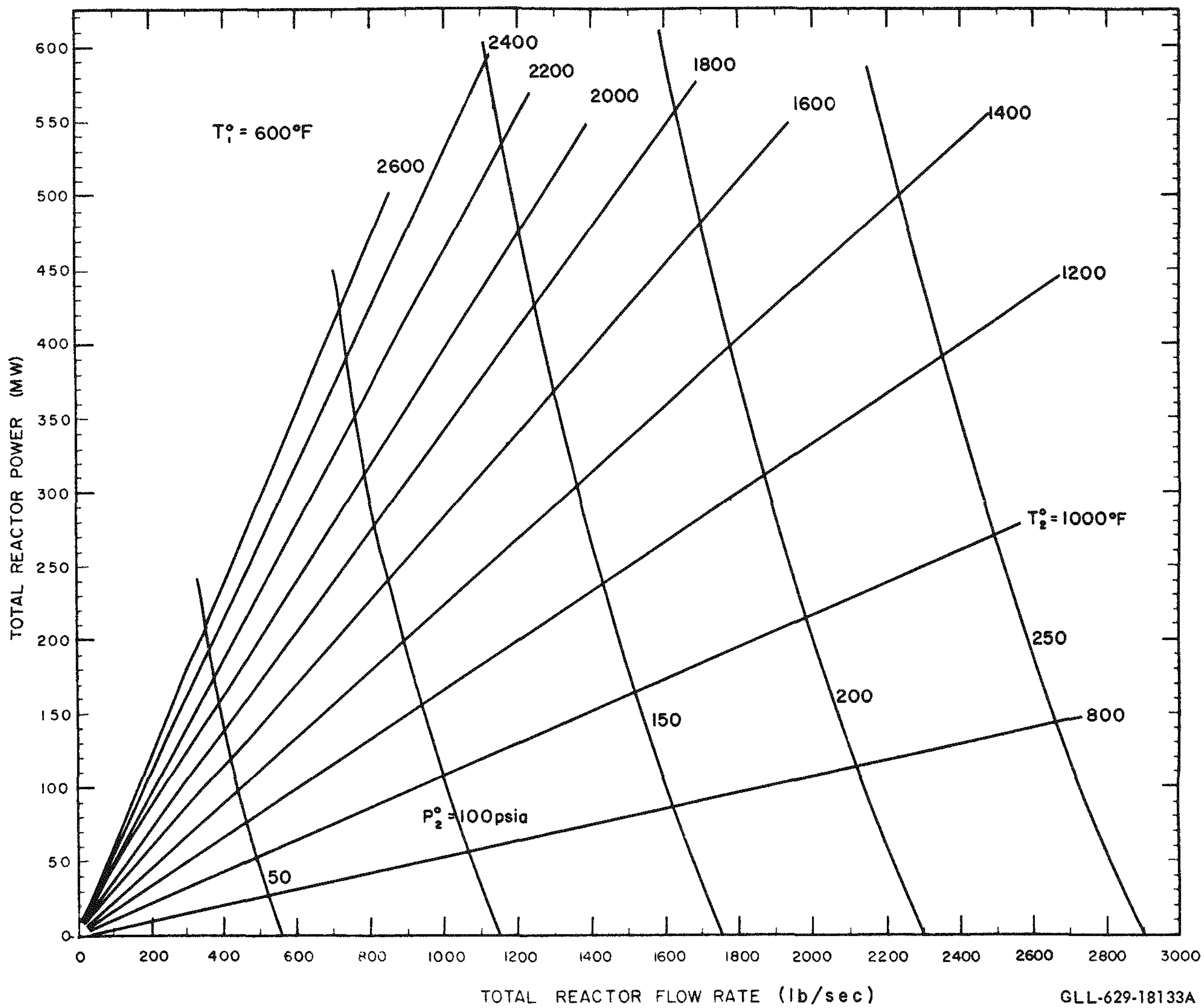

Performance map - lines of constant P_2° and T_2°.

4. Parameter Influence on Performance

Total thrust loss assessment for parameters not analyzed by NOMAC code*	-7.3%
Boundary layer bleed	-3.5%
Entrance (0.4% in pressure)	-0.7%
Offset (misalignment in flow tubes)	-3.0%
Power depression due to rods	-2.0%
Sudden expansion loss (effect of bell-mouthing exit)	+2.9%
All others	-1.0%

Reactor inlet pressure effect on C_f net . . . . . Page I-70
Peak fueled tube wall temperature effect on C_f net . Page I-70
Friction factor effect on C_f net . . . . Page I-70
Heat transfer coefficient effect on C_f net . . . Page I-70
Fueled tube discharge coefficient effect on C_f net . . Page I-70
Fueled tube flow passage diameter effect on C_f net . Page I-70
Fueled tube flow passage diameter effect on C_f net (Γ = const) . . . . Page I-71
Exit nozzle influence parameters . . . . . . Page I-72

---

*But included on page I-4.

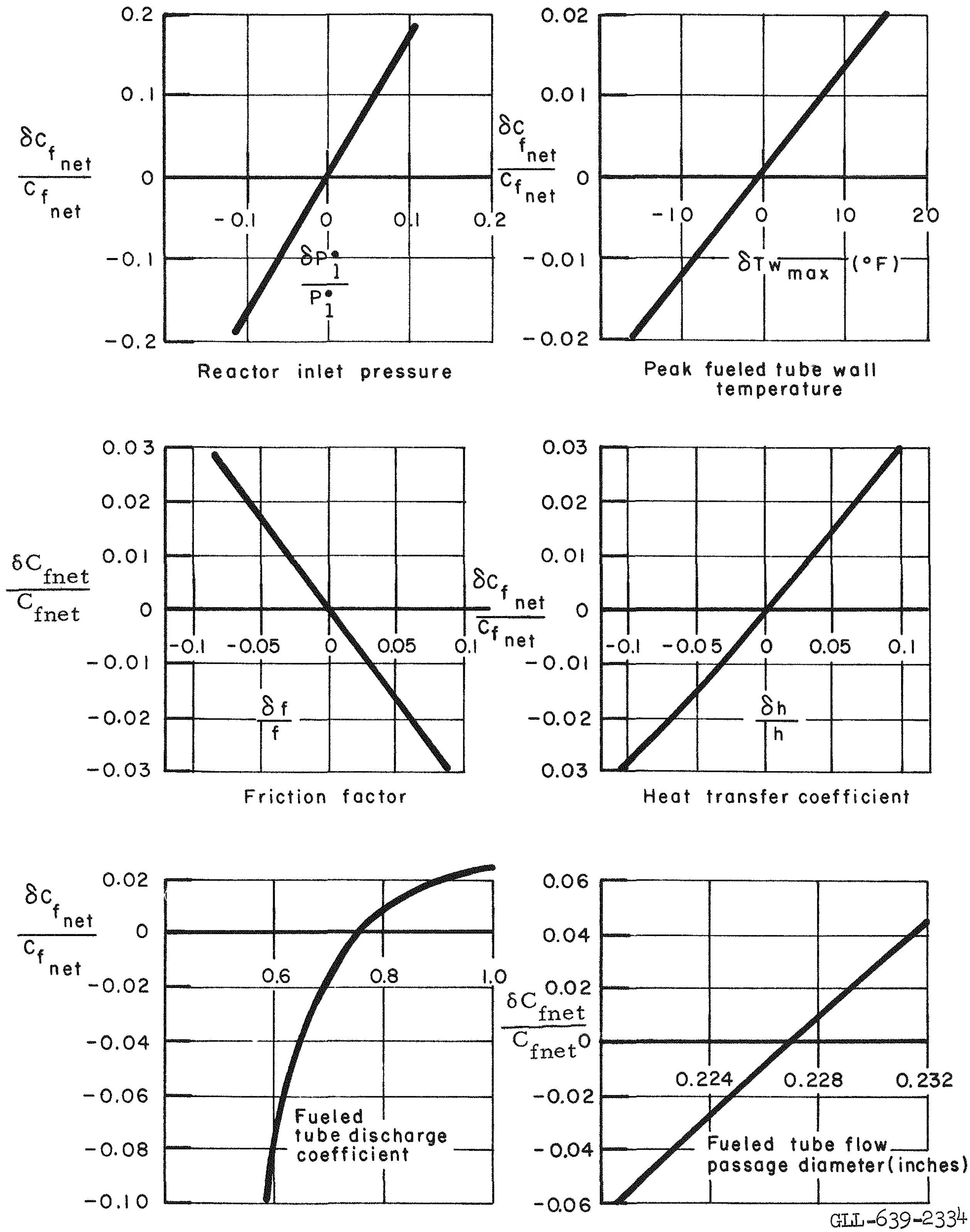

Influence of net engine thrust coefficient at diffuser design point condition.

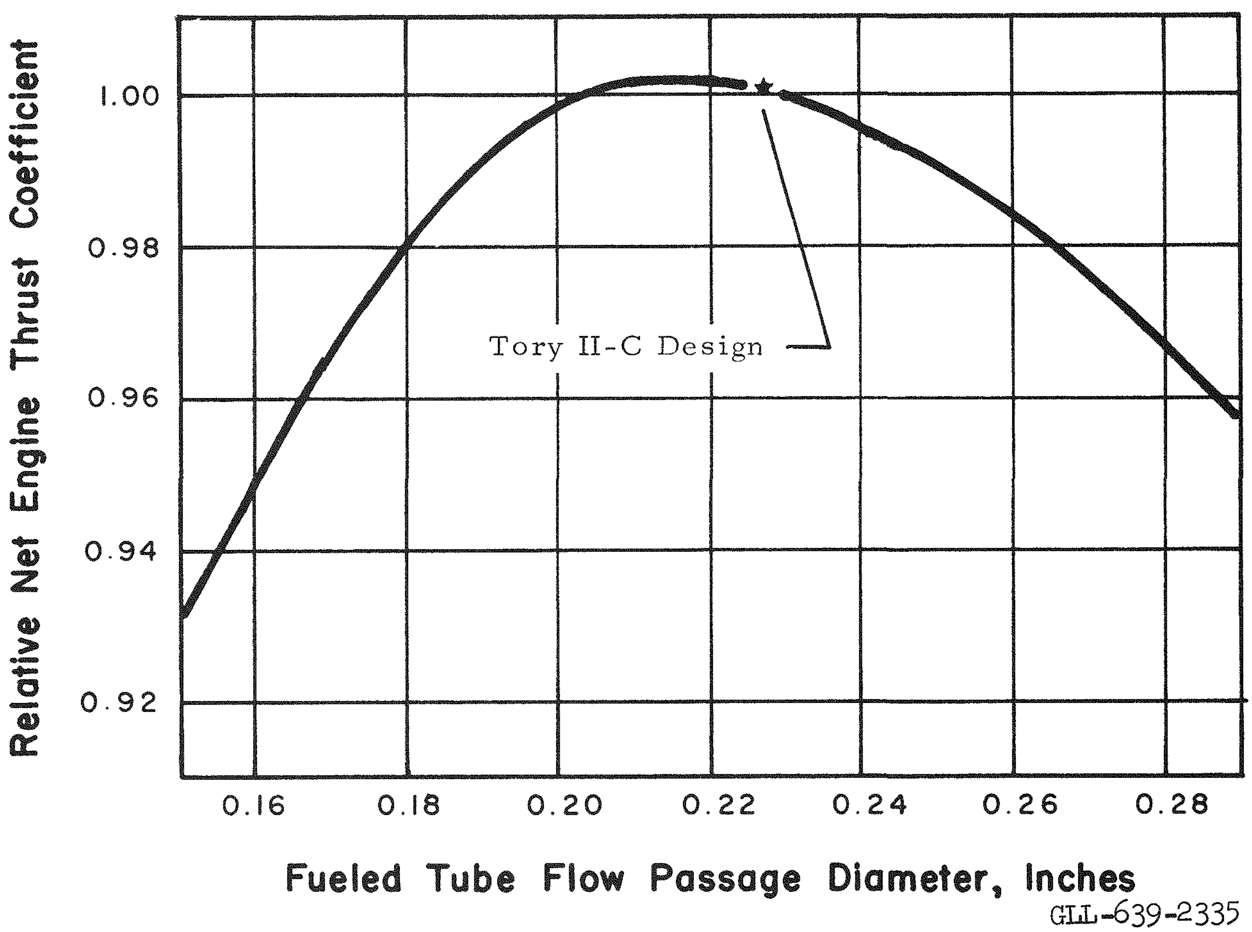

Net engine thrust coefficient vs fueled tube flow passage diameter (reactor porosity kept constant), diffuser design point condition.

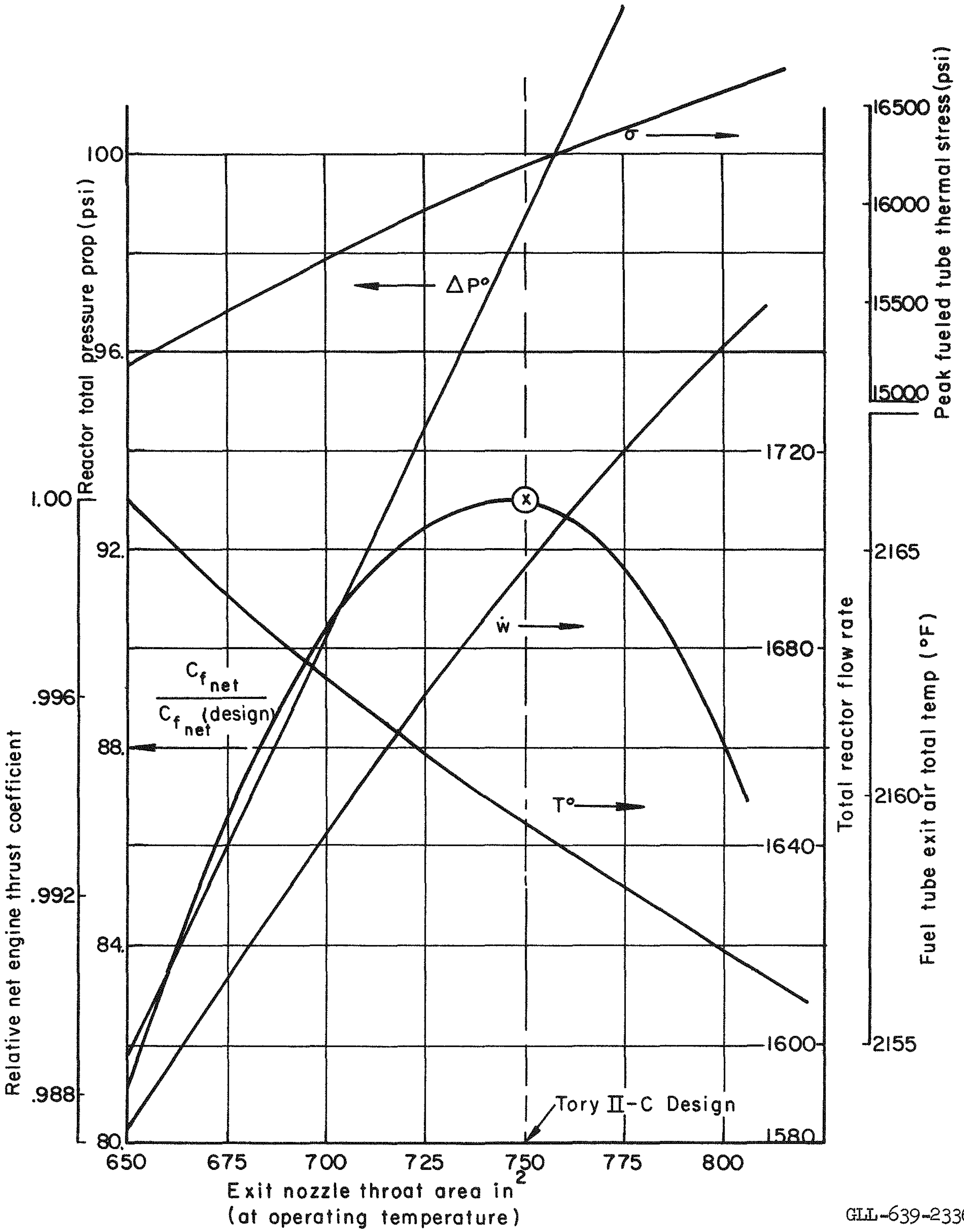

GLL-639-2336

Exit nozzle influence parameters, diffuser design point condition.

5. Analysis and Heat Transfer Data

Inlet Diffuser

Design point of critical operation	Mach 2.8
Pressure recovery ratio	0.80
Bleed fraction	0.04
Momentum recovery of bleed	0.80

Reactor

Fueled Tubes

Number of channels	21,012
Length	64.56 in.
Diameter of flow channel	0.227 in.
Exit discharge coefficient (due to transition losses)	0.76
Porosity	0.5298

Side Reflector Tubes

Number of channels	3888
Length	64.56 in.
Diameter	0.93 in.
Porosity	0.0895

Peripheral Shims (Circular Cooling Channels)

Number of channels	942
Length	62.70 in.
Diameter	0.130 in.
Porosity	0.1559

Peripheral Shims (Key Slots)

Number of channels	120
Length	62.70 in.
Flow area/channel	0.03334 in^2
Wetted perimeter of channel	0.7602 in.

Tie Rod

Number of channels	103
Length	80.9 in.
Diameter of flow channel	0.576 in.
Porosity	0.7391

Guard Tube (Standard Tie Rod)	
Number of channels	876
Length	54.185 in.
Diameter	0.130 in.
Porosity	0.1761
Reflector Inserts (Standard Tie Rod)	
Number of channels	103
Length	10 in.
Flow area per channel	0.5806 in^2
Wetted perimeter of channel	5.529 in.
Control Rod	
Number of components	14
Length of insertion (measured from inlet to control tie rod)	
Nominal 5-hour operating position*	32.3 in.
Fully inserted position	55.8 in.
Flow area per channel (within control tie rod)	0.87713 in^2
Wetted perimeter (within control tie rod)	10.357 in.
Control Tie Rod	
Number of components	18
Length	80.9 in.
Diameter	1.162 in.
Porosity	0.9042
Guard Tube (Control Tie Rod)	
Number of channels	324
Length	54.185 in.
Diameter	0.130 in.
Porosity	0.1761
Reflector Inserts (Control Tie Rod)	
Number of channels	18
Length	10.0 in.
Flow area per channel	0.8504 in^2
Wetted perimeter of channel	8.8813 in.
Side Support Structure (Structure Limit Condition)	
Length	63.81 in.

*Shim control rods

Flow area (total effective)	137.49 in^2
Wetted perimeter (average)	1623.3 in.
Exit Nozzle	
Throat area (at operating conditions)	750.0 in^2
Velocity coefficient	0.98
Discharge coefficient	0.98
Divergence factor	1.00

6. Time Constants and Thermal Capacities

Time Constants**

Symbols

ρ_w	Channel wall material density
C_w	Channel wall specific heat
dV_w	Channel wall element volume
T_w	Channel wall temperature
P_w	Power generated in channel wall element
h	Heat transfer coefficient between channel wall and gas
T_g	Total gas temperature in channel element
dA	Channel wall element heat transfer surface area
X	Channel axial station
t	Time
D	Channel diameter
Γ	Channel porosity

Formulas

The fundamental aerothermodynamic time constant for a step change in power is

$$\tau(t) \equiv \left(\frac{\rho_w C_w D}{4h(t)}\right)\left(\frac{1-\Gamma}{\Gamma}\right).$$

The effective aerothermodynamic time constant for a step change in power is:

$$\tau^*(X,t) \equiv \tau(t)\left[1 + \frac{\frac{2f(t)}{D}\int_0^X \frac{dT_w(X,t)}{dt}\,dX}{\frac{dT_w(X,t)}{dt}}\right].$$

**See Tory II-C Memos 253 and 295.

1. τ^* values were derived from SEA LION for step changes in power at M = 2.8 conditions and are first order approximations.
2. The values presented here were obtained from transients with constant inlet gas temperature. The time constants for variable inlet gas temperatures are somewhat higher.
3. For other airflow conditions,

$$\left(\frac{\tau_0^*}{W_0^{0.8}}\right) \approx \left(\frac{\tau^*}{W^{0.8}}\right) .$$

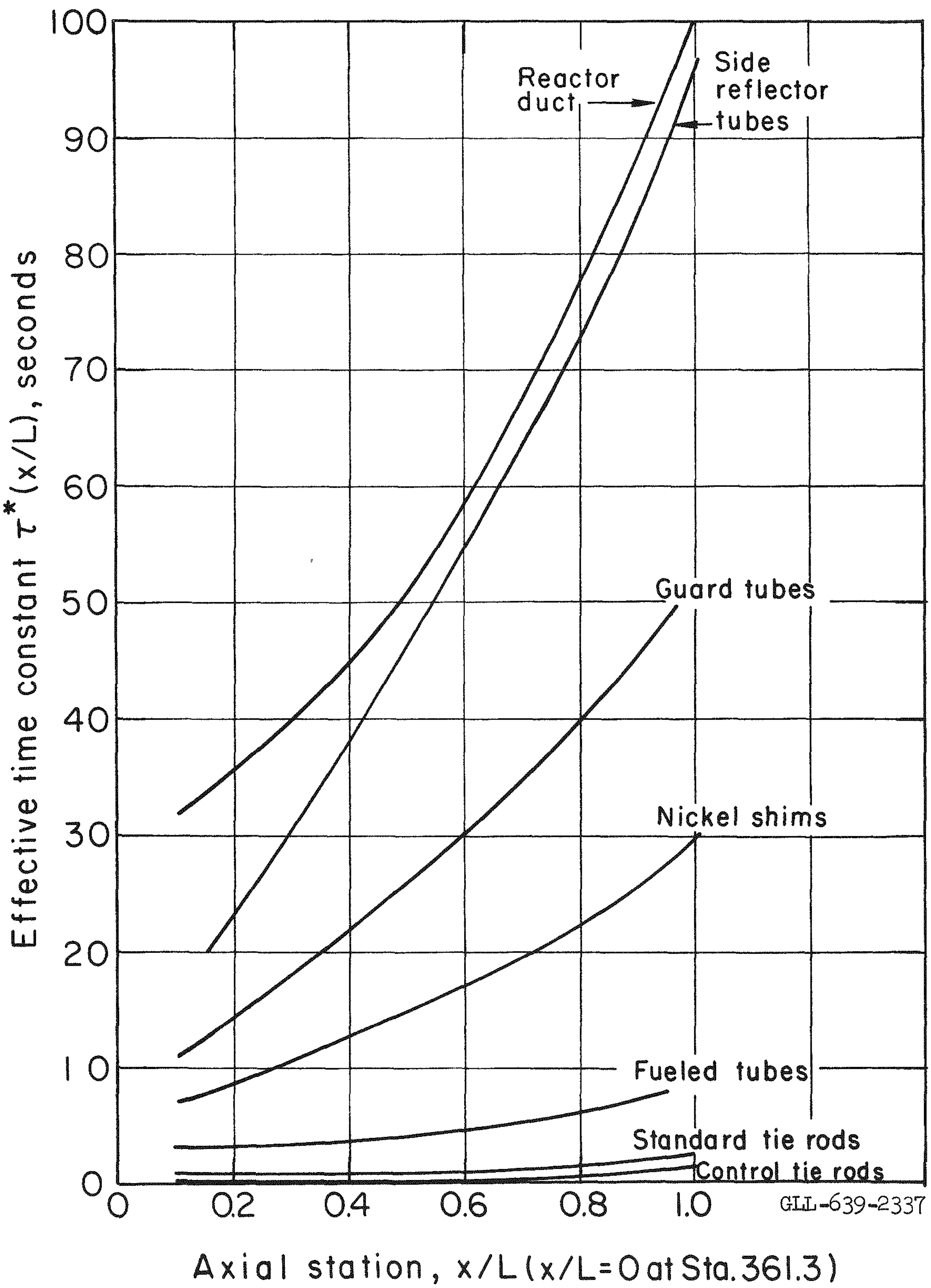

Effective time constants for design point operating condition (see p. I-75).

CHAPTER II – NEUTRONICS*

A. CRITICALITY

Criticality calculations are based upon the following input:

Average reactor temperature	2330°F
Linear expansion in all dimensions	See p. IV-5
Volume fractions	See p. II-5
Total number of tie rods	121
Number of control tie rods of Hastelloy R-235	4
Number of control tie rods of René 41	14
Number of standard tie rods of Hastelloy R-235	36
Number of standard tie rods of René 41	67
Assumed BeO density (percent of theoretical)	
Fueled tubes	99.2%
Guard tubes	97.5%
Front reflector	98.3%
Side reflector	97.3%
Side support system and peripheral shim surface density	See p. III-55
Base block surface density	11.7 g/cm^2
Power distribution	See p. II-16
Critical mass of OyO_2	59.9 kg
Mass of OyO_2 present	63.5 ± 1.0 kg**

Effect on reactivity of factors not considered by ANGIE:

	$\Delta k/k$
Normalization to Spade assembly (includes pedestal effect)	-0.009
Streaming	-0.009
Xenon buildup over 10 hours	-0.023
Thermocouples	-0.010
Background return	+0.004

---

*References: Tory II-C memos 316, 415, 429, 446, 454.

**This uncertainty in OyO_2 mass accounts for the uncertainty in the gamma counting and the statistical error in sorting.

	$\Delta k/k$
Support grid	+0.002
Coolant air	-0.003
Ceramic tube packing efficiency	-0.003
Fuel burnup, 10 hours	-0.001
γ-n contribution	+0.0004
New σ's for Be, O, U^{235}	-0.010
New σ's for René 41, R-235	-0.005
Impurities in fueled tubes	-0.005
Partial insertion of vernier rod	-0.003
Fast period reserve	-0.005
U^{235} enrichment	93.2%
Weight of U^{235} in critical mass	38.5 kg
Gross mean molar fraction: $\frac{\text{All BeO in active core}}{U^{235}}$	362
Mean wt % OyO_2	3.24
Maximum wt % OyO_2 in fueled tubes	8.12
Minimum wt % OyO_2 in fueled tubes	1.23
Approximate number of tube inches having given UO_2 loadings	See p. II-15
Loading class description	See p. II-8
Discrete UO_2 concentration step change	8%
Number of discrete UO_2 concentrations required	26

B. REACTIVITY REQUIREMENTS

	Δk_{eff}
Total reactivity swing required	-0.135
Total temperature effect	-0.074
Nuclear	-0.051
Geometry	-0.023
Xenon override	-0.023
Shutdown	-0.028
Excess at operating temperature	0.005
Errors in temperature effect assuming $\beta = 0.008$	0.010

C. REACTOR CHARACTERISTICS

Prompt lifetime, ℓ*	90×10^{-6} sec
Delayed neutron fraction, β	0.00677
Temperature coefficient $\frac{\Delta k/k}{\Delta T}$	$-5.5 \times 10^{-5}/°C$
Neutron economy*	
Neutrons captured in active core	+0.300
OyO_2	+0.304
René 41 tie rods	+0.092
R-235 tie rods	+0.023
Unfueled BeO	-0.013
Fueled BeO	-0.131
Y_2O_3	+0.009
ZrO_2	+0.002
Shim rods at 5-hour position	+0.015
Neutrons captured in peripheral shims	+0.163
Neutrons captured in side support structure	+0.111
Neutrons captured in base blocks	+0.015
Neutrons captured in front reflector	+0.021
Neutrons captured in cell plates	+0.003
Neutrons captured in aft reflector	+0.001
Neutrons captured in side reflector BeO	-0.003
Total parasitic capture of neutrons in reactor	0.630
Neutrons captured to cause fission	1.000
Neutrons leaking from reactor	0.698
Total neutrons captured and leaking	2.309
Effective number of neutrons generated	2.309

*Neutrons per fission with reactor at high power and temperature. Base problem ANGIE RZ 501; shim rods at the expected operating position. The k_{eff} for this problem was 1.0766.

Delayed neutron characteristics

(Thermal fission of U^{235}):

Group	$\overline{E}$ (MeV)	λ (sec^{-1})	Absolute group yield (n/fiss.)	γ	$\beta_{i,eff}$ [a]	(mod)[b] $\beta_{i,eff}$
1	0.25	0.0124	0.00052	1.090	0.00023	0.00029
2	0.46	0.0305	0.00346	1.063	0.00148	0.00186
3	0.405	0.111	0.00310	1.069	0.00133	0.00167
4	0.45	0.301	0.00624	1.065	0.00267	0.00335
5	0.42	1.13	0.00182	1.068	0.00078	0.00098
6	(0.43)[c]	3.00	0.00066	1.067	0.00028	0.00035
		Totals	0.01580		0.00677	0.00848

[a] $\beta_{i,eff} = \dfrac{\text{Absolute gp. yield}}{\nu} \times \gamma_i$; $\nu = 2.486$ assumed.

[b] This set is to be used when the shim rod worth curves of p. II-6 are used.

[c] Assumed value.

D. CONTROL ROD WORTH

	Predicted	Desired
Shim rods, swing ($\Delta k/k$)	0.169	0.135
Vernier rods, swing ($\Delta k/k$)	0.0078	0.0061
Safety rods, swing ($\Delta k/k$)	0.0078	0.0085
Multiplication constant, k_{eff}, vs shim rod position	See p. II-6	

Radial distribution on materials at axial loading zone D (Sta. 383.748).

Radius[b] (cm)	OyO$_2$ loading (g/in)	Volume Fractions[a]: Fueled tubes	Guard tubes	Tie rods[c]	Control rods[d]	Refl tubes	Nickel shims	Side support[f] + duct: René 41	HA-C	
0										
	0.0277									
14.102		0 4357	0.03828	0 004466	0	0	0	0	0	Standard unit cells
	.0299									
18 332										
	.0323									
20.661										
	.0323									
22.198		0.3906	0 06472	0 006141	0 02189	0	0	0	0	Control unit cell
	.0350									
24.993										
	0379									
28 401										
	.0410									
31.489										
	.0443									
34 234										
	0479									
36.772										
	.0518									
39 245										
	.0560									
41 435		0 4357	0.03828	0 004466	0	0	0	0	0	Standard unit cells
	.0606									
43 655										
	.0656									
45.714										
	.0710									
47.844										
	.0769									
50.094										
	0832									
52 596										
	.0901									
56.137		0.4333	0.04101	0.004784	0	0	0	0	0	Standard unit cells[e]
	0976									
60.153										
	0	0	0	0.008492	0	0.8579	0	0	0	Side reflector
65 264										
	0	0	0	0	0	0	0.659	0	0	
68.578										
	0	0	0	0	0	0	0	0.2228	0 4097	
72 706										

[a] Volume fractions given are fractions of the annular volume contained within the radii

[b] Nominal tube dimensions are assumed Effects of camber and twist are not included

[c] René 41 comprises 66.7% of the tie rods, Hastelloy R-235 accounts for 33 3%

[d] Value given corresponds to 12 shim rods. The vernier rods and their associated tie rods and guard tubes are not included in the present format

[e] Adjusted for mass conservation

[f] Includes springs, wiper bars rails wipers, and duct

GLL-639-2343

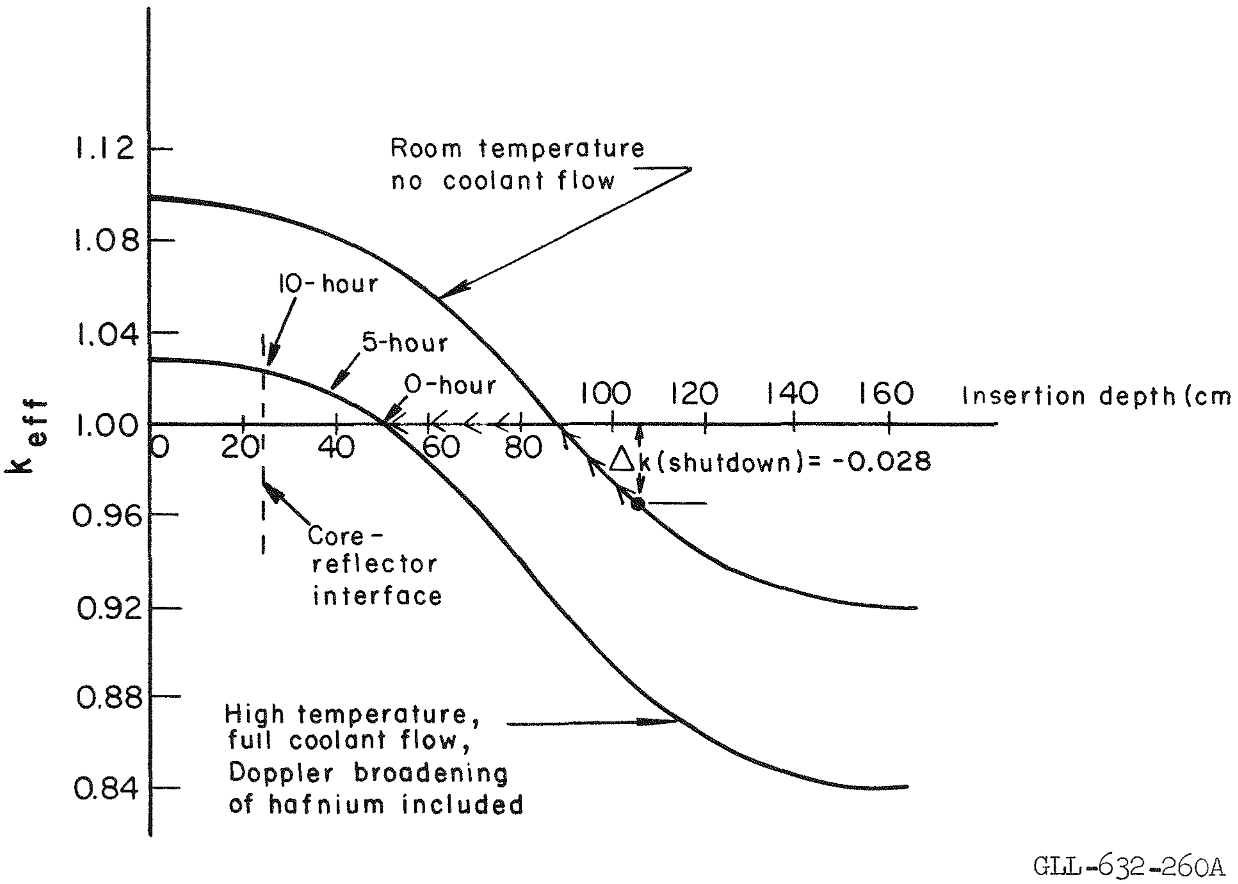

Multiplication constant of reactor vs shim rod position. (Note: $\left|\Delta k/\bar{k}\right|_{40\text{ in.}}^{\text{hot}}$ = 0.135, which is the desired rod worth.)

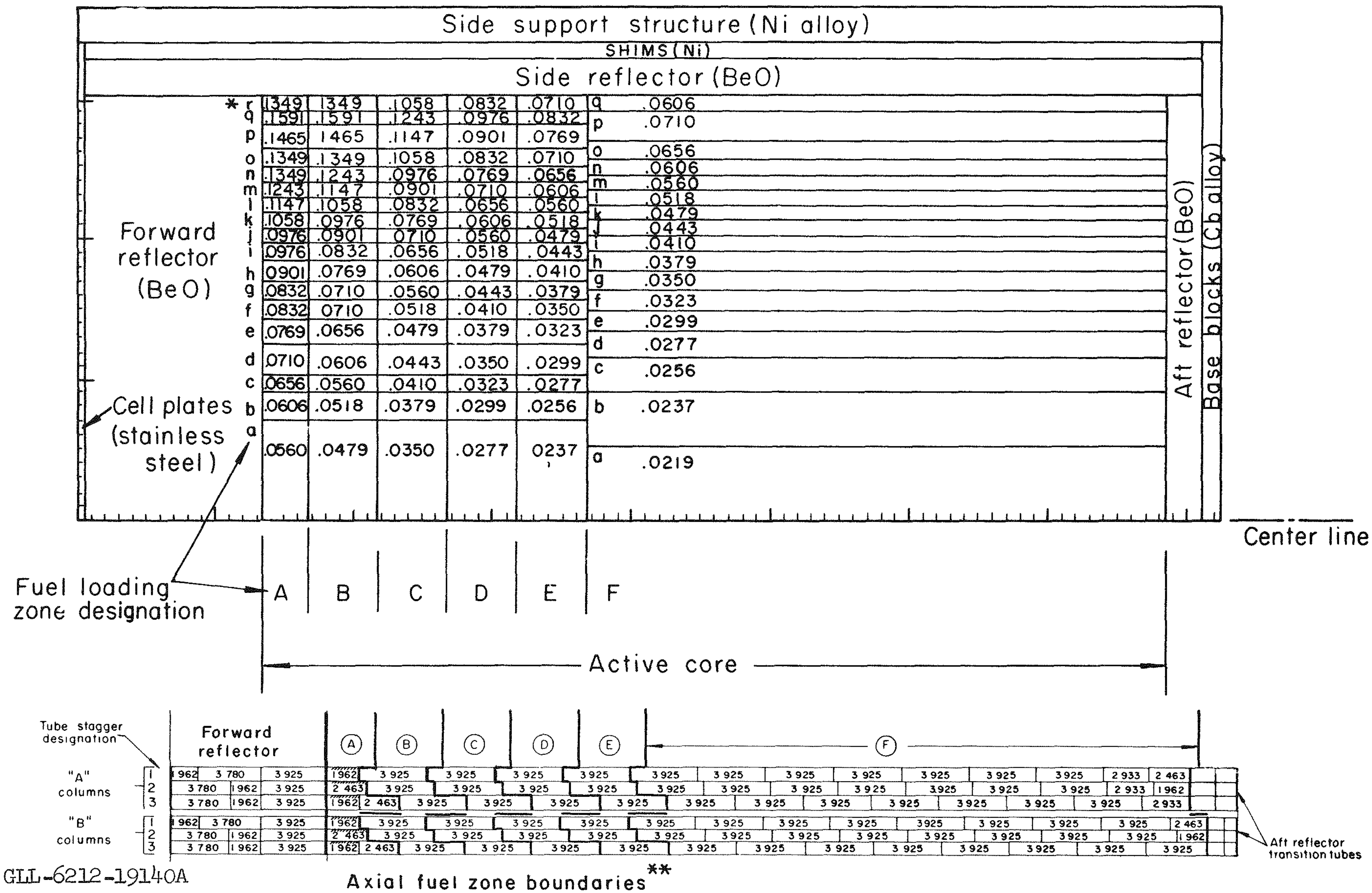

Fuel loading map. *Numbers designate the weight of OyO_2 in grams per inch length of tube. ** See pp. II-9 through II-14 for radial fuel zone boundaries.

Fueled tube class description.

Grams of OyO_2/inch of tube			Wt % OyO_2
Max	Nom	Min	Nom
0.0228	0.0219	0.0211	1.229
.0246	.0237	.0228	1.328
.0266	.0256	.0246	1.433
.0288	.0277	.0266	1.548
.0311	.0299	.0288	1.668
.0336	.0323	.0311	1.799
.0364	.0350	.0336	1.945
.0394	.0379	.0364	2.102
.0426	.0410	.0394	2.269
.0461	.0443	.0426	2.446
.0498	.0479	.0461	2.638
.0538	.0518	.0498	2.845
.0582	.0560	.0538	3.067
.0630	.0606	.0582	3.308
.0682	.0656	.0630	3.567
.0738	.0710	.0682	3.847
.0800	.0769	.0738	4.150
.0866	.0832	.0800	4.470
.0938	.0901	.0866	4.818
.1016	.0976	.0938	5.192
.1100	.1058	.1016	5.597
.1192	.1147	.1100	6.031
.1293	.1243	.1192	6.494
.1405	.1349	.1293	6.997
.1526	.1465	.1405	7.539
0.1655	0.1591	0.1526	8.123

A

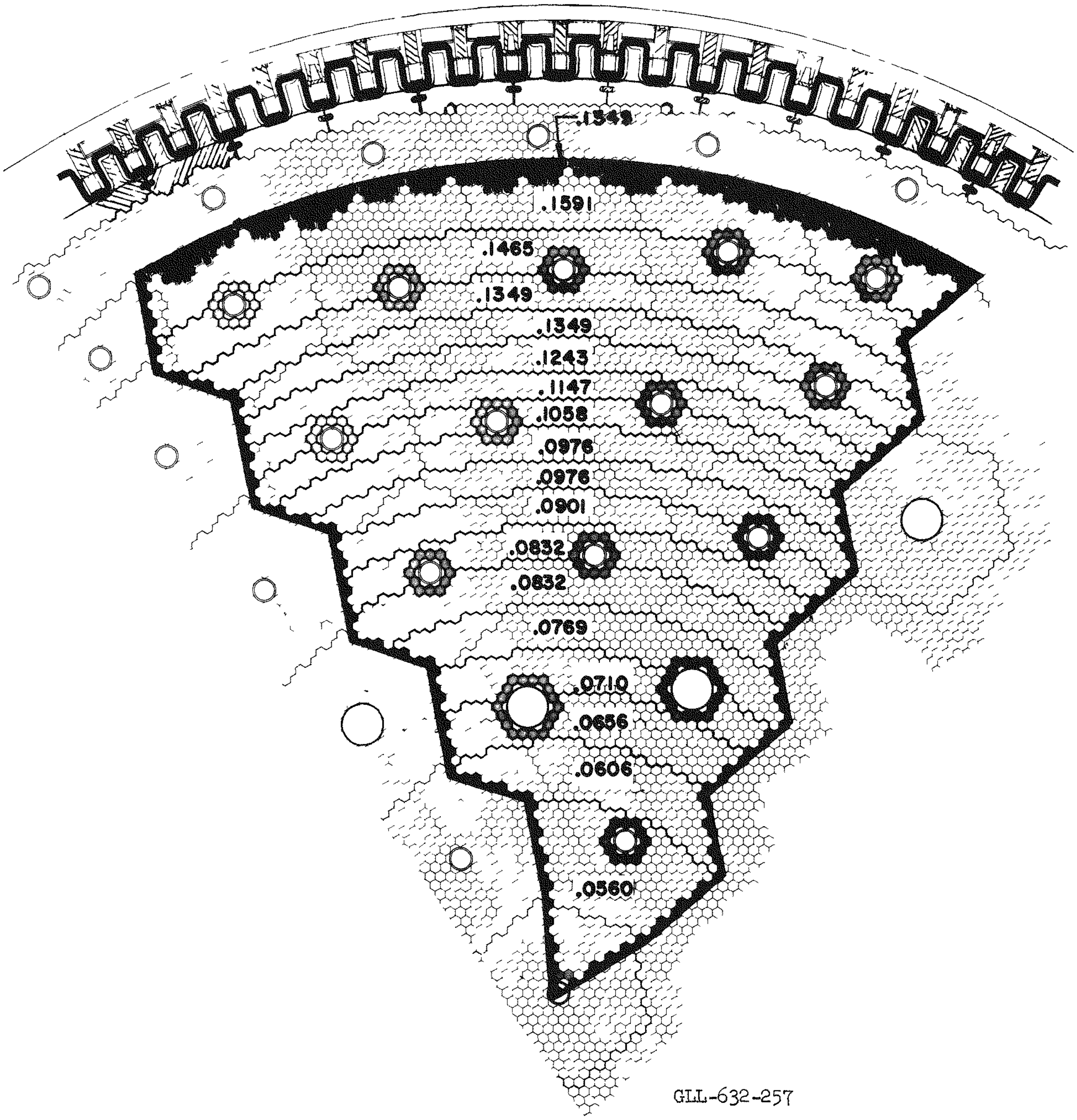

Radial fuel zone boundaries for axial zone A (looking downstream).

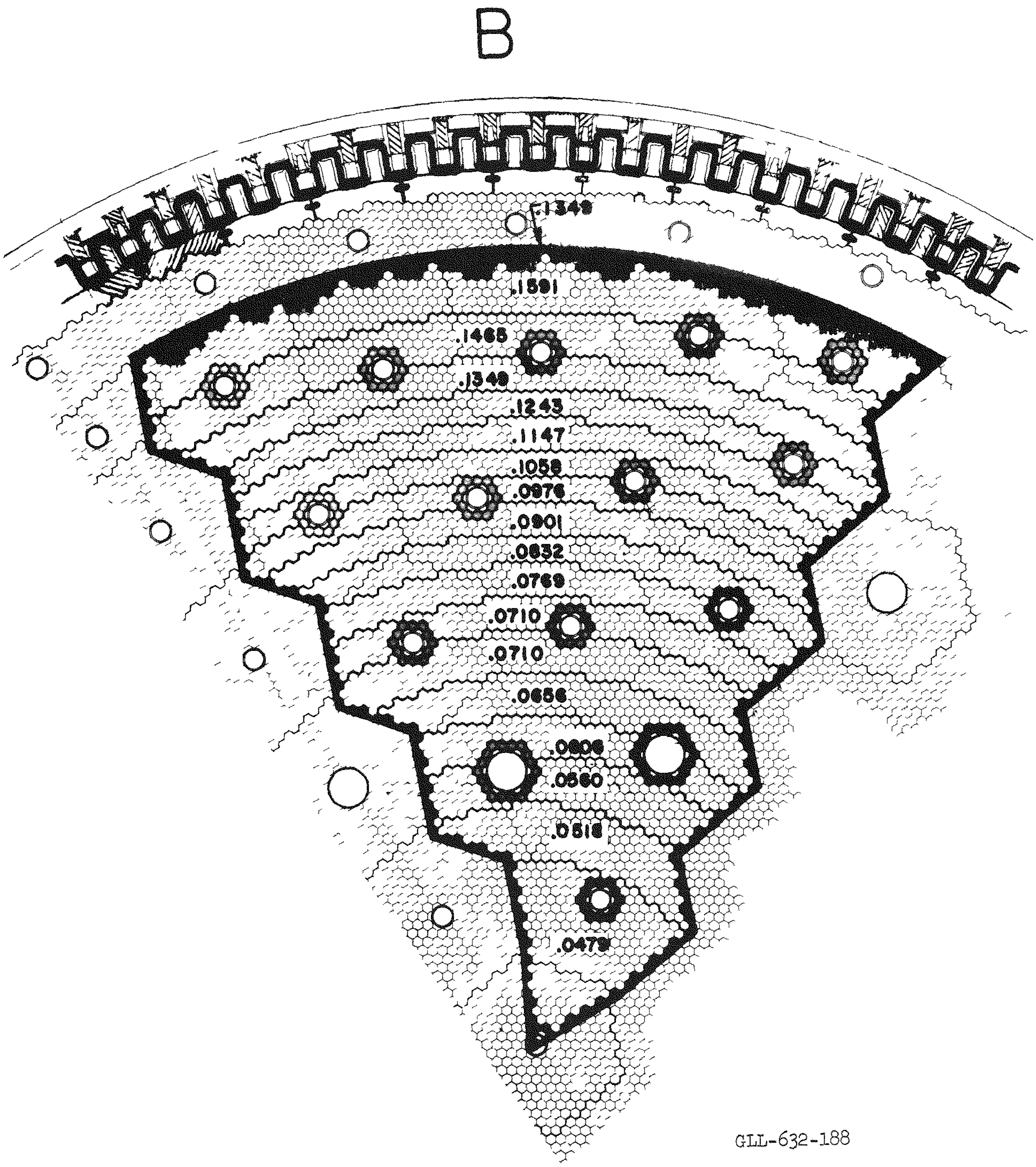

Radial fuel zone boundaries for axial zone B (looking downstream).

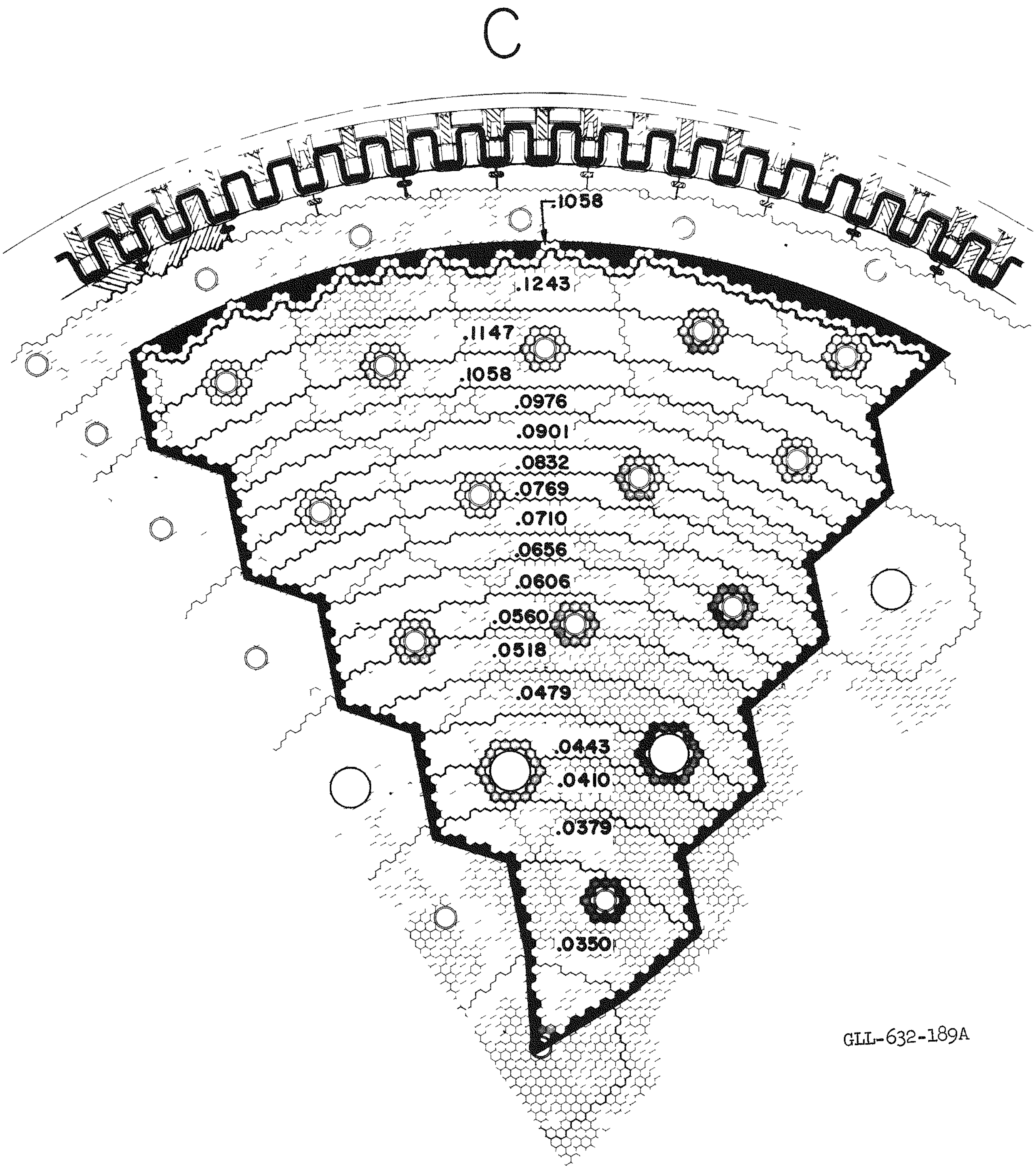

Radial fuel zone boundaries for axial zone C (looking downstream).

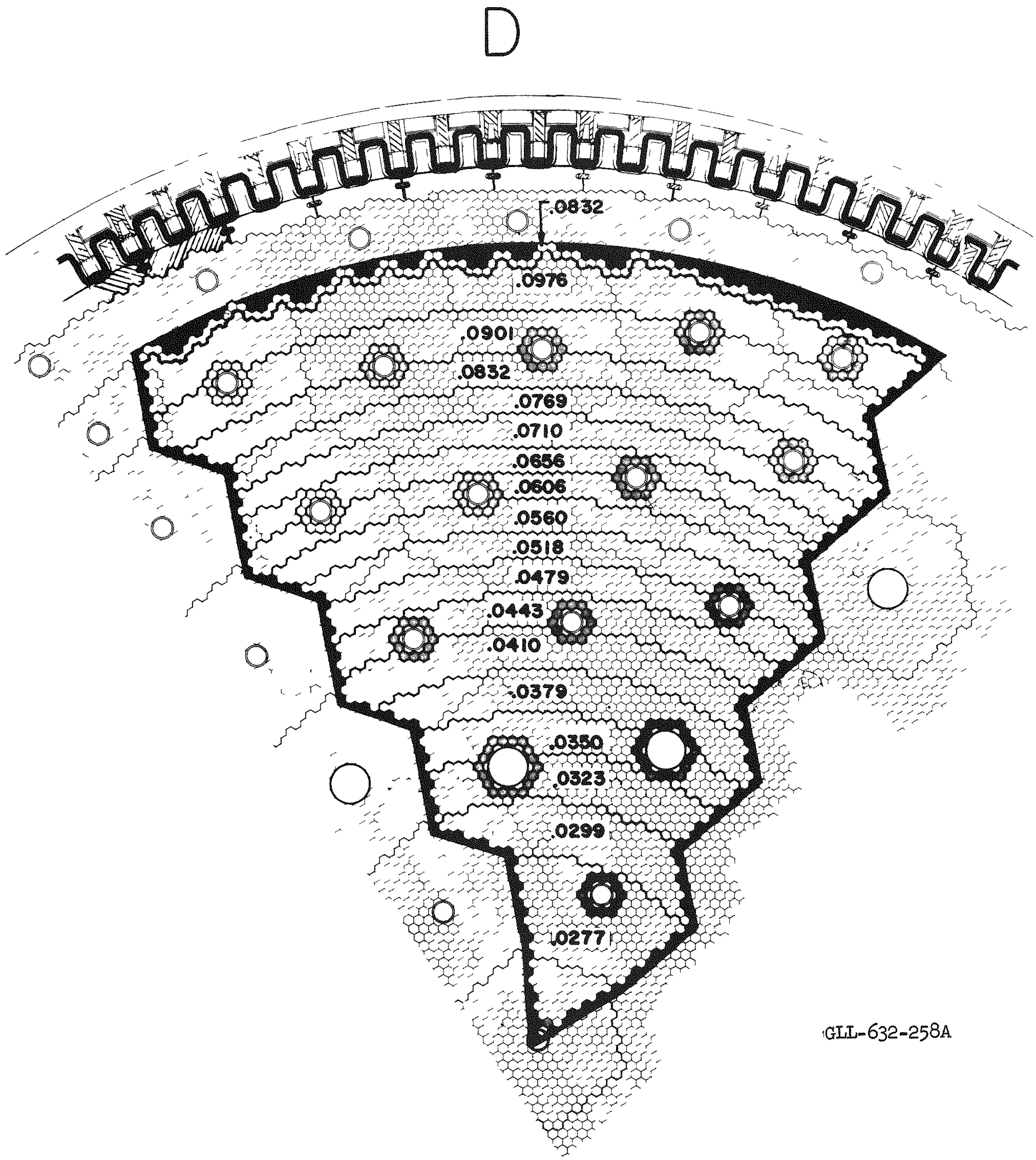

Radial fuel zone boundaries for axial zone D (looking downstream).

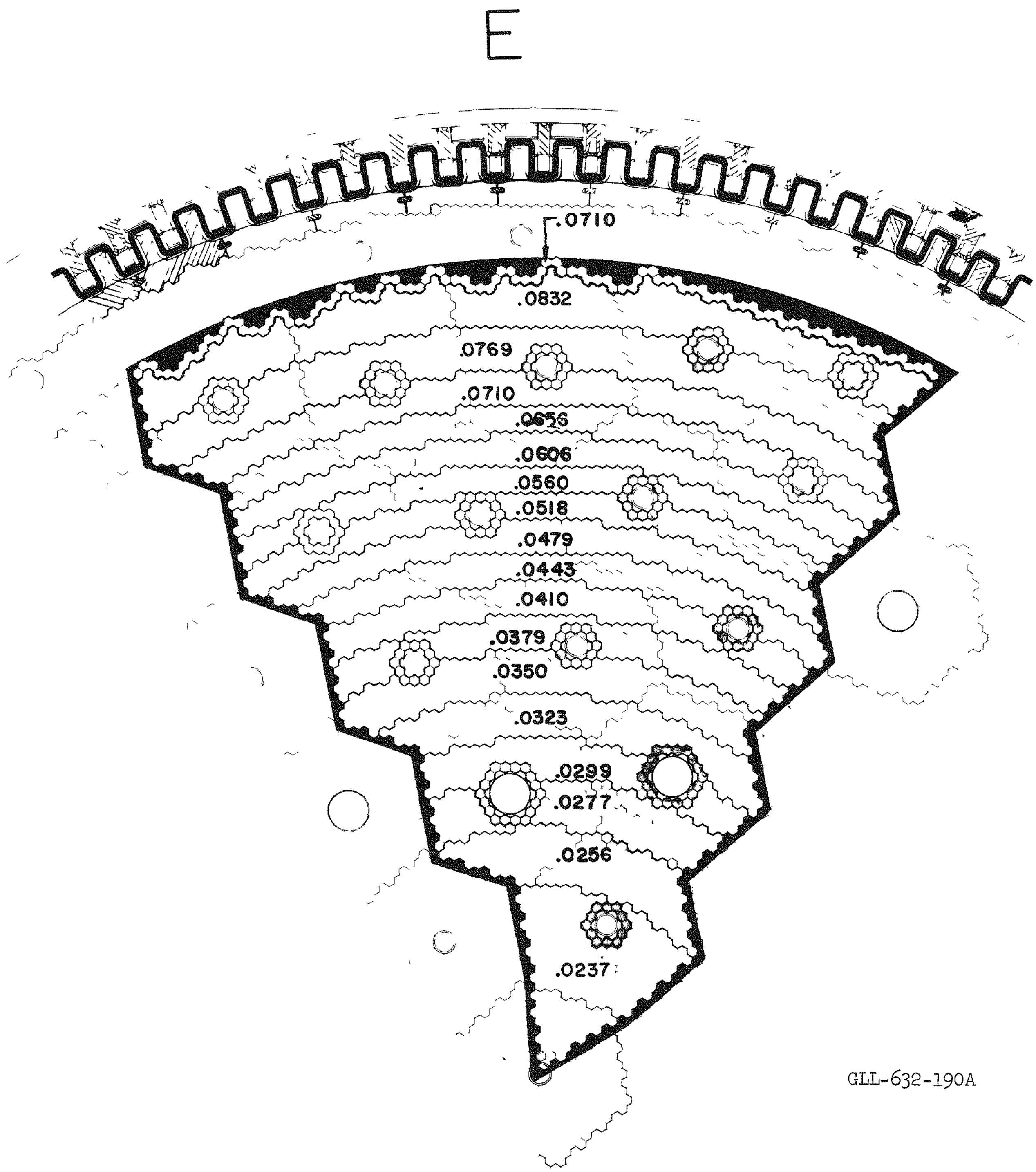

Radial fuel zone boundaries for axial zone E (looking downstream).

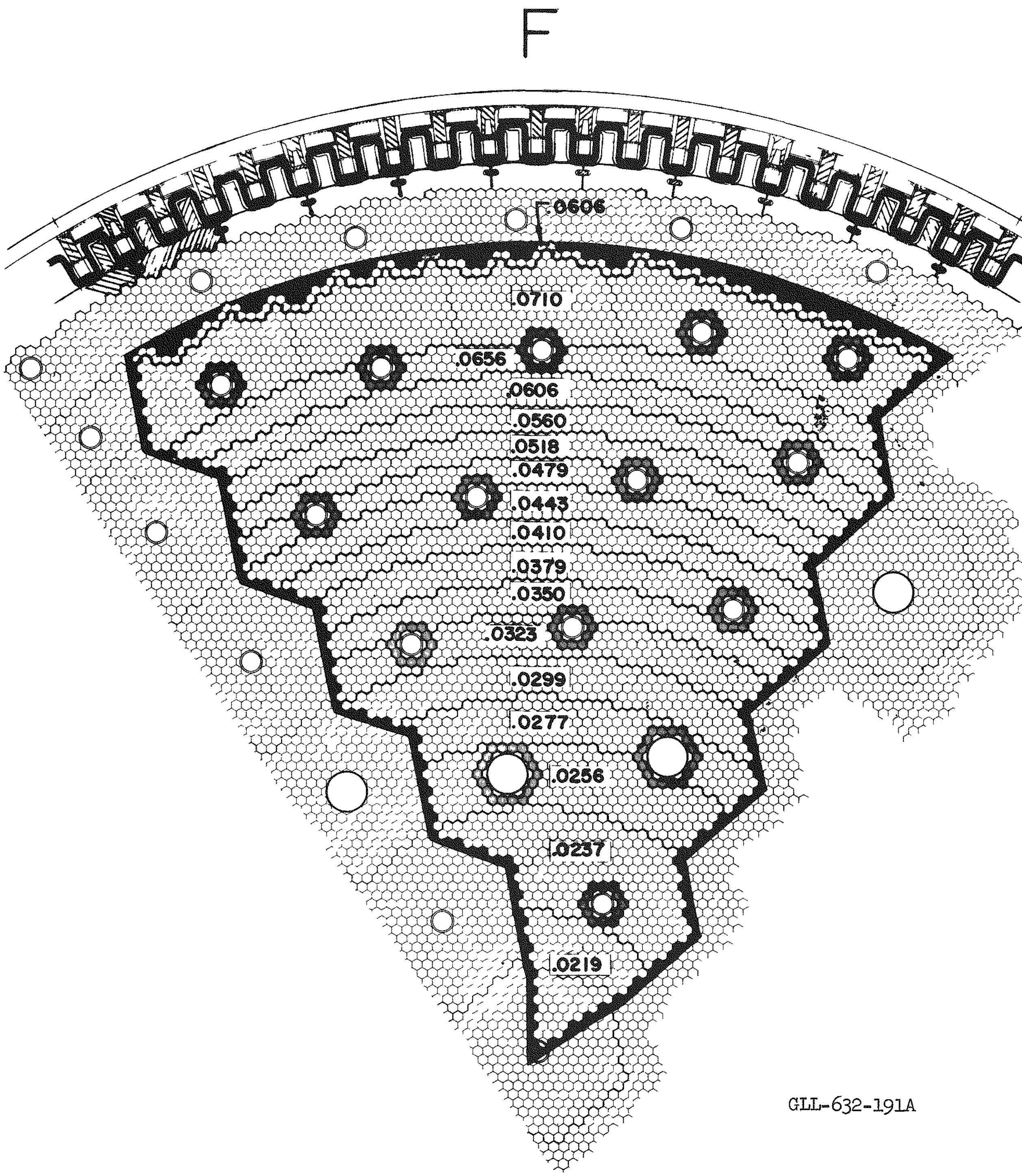

Radial fuel zone boundaries for axial zone F (looking downstream).

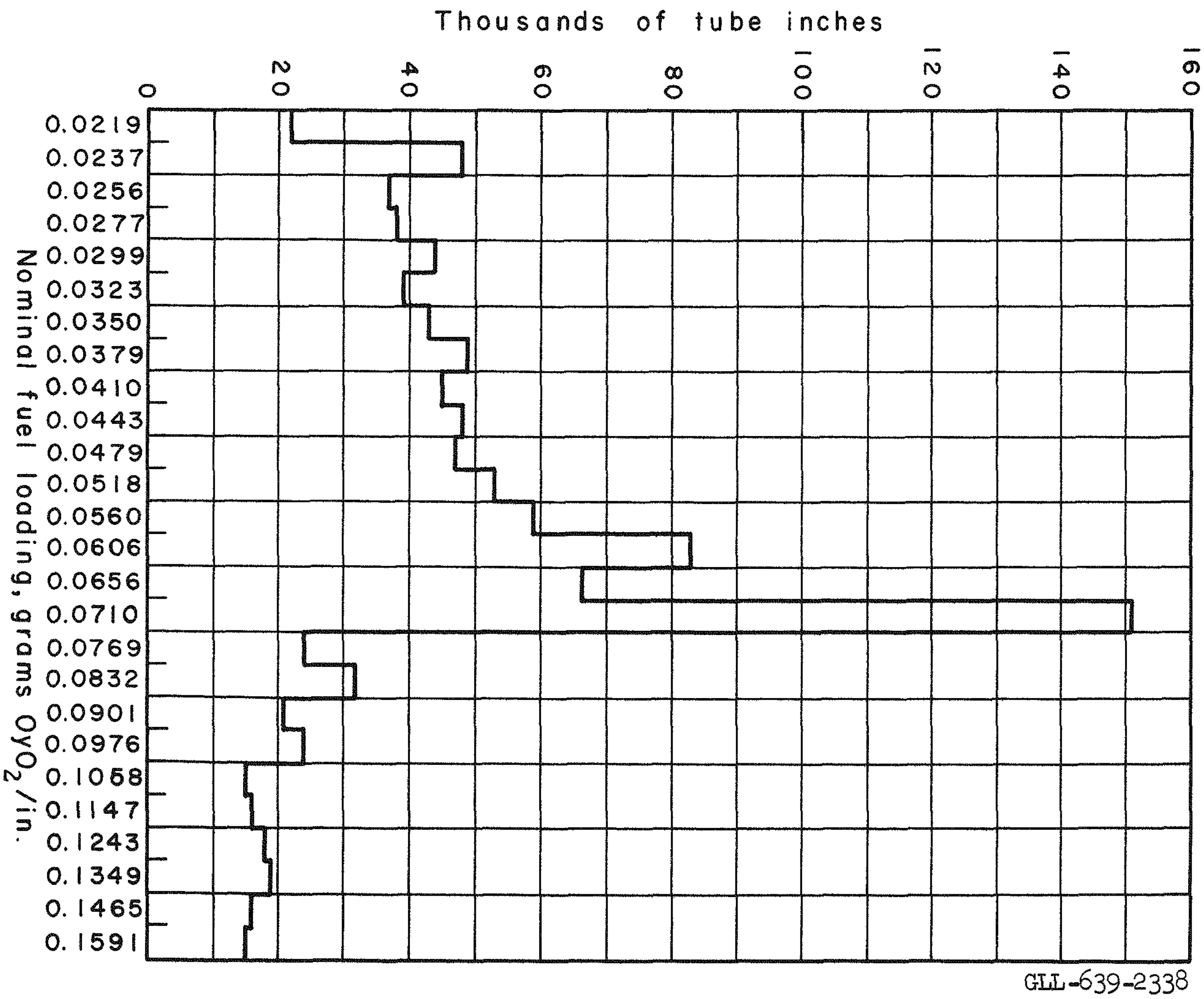

Fuel loading class distribution, expressed in total inches of tube per loading class.

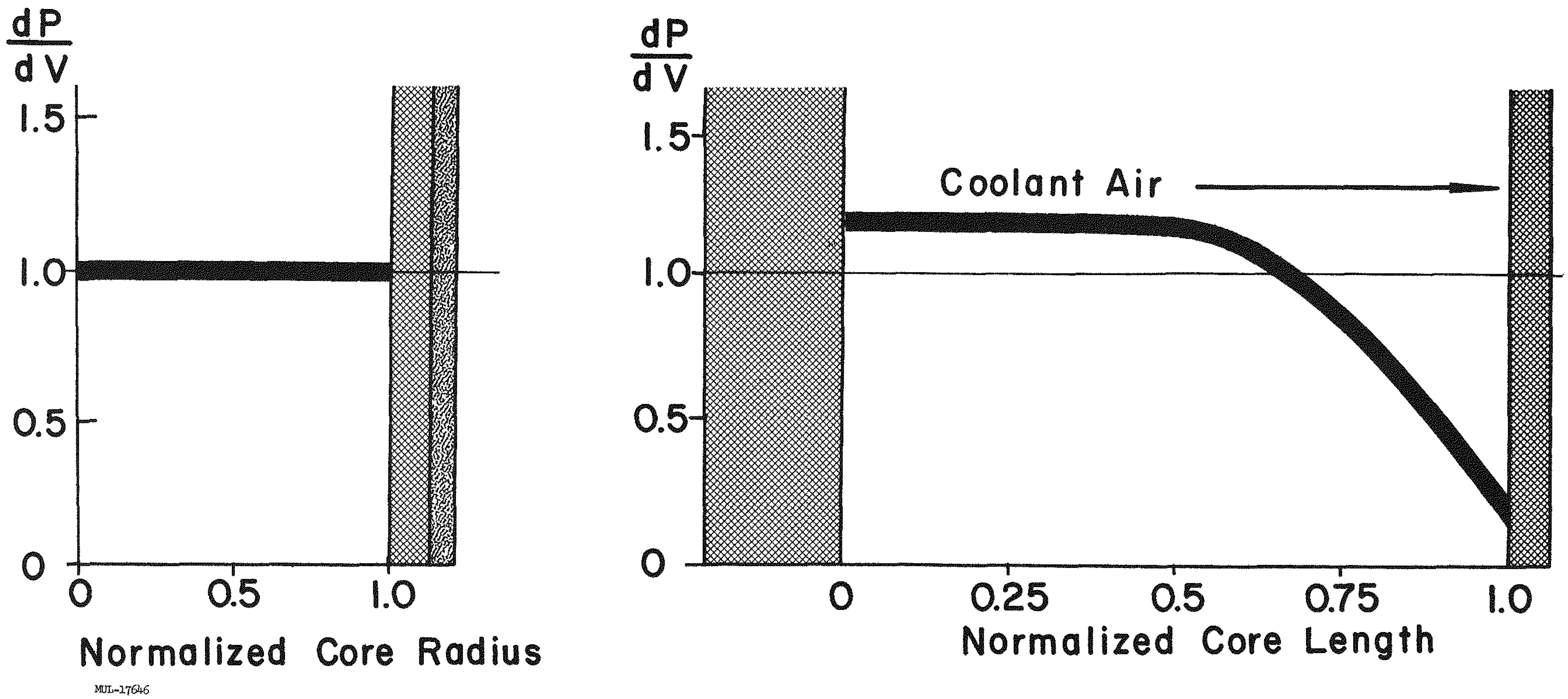

Design power profiles.

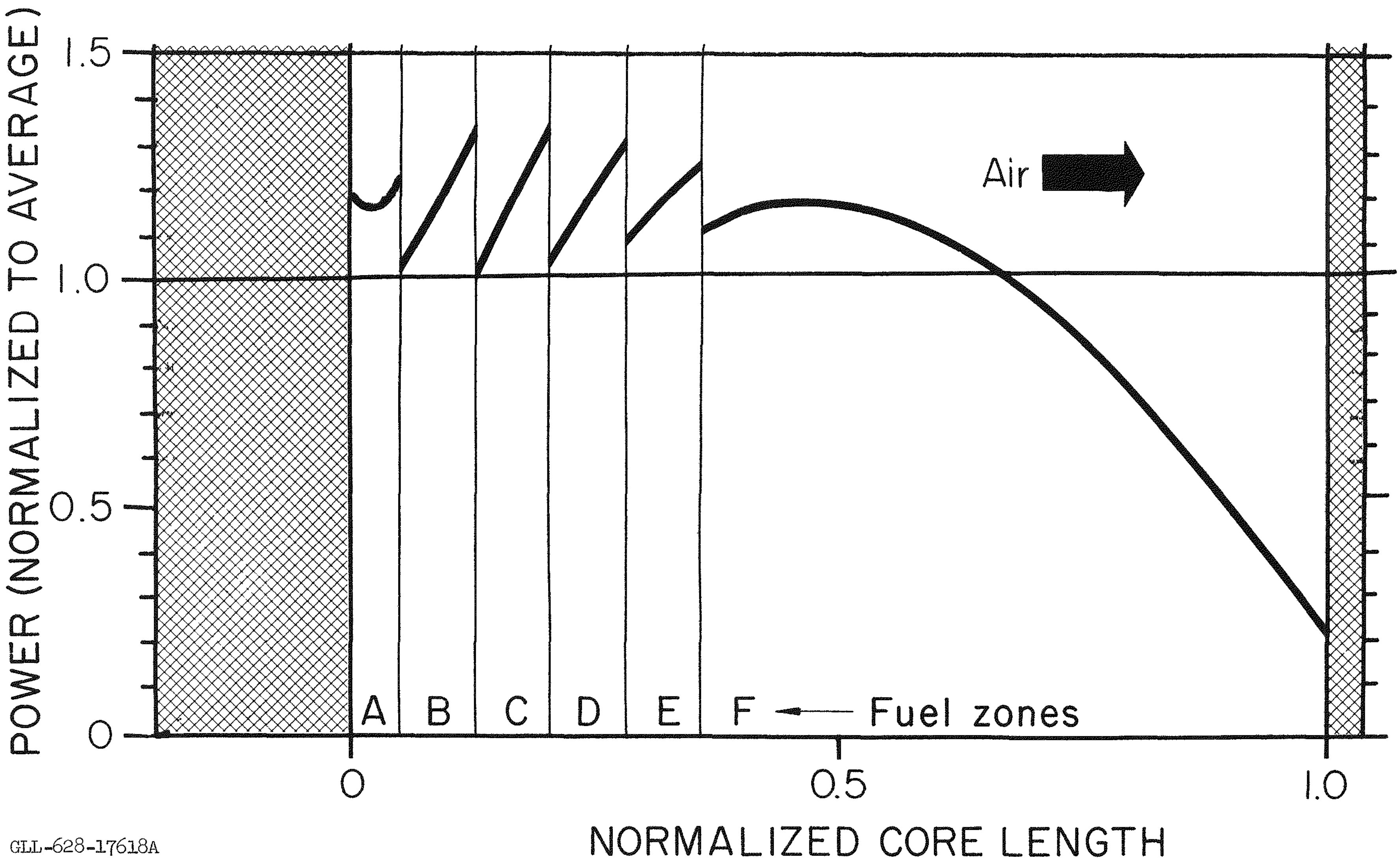

GLL-628-17618A

Realistic axial power profile.

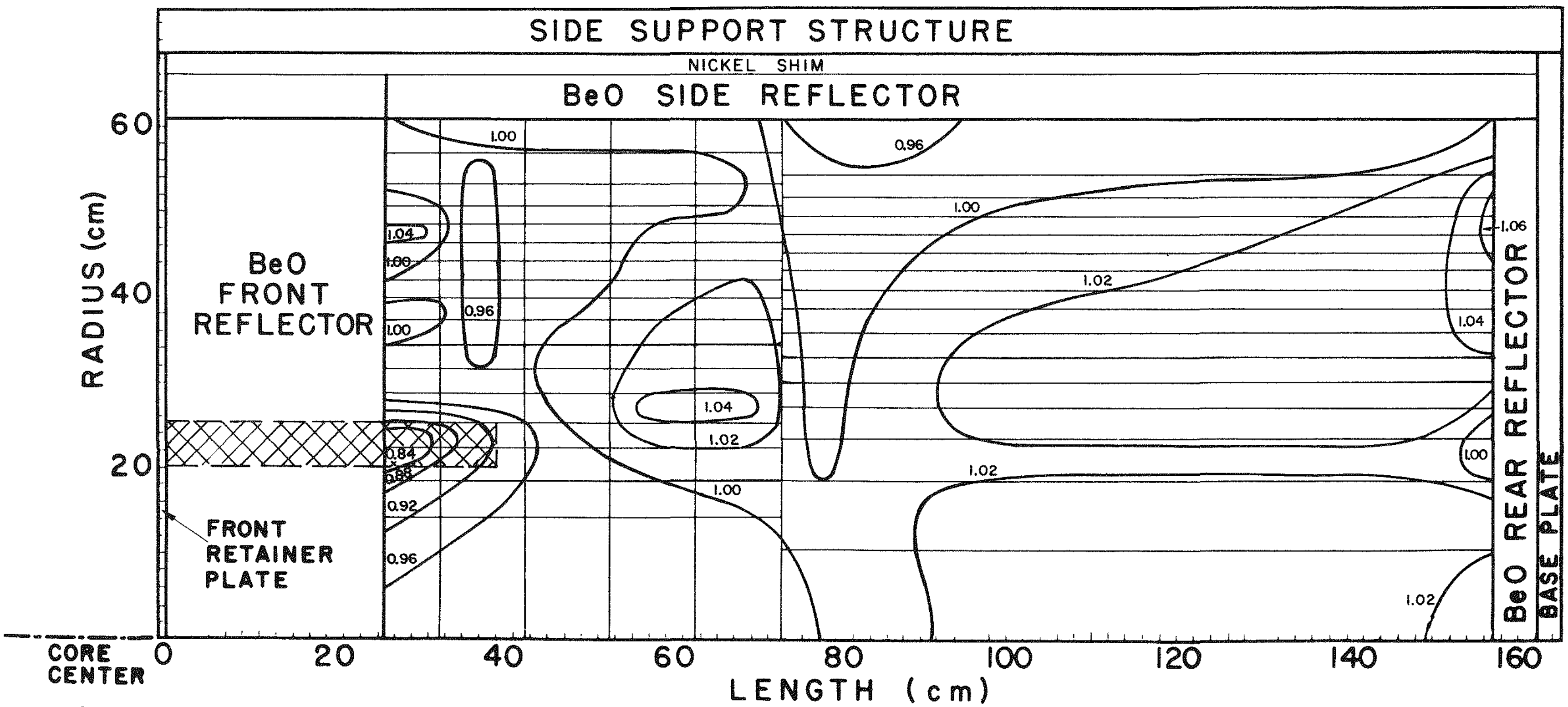

GLL-632-192

Deviation from design power profile (shim rods at 5-hour point).

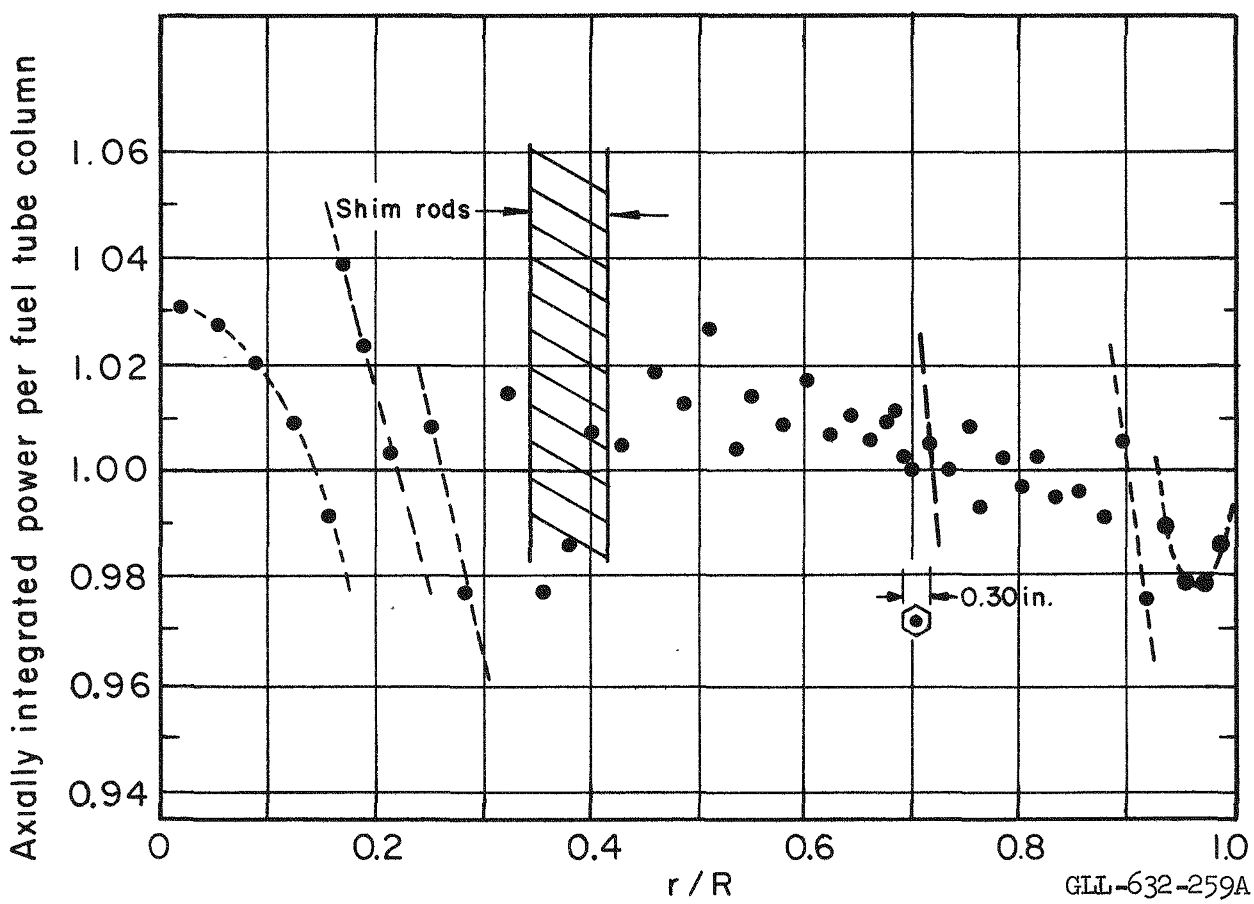

Axially integrated power per fueled tube column (normalized to average).

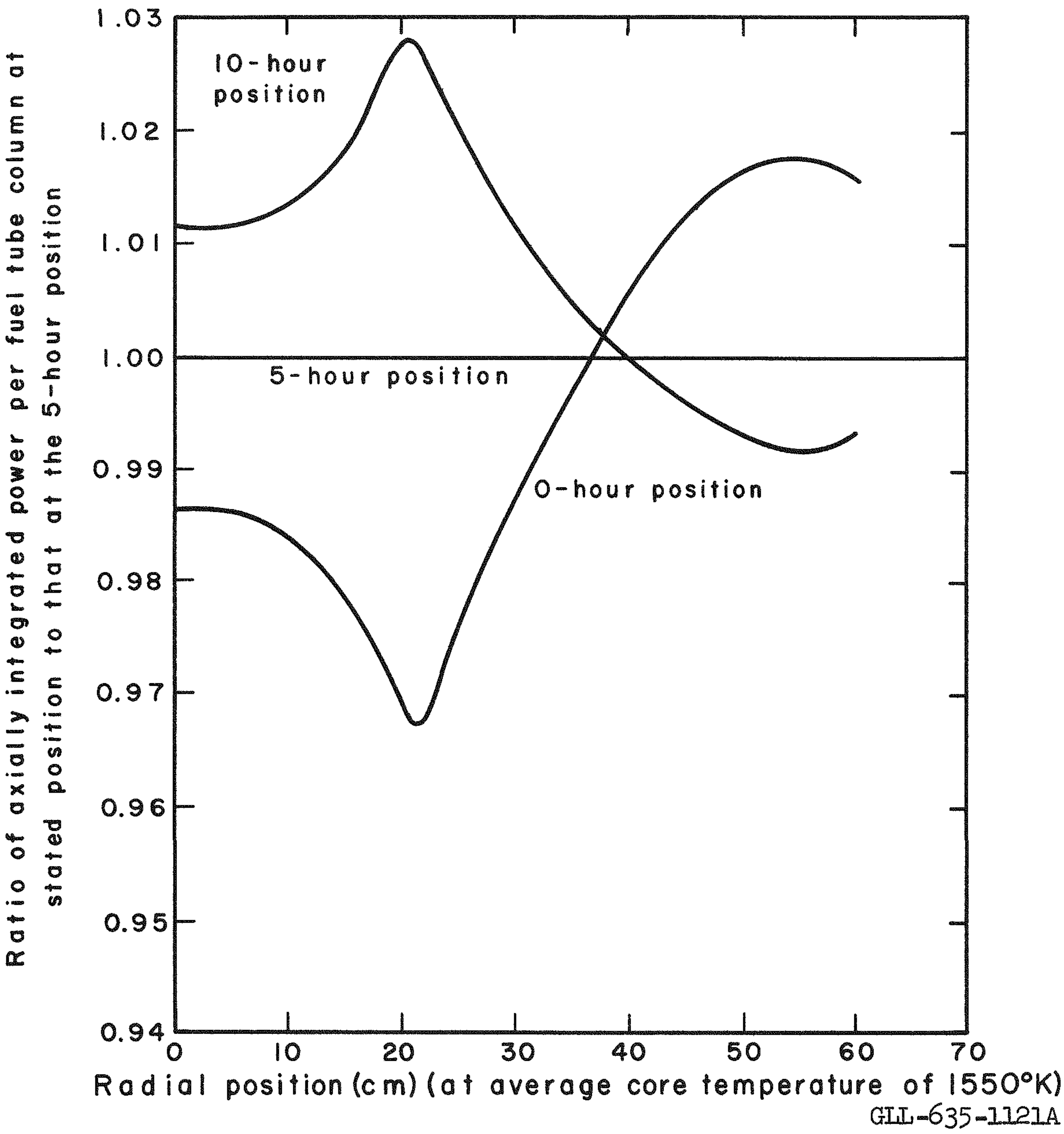

The effect of shim rod movement on axially integrated power per fuel tube column (normalized to the 5-hour shim rod position).

Gamma energy source spectra in the active core at 90% fission product saturation, equivalent to 10 hours steady operation.

	Energy, MeV			S(E), MeV/fission				Composite		
Group	$\bar{E}$	E_{max}	ΔE	Prompt fission	90% fission product decay	Tie rod (n,γ)	Fuel (n,γ)	S(E), MeV/fiss.	S(N), Photons/fiss.	S(E)/ΔE, MeV/fiss. / MeV
1	8.91	10.0	2.057	0	0	0.3397	0	0.3397	0.038	0.165
2	7.08	7.943	1.633	0.0394	0	.2330	0	.2724	.038	.166
3	5.62	6.31	1.298	.1187	0.045	.1434	0	.3071	.054	.236
4	4.47	5.012	1.031	.2889	.261	.0808	0.126	0.7567	.169	0.733
5	3.55	3.981	0.819	.4438	.498	.0435	.205	1.1903	.335	1.453
6	2.82	3.162	.65	.6548	.607	.0478	.255	1.5646	.554	2.407
7	2.24	2.512	.517	.7338	.815	.0408	.300	1.8896	0.843	3.654
8	1.78	1.995	.41	.7594	.818	.0365	.241	1.8549	1.042	4.524
9	1.41	1.585	.326	.890	.768	.0294	.221	1.9084	1.353	5.853
10	1.12	1.259	.259	.7196	.692	.0231	.188	1.6227	1.448	6.265
11	0.891	1.00	.2057	.6189	.573	.0112	.091	1.2941	1.452	6.291
12	.708	0.7943	.1633	.5602	.473	.0089	.066	1.1081	1.565	6.785
13	.562	.631	.1298	.5366	.377	.0071	.047	0.9677	1.721	7.455
14	.447	.5012	.1031	.4997	.316	.0056	.034	.8553	1.913	8.295
15	.355	.3981	.0819	.404	.093	.0044	.022	.5234	1.474	6.390
16	.282	.3162	.065	.2018	.074	.0034	.015	.2942	1.043	4.526
17	.224	.2512	.0517	.1425	.059	.0027	.013	.2172	0.969	4.201
18	.178	.1995	.041	.0826	.047	.0020	.009	.1406	.789	3.429
19	.141	.1585	.0326	.0573	.037	.0015	.007	.1028	.729	3.153
20	.112	.1259	.0259	.0322	0.030	.0011	0.005	.0683	.609	2.630
21	.0891	.100	.02057	.0159	0	.0006	0	.0165	.185	0.802
22	.0708	.0794	.01633	.0078	0	0.0003	0	.0081	.114	.496
23	.0562	.0631	.01298	.0044	0	0	0	.0044	.078	.339
24	.0447	.0501	.01031	.0037	0	0	0	.0037	.082	.359
25	.0355	.0398	.00819	.0049	0	0	0	.0049	.138	.598
26	.0282	.0316	.0065	.0037	0	0	0	.0037	.131	.569
27	.0224	.0251	.00517	.0013	0	0	0	.0013	.058	.251
28	.0178	.020	.0041	.0008	0	0	0	.0008	.045	.195
29	.0141	.0159	.00326	.0006	0	0	0	.0006	.043	.184
30	0.0112	0.0126	0.00259	0.0004	0	0	0	0.0004	0.036	0.154
			TOTAL	7.83	6.58	1.07	1.85	17.32	19.00	

GLL-632-242

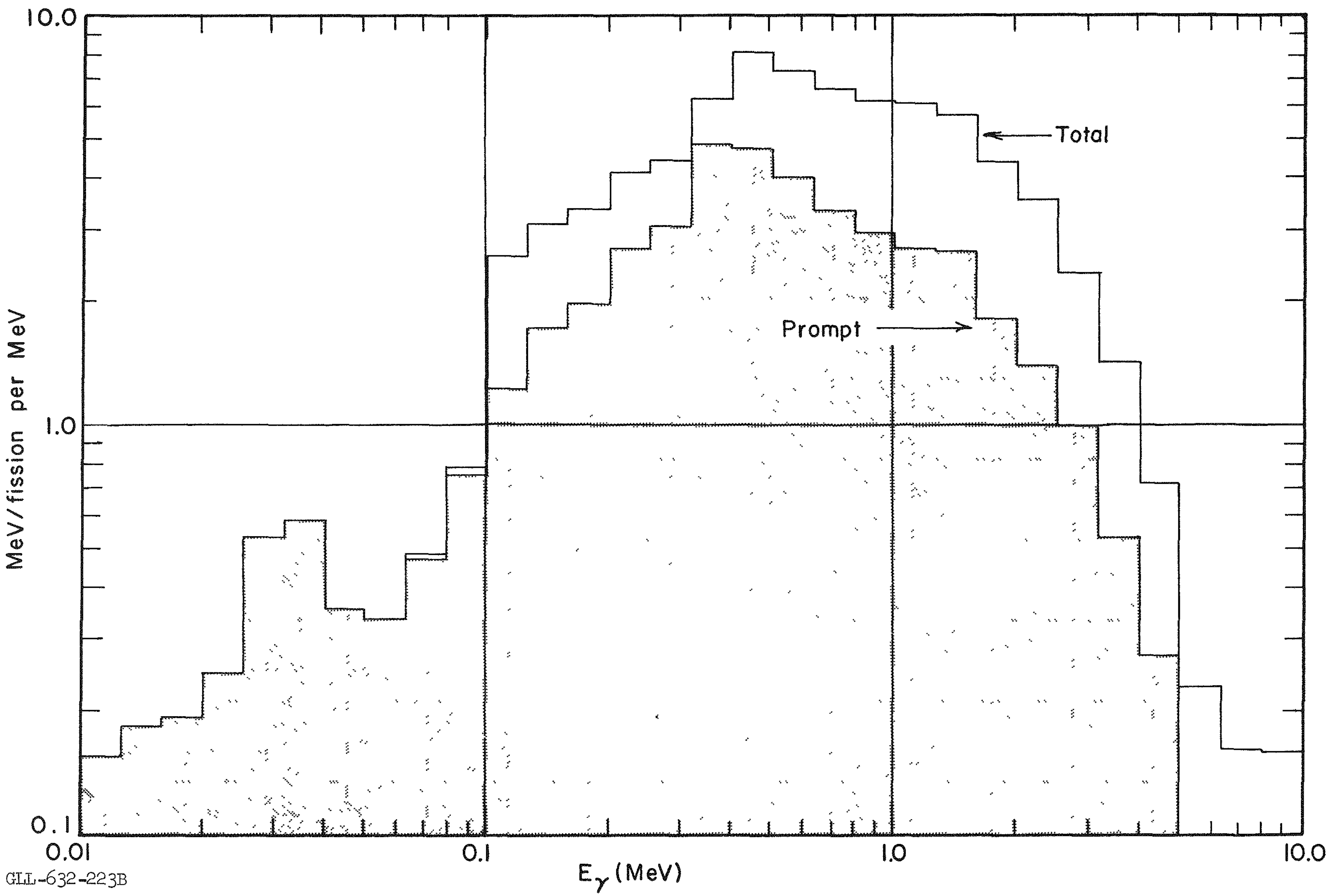

Gamma energy source spectra in the active core 10 hours after start-up.

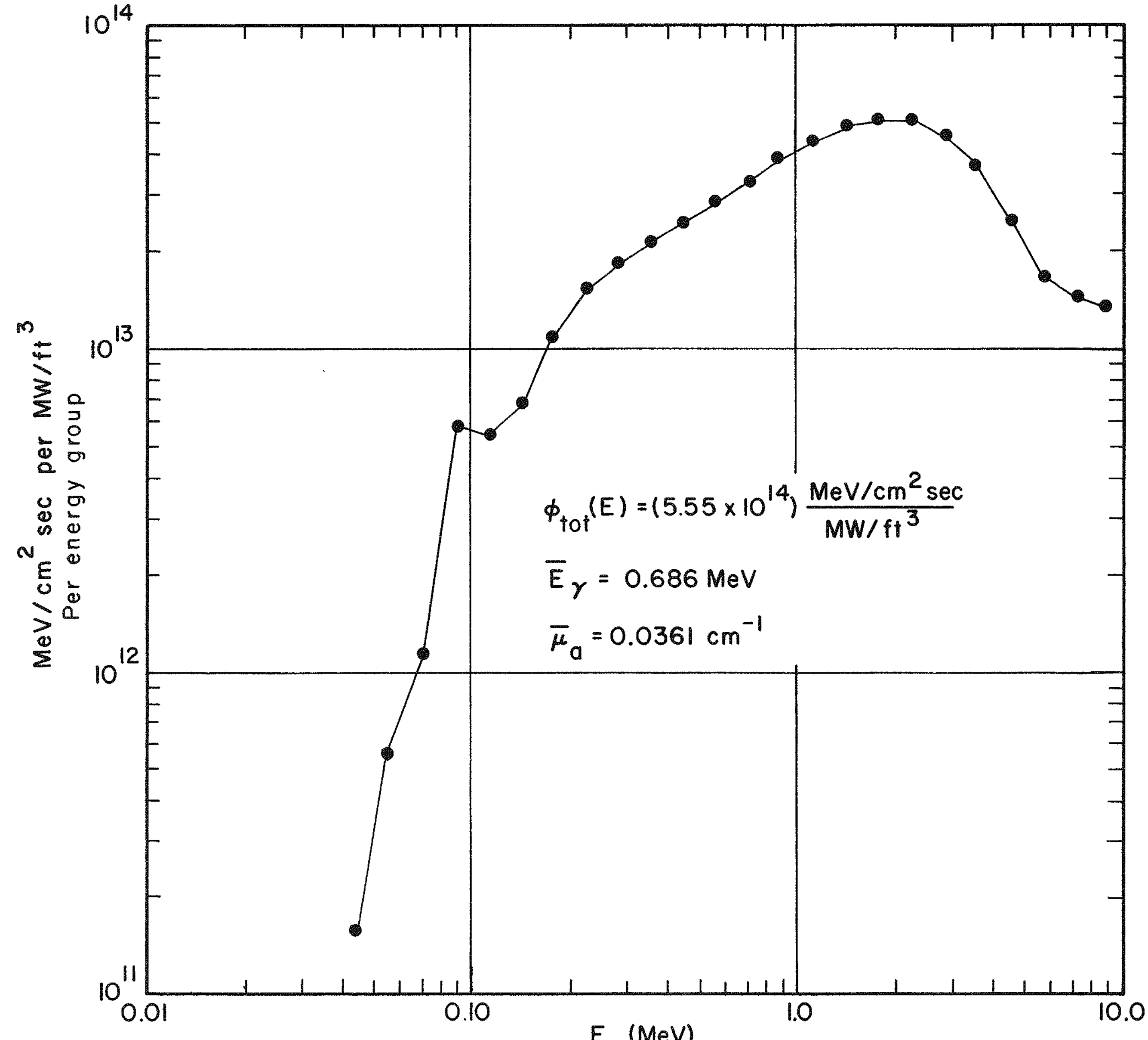

GLL-632-235B

Gamma ray energy flux distribution in the center of the active core normalized to average unit core power density. See page II-21 for energy group widths.

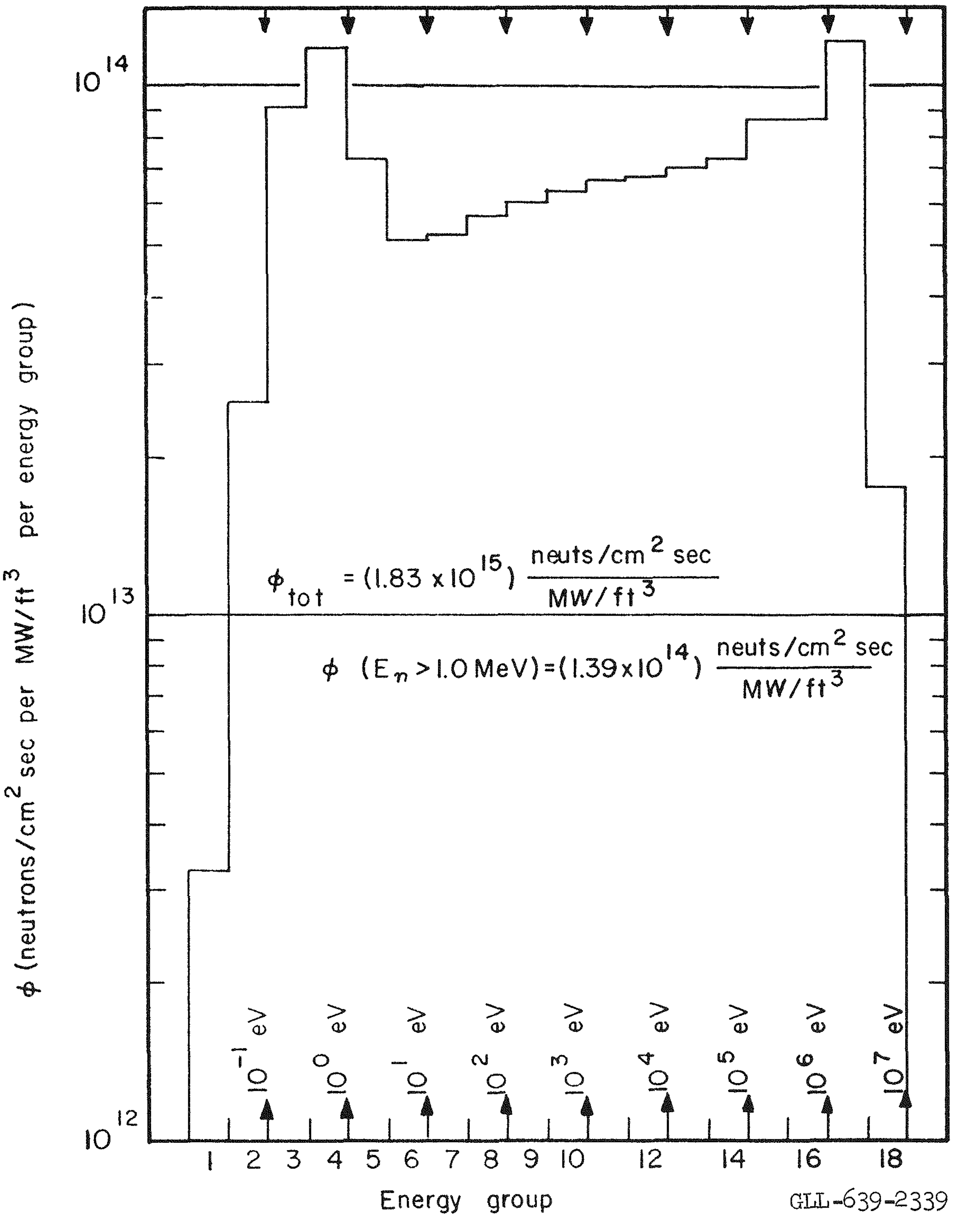

Peak neutron flux distribution in active core (normalized to average unit core power density).

Nuclear heating densities in the active core.

All heating density values are given in MW/ft^3 of solid component material normalized to 1 MW/ft^3 of average core power density based on the hot fueled volume of the active core, $V_c = 54.04\ ft^3$. The heating calculations were performed for 90% fission product saturation, equivalent to 10 hours steady operation.

	Control unit cell at R = 8.5 in.				Standard unit cell at R = 0	
	René 41 tie rod		Guard tubes		René 41 tie rod	Guard tubes
Control rod insertion (in.)	13	40	13	40	–	–
Peak heating density (MW/ft^3 per MW/ft^3)	0.935	1.143	0.319	0.360	1.065	0.285
Peak-to-average ratio[a]	1.47	1.60	1.46	1.55	1.50	1.50
Average heating density[a] (MW/ft^3 per MW/ft^3)	0.648	0.714	0.218	0.232	0.712	0.190
Considered component volume[b] (ft^3)	0.00417	0.00417	0.0424	0.0424	0.00329	0.0294
Total component power (kW per MW/ft^3)	2.70	2.98	9.26	9.85	2.34	5.58

[a] Average was taken over the full length of the hot reactor (L_R = 63.5 in.).

[b] The components were assumed to be hot and to extend the full length of the hot reactor.

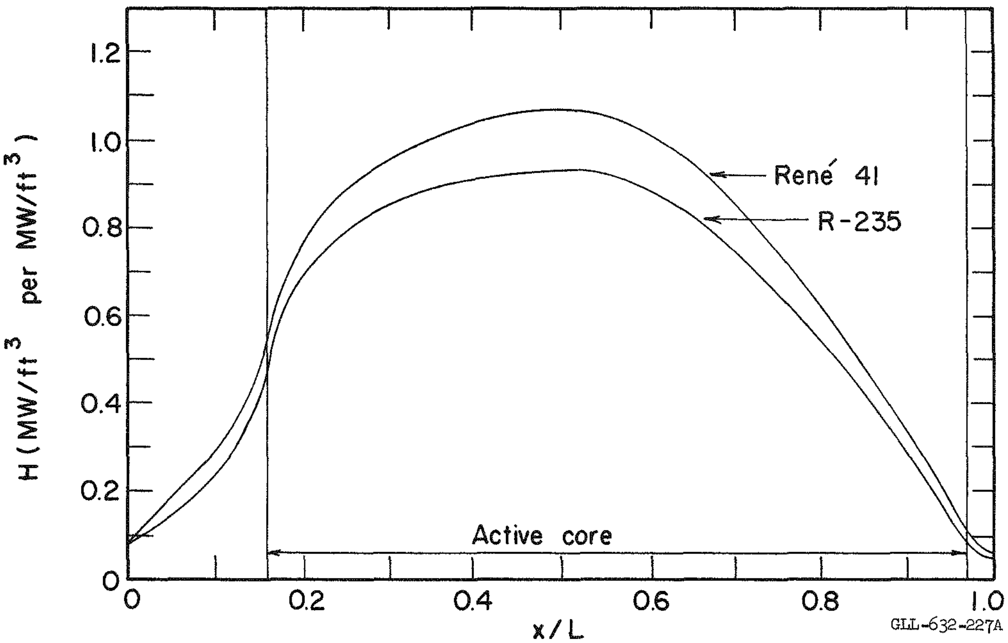

Nuclear heating of standard tie rods at R = 0.

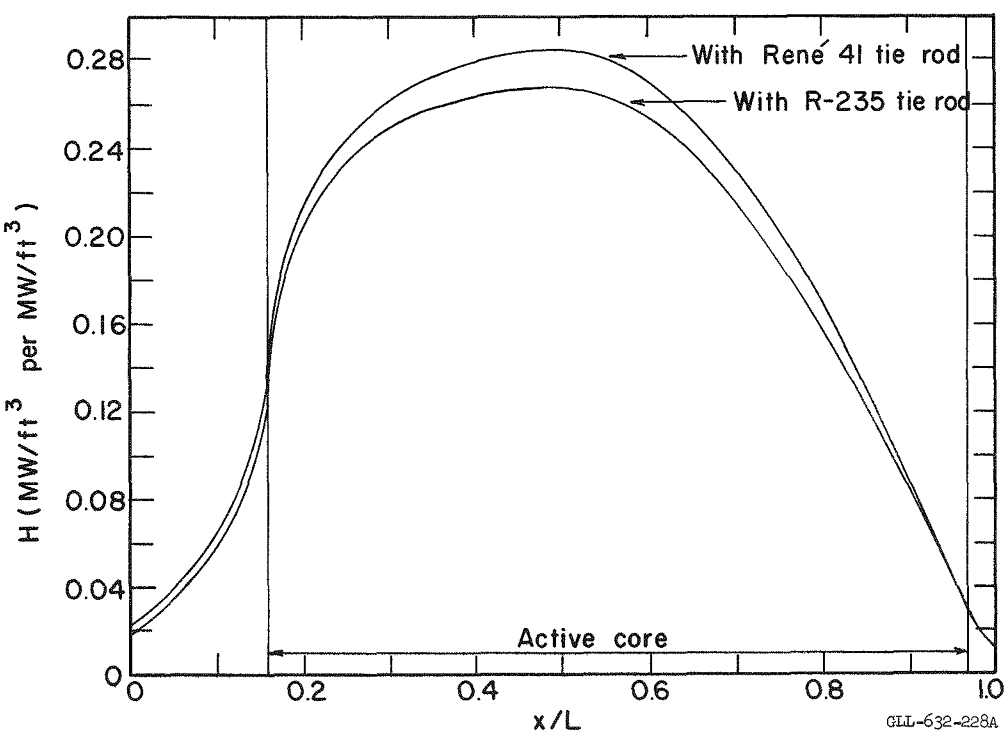

Nuclear heating of guard tubes in standard unit cell at R = 0.

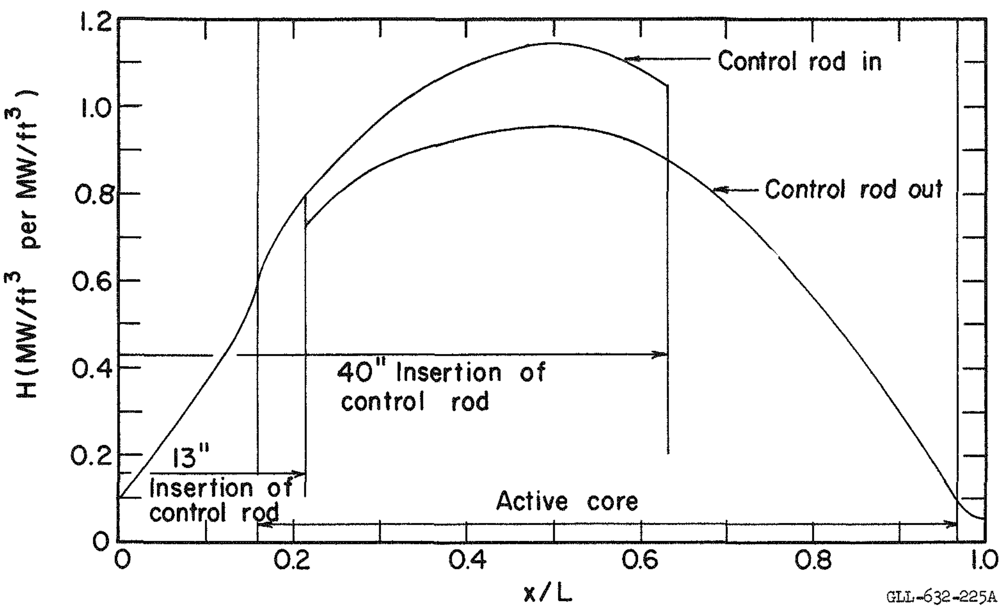

Nuclear heating of René 41 control tie rod at R = 8.92.

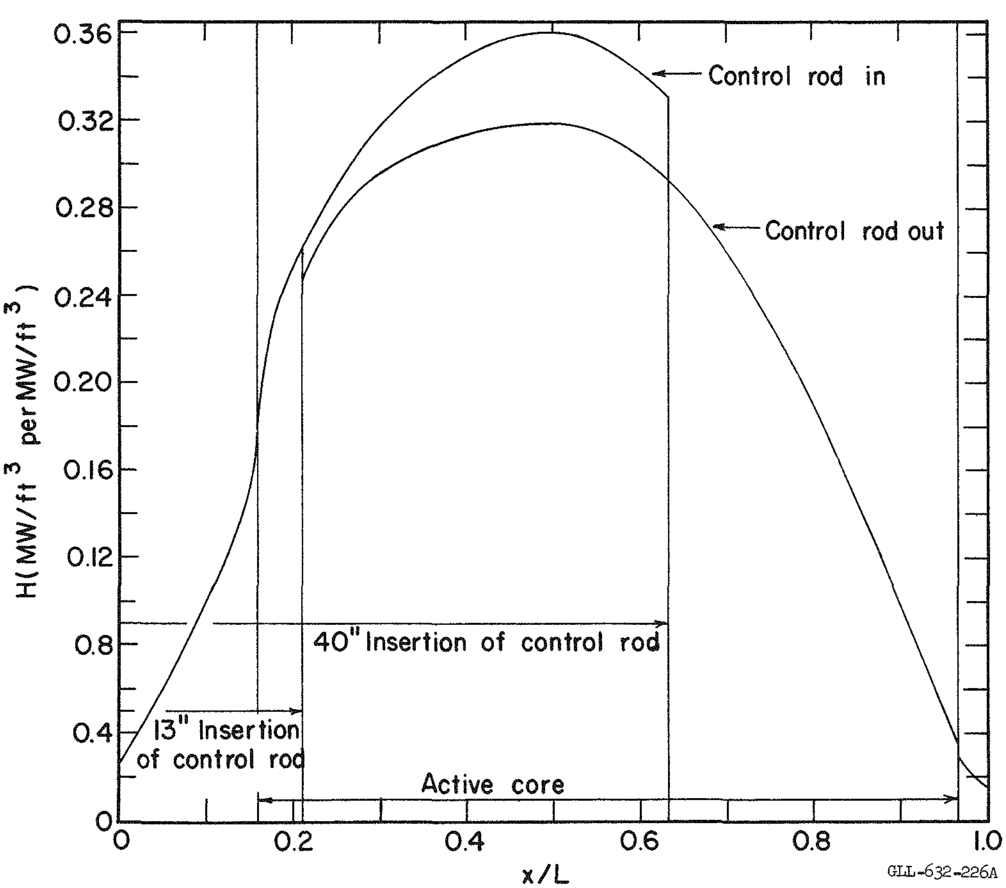

Nuclear heating of guard tubes in control unit cell at R = 8.92.

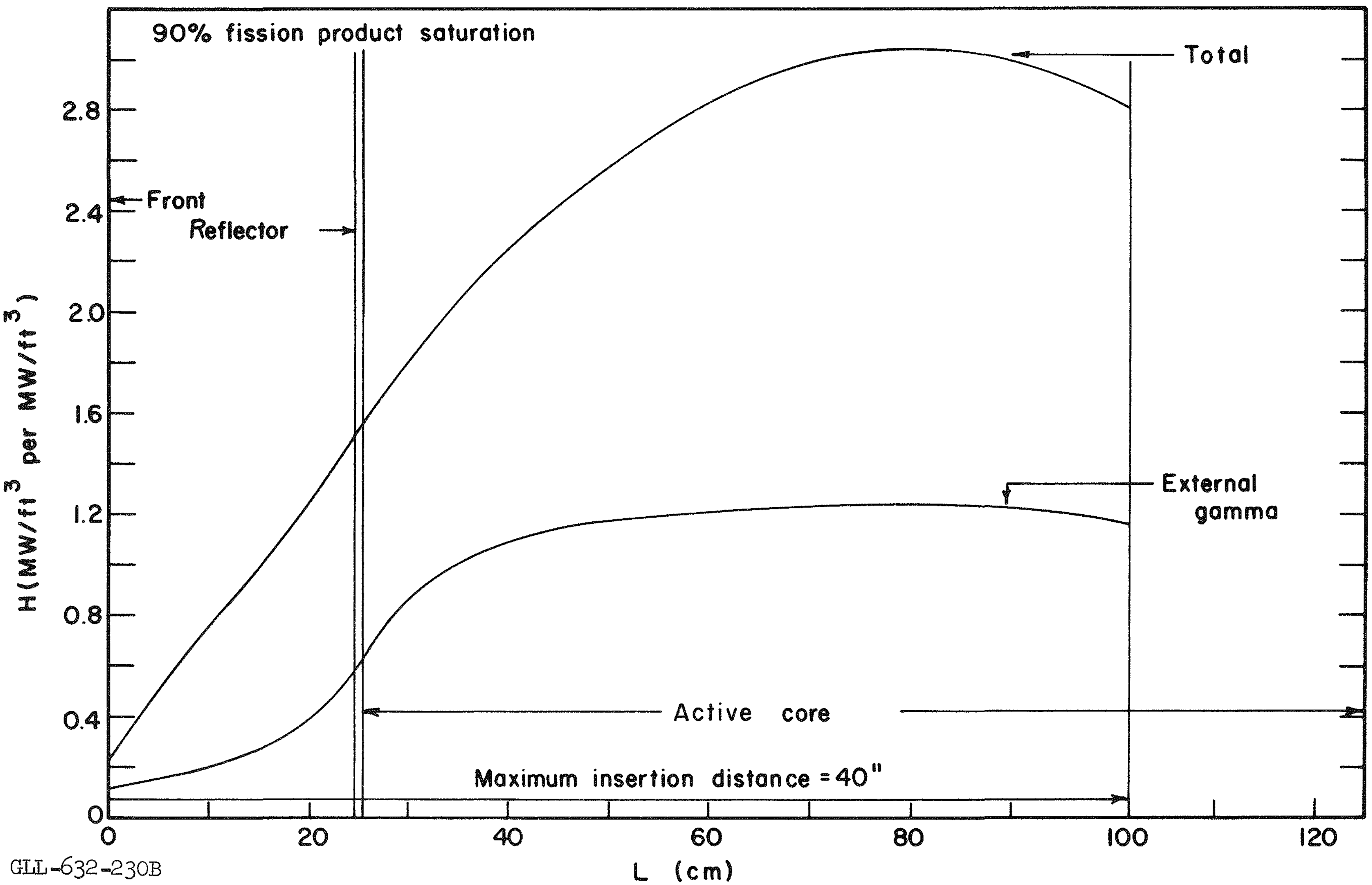

GLL-632-230B

Nuclear heating of control rod (vane 0.080 in. thick).

Nuclear heating density distributions in the side reflector and side support system at axial peak (x/L = 0.5). All heating values given are averaged over the considered zones, and are given in MW/ft^3 of solid component material per MW/ft^3 of average core power density based on core volume of 54.04 ft^3.

R_{max} (cm)	Region thickness (cm)	Region	Core source	Ni (n, γ)	SSS(n, γ)	Fast neutrons	Total
1.005	1.005	BeO	0.0757	0.0096	0.0020	0.0223	0.1096
1.993	0.988	"	.0507	.0109	.0017	.0180	.0813
2.966	0.973	"	.0501	.0133	.0020	.0150	.0804
3.924	0.958	"	.0422	.0138	.0021	.0130	.0711
5.258	1.334	"	.0316	.0177	.0024	.0017	.0634
6.03	0.772	Shims	.0998	.1122	.0117	.0046	.2237
6.802	.772	"	.0638	.1005	.0160	.0040	.1803
7.574	.772	"	.0435	.0733	.0247	.0035	.1415
8.518	0.944	Spring	0.0285	0.0403	0.0405	0.0029	0.1122
11.081	2.563	Void	–	–	–	–	–
11.589	0.508	Rail	0.0229	0.0274	0.0354	0.0025	0.0882
12.701	1.112	Duct	0.0183	0.0172	0.0249	0.0023	0.0627

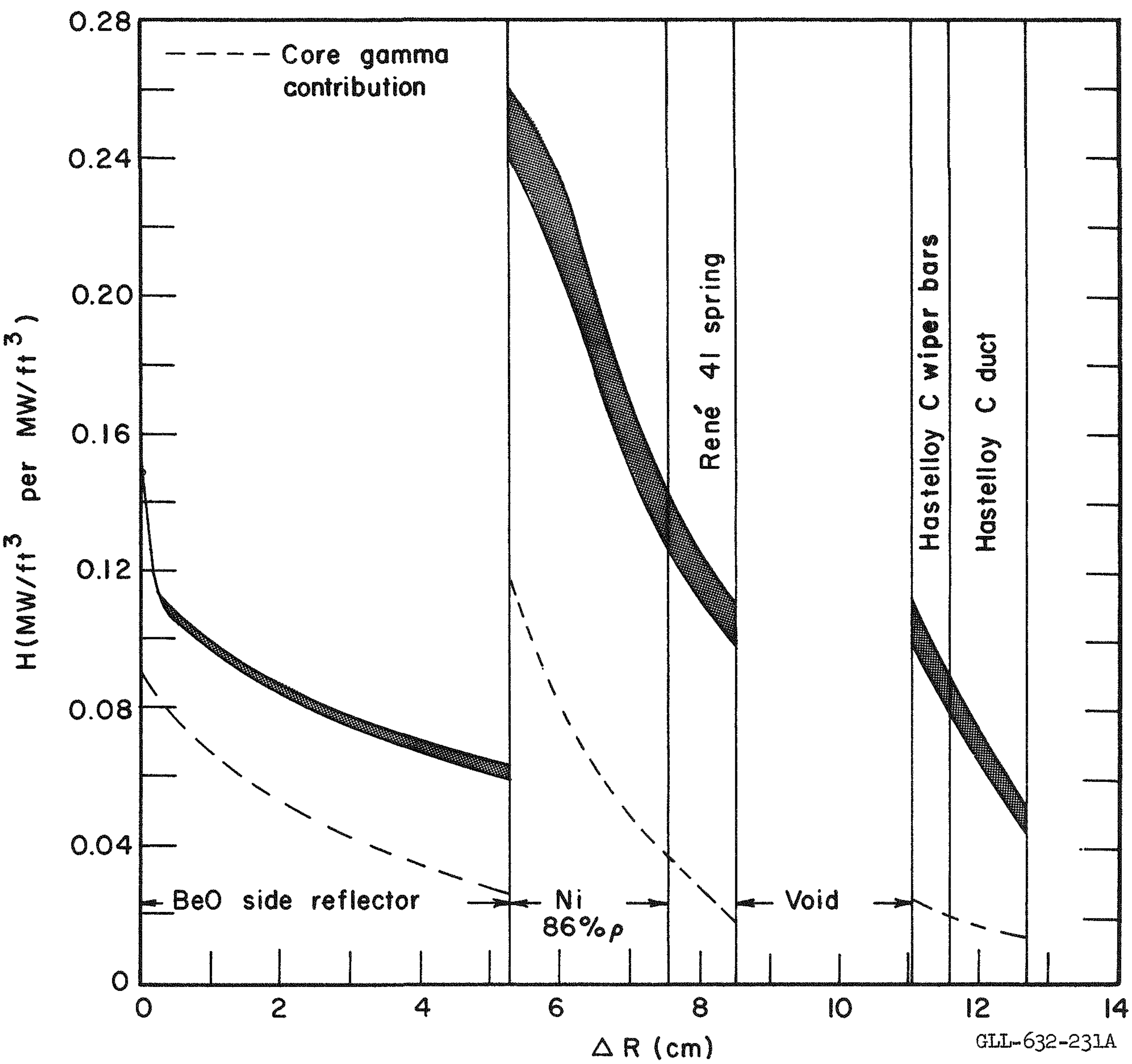

Total heating density distribution in the peripheral region of the reactor midplane. Note: Bands represent uncertainty in nickel nuclear cross sections.

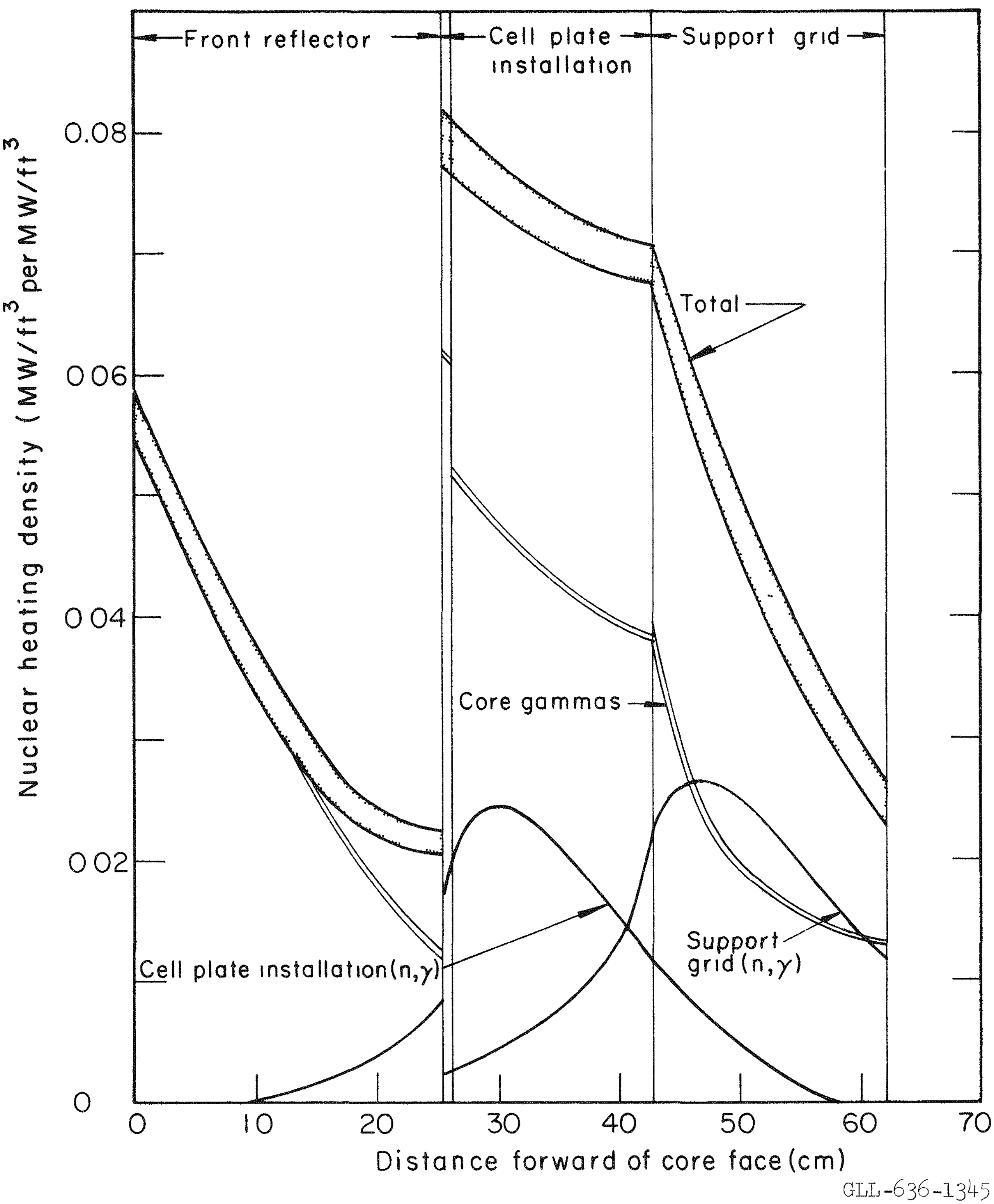

Total nuclear heating density distribution in forward reactor regions at R = 0. Note: Bands represent uncertainty in nickel nuclear cross sections.

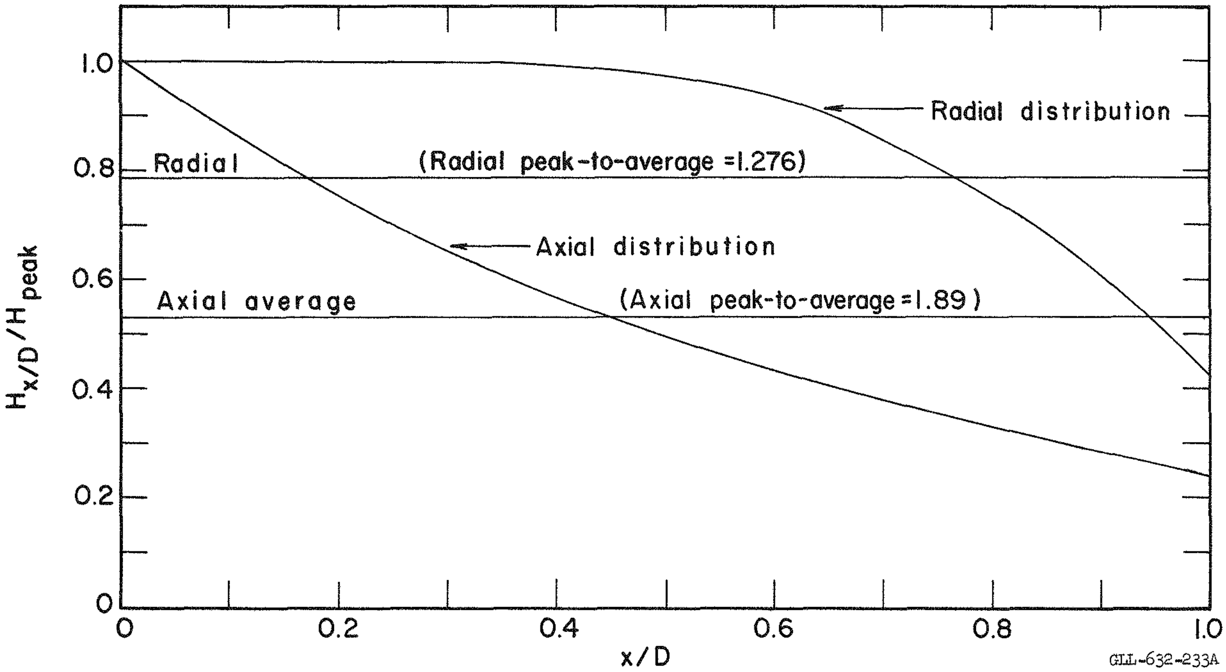

Axial and radial core gamma heating density in the front reflector (normalized to peak).

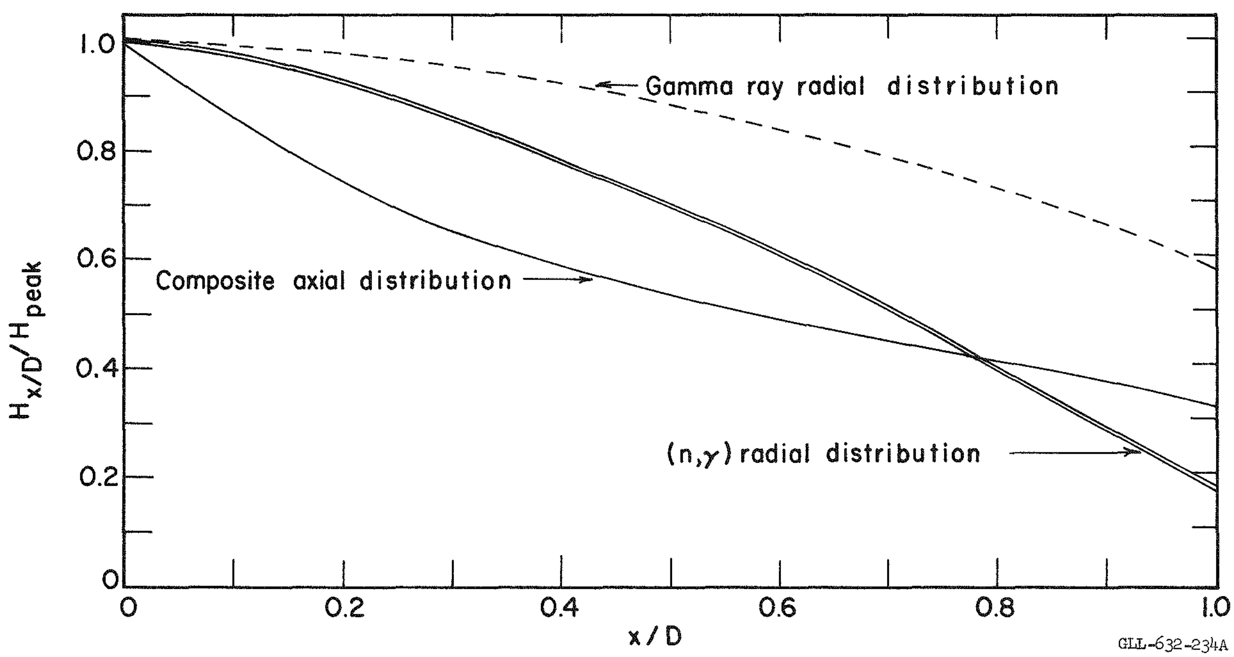

Axial and radial nuclear heating density in support grid and cell plate installation (normalized to peak).

Nuclear heating distribution in aft reactor regions (in MW/ft^3 per MW/ft^3), based on core volume of 54.04 ft^3.

Object \ Sources		Core gammas	Trans. rings (n,γ)	Base block (n,γ)	Cermet cartridge (n,γ)	Total
Aft reflector (BeO)	Peak on axis	0.034	0.007	0.0031	0.0101	0.054
	Average	.022	.000	.0021	.0067	.0308
Transition rings (Cr-MgO)	Peak on axis	.0254	.0144	.0023	.0034	.0455
	Average	.0169	.0096	.0015	.0023	.0303
Cermet cartridge layer (Cr-MgO)	Peak on axis	.071	.0000	.013	.012	.096
	Average	.060	.0000	.008	.008	.076
Base blocks (F-48)	Peak on axis	.056	.0000	.018	.008	.082
	Average	0.049	0.0000	0.012	0.0051	0.066

Radiation leakage summary.

	Forward[a]	Aft[b]	Lateral
Gamma leakage flux averaged over leakage plane (MeV/cm^2 sec per MW/ft^3)[c]	6.31×10^{12}	3.87×10^{13}	2.87×10^{13}
Gamma leakage peak-to-average ratios	1.2	1.31	1.51
Neutron leakage flux averaged over leakage plane (neutrons/cm^2 sec per MW/ft^3)	1.21×10^{13}	1.09×10^{13}	1.12×10^{13}
Neutron leakage peak-to-average ratios	1.97	1.87	1.41
Gamma dose rate averaged over leakage plane (Rads/MWh)	1.43×10^5	9.78×10^5	6.1×10^5
Gamma dose rate averaged over leakage plane (Rads/sec per MW/ft^3)	2.12×10^3	1.45×10^4	9.05×10^3
Neutron dose rate averaged over leakage plane (Rads/MWh)	1.49×10^6	1.85×10^6	1.43×10^6
Neutron dose rate averaged over leakage plane (Rads/sec per MW/ft^3)	2.21×10^4	2.74×10^4	2.19×10^4
Neutron dose peak-to-average ratios	1.42	1.30	1.55
Total dose averaged over leakage plane (Rads/MWh)	1.63×10^6	2.83×10^6	2.09×10^6
Total dose averaged over leakage plane (Rads/sec per MW/ft^3)	2.42×10^4	4.2×10^4	3.1×10^4
Average gamma flux-to-dose conversion (Rads/sec per neutron/cm^2 sec)	3.36×10^{-10}	3.75×10^{-10}	3.26×10^{-10}
Average neutron flux-to-dose conversion (Rads/sec per neutron/cm^2 sec)	1.83×10^{-9}	2.51×10^{-9}	1.96×10^{-9}
Peak total dose at leakage plane (Rads per MWh)	2.29×10^6	3.69×10^6	3.21×10^6
Total dose rate composition averaged over each surface (in percent): Gamma	8.8	34.5	29.2
Fast neutrons	26.5	30.5	42.5
Intermediate	45.6	28.8	26.6
Slow neutrons	19.1	6.2	1.7

[a] Station 360.938 (front surface of cell plates).

[b] Station 425.498 (aft surface of base blocks).

[c] Based on core volume = 54.04 ft^3.

Gamma-ray leakage flux spectra averaged over front, aft, and lateral bounding surfaces, based on core volume of 54.04 ft^3.

$\overline{E}_\gamma$ (MeV)	ΔE (MeV)	E_{max} (MeV)	MeV/cm^2 sec per MW/ft^3 Forward[a]	Aft[b]	Lateral
8.91	2.057	10.0	7.6×10^{11}	1.26×10^{12}	5.16×10^{12}
7.08	1.633	7.943	6.95×10^{11}	2.18×10^{12}	4.69×10^{12}
5.62	1.298	6.310	8.54×10^{11}	3.04×10^{12}	3.06×10^{12}
4.47	1.031	5.012	5.23×10^{11}	4.61×10^{12}	2.04×10^{12}
3.55	0.819	3.981	5.40×10^{11}	5.08×10^{12}	2.25×10^{12}
2.82	0.65	3.162	5.95×10^{11}	4.19×10^{12}	1.92×10^{12}
2.24	0.517	2.512	4.77×10^{11}	4.06×10^{12}	1.48×10^{12}
1.78	0.41	1.995	4.22×10^{11}	3.68×10^{12}	1.37×10^{12}
1.41	0.326	1.585	2.86×10^{11}	3.52×10^{12}	1.32×10^{12}
1.12	0.259	1.259	3.09×10^{11}	2.34×10^{12}	1.05×10^{12}
0.891	0.2057	1.00	2.36×10^{11}	1.55×10^{12}	7.94×10^{11}
0.708	0.1635	0.7943	1.55×10^{11}	1.37×10^{12}	7.18×10^{11}
0.562	0.1298	0.6310	1.01×10^{11}	8.72×10^{11}	7.43×10^{11}
0.447	0.1031	0.5012	8.80×10^{10}	4.51×10^{11}	4.52×10^{11}
0.355	0.0819	0.3981	8.34×10^{10}	2.56×10^{11}	3.53×10^{11}
0.282	0.065	0.3162	4.79×10^{10}	1.35×10^{11}	1.85×10^{11}
0.224	0.0517	0.2512	4.79×10^{10}	4.5×10^{10}	1.06×10^{11}
0.178	0.041	0.1995	3.42×10^{10}	1.5×10^{10}	6.02×10^{10}
0.141	0.0326	0.1585	2.32×10^{10}	–	1.43×10^{10}
0.112	0.0259	0.1259	1.73×10^{10}	–	3.05×10^{9}
0.089	0.02057	0.100	1.34×10^{10}	–	1.15×10^{9}
		Total ϕ	6.31×10^{12}	3.87×10^{13}	2.78×10^{13}
Average gamma energy (MeV)			1.62	1.83	2.03
MeV/fission leaking			0.042	0.26	0.66
Peak-to-average ratio			1.2	1.31	1.51

[a] Station 360.938 (front surface of cell plates).

[b] Station 425.498 (aft surface of base blocks).

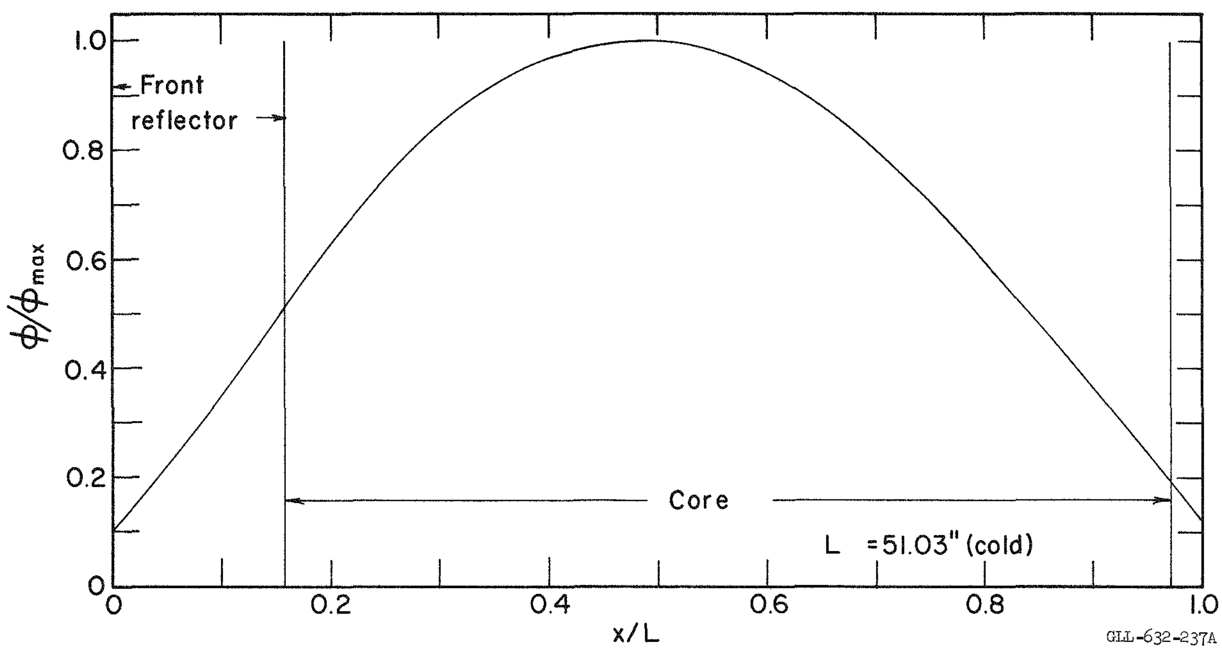

Gamma ray leakage at outer duct surface (normalized to peak in midplane).

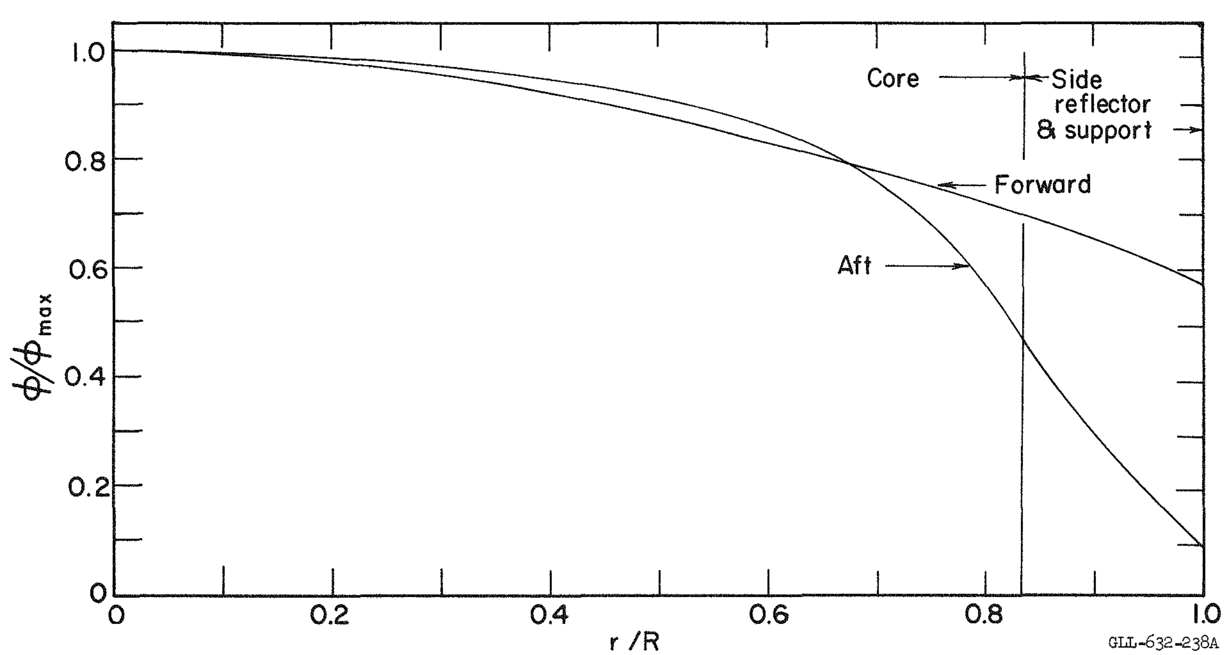

Gamma ray leakage at stations 360.938 and 425.498 (normalized to peak on axis).

. Neutron leakage flux spectra averaged over front, aft, and lateral bounding surfaces, based on core volume of 54.04 ft^3.

Group	E_{max}		Leakage flux (neutrons/cm^2 sec per MW/ft^3)		
			Forward[a]	Aft[b]	Lateral
Slow					
1	0.03162	eV	4.35×10^{10}	4.50×10^{9}	2.22×10^{9}
2	0.10	eV	2.84×10^{11}	6.30×10^{10}	1.64×10^{10}
3	0.3162	eV	9.87×10^{11}	3.51×10^{11}	7.54×10^{10}
4	1.0	eV	1.23×10^{12}	6.20×10^{11}	1.76×10^{11}
Intermediate					
5	3.162	eV	7.54×10^{11}	4.94×10^{11}	2.34×10^{11}
6	10.0	eV	5.43×10^{11}	1.10×10^{11}	1.91×10^{11}
7	31.62	eV	5.48×10^{11}	6.35×10^{10}	3.14×10^{11}
8	0.10	keV	5.64×10^{11}	3.19×10^{11}	3.09×10^{11}
9	0.3162	keV	5.68×10^{11}	3.21×10^{11}	3.24×10^{11}
10	1.00	keV	5.97×10^{11}	6.11×10^{11}	5.53×10^{11}
11	3.162	keV	6.17×10^{11}	6.53×10^{11}	6.17×10^{11}
12	10.0	keV	5.44×10^{11}	6.67×10^{11}	2.72×10^{11}
13	31.62	keV	6.42×10^{11}	7.29×10^{11}	2.77×10^{11}
14	0.1	MeV	6.44×10^{11}	8.18×10^{11}	1.18×10^{12}
Fast					
15	0.3162	MeV	7.77×10^{11}	1.07×10^{12}	1.59×10^{12}
16	1.0	MeV	7.71×10^{11}	1.15×10^{12}	1.99×10^{12}
17	3.162	MeV	1.71×10^{12}	2.37×10^{12}	2.67×10^{12}
18	10.0	MeV	3.18×10^{11}	4.89×10^{11}	3.9×10^{11}
	Total ϕ		1.21×10^{13}	1.09×10^{13}	1.12×10^{13}
% fast			29.0	46.5	60.0
% intermediate			50.0	44.0	37.5
% slow			21.0	9.5	2.5

[a] Station 360.938 (front surface of cell plates).

[b] Station 425.498 (aft surface of base blocks).

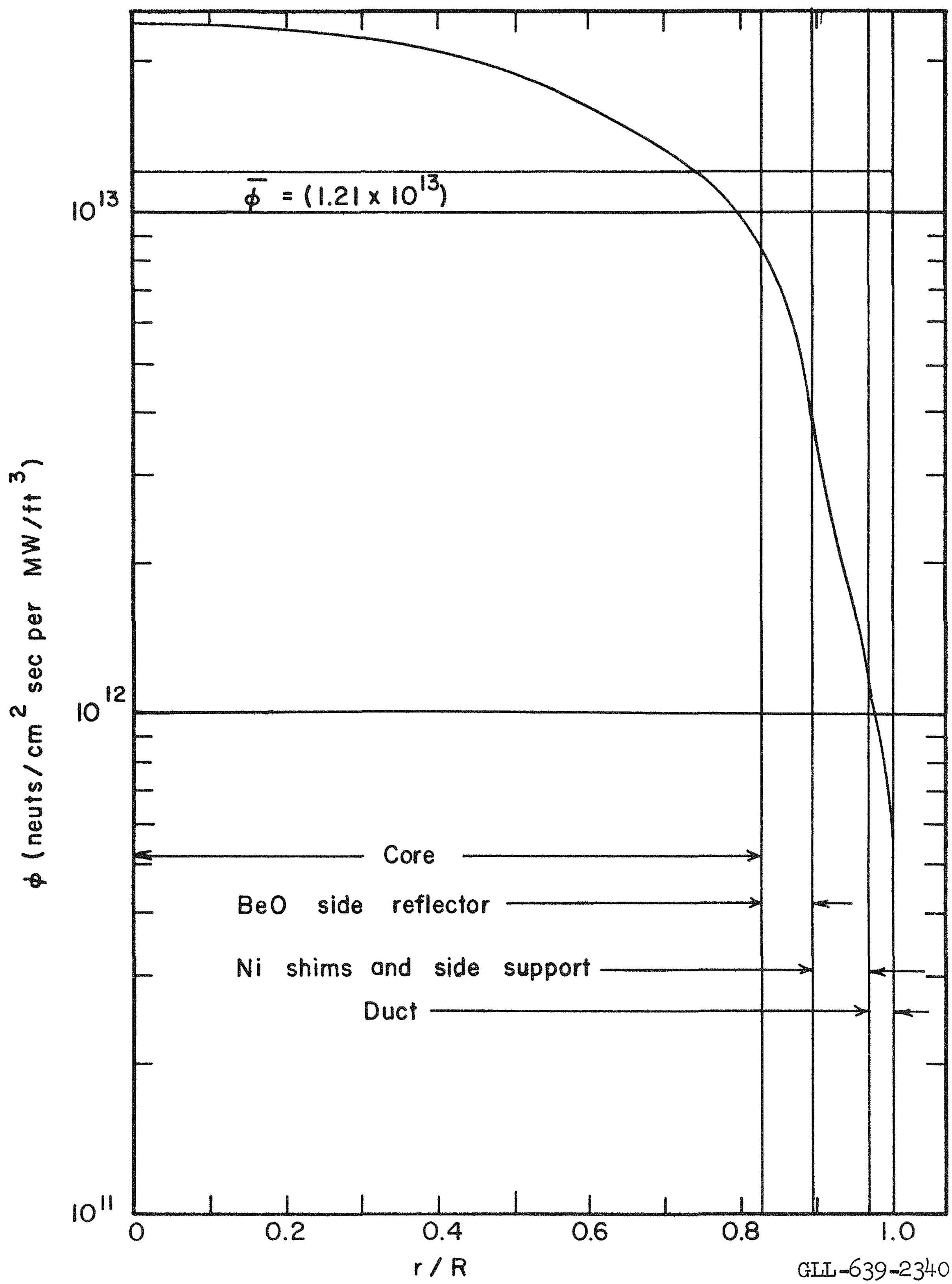

Total neutron aft leakage flux profile (normalized to unit power density).

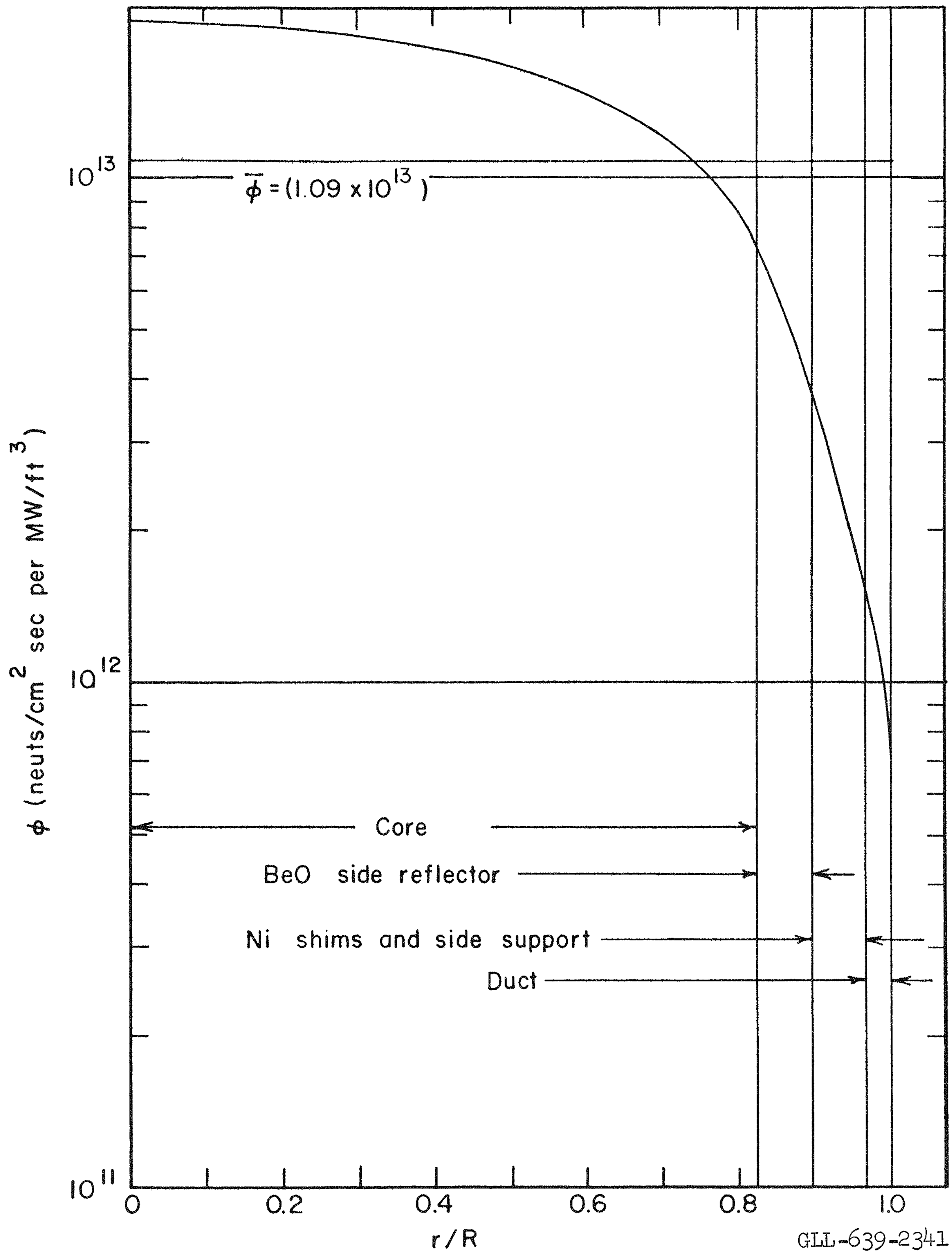

Total neutron forward leakage flux profile (normalized to unit power density).

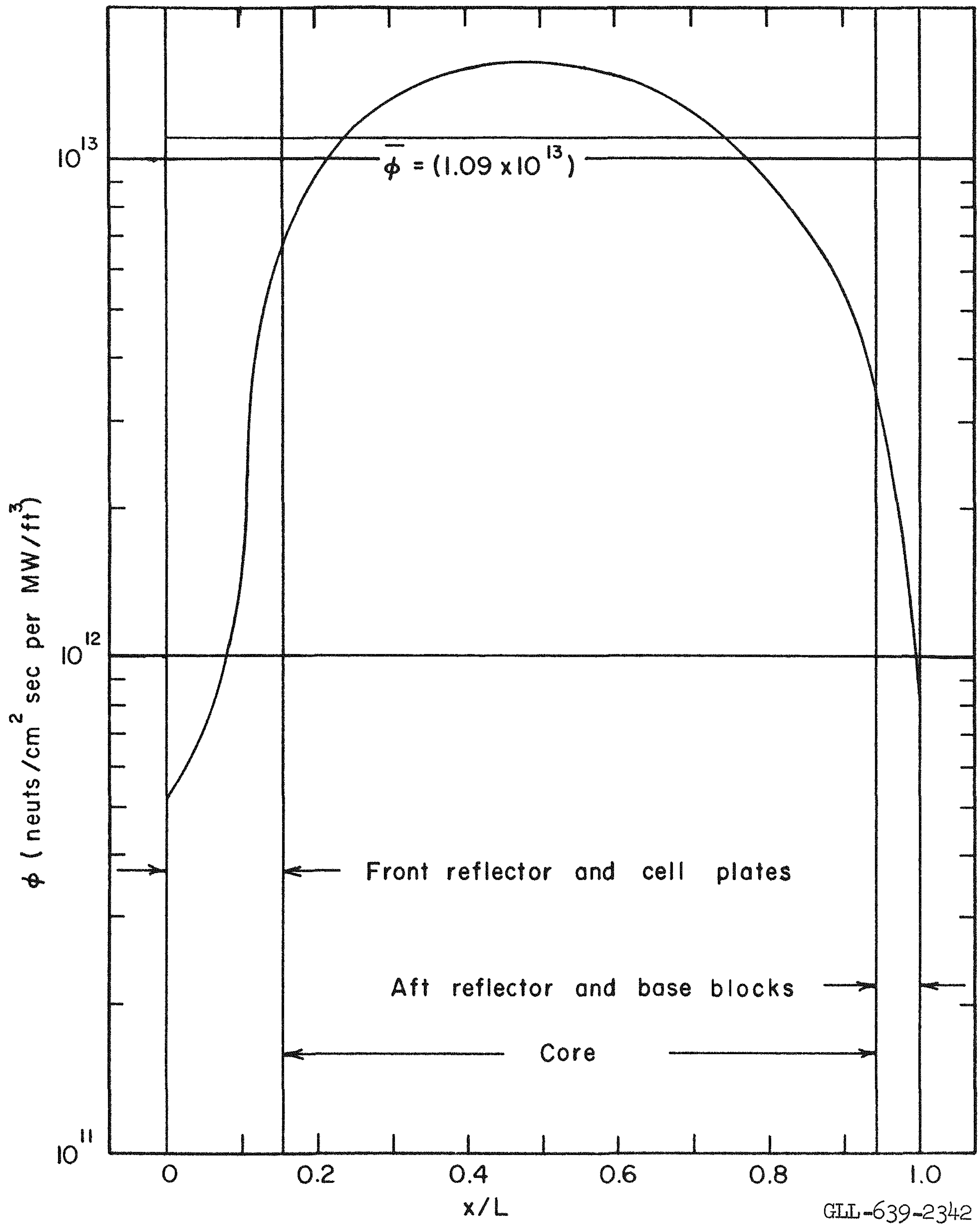

Total lateral neutron leakage flux profile (normalized to unit power density).

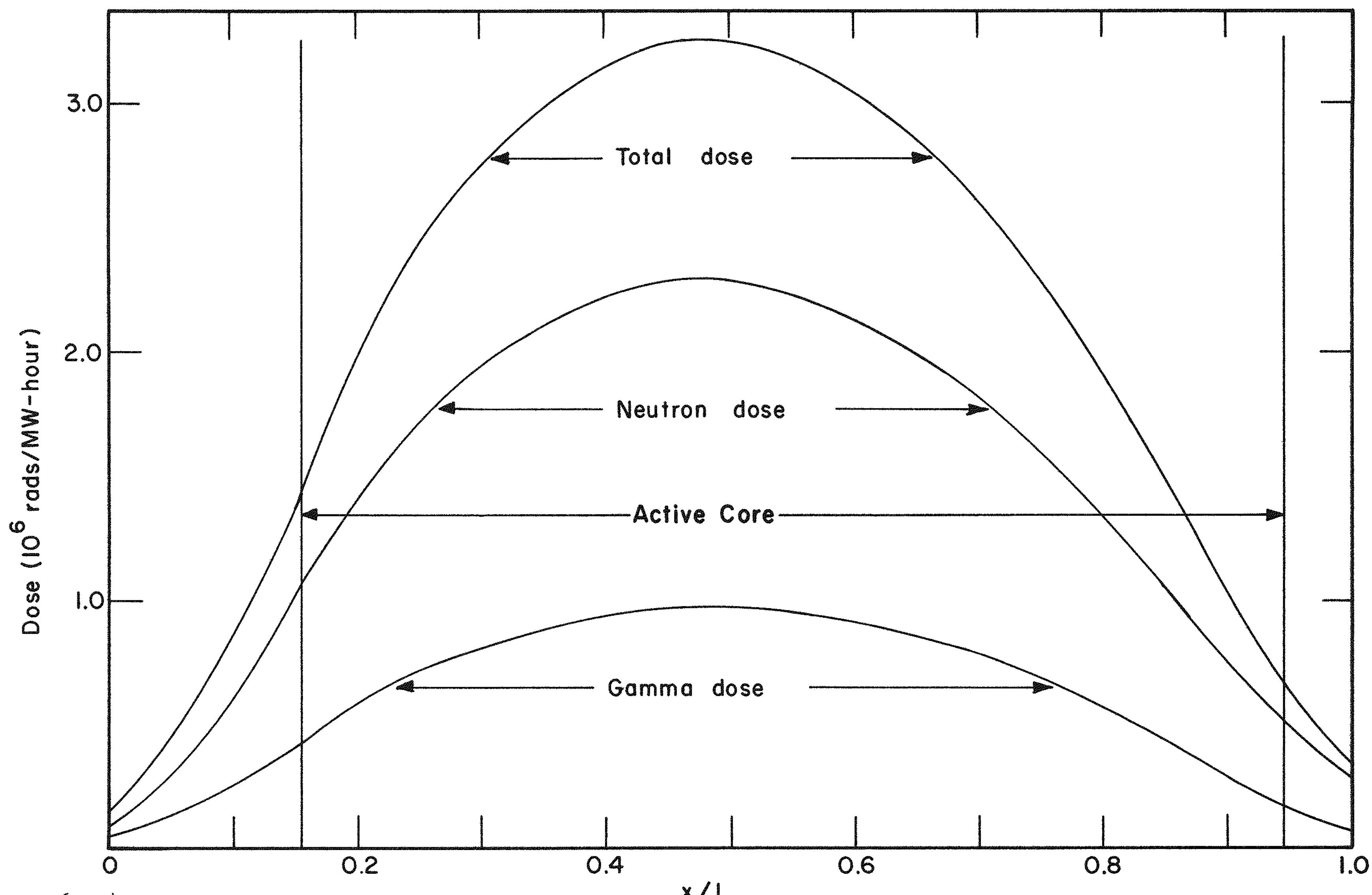

GLL-632-240A

Radiation dose rate at outer duct surface.

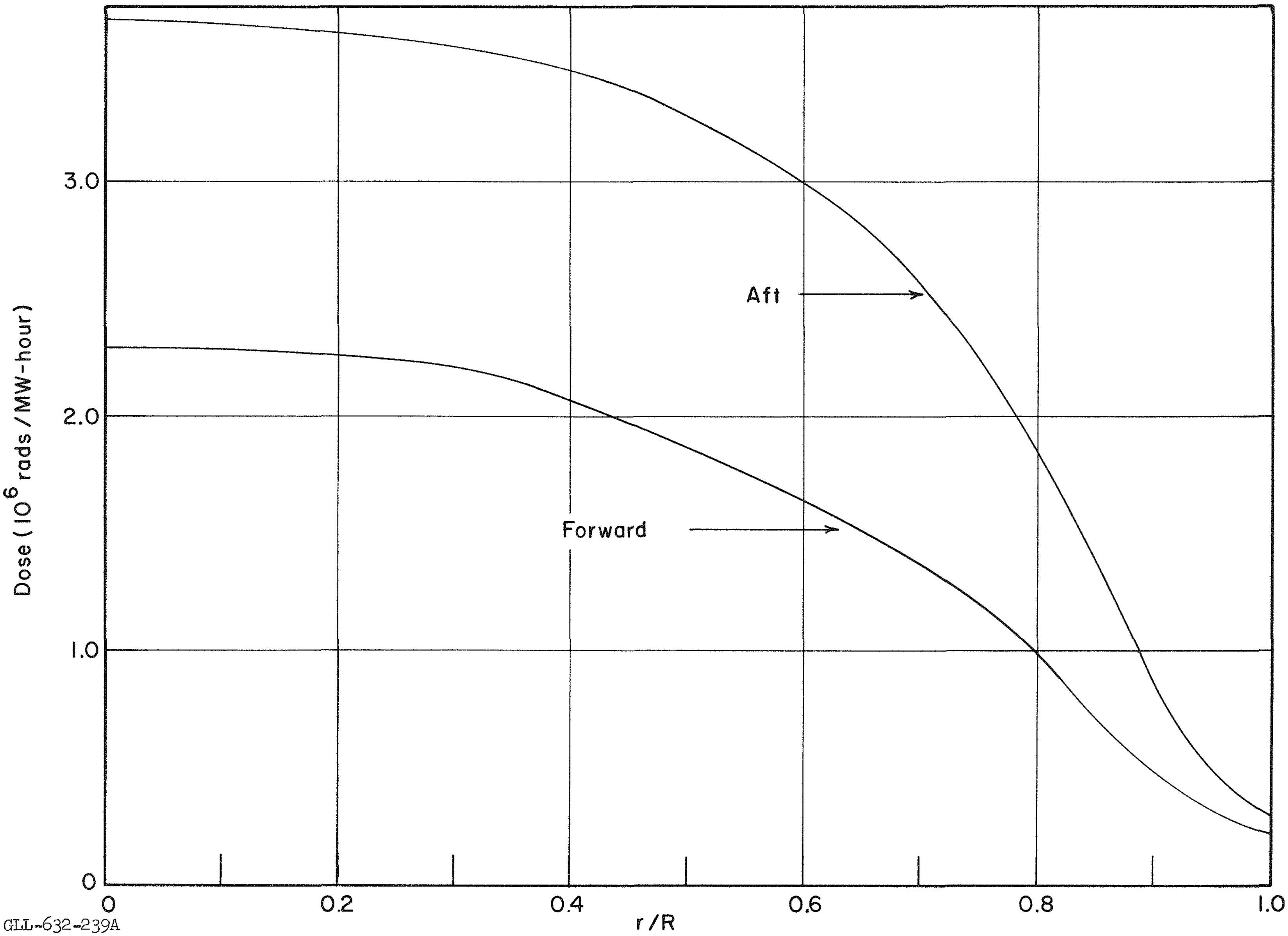

GLL-632-239A

Total radiation dose rate at stations 360.938 (forward) and 425.498 (aft).

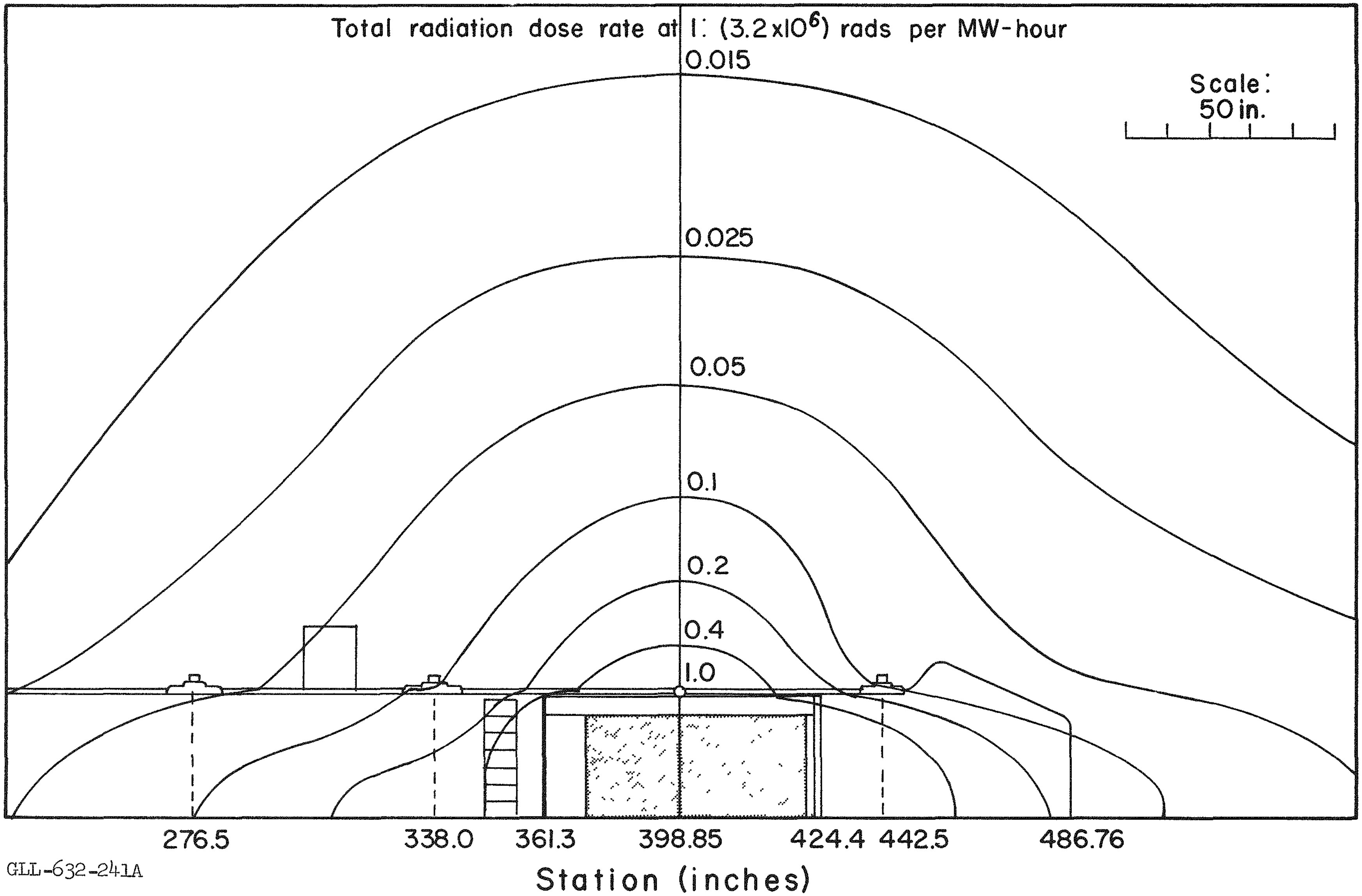

GLL-632-241A

Isodose contour map (normalized to peak). For distances x (in feet) greater than 1000 feet, use

$$\text{Dose (rads/MWh)} = \left[\frac{1.35 \times 10^7}{x^2}\right]\left[0.25\, e^{-0.010(x-2.5)} + 0.75\, e^{-0.015(x-2.5)}\right].$$

UCRL-7315

CHAPTER III - MECHANICAL DESIGN

A. REACTOR ASSEMBLY

Reference drawings	AAA 109471 AAA 109474
Reactor assembly general arrangement	See p. III-3

1. The Reactor

Reactor schematic	See p. III-4
Reactor dimensions	See p. III-5
Reactor weights	See p. IV-2

a. Reflected Core

Overall diameter (ceramic and peripheral shims)	53.42 in. (av)*
Overall area (ceramic and peripheral shims)	2241 in^2
Overall ceramic length	63.075 in.
Volume of the reflected core	81.8 ft^3
Active core diameter	47.46 in. (av)*
Active core area	1769 in^2
Active core length	51.03 in. (av)
Volume of the active core cylinder . . .	52.2 ft^3
Forward reflector thickness	9.667 in.
Aft reflector thickness	2.38 in. (av)
Side reflector thickness (incl. peripheral shims)	2.98 in. (av)*
Peripheral shim thickness	0.97 in. (av)
Tolerances on reactor radii	See p. III-6
Total number of flow channels in the region of the active core	27,030
Number of fueled channels	20,952
Number of guard tube channels	1,200
Number of side reflector BeO channels . .	3,888
Number of peripheral shim channels . .	1062
Number of wireways in active core . .	60
Number of wireways in side reflector . .	3
Total area of flow channels	952.30 in^2
Area of fueled channels	850.37 in^2

*Most probable dimension, based on 90,000 production tubes.

Area of guard tube channels	15.92 in^2
Area of side reflector BeO channels . .	26.41 in^2
Area of peripheral shim channels . . .	16.50 in^2
Area of flow channels through tie rods* . .	43.35 in^2
Area of wireway channels in active core . .	2.43 in^2
Area of wireway channels in side reflector .	0.12 in^2
Core porosity: $\frac{\text{total area of fueled channels}}{\text{area of the active core circle}}$	0.4813
Reactor porosity: $\frac{\text{total area of fueled channels}}{\text{area of the reflected core circle}}$	0.3802
"Missile" porosity: $\frac{\text{total area of fueled channels}}{\text{area within the reactor duct o.d.}}$	0.3406
Total number of ceramic tubes	465,000 (see p. III-23)
Unit cell arrangement	See pp. III-15, 16
Unit cell cross sections	See pp. III-9 to 14
Reflected core area analyses	See pp. III-18, 19

*Assumes control rods inserted.

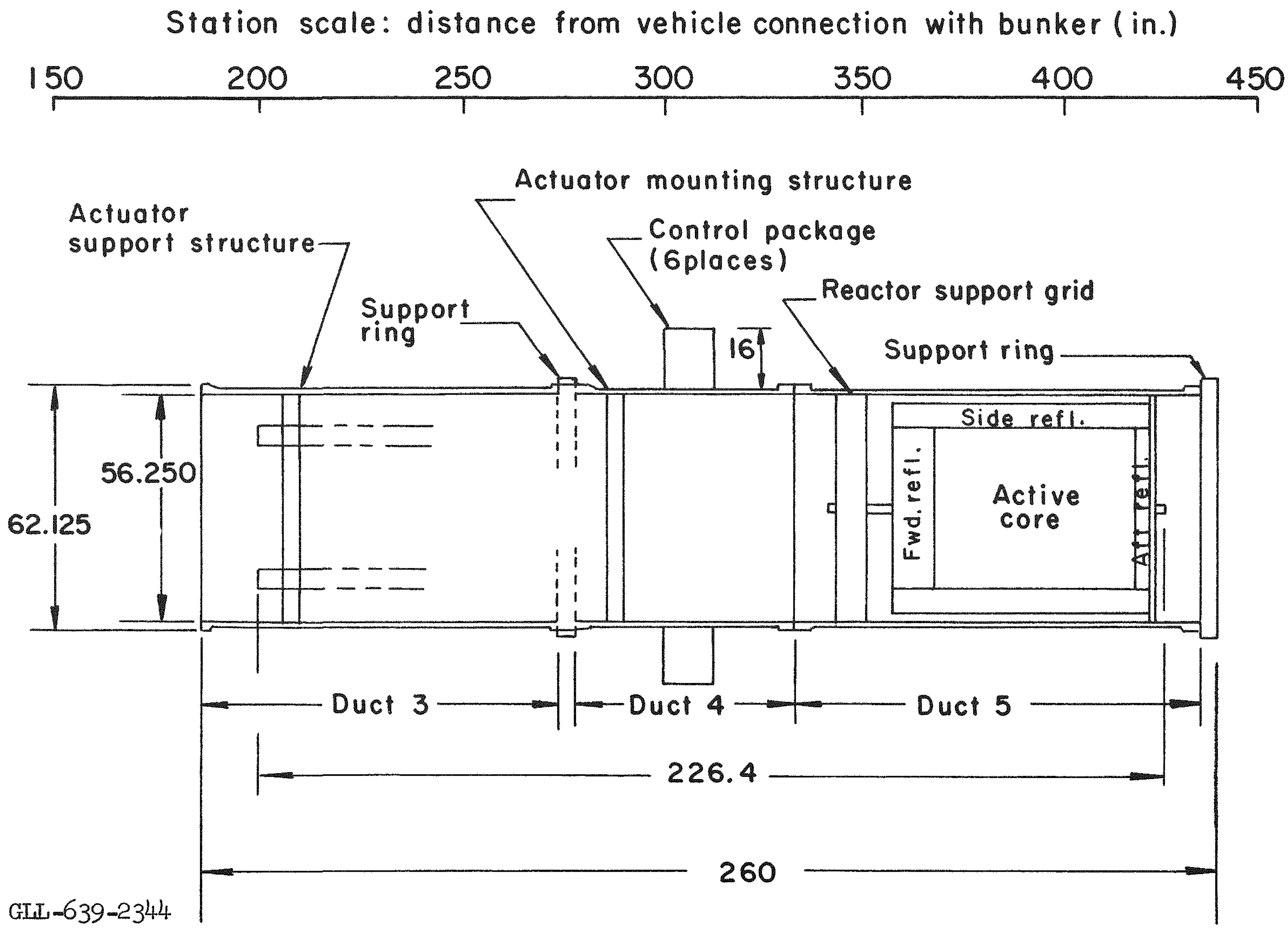

Reactor assembly, general arrangement. All dimensions are in inches.

CONFIDENTIAL R D

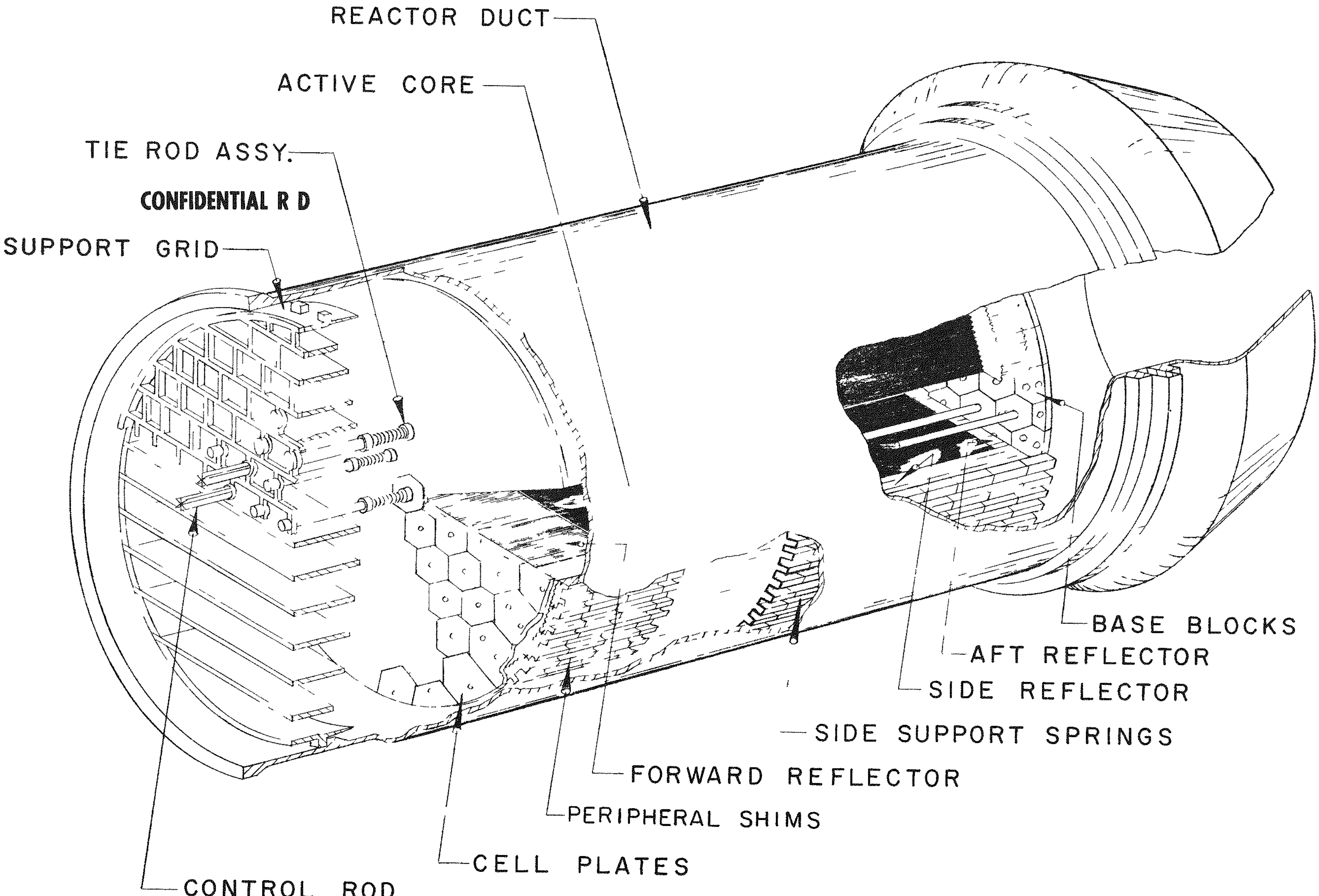

GLL-627-17544B

Reactor schematic.

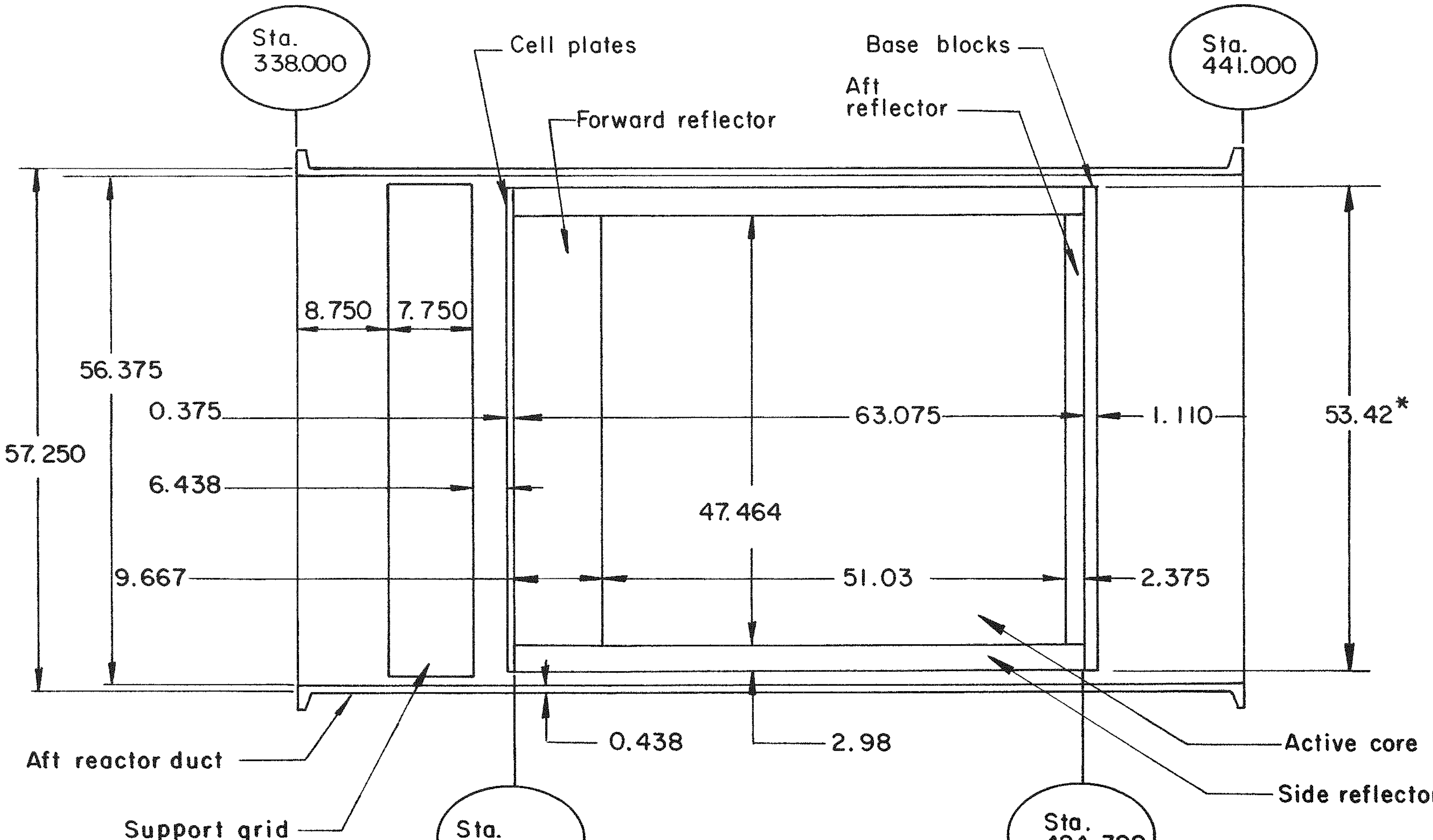

GLL-639-2345

Reactor dimensions. * Most probable dimension, based on stacking allowance of 0.0004 in./tube.

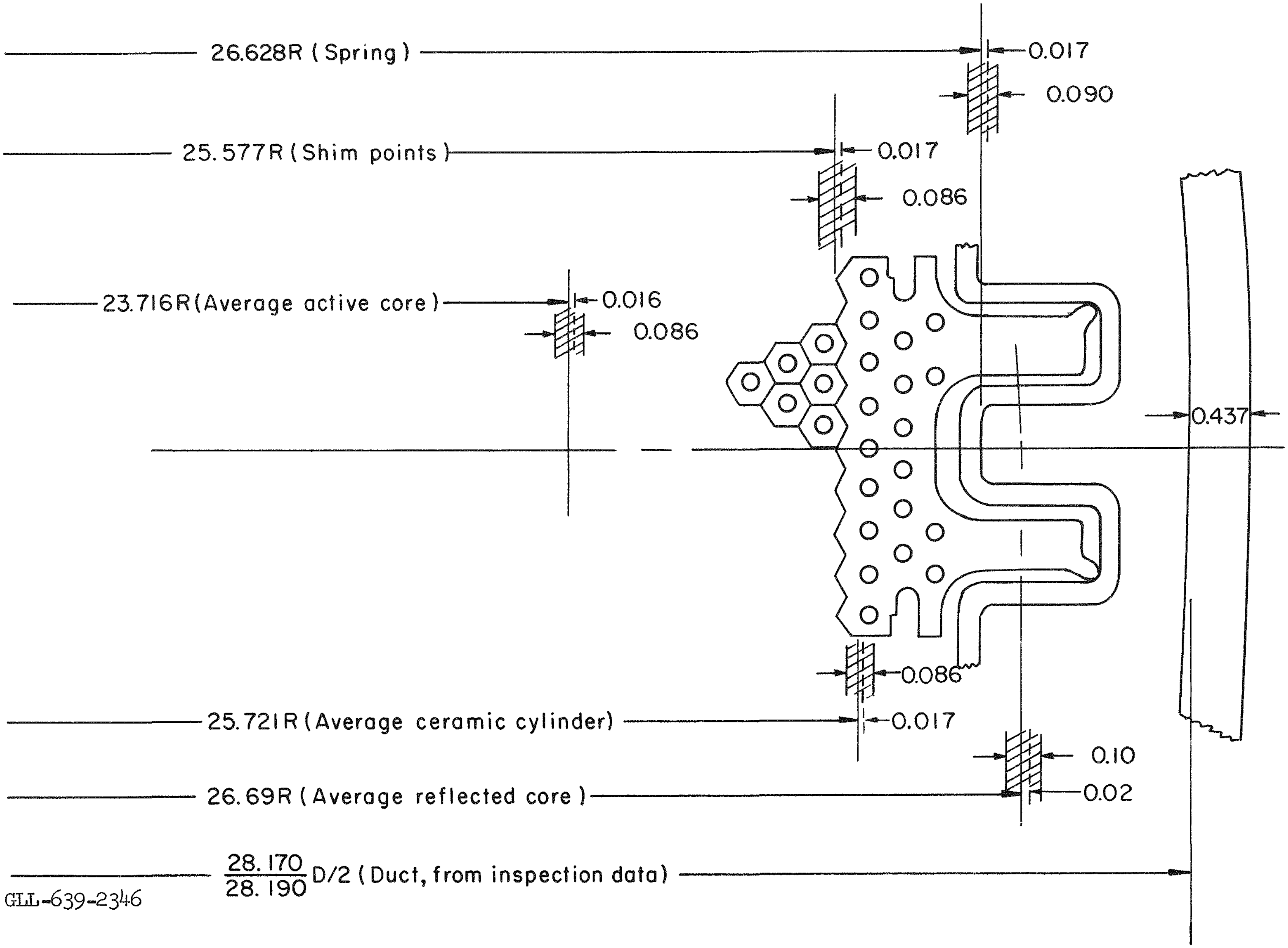

Tolerances on reactor radii at 70°F. Both nominal and most probable radii are shown, the latter (dashed lines) being based on 0.2972 in. average tube cross-flats dimension to allow for buildup on stacking, as discussed on the following page. (All dimensions in inches, R = radius, D/2 = 1/2 diam.)

Calculation of Radii in Fig. III-4.

A stacking allowance of 0.0004 in. per tube is included, as measured in a stackup of production tubes.

Effective core and reflected core radii were calculated from the number of tube positions, the nominal tube area, and the 0.0004-inch buildup per tube.

The spring radius was calculated from the actual part dimension in the two planes of symmetry. The thickness of ceramic was obtained by a tube count, and the distance across the shim and spring assembly was measured on a large scale lofting of the side support region. The two measurements differed by 2 mils. The average is reported.

The tolerance bands were obtained by combining the spring and shim tolerances with the specified ±0.0005 in. allowable on the tube average dimension.

Based on the first 90,000 production tubes, the most probable tube cross-flats dimension is 0.2972 in.

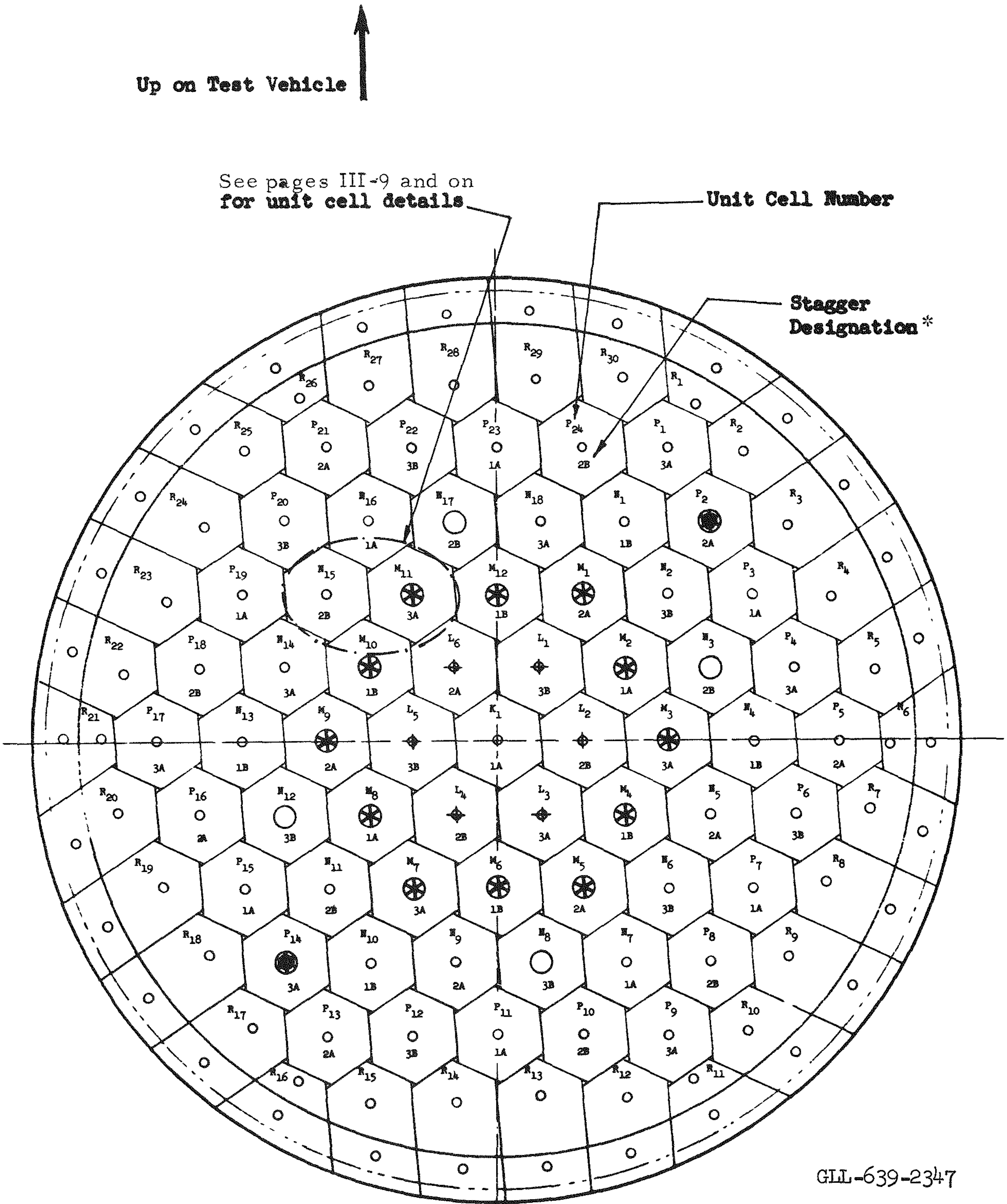

○ **Standard Tie Rod**

⊛ **Control Tie Rod (Shim)**

● **Control Tie Rod (Vernier)**

◯ **Spare Control Tie Rod**

⌖ **Safety Rod**

<u>Arrangement and Designation of Unit Cells</u>

View looking downstream

* The imaginary tube column located at the center of the tie rod has the stagger designation shown. See Fig. III-16.

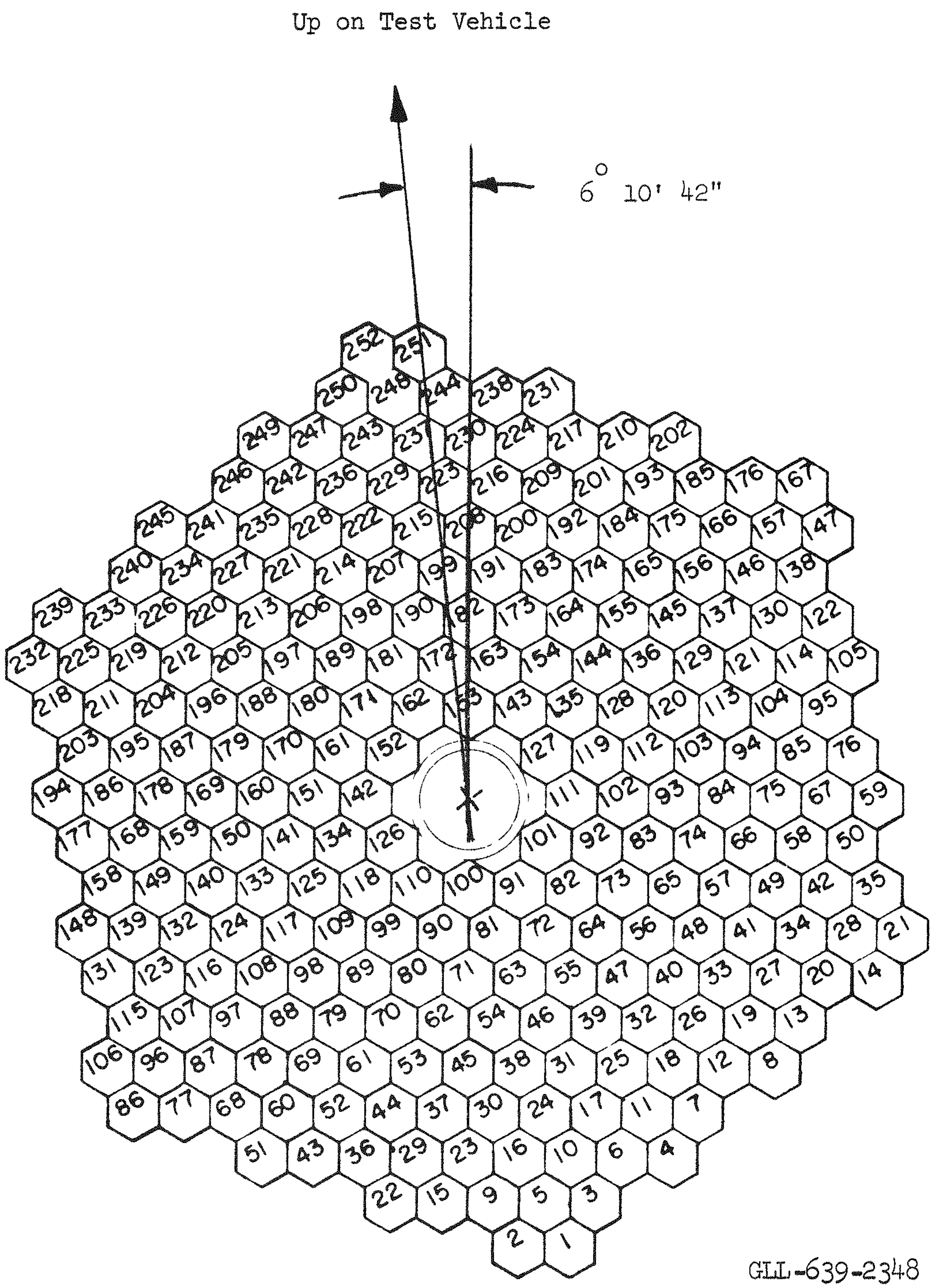

GLL-639-2348

Unit cell arrangement and numbering system. View looking downstream. Applicable to K, L, M, N, and P, unit cells except that inner "ring" of tubes is omitted in control cells.

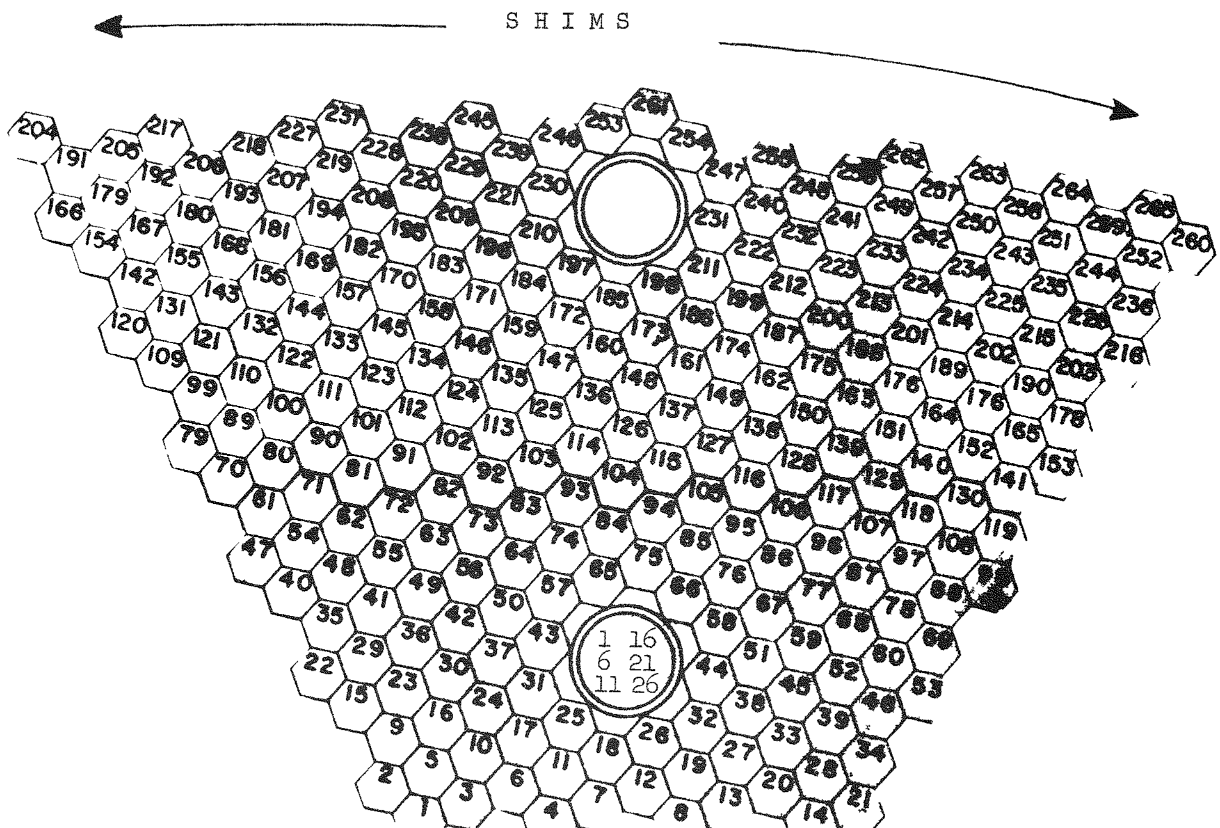

GLL-639-2349

Unit cell arrangement and numbering system. View looking downstream. Applicable to R_1, R_6, R_{11}, R_{16}, R_{21}, and R_{26} peripheral cells.

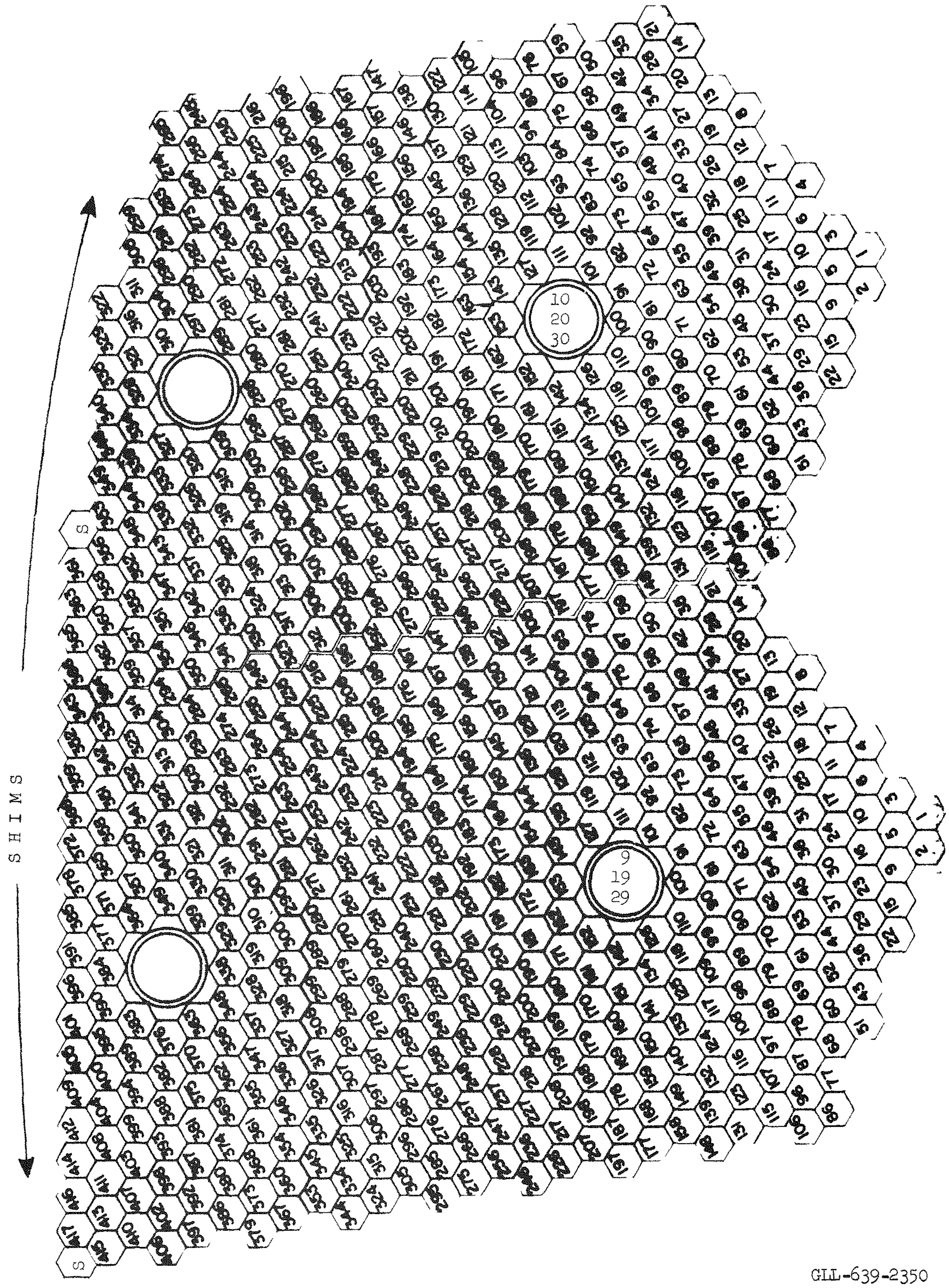

GLL-639-2350

Unit cell arrangement and numbering system. View looking downstream. Applicable to R_9, R_{10}, R_{19}, R_{20}, R_{29}, and R_{30}, peripheral cells.

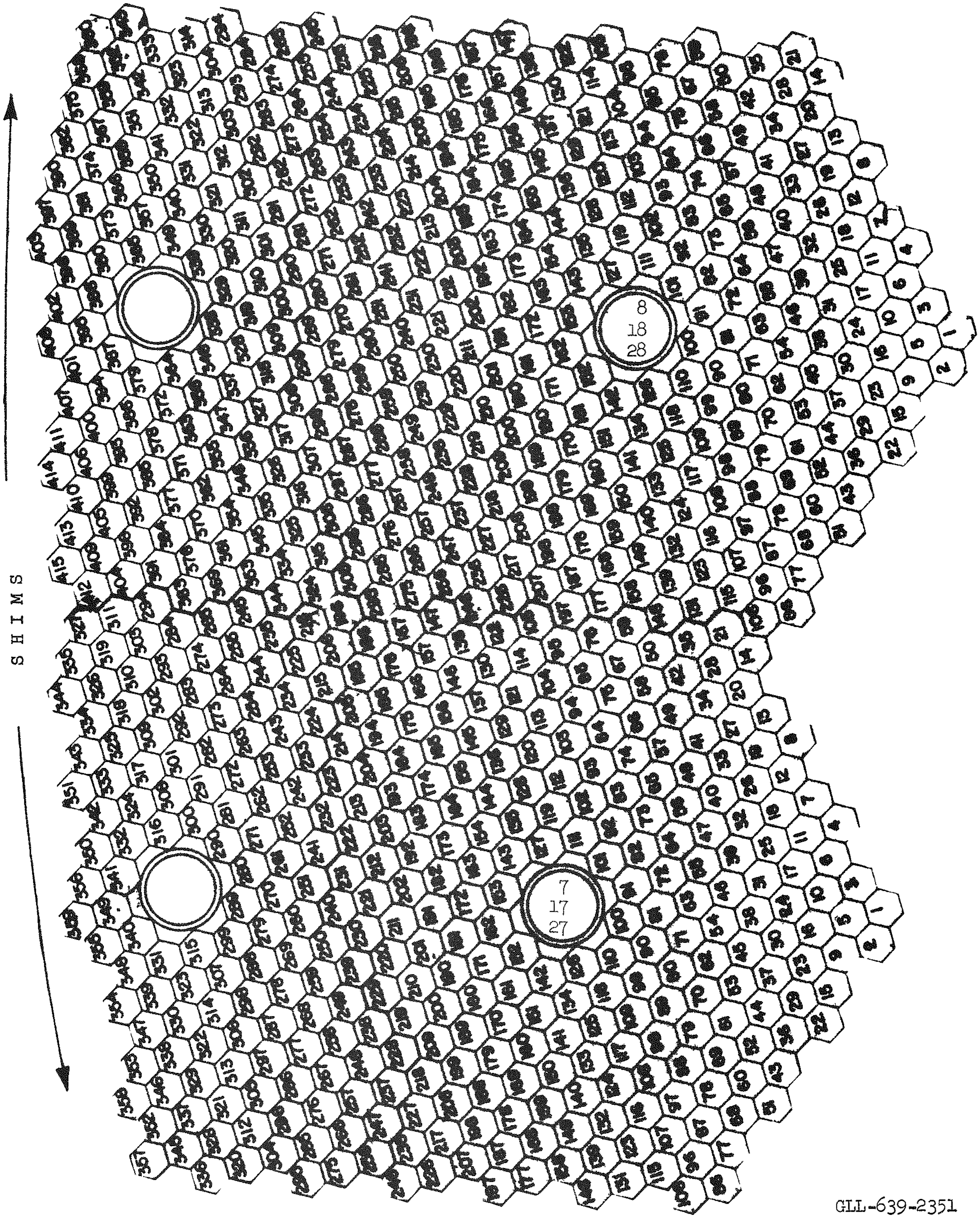

GLL-639-2351

Unit cell arrangement and numbering system. View looking downstream. Applicable to R_7, R_8, R_{17}, R_{18}, [redacted] R_{27}, and R_{28}, peripheral cells.

UNIVERSITY OF CALIFORNIA
Lawrence Radiation Laboratory
Livermore, California

August 27, 1964

TO: Distribution

FROM: Technical Information Division

RE: UCRL-7315, entitled "Tory II-C Data Book," by Carl E. Walter and Parker C. Smiley. [Nuclear Reactors for Ram-Jet Propulsion, C-90, M-3679 (30th Ed.)] (Report: SRD)

ERRATA

Please make the following corrections to the Tory II-C Data Book, UCRL-7315:

Page I-1 Add Note: "Information in this chapter has been slightly modified and presented in UCRL-7933."

Page I-70 Friction factor curve: Ordinate should read:

$$"\frac{\delta C_{fnet}}{C_{fnet}}."$$

Fueled tube flow passage diameter: Label ordinate

$$"\frac{\delta C_{fnet}}{C_{fnet}}."$$

Page II-9, 10 Outside fuel zone (.1349) should be unshaded as the .1058 zone on page II-11.

This document contains confidential restricted data relating to civilian applications of atomic energy.

RESTRICTED DATA

This document contains restricted data as defined in the Atomic Energy Act of 1954. Its transmittal or the disclosure of its contents in any manner to an unauthorized person is prohibited.

GROUP 1: Excluded from Automatic Downgrading and Declassification.

Page II-43 "Dose (rads/MWh) = $\left[\frac{1.35 \times 10^7}{x^2}\right.$ 0.25. . ."

should read:

"Dose (rads/MWh) = $\frac{1.35 \times 10^7}{x^2}\left[0.25. . .\right.$"

Page III-10 Add "R_{16}" to caption between "R_{11}" and "R_{21}."

Page III-12 Cross out "R_{19}" in caption.

Page III-20 "Aft reflector transition tubes" should read "aft reflector transition cartridges."

Page III-21 The right hand tie rod should be moved 1 tube in the five o'clock direction. The two perpendicular center lines should be rotated to correspond to the new position of the tie rod.

Page III-26 Guard tube reference drawing: add "62-128625."

Page III-40 Inside diameter "0.0576" should read "0.576."

Page III-82 Add note: " Information on pages III-82-84, -87, -94 has been revised. See Tory II-C Memo 748."

Page III-85, -86 Mark out everything on these pages. Add note: "Aft pressure and temperature rake was replaced by 2 air-cooled delta-shaped cantilever rakes. Dwg. No. 64-107275 and 64-107307."

Pages VI-9-14 In note 1, "MEL 523" should read "MEL 573."

Page VI-31 Ordinate of σ_u, σ_y curve: "stress, psi $\times 10^{-6}$" should read "stress, psi $\times 10^{-3}$."

Page VI-37 σ_u, σ_y curve: Top curve should be labeled "σ_u" instead of "σ_y." On "E" curve "psi $\times 10^{-3}$" should read "psi $\times 10^{-6}$."

Page VI-39 "E" curve ordinate: "psi $\times 10^{-3}$" should read "psi $\times 10^{-6}$."

Page VI-41 C_p curve: "Btu/lb-°F $\times 10^{-2}$" should read "Btu/lb-°F $\times 10^{2}$."

Page VI-43 Tensile properties: base line on ordinate should be labeled "0" instead of "10."

According to our records you have copy(s)__________Series____transmitted ____________________.

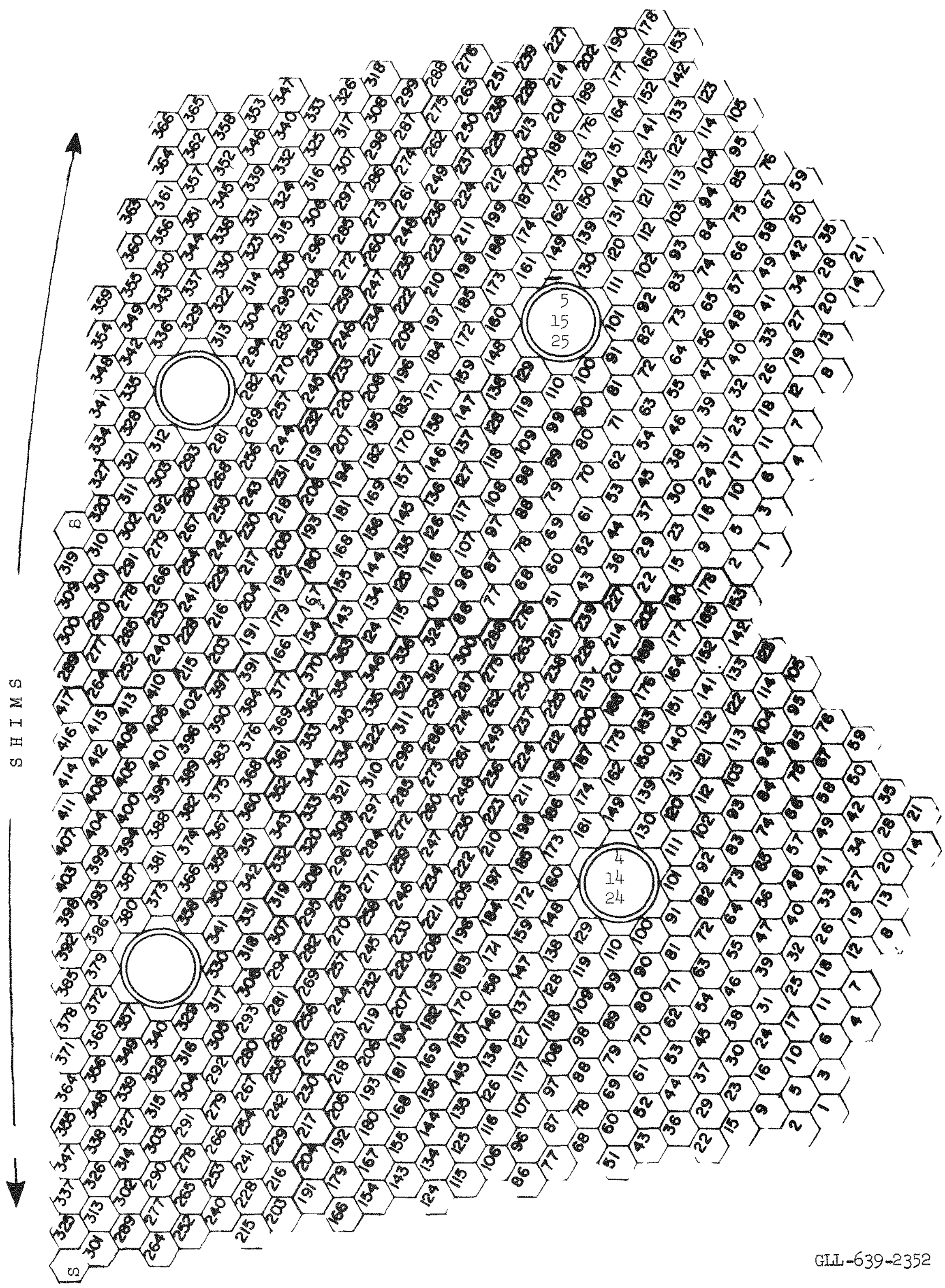

Unit cell arrangement and numbering system. View looking downstream. Applicable to R_4, R_5, R_{14}, R_{15}, R_{24}, and R_{25}, peripheral cells.

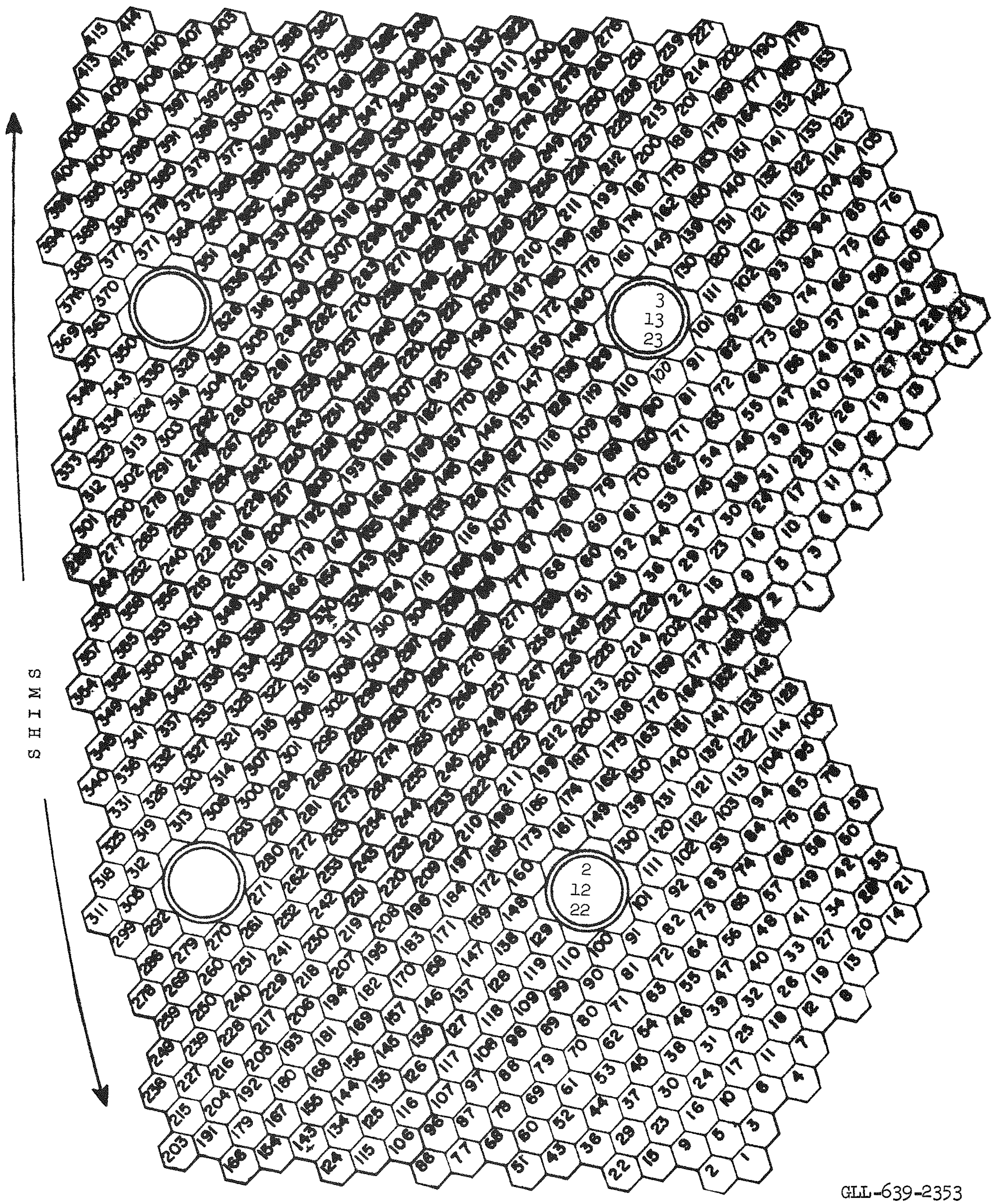

GLL-639-2353

Unit cell arrangement and numbering system. View looking downstream. Applicable to R_2, R_3, R_{12}, R_{13}, R_{22}, and R_{23}, peripheral cells.

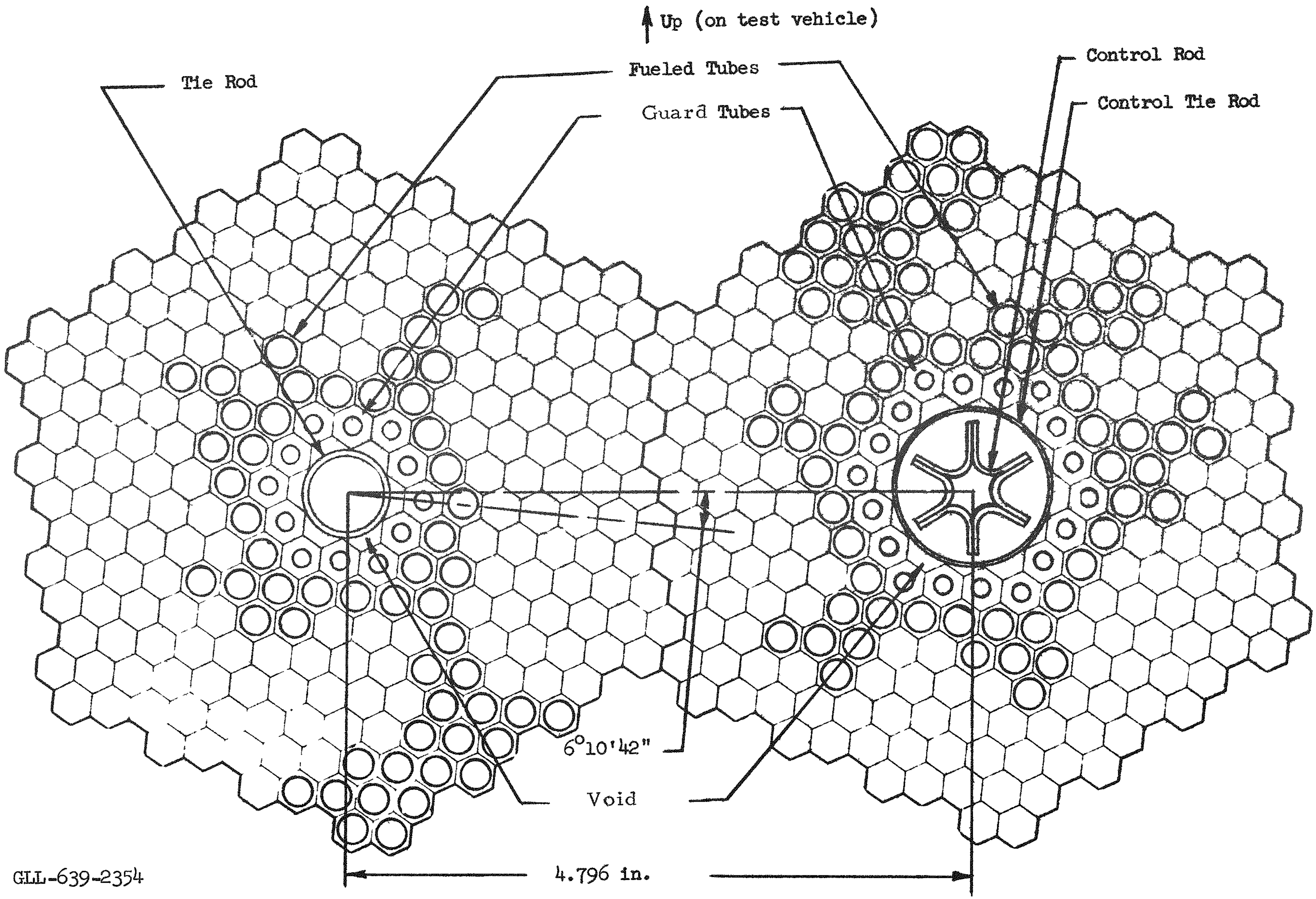

GLL-639-2354

Standard and control unit cells in the region of the active core. View looking downstream.

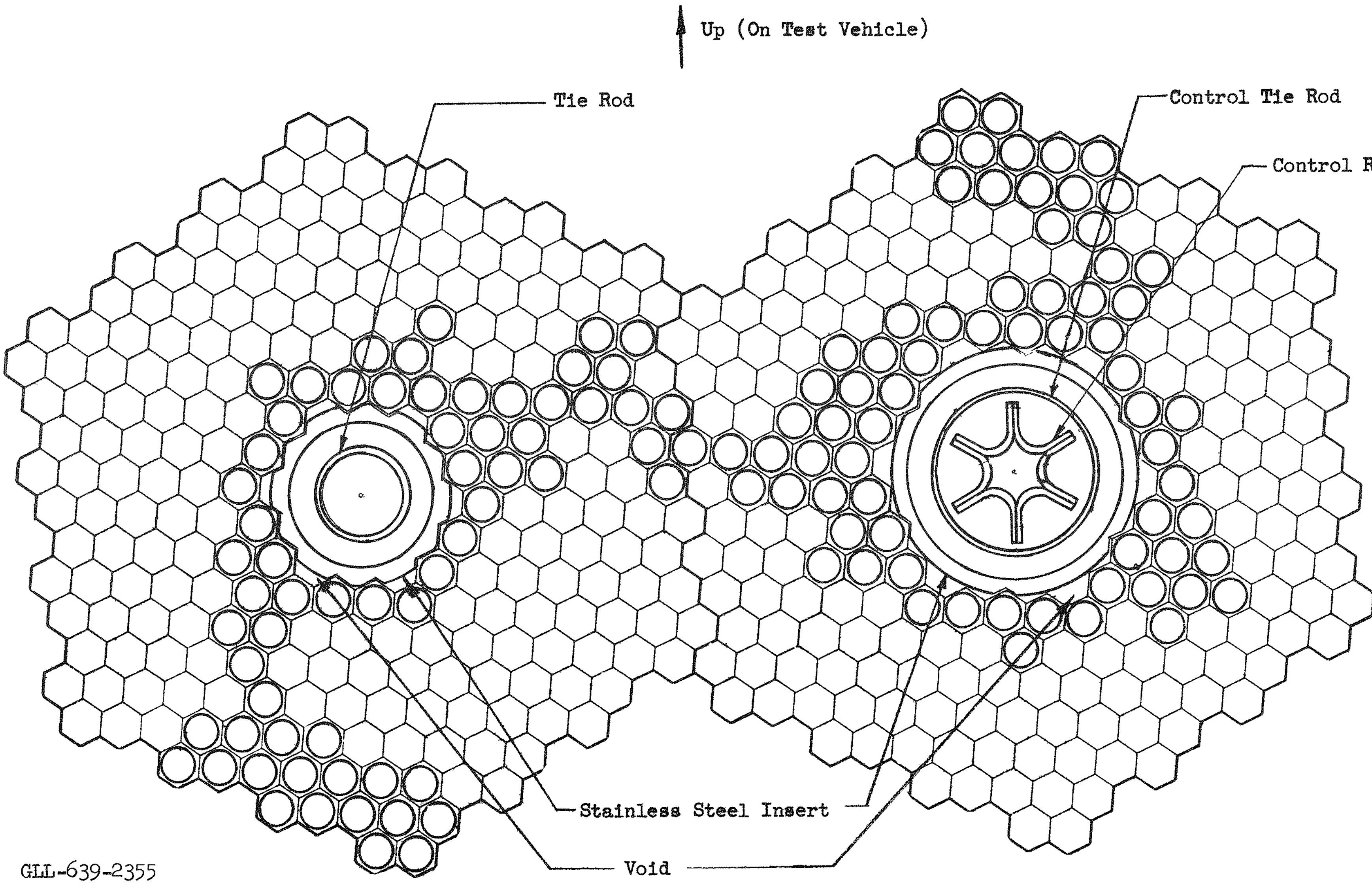

Standard and control unit cells. Typical cross-section in the region of the forward reflector. View looking downstream.

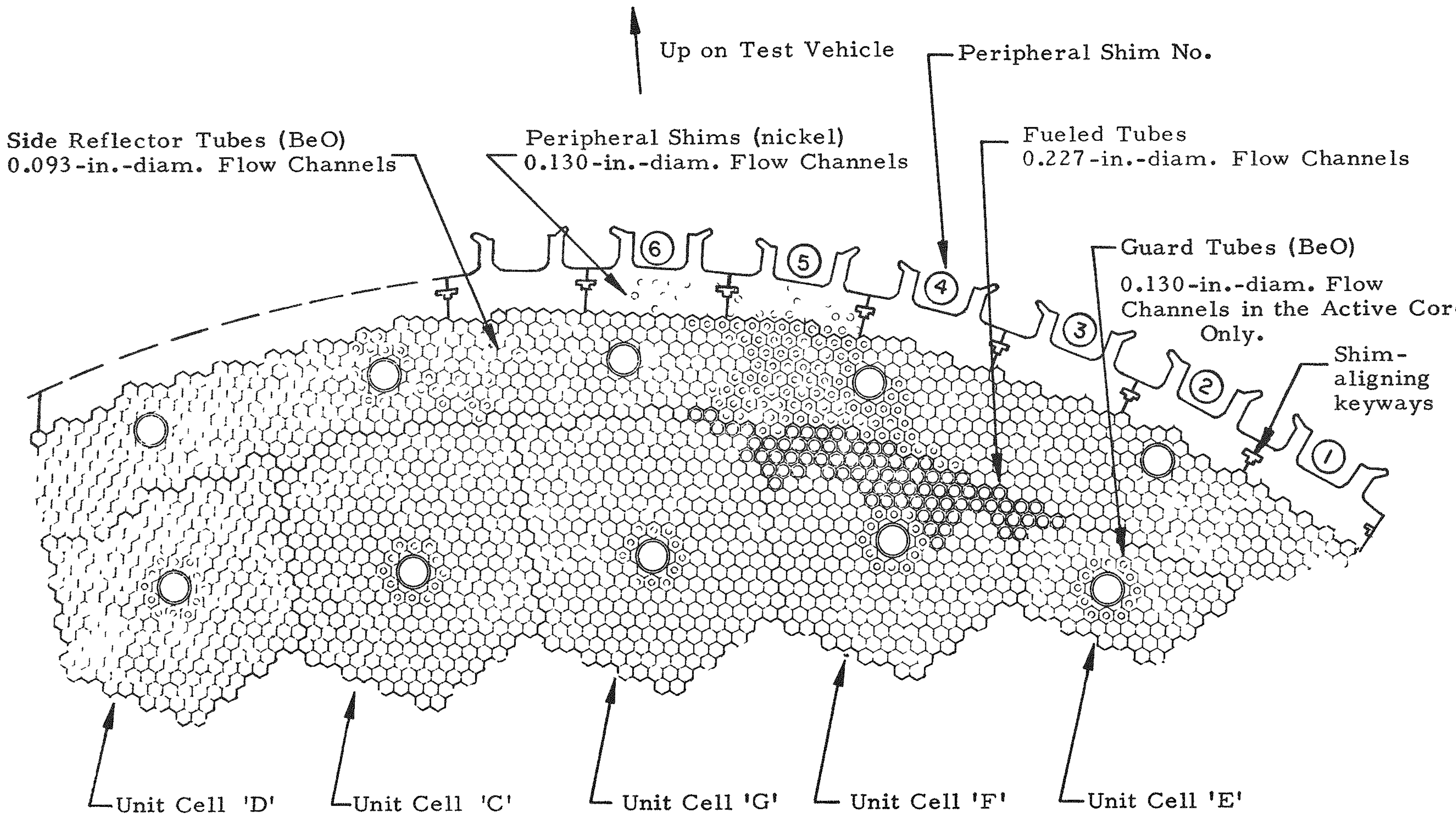

GLL-6110-14683A

Reflected core periphery. Typical sextant "in the region of the active core". View looking downstream showing designation of typical active core peripheral unit cells and of peripheral shims.

Frontal Areas in a Typical Section in the Region of the ACTIVE CORE

					Active Core Peripheral Cells									
	Standard unit cell (43 each)		Control unit cell (18 each)		C (6 each)		D (6 each)		E (6 each)		F (6 each)		G (6 each)	
Number of tube column positions (1)	259		259		308		245		105		245		308	
Number of tube columns	252		240		301		238		98		238		301	
Fueled tube columns	240		222		289		226		86		226		289	
Unfueled tube columns	12		18		12		12		12		12		12	
Peripheral shim flow channels														
Frontal area breakdown	Area in^2	Relative area %	Area in^2	Relative area, %	Area in^2	Relative area %	Area in^2	Relative area %	Area in^2	Relative area, %	Area in^2	Relative area %	Area in^2	Relative area %
Total solids	9 4581	47 675	9 3890	47 326	11 2183	47 551	8 9552	47 719	3 9263	48 819	8 9552	47 719	11 2183	47 551
Fueled BeO (2)	*8 6210*	*43 455*	*7 9745*	*40 196*	*10 3812*	*44 003*	*8 1181*	*43 258*	*3 0892*	*38 410*	*8 1181*	*43 258*	*10 3812*	*44 003*
Unfueled BeO	0 7451	3 756	1 1177	5 634	0 7451	3 158	0 7451	3 970	0 7451	9 264	0 7451	3 970	0 7451	3 158
Tie rod	0 0920	0 464	0 1123	0 566	0 0920	0 390	0 0920	0 490	0 0920	1 144	0 0920	0 490	0 0920	0 390
Control rod			0 1845	0 930										
Peripheral shim Ni														
(Nickel within a 52 882 in. diam circle)														
Total voids	10 3808	52 325	10 4499	52 674	12 3739	52 449	9 8114	52 281	4 1163	51 181	9 8114	52 281	12 3739	52 449
Fueled flow channels	9 7128	48 958	8 9846	45 288	11 6961	49 576	9 1464	48 738	3 4805	43 276	9 1464	48 738	11 6961	49 576
Unfueled flow channels	0 1592	0 802	0 2389	1 204	0 1592	0 675	0 1592	0 848	0 1592	1 979	0 1592	0 848	0 1592	0 675
Peripheral shim flow channels														
Flow channels inside tie rod	0 2606	1 314	0 8760[(3)]	4 416	0 2606	1 105	0 2606	1 389	0 2606	3 240	0 2606	1 389	0 2606	1 105
Voids between BeO and tie rod	0 1873	0 944	0 2888	1 456	0 1873	0 794	0 1873	0 998	0 1873	2 329	0 1873	0 998	0 1873	0 794
Other nonflow voids in BeO	*0 0609*	*0 307*	*0 0616*	*0 310*	*0 0707*	*0 300*	*0 0579*	*0 308*	*0 0287*	*0 357*	*0 0579*	*0 308*	*0 0707*	*0 300*
Nonflow voids surrounding shims														
Flow channel in peripheral shims within a 52 882 in diam circle														
TOTALS	19 8389	100 000	19 8389	100 000	23 5922	100 000	18 7666	100 000	8 0426	100 000	18 7666	100 000	23 5922	100 000

			Side Reflector							
	Total active core		Unfueled BeO		Peripheral shims		Total side reflector		Total reflected core	
Number of tube column positions (1)	23,065		4098				4098		27 163	
Number of tube columns	22 212		3888				3888		26,100	
Fueled tube columns	21 012								21,012	
Unfueled tube columns	1 200		3888				3888		5,088	
Peripheral shim flow channels					1062				1 062	
Frontal area breakdown	Area in^2	Relative area, %	Area in^2	Relative area, %	Area in^2	Relative area, %	Area in^2	Relative area, %	Area in^2	Relative area, %
Total solids	840 6021	47 580	271 3625	87 034	140 6418	88 901	412 0043	87 662	1253 3444	56 035
Fueled BeO (2)	*754 7708*	*42 722*							*754 7708*	*33 744*
Unfueled BeO	74 5109	4 218	268 6025	86 149			268 6025	57 150	343 1134	15 340
Tie rod	8 7374	0 495	2 7600	0 885			2 7600	0 587	11 4974	0 514
Control rod	2 5830[(4)]	0 146							2 5830	0 115
Peripheral shim Ni					140 6418	88 901	140 6418	29 924	140 6418	6 288
(Nickel within a 52 882 in. diam circle)					(89 7648)	(56 741)	(89 7649)	(19,099)		
Total voids	926 1320	52 420	40 4256	12 966	17 5604	11 199	57 9860	12 338	983 3800	43 965
Fueled flow channels	850 3662	48 132							850 3662	38 018
Unfueled flow channels	15 9218	0 901	26 4112	8 471			26 4112	5 615	42 3330	1 893
Peripheral shim flow channels					16 5044	10 432	16 5044	3 512	16 5044	0 738
Flow channels inside tie rod	35 5298[(4)]	2 011	7 8180	2 507			7 8180	1 663	43 3478	1 938
Voids between BeO and tie rod	18 8713	1 068	5 6190	1 802			5 6190	1 196	24 4903	1 095
Other nonflow voids in BeO	5 4429	*0 308*	*0 5774*	*0 185*			0 5774	0 123	6 0203	0 269
Nonflow voids surrounding shims					1 0560	0 667	1 0560	0 225	1 0560	0 047
Flow channel in peripheral shims within a 52 882 in diam circle					(16 5044)	(10 432)	(16 5044)	(3 512)		
TOTALS	1766 7341	100 000	311 7881	100 000	158 2022	100 000	469 9903	100 000	2236 7244	100 000

(1) The number of tube column positions is the number of tube columns which would fill the area within the nickel peripheral shims including areas taken up by tie rods

(2) Thermocouple wireways (unfueled tubes) omitted from this tabulation

(3) With control rods in

(4) With 14 control rods in

GLL-633-393

Frontal Areas in a Typical
Section in the Region of the FORWARD REFLECTOR

	Standard unit cell (43 each)		Control unit cell (18 each)		Peripheral Cells Within the Active Core Circle (47 524 in dian) C (6 each)		D (6 each)		F (6 each)		F (6 each)		G (6 each)	
Number of tube column positions (1)	259		259		308		245		105		245		308	
Number of 0 227 i d tube columns	240		222		289		226		86		?26		289	
Number of side re flector tube columns														
Peripheral sh m flow channels														
Typical frontal area breakdown (2)	Area in^2	Relative area %	Area in^2	Relative area %	Area in^2	Relative area %	Area in^2	Relative area %	Area in^2	Relative area %	Area n^2	Relat ve area %	Area in^2	Relat ve area %
Total solids	9 0709	45 723	8 7793	44 253	10 8311	45 910	8 5680	45 656	3 5387	43 999	8 5680	45 656	10 8311	45 910
BeO	8 6213	43 456	7 9742	40 195	10 3815	44 004	8 1184	43 260	3 0891	38 409	8 1184	43 260	10 3815	44 004
Tie rod	*0 0920*	*0 464*	*0 1123*	*0 566*	*0 0920*	*0 390*	*0 0920*	*0 490*	*0 0920*	*1 144*	*0 0920*	*0 490*	*0 0920*	*0 390*
Control rod			0 1845	0 930										
Reflector insert	0 3576	1 803	0 5083	2 562	0 3576	1 516	0 35 6	1 906	0 3576	4 446	0 35 6	1 906	0 35 6	1 516
Peripheral shim														
Total voids	10 7680	54 277	11 0596	55 747	12 7611	54 090	10 1986	54 344	4 5039	56 001	10 1986	54 344	12 7611	54 090
BeO flow channel	9 7128	48 958	8 9843	45 286	11 6958	49 575	9 1462	48 37	3 4804	43 275	9 1462	48 737	11 6958	49 575
Inside tie rod	0 2606	1 314	0 8 60[3]	4 416	0 2606	1 105	0 2606	1 389	0 2606	3 240	0 2606	1 389	0 2606	1 105
Between tie rod and nsert	0 5805	2 926	0 8504	4 287	0 5805	2 460	0 5805	3 093	0 5805	7 218	0 5805	3 093	0 5805	2 460
Peripheral shim flow channels														
Nonflow voids nsert and B O	0 1658	0 836	0 3038	1 531	0 1658	0 703	0 1658	0 883	0 1658	2 062	0 1658	0 883	0 1658	0 703
Other nonflow o ds n BeO	0 0483	0 243	0 0451	0 22	0 0584	0 24	0 0455	0 242	0 0166	0 206	0 0455	0 242	0 0584	0 247
Nonflow o d a ound shims														
TOTALS	19 8380	100 000	19 8389	100 000	23 5922	100 000	18 7666	100 000	8 0426	100 000	18 7666	100 000	23 5922	100 000

	Total within the active core circle		Side Reflector: S de reflector BeO		Peripheral shims		Total side reflector		Total reflected core	
Number of tube column positions (1)	23 065		4098				4098		27 163	
Number of 0 227 i d tube columns	21 012								21 012	
Number of side re flector tube columns			3528				3528		3 528	
Peripheral sh m flow channels					1062				1 062	
Typical frontal area breakdown (2)	Area in^2	Relative area %	Area in^2	Relative area %	Area in^2	Relative area %	Area in^2	Relative area %	Area in^2	Relative area %
Total solids	801 3595	45 358	250 3409	80 292	140 6418	88 901	390 9827	83 189	1192 3422	53 308
BeO	754 7849	42 722	243 7319	78 172			243 7319	51 859	998 5168	44 642
Tie rod	*8 7374*	*0 495*	*2 7600*	*0 885*			*2 7600*	*0 587*	*11 4974*	*0 514*
Control rod	2 5830[4]	0 146							2 5830	0 115
Reflector insert	35 2542	1 995	3 8490	1 234			3 8490	0 819	39 1032	1 748
Peripheral shim					140 6418	88 901	140 6418	29 924	140 6418	6 288
Total voids	965 3746	54 942	61 4472	19 708	1[illegible] 5604	11 099	79 0076	16 810	1044 3822	46 692
BeO flow channel	850 3542	48 431	23 9657	7 686			23 9657	5 099	874 3199	39 089
Inside tie rod	35 5298[4]	2 011	8180	2 507			7 8180	1 663	43 3478	1 938
Between tie rod and nsert	57 6837	3 265	17 4150	5 586			17 4150	3 705	75 0987	3 358
Peripheral shim flow channels					16 5044	10 432	16 5044	3 512	16 5044	0 738
Nonflow voids nsert and B O	1 5718	0 995	11 5560	3 706			11 5560	2 459	29 1278	1 302
Other nonflow o ds n BeO	4 2351	0 240	0 6925	0 222			0 6925	0 147	4 9276	0 220
Nonflow o d a ound shims					1 0560	0 667	1 0560	0 225	1 0560	0 047
TOTALS	1766 7341	100 000	311 7881	100 000	158 2022	100 000	469 9903	100 000	2236 7244	100 000

GLL-639-2357

(1) The number of tube columns which would fill the total area within the Ni shims including the areas taken up by tie rods and reflector inserts.

(2) Does not consider the nickel tubes or atypical inserts

(3) Assuming 14 control rods to be in

(4) Assuming control rod to be in

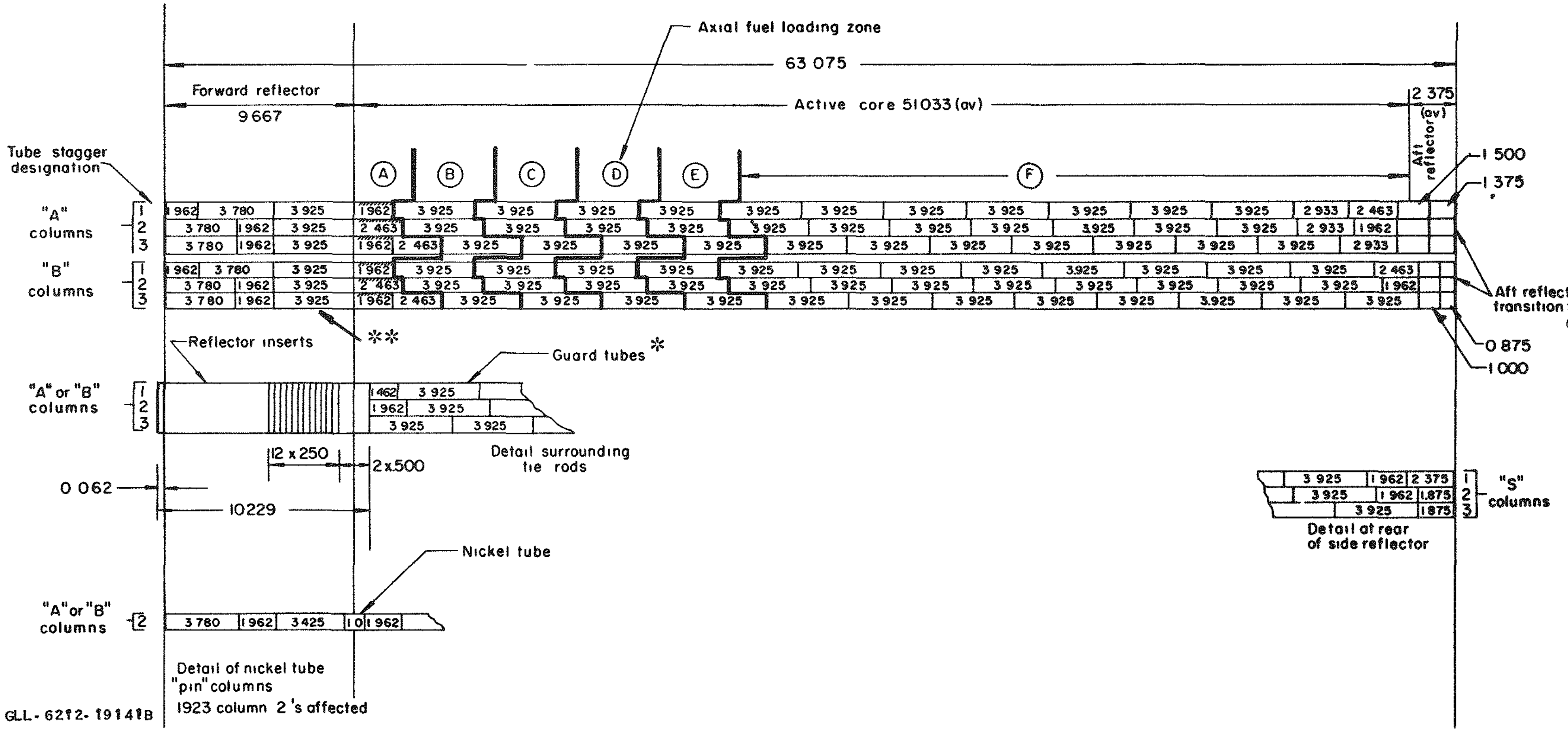

Tube Stagger Arrangements

*3.925-inch guard tubes are notched so that they break in the center with a thermal gradient rather than load the fueled tubes.

**These tubes are chamferred on both ends.

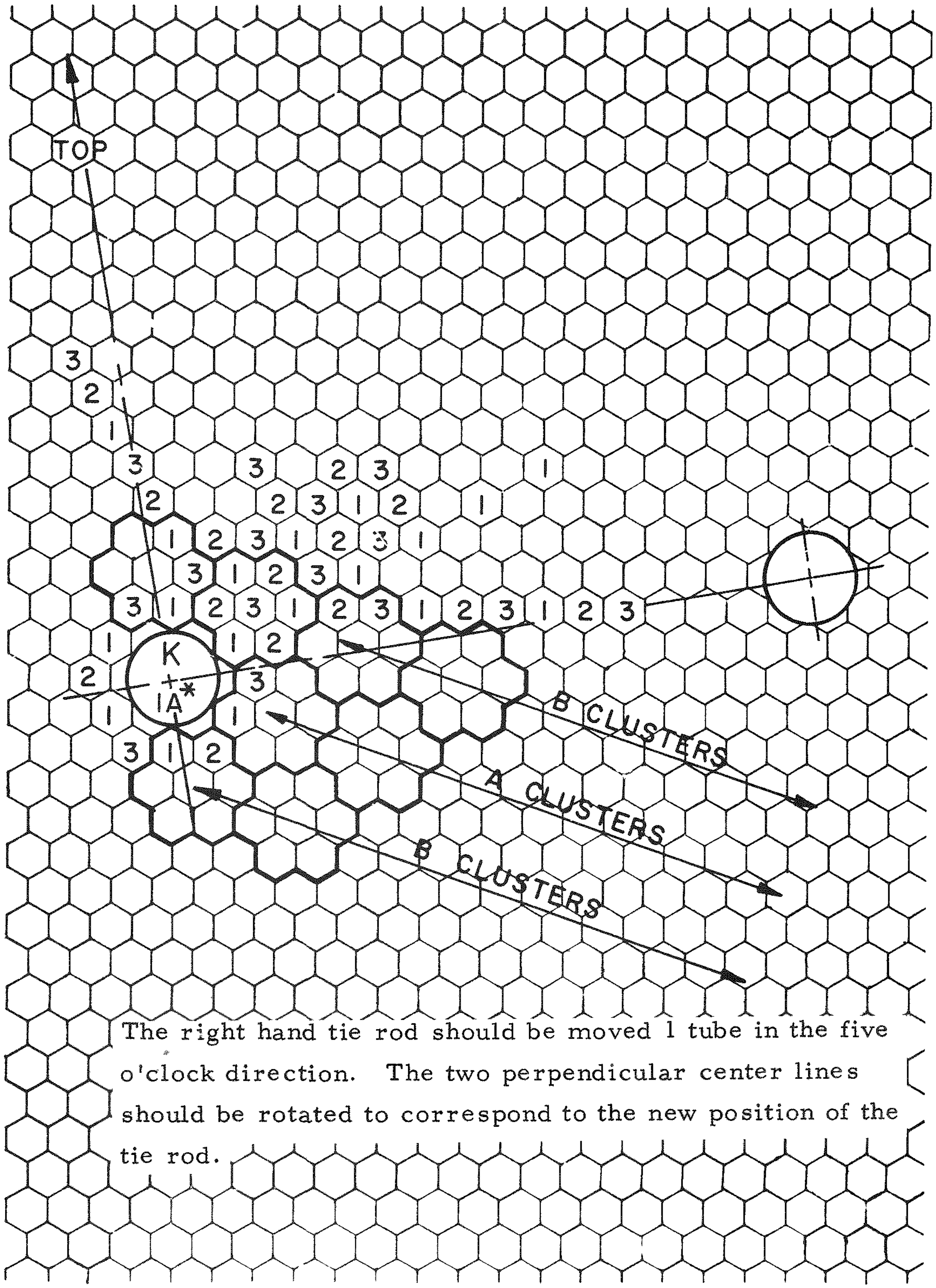

GLL-639-2358

Tube cluster and stagger arrangement. View looking down stream. *In a "1A" unit cell, the center tube column would be 1 and the center 7 tube cluster would be A, if not replaced by a tie rod. See page III-8.

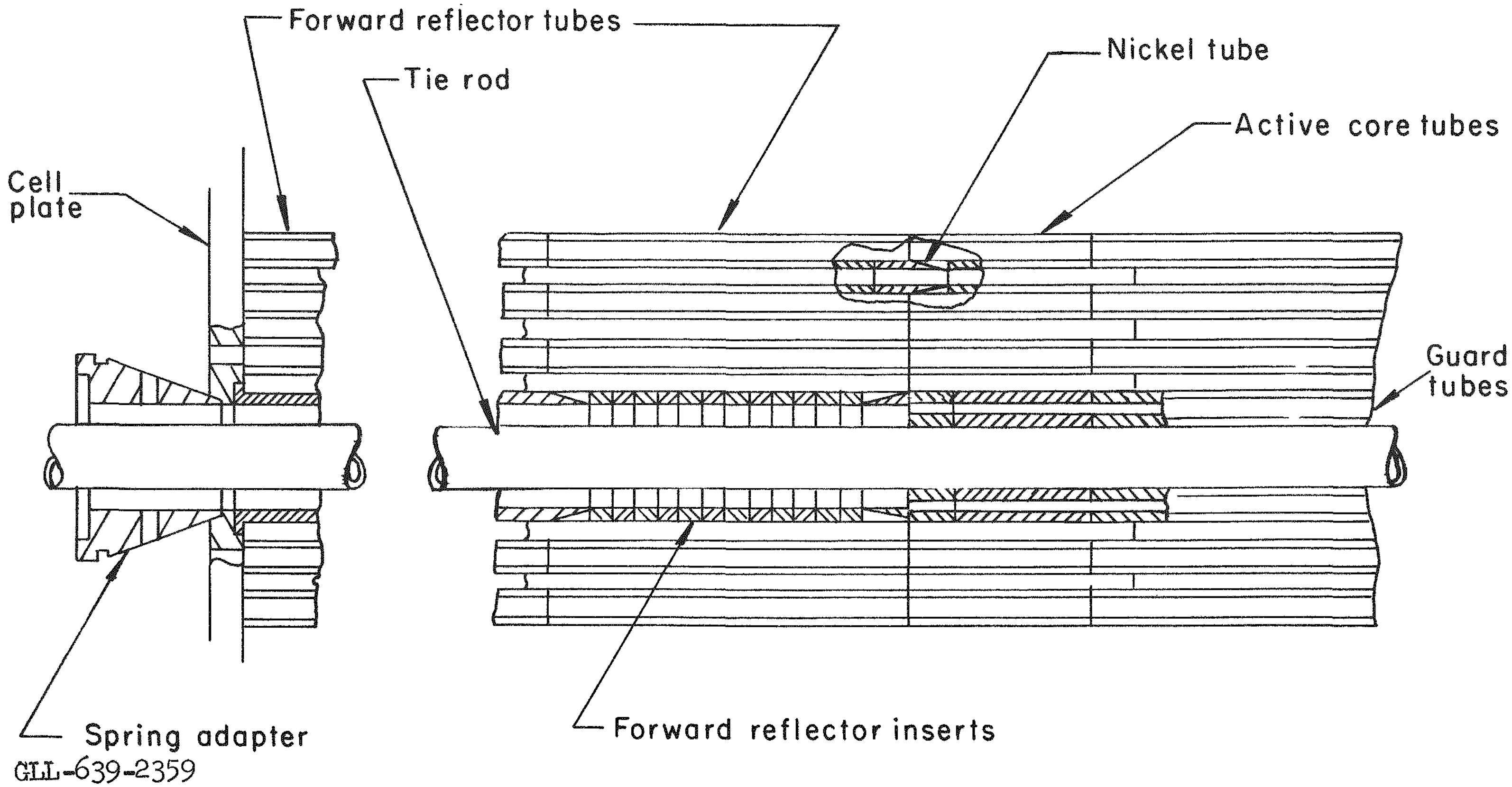

Forward reflector – active core interface. Section through a standard unit cell.

Ceramic tube quantities (dimensions in inches):

	Hole diam.	Size code	Length	No. of tubes	Tube-inches
Fueled	0.227	R	1.962	22,604	44,349.048
		S	2.463	19,298	47,530.974
		T	2.933	10,479	30,734.907
		U	3.925	240,947	945,716.975
			Total fueled	293,328	1,068,331.904
Unfueled	0.227	B1	1.000	11,088	11,088.000
		C1	1.500	11,124	16,686.000
		E1	1.962	21,081	41,360.922
		F1	2.375	3	7.125
		G1	2.463	60	147.780
		H1	2.933	33	96.789
		J1	3.780	21,015	79,436.700
		K1	3.925 (C)	20,115	78,951.375
		L1	3.425 (C)	1,623	5,558.775
				86,142	233,333.466
	0.130	A2	1.462	408	596.496
		E2	1.962	792	1,553.904
		G2	2.463	402	990.126
		H2	2.933	608	1,783.264
		K2	3.925	14,191	55,699.675
				16,401	60,623.465
	0.093	A3	1.462	108	157.896
		D3	1.875	2,610	4,893.750
		E3	1.962	8,877	17,416.674
		F3	2.375	1,275	3,028.125
		G3	2.463	2,058	5,068.854
		J3	3.780	3,525	13,324.500
		K3	3.925	46,743	183,466.275
		K4	3.925 (C)	3,228	12,669.900
		L3	3.425 (C)	300	1,027.500
				68,724	241,053.474
			Total unfueled	171,267	535,010.405
			Total reactor	464,595	1,603,342.309

(C). Chamfered tubes.

Fuel loading distribution.

Size Code → Length in. → Loading, (g OyO_2/in.)	R 1.962 Quantity	R 1.962 Tube-in.	S 2.463 Quantity	S 2.463 Tube-in.	T 2.933 Quantity	T 2.933 Tube-in.	U 3.925 Quantity	U 3.925 Tube-in.	Total Quantity	Total Tube-in.	Total fuel (g OyO_2)
0.0219	225	441.5	234	576.3	336	985.5	5,136	20,158.8	5,931	22,162.1	485
.0237	450	882.9	436	1073.9	696	2041.4	11,138	43,716.6	12,720	47,714.8	1,131
.0256	339	665.1	348	857.1	495	1451.8	8,607	33,782.5	9,789	36,756.6	941
.0277	312	612.1	318	783.2	470	1378.5	8,974	35,223.0	10,074	37,996.8	1,053
.0299	386	757.3	384	945.8	580	1701.1	10,252	40,239.1	11,602	43,643.4	1,305
.0323	330	647.5	330	812.8	508	1490.0	9,236	36,251.3	10,404	39,201.5	1,266
.0350	325	637.6	324	798.0	484	1419.6	10,278	40,341.1	11,411	43,196.4	1,512
.0379	393	771.1	384	945.8	570	1671.8	11,652	45,734.1	12,999	49,122.8	1,862
.0410	345	676.9	348	857.1	529	1551.6	10,751	42,197.7	11,973	45,283.2	1,857
.0443	391	767.1	378	931.0	589	1727.5	11,377	44,654.7	12,735	48,080.4	2,130
.0479	300	588.6	326	802.9	436	1278.8	11,356	44,572.3	12,418	47,242.6	2,263
.0518	380	745.6	367	903.9	598	1753.9	12,528	49,172.4	13,873	52.575.8	2,723
.0560	1254	2460.3	1089	2682.2	602	1765.7	13,314	52,257.4	16,259	59,165.7	3,313
.0606	1349	2646.7	1171	2884.1	979	2871.4	19,063	74,822.3	22,562	83,224.6	5,043
.0656	1055	2069.9	952	2344.8	763	2237.9	15,211	59,703.2	17,981	66,355.7	4,353
.0710	1767	3466.9	1673	4120.6	1877	5505.2	35,096	137,751.8	40,413	150,844.5	10,710
.0769	808	1585.3	585	1438.4			5,422	21,281.4	6,814	24,305.4	1,869
.0832	1537	3015.6	1211	2982.7			6,534	25,646.0	9,282	31,644.2	2,633
.0901	778	1526.4	632	1556.6			4,546	17,843.0	5,956	20,926.1	1,885
.0976	1700	3335.4	1309	3224.1			4,521	17,744.9	7,530	24,304.4	2,372
.1058	775	1481.3	553	1362.1			3,191	12,524.7	4,499	15,368.0	1,626
.1147	747	1465.6	602	1482.7			3,388	13,297.9	4,737	16,246.2	1,863
.1243	970	1903.1	741	1825.1			3,541	13,898.4	5,252	17,626.6	2,191
.1349	2609	5118.9	2034	5009.7			2,175	8,536.9	6,818	18,665.5	2,518
.1465	1552	3045.0	1252	3083.7			2,102	8,250.4	4,906	14,379.0	2,107
0.1591	1607	3152.9	1378	3394.0			2,245	8,811.6	5,230	15,358.6	2,444
Totals	22,664	44,467	19,358	47,679	10,512	30,832	241,634	948,413	294,186	1,071,391	63,450*

*Subtract 160 g for fueled tubes replaced by unfueled thermocouple wireways.

Note: Nickel tubes taken into account.

GLL-639-2360

i. Fueled tubes

Material	BeO + Horseradish (see LRL Spec. MEL 573)
Density	See p. VI-11
Total number of fueled tubes . .	See p. III-23
Fuel loadings .	See p. III-24

Reference drawings	Size code	Length (in.)	Volume (in^3)	Approx. weight (g)
62-102879-1	R	1.962	0.0701	3.63
62-102879-2	S	2.463	0.0880	4.56
62-102879-3	T	2.933	0.1048	5.43
62-102879-4	U	3.925	0.1402	7.26

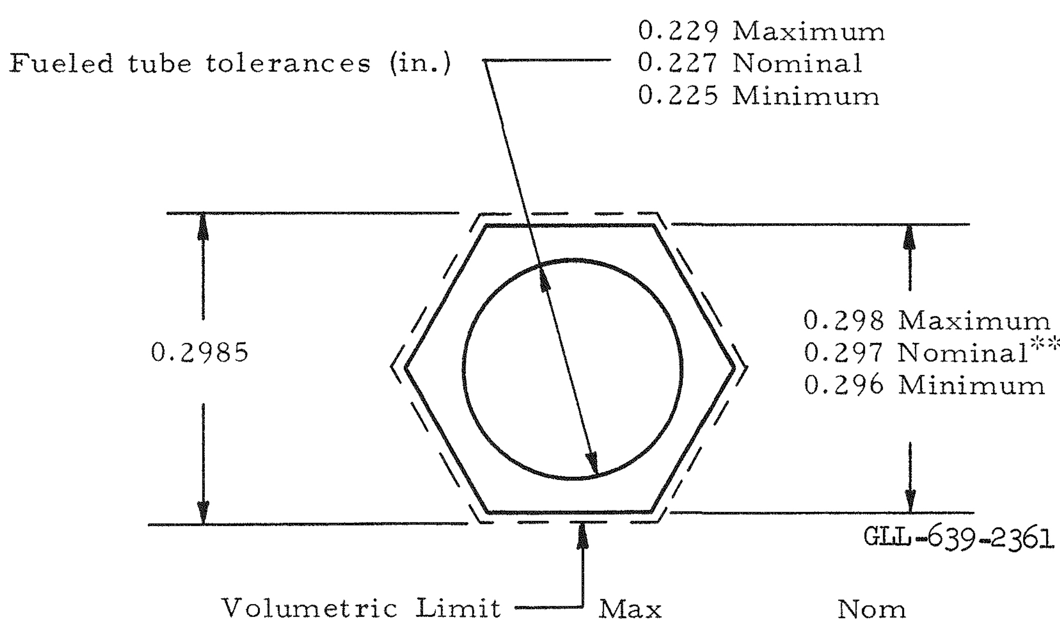

	Max	Nom	Min
Hole area, in^2	0.0412	0.0405	0.0398
BeO area, in^2	0.0371	0.0359	0.0347
Total area, in^2	0.0769	0.0764	0.0759
Porosity: $\frac{\text{Hole area}}{\text{Total area}}$	0.5428	0.5298	0.5170

---

*Not allowing for thermocouple wireways.

**In considering a matrix of seven or more tubes, a stacking allowance of 0.0004 in./tube should be added to the flat-to-flat dimension.

ii. Unfueled Tubes

Material	BeO
Theoretical density	3.01 g/cc
Minimum specified density (96.3% theoretical)	2.90 g/cc
Total number of unfueled tubes	171,267 (see p. III-23 for breakdown)

	Forward reflector	Guard tubes	Side reflector
Nominal hole diameter, in.	0.227	0.130	0.093
Nominal distance across flats, in.*	0.297	0.295	0.296
Reference drawing	62-102881	62-102883 62-128625	62-105506
Hole area, in^2	0.0405	0.0133	0.0068
BeO area, in^2	0.0359	0.0621	0.0691
Weight/linear inch, g (nominal dimensions):			
@ Theoretical density	1.771	3.061	3.405
@ 96.3% theoretical density	1.707	2.952	3.283
Porosity:			
$\frac{\text{Hole area}}{\text{Total area}}$	0.5298	0.1764	0.0895

*In considering a matrix of seven or more tubes a combined tolerance buildup of 0.0004 in. across flats per tube is assumed. Therefore, flat-to-flat dimensions of 0.2974 and 0.2964 for forward and side reflector tubes, respectively, should be used for dimensional analyses.

iii. Nickel Tubes

Location	See pp. III-22, 28
Material	Nickel 200
Configuration	See p. III-27
Number of tubes in active core region . .	1620
Number of tubes in side reflector region .	303

Weight of tubes in active core region . .	13.3 lb
Weight of tubes in side reflector region . .	2.49 lb
Void outside nickel tube	0.00889 in^3
Density	8.86 g/cm^3

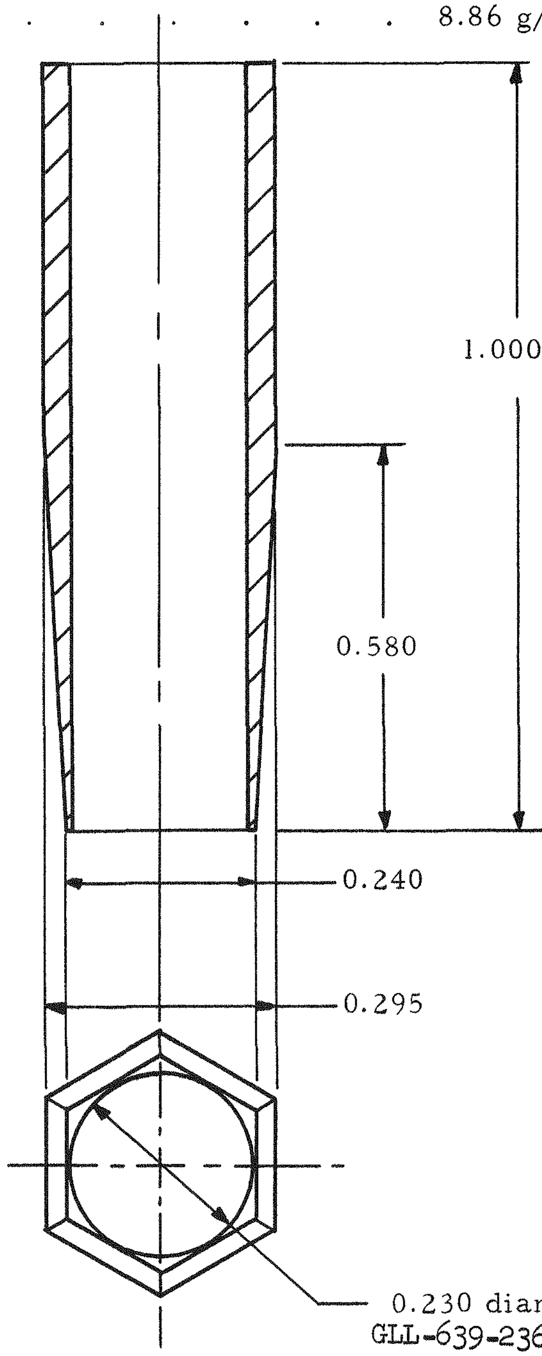

Nickel tube, used to prevent gross misalignment between front reflector and active core (all dimensions in in.).

Arrangement of Nickel Tubes

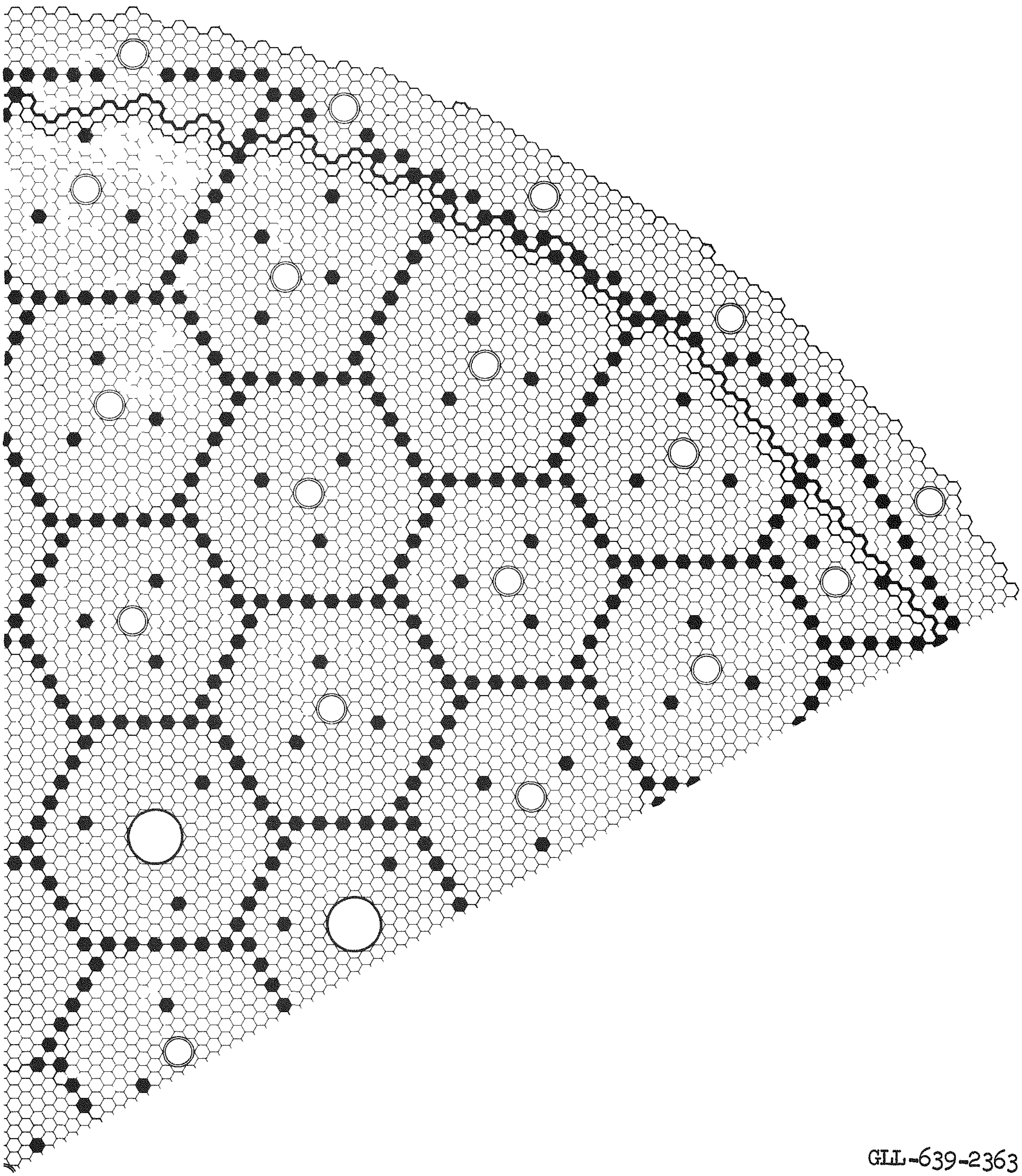

GLL-639-2363

iv. Peripheral Shims

Location, arrangement, and cross sections of shims	See pp. III-17, 32, 56
Material	Grade "A" nickel
Average annular thickness	0.96 in.
Frontal areas	See p. III-18
Total number of flow channels	1062
Number of standard flow channels . . .	942
Number of flow channels adjacent to alignment keys	120
Standard flow channel diameter . . .	0.130 in.
Total porosity	0.1053
Flow porosity (within a 26.441-in. radius) .	0.1559
Length of shim "column"	62.564 in.
Shim lengths	3.925 in. (15 per column)*
	1.205 in. (1 per column)
	2.384 in. (1 per column)
Circumferential gap between shims . . .	0.040 in.
Shim quantities, weights, volumes . . .	See p. III-31

* The aftmost shim is of modified design due to base block and side support spring requirements.

Peripheral shim data. See p. III-17 for shim identification.

Shim No.	Length (in.)	Drawing No.	No. of flow channels (0.130 in.-diam)	No. of flow channels at keyways	Material* frontal area (in^2)	Volume* (in^3)	Weight* (lb)	Quantity
1	1.205	62-111532	14	2	2.16	2.60	0.83	6
	2.384					5.15	1.65	6
	3.925 (std)					8.48	2.72	84
	3.925 (aft)					7.39	2.37	6
2	1.205	62-111533	13	2	2.21	2.66	0.85	12
	2.384					5.26	1.69	12
	3.925 (std)					8.66	2.78	168
	3.925 (aft)					7.58	2.43	6 (rh)
								6 (lh)
3	1.205	62-111535	17	2	2.42	2.92	0.94	12
	2.384					5.77	1.85	12
	3.925 (std)					9.49	3.05	168
	3.925 (aft)					8.41	2.70	6 (rh)
								6 (lh)
4	1.205	62-111537	15	2	2.34	2.82	0.91	12
	2.384					5.57	1.79	12
	3.925 (std)					9.17	2.94	168
	3.925 (aft)					8.07	2.59	6 (rh)
								6 (lh)
5	1.205	62-111538	17	2	2.40	2.89	0.93	12
	2.384					5.72	1.84	12
	3.925 (std)					9.42	3.02	168
	3.925 (aft)					8.33	2.67	6 (rh)
								6 (lh)
6	1.205	62-111540	19	2	2.56	3.08	0.99	6
	2.384					6.10	1.96	6
	3.925 (std)					10.05	3.23	84
	3.925 (aft)					9.09	2.92	6
			Reactor totals		140.6	8733	2803	1020

*Including keys.

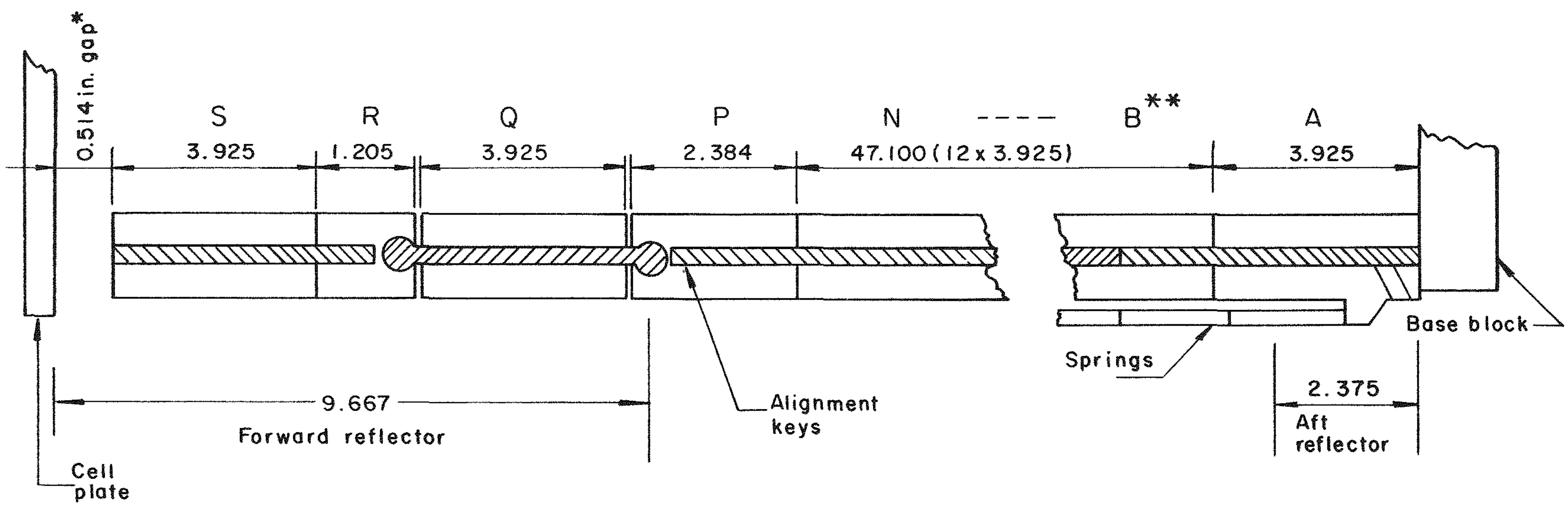

**Except "I"

GLL-639-2364

Longitudinal arrangement of peripheral shims. * Gap will be distributed between shims.

v. Aft Reflector

Material	Chromium-5% MgO
Aft reflector configuration and part arrangement	See p. III-34
Aft reflector Cr-MgO transition part volumes, weights, and quantities . .	See p. III-35
Average aft reflector thickness . . .	2.375 in.
Aft reflector volume	4219.7 in^3
Volume fractions	
BeO	0.236
Chromium parts	0.195
Tie rod material	0.006
Void	0.563
	1.000

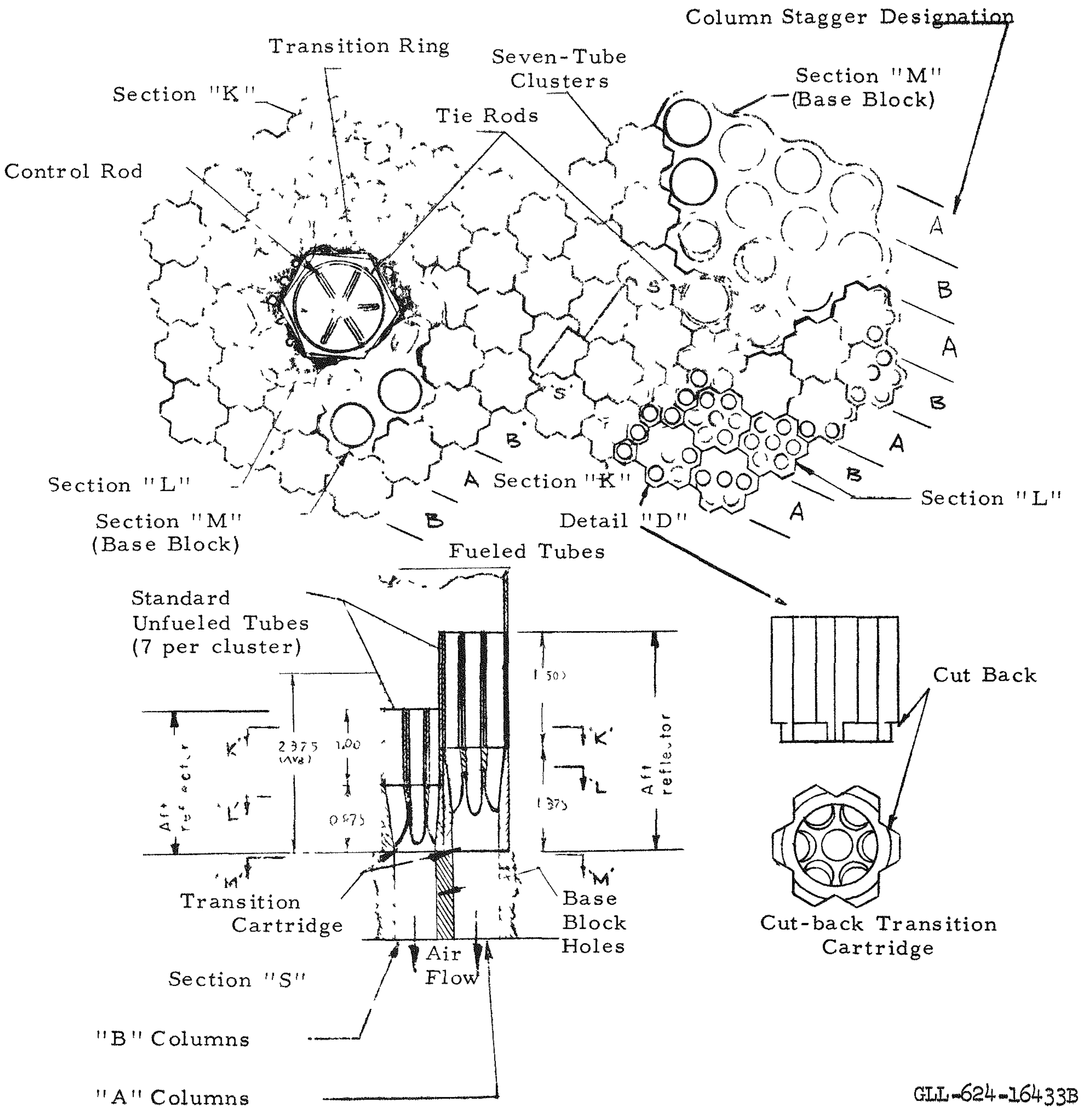

Aft reflector general arrangement, view looking downstream.

Aft reflector transition parts: weights, volumes, and quantities.

Item	Length, in.	Drawing No.	Quantity	Volume each, in^3	Weight each, lb	Total weight, lb
Cartridge, std.	1.375	62-116987	590	0.324	0.0766	45.1
	0.875		578	0.196	0.0464	26.8
Cartridge, std., cut back	1.375	62-116991	740	0.313	0.0741	54.8
	0.875		748	0.186	0.0440	33.0
Cartridge, type A	1.375	62-116990	218	0.329	0.0779	16.9
	0.875		208	0.200	0.0471	9.7
Cartridge, type A, cut back	1.375	62-116988	8	0.320	0.0755	0.6
	0.875		4	0.189	0.0447	0.2
Tube, type B (1)	1.375	62-102685	52	0.057	0.0136	0.7
	0.875	62-102410	56	0.038	0.0090	0.5
Tube, type B (2)	1.375	62-102688	52	0.057	0.0136	0.7
	0.875	62-102413	56	0.038	0.0090	0.5
Rings	1.375	62-109494	10	0.953	0.226	2.3
	1.375	62-109496	8	1.123	0.266	2.1
Totals			3328			194

vi. Forward Reflector Inserts

Material	Stainless steel type 410	
Weight	120 lb	
Length of insert "stack"	10.23 in.	
Number of inserts per standard tie rod .	15	
Number of inserts per control tie rod . .	15	
Total number of inserts	1815	
	Standard insert	Control rod insert
I. d.	1.090 in.	1.605 in.
Nominal radial clearance between insert and tie rod	0.210 in.	0.191 in.
Nominal radial clearance between insert and BeO	0.005 in.	0.005 in.

Insert type	Drawing No.	Length	Max mat'l frontal area	Quantity
Standard Insert				
Key block	AAA62-117000	6.164 in.	0.485 in^2	103
Tie rod	AAA62-116971	0.250 in.	0.188 in^2	1,236
Insert "A"	AAA62-111893	1.000 in.	0.698 in^2	103
Core face	AAA62-116116	0.500 in.	0.382 in^2	103
			Total	1,545
Control Rod Insert				
Key block	AAA62-116970	6.164 in.	0.602 in^2	18
Tie rod	L13C4112	0.250 in.	0.446 in^2	216
Insert "B"	AAA62-111895	0.500 in.	1.254 in^2	18
Core face	L13C4123	0.500 in.	0.434 in^2	18
			Total	270

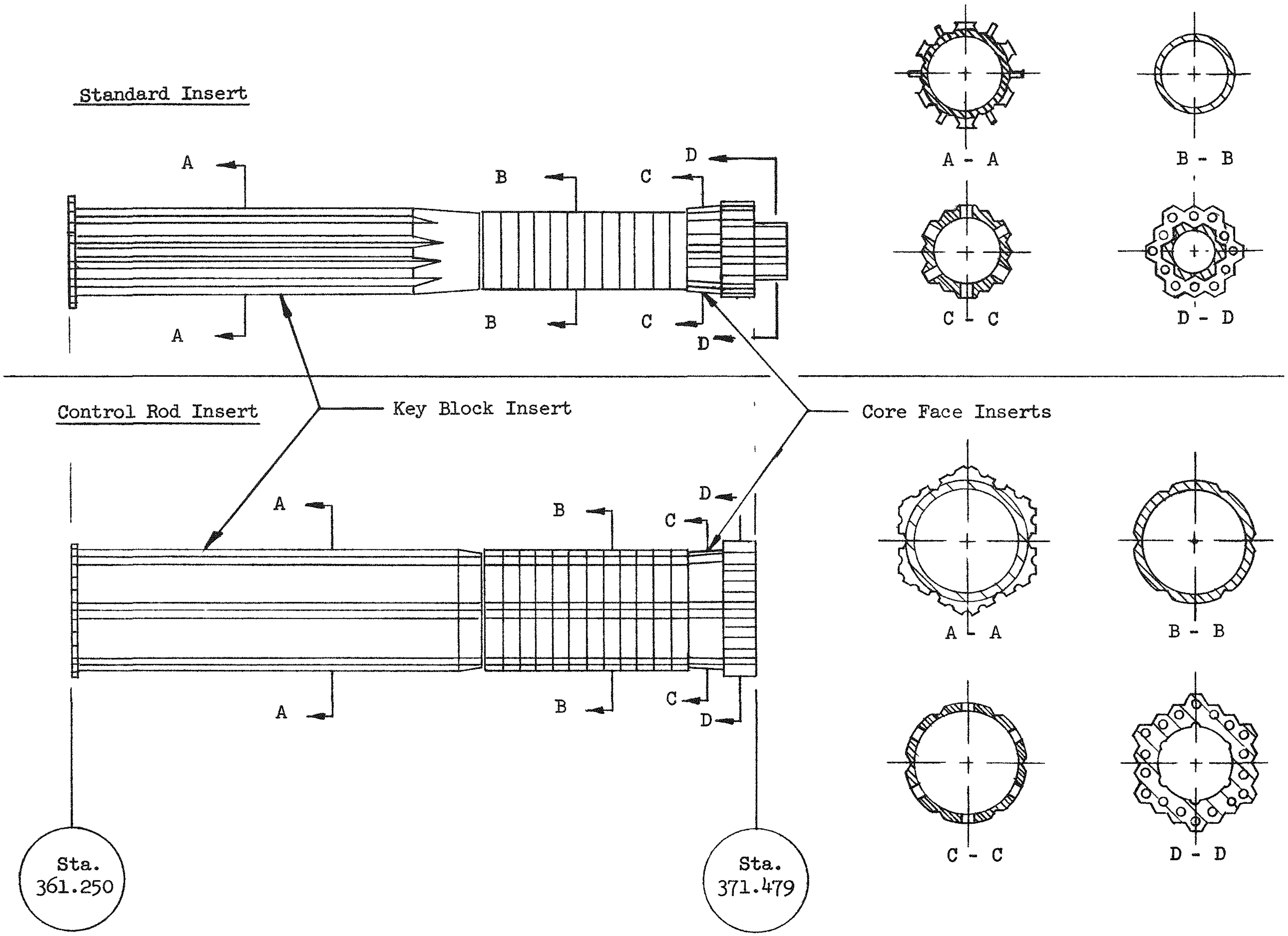

GLL-639-2365

Forward reflector inserts.

b. Tie Rod Assembly

Materials	René 41 and Hastelloy R-235	
Total weight, lb	325	
Total number of tie rods	121	
	Standard tie rod	Control tie rod
Assembly drawing number	L16B9984	62-100009
Length of assembly, in.	80.70	80.875
Total number of tie rods	103	18
Number of René 41 tie rods	69	12
Number of R-235 tie rods	34	6
Tie rod o.d., in.	0.670	1.222
Tie rod i.d., in.	0.576	1.162
Wall thickness, in.	0.047	0.030
Minimum i.d. at forward end, in.	0.477	1.162
Aft flange o.d., in.	1.100	1.600
Aft flange length, in.	0.500	0.500
Average tie rod weight, lb/in.	0.0267	0.0297
Tie rod nut		
I.d., in.	0.600	1.314
O.d., in.	1.000	1.480
Flange diameter	1.375	2.062
Length, in.	2.030	2.093
Threads	0.675-7 (rh)	0.693-8 (rh)
Insulating cup		
Material	Platinum-5% Ruthenium, coated	
I.d., in.	1.102	1.634
Depth, in.	0.850	0.850
Wall thickness, in.	0.044	0.060
Weight, lb	0.094	0.139
Coating	Rokide "A", 0.010 in. thick	
Insulating washers		
Material	Hastelloy "C"	
Number of washers per tie rod	5	5
O.d., in.	1.107	1.648
I.d., in. (small)	0.676	1.441
I.d., in. (large)	0.698	1.258
Thickness, in.	0.06	0.06

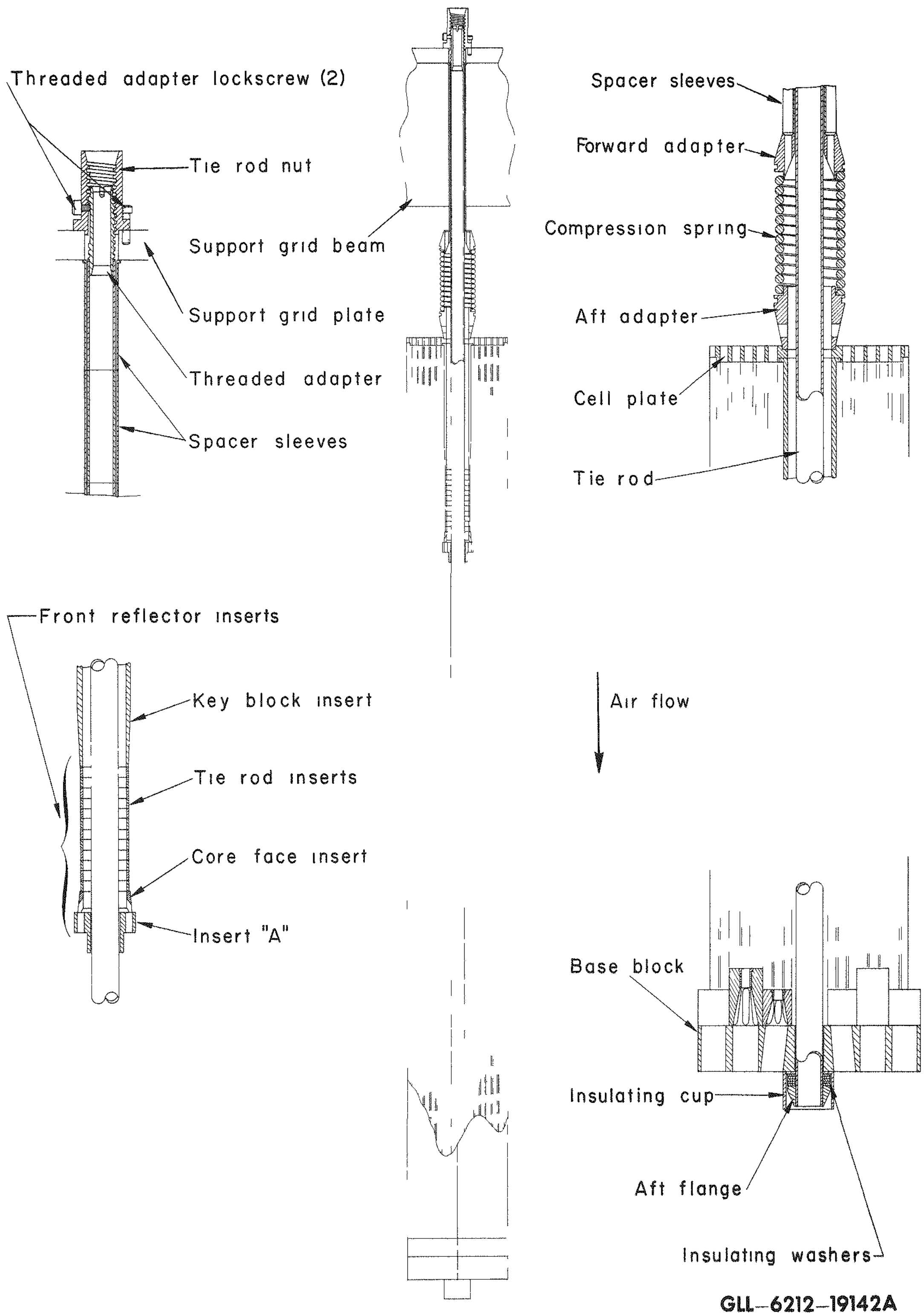

Standard tie rod assembly (not to scale).

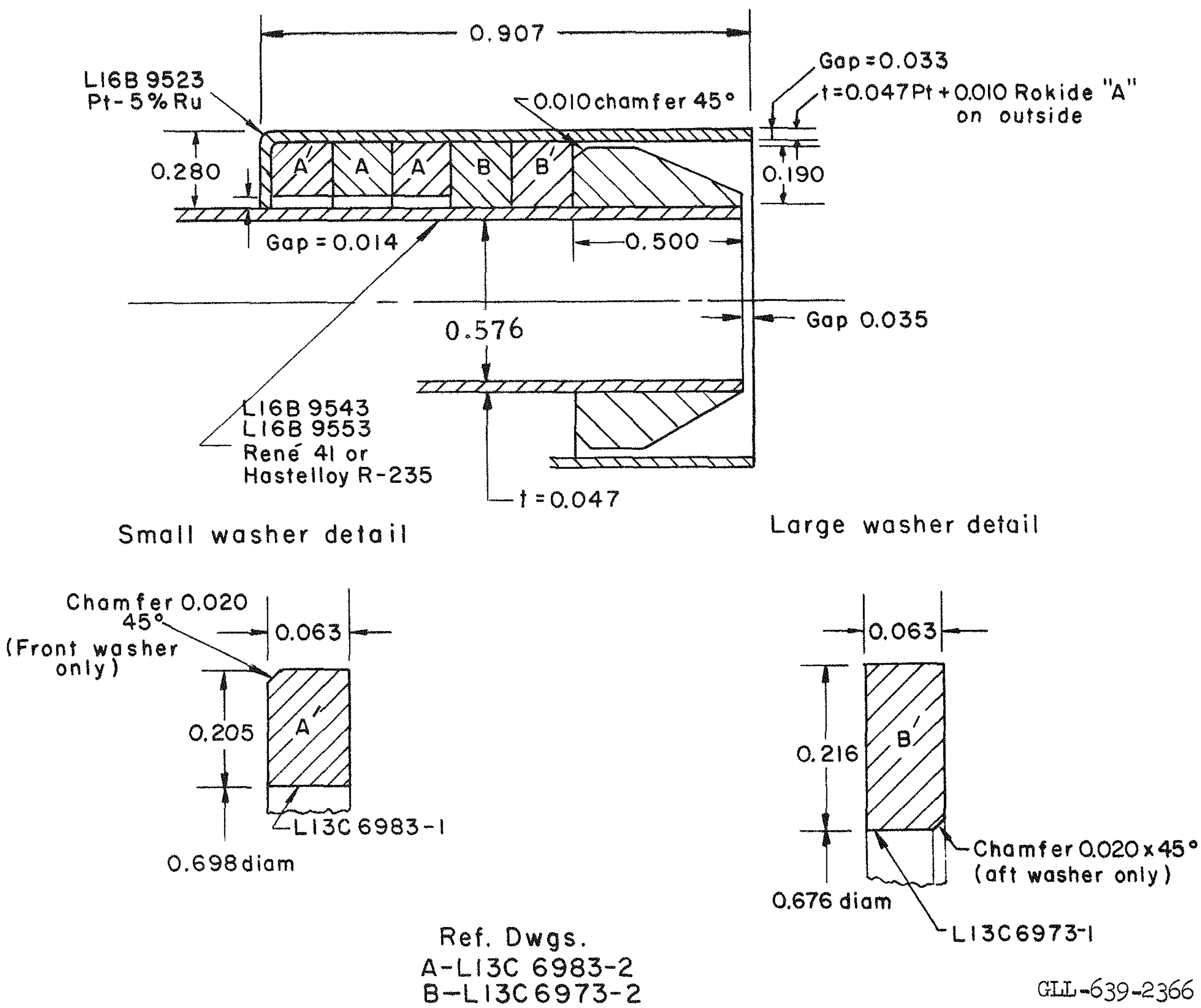

Standard tie rod: aft end detail (all dimensions in inches).

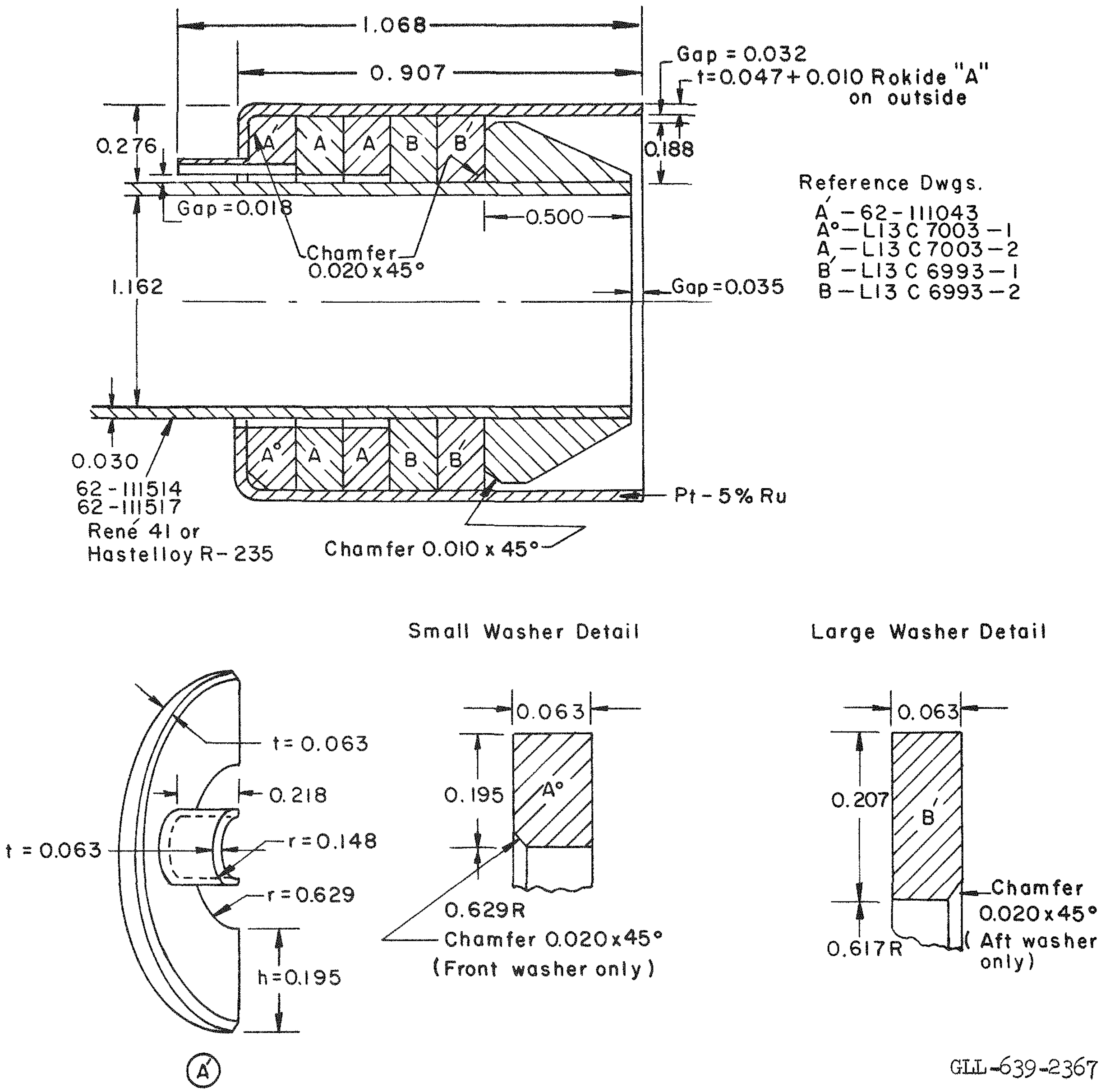

Control tie rod: aft end detail (all dimensions in inches). Note all washers are semi-circular.

c. Cell Plate Installation*

Quantity	91	
Total weight, lb	287	
i. Cell Plate		
Material	SS type 410	
Thickness, in.	0.375	
Additional data	See p. III-44	
Nominal hole diam, active core, in.	0.232	
Nominal hole diam, side reflector, in.	0.232	

	Standard tie rod	Control tie rod
ii. Aft Adapter		
Material	SS type 410	SS type 410
Drawing number	61-914916	61-914948
Number of adapters	103	18
Weight, ea., lb	0.2	0.2
Maximum o. d., in.	1.7	2.0
I. d., in.	1.1	1.6
iii. Compression Spring		
Material	Inconel X	Inconel X
Drawing number	63-107552	63-107554
Number of springs	103	18
O. d., in.	1.75	2.06
I. d., in.	1.32	1.60
Wire diameter, in.	0.207	0.225
Spring constant, lb/in.	62.4	56.8
Free length, in.	5.297	5.81
Fully compressed length, in.	2.90	2.93
Assembly preload, lb	135	139
iv. Forward Adapter		
Material	SS type 410	SS type 410
Drawing number	61-914917	61-914949
Number of adapters	103	18
Weight, ea., lb	0.1	0.1
Maximum o. d., in.	1.7	2.0
I. d., in.	1.1	1.6

*See page III-39 for sketch.

v. Spacer Sleeves

	Standard	Control cell
Material	SS type 410	SS type 410
Drawing number	62-100862 62-100858	62-100054
Total number of spacers . .	309	54
Number of spacer/tie rod . .	3	3
O. d., in.	0.800	1.562
I. d., in.	0.710	1.262
Wall thickness, in.	0.045	0.150 max 0.050 min
Nom. length of spacer "stack," in.	7.9	8.1
Nom. length of each spacer, in. .	2.635	2.710

Cell plate data.

Type	Number of each type	Drawing number	Number of flow channels*	Total frontal area, (in^2)	Total porosity	Weight each,** (lb)	Total weight, (lb)
A (standard cell)	43	L16B1424F	217 holes 42 slots	19.5	0.561	0.82	35
B (control cell)	18	L13C4514E	199 holes 42 slots	19.5	0.578	0.75	13
Reactor Periphery:							
C	6	L13C6836C	421 holes 60 slots	41.3	0.504	1.50	9
D	6	L13C6846C	365 holes 54 slots	32.1	0.571	1.31	8
E	6	L13C6856C	308 holes 52 slots	30.8	0.516	1.15	7
F	6	L13C6816C	378 holes 56 slots	37.9	0.500	1.34	8
G	6	L13C6826C	429 holes 55 slots	37.6	0.561	1.52	9
						Total reactor	89

*Not all flow channels are the same size since the tie rod holes are included in this tabulation.

**Weights are based on representative parts.

d. Base Blocks

Number of base blocks	91
Location, arrangement, and identification	See p. III-47
Material	79Cb-15W-5Mo-1Zr (Du Pont D-40) coated
Coating	Dual cycle Si/Cr-FeB
Coating thickness, in.	0.005
Base block thickness, in.	1.110 (uncoated)
Additional base block data	See p. III-46

Base block data.

Block type	No. of each type	Drawing No.	No. of flow passages	Overall frontal area* (in^2)	Total porosity	Weight each** (lb)	Total weight (lb)
A (standard block)	43	L12E9444	36	20.127	0.523	3.40	146.2
B (control block)	18	L16B2784	36	20.127	0.536	3.11	56.0
C	6	L16B7966	199	36.11	0.448	8.07	48.4
D	6	L16B7976	194	32.18	0.391	7.33	44.0
E	6	L16B7986	248	25.921	0.297	7.18	43.1
F	6	L16B7996	208	32.53	0.388	7.70	46.2
G	6	L16B8006	207	36.89	0.424	8.19	49.1
Total	91						433.0

*Not all flow passages are the same size. All "flow" passages in the peripheral base blocks are included above but not all have flow.

**Weights are based on representative parts and include coating weight.

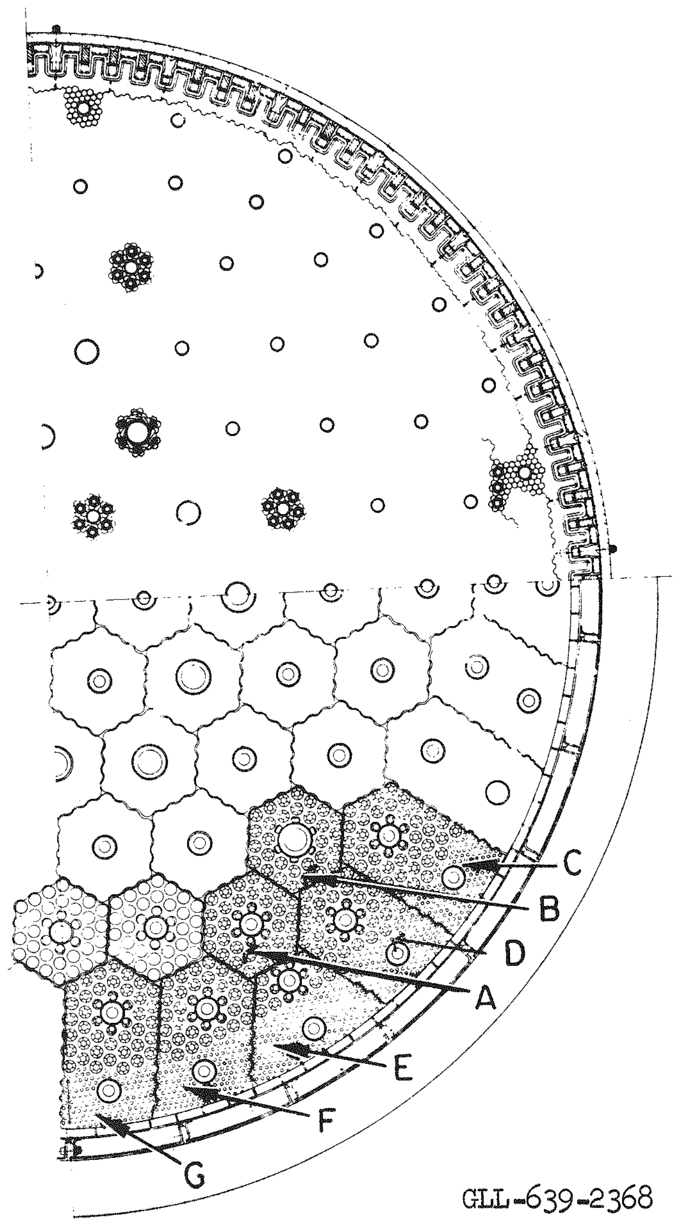

GLL-639-2368

Base block arrangement. View looking upstream. Note: Peripheral repeats (without inversion) each 60°.

e. Support Grid

Drawing number	62-109561
Weight	900 lb
Porosity: at front plate	0.74
at beams	0.83
Total depth of grid	8.50 in.
Beam orientation	Horizontal
Number of key positions (ring to duct)	12 radial (pins)
i. Ring	
Material	Hastelloy "C"
Drawing number	AAA61-133958
Maximum o. d.	56.062 in.
"Root" diameter	54.686 in.
I. d.	53.250 in.
Number of lugs	96
Circumferential lug width	0.938 in.
Axial lug depth	1.50 in.
Axial depth of ring	7.00 in.
Axial depth of beam grooves	2.00 in.
ii. Beams	
Material	René 41
Drawing number	AAA62-108279
Number of beams	12
Beam thickness	0.500 in.
Depth of beam	7.75 in.*
Method of assembly to ring	Tongue and groove
Axial depth of tongue	2.0 in.
Length of beams: longest beam	54.5 in.
shortest beam	30.9 in.
Beam spacing, o. c.: max	4.678 in.
min	3.208 in.

---

*The depth of several short beams has been decreased to control the deflection pattern of the support grid.

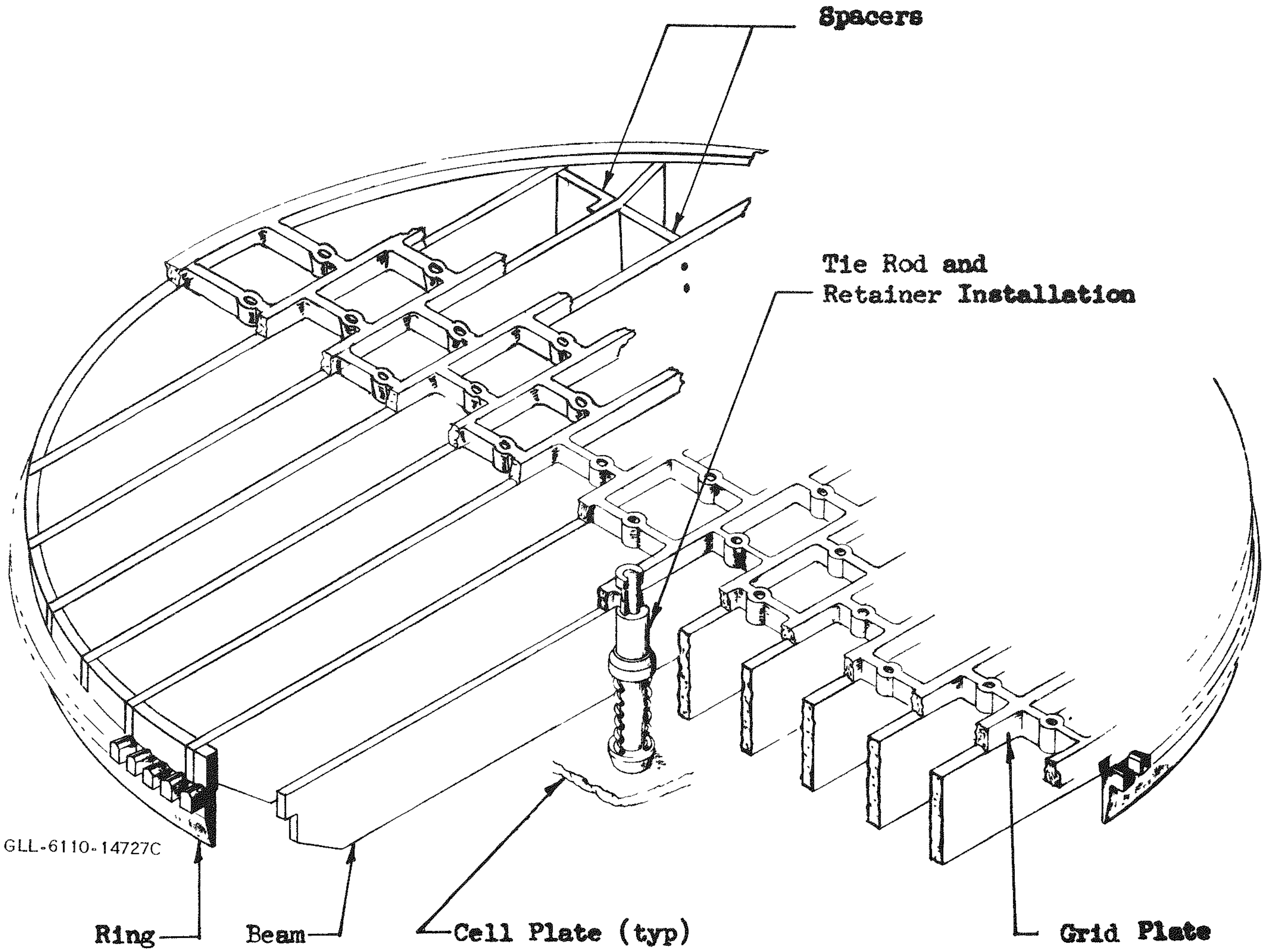

Support grid.

iii. Grid Plate

Material	René 41	
Drawing number	62-103338	
Thickness, in.	0.75	
Method of assembly	Bolted to ring and beams	

iv. Spacers

	Outer	Inner
Material	Hastelloy C	Same
Drawing number	62-108275	62-108278
Number of spacers	2	2

v. Ring Pin

Material	René 41
Drawing number	62-127080
Number of ring pins	12
Diameter	0.500 in.

f. Side Support System

Note: The nickel shims and aft reactor duct are, by definition, not part of the side support system, although many analyses of the system include these components. Unless otherwise stated, the following data does not consider the shims or the duct.

Assembly drawing number	See reactor assembly
Length of the system (from Sta. 361.313)	63.075 in.
Thickness (from av shim o. d. to duct i. d.) . . .	1.56 in.
Total frontal area	268.5 in^2
Material frontal area	100.7 in^2
Weight of the system	31 lb/axial in.
Surface density and weight data	See p. III-55
Preload	17 psi max 8 psi min

i. Spring Segment

Reference drawing	62-109268
Material	René 41
Number of springs	32
Width (axial), in.	
Standard	1.952
First	1.200
Sixth	1.387
Material thickness	0.150 in.
Depth (radial)	1.00 in. (center to center)
Pitch of spring corrugations	1.40 in. (3°)
Spring deflection characteristics	See p. III-54

ii. Support Rail

Reference drawings	Fwd AAA62-127093 Std AAA62-127098
Material	René 41
Number of support rails	510
Rail length	3.792 in.
Rail height (radial)	1.200 in.
Rail width	0.510 in.

iii. Wiper Bars

Reference drawing	
Wiper bar assembly, short	AAA63-109518
Material	Hastelloy "C"
Number of wiper bars	90
Long wiper bars	60
Short wiper bars	30
Wiper bar lengths	
Long wiper bar	76.184 in.
Short wiper bar	64.987 in.
Wiper bar height (radial)	1.10 in.
Wiper bar width	0.375 in.

iv. Wipers

	Wing wipers	Bar wipers	Rail wipers
Reference drawings	63-107561 63-107557	63-107561 63-107557	63-102788
Material	René 41	René 41	René 41
Number of wipers (circumferentially)	60	120	30
Total number of wipers	600	1200	300
Stock thickness, in.	0.022	0.022	0.022
Width	See p. III-53		

Wiper Widths

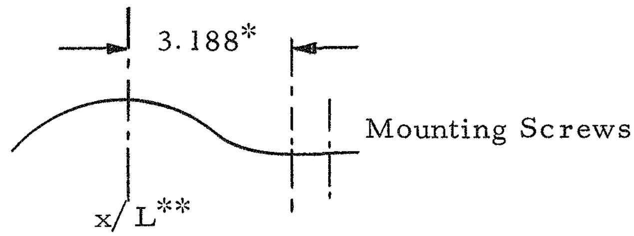

Wiper No.	x/L	Widths (in.) Bar	Wing	Rail
1	0.047	0.285	0.675	
	.059			0.345
2	.142	.285	.800	
	.155			.345
3	.237	.315	.900	
	.250			.345
4	.332	.310	.900	
	.345			.315
5	.427	.320	.950	
	.440			.315
6	.522	.275	.925	
	.535			.315
7	.618	.295	.950	
	.643			.290
8	.713	.315	.950	
	.738			.290
9	.808	.315	.975	
	.833			.290
10	.903	0.320	0.950	
	0.928			0.290

* Structural limit condition.

** x/L = 0 @ Sta. 361.3; L = 63.075.

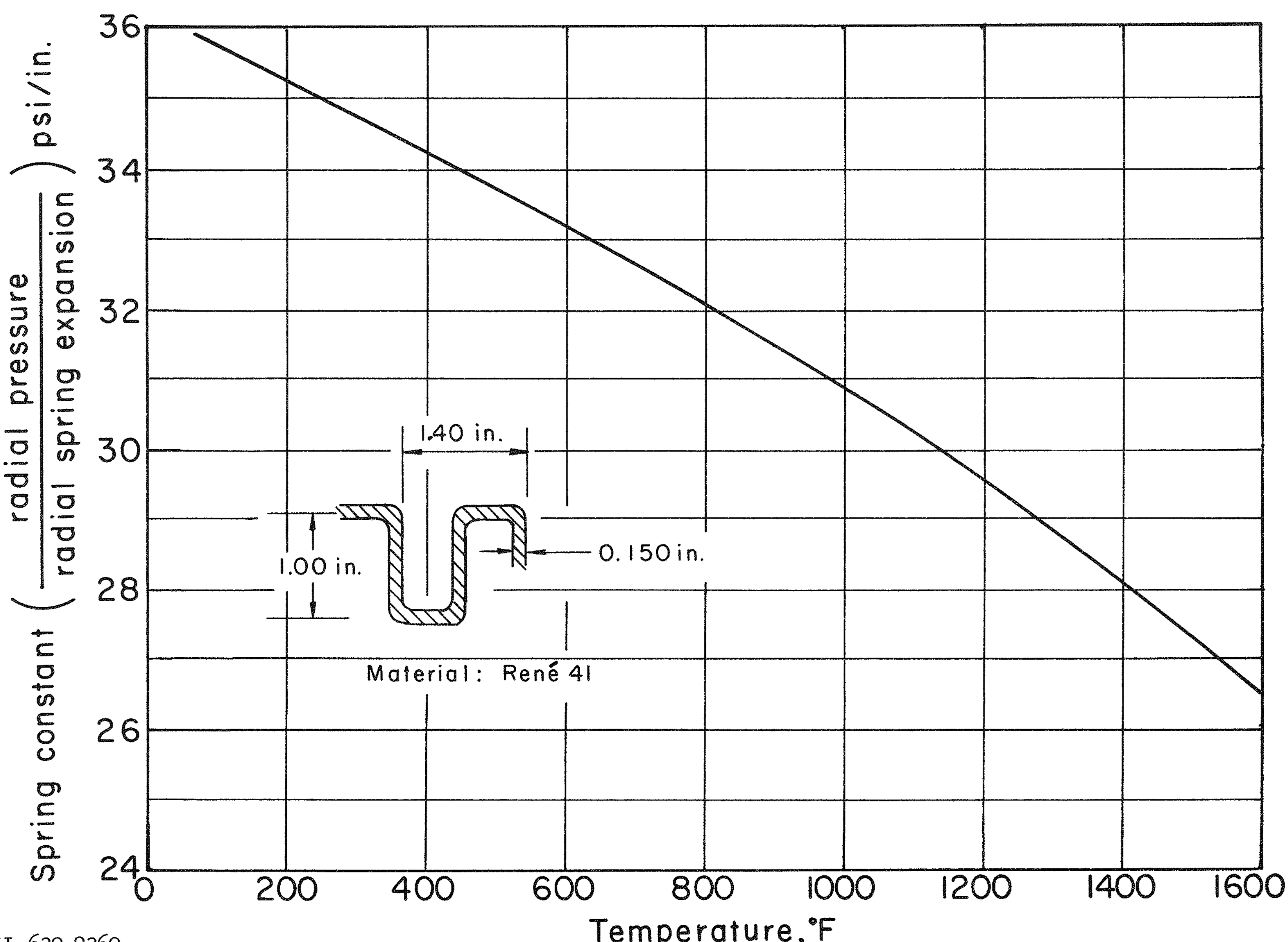

GLL-639-2369

Side support spring constant vs temperature.

Weight and surface density data for reactor components outside the BeO.

Component	Average material frontal area, in^2 6°	Average material frontal area, in^2 Total	Density, lb/in^3 (g/cm^3)	Weight, lb/axial inch 6°	Weight, lb/axial inch Total	Approx average radius (cold) (in.)	Surface density at approx average radius (g/cm^2)	Equiv. radial thickness, (cm)
Nickel shims* (Flow porosity within R = 26.441 : 0.1559)	2.344	140.64	0.321 (8.88)	0.752	45.15	26.3	19.21	2.33
Corrugated spring	0.966	57.96		0.288	17.27	27.1	7.13	0.87
Bar wipers	0.018	1.10	0.298 (8.25)	0.005	0.33	26.9	0.14	0.02
Wing wipers	0.044	2.65		0.013	0.79	27.8	0.32	0.04
Wing wiper supports	0.012	0.70		0.003	0.21	28.0	0.08	0.01
Support rails	0.171	10.27		0.051	3.06	27.8	1.23	0.15
Total René 41	1.21	72.7		0.36	21.7	27.5	8.9	1.1
Wiper bars	0.502	30.12	0.323 (8.94)	0.162	9.72	27.6	3.94	0.44
Aft reactor duct**	1.301	78.06		0.420	25.21	28.4	9.93	1.11
Total Hastelloy C	1.803	108.18		0.582	34.93	28.0	13.87	1.55
Totals	5.36	321.5		1.69	101.78	27.3	42.0	

*Material frontal area is for complete shim.

**Not part of the side support system.

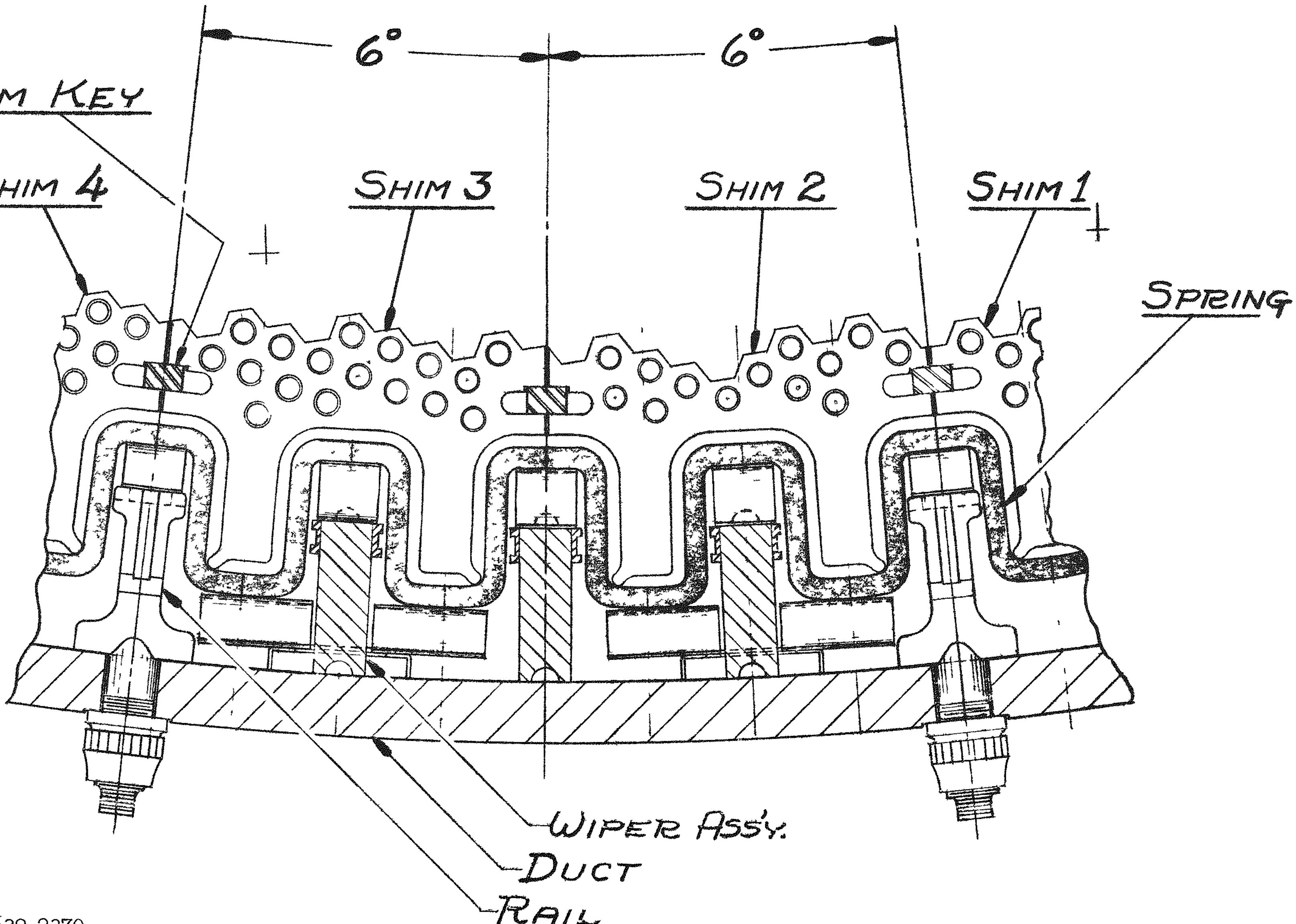

GLL-639-2370

Side support system.

g. Duct shroud

Purpose	Prevent reactor exhaust gas from contacting duct
Drawing number	See reactor assembly
Material	René 41
Weight	48 lb
I. d.	54.356 in.
Thickness	0.025 in.
Length	13.289 in.
Sketch	Attached to wiper bars

h. Control Rod*

Drawing number	62-115610
Absorber material	Hafnium
Minimum number of shim control rods	12
Maximum number of shim control rods	16
Number of vernier control rods	2
Weight each, lb	5.7
Rod shape	See p. III-58
Rod length, in.	63.25
Stroke, in.	40
Location of rod tip in the full-out position	Sta. 361.313 (forward face of forward reflector)
Maximum diameter, in.	1.130
"Leaf thickness," in.	0.084
Cross-sectional area, in^2	0.1845
Volume of absorber, in^3	12.0

*Each control rod has a central René 41 safety strap, 0.375 in. × 0.050 in. which is attached to the slider. The strap is designed to prevent the control rod from leaving the reactor should it break.

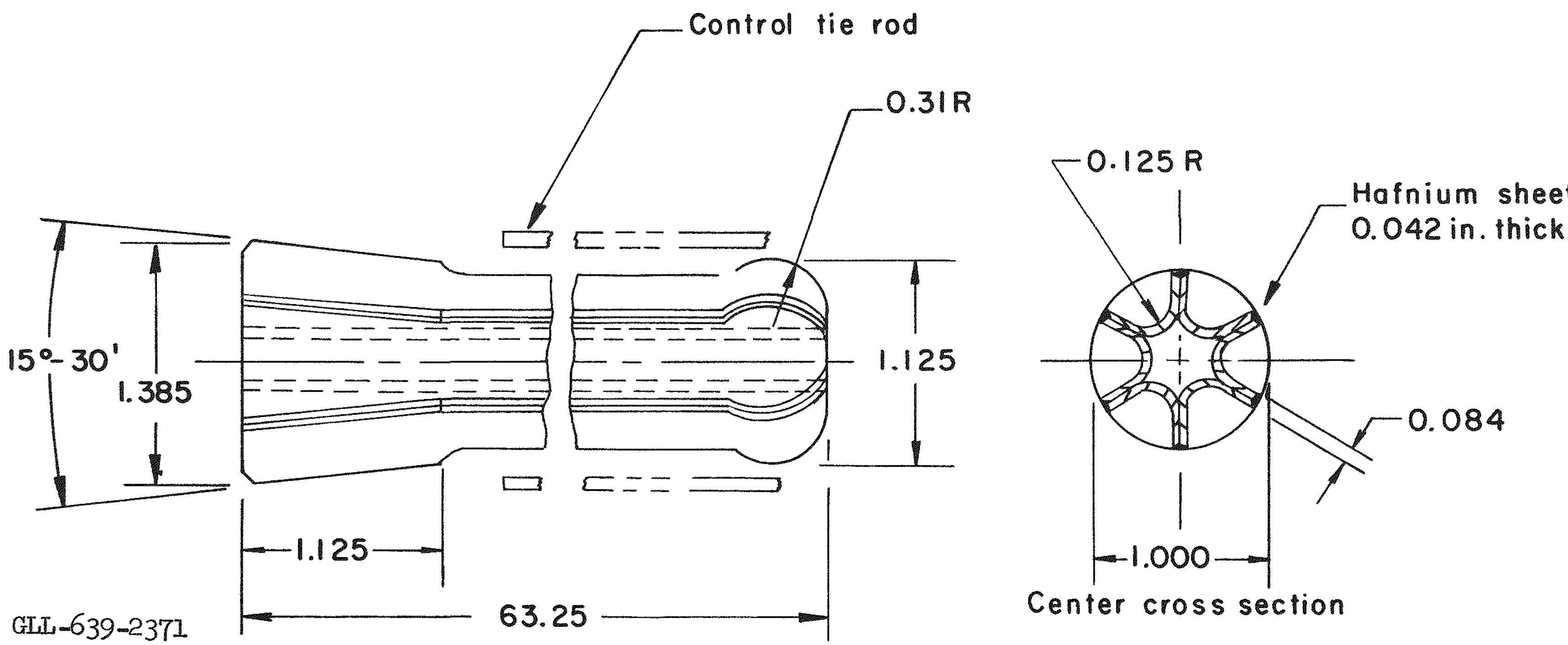

Control rod details (dimensions in inches).

i. Aft Reactor Duct

Drawing number	L16B3635
Material	Hastelloy "C"
Weight	4050 lb
Length	103.0 in. (from Sta. 338.00)
O. d. at reactor	57.250 in.
I. d. at reactor	56.375 in.
Flange o. d.	62.125 in.
Flange i. d.	56.250 in. (fwd. flange)
	56.375 in. (aft flange)
Number of support lugs (see p. III-60)	96 (at Sta. 351.00)
Lug height (radial)	0.730 in.
Lug width (circumferential)	0.896 in.
Lug depth (axial)	1.25+ in.
Number of instrumentation pass-through glands .	56 front
	8 rear

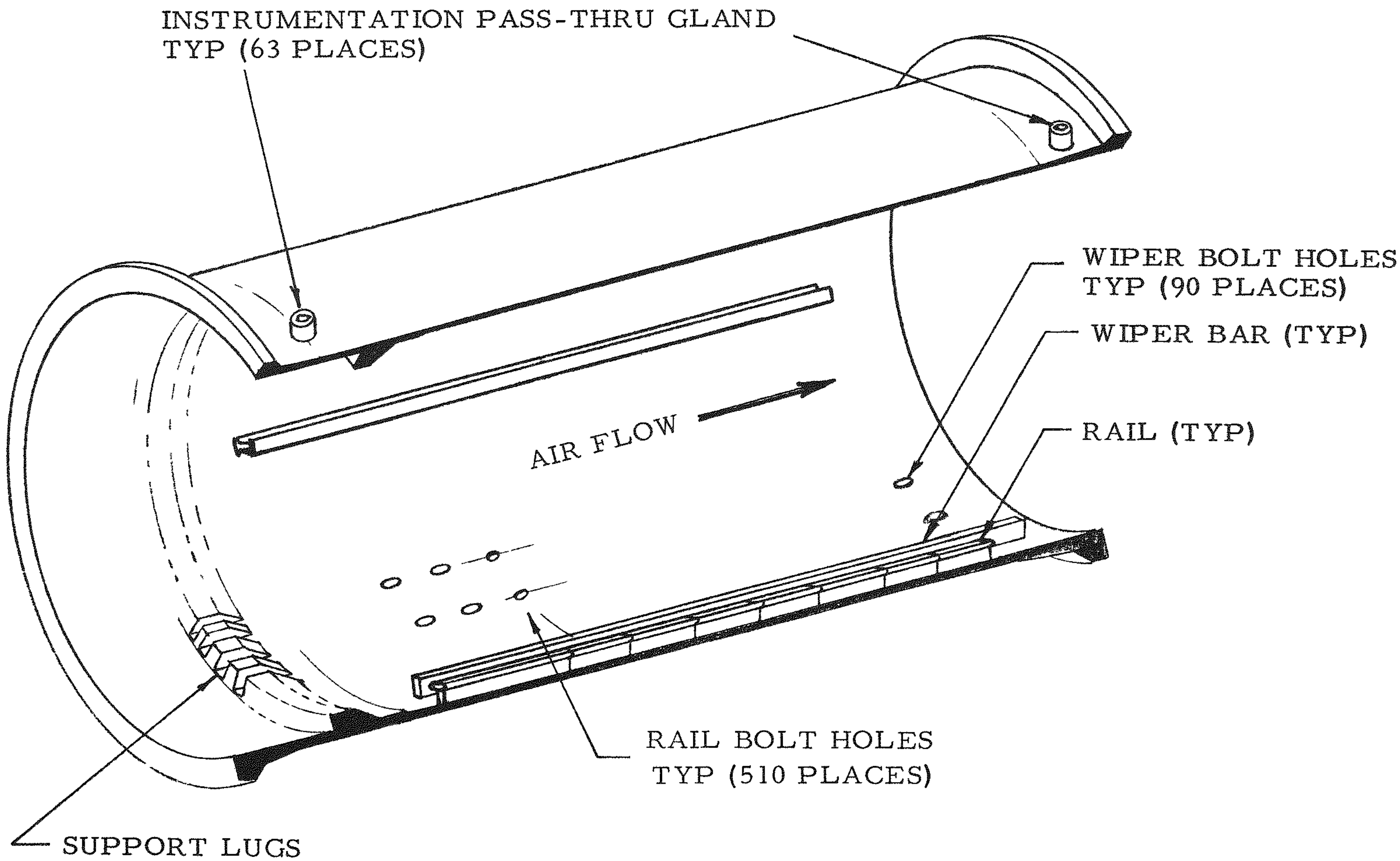

GLL-639-2372

Aft reactor duct.

2. Reactor Control System

Assembly drawing	62-126126	
Pneumatic system schematic	See p. III-65	
Control system arrangement	See p. III-66	
Actuator assembly schematic	See p. III-67	

a. Control Rod Actuator

i. Environment

Duct air temperature	0 to 1060°F
Duct air pressure	12 to 360 psia
Duct air velocity, max	100 ft/sec
Total radiation dose at Sta. 283	10^8 rads
Fast neutron dose	5×10^7 rads
Slow neutron dose	3×10^7 rads
Gamma dose	2×10^7 rads

ii. Actuator Mechanical Arrangement

	Shim	Vernier
Purpose	Large slow reactivity adjustments	Power control, fast reset, and calibration
Number of actuators	4	2
Number of control rods per actuator	3	1
Max cross-sectional area	95 in^2	55 in^2
Actuator weight	240 lb	220 lb
Weight of slider	17 lb	12 lb
Weight of control rods	18 lb	6 lb
Overall length (rack extended)	124 in.	Same
Servo drive	Rack & pinion	Same
Scram drive	Pneumatic piston, 10 in^2 area	Same
Stroke	40 in.	Same
Maximum overtravel		
Forward	1.5 in.	Same
Aft	3 in.	Same
Clutch	Torque limiting (pressure release on scram)	None
Transmission	56:1 two-stage planetary	None

	Shim	Vernier
Motor	Fixed displacement gear	Same
Servo control valve type .	Two-stage, four-way electro-pneumatic	Same
Position transducer type .	Linear variable differential transducer (LVDT)	Same
Full-in snubber type . .	Pneumatic	Same
Full-out snubber type .	Helical spring	Same
Scram lock	Spring-loaded pin	Same
Actuator mounting location .	Sta. 283	Same
Mechanical connection .	Three 3/4-in. bolts	Same
Electrical connection .	Ten pins at interface	Same
Pneumatic connection .	"K" seals at interface	Same

b. Supply and Control Package

Power medium	Air	Air
Air storage capacity (supplies both systems) . . .	5522 ft^3 @ 3600 psi or 103,000 lb at 60°F	
Filter	10-micron	
Servo supply pressure . . .	712 to 1060 psia	Same
Scram supply pressure . . .	1000 psia	Same
Servo pressure differential . .	700 psid	Same
Scram pressure differential .	1000 to 625 psid	Same
Maximum servo air temperature .	1060°F	Same
Maximum scram air temperature .	580°F	Same
Servo air pressure relief valve setting	1260 psia	Same
Scram air pressure relief valve setting	1200 psia	Same
Scram air orifice control valve .	Variable area controlled by duct pressure	Same
Receiver volume No. 1 . . .	900 in^3	Same
Receiver volume No. 2 . . .	37 in^3	None

c. Operational Characteristics

	Shim	Vernier
Operating flow rate per actuator at 700 psid	300 scfm, max	Same
Null flow rate per actuator at 700 psid	50 scfm, max	Same
Scram regulator flow rate @ 50 psid	0.43 pps	Same
Servo control valve requirements .	48 V, 0.6 A	Same
Servo supply valve requirements .	6 V, 0.8 A	Same
Clutch valve	48 V, 0.6 A	Same
Scram valve	48 V, 0.3 A	Same
Motor stall torque	±250 in.-lb	Same
LVDT		
Voltage	10 V rms	Same
Output gain	0.5 V/in.	Same
Output linearity (over environmental range) . .	±5%	Same
Resolution	±0.02 in. max	Same
Design friction load on control rod and slider	75 lb	25 lb
Aerodynamic load on control rod and slider	210 lb	70 lb
Rod position demand signals		
Full-out	+20 V dc	+10 V dc
Mid	+10	0
Full-in	0	-10
Stroke-to-signal ratio	2 in./V	2 in./V
Acceleration capability	15 g's	30 g's
Normal velocity	0.67 in./sec	1 in./sec
Saturation velocity	3 in./sec	170 in./sec
Deceleration, full-in	50 g's	100 g's
Deceleration, full-out	50 g's	50 g's
Scram insertion time	3 sec max	1.4 sec max
Stiffness	0.004 in./1000 lb	0.2 in./1000 lb
Closed-loop frequency	15 cps for ±0.2 in. demand amplitude; phase shift less than 90°	1 to 4 cps for 0.06 in. demand amplitude; phase shift less than 90°

	Shim	Vernier
Overtravel on step demand, greater of	2% or 0.02 in.	12% or 0.1 in.
Repeatability of position to signal .	± 0.02 in.	Same
Minimum gain margin . . .	6 dB	Same
Minimum phase margin . .	50°	Same
Result of electrical power failure .	Control rod is inserted due to mechanically biased servo valve	Same
Full stroke time: out . . .	120 sec max	–
in . . .	40 sec max (limited mechanically and electrically)	–

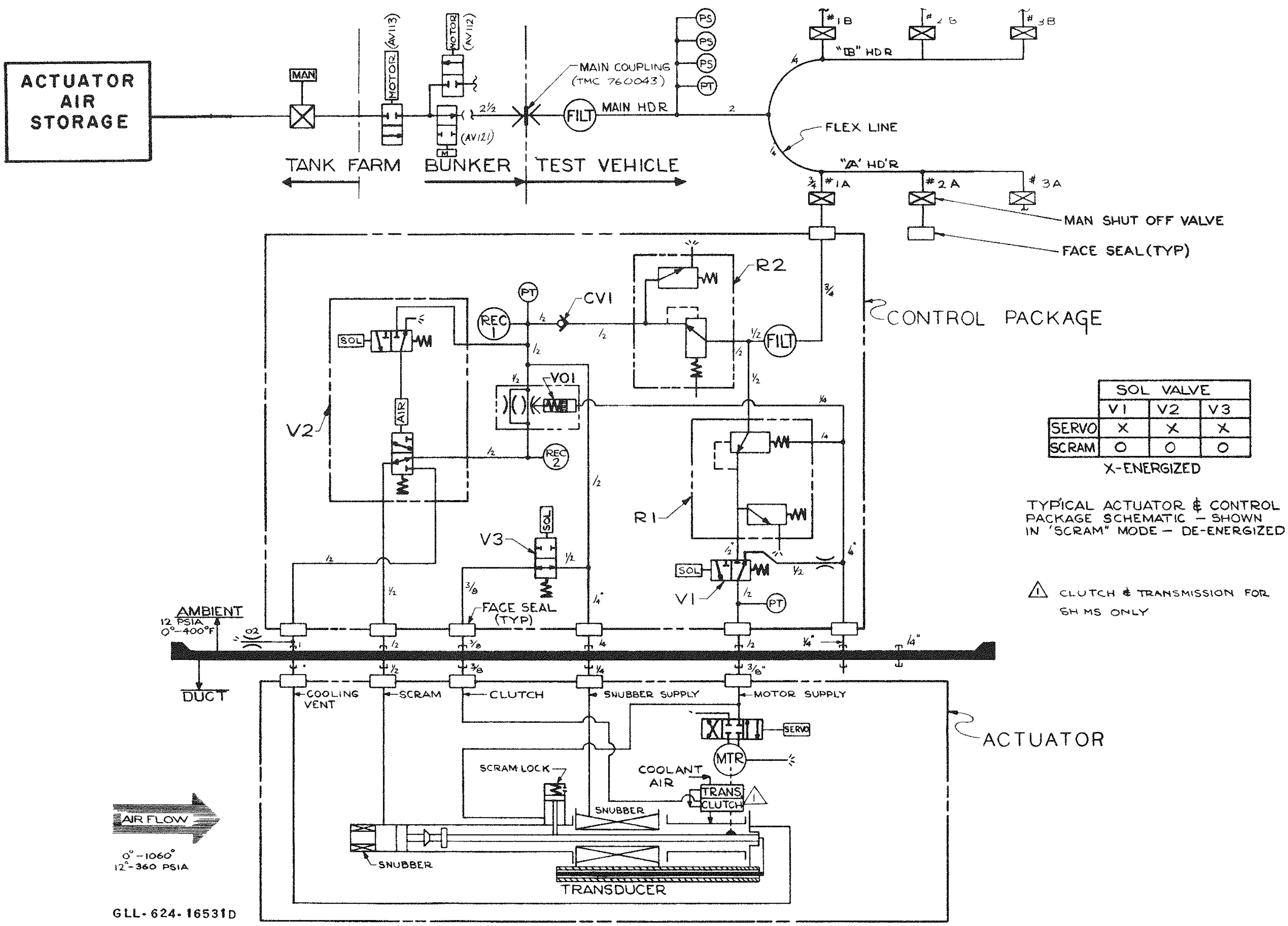

Reactor control system, pneumatic schematic.

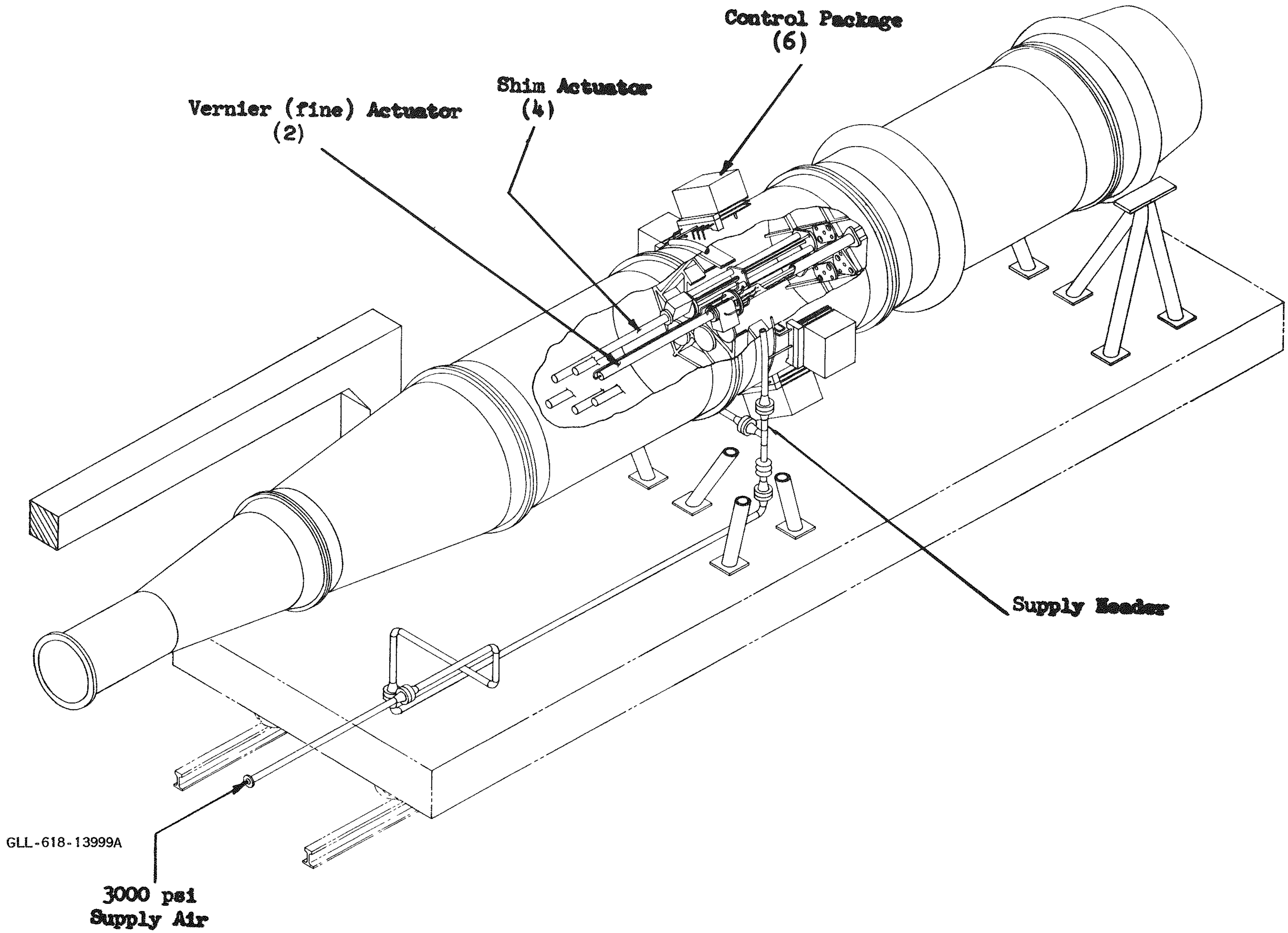

Reactor control system, general arrangement.

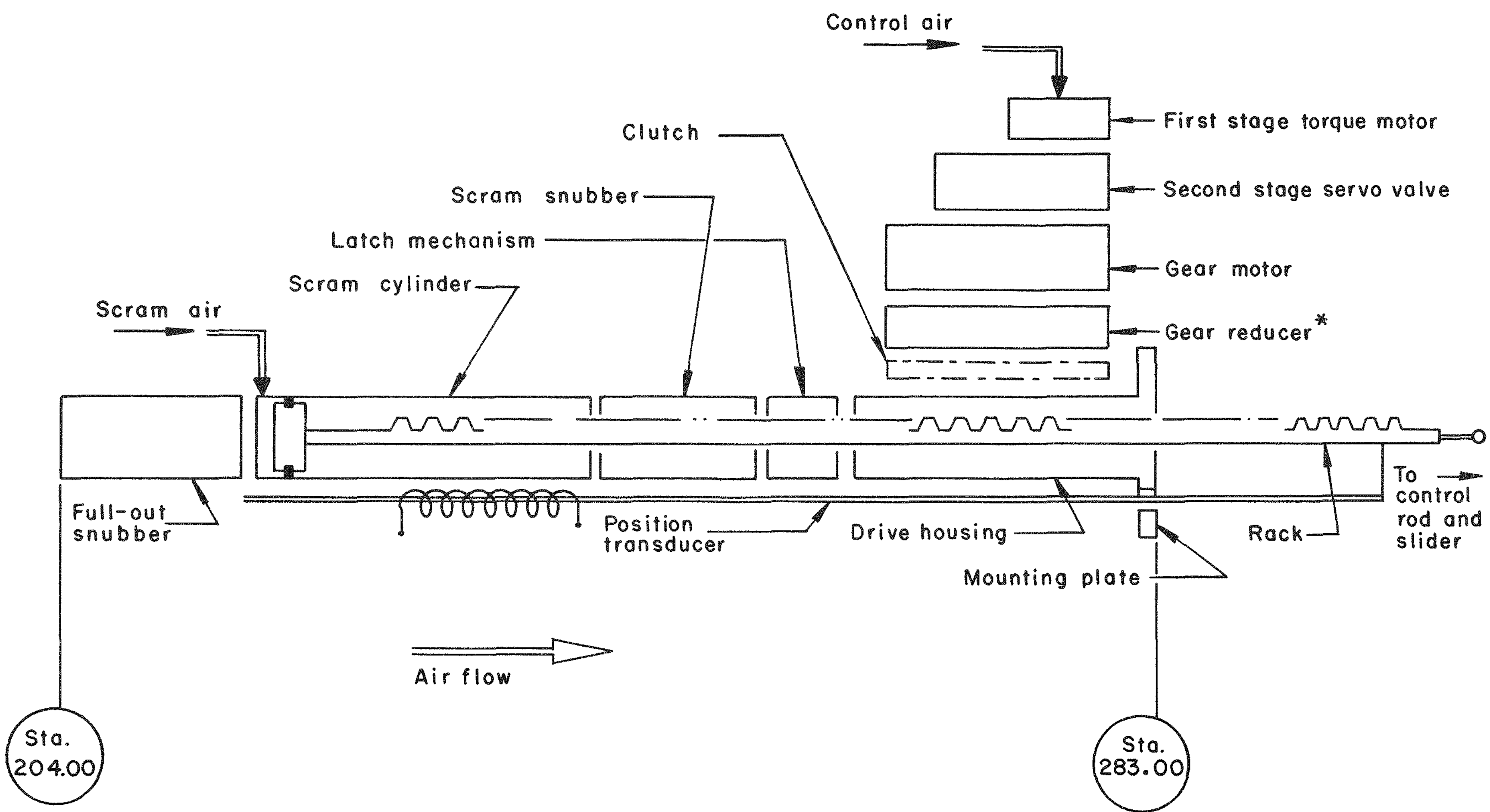

GLL-639-2373

Control actuator assembly. *The clutch and gear reducer appear on the shim actuator only.

3. Reactor Safety System

Purpose	Provide added safety for personnel. Allow checkout of control actuators. Shut down reactor in case of certain control system failure
Safety system sketch	See p. III-70
Environment, duct interior	Same as control actuator, see p. III-61
Environment, duct exterior	
Ambient temperature	0-120°F
Duct wall temperature	0-1100°F
Safety rod	
Drawing number	62-119024
Sketch	See p. III-71
Absorber material	Boron-10 carbide
Structural material	Hastelloy X
Number of rods	6
Configuration	Boron carbide-filled tube
Absorber length	45.75 in.
Overall length	47.25 in.
Absorber diameter	0.350 in.
Absorber area, minimum	0.0962 in^2
Absorber volume, minimum	4.40 in^3
Absorber weight, minimum	0.374 lb
Tube o. d.	0.400 in.
Tube area	0.0239 in.
Total weight	0.742 lb
Power source	
Drive system, arrangement	See p. III-72
Motor type	Dc Class C
Number of motors	2
Flexible cable type	"Teleflex"

Flexible cable o. d.	0.338 in.
Drive mode	Drive wheel engages helix on cable
Gear ratio	941:1
External lock	
Purpose	Prevent accidental removal of safety rod when personnel are present
Type	Removable mechanical stop
Operation	Manual
"Locked" position indicator	Red pennant
Rod position transducer type	Potentiometer
Operational characteristics	
Insertion depth in reflected reactor core	45 ± 1 in.
Travel	65 in.
Position transducer accuracy	±0.125 in.
Cable operating temperature, max	1200°F
Motor operating temperature, max	300°F
Maximum safety rod velocity (approx)	65 in./min

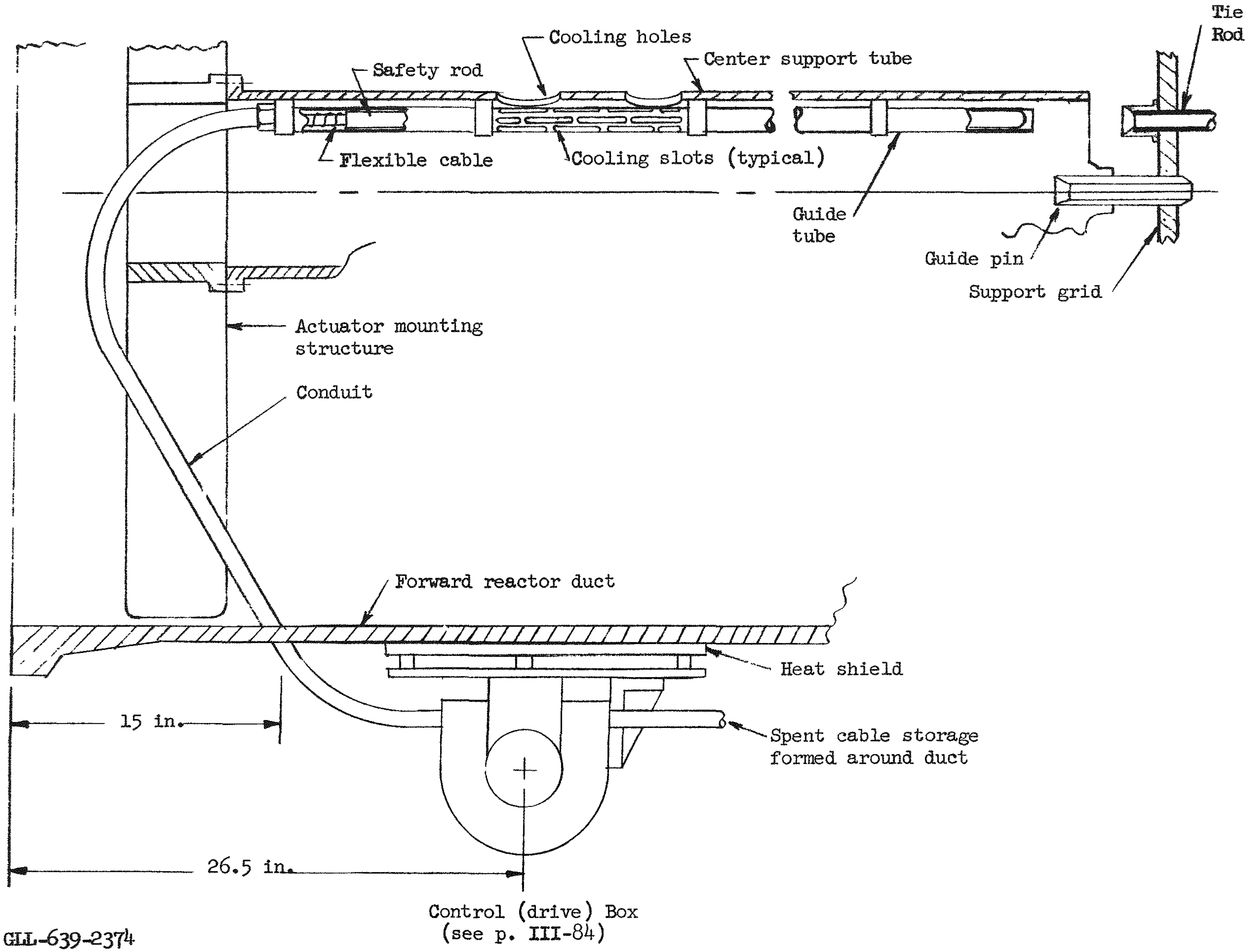

Reactor safety system general arrangement.

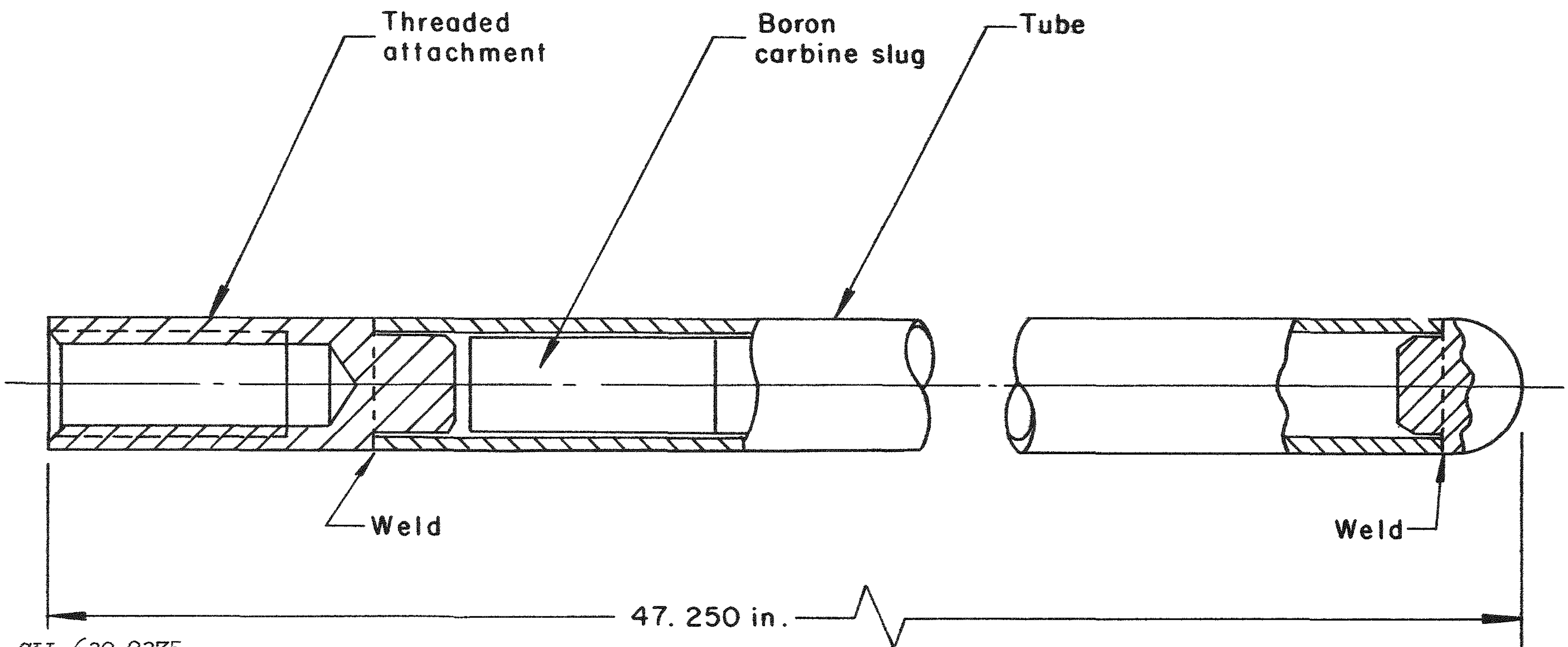

GLL-639-2375

Safety rod.

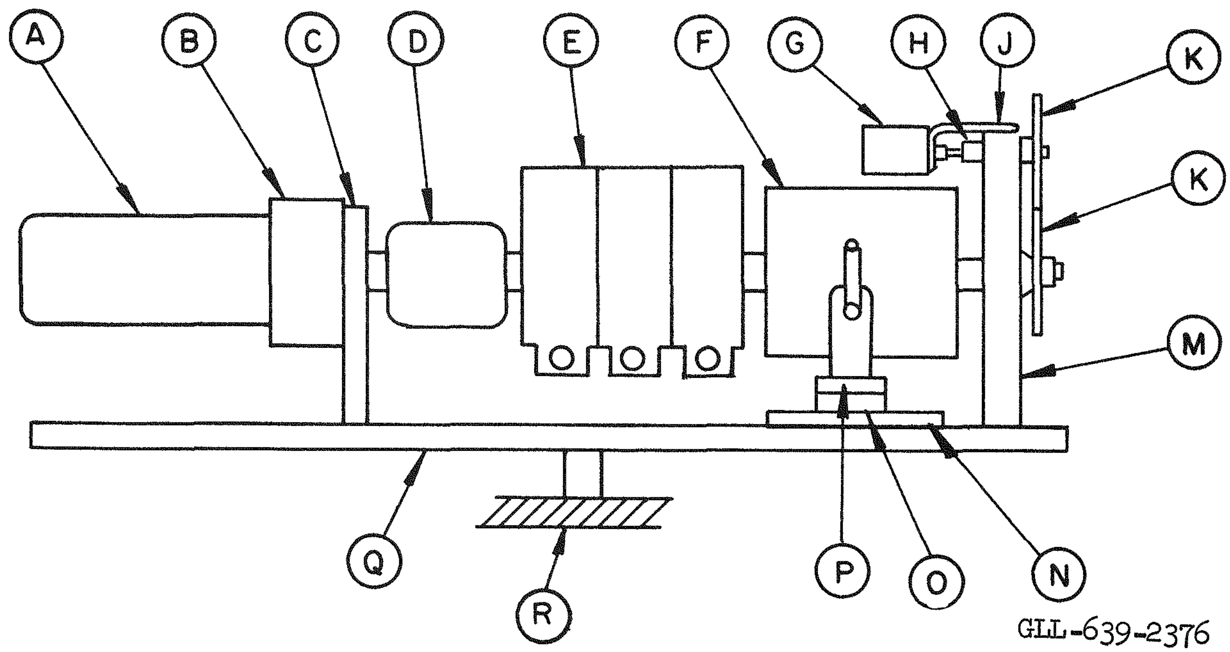

A. Electric drive motor

B. Gear speed reducer

C. Motor-reducer mounting bracket

D. Coupler – manual safety stop

E. Ganged Teleflex control boxes

F. Automatic safety stop, drum

G. Potentiometer

H. Potentiometer coupler and shaft extension

J. Potentiometer mounting bracket

K. Potentiometer gears

M. End support bracket

N. Lower "V" slide

O. Upper "V" slide

P. Microswitch support plate

Q. System mounting plate

R. Duct wall

Reactor safety system drive components.

B. TEST VEHICLE

1. Flat Car

Overall length of flat car	36.5 ft
Overall width of flat car	10 ft
Flat car bed (bottom of support pads) height above tracks in unloaded condition	34.625 in.
Height above tracks to duct centerline	8 ft
Flat car material	AISI 1020 steel
Method of fabrication	Weldment
Total weight of flat car (including duct support stands)	34,300 lb
Trucks	7,400 lb
Structural floor	25,100 lb
Support stands	1,800 lb
Wireway with cabling	3,500 lb
Thickness of flat car deck	0.375 in.
Distance between double axles	30 in.
Distance between front and rear axles	354 in.
Lifting lug material	AISI 1020 steel
Distance between lifting lugs	85.5 in.
Minimum track curvature	250 ft radius

2. Brake System

Brake location	Front truck wheels
Brake application method	Springs
Brake release method	Pneumatic
Brake fluid	Nitrogen
Nitrogen storage in cylinder	222 scf
Schematic of brake system	See p. III-74
Brake shoes	
Number	4
Material	Low carbon H. R. steel
Radius of curvature	10 in.
Length	8 in.
Width	3.093 in.
Distance from pin centerline to brake shoe surface	2.718 in.

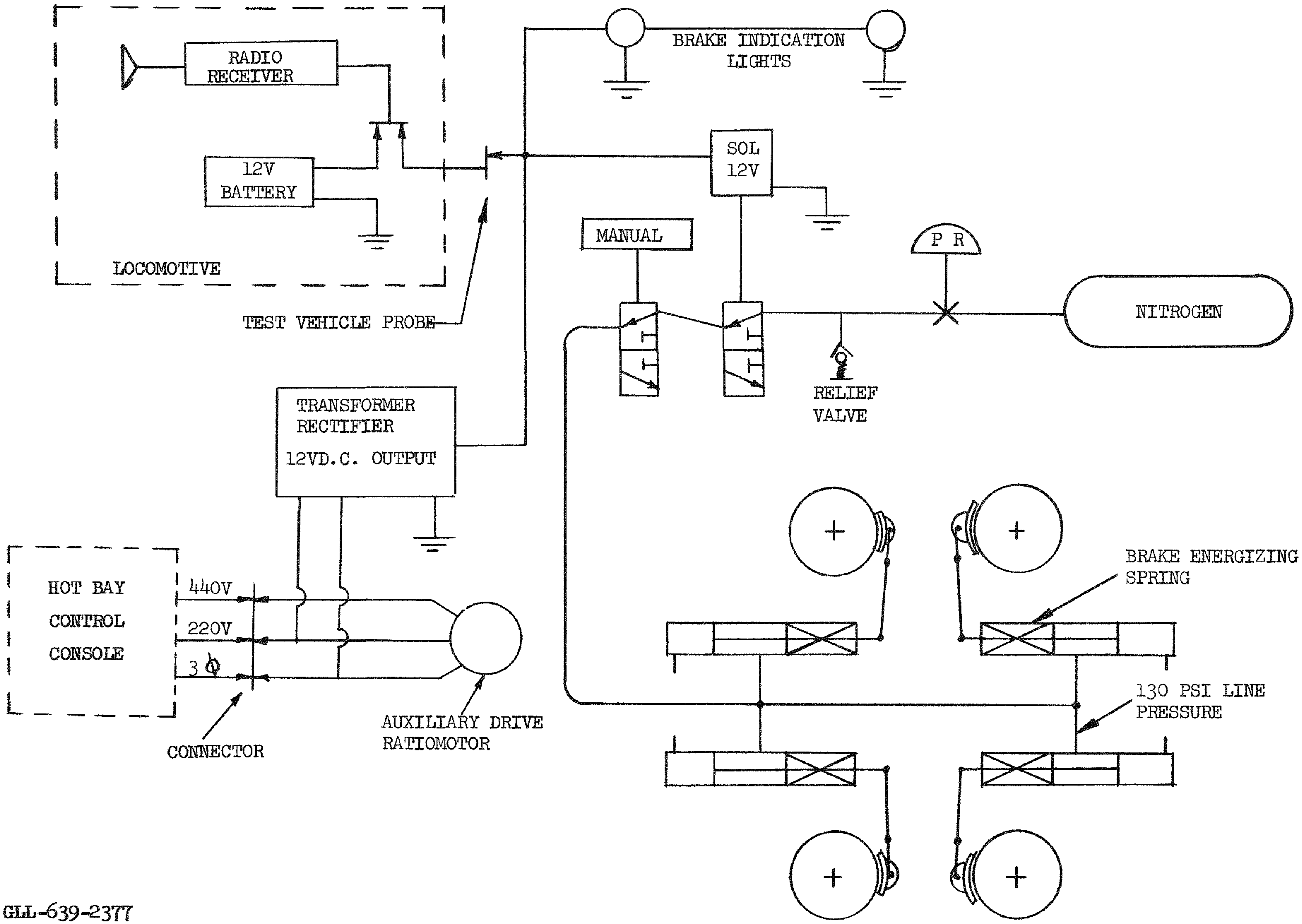

GLL-639-2377

Schematic diagram of brake system and auxiliary drive system.

Pneumatic cylinder	
Size	3.25 in. diam
Type	Double action
Stroke	2 in.
Rod diameter	1 in.
Sealing material	Hycar rubber
Length of cylinder assembly	27 in.
Brake solenoid power (max)	12 V dc, 8 A
Brake shoe design force	6000 lb per wheel
Brake shoe design speed	3 mph
Friction coefficient between wheel & shoe	0.20
Friction coefficient between wheel & track	0.20
Braking distance at 3 mph	117 ft
Response time of brake system	1-3 sec
Horizontal force needed to cause brakes to slip*	4,800 lb
Locomotive drawbar pull	8,000 lb

3. Right Outrigger Wheels

Number of outrigger wheels	2
Distance between outrigger wheels	99.562 in.
Rail height above track	10 in.
Purpose	Vertical & lateral alignment to ± 0.005 in.
Wheel diameter	10 in.
Wheel thickness	2.25 in.
Wheel material	AISI 4140 steel
Distance between right outrigger wheels	166 in.
Location of forward outrigger wheel	Sta. 276.5
Location of aft outrigger wheel	Sta. 442.5

---

*Slipping occurs between brake shoe & brake drum so that wheels turn on track. Brake pressure is removed by a cam actuated by a special rail at test bunker.

Lateral alignment wheels	
Number	4
Location	2 at each outrigger wheel
Diameter	3.5 in.
Thickness	2 in.
4. Left Outrigger Wheels*	
Number of outrigger wheels	2
Purpose	Vertical alignment
Distance between left outrigger wheels . . .	166 in.
Location of forward outrigger wheel	Sta. 276.5
Location of aft outrigger wheel	Sta. 442.5
5. Truck Assembly	
Track gage (STD)	56.5 in.
Rail type	90# A.R.A. Type "A" rail
Wheel and axle assemblies	2
Axle material	AISI C1042 steel
Axle length	68.875 in.
Wheel dimensions	
Outer diameter	24 in.
Running diameter	20 in.
Width	10.812 in.
Wheel material	Cast AISI 1020 Stl.
Wheel bearings	Tapered roller bearings
Distance between double axles	30 in.
Springs	
Number per truck assembly	8
Outside diameter	6.25 in.
Wire diameter	1.25 in.
Free height	8 in.
Solid height	6 in.

---

*Wheel description same as for right outrigger wheels.

Spring constant	9,500 lb/in.
Capacity at 7.25 in.	5,000 lb
Capacity at solid height	19,000 lb

6. Auxiliary Drive

Motor	Boston Ratiomotor
Type	Worm gear reducer with roller chain drive
Power rating	0.5 hp
Maximum load rating	0.21 hp @ 1.5 rpm
Running speed	1800 rpm
Test vehicle speed at full motor power	5 fpm
Location of auxiliary drive	Rear left corner of flat car
Power supply	208-V, 3-ϕ
Line used between supply and motor	80 ft 14/4 600-V type PVC cable
Mechanical linkage	
Coupling	Square clutch coupling and roller chain
Drive ratio of motor to wheels	3
Coupling engagement method	Manual lever (normally dis-engaged)

7. Wireway

Length	44 ft 6 in.
Height	18 in.
Width	16 in.
Metal thickness	0.25 in.
Material	AISI 1020 steel

8. Nozzle Cooling Air Pipe

Pipe size	8 in. schedule 40 (8.625 in. o.d.)
Inside diameter	7.981 in.
Pipe type	ASTM B241-58T alloy GS11A
Length	48 ft
Pipe material	6061-T6 Al

9. Control Air Pipe

Pipe size	2.375 in.
Inside diameter	1.503 in.
Pipe type	5400 psi double extra strong
Length	32 ft
Pipe material	304 stainless steel

10. Duct Support System

Forward support location	Sta. 276.5
Aft support location	Sta. 442.5
Height	Trunnion center line 59.625 in. from deck
Material	AISI 4140 steel
Support arrangement	See p. III-80

11. Duct System

a. Forward Inlet Duct (No. 1)

Length	100.250 in.
I. d. at forward flange	23 in.
Wall thickness	0.625 in.
I. d. at aft flange	37.448 in.
Length of cylindrical section	41 in.
Material	Hastelloy C
Weight	2580 lb

b. Diffuser Grid

Length	5.00 in.
O. d.	37.624 in.
Number of flow passages	241
Flow passage throat diameter	1.170 in.
Total throat area	258.0 in^2
Porosity	23%
Material	A-286
Weight	800 lb
Discharge coefficient	0.9995

c. Aft Inlet Duct (No. 2)

Length	84.250 in.
I. d. forward flange	37.672 in.
I. d. at aft flange	56.250 in.
Wall thickness	0.625 in.
Material	Hastelloy C
Weight	3650 lb

d. Access Duct (No. 3)

Length	91.00 in.
I. d.	56.250 in.
Wall thickness	0.625 in.
Number of manholes	2
Manhole i. d.	17.500 in.
Material	Hastelloy C
Weight	4900 lb

e. Controls Duct (No. 4)

Length	60.00 in.
I. d.	56.250 in.
Wall thickness	0.625 in.
Material	Hastelloy C
Weight	3500 lb

f. Reactor Duct (No. 5)

Length	103.00 in.
I. d.	56.375 in.
Wall thickness	0.437 in.
Number of rail mounting holes	510
Diameter of rail mounting holes	0.500 in.
Axial distance between mounting holes	3.85 in.
Material	Hastelloy C
Weight	4050 lb

g. Nozzle (No. 6)

Nozzle type	Convergent, double-wall, air-cooled

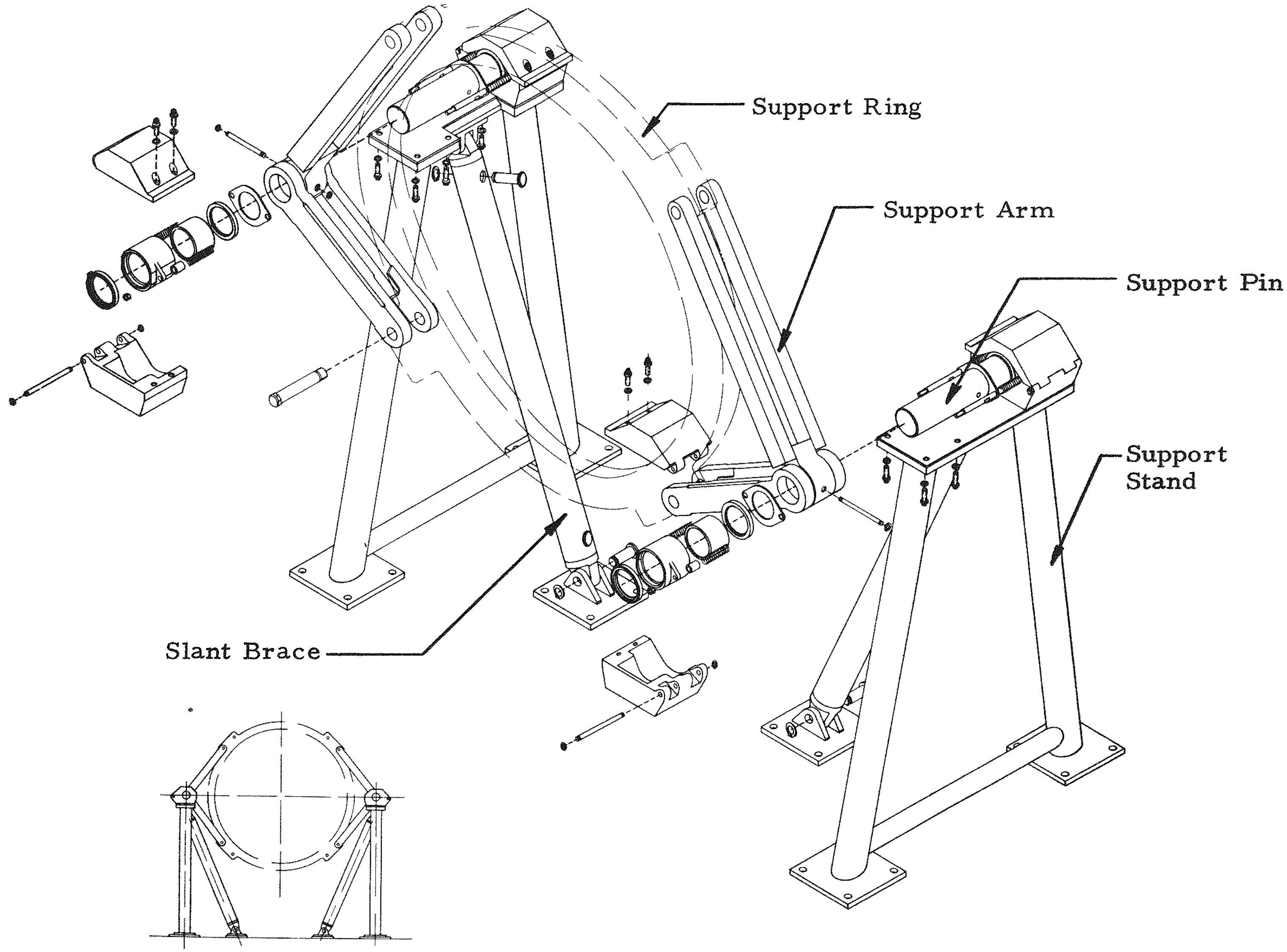

Support stand assembly.

Nozzle weight	1700 lb
Material of primary nozzle	Hastelloy C
Material of cooling shroud	SS type 321
Length of nozzle	42.76 in.
Entrance diameter	56.125 in.
Throat diameter	30.80 in.
Throat area	745 in^2
Throat area (hot)	758 in^2
Method of attachment	56-bolt flange
Cooling air pressure limit	150 psi
Primary air pressure limit	250 psi
Primary nozzle wall temperature limit . .	1500°F

C. INSTRUMENTATION

1. Nonnuclear

Total Number of Data Channels	374
Strain	20
Displacement	16
Acceleration	11
Stagnation pressure	42
Static pressure (wall)	16
Static pressure	12
Transient pressure	4
Stagnation temperature	23
Reactor component temperature (see p. III-9 et seq.)	153
Control actuator component temperature	22
Miscellaneous component temperature	34
Transducer Types	
Strain gage	SR-4
Displacement gage	LVDT
Accelerometer	Ceramic, self-checking
Pressure transducer	Bonded strain gage
Thermocouple	Pt-10 Rh/Pt Cr/Alumel
Transducer Temperature Limit	
Strain gage	1100°F
Displacement gage	400°F
Accelerometer	120°F
Pressure transducer	120°F
Thermocouple	
Pt/Pt-10 Rh	2700°F
Cr/Alumel	1800°F

note: " Information on pages III-82-84, -87, -94 has been revised. See Tory II-C Memo 748."

Instrumentation Summary

Station*	Measurement**	Purpose
-1000	6 P° 2 P 4 T°	(No. 0' rake) in 24-in. bypass line for facility checkout
-297	6 P° 2 P 4 T° 2 P_w	(No. 0 rake) in 36-in. mainline for flow control
0	2 E 2 T	Clamp strain and temperature
	1 D_y 1 D_x	Duct displacement with respect to ground
86	8 P° 2 P 2 T°	(No. 2 rake) aid in flow control and calibration of No. 0 rake
95	2 P_w	Static pressure before grid
100	2 E	Flange strain (fillet radius)
184	1 A_x 1 A_y 1 A_z	Triaxial acceleration on flange
248	4 P° 2 P 2 P_w 2 T	(No. 4 rake) control actuator operating conditions
250	1 A_y 1 A_x	Shim actuator housing acceleration
278	8 E	Flange, bolt, and support arm strain
	22 T	Actuator temperature
	2 T	Support ring temperature
328	2 P_f	Static transient pressure (short-coupled)
338	1 A_x 1 A_y 1 A_z	Triaxial acceleration on flange

* See p. xvii for station numbers. Negative station numbers give number of inches forward of station 0.

** x, y, z refer to tranverse, vertical and axial components respectively, pages III-83 and III-84 only.

Station	Measurement	Purpose
348	8 P°	(No. rake) pressure at support grid
	4 P	
375	2 D_y	Displacement between duct and car (1), car and ground (1)
380	2 D_y	Displacement between duct and reflected core (2)
	1 D_x	Displacement between car and ground
	1 P_w	Pressure in side support annulus
381	2 T	Temperature of outside duct wall opposite wiper
Reactor	176 T	Temperature throughout reactor (see p. III-90)
397	2 T	Temperature of outside duct wall on nut
398	4 T	Temperature of outside duct wall opposite wiper bar (2), opposite rail (2)
407	4 P_w	Static pressure in side support annulus
	2 D_x	Displacement between duct and reflected core
	2 D_y	Displacement between duct and reflected core
	8 T	Temperature of outside duct wall opposite wiper (2), opposite wiper bar (2), opposite rail (2), on nut (2)
418	2 D_y	Displacement between duct and car (1), car and ground (1)
422	1 P_w	Static pressure in side support annulus
	2 D_y	Displacement between duct and reflected core
	1 D_x	Displacement between duct and car
	2 T	Temperature on outside duct wall opposite wiper bar
433	2 P_f	Static transient pressure (short-coupled, high response)
441	6 T	Temperature of aft support ring
	1 $A_{x,y,z}$	Triaxial acceleration of aft support ring
	6 E	Flange, support arm, and nozzle strain

Station	Measurement	Purpose
448	10 P° 12 T°	(N6.. 10 rake) temperature and pressure of reactor exit air (rake vertical)
Nozzle	4 T 4 P_w	Inner nozzle wall temperature Exhaust air static pressure

Aft Pressure and Temperature Rake

Purpose	Measure total pressure and total temperature in nozzle region
Drawing number	62-128279
Sketch	See p. III-86
Number of pressure taps	10
Number of thermocouples	12
Material	D-36 (columbium alloy)
Weight	27 lb
Frontal area	66 in^2
Pressure tubes	0.250-in. o.d.; 0.049-in. wall
Pressure tube material	D-36
Coating	Si/CrFeB
Coating thickness	0.005 in. max

↓

note: "Aft pressure and temperature rake was replaced by 2 air-cooled delta-shaped cantilever rakes. Dwg. No. 64-107275 and 64-107307."

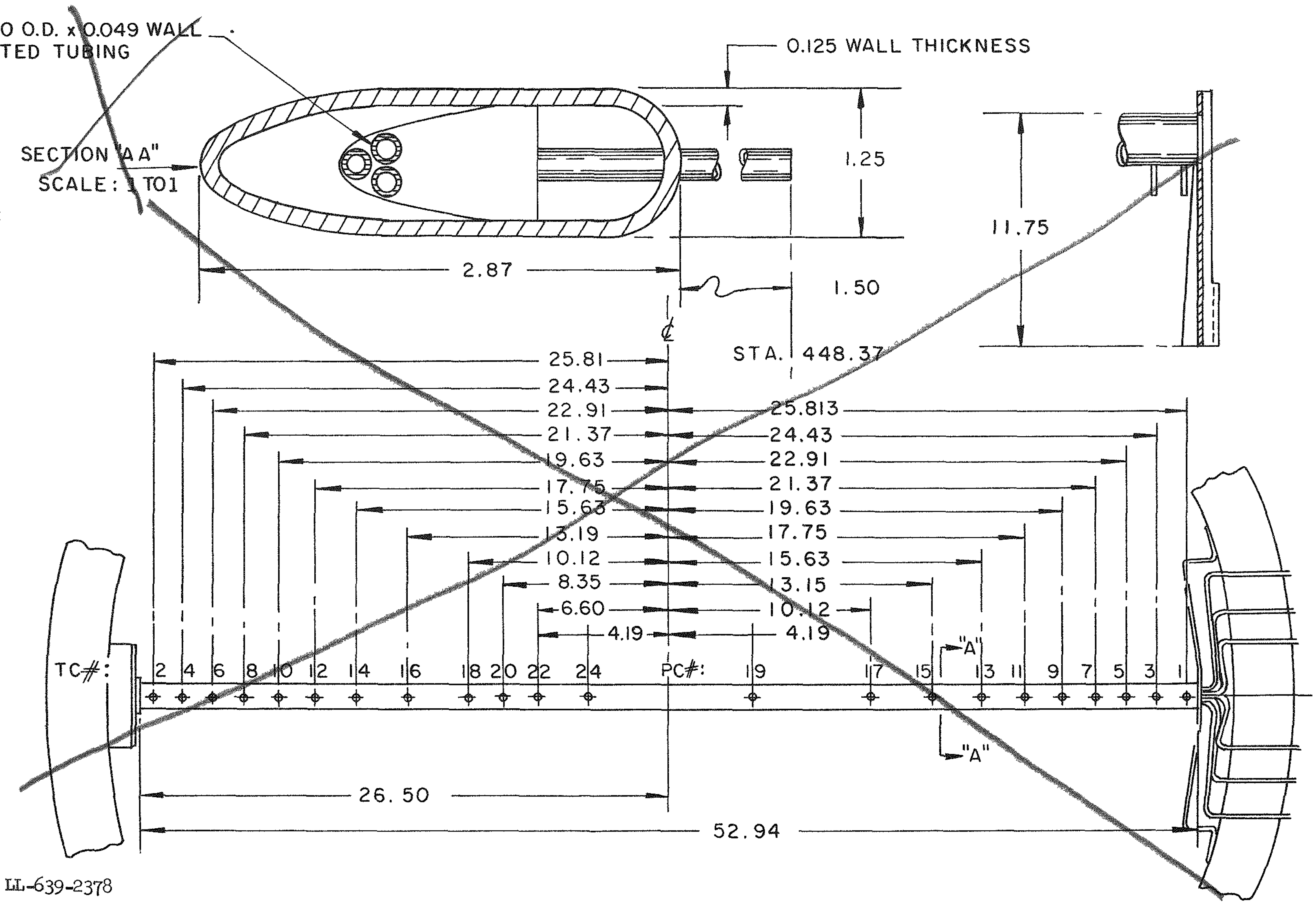

Aft pressure, temperature rake (dimensions in inches).

note: "Aft pressure and temperature rake was replaced by 2 air-cooled delta-shaped cantilever rakes. Dwg. No. 64-107275 and 64-107307."

2. Reactor Thermocouples

Outer Sheath

Material	Pt-12% Rh
O. d.	0.062 in.
Minimum wall thickness	0.006 in.

Inner Sheath

Material	Thermocouple grade Pt
O. d.	0.025 in.
Wall thickness	0.005 in.

Center Wire

Material	Thermocouple grade Pt-10% Rh
Minimum o. d.	0.005 in.

Total thermocouple length in active core	373.9 ft
Thermocouple weight per foot of wire	7.42 g/ft
Total thermocouple weight in active core	2.776 kg
Total weight of platinum in active core	2.17 kg
Total weight of rhodium in active core	0.228 kg
Total weight of MgO in active core	0.378 kg
Thermocouple weight distribution	See p. III-88

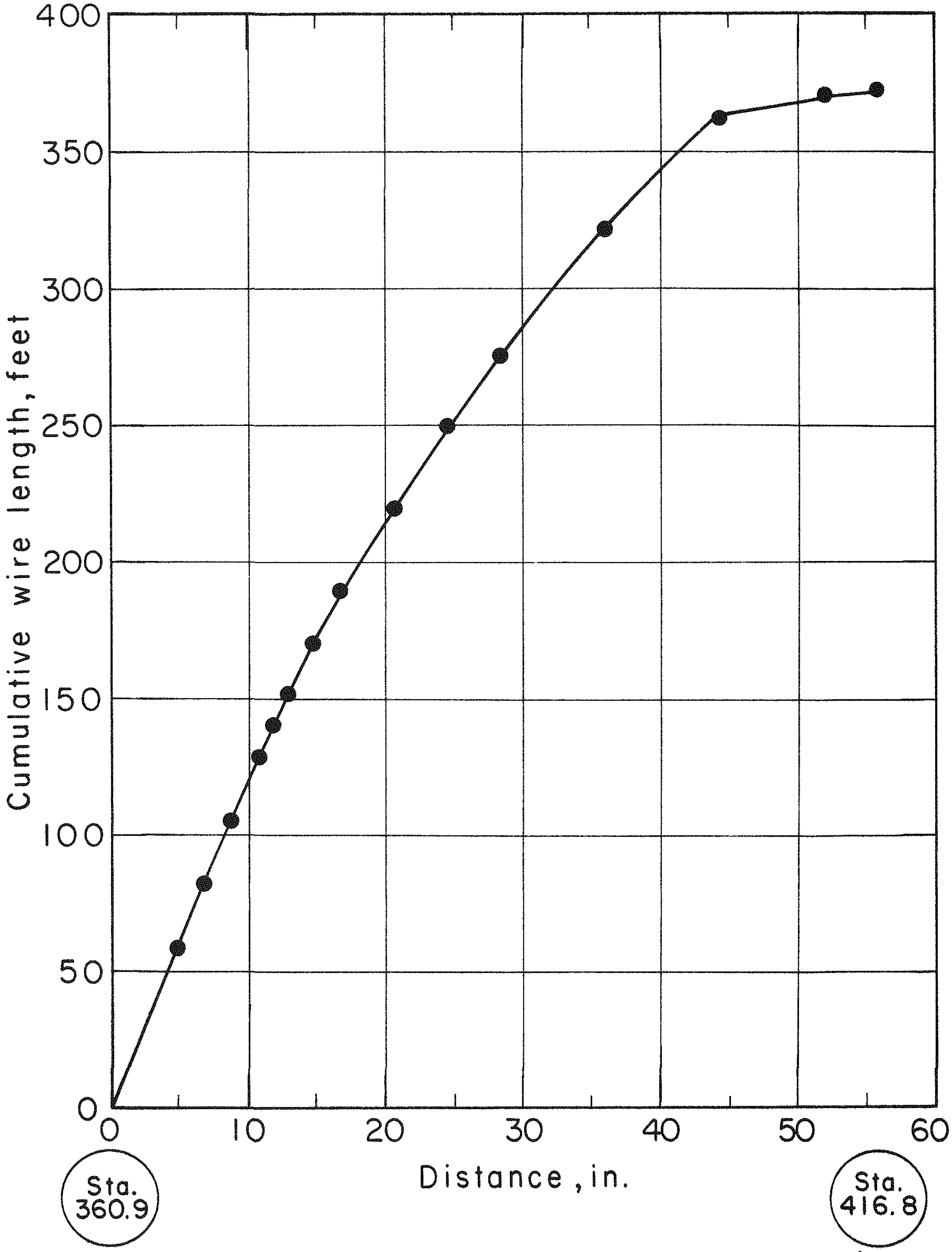

Cumulative thermocouple wire distribution in reactor (cf. Tory II-C memo No. 331).

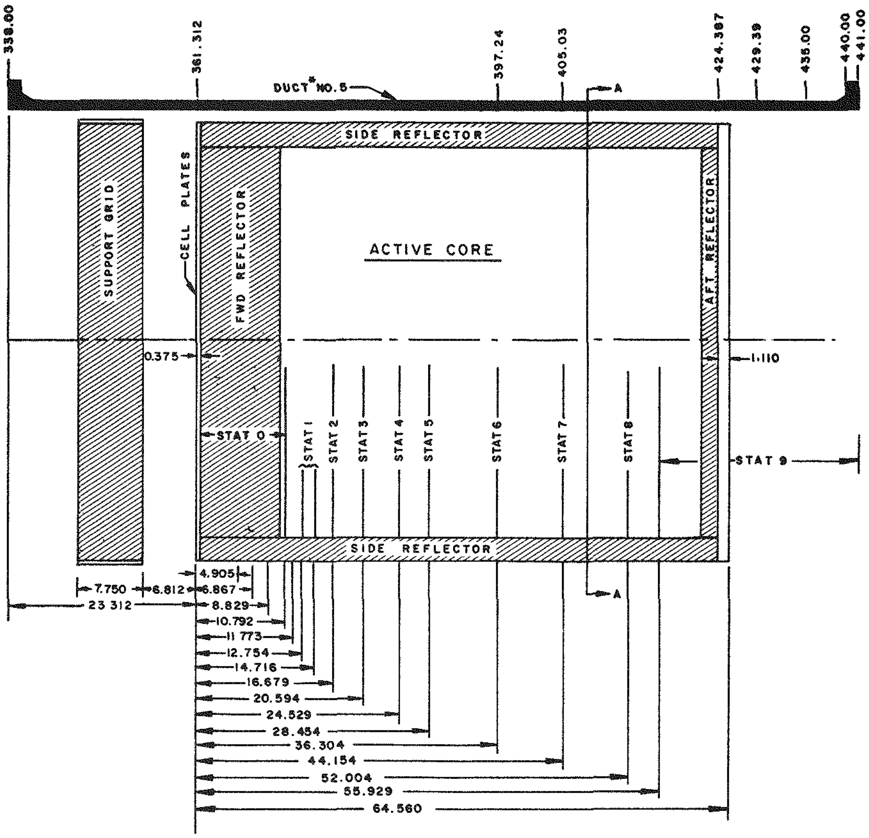

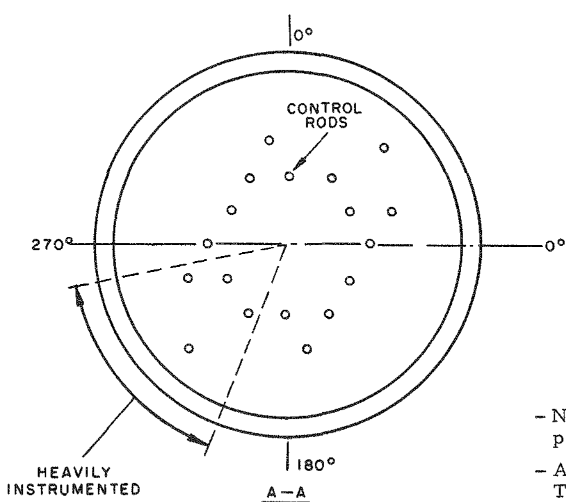

NUMBERING SYSTEM

XX X XX

- ITEM NUMBER
- DEFINED STATION
- PARAMETER DESIGNATION

PARAMETERS

10	FUELED TUBES
11	UNFUELED TUBES
12	TIE RODS
13	SIDE SUPPORT SPRINGS
14	AFT SHROUD
15	SHIMS (NICKEL)
16	SUPPORT GRID
17	BASE BLOCK
18	SIDE SUPPORT ANNULUS
19	DUCT WALL

GLL-639-2380

- Numbering starts at center of reactor and proceeds clockwise at each radius
- All tube temperatures are measured in Type 2A or 2B columns (see p. III-20)
- Thermocouple wires are located in Type 1A or 1B columns. The entire column uses 0.227-in.-diam. unfueled tubes when wires are present

Reactor thermocouple location.

Reactor thermocouple locations.*

Station No.	Transducer No.	θ (deg)	Radius (in.)	Unit cell No.	Tube No.
365.8	11001	55	1.6	K	145
367.8	11002	55	1.6	K	145
369.8	11003	55	1.6	K	145
371.7	10004	$50\frac{1}{2}$	16.5	P_2	6
	10005	55	1.6	K	145
	10006	$127\frac{1}{2}$	19.3	R_9	30
	10007	227	8.1	M_8	19
	10008	240	19.8	R_{18}	28
372.7	10009	55	1.6	K	145
373.7	10101	55	1.6	K	145
	11102	$64\frac{1}{2}$	8.8	M_2	90
	10103	$76\frac{1}{2}$	21.0	R_5	38
	10104	79	8.8	M_3	235
	10105	136	23.2	R_{10}	229
	11106	206	4.4	L_4	127
	11107	206	10.0	M_7	81
	10109	226	1.6	K	88
	11110	226	18.1	P_{14}	81
	11112	240	25.2	R_{19}	410
	10113	$244\frac{1}{2}$	13.5	N_{12}	30
	11114				
	10115	310	17.6	P_{20}	77
375.7	11116	44	16.6	P_2	99
	10117	55	1.6	K	145
	10118	60	19.9	P_3	147
	11119	$68\frac{1}{2}$	13.6	N_3	102
	10120	$203\frac{1}{2}$	6.8	L_4	23
	11121	210	13.9	N_{10}	143
	10122	222	12.0	N_{11}	49
	10123	226	22.0	R_{17}	120
	10124	232	18.0	P_{14}	233

*See page III-89, III-8, and III-20 for numbering system.

Station No.	Transducer No.	θ (deg)	Radius (in.)	Unit cell No.	Tube No.
	10125	251	17.7	P_{16}	24
	11126	255	24.3	R_{20}	308
377.6	10201	$50\frac{1}{2}$	1.6	K	145
	11202	$64\frac{1}{2}$	8.8	M_2	90
	10203	$76\frac{1}{2}$	21.0	R_5	38
	10204	79	8.8	M_3	235
	10205	136	23.2	R_{10}	229
	11206	206	9.0	M_7	135
	10207	211	16.6	N_{10}	60
	10208	226	1.6	K	88
	10209	230	22.5	R_{18}	237
	10210	$244\frac{1}{2}$	13.5	N_{12}	30
	10211	252	22.3	R_{19}	138
	10212	$256\frac{1}{2}$	20.7	R_{20}	116
	10213	310	17.6	P_{20}	77
381.5	11301	$64\frac{1}{2}$	8.8	M_2	90
	10302	$76\frac{1}{2}$	21.0	R_5	38
	10303	79	8.8	M_3	235
	10304	136	23.2	R_{10}	229
	10305	226	1.6	K	88
	10306	$244\frac{1}{2}$	13.5	N_{12}	30
	10307	310	17.6	P_{20}	77
385.5	11401	$64\frac{1}{2}$	8.8	M_2	171
	10402	$76\frac{1}{2}$	21.0	R_5	38
	10403	$81\frac{1}{2}$	8.8	M_3	214
	10404	133	23.2	R_{10}	284
	10405	226	1.6	K	88
	10406	$244\frac{1}{2}$	14.1	N_{12}	29
	10407	310	18.2	P_{20}	106
389.4	11501	$64\frac{1}{2}$	8.8	M_2	171
	10502	$76\frac{1}{2}$	21.0	R_5	38
	10503	$81\frac{1}{2}$	8.8	M_3	214
	10504	133	23.2	R_{10}	284
	10505	226	1.6	K	88

Station No.	Transducer No.	θ (deg)	Radius (in.)	Unit cell No.	Tube No.
389.4	11507	240	25.2	R_{19}	410
	11508	241	24.0	R_{19}	360
	10509	$244\frac{1}{2}$	14.1	N_{12}	29
	10510	252	22.3	R_{19}	138
	10511	310	17.6	P_{20}	106
397.2	10601	$50\frac{1}{2}$	16.5	P_2	6
	11602	$64\frac{1}{2}$	8.8	M_2	171
	10603	$76\frac{1}{2}$	21.0	R_5	38
	10604	$81\frac{1}{2}$	9.1	M_3	214
	14605	93	27.3	No. 11 rail	
	13606	51	26.9	Row 11 spring	
	15607	84	26.4	F-59 shim	
	10609	133	23.2	R_{10}	284
	14610	177	27.3	No. 11 rail	
	13611	171	26.4	Row 11 spring	
	15612	174	26.4	F-14 shim	
	10614	226	1.6	K	88
	10615	232	18.0	P_{14}	233
	10616	$244\frac{1}{2}$	13.5	N_{12}	29
	10617	310	18.2	P_{20}	106
405.1	10701	6	15.9	P_{23}	41
	10702	$15\frac{1}{2}$	19.0	P_{24}	208
	10703	26	15.8	N_1	222
	11704	44	16.6	P_2	99
	10705	$50\frac{1}{2}$	16.5	P_2	6
	10706	60	19.9	P_3	147
	11707	62	9.2	M_2	119
	11708	$68\frac{1}{2}$	13.6	N_3	102
	10709	$76\frac{1}{2}$	21.0	R_5	38
	10710	$81\frac{1}{2}$	9.1	M_3	214
	10711	92	16.1	N_4	66
	14712	93	27.3	No. 13 rail	
	13713	51	26.9	Row 7 spring	

Station No.	Transducer No.	θ (deg)	Radius (in.)	Unit cell No.	Tube No.
405.1	15714	84	26.4	D-59 shim	
	10716	103	16.2	P_6	188
	10717	124	13.6	N_6	137
	10718	$127\frac{1}{2}$	19.3	R_9	30
	10719	133	23.2	R_{10}	284
	10720	153	16.0	N_7	38
	10721	165	19.3	P_{10}	24
	14722	177	27.3	No. 13 rail	
	13723	171	26.9	Row 7 spring	
	15724	174	26.4	D-14 shim	
	10726	196	17.2	P_{11}	140
	10727	$203\frac{1}{2}$	6.8	L_4	23
	11728	206	10.0	M_7	81
	10729	207	1.6	K	61
	11730	207	4.4	L_4	127
	11731	$208\frac{1}{2}$	9.0	M_7	135
	11733	210	13.9	N_{10}	143
	10734	211	16.6	N_{10}	60
	11735	211	23.4	R_{16}	75
	10736	222	12.0	N_{11}	49
	10737	225	22.0	R_{17}	120
	11738	226	18.4	P_{14}	81
	10739	227	8.1	M_8	19
	10740	230	22.5	R_{18}	237
	10741	232	18.0	P_{14}	233
	10742	240	19.8	R_{18}	28
	11743	$240\frac{1}{2}$	25.2	R_{19}	410
	10745	$242\frac{1}{2}$	13.8	N_{12}	9
	11746	246	8.0	M_8	171
	10747	251	17.7	P_{16}	24
	10748	252	22.3	R_{19}	138
	11749	255	24.3	R_{20}	308
	10750	$256\frac{1}{2}$	20.7	R_{20}	116

Station No.	Transducer No.	θ (deg)	Radius (in.)	Unit cell No.	Tube No.
	10751	273	17.7	P_{17}	137
	10752	291	14.5	N_{14}	212
	10753	309	17.6	P_{20}	106
	10754	310	14.5	N_{15}	204
	10755	334	16.1	N_{16}	223
	10756	349	16.4	P_{22}	57
412.9	11801	62	9.2	M_2	119
	10802	$76\frac{1}{2}$	21.0	R_5	38
	10803	$81\frac{1}{2}$	9.1	M_3	214
	10804	133	23.2	R_{10}	284
	10805	207	1.6	K	61
	10806				
	10807	309	17.6	P_{20}	106
416.9	11901	62	9.2	M_2	119
	10902	$76\frac{1}{2}$	21.0	R_5	38
	10903	$81\frac{1}{2}$	9.1	M_3	214
	10904	133	23.2	R_{10}	284
	10905	207	1.6	K	61
	10906	$242\frac{1}{2}$	13.8	N_{12}	9
	10907	309	17.6	P_{20}	106
424.4	18908	93	28.0	SS air near duct	
	18909	177	28.0	SS air near duct	
	18910	273	28.0	SS air near duct	
	18911	357	28.0	SS air near duct	

Inner duct wall thermocouple location

Station No.	Transducer No.	θ (deg)	Station No.	Transducer No.	θ (deg)
431.0	05512	6	435.0	05518	186
	05513	126		05519	248
	05514	248		05520	306
435.0	05515	6	440.0	05521	6
	05516	68		05522	126
	05517	126		05523	248

Summary of nuclear instrumentation. (See p. III-97 for general arrangement.)

Nomenclature	Detector type	No.	Purpose	Sensitivity	Location: Extended	Location: Retracted	Range,* watts of reactor power (approx)
BF_3	N Wood G20-12 detector	2	Monitor power level in the very low power range	20 cps/nv	10 ft above ground 8 ft from core center line	Bunker	10^{-5} to 10^{2}
"S" Series	Cluster of 3 (A, B, C) fission chambers	2	" "	A: 1 cps/nv B: 0.1 cps/nv C: 0.01 cps/nv	Under test vehicle	"	10^{-4} to 10^{6}
Low log N	Westinghouse 6377 compensated ion chambers	3	Closed-loop control in intermediate range	4×10^{-14} A/nv	"	"	10^{0} to 10^{9}
High log N	" "	3	Closed-loop control in full power range	"	40 ft from center of core reactor	"	10^{1} to 10^{10}
Micromicro ammeter	" "	3	Collection of experimental data	"	"	"	10^{-2} to 10^{10}

*See p. III-98.

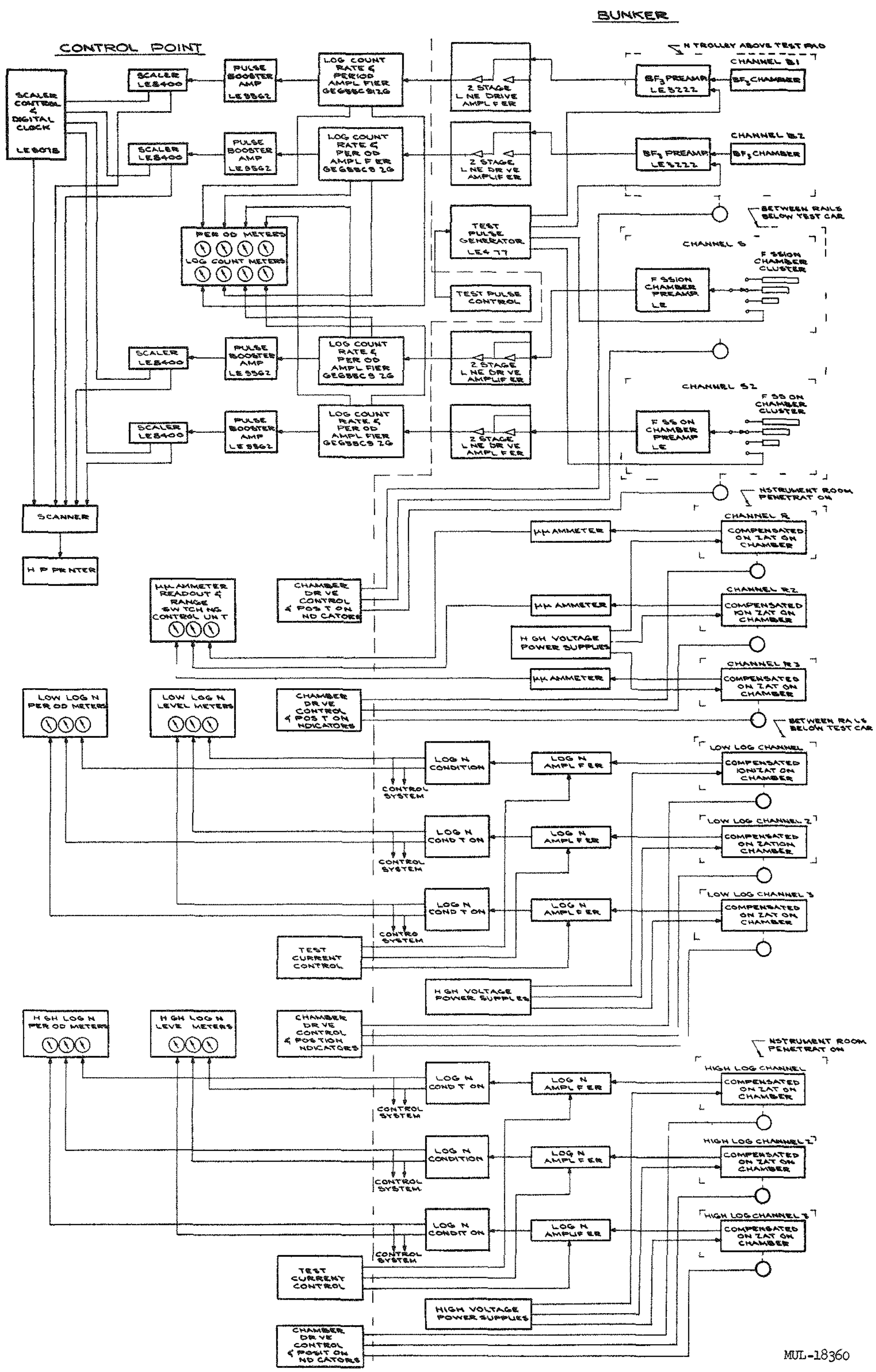

Block diagram of the nuclear instrumentation system.

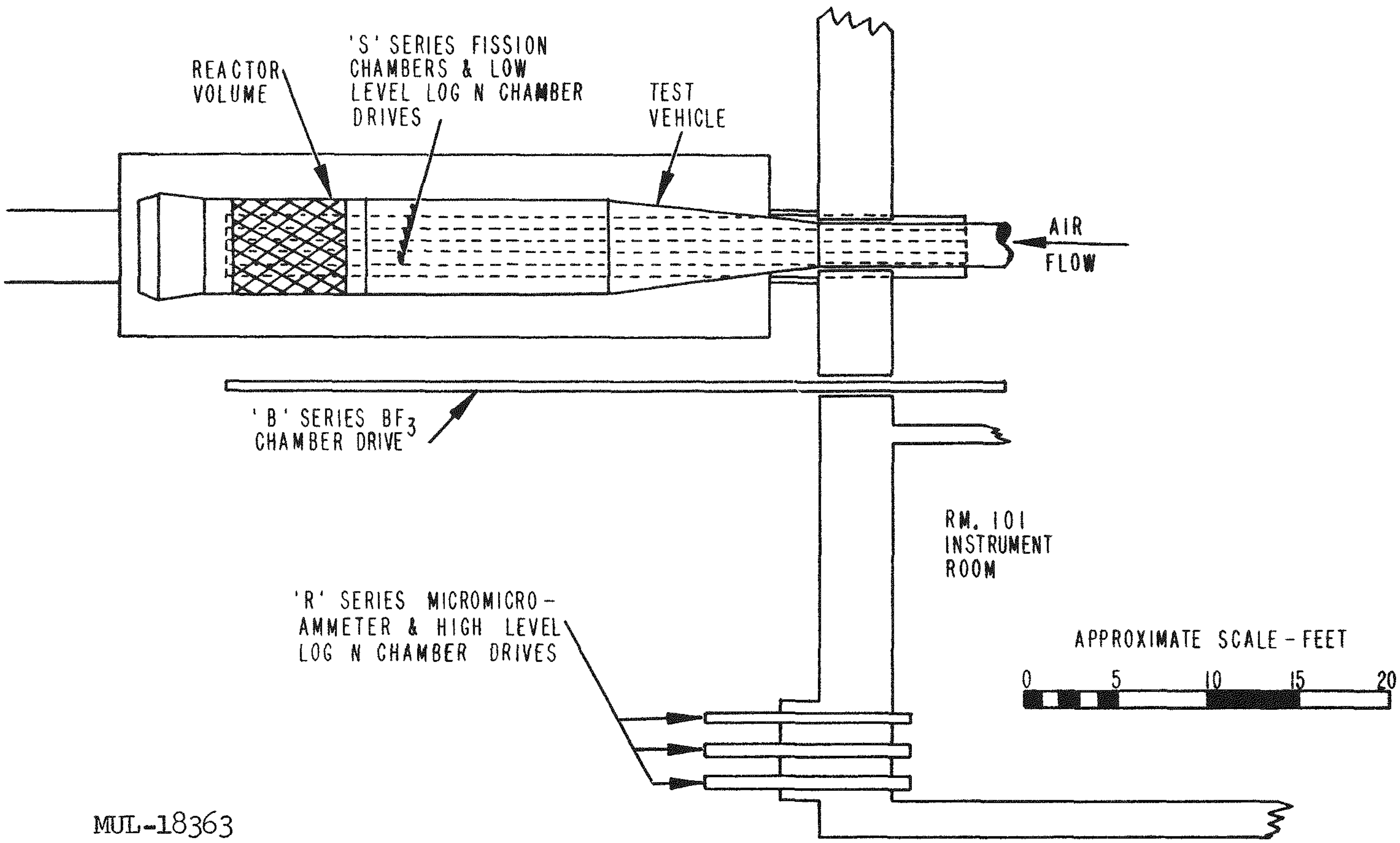

MUL-18363

Nuclear detector system arrangement.

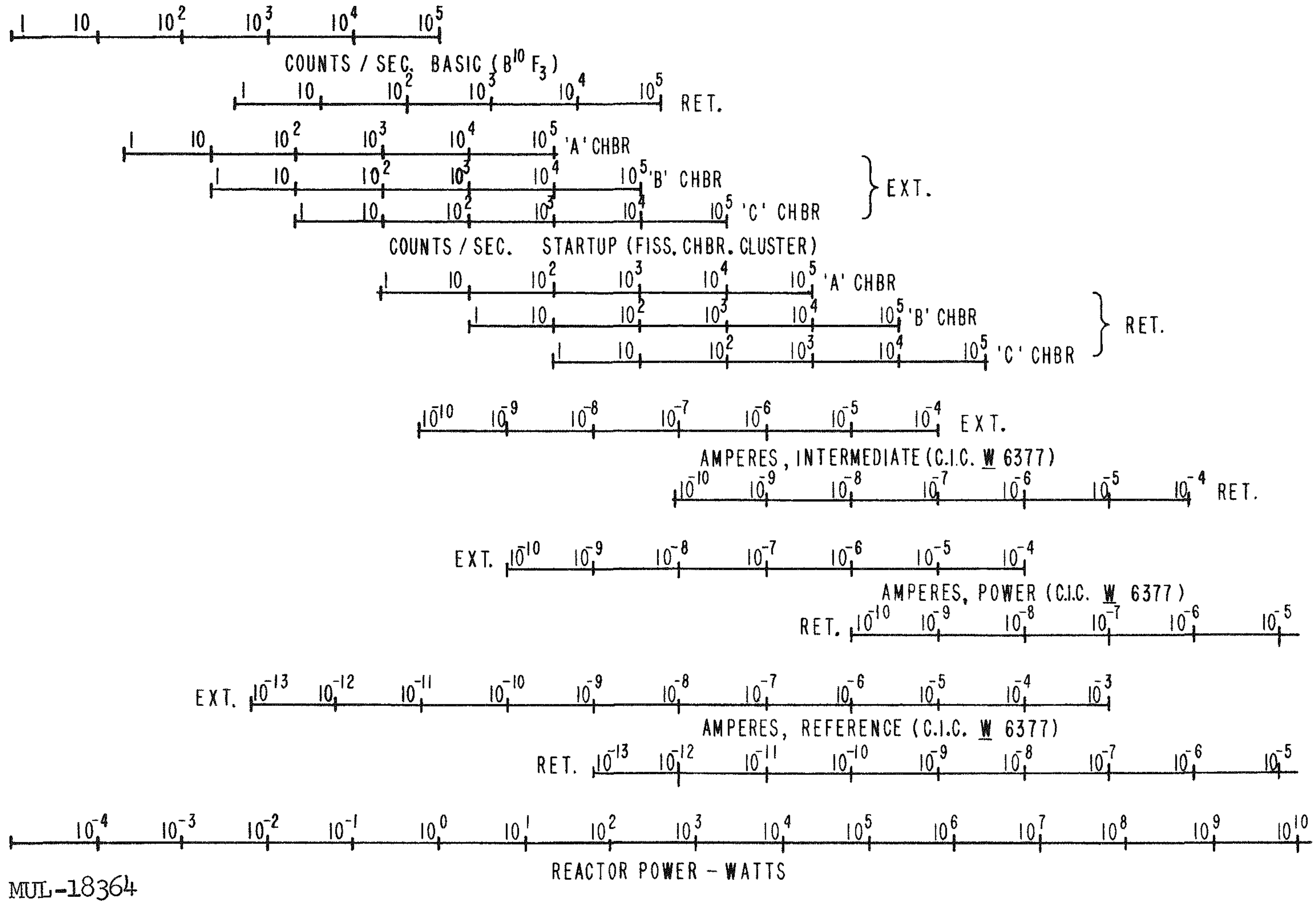

Estimated detector power range chart.

D. TEST FACILITY

1. Site 401 Description

Location	28 miles northwest of Mercury
Site plan	See p. III-100
Size	4 square miles
Elevation	4400 feet
Winds	
Summer	Southerly
Winter	Northerly
Average temperature and humidity	
Summer	75°F, 20% RH
Winter	45°F, 33% RH
Distances	
Control building to test bunker . . .	8450 feet
Control building to disassembly building .	4380 feet
Disassembly building to test bunker .	8190 feet
Disassembly building to check station .	2300 feet
Commercial power high line rating . .	6 MW
Commercial power system	3 MW at 69 kV, 3-phase
Utility power system	3 diesel generators, 125 kVA, 480 V, 3-phase
Instrument power system	2 diesel generators, 75 kVA, 480 V, 1-phase
Location of generators	In power house

2. Test Air System

Piping schematic	See p. III-101
Piping design life	100,000 hours
Allowable stress	50% of minimum yield strength
Maximum flow	1900 lb/sec
Maximum temperature (at station 0) . .	1060°F
Maximum pressure (at station 0) . .	560 psi
Relief valve pressure set points (2 valves) .	730 psi & 740 psi
Flow capacity for each relief valve . .	6225 lb/sec (0°F air)

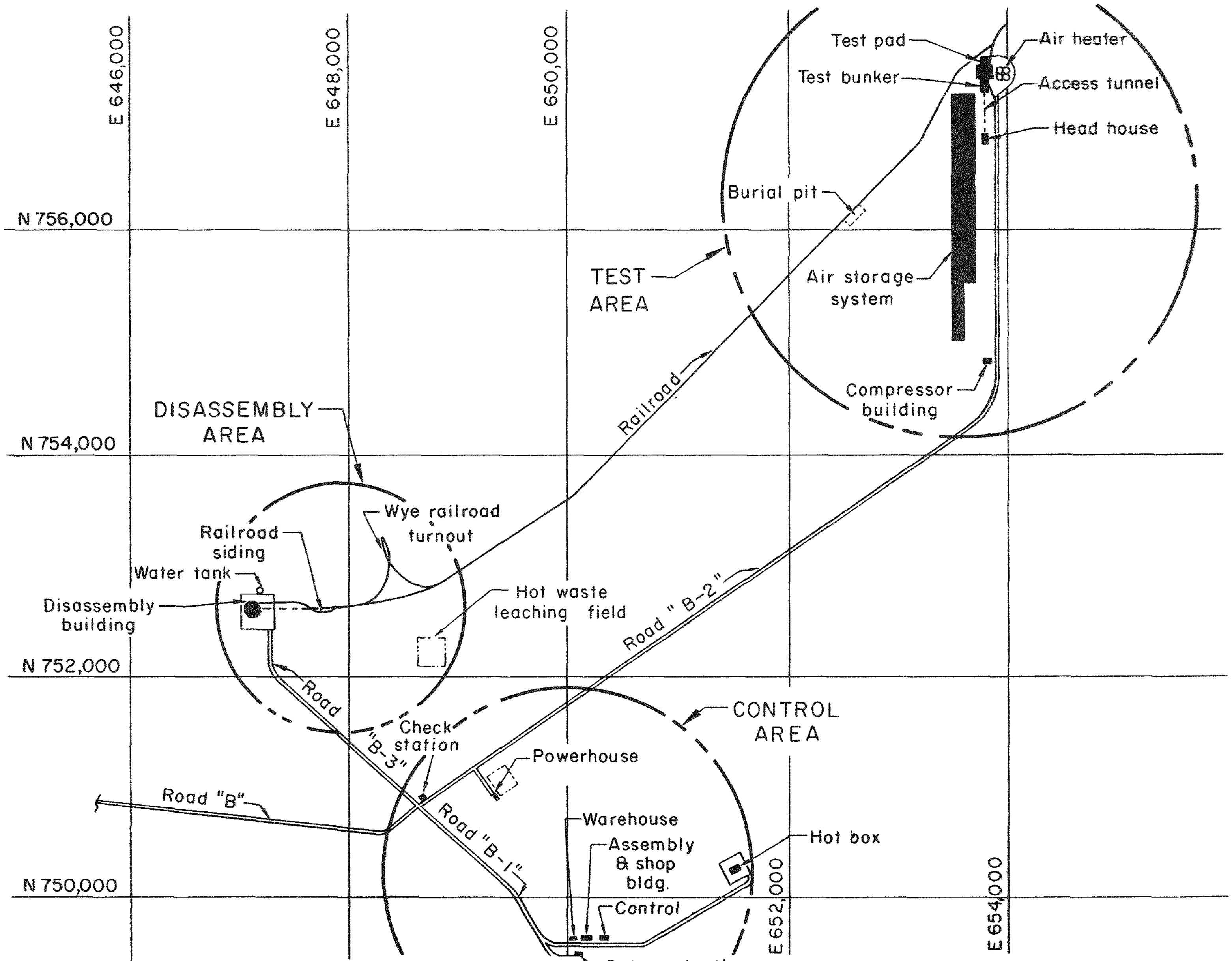

MUL-18415

Site 401 plan.

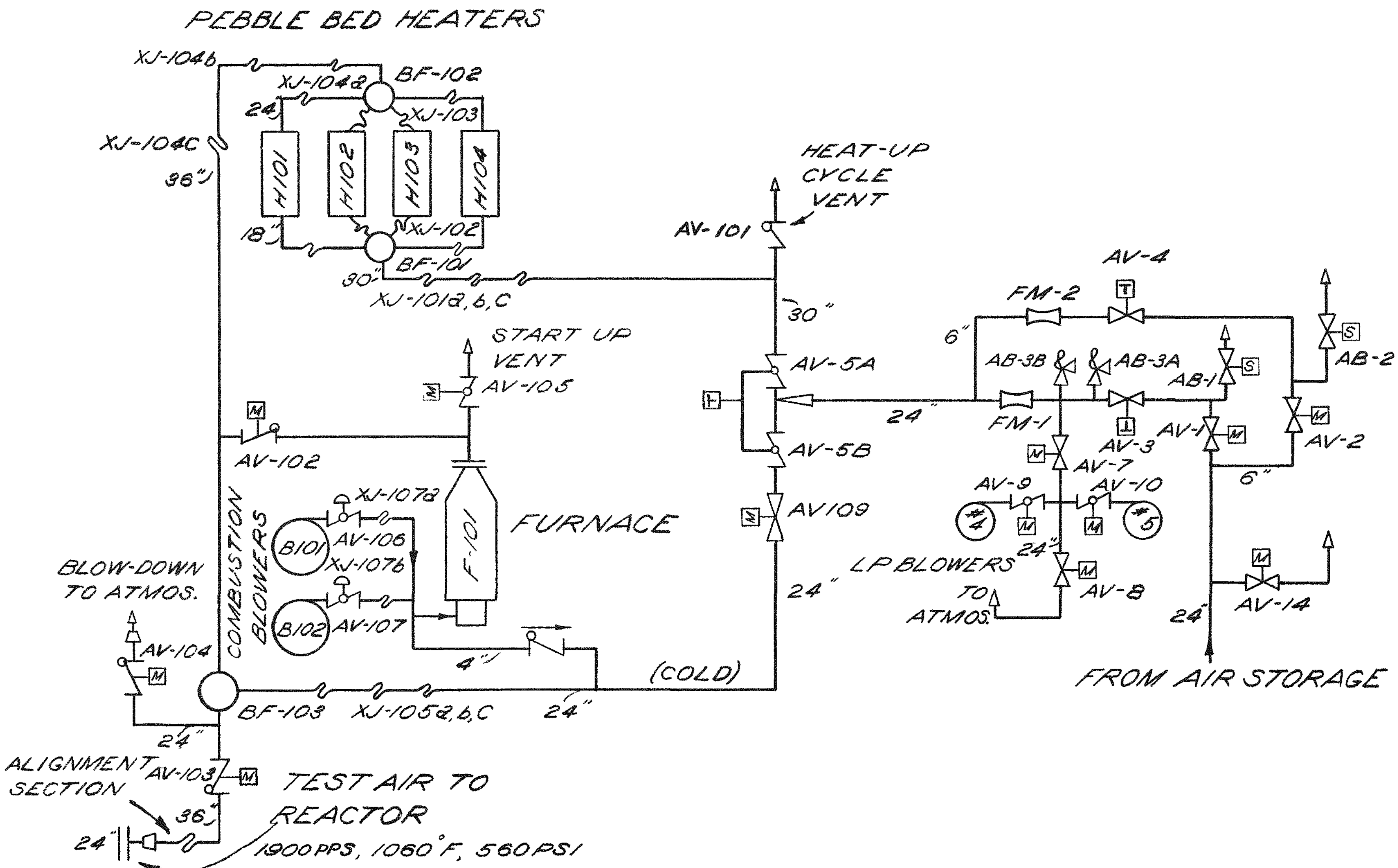

GLL-639-2381

Bunker air piping.

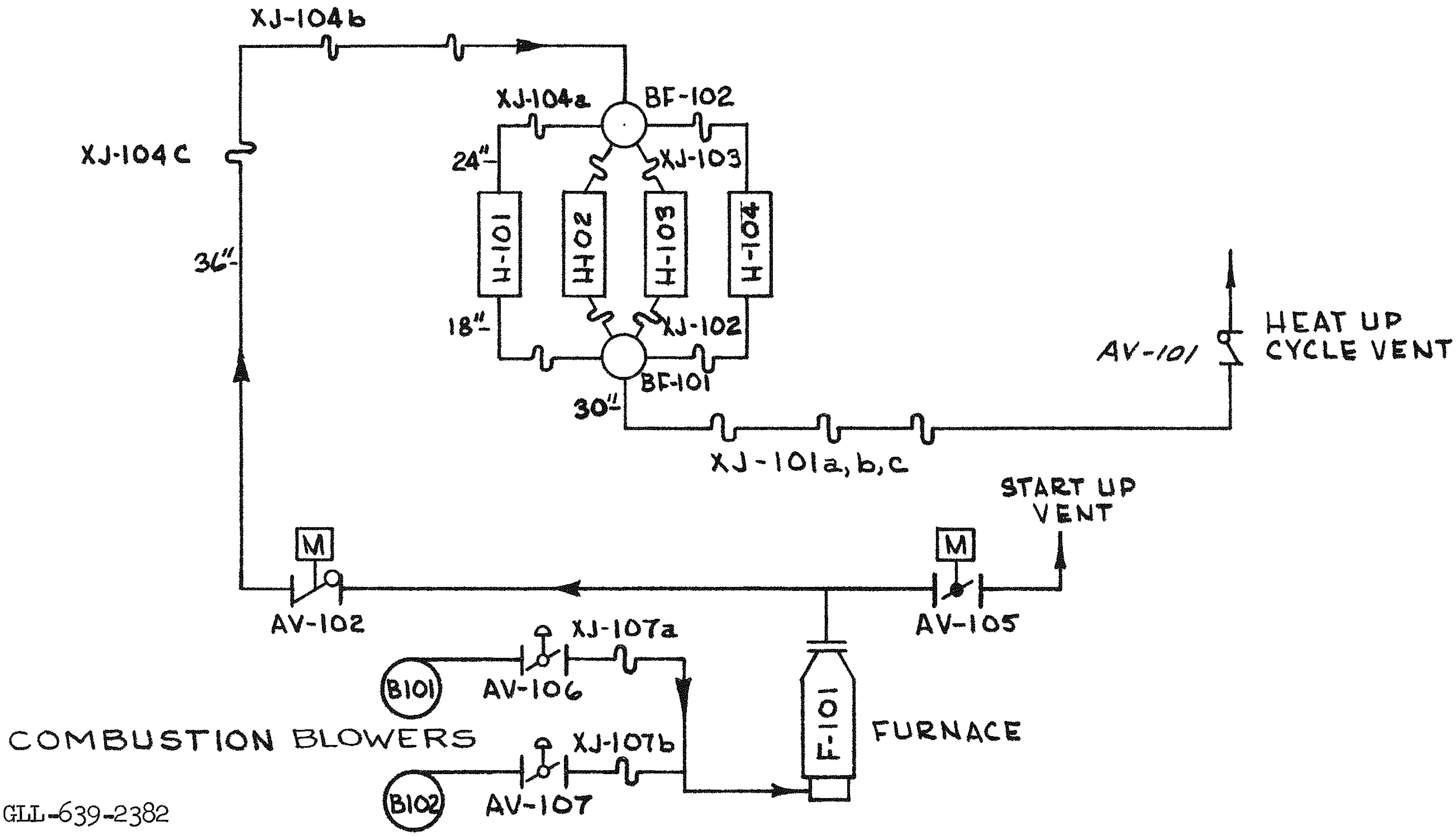

GLL-639-2382

Bunker air piping, showing flow during heat-up cycle.

Flow meter ranges	
FM 2	0-450 lb/sec
FM 1B	450-1200 lb/sec
FM 1	1200-2000 lb/sec
Test air cutoff pressure	920 psi
Nozzle cooling air	75 lb/sec @ 150 psi
Actuator control air	3 lb/sec @ 3600 psi
Actuator air cutoff pressure	1300 psi
Steady-state test air	
Power for two low-pressure blowers . .	900 hp
Maximum flow	23 lb/sec
Blower discharge pressure	7.25 psig

3. Air Storage System

Storage area I	30 casings, each 580 ft long
Casing size	9-5/8 in. o.d. × 0.472 in. wall
Casing material	API-N80
Volume	7542 ± 31 ft^3
Storage capacity (60°F & 3600 psi) . .	140,900 lb
Storage area II	12 casings, each 1685 ft long and 36 casings, each 2252 ft long
Casing size	10-3/4 in. o.d. × 0.400 in. wall
Casing material	API-P110
Volume	55,331 ± 192 ft^3
Storage capacity (60°F & 3600 psi) . .	1,034,000 lb
Actuator air storage	6 casings, each 1685 ft long
Casing size	10-3/4 in. o.d. × 0.400 in. wall
Casing material	API-P110
Volume	5522 ± 20 ft^3
Storage capacity (60°F & 3600 psi) . .	103,200 lb

4. Air Compression System

Number of compressors	3
Normal delivery pressure	4000 psi
Power for two 4-stage compressors . . .	900 hp
Capacity of two 4-stage compressors . .	1.8 lb/sec
Power for one 5-stage compressor . . .	700 hp
Capacity of 5-stage compressor	1.4 lb/sec
Air storage recharge time (all compressors)	
From ambient to 3600 psi	102 hours
From 920 psi cutoff to 3600 psi . . .	76 hours
Air storage recharge time (5-stage compressor only)	
From ambient to 3600 psi	232 hours
From 920 psi cutoff to 3600 psi . . .	174 hours
Actuator air storage recharge time (5-stage compressor only)	
From ambient to 3600 psi	20 hours
From 1300 cutoff to 3600 psi	13 hours
Number of air driers	3
Rate of water removal (3 driers) . . .	6.8 lb/hour at 2000 psi
Moisture content in stored air	0.001% wt
Dew point temperature	-72°F

5. Air Heater (Stored Energy, Pebble Bed)

Sketch	See p. III-106
Heater design life	100 test runs
Number and arrangement	4 vessels in parallel
Total heat mass weight	1,900,000 lb
Form of heat mass	1-in.-diam, 405 SS balls
Ball stack (each vessel)	103.8 ft^2 by 16.8 ft high
Porosity of heat mass	0.37
Liner material	
Ends	410 SS
Heat mass region	405 SS
Liner inside diameter	138 in.
Vessel material	T-1 steel
Vessel inside diameter	156 in.
Vessel design pressure	700 psi
Insulation material	B & W Kaowool
Packing density	12 lb/ft^3
Rating	2000°F continuous
Estimated heat loss (heat mass at 1200°F) .	140 Btu/hour-ft^2
Maximum flow pressure drop (1200°F) . .	22 psi
Pressure drop for top ball layer to roll . .	25 psi
Pressure drop for 1/2 to 3/4 bed lifting . .	32 psi
Flow rate at which bed flotation results . .	130% of design

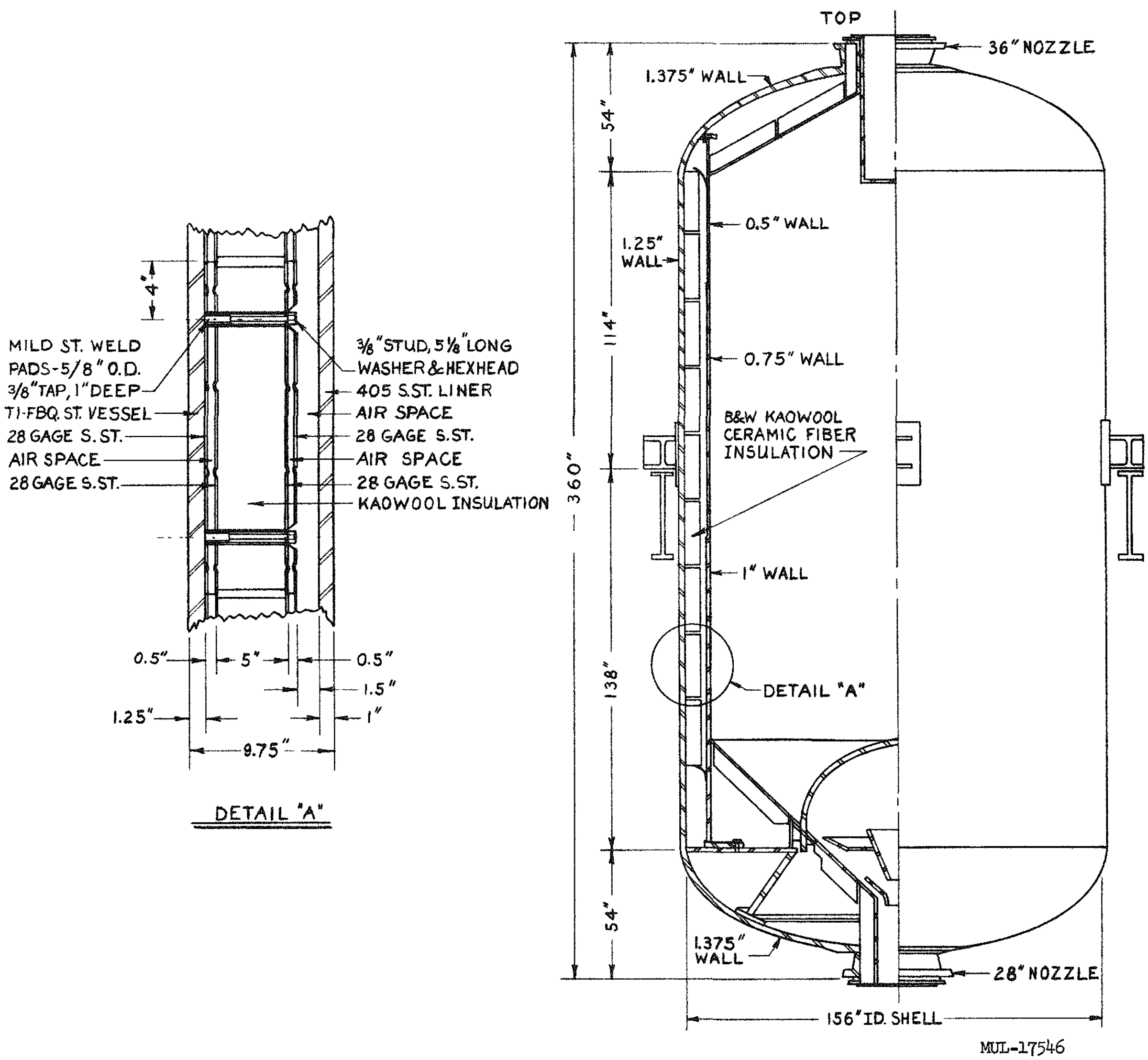

Pebble bed heater vessel.

6. Air Heater Furnace

Type	Oil-fired
Combustion gas temperature	1250°F
Combustion gas flow rate	30 lb/sec
Fuel	Fuel oil,No. 2
Heating value	139,000 Btu/gal
Flow rate	3 gal/min
Storage	20,000 gal
Time to heat heaters	30 hours

7. Test Bunker

Concrete wall thickness	
North	48 in.
Others	18 in.
Overpressure required to blow out relief panel .	0.1 psi
Distance from tunnel entrance to zero point .	500 ft

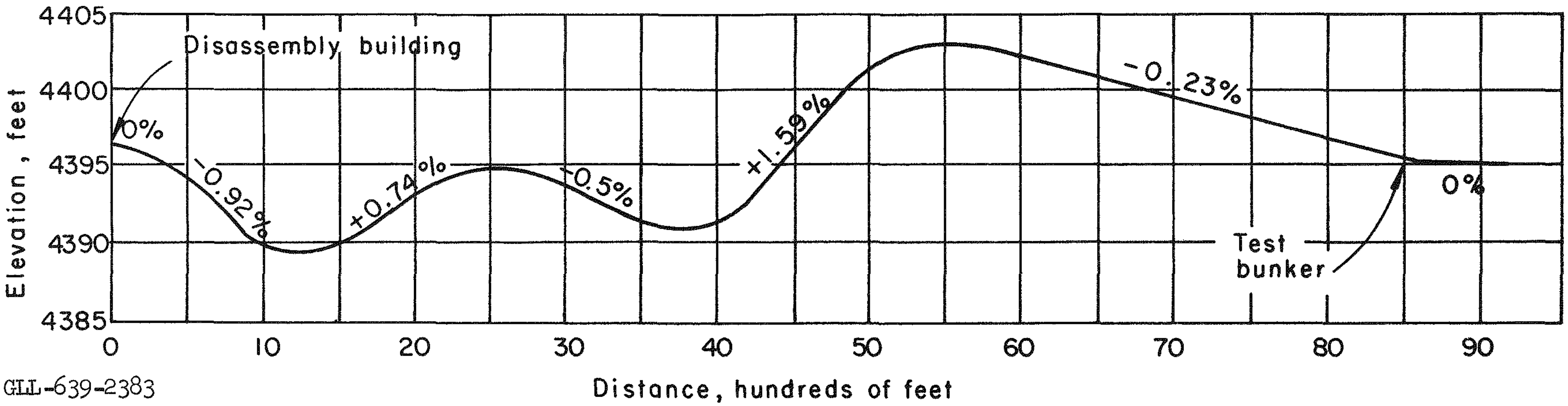

GLL-639-2383

Main line railroad profile, disassembly building to test bunker.

E. LOCOMOTIVE

1. Power Plant

Voltage	115 V dc
Ampere-hour rating	1009 ampere-hours
Control	Electrical, local & remote
Max drawbar pull (at standstill)	8000 lb

2. Locomotive Coupler

No. of couplers	2 (one on each end)
Location of jaws above tracks	23 in.
Jaw material	Low-carbon, hot-rolled steel mostly 0.75-in. plate

CHAPTER IV - DESIGN ENVIRONMENT AND ANALYSIS

A. ACCELERATIONS OF REACTOR VEHICLE[1]

	Design criteria	Structural capability
Flight[2,3]		
Longitudinal	+6.0 to -0.32 g	See note
Lateral	1.5 g	4.0
Vertical	+4.0 to -0.5 g	4.0
Ground handling[2]		
Longitudinal	±5.0[4] g	See note
Lateral	0.5 g	4.0
Vertical	+2.7 to - 1.0 g	4.0

Note:

Support structure for axial loads is designed to withstand a force equivalent to 24 times the weight of the supported mass for a period of 10 hours. Its capability for any phase of operation introducing forward acceleration loads or combinations of axial pressure drop and forward acceleration may be judged by comparison with this figure.

Aft acceleration without pressure drop is permissible up to 1 g, or with handling fixtures, up to 5 g. The aft acceleration tolerance is increased by axial pressure drop.

---

[1] Accelerations are positive upward or forward.

[2] Earth's gravity, 1 g, is included.

[3] At operating temperatures.

[4] With handling fixtures.

B. WEIGHTS AND CG LOCATIONS

	Wt., lb			CG Station
1. Reactor			18,700	390.2
a. Reflected Core		10,575		394.2
Active core	4,760			
Fueled BeO 4,360				
Unfueled BeO 400				
Side reflector	4,604			
BeO 1,769				
Nickel tubes 2				
Forward reflector inserts 30				
Peripheral shims 2,803				
Forward reflector	911			
BeO 775				
Nickel tubes 16				
Forward reflector inserts 120				
Aft reflector	300			
BeO 106				
Cr-MgO 194				
b. Tie Rods		325		370.9
Standard	263			
Control	62			
c. Retainer Assembly		287		331.6
Cell plates	89			
Retainer springs	81			
Spring adapters and spacers	117			
d. Base Blocks		433		424.9
e. Support Grid		900		349.3
f. Side Support System		2,100		393.1
Spring segments	1,150			
Rails and wiper assembly	211			
Wipers	70			
Wiper Bars	670			
g. Aft Reactor Duct		4,050		388.7
h. Shroud		48		431
2. Test Vehicle	See page IV-3			

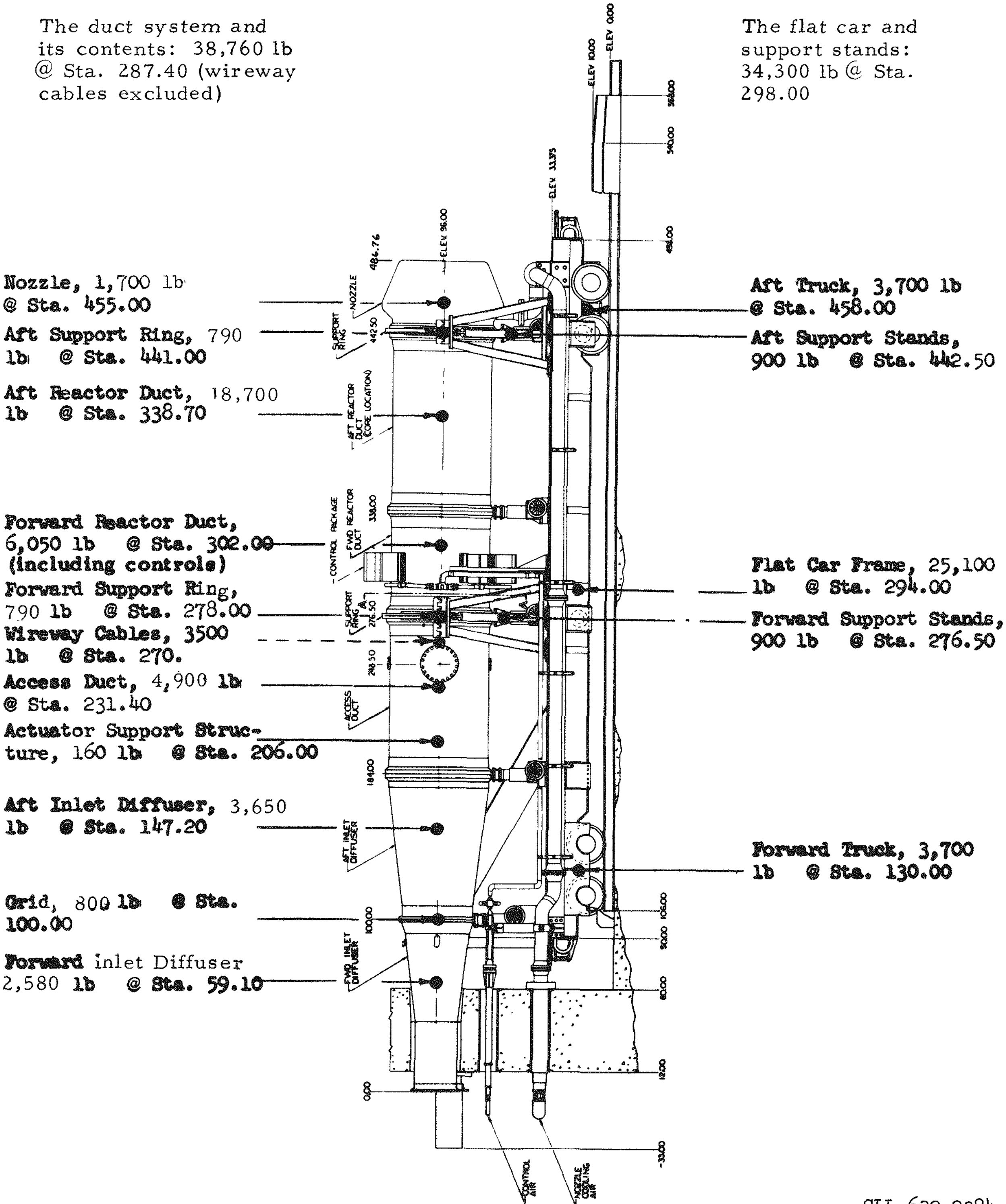

GLL-639-2384

Weights and CG locations of test vehicle components.

C. COMPONENT ANALYSIS

1. Reflected Core

Radial preload on reflected core at 70°F[1]	12 psi
Maximum radial preload by spring on reflected core at operating temperatures[1]	14 to 17 psi
Minimum radial preload required for stability in flight environment	12 psi
Axial preload on reflected core	10,600 lb
Minimum axial preload required for stability	8,800 lb
Radial expansion	See p. IV-6
Maximum radial reflected core expansion (70 to 2500°F, includes peripheral shims and corrugated spring)	0.687 in.
Maximum radial reflected core expansion (70 to 2850°F, includes peripheral shims and corrugated spring)	0.767 in.
Maximum axial reflected core expansion (70 to 2500°F, includes cell plates and base blocks)	0.700 in.

2. Reactor Components

Fueled tubes	
Temperature distribution	See p. I-6, 20, 34, 48
Thermal stress	See p. IV-6
Tie rods	
Nominal axial stress due to axial load	27,100 psi
Maximum axial stress due to bending (at R = 26 in.)	17,000 psi
Maximum thermal stress (at R = 0)	4,450 psi
Factor of safety[2] (considers radiation aging effects)	1.3
Cell plates	
Maximum bending stress (at 70°F)	12,600 psi
Maximum thermal stress	6,000 psi
Factor of safety (based on σ_y at 70°F)	7
Base blocks	
Maximum bending stress	8,000 psi
Factor of safety (based on σ_y at 2500°F)	3

---

[1] Design.

[2] Based on 10-hour rupture stress at operating temperature.

Side support spring

Maximum bending stress	60,000 psi
Maximum thermal stress	4,000 psi
Factor of safety[1]	1.5

Side support rails

Maximum bending stress	60,000 psi
Maximum thermal stress	6,000 psi
Factor of safety[1]	1.5

Control rods

Maximum axial stress	7,000 psi
Maximum thermal stress	1,700 psi
Factor of safety (based on σ_u at operating temperature)	3.2

Support grid

Maximum deflection (thermal and mechanical)	0.140 in.
Lateral natural frequency of beams (under load)	>300 cps
Design load on center beams	30,000 lb
Minimum buckling load on center beams with front plate	100,000 lb

	Center beam		Front plate[2]	
	Aft surface	Fwd surface (@ bolt hole)	Web at tie rod hole	Tie rod bolt hole
Bending stress, σ_1, kpsi	+38	-38	∓9	∓9
Thermal stress, kpsi	+10	None	-5	0
Stress conc. factor	None	2.0	2.0	2.4
Maximum elastic stress, kpsi	+48	-76	-23	±21.6
Approx. temperature, °F	1250	1130	1120	1120
Safety factor (dead load) σ_y/σ_1	2.8	>2.9	12	12

3. Test Vehicle

Duct system natural frequency	18, 48, 66, 120, 150 cps

[1] Based on 10-hour rupture stress at operating temperature.

[2] Based on evenly distributed load; load concentration factor 1.5.

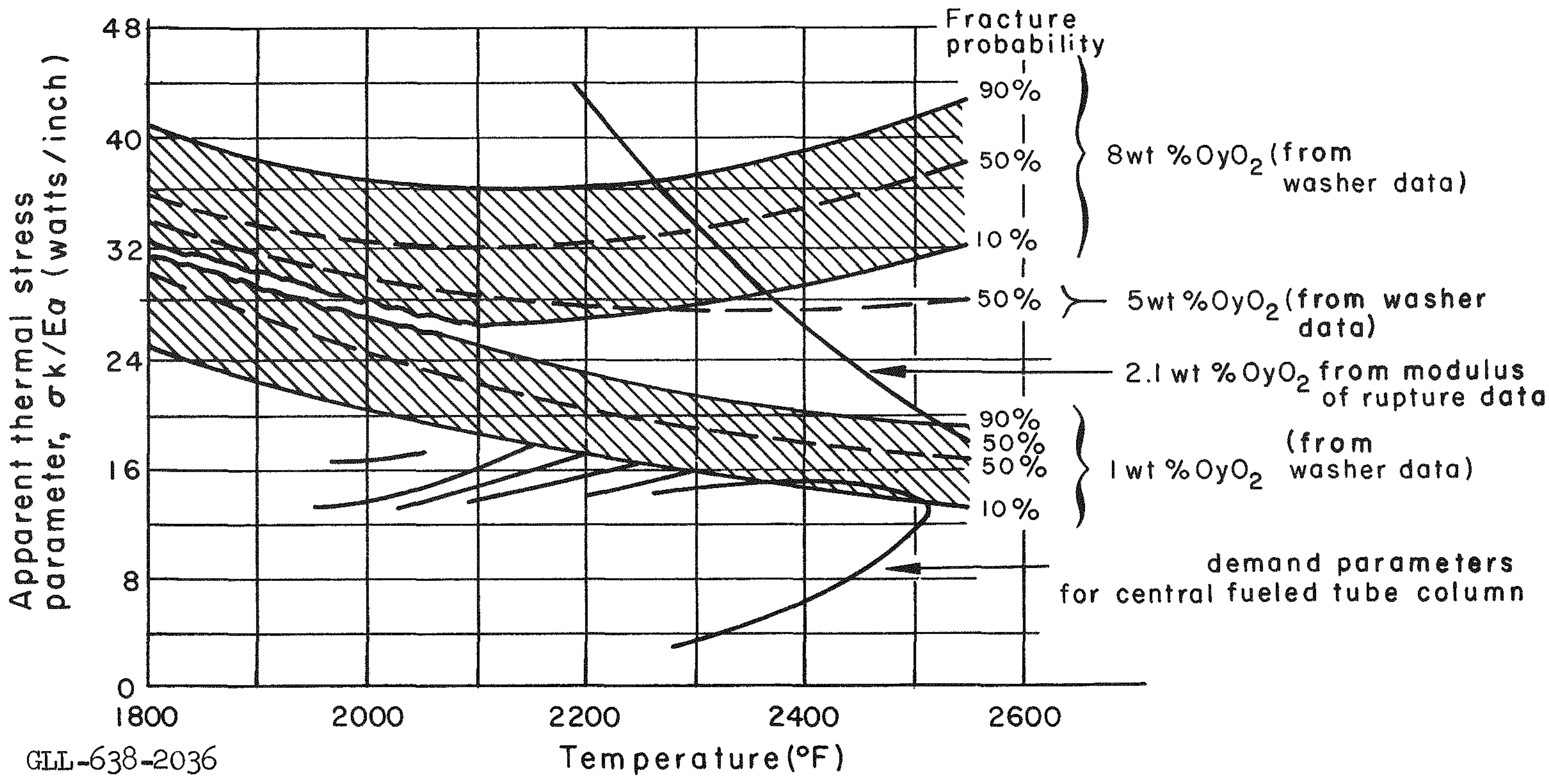

GLL-638-2036

Predicted thermal stress demands and characteristics of fueled tubes. (Washer data is obtained in special thermal stress apparatus (Ref UCRL-6852).)

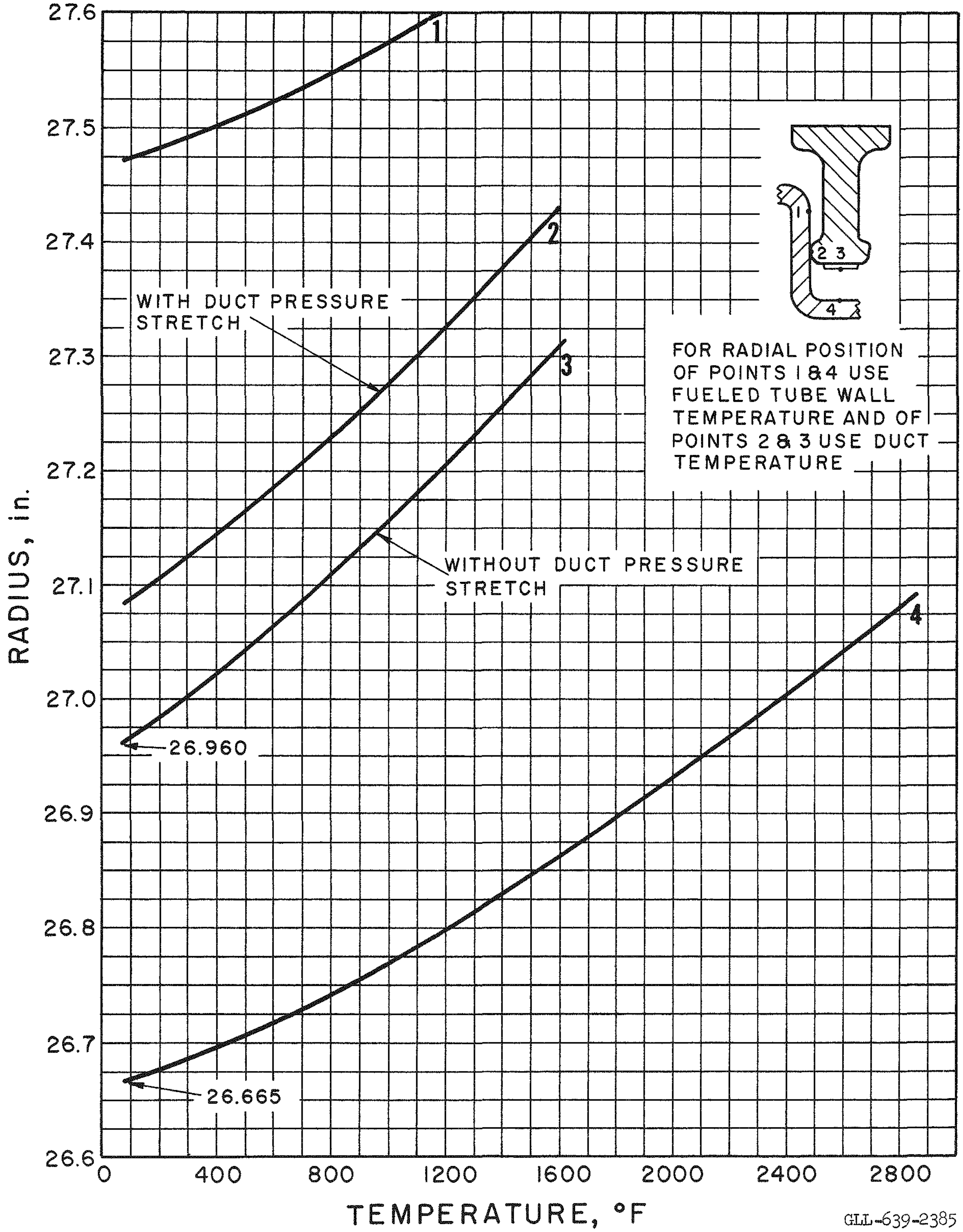

Effect of temperature on critical side support radii.

Duct Flange Analysis

		Calculated max expected stress (kpsi)	Experimental max stress (kpsi)	Factor of safety based on yield strength at 1100°F	Temp at position of max stress (°F)
Forward Diffuser	Fwd flange	14.9	--	2.0	900
	Plate section	16.5	--	2.2	1000
	Aft flange	24.6	24.0[1]	1.1[2]	800
Aft Diffuser	Fwd flange	20.9	18.5	1.5[2]	800
	Plate section	15.8	--	2.3	1000
	Aft flange	22.7	25.0[1]	1.4[2]	800
Access Duct	Fwd flange	25.9	23.6[1]	1.2[2]	800
	Plate section	15.8	--	2.4	950
	Aft flange	25.9	23.6[1]	1.3[2]	800
Forward Reactor Duct	Fwd flange	25.9	24.0	1.4[2]	800
	Plate section	15.8	--	2.3	1100
	Aft flange	25.9	24.0	1.3[2]	1100
Aft Reactor Duct	Fwd flange	25.7	--	1.4	1100
	Plate section	22.6	--	1.6	1400
	Aft flange	17.8	18.5	1.7[2]	1200
Nozzle	Fwd flange	26.2	--	1.1[3]	1200
	Plate section	22.1	--	1.6[3]	1400

[1]Maximum predicted stress and the maximum experimental stress do not occur at the same position.

[2]Based on experimental values.

[3]Based on properties at 1400°F.

CHAPTER V – OPERATION

A. PROPOSED TEST PLAN

1. Critical Experiments at Livermore

    Determine critical control rod position.

    Determine spatial power distribution with fission detector.

    Determine differential rod worth by rod bump method.

    Determine reactivity temperature coefficient by heating reactor to 200°F.

    Study power distribution at simulated design wall temperature (poison core with boron strips).

*2. Subsystem Checkout at NTS

    Mate test vehicle to facility.

    Check out data collection system from transducers to recording equipment.

    Complete checkout of reactor control system.

    Verify location of thermocouples with hot probe.

*3. Cold Blowdown Through Reactor

    Observe and check air pressure instrumentation.

    Observe reactor and duct system vibration characteristics.

4. Critical Experiment at Room Temperature

    Recheck critical rod bank height.

    Check start-up nuclear instrumentation.

    Determine count rate vs absolute power level by foil irradiation.

5. Zero Power Reactor Control Dynamics

    Measure open-loop reactor transfer function.

    Determine power level response to step insertions of ion chamber demand.

6. Critical Experiment at Elevated Temperatures

    Heat reactor to 950°F with low pressure blower air.

    Check temperature instrumentation.

    Determine critical rod bank height.

7. Intermediate Power Test

    Proof-test reactor at design wall temperature and one-third power.

    Check reactor heat transfer and air flow behavior.

---

*Tests 2 and 3 are performed first with reactor controls and simulated reactor, then repeated with reactor.

8. Full Power Tests

B. TYPICAL REACTOR OPERATION SEQUENCE

Temperature, flow vs time . . . . See p. V-4

Event	Time
Start air storage compressors	X - 85 hours
Start checkout of facility instrumentation	X - 80 hours
Start checkout of facility equipment	X - 55 hours
Start hot air furnace	X - 40 hours
Hold prerun meeting	X - 24 hours
Conduct analog runs	X - 20 hours
Limit access to test area	X - 4 hours
Hold prerun meeting	X - 2 hours
Manually check position of air supply valves	X - 1-1/2 hours
Unlock master block valves	X - 1 hour
Clear test area of all personnel	X - 1 hour
Review operating and emergency procedures at control point	X - 45 minutes
Bring reactor critical	X - 30 minutes
Increase power to about 1 MW and transfer to closed loop control	X - 20 minutes
Start low pressure blowers (23 lb/sec)	X - 10 minutes
Start process recorders on low speed	X - 9 minutes
Raise inlet air temperature to test condition	X - 8 minutes
Divert low pressure blower air	X - 30 seconds
Shift process recorders to high speed	X - 10 seconds
Start air flow from main air supply	X
Increase reactor temperature to 2200°F	
Start nozzle cooling flow	
Start automatic air flow program	X + 2 minutes
Increase core temperature to 2500°F	X + 2 minutes
Shut down reactor	
Reduce air flow to 50 lb/sec	
Reduce inlet air temperature	
Shut down nozzle cooling flow	
Return low pressure blower air to reactor	

Shut down main air supply

Secure

C. NUCLEAR CONTROL MODES

1. Manual Mode

Reactivity change rate: Vernier . .	±1 ¢/sec
Shim . . .	+5 to +20 ¢/sec
Action in case of malfunction . . .	Rods are held in present position automatically. Operator may scram rods

2. Automatic Log Power Mode

Control range	100 watts to 10× design power
Power monitor	6 compensated ion chambers (CIC's)
CIC location, 100 W to 10 MW . . .	3 at 10 ft from core
Greater than 500 kW . .	3 at 50 ft from core
Logarithmic output (proportional to $\log_{10}$ power)	1.6 volts/decade
Power ramps available	±5, 10, 30, 60 sec
Power excursion rate limiter (PERL) .	Limits positive rate of change of power to pre-set ramp

3. Automatic Reactor Core Temperature Mode

Control means	Δ Log power determined by temperature demand
Number of thermocouples . . .	12
Location of thermocouples . . .	x/L = 0.7
Thermocouple failure limit before complete system failure	11
Thermocouple failure limit for control without operator action . .	5
Rate of change of power demand, max .	5-second period
Temperature ramps available on automatic control panel	5, 10, 15°F/sec

4. Automatic Fast Reset Mode

Purpose	Holds reactor at pre-determined power level to allow time for correction

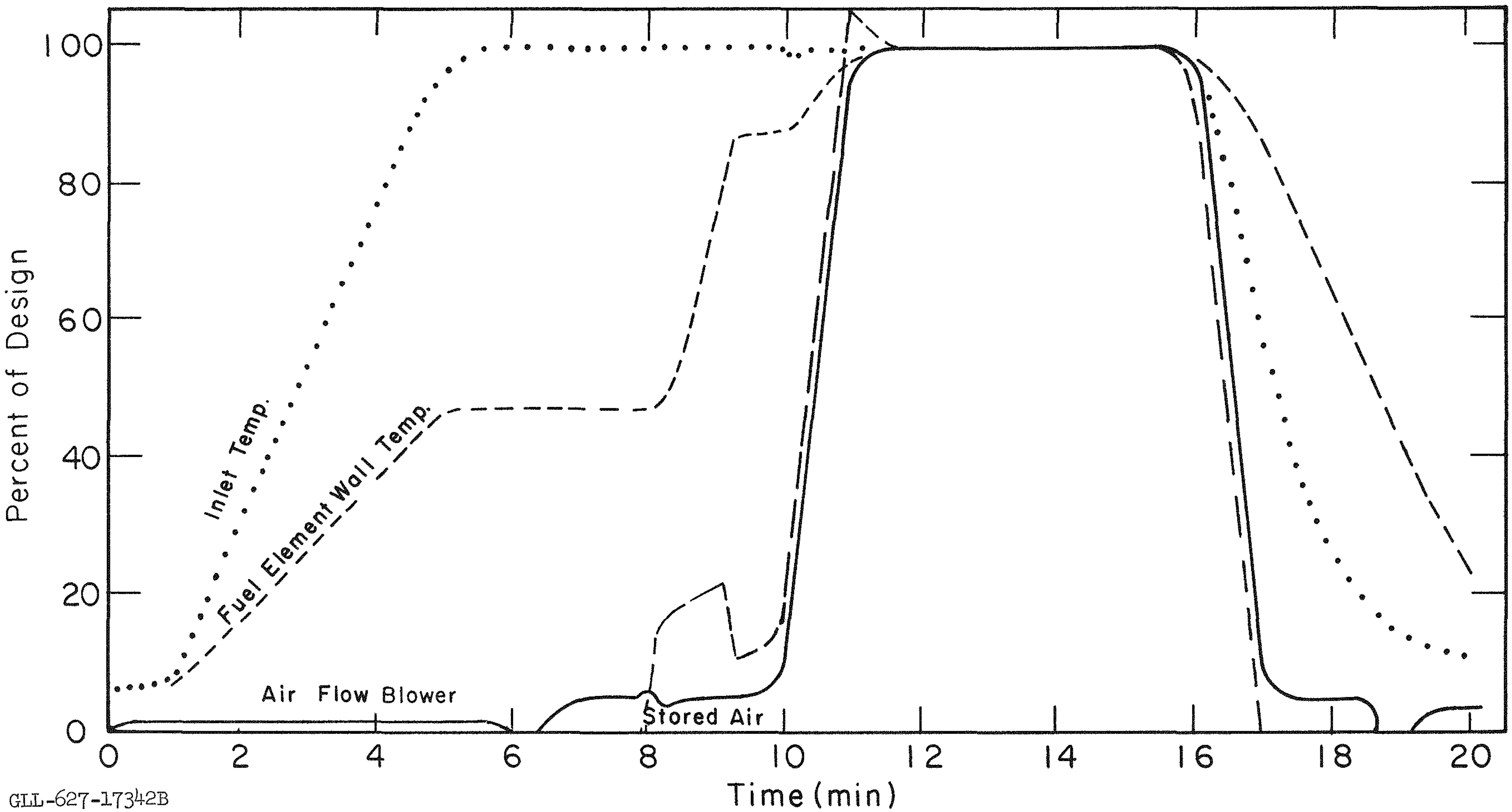

Typical test sequence.

Initiation	Initiated manually or when 2 of 3 log power currents or period circuits exceed a preset value. For automatic control, power limit is set at 1.2 times demand power
Rate of change of reactivity: Safety rod .	93 ¢/sec
Shims . .	31 ¢/sec
Safety rod withdrawal rate . . .	+2.5 ¢/sec

5. Scram Mode

Initiation conditions	Manual. Individual actuator scrams if its supply pressure drops below 800 psi. 2 of 3 period amplifiers exceed a preset period. 2 of 3 log power amplifiers exceed a preset power level. Power demand circuit failure

D. AIR FLOW RATE CONTROL

High range	1300 to 2000 lb/sec
Control valve	AV3
Flow rate sensor	Pressure and temperature downstream of AV103 or upstream of AV104
Intermediate range	450 to 1300 lb/sec
Control valve	AV4
Flow rate sensor	Venturi FM1 or pressure at Station O or near AV104
Low range	0 to 450 lb/sec
Control valve	AV4
Flow rate sensor	Venturi FM2 or pressure downstream of AV103 or upstream of AV104
Automatic valve position control . . .	Feed forward prediction and feed back error; no temperature correction in intermediate and low ranges

Accident control

High and intermediate ranges, manual servo or automatic control	Valve position is controlled so that pressure rate never exceeds a preset level (non-locking)
All ranges	Control reverts to manual override if pressure level, rate, or valve position error exceed preset value (locking)

E. AIR TEMPERATURE CONTROL

Butterfly control valves (mechanically linked)	AV5A, AV5B
Total area of valve openings (constant)	243 in^2 ± 3%
Automatic valve position control	Position predictor plus error feedback
Automatic temperature ramps	100, 150, or 200°F/min
Temperature sensors	3 chromel-alumel thermocouples downstream of AV103
Control process time delay constant	0.5 sec at design
Manual valve position control	
Manual override (hydraulic slewing) rate	Full stroke in 50 sec
Manual servo rates	Full stroke in 1, 2, or 4 min

F. OPERATING LIMITS

1. Reactor Temperatures

Maximum fueled tube wall temperature (T_w)	2850°F
Maximum fueled tube wall temperature at design point	2825°F
Maximum temperature difference: $T_w - T_{ig}$	1900°F
Operating envelope for T_w vs T_{duct}	See p. V-8

2. Experiment Duration

Design maximum length of full power run	7 minutes
Planned length of full power run . .	5 minutes
Minimum time to attain full flow rate	1.25 minutes
Minimum time to attain desired inlet temperature	1.25 minutes
Maximum number of full power runs	10
Maximum integrated power per run .	50 MW-hours
Minimum time between full power runs	2 weeks
Maximum number of temperature cycles (including full power runs) . .	35

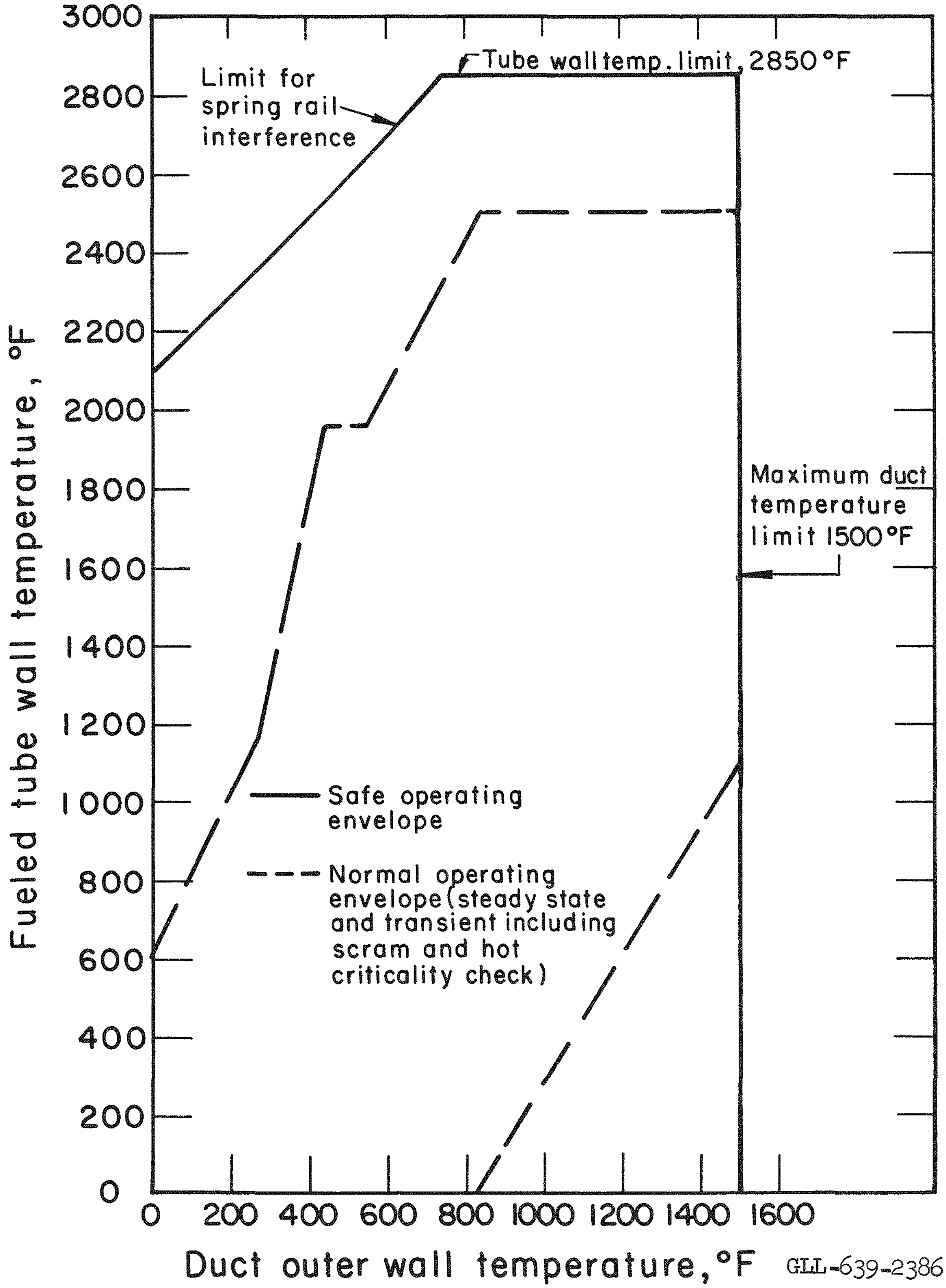

Fueled tube, duct temperature operating envelope at x/l = .7).

CHAPTER VI. MATERIAL PROPERTIES

Material properties depend upon many variables such as condition, prior history, and method of manufacture. It is difficult to set down in a concise manner all the properties of interest. Further, data is not available in most cases for the particular set of conditions applicable to the reactor.

Wherever possible, LRL data obtained under a specific set of conditions are used. Often data from manufacturers' brochures or general material handbooks is quoted. The data in this chapter must therefore be considered only as a general statement of material properties.

When not otherwise noted, properties are those exhibited at room temperature.

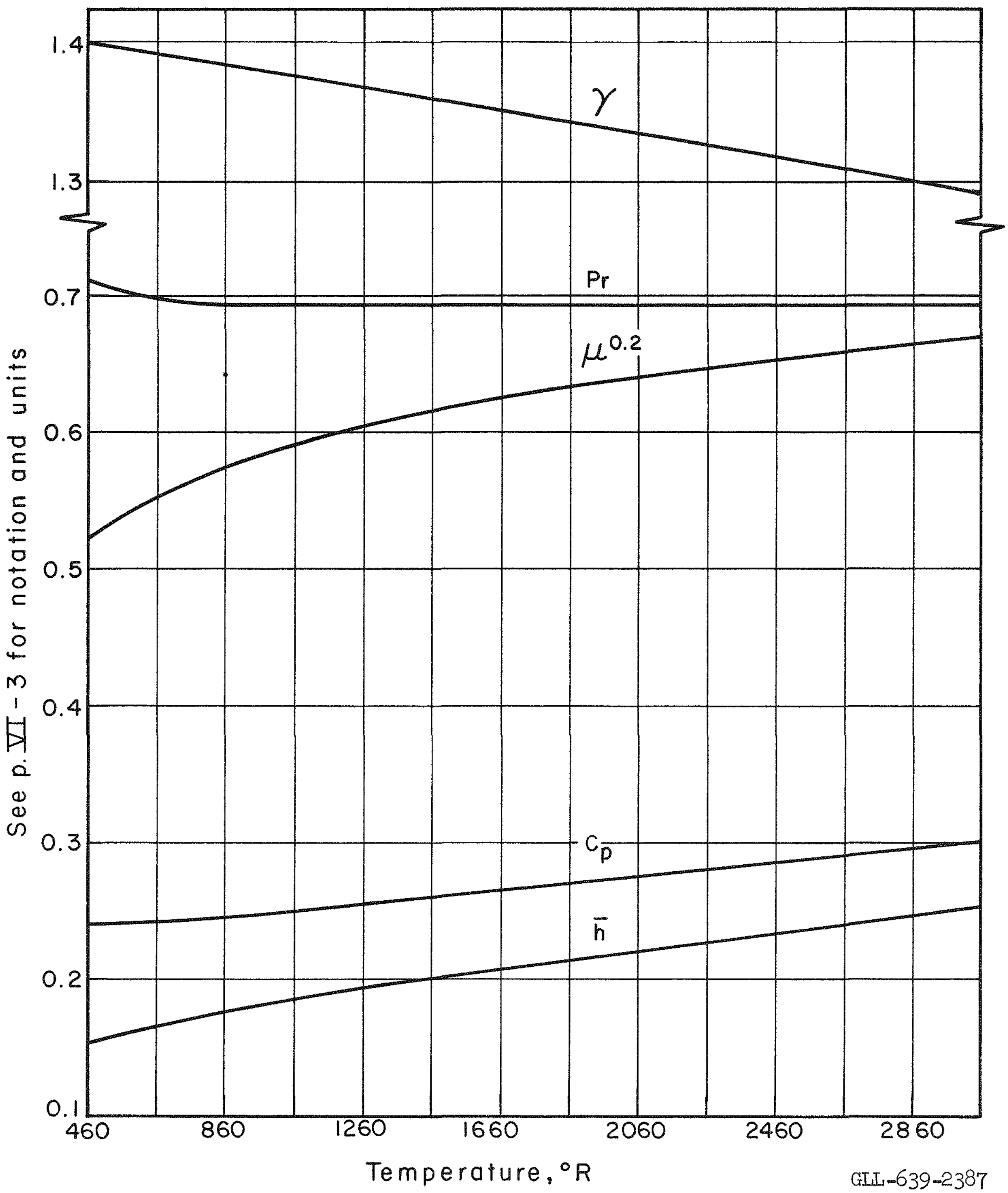

Properties of air (at 1 atmosphere pressure, used by FLOSS codes).

Notation and units used on p. VI-2 and in formulas below:

$\hat{\gamma}$	Specific heat ratio
μ	Dynamic viscosity, lb/hr-ft
h	Film coefficient, Btu/hr-ft^2-°R
$\overline{h}$	Gas film property group (see definition below)
C_p	Specific heat at constant pressure, Btu/lb-°F
G	Mass flow rate, lb/ft^2-hr (evaluate at bulk velocity, T_b, and static pressure)
D	Hydraulic diameter, ft
T_b	Bulk air static temperature, °R
T_b°	Bulk air stagnation temperature, °R
T_f	Mean film static temperature, °R
T_w	Wall temperature, °R
f	Friction factor
q	Heat flux, Btu/hr-ft^2
Pr	Prandtl number

Formulas:

$$h = 0.0205\,\overline{h}\left(\frac{G^{0.8}}{D^{0.2}}\right)\left(\frac{T_b}{T_f}\right)^{0.8}$$

where

$$\overline{h} = C_p\,\frac{\mu^{0.2}}{Pr^{0.6}} \qquad \text{(evaluate } \overline{h} \text{ at } T_f \text{ on p. VI-2)},$$

$$T_f = (T_w + T_b)/2.$$

$$f = 0.046\left(\frac{\mu}{GD}\right)^{0.2}\left(\frac{T_f}{T_b}\right)^{0.2} \qquad \text{(evaluate } \mu \text{ at } T_f \text{ on p. VI-2)},$$

$$q = h\,(T_w - T_b^\circ).$$

References:

1. "Table of Thermal Properties of Gases," NBS Circular 564, November 1955.
2. P.M. Uthe, "A Summary of Tory II-A Aerothermodynamics," PTN 208, 1 July 1960.

B. PROPERTIES OF CERAMICS AND CERMETS

1. BeO Properties

Use	Unfueled ceramic tubes
Powder specification	MEL 292
Ceramic tube specification	MEL 523
Powder producer	Brush Beryllium
Tube producer	Coors
Melting point	4620°F
Theoretical density	3.010 g/cc
Average density of 0.227-in.-diam-bore tubes	98.3%
Average density of 0.130-in.-diam-bore tubes	97.7%
Average density of 0.093-in.-diam-bore tubes	97.1%
Average modulus of rupture (0.227-in.-diam-bore tubes)	39,000 psi
Standard deviation of modulus of rupture	7,500 psi
Average modulus of rupture at temperature	See p. VI-5
Thermal expansion	See p. VI-6
Thermal conductivity	See p. VI-7
Dynamic modulus of elasticity	See p. VI-7
Dynamic Poisson's ratio	0.3
Thermal stress property group $E\alpha/k(1 - \nu)$	See p. VI-7
Specific heat	See p. VI-8
Powder chemical analysis	See p. VI-9
Tube chemical analysis	See p. VI-9

References:

1. D. K. Smith, "Density of BeO," Tory II-C Memo 334 dated June 1962.
2. J. Lillie, "Some Properties of BeO," UCRL-6457 dated May 1961.
3. Reactor Handbook, 2nd Ed., Vol. 1, "Materials."
4. W. Wells, personal communication.

BeO(Contd.)

Average modulus of rupture for 0.227-in.-diam-bore ceramic tubes.

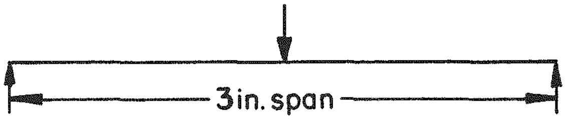

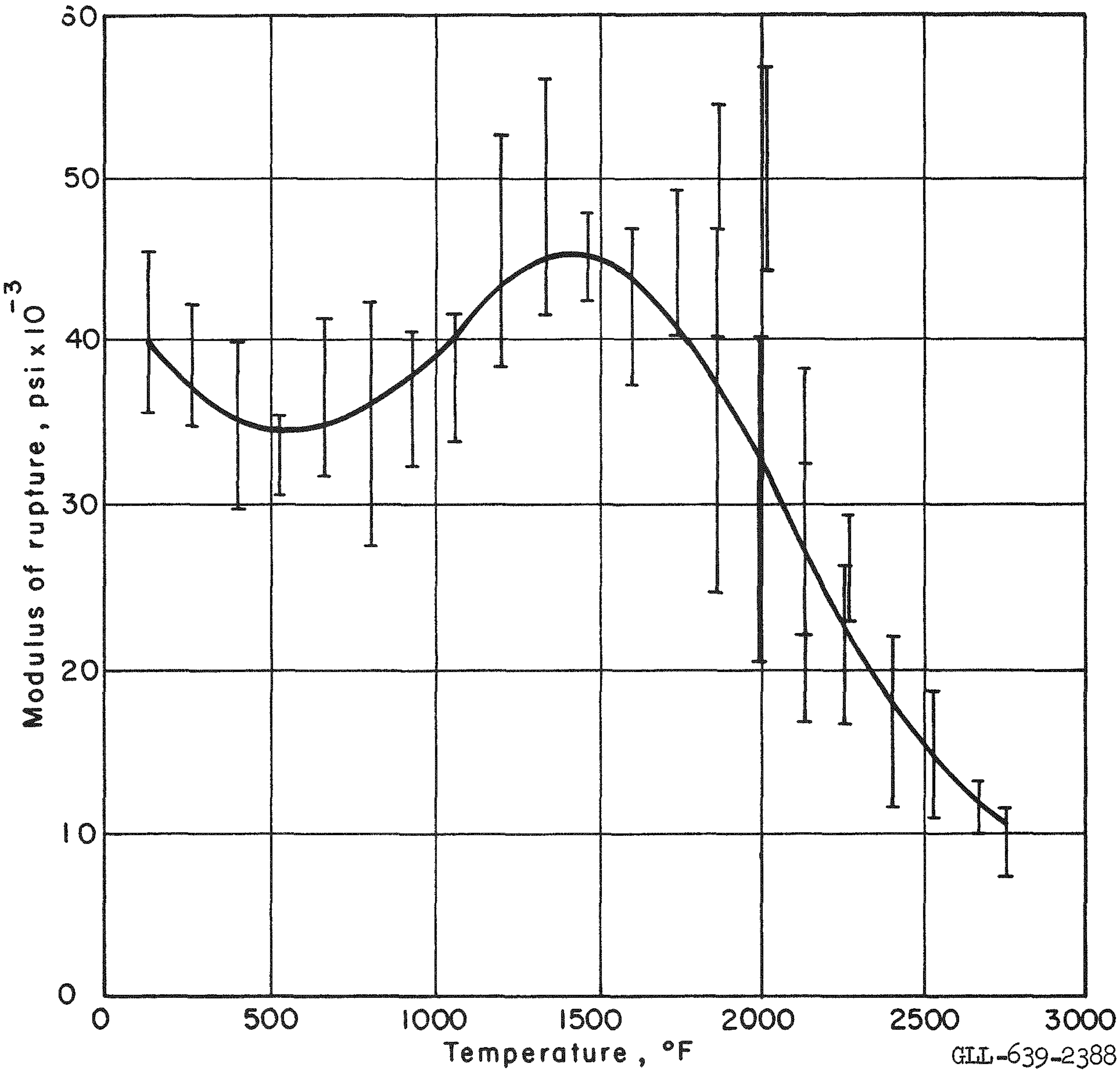

BeO (Contd.)

Thermal Expansion — Average properties for several types of BeO (Ref: UCRL-6457).

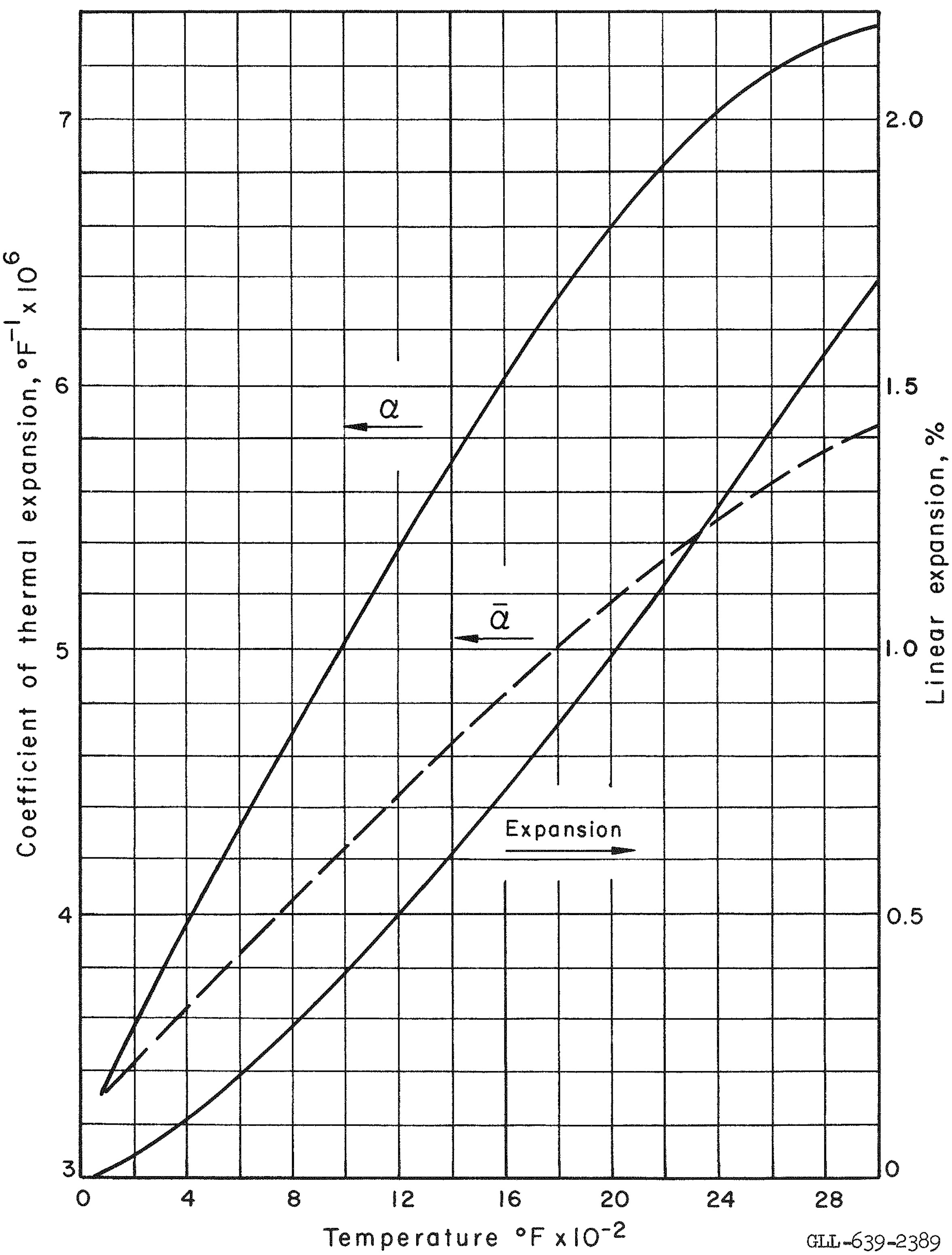

GLL-639-2389

BeO (Contd.)

Thermal conductivity, dynamic modulus of elasticity, and thermal stress property group, $E\alpha/k(1-\nu)$; 98% theoretical density, $\nu = 0.3$. Note: E increases 3% and k increases 2% for an increase in density of 1%.

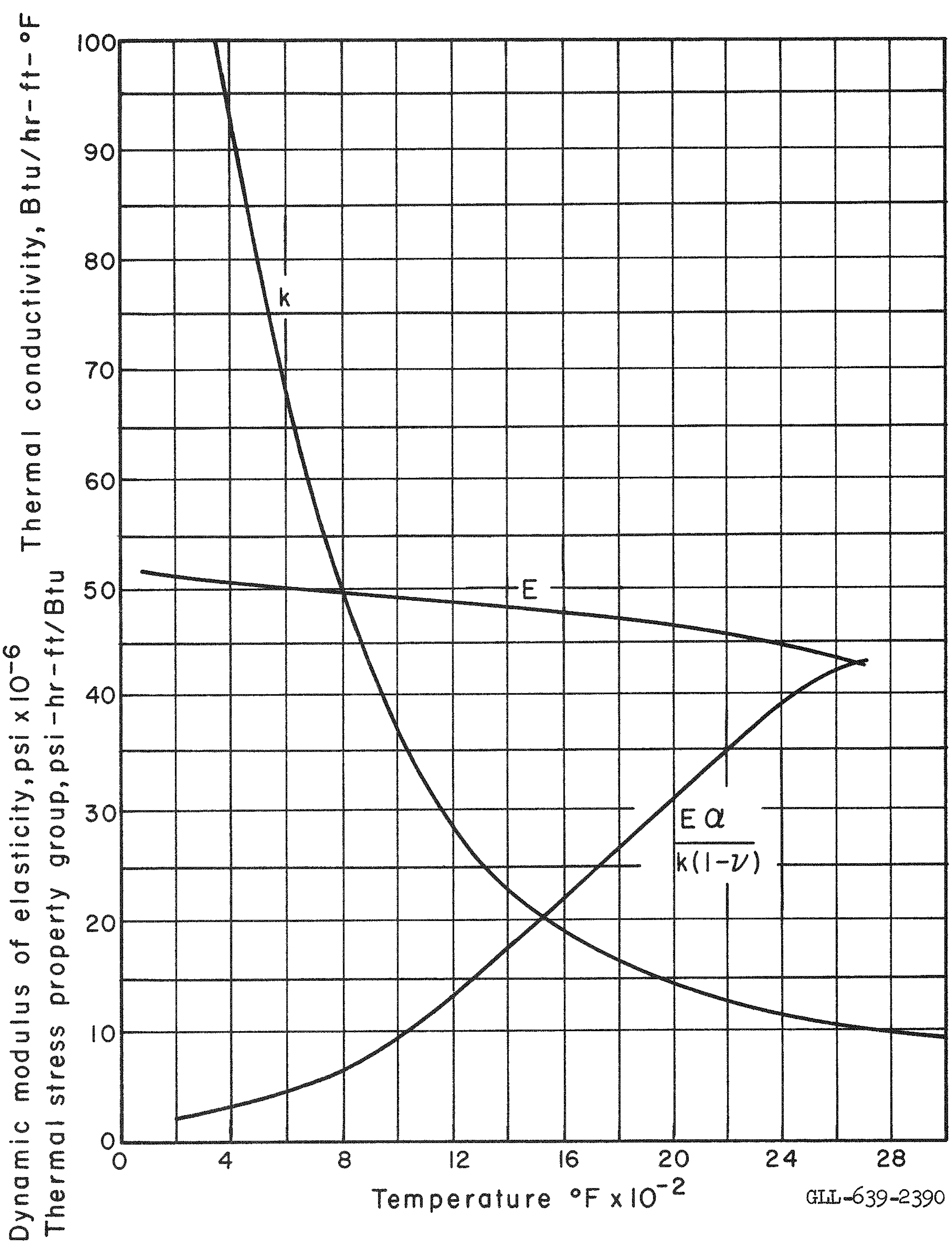

BeO (Contd.)

Specific Heat (Ref.: Reactor Handbook)

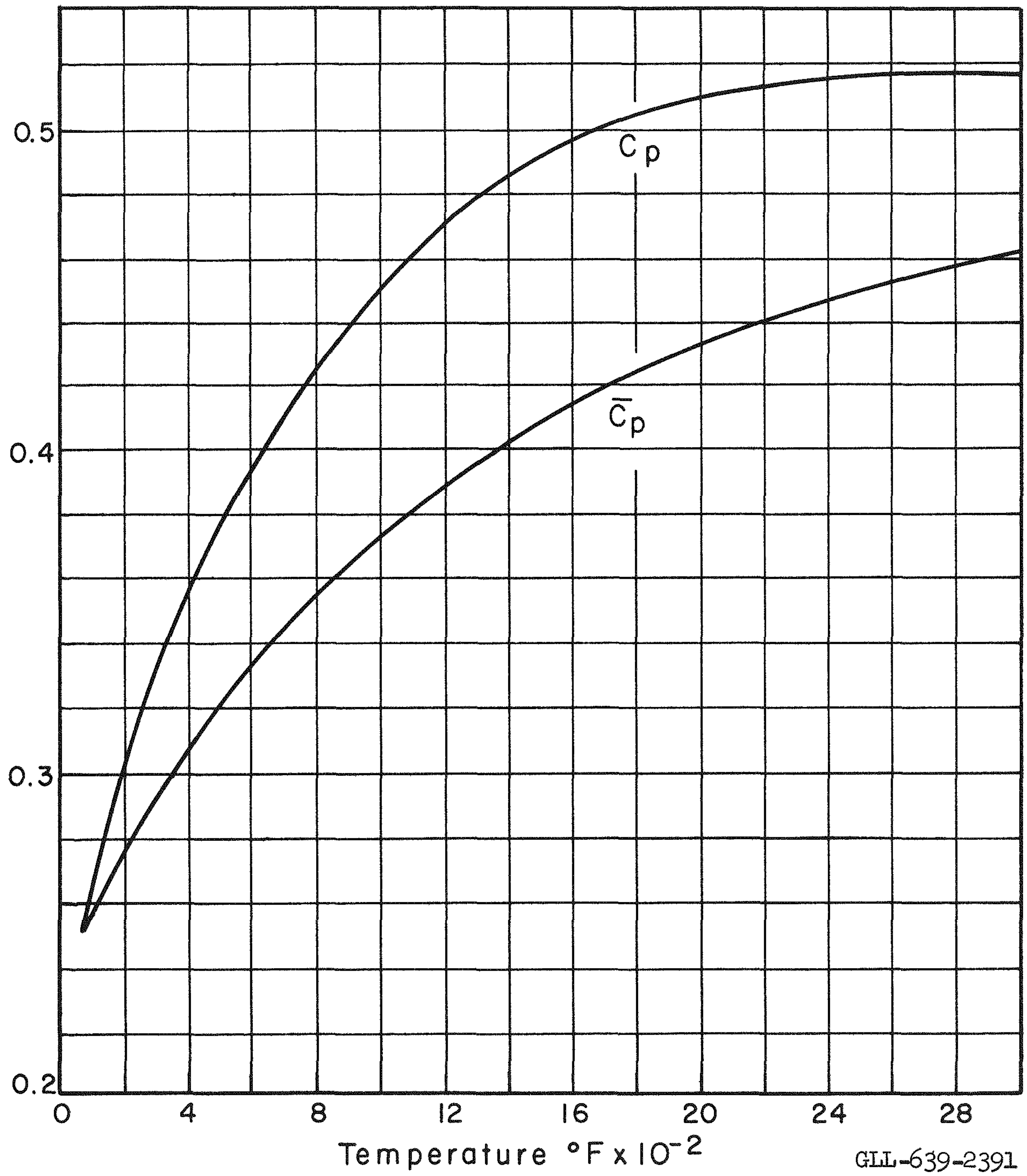

GLL-639-2391

BeO (Contd.)

BeO Powder and Tube Chemical Analysis[1,2]

Element	Average concentration (ppm)		Standard deviation (ppm)		Maximum concentration analyzed (ppm)		c/q	
	Powder	Tube	Powder	Tube	Powder	Tube	Powder	Tube
Chromium	2	7	2.6	20	18	55		
Copper	1	4	0.5	1	7	8		
Iron	16	25	10	64	75	150		
Nickel	2	7	1.3	18	10	50		
Magnesium	27	15	13	19	90	60		
Calcium	9	12	5	23	50	40		
Aluminum	22	60	13	78	70	200		
Silicon	37	47	18	70	90	150		
Sulfur	798	149	278	12	1500	150		
Boron	0.4				0.4		0.1	
Cadmium	0.6				0.6		.1	
Cobalt	1.2				1.2		.1	
Lithium	2		0.33		4		.1	
Manganese	2		0.62		6		.1	
Sodium	14	13	7	17	50	50	.3	0.25
Titanium	5	12	0.4	9	10	40	.1	0.25
Silver	5				5		0.1	
						Sum	1.0	0.5

1. See Specification MEL 292 and MEL 573 for definitions and limits specified.

2. Values are high since nondetectable elements are computed as being present in the amount of the detection threshold. See Tory II-C Memo 338.

2. Fueled BeO Properties

Use in reactor	Fueled tubes
Ceramic tube specification	MEL 523
Fuel composition	"Horseradish"
Tube producer	Coors
Theoretical density	See p. VI-11
Average tube density	See p. VI-11
Average modulus of rupture	38,700 psi
Typical product variation of modulus of rupture	See p. VI-12
Average modulus of rupture at temperature . .	See p. VI-13
Thermal expansion	*
Thermal conductivity	*
Dynamic modulus of elasticity	*
Dynamic Poisson's ratio	*
Thermal stress property group $E\alpha/k(1-\nu)$ . .	*
Specific heat	*
Tube chemical analysis	See p. VI-14

References:

1. E. Robinson, personal communication.
2. W. Moran, memorandum dated February 19, 1963.
3. J. Collins, personal communication.

* See BeO property values. No data on fueled BeO tubes available.

Fueled BeO (Contd.)

Density of Fueled Tubes

Curves are based on nominal tube cross-sectional area and nominal Horse-radish composition.

Data points are measured average values (averaged in size groups).

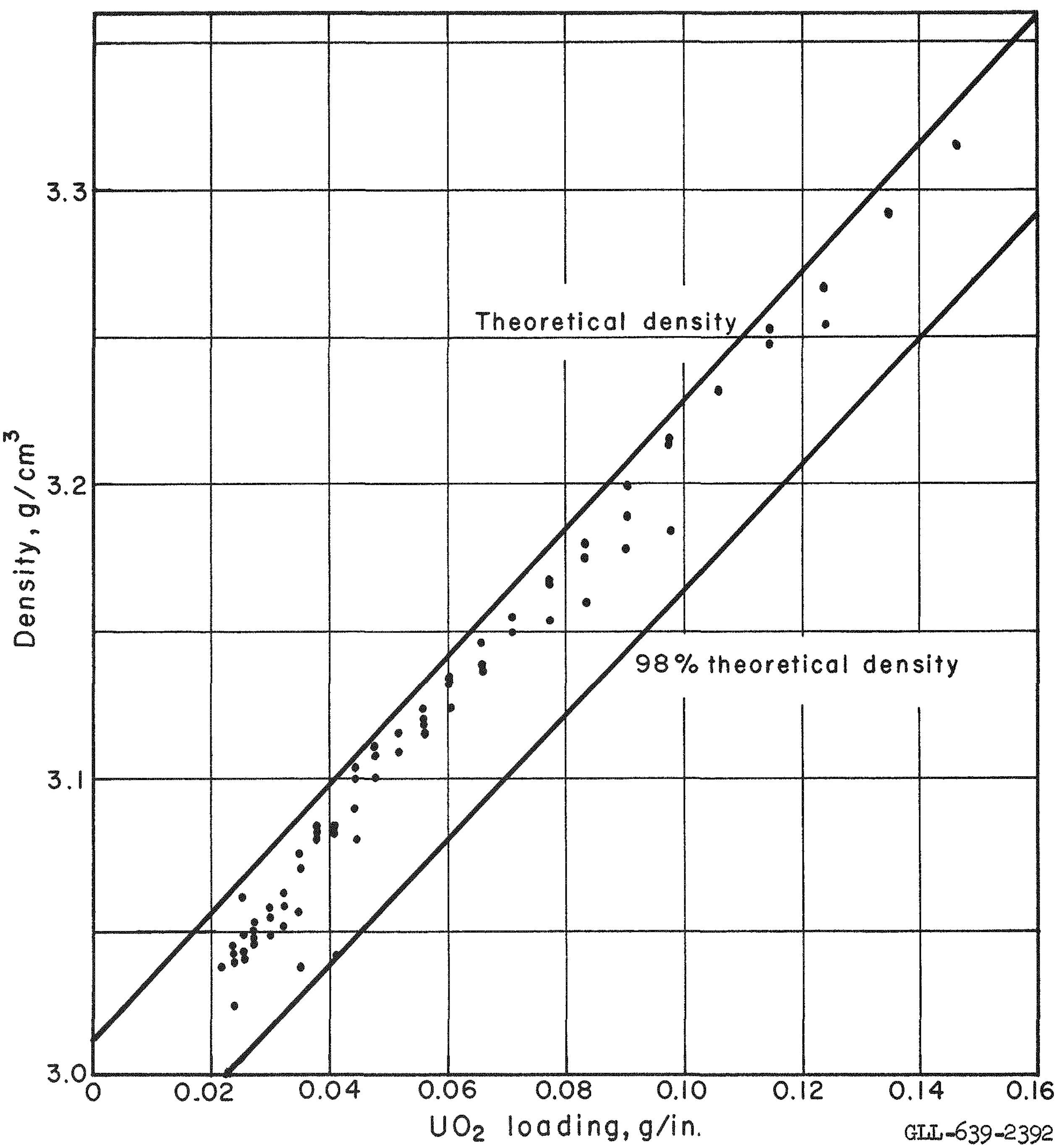

Fueled BeO (Contd.)

Typical (Coors) product variation of modulus of rupture at room temperature (large range of fuel loadings).

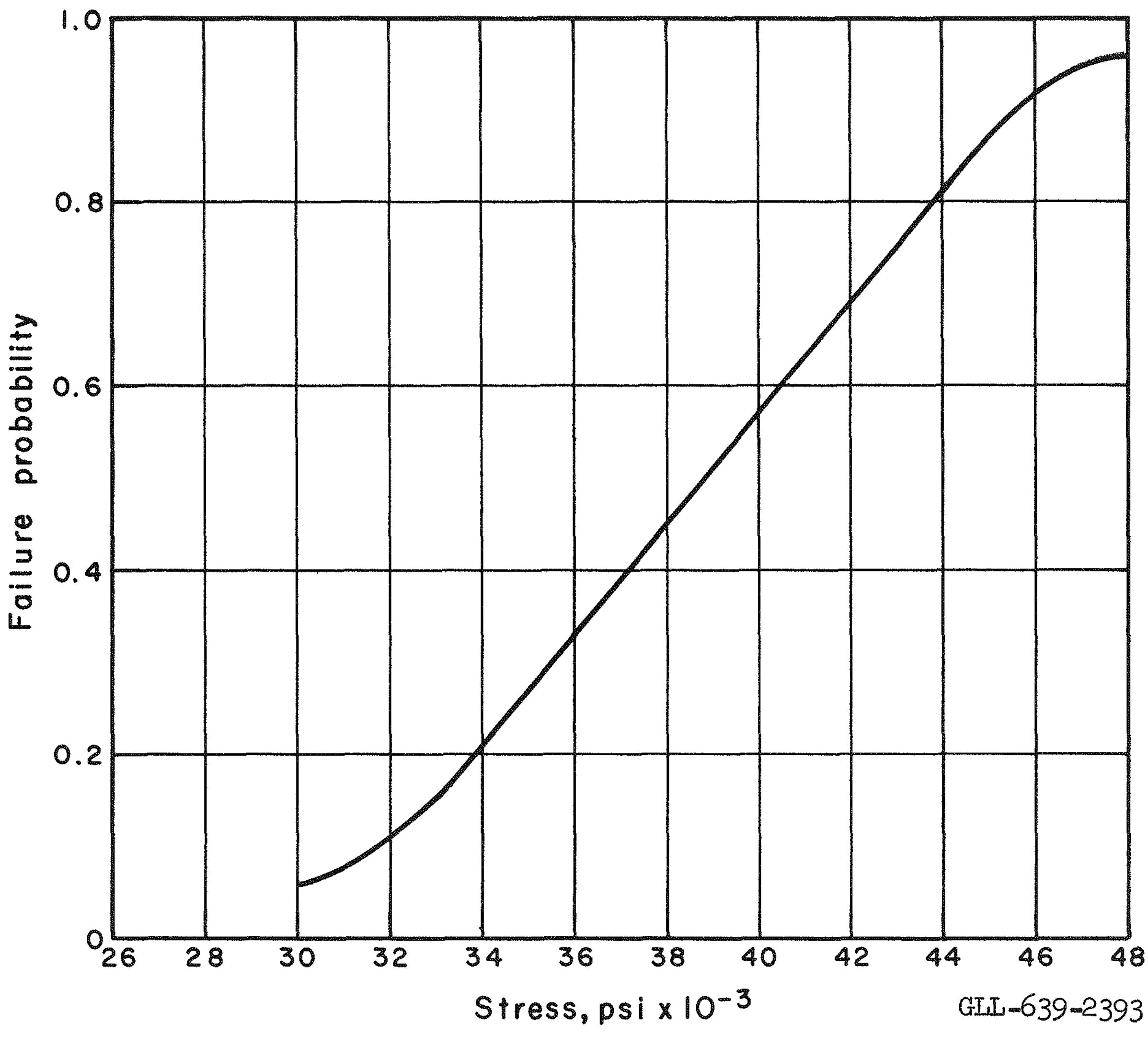

Fueled BeO (Contd.)

Corrected average modulus of rupture of fueled tubes. Using the curve on page VI-12, a correction is applied in accordance with the position of the tube batch tested relative to the stress value for 50% probability of failure.

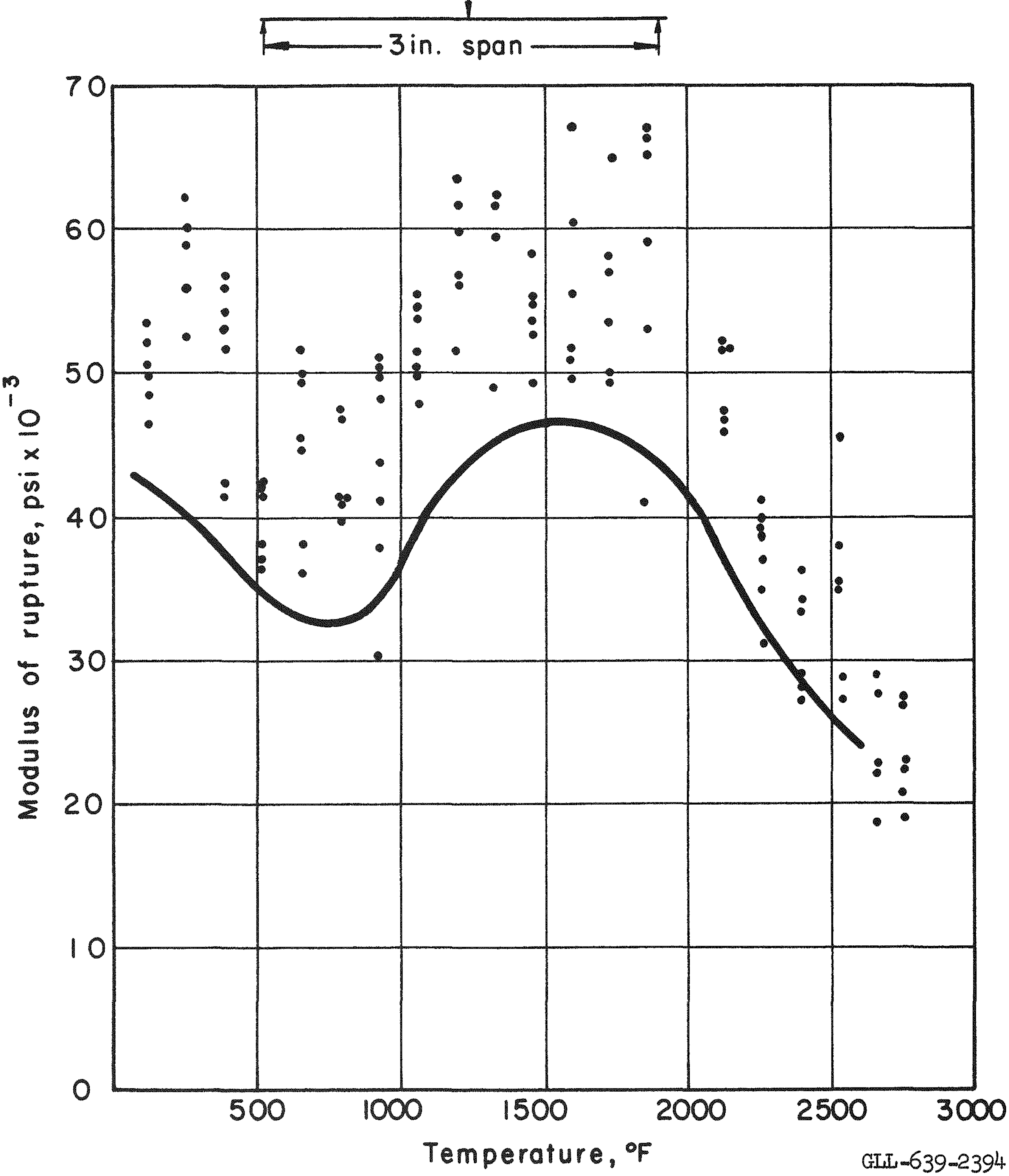

Fueled BeO (Contd.)

Fueled tube chemical analysis[1,2]
(with exception of UO_2, Y_2O_3, and ZrO_2)

Element	Average concentration (ppm)	Standard deviation (ppm)	Maximum concentration analyzed (ppm)	c/q
Chromium	5	0.3	10	
Copper	4	0.5	5	
Iron	34	23		
Nickel	4	0.2	5	
Magnesium	36	26	150	
Calcium	12	31		
Aluminum	40	25	155	
Silicon	61	49	200	
Sulfur	159			
Boron	0.4	0.02	0.4	0.1
Cadmium	0.6	.03	0.6	.1
Cobalt	1.2	.05	1.2	.1
Lithium	2	.1	2	.1
Manganese	2	0.1	2	.1
Sodium	1.0	7	60	.2
Titanium	5	0.2	5	.1
Silver	5	.2	5	.1
Gadolinium	0.1	.00	0.1	.1
Samarium	0.5	.05	1	.1
Europium	0.8	.04	0.8	.1
Indium	2	.1	2	.1
Dysprosium	3	.3	6	.1
Tin	3	.1	3	.1
Hafnium	3	.1	3	.1
Gold	3	.1	3	.1
Rhodium	4	.2	4	.1
Erbium	5	0.2	5	0.1
			Sum	1.9

1. See MEL 523 for definitions and limits specified.
2. Nondetectable elements are computed as being present in the amount of the detection threshold.

3. Carbon P-56 HT Properties

Use	Slider bearings
Characteristics	Graphite, medium-hard, chemical salt impregnated, oxidation resistant
Density	1.65 g/cc
Porosity	14%
Coefficient of thermal expansion	2.73×10^{-6} °F^{-1}
Modulus of elasticity	1×10^{6} psi
Compressive strength	18,000 psi
Tensile strength	2,200 psi
Modulus of rupture	6,500 psi
Elastic compressive deformation	1.8%
Hardness (Shore scleroscope)	65
Maximum recommended temperature in air	1100°F

4. Carbon P-303C Properties

Use	Control actuator seals and bearings
Characteristics	Carbon, hard, oxidation resistant
Density	1.84 g/cc
Porosity	4%
Coefficient of thermal expansion	2.02×10^{-6} °F^{-1}
Modulus of elasticity	1.2×10^{6} psi
Compressive strength	18,000 psi
Tensile strength	2,200 psi
Modulus of rupture	8,500 psi
Elastic compressive deformation	1.5%
Hardness (Shore scleroscope)	78
Maximum recommended temperature in air	1000°F

Reference: Pure Carbon Co., Inc., brochure.

5. Chrome 2400-30 Properties

Use in reactor	Transition rings and cartridges
Specification	MEL 624
Stock	Extruded rod
Ambient air ignition temperature	3000°F
Melting point	3400°F (chromium)
Density	6.55 g/cm^3
Hardness (Brinell)	100
Impact transition temperature	415°F
Chemical composition	
Cr	95%
MgO	5%
Modulus of elasticity	32×10^6 psi
Coefficient of thermal expansion	See p. VI-17
Thermal conductivity	See p. VI-17
Ultimate strength	See p. VI-17
Yield strength	See p. VI-17
Elongation	See p. VI-17
Creep strength	See p. VI-17
Oxidation resistance	See p. VI-17

References: Memo by E. Platt dated January 16, 1963.
W. Hay, personal communication.

Chrome — 2400-30

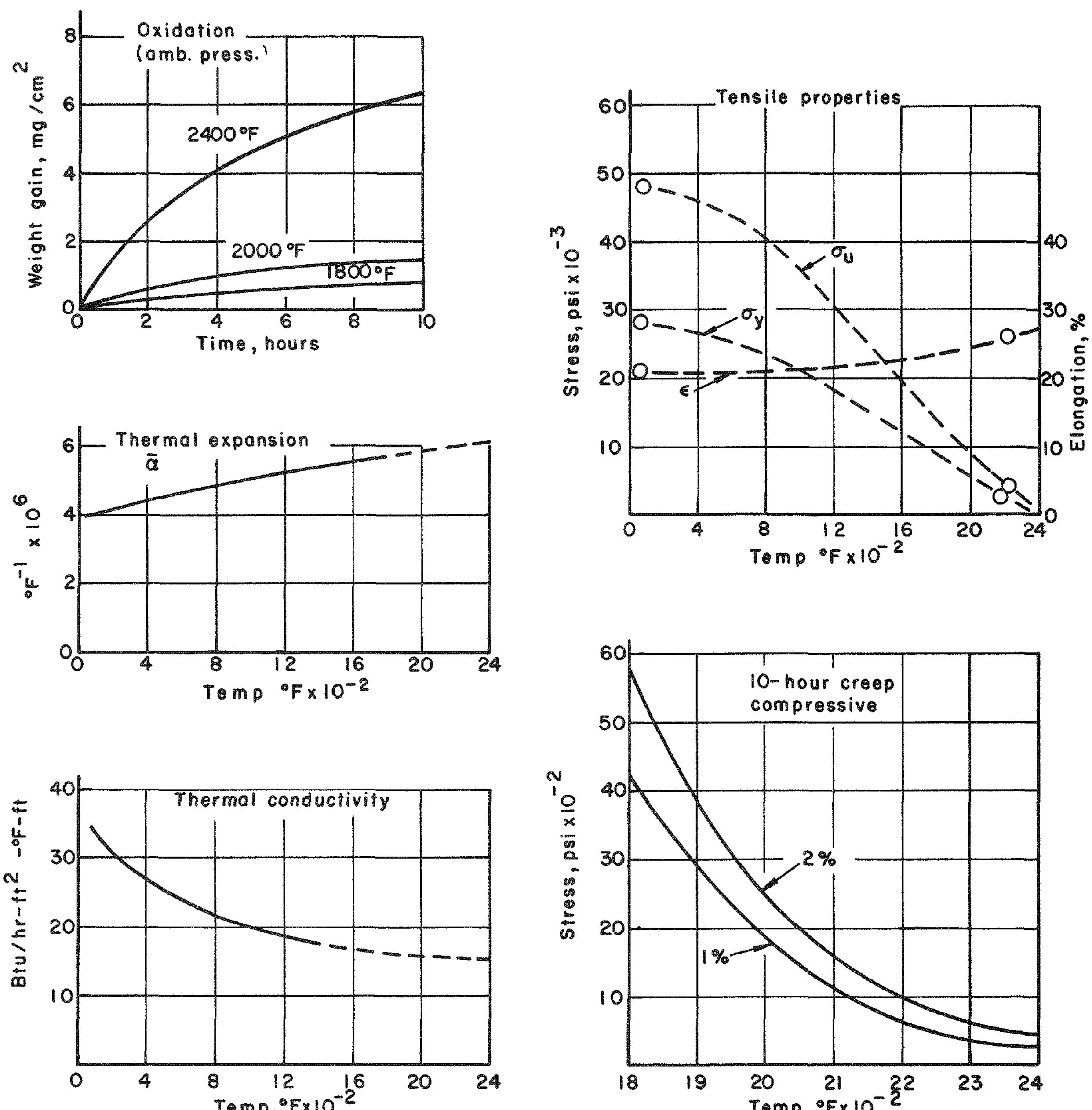

GLL-639-2395

C. PROPERTIES OF COATINGS

1. Alumina Coating Properties

Use in reactor	Insulating cup, transition parts, base blocks
Specification	MEL 706 (insulating cup)
Process	Plasma spray
Density	3.3 g/cm^3
Thickness	0.010 inch (insulating cup)
Thermal conductivity	2 Btu/hr-ft-°F above 1022°F

2. Si/Cr-FeB Coating Properties

Use in reactor	Base blocks
Specification	MEL 623
Process	Two-cycle pack diffusion
Total coating thickness	5 mils
First cycle coating thickness	2.6 mils
First cycle coating density	19 mg/cm^2
Second cycle coating thickness	2.4 mils
Second cycle coating density	25 mg/cm^2
First cycle pack constituents	
Alumina	30%
Silicon	60%
Potassium acid flouride	10%
Second cycle pack constituents	
Alumina	33%
Chromium	30%
Ferro-boron	30%
Potassium iodide	7%
Process temperature and time	
First cycle	4 hr @ 2300°F
Second cycle	8 hr @ 2200°F

Life of Si/Cr-FeB coating on D-40 in cyclic tests, in static* air. (*Ignition failures occurred in high-rate airflow test.)

____________________ No failures, tests discontinued

-----------o------------- Failure (coating loss in excess of 1/8-in.-diam spot)

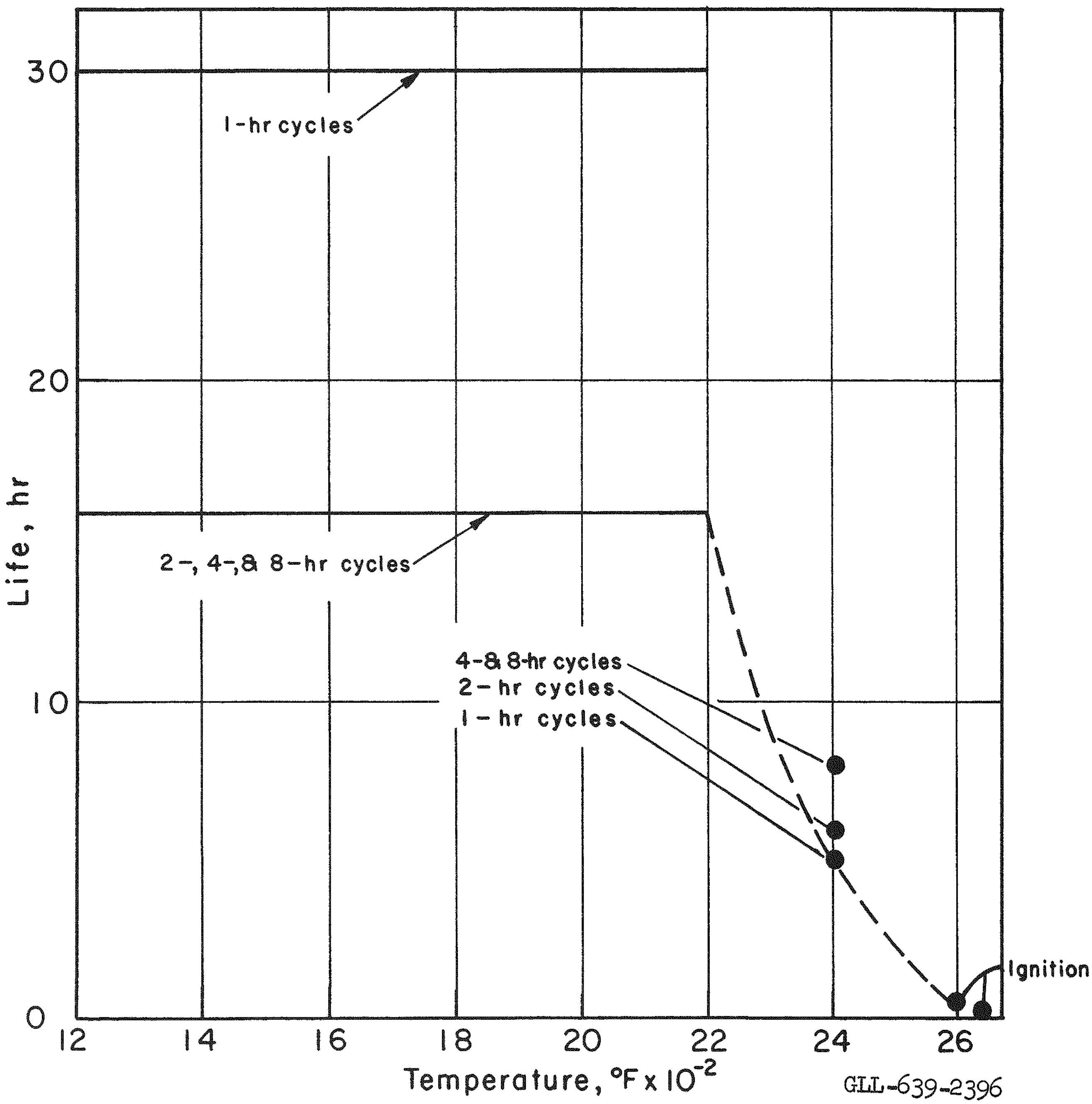

GLL-639-2396

D. PROPERTIES OF COBALT ALLOYS

1. Haynes 25 Properties (L-605)

Use	Control actuator rack
Stock	Bar, pinion 15% cold reduced
Melting point	2425°F
Density	9.13 g/cm^3
Specific heat	0.092 Btu/lb-°F
Poisson's ratio	0.29
Modulus of elasticity	See p. VI-21
Mean coefficient of thermal expansion	See p. VI-21
Thermal conductivity	See p. VI-21
Ultimate strength	See p. VI-21
Yield strength	See p. VI-21
Creep rupture strength	See p. VI-21
Impact strength (C. V. @ 0°F)	150 ft-lb
Hardness (Rockwell C) (15% cold reduced)	31
Heat treatment	Aged 4 hr @ 1200°F
Chemical composition	
Cobalt	49.4%
Chromium	20%
Tungsten	15%
Nickel	10%
Iron	3% (max)
Manganese	1.5%
Silicon	1%
Carbon	0.1%

Reference: ARDC-TR-59-66.

Haynes 25 Properties (continued)

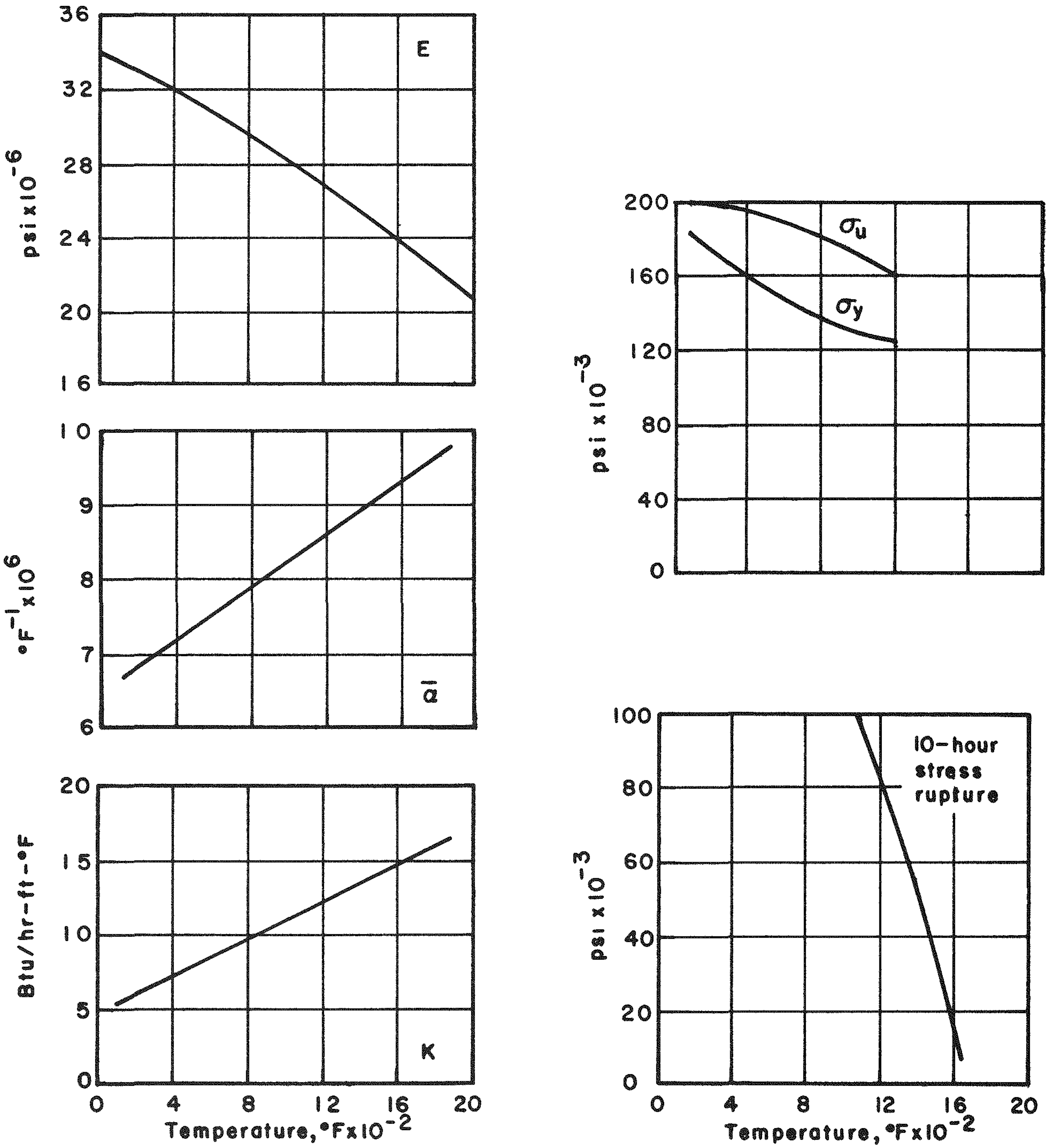

GLL-639-2397

2. Stellite 68 Properties

Use	Servo valve and miscellaneous actuator parts
Melting point	2470°F
Density	8.38 g/cm^3
Poisson's ratio	0.27
Modulus of elasticity (70 to 600°F)	30.4×10^6 psi
Mean coefficient of thermal expansion	7.7 in./in.-°F @ 70°F 9.7 in./in.-°F @ 1000°F
Thermal conductivity	8.6 Btu/hr-ft-°F
Ultimate strength @ 1500°F	70,000 psi
Impact strength (Charpy, unnotched)	65
Hardness (Rockwell C)	37
Chemical composition	
Cobalt	52.7%
Chromium	30%
Tungsten	4.5%
Nickel	3.0%
Iron	3.0%
Carbon	1.1%
Silicon	2.0% (max)
Molybdenum	1.5% (max)
Manganese	2.0% (max)

Reference: ARDC-TR-59-66.

E. PROPERTIES OF COLUMBIUM ALLOYS

1. D-36 Properties

Use	Instrument rake
Stock	Sheet and plate
Condition	Recrystallized
Melting point	3500°F
Melting point of Cb_2O_5	2570°F
Density	7.95 g/cm^3
Poisson's ratio	0.25
Modulus of elasticity	16.5×10^6 psi
Mean coefficient of thermal expansion	4×10^{-6} $°F^{-1}$
Thermal conductivity	Use D-40 properties
Ultimate strength	See p. VI-24
Yield strength	See p. VI-24
Elongation	> 2%
Creep rupture strength, 1 hour @ 2000°F	18,000 psi
Creep rupture strength, 1 hour @ 2200°F	7,000 psi
Chemical composition	
Columbium	85%
Titanium	10%
Zirconium	5%
Carbon	50 ppm
Nitrogen	100 ppm
Oxygen	400 ppm

D-36 properties (continued)

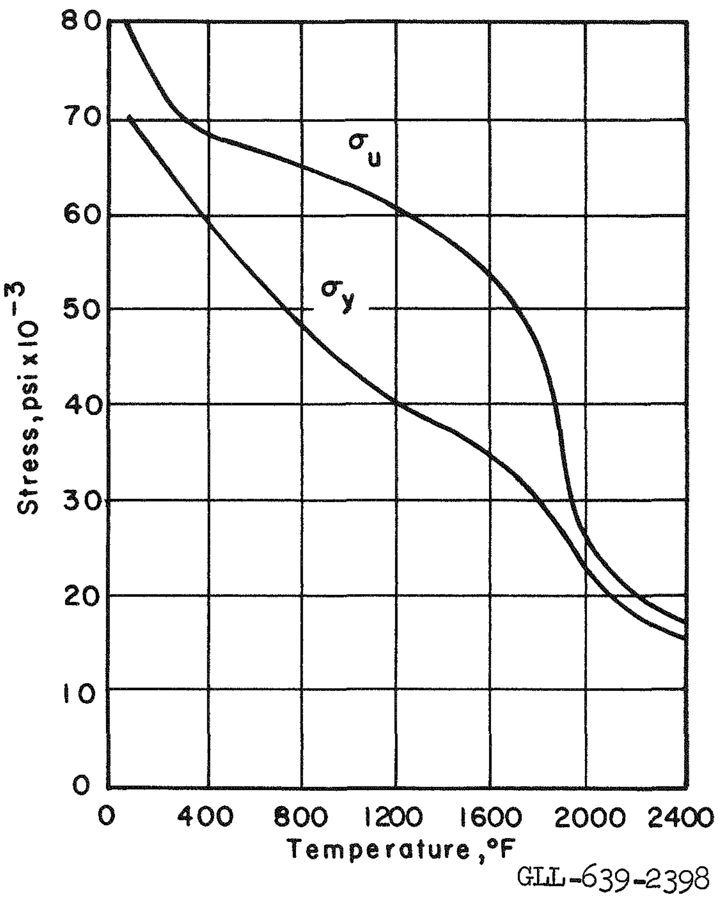

Reference: Dupont Metal Products Data Sheet No. 1.

2. D-40 Properties (F-48)

Use	Base blocks
Specification	MEL 504
Stock	Plate
Melting point	4350°F
Melting point of Cb_2O_5	2570°F
Density	9.42 g/cm^3
Poisson's ratio	0.25
Modulus of elasticity	See p. VI-26
Mean coefficient of thermal expansion	See p. VI-26
Thermal conductivity @ 1600°F	34.8 Btu/hr-ft-°F
Ultimate strength	See p. VI-26
Yield strength	See p. VI-26
Elongation	See p. VI-26
Impact transition temperature	800°F
Creep rupture strength 3.7 hr @ 2200°F	30,000 psi
Creep strength, 1%, 10 hr @ 2200°F	14,000 psi
Creep strength, 1%, 10 hr @ 2500°F	6,000 psi
Hardness (DPH)	250
Heat treatment	Recrystallized, 20%
Oxidation resistance	See p. VI-27
Chemical composition	
Columbium	79%
Tungsten	15%
Molybdenum	5%
Zirconium	1%
Carbon	400-500 ppm
Oxygen	200-400 ppm
Nitrogen	20-40 ppm

Columbium Alloy Cb 15W5Mo 1 Zr
(D-40)

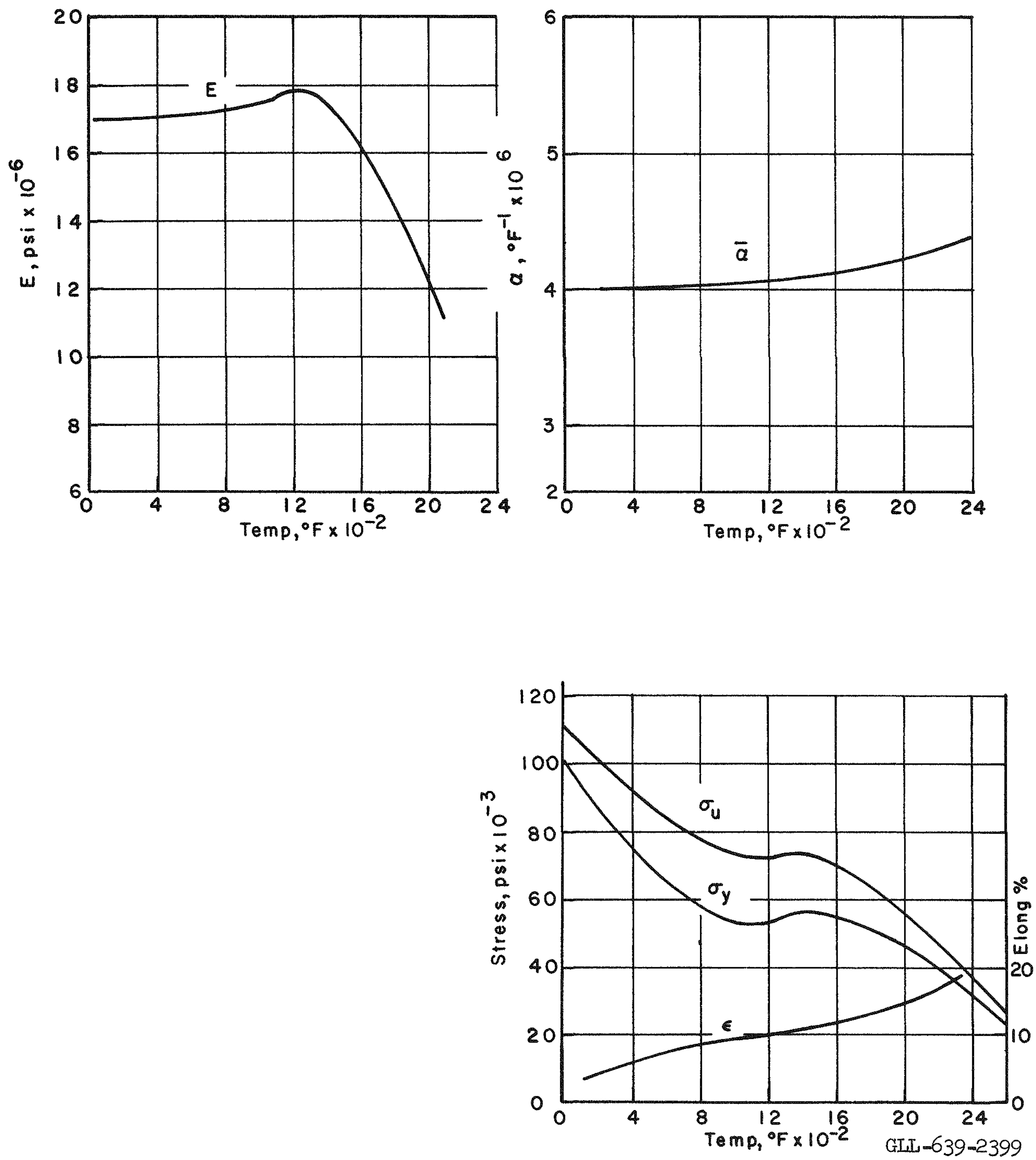

D-40 Properties (Contd.)

Life of uncoated D-40 in static air.

Failure defined at time for 0.005 in. metal recession to occur.

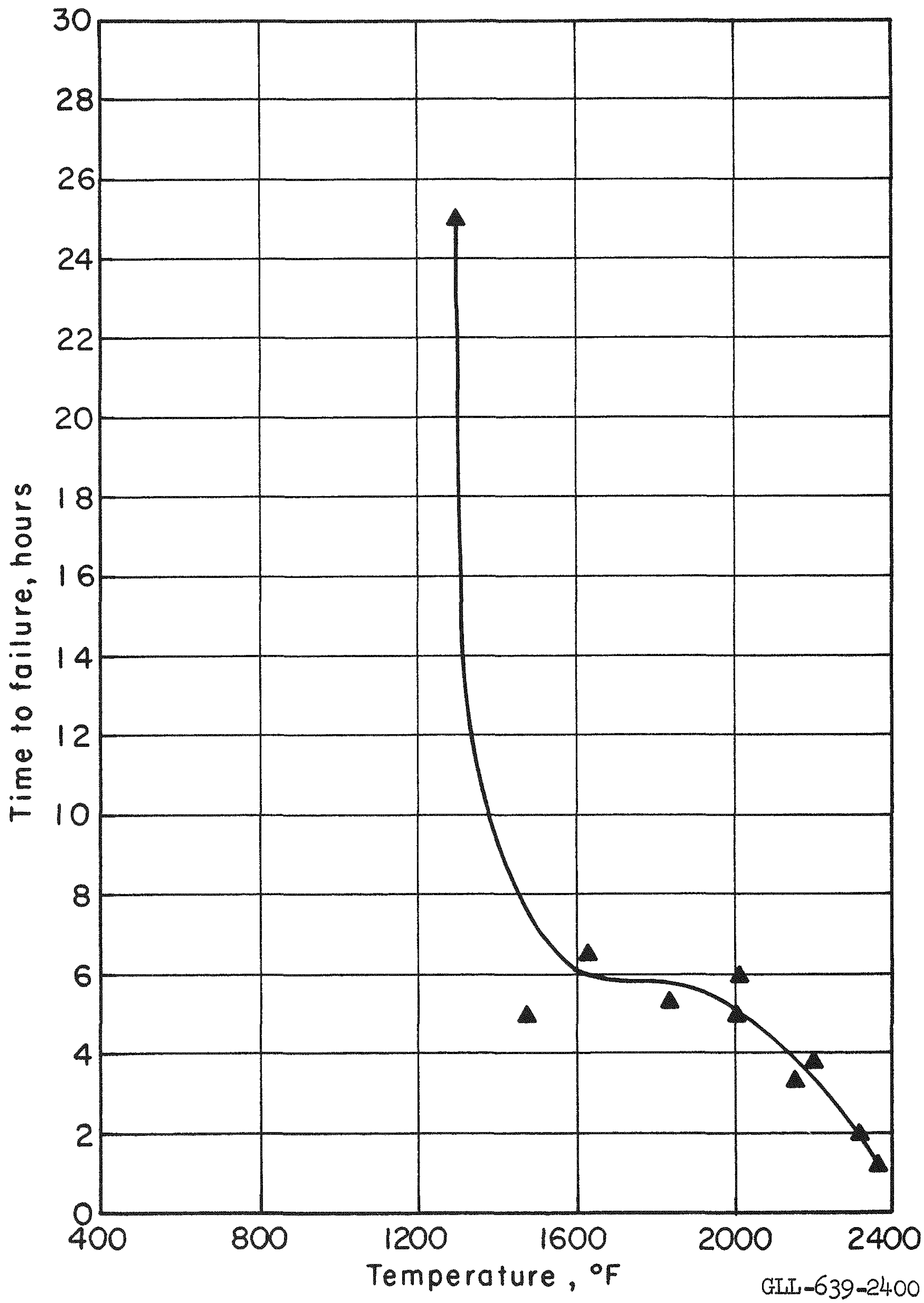

F. PROPERTIES OF FERROUS ALLOYS

1. Mild Steel Properties

Use	Blowdown ducts
Specification	ASTM A-350/LF2 A285/Grade C
Stock	Ring forging, plate
Melting point	2800°F
Density	7.85 g/cm^3
Specific heat	0.12 Btu/lb-°F
Poisson's ratio	0.29
Modulus of elasticity	30×10^6 psi
Mean coefficient of thermal expansion	See p. VI-29
Thermal conductivity	See p. VI-29
Ultimate strength	See p. VI-29
Yield strength	See p. VI-29
Chemical composition	
Iron	98%
Manganese	1.3%
Carbon	0.25%

Mild Steel

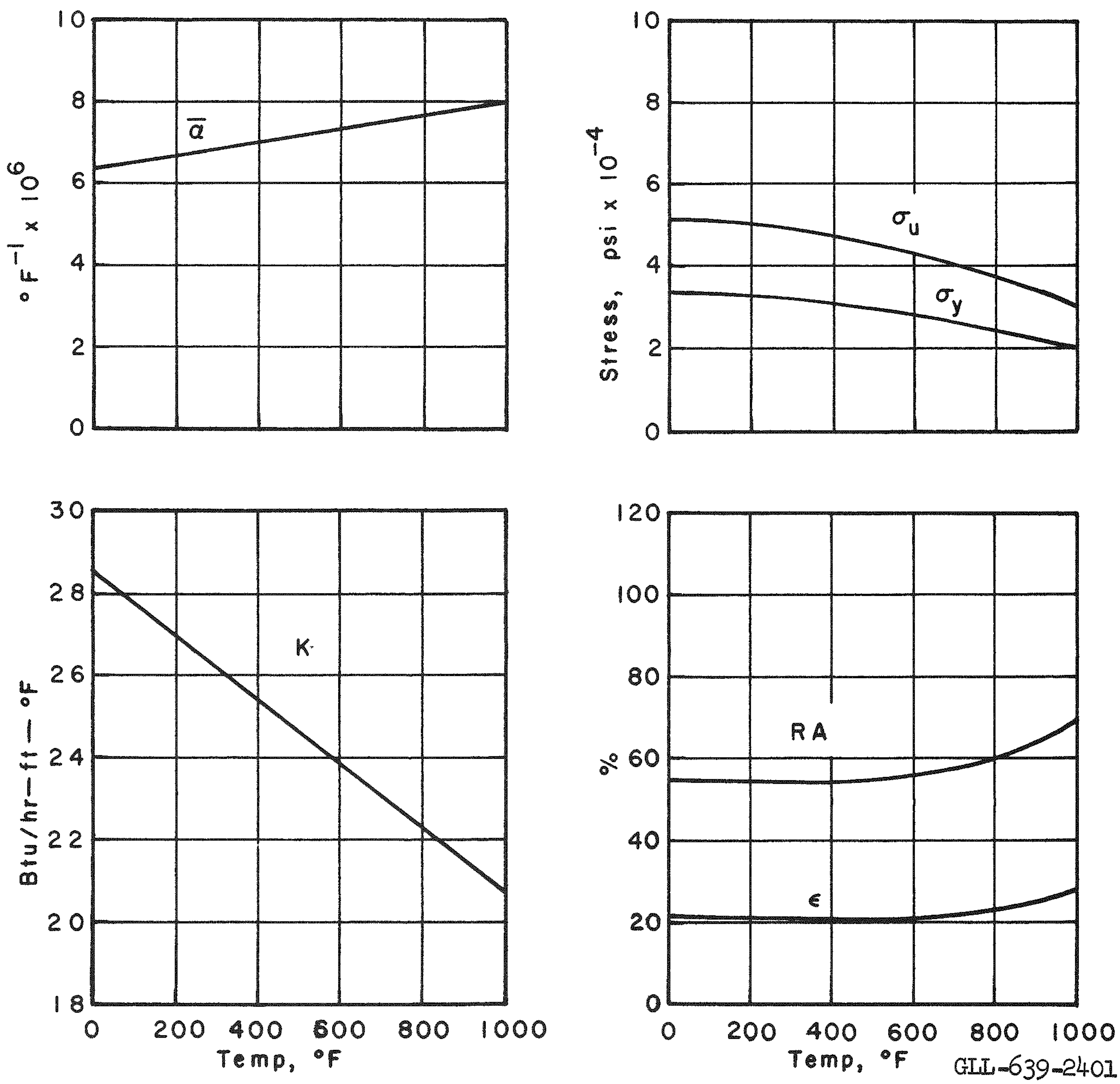
10
8
6
4
2
0
°F^{-1} x 10^6
$\bar{\alpha}$
Stress, psi x 10^{-4}
σ_u
σ_y
30
28
26
24
22
20
18
Btu/hr—ft—°F
K
0
200
400
600
800
1000
Temp, °F
120
100
80
60
40
%
RA
ϵ
GLL-639-2401

2. Stainless Steel Type 347 Properties

Use	Control actuator
Melting point	2550°F
Density	8.05 g/cm^3
Specific heat	0.12 Btu/lb-°F
Modulus of elasticity	See p. VI-31
Mean coefficient of thermal expansion	See p. VI-31
Thermal conductivity	See p. VI-31
Ultimate strength	See p. VI-31
Yield strength	See p. VI-31
Creep rupture strength	See p. VI-31
Hardness (Brinell)	200
Heat treatment	1800°F/1/2 hr, WQ
Chemical composition	
Iron	70%
Chromium	18%
Nickel	12%
Manganese	2% max
Silicon	1% max
Columbium	0.8% max
Carbon	0.08% max

347 Stainless

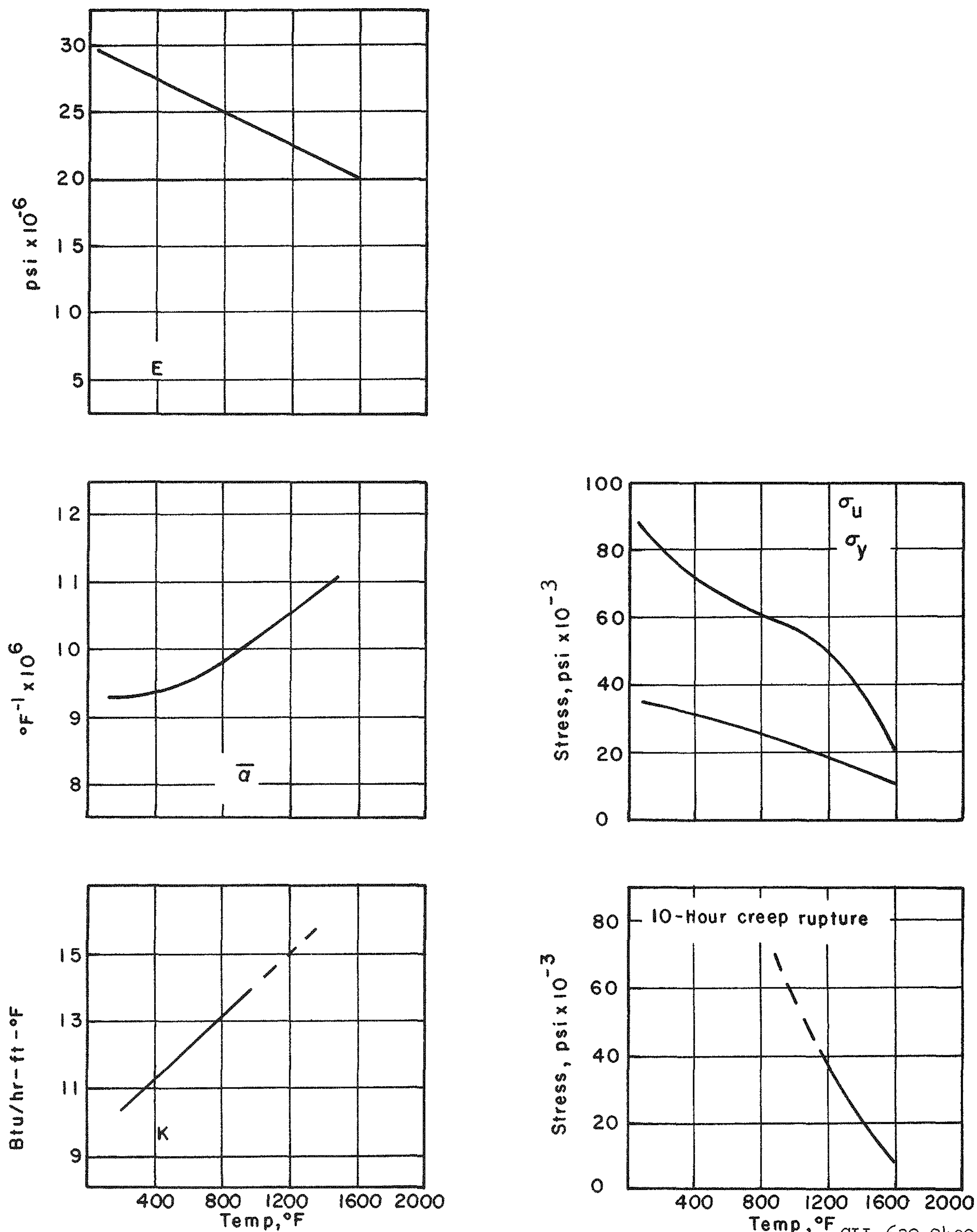

GLL-639-2402

3. Stainless Steel Type 405 Properties

Use	Facility air heater
Specification	NECO 292-62-3
Stock	Forgings
Melting point	2700°F
Density	7.78 g/cm^3
Heat capacity	See p. VI-33
Modulus of elasticity	29×10^6 psi
Mean coefficient of thermal expansion	See p. VI-35
Thermal conductivity	See p. VI-35
Ultimate strength	60,000 psi
Yield strength	32,000 psi
Elongation (in 2 in.)	20%
Impact strength	25 ft-lb
Hardness (Rockwell B)	90
Heat treatment	Not hardenable
Chemical composition*	
Iron	85%
Chromium	12%
Nickel	1% max
Silicon	1% max
Manganese	1% max
Aluminum	0.20%
Carbon	0.12% max
Phosphorus	0.04% max

*Modified from usual composition for this application.

Stainless Steel Type 405 (Contd.)

Heat Capacity

Reference: Thermotest Laboratories Report No. 61-1166, June 1961.

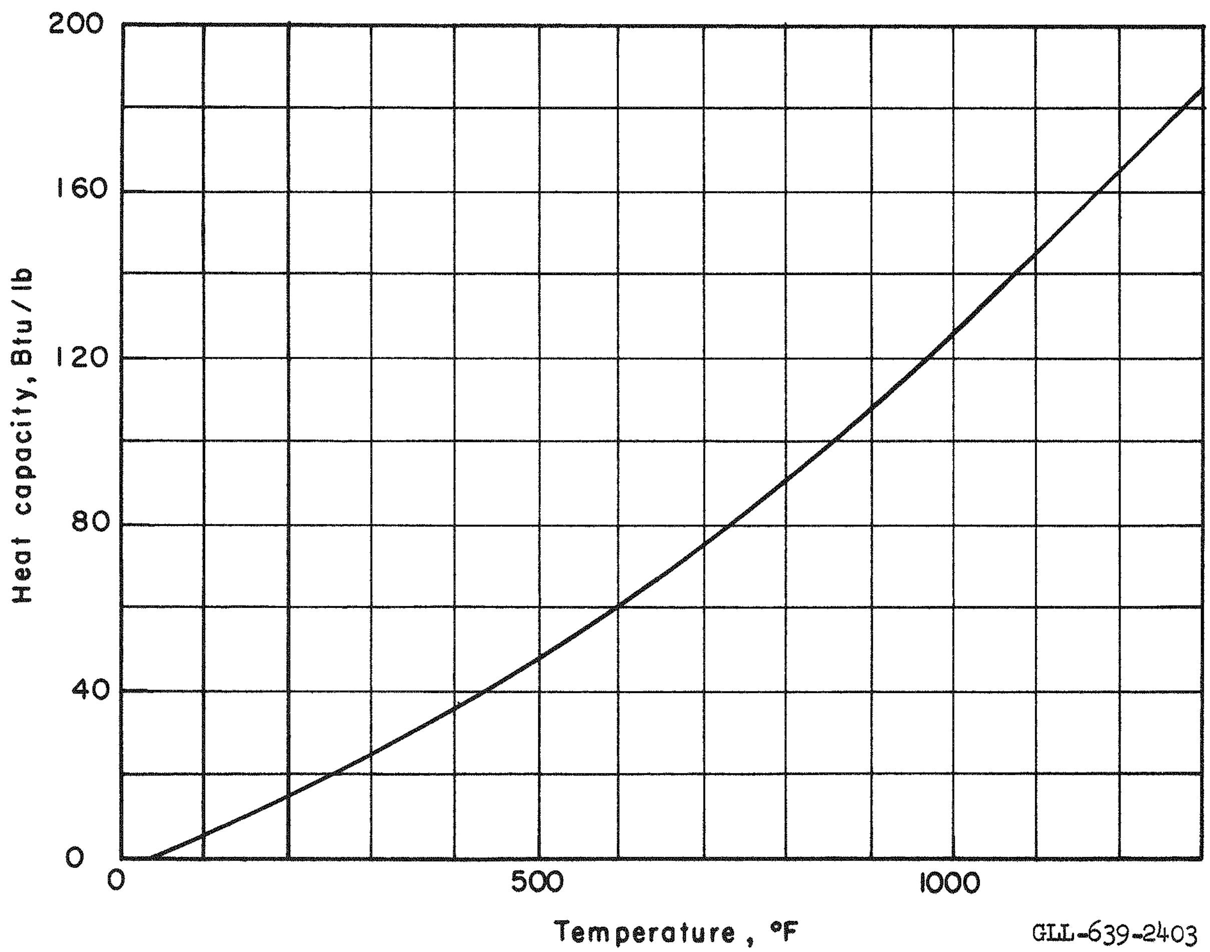

GLL-639-2403

4. Stainless Steel Type 410 Properties

Use	Cell plates, adapters, and reflector inserts
Specification	MEL 603
Melting point	2700°F
Density	7.75 g/cm^3
Specific heat	0.11 Btu/lb-°F
Modulus of elasticity	See p. VI-35
Mean coefficient of thermal expansion	See p. VI-35
Thermal conductivity	See p. VI-35
Ultimate strength	See p. VI-35
Yield strength	See p. VI-35
Creep rupture strength	See p. VI-35
Chemical composition	
Iron	78%
Chromium	12%

References:

1. Reactor Handbook, Vol. 3, Sec. 1, 1st Ed., p. 276.
2. Carpenter Steel Brochure.
3. Metals Handbook, Vol. 1, 8th Ed., p. 422.

410 Stainless Steel

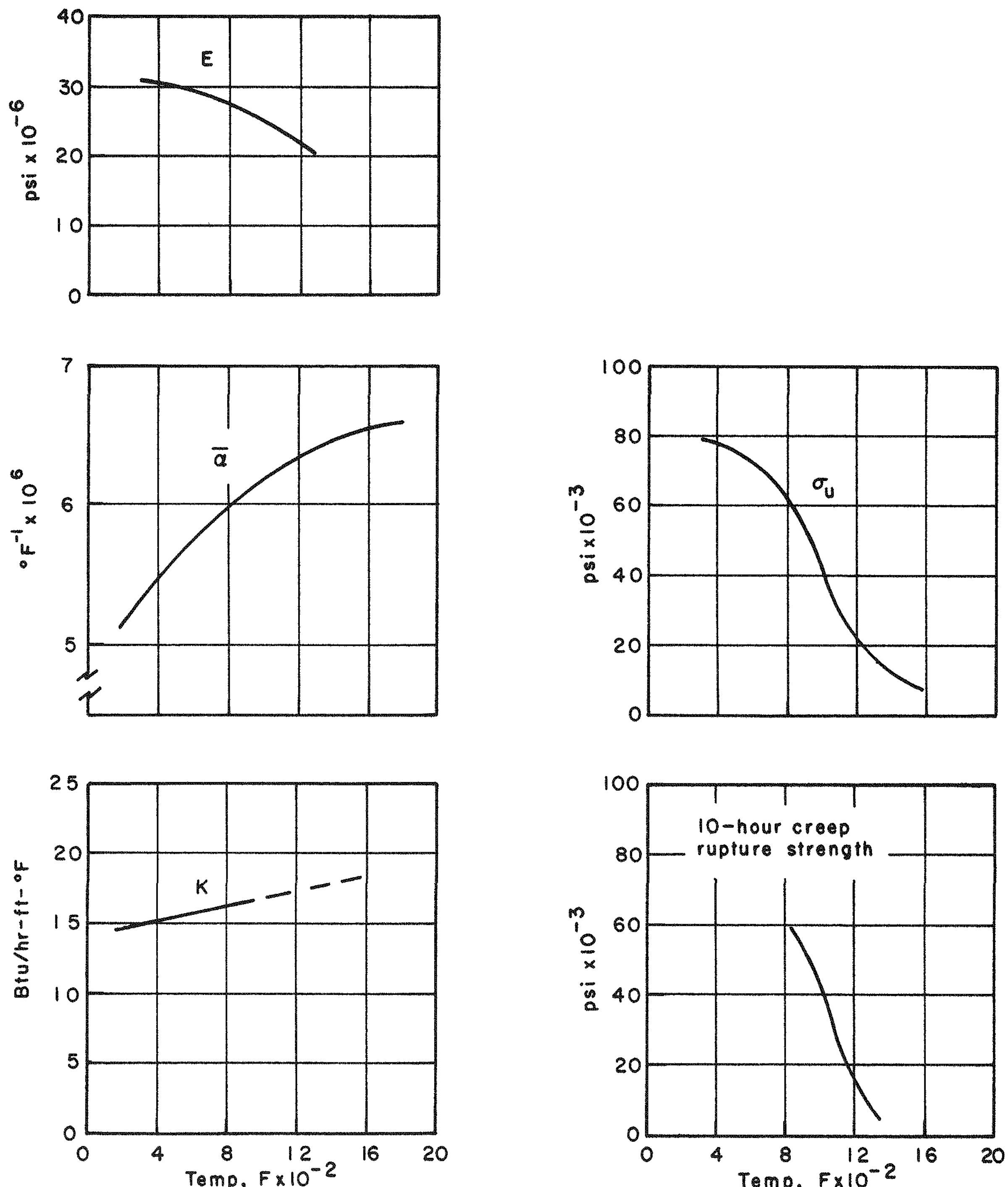

GLL-639-2404

5. Nickel Chromium Steel A-286 Properties

Use	Aerodynamic grid
Stock	Forgings
Melting Point	2500°F
Density	7.94 g/cm^3
Specific heat	0.11 Btu/lb-°F
Poisson's ratio	0.306
Modulus of elasticity	See p. VI-37
Mean coefficient of thermal expansion	See p. VI-37
Thermal conductivity	See p. VI-37
Ultimate strength	See p. VI-37
Yield strength	See p. VI-37
Elongation	See p. VI-37
Impact strength (Charpy)	65 ft-lb
Impact strength (1200°F) (Charpy)	38 ft-lb
Hardness (Rockwell C)	28
Heat treatment	ST 1800°F, 1 hr, WQ Age 1325°F, 16 hr, AC
Chemical composition	
Iron	54%
Nickel	25%
Chromium	15%
Titanium	2%
Manganese	1.5%
Molybdenum	1.3%
Vanadium	0.3%

Reference: Allegheny Ludlum Brochure, ARDC-TR-59-66.

Nickel Chromium Steel A-286

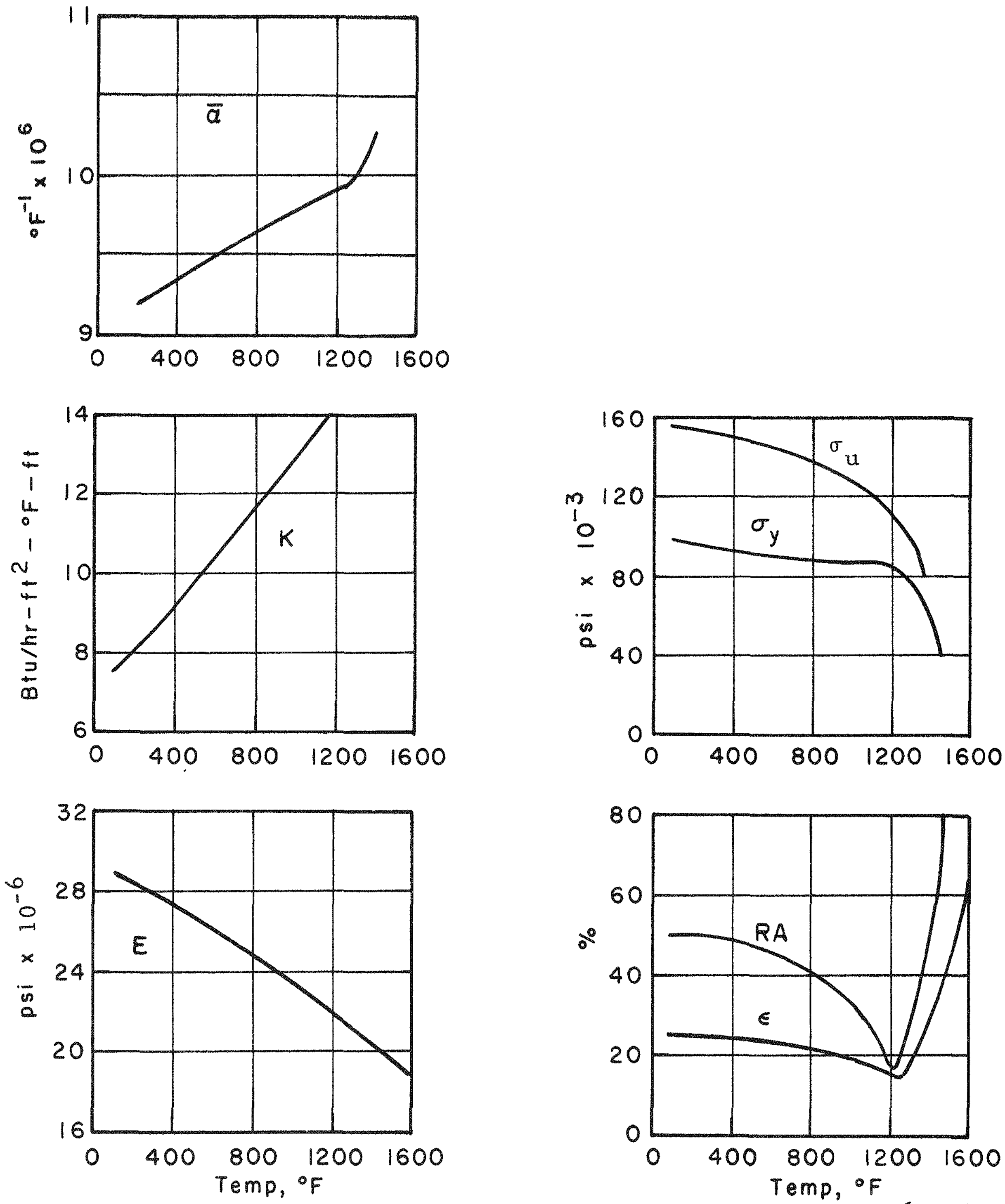

GLL-639-2405

6. Ultra High Strength Steel (Vascojet 1000)

Use	Duct bolts
Stock	Forgings
Density	7.75 g/cm^3
Poisson's ratio	0.281
Modulus of elasticity	See p. VI-39
Mean coefficient of thermal expansion	See p. VI-39
Thermal conductivity	See p. VI-39
Ultimate strength	See p. VI-39
Yield strength	See p. VI-39
Elongation	See p. VI-39
Impact strength (Izod)	19 ft-lb
Impact strength (Izod, 1000°F)	30 ft-lb
Hardness (Rockwell C)	53
Heat treatment	Austenize 1850°F, 45 min AC Triple temper 1025°F, 2 hr AC
Chemical composition	
Iron	93%
Chromium	5%
Molybdenum	1.3%
Vanadium	0.5%
Carbon	0.4%

References:

1. Vanadium-Alloys Brochure.
2. ARDC-TR-59-66.

Vascojet 1000

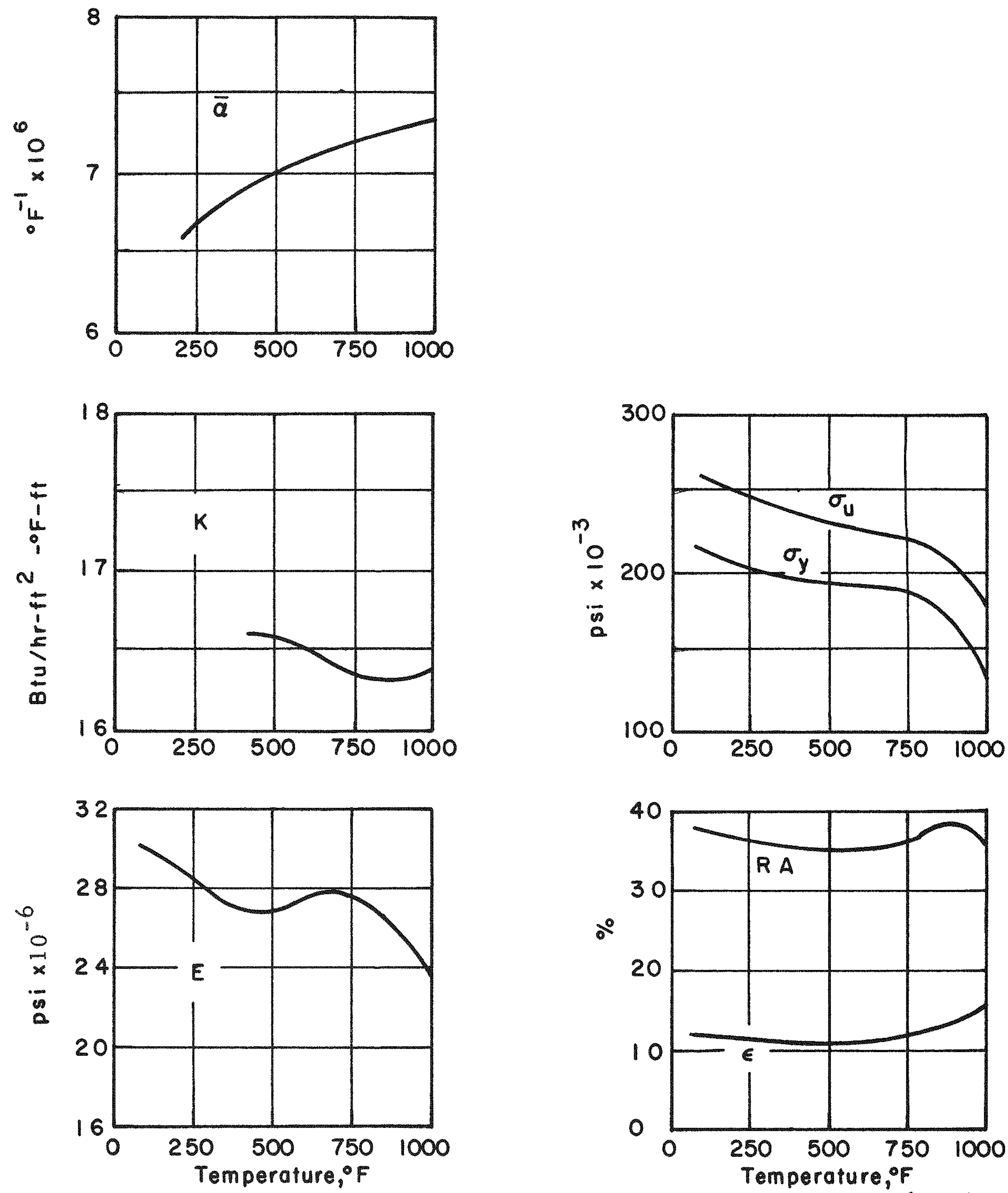

GLL-639-2406

G. PROPERTIES OF HAFNIUM

Use	Control rods
Specification	MEL 534
Stock	Sheet
Melting point	3978°F
Density	12.9 g/cm^3
Specific heat	See p. VI-41
Poisson's ratio	0.29
Modulus of elasticity	See p. VI-41
Mean coefficient of thermal expansion	See p. VI-41
Thermal conductivity	See p. VI-41
Ultimate strength	See p. VI-41
Yield strength	See p. VI-41
Elongation	See p. VI-41
Impact strength (Izod, 0°F)	2.5 ft-lb
Hardness (Rockwell A)	55
Oxidation characteristics	See p. VI-41
Heat treatment	Annealed
Thermal neutron absorption cross section	100 b
Resonance integral	2000 b
Chemical composition	
Hafnium	96.5%
Zirconium	3.5%
Aluminum	50
Copper	50
Iron	200
Oxygen	180
Nitrogen	100
Tungsten	100
Titanium	50
Hydrogen	25
Uranium	20

Hafnium

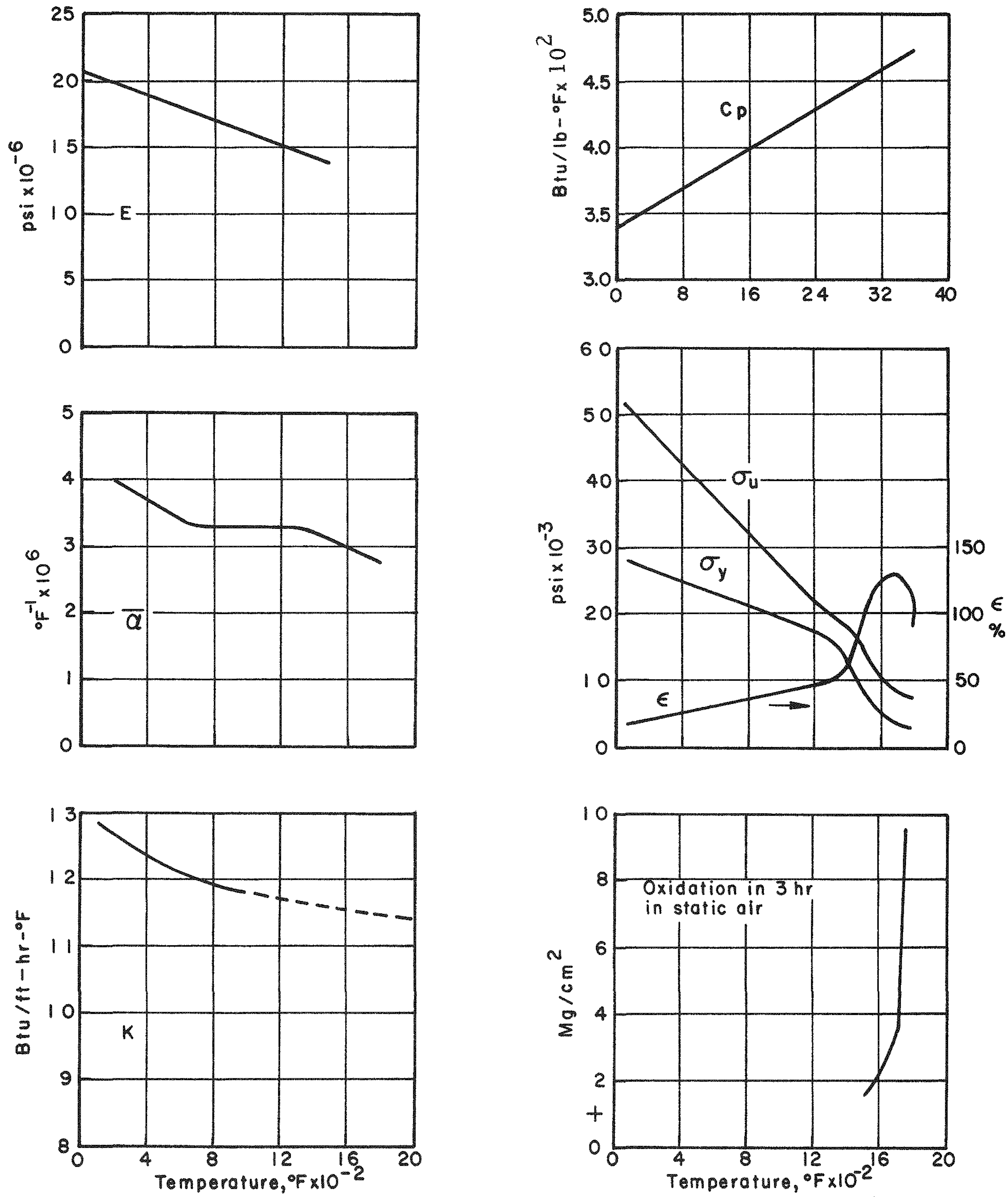

GLL-639-2407

H. PROPERTIES OF NICKEL ALLOYS

1. Nickel Grade 200 Properties

Use	Peripheral shims
Specification	MEL 606
Stock	Bar
Melting point	2615°F
Density	8.92 g/cm^3
Specific heat	0.13 Btu/lb-°F
Poisson's ratio	0.31
Modulus of elasticity[1]	See p. VI-43
Mean coefficient of thermal expansion[2]	See p. VI-43
Thermal conductivity[3]	See p. VI-43
Ultimate strength[4]	See p. VI-43
Yield strength[4]	See p. VI-43
Elongation[4]	See p. VI-43
Creep rupture strength[4]	See p. VI-43
Hardness (Brinell)	90
Heat treatment	Anneal 1500°F 1/4 hr, AC
Chemical composition	
Nickel	99.2% min
Cobalt	0.3% max
Manganese	0.25% max
Iron	0.15% max
Carbon	600 ppm max
Copper	500 ppm max
Silicon	500 ppm max
Sulfur	50 ppm max

1. Reactor Handbook, 2nd Ed., Vol. I, p. 644.
2. Jordan and Swanger, B.J.S. Research 5, 1291, 1930, MBS Cir. 592, p. 20.
3. WADC-TR-58-476, Vol. I.
4. LRL – Metcut Report No. 511-4039-1.

Nickel

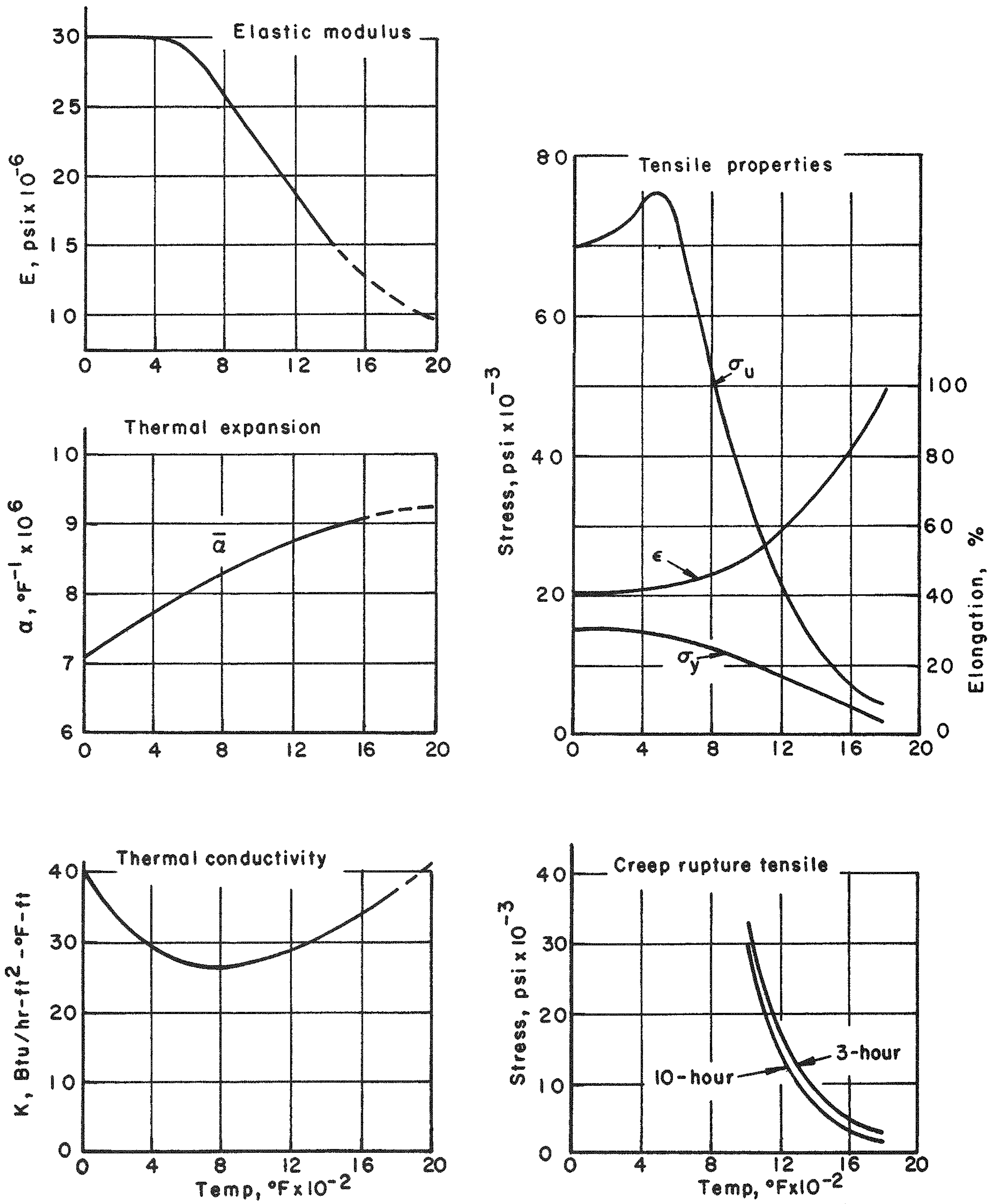

GLL-639-2408

2. Hastelloy B Properties

Use	Control actuators, pinion spacers
Stock	Bar
Melting point	2408°F
Density	9.24 g/cm^3
Specific heat	0.091 Btu/lb-°F
Modulus of elasticity	30×10^6 psi
Mean coefficient of thermal expansion	See p. VI-45
Thermal conductivity	See p. VI-45
Ultimate strength	See p. VI-45
Yield strength	See p. VI-45
Creep rupture strength	See p. VI-45
Impact strength (Izod)	58-62 ft-lb
Hardness (Brinell)	205
Heat treatment	2125°F AC
Chemical composition	
Nickel	61%
Molybdenum	28%
Iron	5.5%
Cobalt	2.5% max
Chromium	1% max
Silicon	1% max
Carbon	0.05% max

Hastelloy B

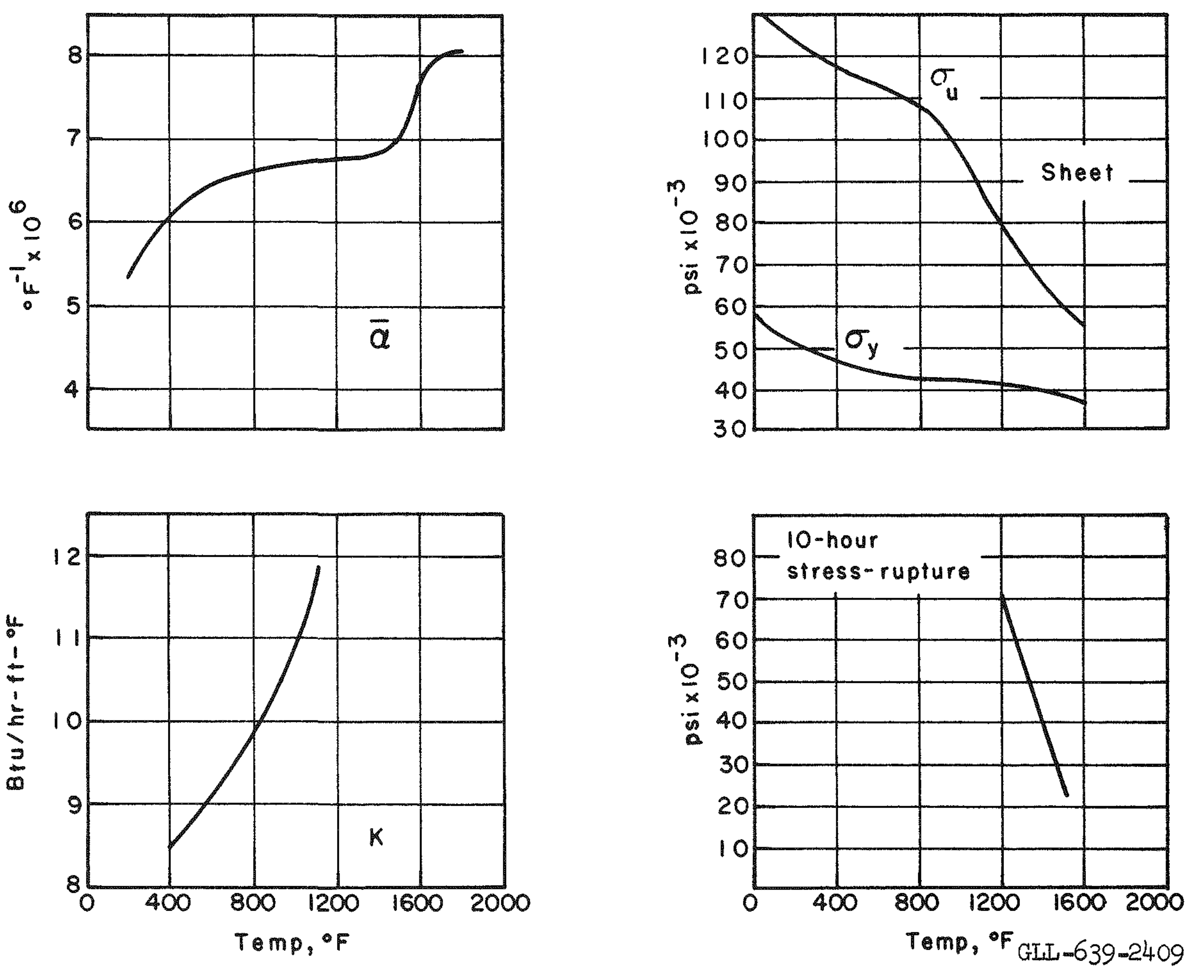

GLL-639-2409

3. Hastelloy C Properties

Use	Ducts
Stock	Plate, forgings
Melting point	2380°F
Density	8.94 g/cm^3
Specific heat	0.092 Btu/lb-°F
Poisson's ratio	0.3
Modulus of elasticity	See p. VI-47
Mean coefficient of thermal expansion	See p. VI-47
Thermal conductivity	See p. VI-47
Ultimate strength	See p. VI-47
Yield strength	See p. VI-47
Elongation	See p. VI-47
Creep rupture strength (10 hr @ 1500°F)	25,000 psi
Impact strength (Izod)	65 ft-lb
Impact strength (Izod, 1500°F)	47 ft-lb
Hardness (Rockwell C)	22
Heat treatment	ST 2225°F, 2 hr, WQ

Chemical composition

Nickel	56%
Chromium	16%
Molybdenum	16%
Iron	5%
Tungsten	4%
Cobalt	1.5%
Silicon	0.6%
Manganese	0.6%

Hastelloy C

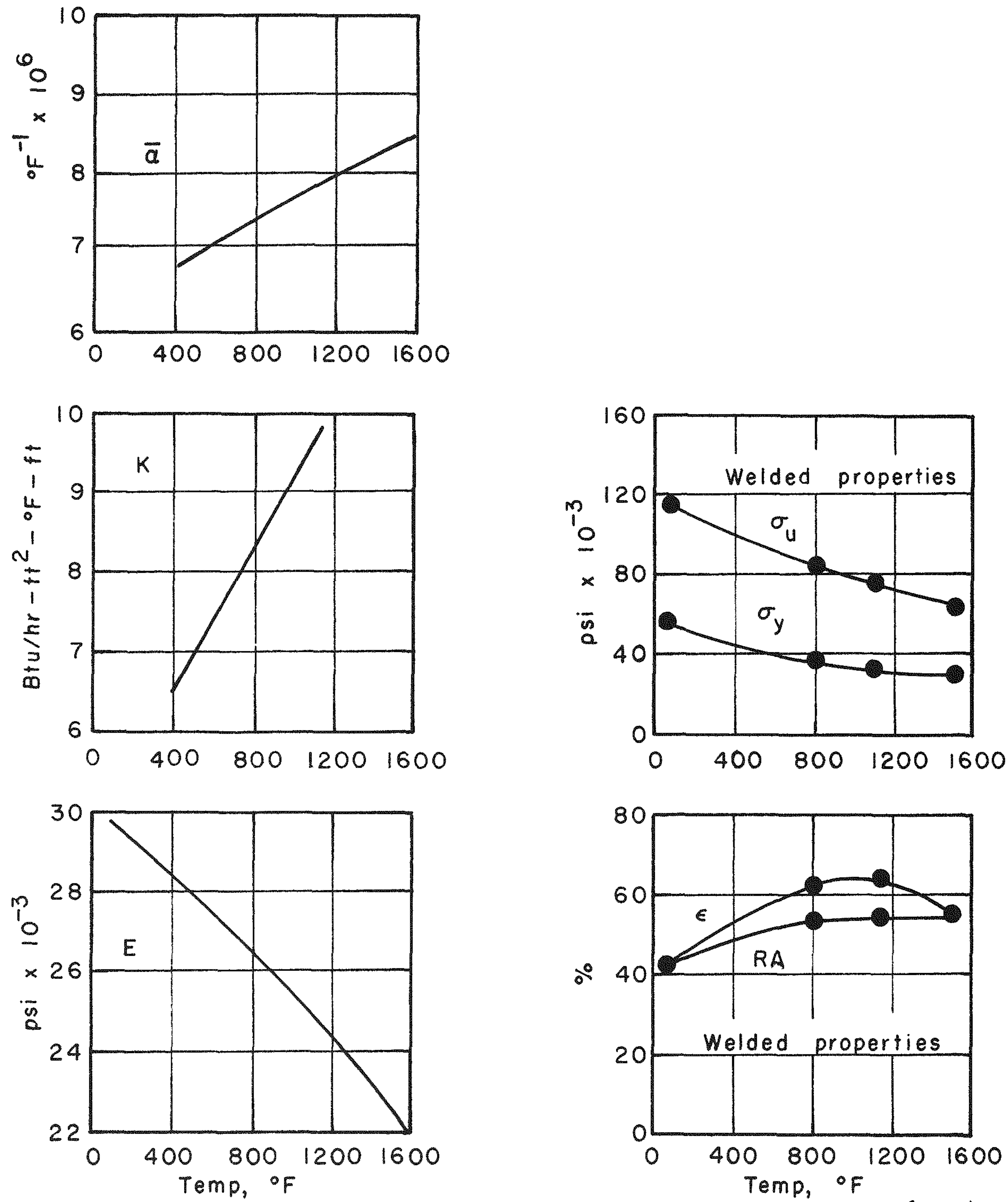

GLL-639-2410

4. Hastelloy X Properties

Use	Control actuator, guide system
Melting point	2350°F
Density	8.23 g/cm^3
Specific heat	0.105 Btu/lb-°F
Modulus of elasticity	See p. VI-49
Mean coefficient of thermal expansion	See p. VI-49
Thermal conductivity	See p. VI-49
Ultimate strength	See p. VI-49
Yield strength	See p. VI-49
Elongation in 1 in. (sheet, 70-1500°F)	60%
Elongation in 1 in. (casting, 70-1500°F)	10%
Hardness (Rockwell B)	90
Heat treatment	2175°F, 1/2 hr, WQ
Chemical composition	
Nickel	47%
Chromium	22%
Iron	18%
Molybdenum	10%
Cobalt	2%
Tungsten	0.5%
Carbon	0.1%

Hastelloy X

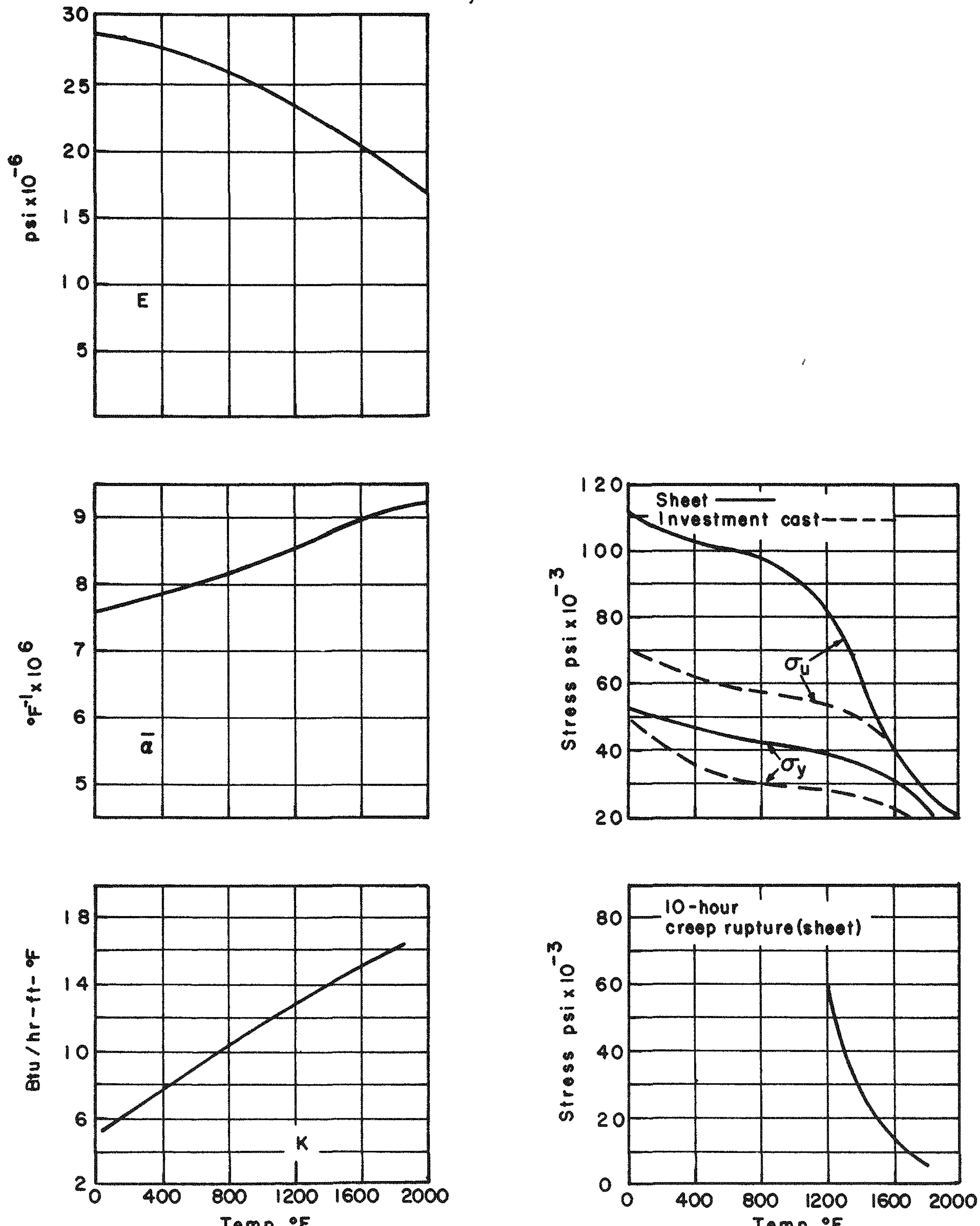

GLL-639-2411

5. Hastelloy R-235 Properties

Use	Tie rods
Specification	MEL 333
Stock	Welded tubing
Melting point	2400°F
Density	8.23 g/cm^3
Specific heat	0.11 Btu/lb-°F
Poisson's ratio	0.3
Modulus of elasticity	See p. VI-51
Mean coefficient of thermal expansion	See p. VI-51
Thermal conductivity	See p. VI-51
Ultimate strength	See p. VI-51
Elongation	See p. VI-51
Creep rupture strength	See p. VI-51
Impact strength (Charpy)	31 ft-lb
Hardness (Rockwell C)	31
Heat treatment	ST 1975°F, 1/2 hr, WQ Age 1400°F, 16 hr, AC
Chemical composition	
Nickel	64%
Chromium	14%
Iron	10%
Molybdenum	5.5%
Cobalt	2.5%
Titanium	2.5%
Aluminum	2%
Manganese	1%
Silicon	1%
Carbon	0.16%

References: H. Conrad, "Heat Treatment of R-235 and René 41," Dec. 1960.
Haynes Stellite Co. Brochure (March 1958).

Hastelloy R-235

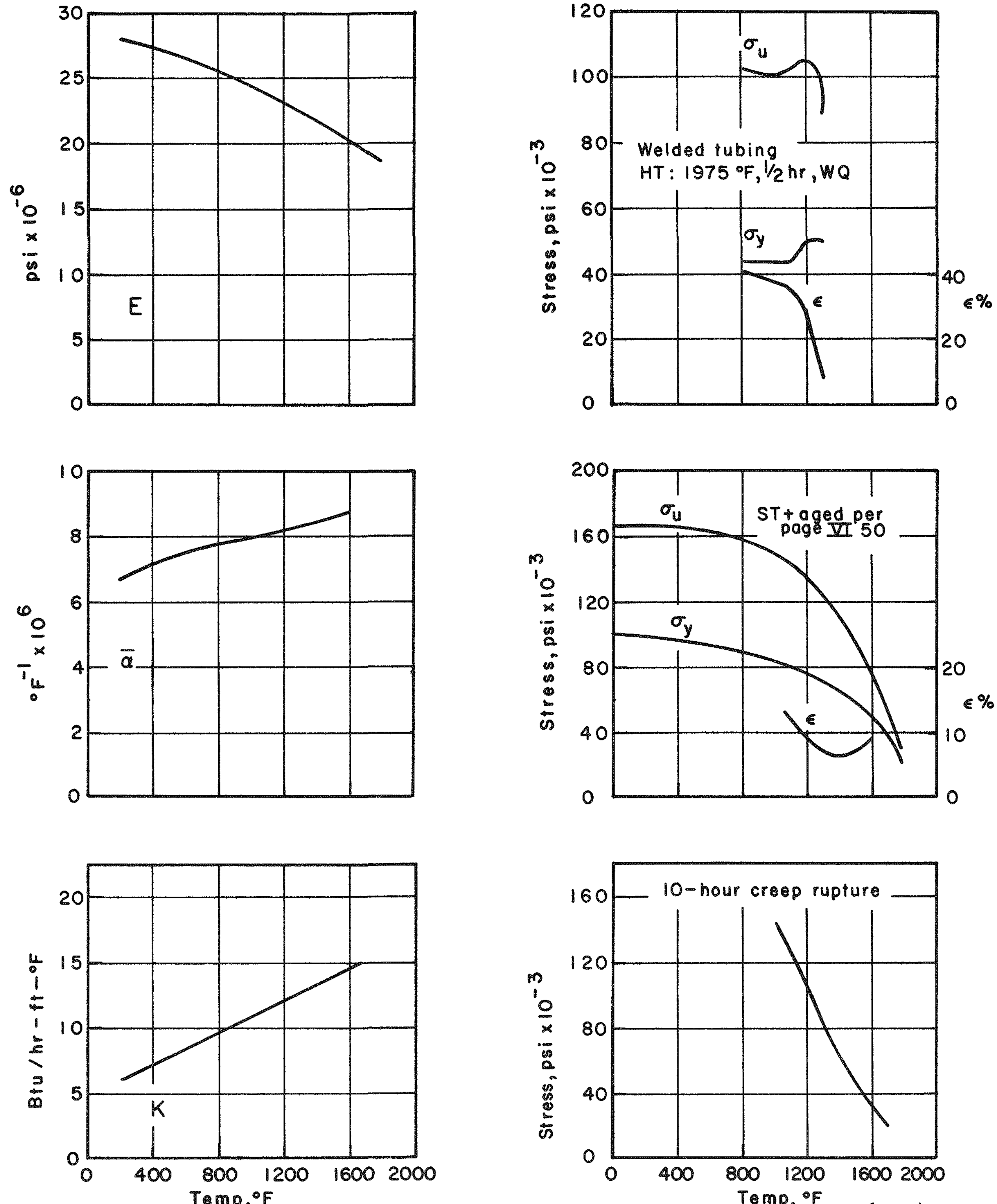

GLL-639-2412

6. René 41 Properties

Use	Tie rods, compression spring, garter spring, support grid, rails, and wipers
Melting point	2400°F
Density	8.28 g/cm^3
Specific heat	0.11 Btu/lb-°F
Poisson's ratio	0.31 @ 80°F, 0.35 @ 1700°F
Modulus of elasticity	See p. VI-53
Mean coefficient of thermal expansion	See p. VI-53
Thermal conductivity	See p. VI-53
Ultimate strength	See p. VI-53
Yield strength	See p. VI-53
Elongation	See p. VI-53
Creep rupture strength	See p. VI-53
Hardness (Rockwell C)	42
Heat treatment	ST 1975°F, 1/2 hr, WQ Age 1400°F, 16 hr, AC
Chemical composition (typical)	
Nickel	54%
Chromium	19.5%
Cobalt	11.1%
Molybdenum	9.8%
Titanium	3.1%
Aluminum	1.5%
Iron	0.8%
Silicon	0.2%
Carbon	0.1%
Manganese	500 ppm
Silicon	100 ppm
Boron	40 ppm
Phosphorus	10 ppm

Reference: H. Conrad, "Heat Treatment of R-235 and René 41," Dec. 1960.

René 41

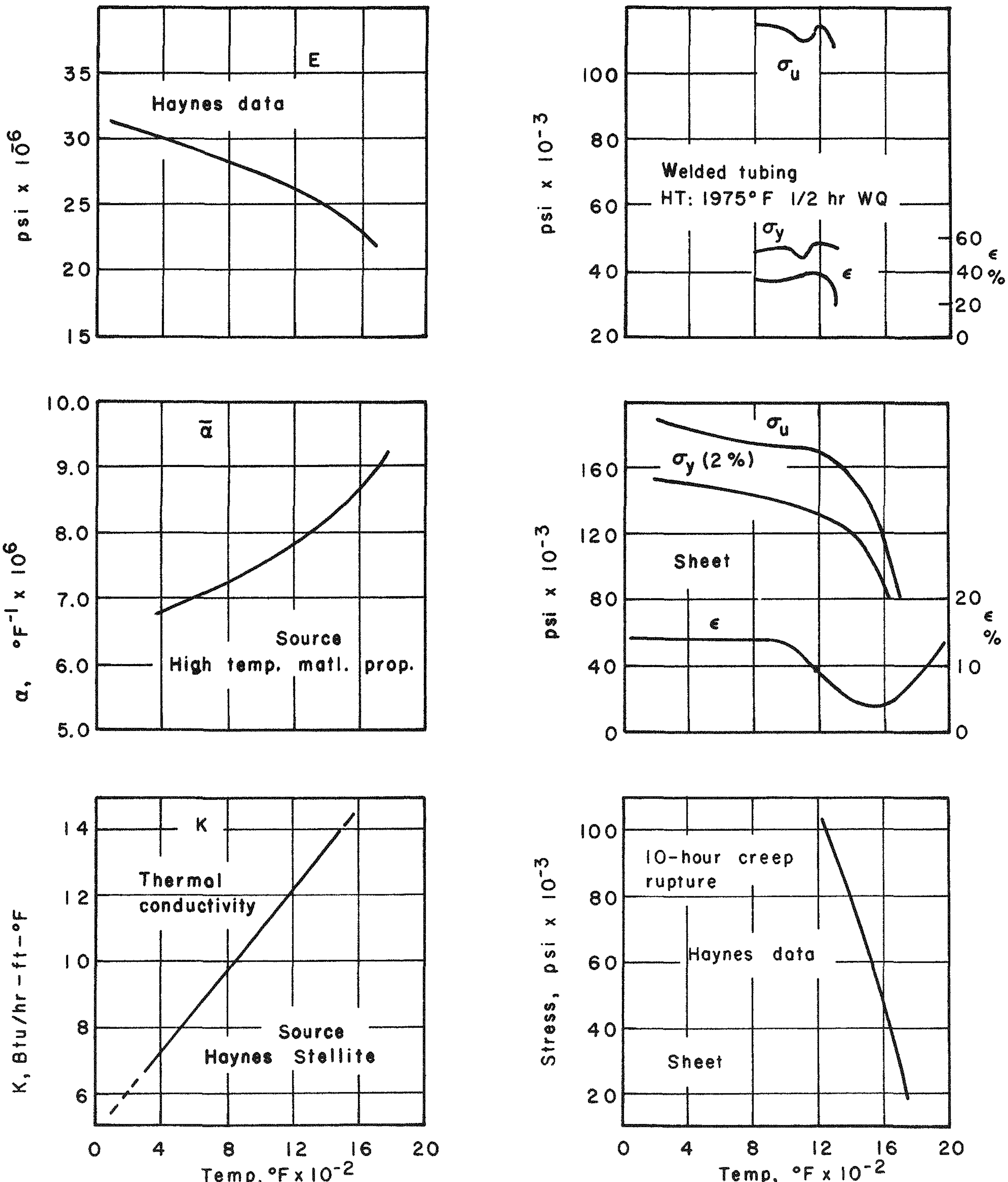

GLL-639-2413

7. Inconel X Properties

Use	Control actuator
Melting point	2540°F
Density	8.3 g/cm^3
Specific heat	0.13 Btu/lb-°F
Poisson's ratio	0.29
Modulus of elasticity	See p. VI-55
Mean coefficient of thermal expansion	See p. VI-55
Thermal conductivity	See p. VI-55
Ultimate strength	See p. VI-55
Yield strength	See p. VI-55
Elongation	See p. VI-55
Hardness (Brinell)	300-360
Heat treatment	1625°F/24 hr, AC 1300°F/20 hr, AC

Chemical composition

Nickel	74%
Chromium	15%
Iron	7%
Titanium	2.5%
Columbium	1%
Aluminum	0.7%

Inconel X

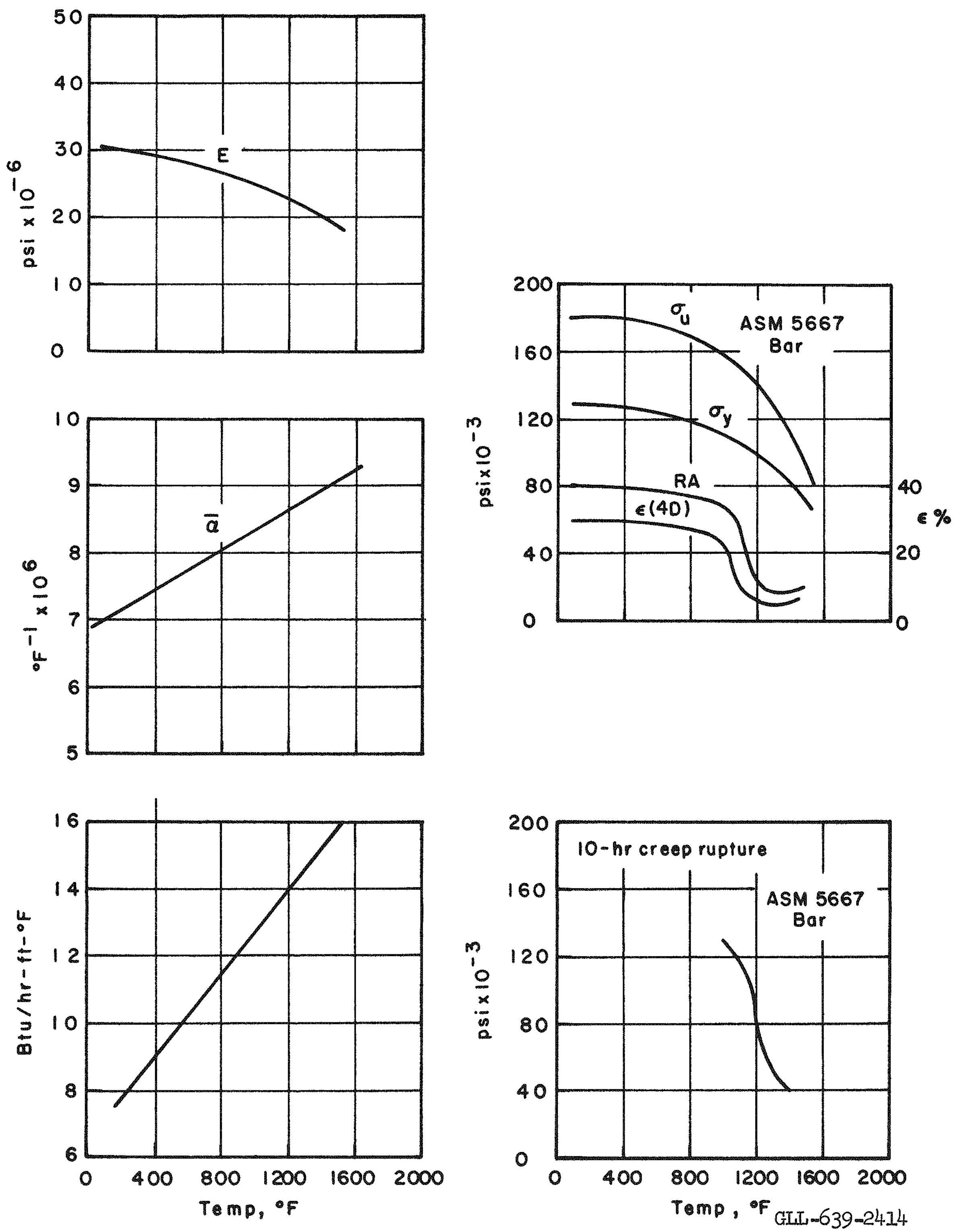
50
40
30
20
10
0
psi x 10^{-6}
E
10
9
8
7
6
5
°F^{-1} x 10^{6}
$\bar{\alpha}$
16
14
12
10
8
6
Btu/hr-ft-°F
0 400 800 1200 1600 2000
Temp, °F
200
160
120
80
40
0
psi x 10^{-3}
σ_u
ASM 5667
Bar
σ_y
RA
ϵ(4D)
40
20
0
ϵ %
200
160
120
80
40
0
psi x 10^{-3}
10-hr creep rupture
ASM 5667
Bar
0 400 800 1200 1600 2000
Temp, °F
GLL-639-2414

J. Platinum Alloys

1. Pt-5 Ru Properties

Use	Tie rod insulating cup
Specification	MEL 611
Stock	Sheet
Melting point (estimated)	3300°F
Density	20.67 g/cm^3
Modulus of elasticity[1]	See p. VI-57
Mean coefficient of thermal expansion[2]	See p. VI-57
Thermal conductivity[2]	See p. VI-57
Ultimate strength[1]	See p. VI-57
Yield strength[1]	See p. VI-57
Elongation[1]	See p. VI-57
Creep rupture strength[1]	See p. VI-57
Hardness (Brinell)	130
Heat treatment	Anneal
Chemical composition	
Platinum	95%
Ruthenium	5%

1. LRL – Metcut Report No. 511-4101-1.
2. LRL – Southern Research Report No. 5638-1409, 1410I.

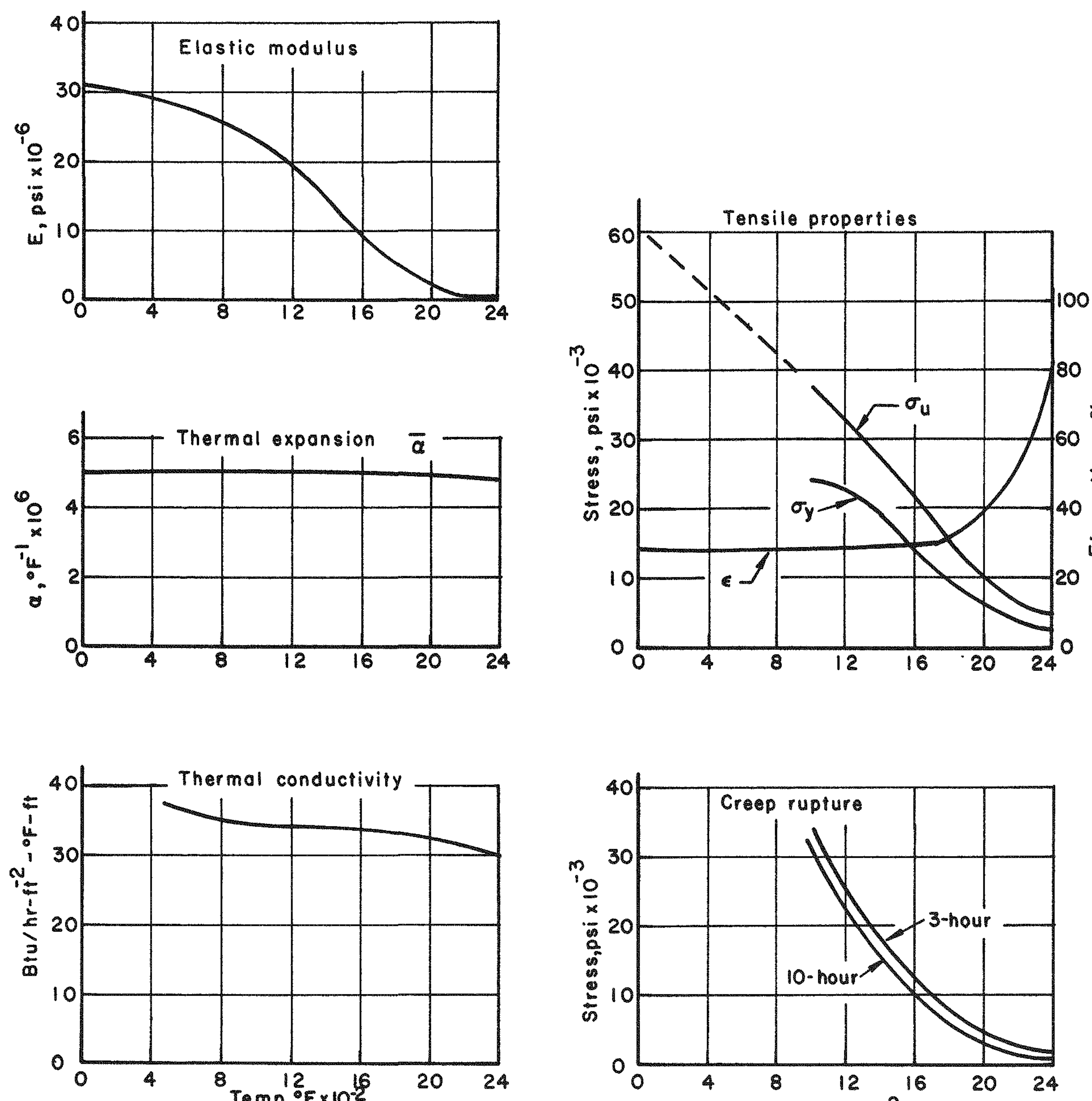
Elastic modulus
E, psi x 10^-6
Thermal expansion
ᾱ
α, °F^-1 x 10^6
Thermal conductivity
Btu/hr-ft^-2-°F-ft
Temp, °F x 10^-2
Tensile properties
Stress, psi x 10^-3
Elongation, %
σu
σy
ε
Creep rupture
Stress, psi x 10^-3
3-hour
10-hour
Temp, °F x 10^-2

GLL-639-2415

APPENDIX A

LIST OF TORY II-C MEMORANDA BY NUMBER

Memo No.	Subject	Author	Month
	1959		
1.	Description of the Tory II-C Reactor	H. Reynolds	January
2.	Early Progress on Neutronics	L. Russell	July
3.	Porosity Definition	H. Reynolds	July
4.	Tory II-C Objectives	H. Reynolds	July
5.	Power Distribution for $dT_w/dx \geq 0$	P. Uthe	August
6.	Field Strength from Gamma Activity of Tray Reactor Section	L. Russell	September
7.	Modular Alike Reactor	C. Walter	October
8.	Comparison of Generic Reactor Systems for Tory II-C	C. Walter	October
9.	Some General Neutronic Calculations on Tory II-C Type Cylindrical Reactors	L. Russell	October
10.	Design Proposal for a Tory II-C Reactor Containing No Metal Parts	W. Wells	November
11.	Metal Volume Fraction in an Alike-Integral Reactor	C. Walter	November
12.	Progress Report: Aerothermodynamics	P. Uthe	December
	1960		
13.	Progress Report: Neutronics	L. Russell	January
14.	Performance	M. Mintz	January
15.	Summary of Tray Reactor Design	J. Cox	January
16.	Tory II-C Performance Choice	H. Reynolds	February
18.	Progress Report: Neutronics	L. Russell	March
19.	Axial Support	W. Wells	March
20.	Reactor Pressure Drop for Structural Considerations	T. Tyson	March
21.	Structural Materials Selection for Reactor Axial Load	C. Walter	May
23.	Performance	H. Reynolds	May
24.	Progress Report: Neutronics	L. Russell	June
25.	Structural and Stability Requirements of the Ceramic Matrix in a Reactor without Internal Structure	P. Mohr	July

Memo No.	Subject	Author	Month
	(1960 contd.)		
26.	Survey of Gamma Heat Deposition in Tory II-C	A. Lorenz	July
27.	Calculation of Thermal Stress in Side Reflector Configuration	L. Deverall	August
28.	Tory II-C Design Analysis	P. Uthe	August
29.	Fueled Tube Hole Non-Symmetry as Regards Thermal Stress	P. Uthe	August
30.	Preliminary Study of Non-Nuclear Instrumentation	T. Rehder	September
31.	Material Frontal Area in a Standard Unit Cell	W. O'Neal	September
32.	Operations	P. Uthe	September
33.	BeO Thermal Stress	P. Uthe	September
34.	Reactor Side Support Design	J. Cox	October
35.	Structural Composition Outline for the Tory II-C-2 Reactor	P. Mohr	October
36.	Performance	P. Uthe	October
37.	Preliminary Design of Reactor Duct and Support Grid	E. Jackson	October
38.	Review of Tory II-C Memos	C. Walter	October
39.	Constraints on Reactor Operating Conditions	C. Walter	October
40.	Description of Tory II-C Neutronics	L. Russell	October
41.	Control Rod Design	J. Hovingh	October
42.	Reactor Design Information	J. Cox	October
43.	Schedule for Tory II-C Reactor Experiment	C. Walter	November
44.	Review of II-C Instrumentation Requirements	T. Rehder	November
46.	Preliminary Design Specification for Reactor Control Actuator	R. Finnigan	December
47.	Design Ground and Flight Loads	E. Arbtin	December
48.	Design Analysis Responsibilities	P. Uthe	December
	1961		
49.	Front Reflector Thickness	C. Walter	January
50.	Unit Cell Design	C. Walter	January

Memo No.	Subject	Author	Month
	(1961 contd.)		
51.	Maximum Material Temperatures in Tie Rods and Inserts	R. Var	January
52.	Tory II-C Nomenclature	H. Stern	January
53.	Material Frontal Area in a Standard Unit Cell	W. O'Neal	January
54.	Tory II-C Data Book	H. Stern	January
55.	Neutronic Description of January 1961 Reactor Configuration	L. Russell	January
56.	Fuel Element Size	P. Uthe	January
57.	Test Report: Glazed Bonded Tubes	W. O'Neal	January
58.	Control Actuator Mounting System	E. Jackson	January
59.	Reactor Assembly and Disassembly	C. Walter	January
60.	Tests on Coated and Uncoated F-48 Columbium Alloys	R. Werner	February
61.	Performance	M. Uthe	February
62.	Reactor Test Run Time	H. Reynolds	February
63.	Number of Flow Channels in Reactor	W. O'Neal	February
64.	Material Frontal Area in a Standard Unit Cell	W. O'Neal	February
65.	Critical Mass	E. Goldberg	February
66.	Tory II-C Subassembly Tests	P. Uthe	February
68.	Mockup Reactor	P. Uthe	February
69.	Material Frontal Area in a Control Unit Cell	W. O'Neal	February
70.	Hybrid Equivalent Hydraulic Flow Channels	M. Mintz	February
71.	Fuel Element Size	P. Uthe	February
72.	Control Console Design	C. Barnett	March
73.	Reactor Assembly	A. Williams	March
74.	Nuclear Heating in Tie Rods	A. Lorenz	March
75.	Thermal Analysis of Control Rod	L. Deverall	March
76.	Number of Flow Channels in Reactor	W. O'Neal	March
77.	Heating of Hafnium Control Rods	A. Lorenz	March
78.	Neutronic Aspects of Control Rods	E. Goldberg	March
79.	Reactor After Cooling	H. Reynolds	March

Memo No.	Subject	Author	Month
	(1961 contd.)		
80.	Tie Rod Temperatures Along Several Radial Positions	N. Balling	March
81.	Side Reflector Design	P. Uthe	March
82.	Sudden Expansion Losses in Turbulent Air Flow	M. Mintz	March
83.	Schedule for Reactor Experiment	C. Walter	March
84.	Performance	P. Uthe	April
85.	New Temperature Distribution for Control Rod	L. Deverall	April
86.	Pebble Bed Heater (Preliminary)	P. Uthe	April
87.	Reactor Assembly Drawing	J. Cox	April
88.	Chance-Vought Information Request	P. Uthe	April
89.	Critical Mass	E. Goldberg	April
90.	Support Grid Aerothermodynamics (Preliminary)	R. Var	April
91.	Design of Side Support Springs	J. Cox	April
92.	Facilities Committee	C. Walter	April
93.	Fuel Loading Request	R. Var	April
94.	Reactor Control Actuators and Pneumatic Sub-System Configuration	J. Day	May
95.	Criticality Adjustments	L. Russell	April
96.	Mechanical Properties of F-48	J. Cox	April
97.	Tie Rod Flange Temperature Distribution	W. O'Neal	April
98.	Reactor Duct Cooling Requirement	P. Uthe	May
99.	Facilities Committee	C. Walter	May
100.	Nuclear Heating of Reactor Side Support Components	A. Lorenz	May
101.	Foil Self-Shielding Calculations for Europium, Gadolinium, and Samarium	R. Fries	May
102.	Nuclear Heating of Unfueled BeO	A. Lorenz	May
103.	Pneumatic Control Rod Simulation	S. Ross	May
104.	Position Limits in Simulation	S. Ross	May
105.	Angie Results on Reactor Configuration Having a Side Support Structure and Control Rod Holes	K. Russell	May
106.	Engineering Status Meeting Report	W. Myers	June

Memo No.	Subject	Author	Month
	(1961 contd.)		
107.	Addendum to Tory II-C Memo No. 97	W. O'Neal	June
108.	Reactor Safety System Requirement	H. Reynolds	June
109.	Hafnium Oxidation Studies	J. Hovingh	June
110.	Pneumatic Actuator Simulation	S. Ross	June
111.	Revision and Summary of Nuclear Heating Values	A. Lorenz	June
112.	Results of 13 June 1961 Assembly and Crit Meeting	H. Reynolds	June
113.	Duct Dimensions	H. Reynolds	June
114.	Fuel Loading Classes	H. Reynolds	June
115.	Temperature Analyses of Peripheral Shims	W. O'Neal	June
116.	Mass Perturbations of Reactor Materials	L. Russell	June
117.	Nuclear Heating of 80 Mil Asterisk-Shaped Hafnium Control Rod	A. Lorenz	June
118.	Proposed Reactor Safety System	J. Cox	June
119.	Shim Rod and Flow Valve, AV-3 Simulation	S. Ross	June
120.	Ramjet Performance Calculations	M. Mintz	June
121.	Performance	P. Uthe	June
122.	On - Line δK Computer for Nevada Site	S. Ross	June
123.	Results of Instrumentation Group Meeting	C. Barnett	June
124.	Control Systems Philosophy	R. Finnigan	July
125.	Static, Dynamic, and Thermal Design Considerations of the Test Vehicle, Duct, and Mounting System	A. Miller	July
126.	Nuclear Heating of Fueled BeO	A. Lorenz	July
127.	Typical Weight and Surface Density of Side Support System	C. Walter	July
128.	Temperature Analysis of Peripheral Shims	R. Var	July
129.	Schedule for Tory II-C Manuals	H. Reynolds	July
130.	Preheater Facility	M. Mintz	July
131.	Base Plates	R. Werner	July

Memo No.	Subject	Author	Month
	(1961 contd.)		
132.	Ideas on Control Philosophy	C. Barnett	July
134.	Mechanical Properties of Hastelloy Alloy C	E. Jackson	July
135.	Tolerance Specifications for the Side Reflector BeO Tubes	R. Var	July
136.	Thermal Stress in Fueled Tubes Adjacent to Tie Rods	L. Deverall	August
137.	Preliminary Report of Reflector Experiments	A. Cole	August
138.	Duct Bolted Joints	S. Giampapa	August
139.	Hastelloy C Evaluation Programs	E. Jackson	August
140.	Notes on Assembly Slice Test, Phase 2	G. Patraw	August
141.	Reactor Safety System	C. Walter	August
142.	Natural Frequencies of Distributed Systems by Finite Differences Implemented by Computer Program	A. Miller	August
143.	Use of Silicon Containing Steel Balls in Pebble Bed Heater	J. Kane	August
144.	Critical Review of Chance-Vought SLAM Design	T. Tyson	August
145.	Suggested Placement of Thermocouples in Reactor	V. Hampel	August
146.	Tube Column, Reflector Cartridge, and Unit Cell Designations	H. Stern	August
147.	Fuel Loading Map	V. Hampel	August
149.	Exit Nozzle Area	H. Reynolds	August
150.	Increase in Diameter of Reactor Due to Tolerance Buildup of Fueled Tubes	W. O'Neal	August
151.	Bendix Liaison Meeting, August 1961, Control Actuator Development	J. Day	August
152.	Checkout Facility Control Group, NTS	R. Finnigan	August
153.	Exit Nozzle Design	M. Mintz	August
154.	Fuel Loading Request	R. Var	August
155.	Analysis of Silicon Iron Pebble Bed Heater	M. Mintz	August
156.	Ceramic Tube Quantities	H. Stern	August
157.	Status of Control Rod Systems: Neutronic Aspects	E. Goldberg	August

Memo No.	Subject	Author	Month
	(1961 contd.)		
158.	Side Reflector Nickel Shims	M. Mintz	August
159.	Transformation from NOMAC to SEA LION Geometry	H. Rodean	September
160.	F-48 Mechanical Properties	J. Cox	September
161.	Production of Photo-Neutrons by the Be^9 (γ, n) Reaction	A. Lorenz	September
162.	Non-nuclear Instrumentation	C. Barnett	September
163.	Nozzle Cooling Air Requirements	J. Behne	September
164.	Control Rod Heating (see Addendum 10-10-61)	S. Kellman	September
165.	Geometric Representation of Reactor in Machine Codes	V. Hampel	June
166.	Inlet Grid Throat Area	D. Corallo	September
167.	Dynamic Analog of Test Vehicle	A. Weston	September
168.	Transient Aerothermodynamic Analysis of a Gas-Cooled Reactor – 1. Single Conduit Response to Step and Sinusoidal Inputs	H. Rodean	September
169.	Transient Aerothermodynamic Analysis of a Gas-Cooled Reactor – 2. Thermal Coupling between Adjacent Conduits	H. Rodean	September
170.	Aerothermodynamic Time Constants of the Reactor	H. Rodean	September
171.	Review and Status of the Tory II-C Reactor Experiment	C. Walter	September
172.	Neutron Absorption by Tie Rods	A. Lorenz	August
173.	Temperature and Stress Analysis – Tie Rod Fastener	W. O'Neal	September
174.	Highlights of Visit to Bendix Research Laboratory	C. Walter	September
175.	Request for Instrumentation to Measure Reactor Radial Expansion	V. Hampel	September
176.	Duct Joint Bolts H-11 (Vasco Jet 1000)	S. Giampapa	October
177.	Preliminary Results: Computation of Natural Frequencies of Test Vehicle Car Frame	A. Miller	October

Memo No.	Subject	Author	Month
	(1961 contd.)		
178.	Bendix Liaison Meeting, September 1961, Control Actuator	J. Day	October
179.	Neutronic Calculations for Reactor Assembly Operations	J. Scott	October
180.	Analysis of Temperatures in the First Row of Ceramic Tubes Adjacent to the Active Core	L. Deverall	October
181.	Specification for Control Actuator Aft Guide Section	J. Day	October
182.	Thermocouple Averaging Device	C. Barnett	October
183.	Thermal Stress in BeO Cartridge (Sunflower)	W. O'Neal	October
184.	Input Data and Analytical Results for Duct Joints	S. Giampapa	October
185.	Snowflake Stress Analysis (Transition Section)	W. O'Neal	October
186.	Nuclear Heating of BeO Tubes and Tie Rods	A. Lorenz	October
187.	Tie Rod Development Program Status	W. O'Neal	October
188.	Temperature Distribution in Control Rod	L. Deverall	September
189.	Support Grid Status	E. Jackson	October
190.	Transient Aerothermodynamics Analysis of a Gas-Cooled Reactor – 3. Aerothermodynamics Time Constant Variation with Conduit Station	H. Rodean	October
191.	Location of Reactor Inlet Pressure and Temperature Measuring Station	D. Peschel	October
192.	Reactor Safety and Hazards Manual	E. Goldberg	October
193.	Compatibility Test of Reactor Material	R. Werner	October
194.	Radiative Capture Data	A. Lorenz	October
195.	Gamma Energy Source in the Active Core	A. Lorenz	October
196.	Side Support System Dynamics	E. Platt	October
197.	Constraints on Reactor Operating Conditions. Part II: Revised Ground and Flight Loads to be Used for Basis of Reactor Design	E. Arbtin	November

Memo No.	Subject	Author	Month
	(1961 contd.)		
198.	Reactor Safety System	C. Walter	November
199.	Bendix Liaison Meeting, October 1961, Control Actuator Development	J. Day	November
200.	Control Room Features Desired	C. Barnett	November
201.	Side Support Design	E. Platt	November
202.	Dimensions of Slice Test Steatite Tubes	W. O'Neal	November
203.	Transient Aerothermodynamic Analysis of a Gas-Cooled Reactor – 4. The Effect of Variable Reactor Air Flow	H. Rodean	November
204.	Lumped Parameter Heat Balance Equation for the Reactor	H. Rodean	November
205.	Proposed Nuclear Instrument System	G. St. Leger-Barter	November
206.	Modifications to AV3, AV4, AV5 Valves and Controls	D. Peschel	November
207.	SEA LION Analysis of Typical Reactor Test	H. Rodean	November
208.	Typical Weight and Surface Density of Metal Components External to the BeO Side Reflector	R. Cole	November
209.	Effect of Tube Tolerances and Camber on Reactor Dimensions	C. Walter	November
210.	Transient Aerothermodynamic Analsis of a Gas-Cooled Reactor – 5. Applicability of Steady Gas Flow Equations	H. Rodean	November
211.	Current Status of Base Plate Coating Program	R. Werner	November
212.	Tie Rod and Control Rod Parameters	R. Var	November
213.	SEA LION Results for Chance-Vought Missile Boost Trajectory	H. Rodean	November
214.	Summary of Recent Oxidation Test of Coatings on F-48 Alloy	G. Rynders	November
215.	Dimensional Analysis of 163 LRL "Chicken Fat" Tubes	J. Collins	November
216.	On Camber	G. Patraw	November
217.	Base Plate Temperature Profile	M. Mintz	December

Memo No.	Subject	Author	Month
	(1961 contd.)		
218.	Estimated Effective Ceramic Tube Size	E. Platt	December
219.	Vibration Instrumentation	C. Barnett	December
220.	LRL Radiation Monitor Network at Site 401	E. Goldberg	December
221.	Failure Protection in Control Actuator	J. Day	December
222.	Dimensions and Chemical Analysis of Tie Rods	V. Hampel	December
223.	Bunker Quick Disconnect and Alignment Section Requirement	J. Pitts	December
224.	Stress in Base Plates at Rear of Side Reflector	L. Deverall	December
225.	Control Rod System	E. Goldberg	December
226.	Base Plate Thermal Stress	M. Uthe	December
227.	Fueled Tube Samples for Post Mortem Testing	A. Williams	December
228.	Critical Experiment, Summary of Measurements Requested at Livermore	C. Barnett	December
229.	Bendix Liaison Meeting, December 1961, Control Actuator Development	R. Hollstien	December
230.	Modulus of Rupture Testing	J. Collins	December
231.	Hafnium Blowdown Test	J. Hovingh	December
232.	Number of Fueled Flow Channels	H. Stern	December
	1962		
233.	Summary of Side Support Requirements	C. Walter	January
234.	Support Grid Aerothermodynamics	R. Var	January
235.	Review of NTS Air Flow Rate Metering System	R. McConnell	January
236.	Tory II-C System Component Review	B. Myers	January
237.	Personnel Assignment	B. Myers	January
238.	SEA LION Analysis of Typical Reactor Test	H. Rodean	January
239.	Aft Reflector and Reflected Core Length Changes	W. O'Neal	January
240.	Transition Tube Design	W. O'Neal	January
241.	Preliminary Objectives – Digital Reactor Test Data Reduction	T. Varljen	January

Memo No.	Subject	Author	Month
	(1962 contd.)		
242.	Process Air Temperature Probe Response	R. McConnell	January
243.	Effects of Bent Tie Rod on Control Rod	J. Hovingh	January
244.	On Pressure Drop Caused by Draining and Filling Heater Vessel Insulation Containers	W. Wells	January
245.	Ceramic Tube Quantities	H. Stern	January
246.	Steady State Elastic Thermal Stress in Control Rods	J. Hovingh	January
247.	Test Vehicle Assembly	J. Behne	January
248.	Summary of Unit Cell Tests	N. Brown	January
249.	Heating of Reactor Peripheral Regions (Preliminary)	A. Lorenz	January
250.	Comments on Control Systems Requirements	C. Barnett	January
251.	Control Console	G. St. Leger-Barter	January
252.	Preparation of Refined Fuel Loading Map	V. Hampel	January
253.	Transient Aerothermodynamic Analysis of a Gas-Cooled Reactor – 6. Redefinition of Aerothermodynamic Time Constant Variation with Conduit Station	H. Rodean	February
254.	Typical Weight and Surface Density of Metal Parts External to the BeO Side Reflector	R. Cole	February
255.	Base Plate Tests	H. Reynolds	February
256.	Sintering Studies on Thin Wall BeO Tubes	W. Sandholtz	January
257.	Scram, Annunciator, and Alarm System	G. St. Leger-Barter	February
258.	Tory II-C Performance	M. Mintz	February
259.	Barrel Angle at Reflected Core Periphery	W. O'Neal	February
260.	Temperature Analysis of Shim Finger	W. O'Neal	February
261.	Transient Heat Balance Equation for the Reactor at Axial Station $x/L = 0.70$	H. Rodean	February

Memo No.	Subject	Author	Month
	(1962 contd.)		
262.	Loads Induced on Control Rod by a Bent Tie Rod	J. Hovingh	February
263.	Tie Rod Weights and Properties	W. O'Neal	February
264.	Stress Analysis of Peripheral Shims	W. O'Neal	February
265.	Stresses in Standard Unit Cell Plate	L. Yost	February
266.	Information Concerning Boron Steel Strips to be Used in Critical Experiment	C. Barnett	February
267.	Instrumentation Required on the Duct and in the Reactor Side Support Region	E. Arbtin	February
268.	Horseradish Composition	A. Rothman	February
269.	Calculational Effects of a Control Rod and Infinite Cylindrical Geometry	R. Freis	February
270.	Range Selection for Air Flow Rate Metering System	R. McConnell	February
271.	Heating of Peripheral Reactor Regions	A. Lorenz	February
272.	Cracking of Coors BeO Tubes	E. Robinson	February
273.	Modified Control System for AV5 Temperature Control Valves	J. Wood	February
274.	Aerodynamic Grid Design	B. Rose	February
275.	Bendix Liaison Meeting, February 1962, Control Actuator Development	J. Day	February
276.	Effect of Horseradish on Reactivity and Local Power Density	V. Hampel	March
277.	Review and Status of Components Included in the Actuator Control Package	D. Buddington	February
278.	Water Content of Air of Three Trans-Pacific Routes	E. Arbtin	February
279.	Buckling of Control Rod	J. Hovingh	February
280.	AV5 Actuator Torque Requirements	J. Day	March
281.	Preliminary Heat Transfer Analysis of Side Support System (III)	N. Balling	March
282.	Transient Aerothermodynamic Analysis of a Gas-Cooled Reactor – 7. Prediction of Steady State and Transient Operating Envelopes	H. Rodean	March

Memo No.	Subject	Author	Month
	(1962 contd.)		
283.	Ceramic Tube Fabrication and Requirements Review	C. Walter	March
284.	Doppler-Broadening in Control Rod	C. Donaghy	March
285.	IBM 7090 Code Swindler	J. Collins	March
286.	Preliminary Dimensional Analysis of Coors Tubes	J. Collins	March
287.	Reviewed Aerodynamic Grid Throat Area and Hole Contour	J. Pitts	March
288.	Density of Horseradish Tubes	A. Rothman	March
289.	Steady-State and Transient Operating Envelopes of the Reactor	H. Rodean	March
290.	Support Grid Test Plan	G. Patraw	March
291.	Exit Gas Pressure and Temperature Probe Location	C. Barnett	March
292.	Side Reflector Tube Size Change	A. Miller	March
293.	Nuclear Heating of Base Plate Coating (Preliminary)	A. Lorenz	March
294.	Automatic Data Acquisition Requirements for the Livermore Critical Experiment	T. Varljen	March
295.	Time Constants for Reactor Components	H. Rodean	March
296.	Restriction on Core and Duct Temperatures to Satisfy Side Support System Requirements	E. Arbtin	March
297.	Axial Variation of the Maximum Internal Control Rod Temperature and Aerodynamic Loads on the Control Rod	J. Hovingh	March
298.	Effect of Xenon 135 Buildup on Reactivity and Spatial Power Profile	V. Hampel	March
299.	Operations and Test Programs	C. Barnett	March
300.	Cutback Tubes Review	C. Walter	April
301.	Tie Rod Unfueled BeO Peripheral Elements	M. Mintz	April
302.	Monte Carlo Analyses of Control Rod Configurations	K. Russell	April
303.	Control Rod Pressure Drop Analysis	M. Mintz	April

Memo No.	Subject	Author	Month
	(1962 contd.)		
304.	Program for Procurement of Side Support Springs	E. Arbtin	April
305.	Control Rod Stop	W. O'Neal	April
306.	Preliminary Core Dimensional Test Results	G. Patraw	April
307.	Geometric and Neutronic Representation in Machine Codes, Preparatory to the Determination of the Critical Mass and Final Fuel Maps	V. Hampel	May
308.	Guard Tube Insulation	W. O'Neal	April
309.	Revised Lumped Parameter Heat Balance Equation for the Reactor	H. Rodean	April
310.	Monitoring of Impurity Levels in Ceramic Tubes	V. Hampel	April
311.	Transient Behavior of the Pebble Bed Heater	M. Mintz	April
312.	Results of Examination and Testing of Silicide Coatings Prepared by Boeing Fluidized BeO Process	J. Rynders	
313.	Maximum Explosion Yield of the Reactor	E. Goldberg	April
314.	Estimated Time that Exit Air May Be at or Near Design Temperature	C. Barnett	April
315.	Dynamic Measurements on Test Vehicle	C. Walter	April
316.	Basic Considerations Preparatory to the Determination of the Final Fuel Maps	V. Hampel	May
317.	Reactor Neutron Economy and Flux Spectra	V. Hampel	May
318.	Use of Additives in the Fabrication of Fuel Elements	J. Kane	May
319.	IBM 7090 Code Swindler 3, 4	J. Burke	May
320.	Reactor Safety System	E. Jackson	May
321.	Actuator Guide System Convection Coefficient	E. Jackson	
322.	Reduction of Data on Swindler Code	J. Burke	May
323.	Full Length Tie Rod Tests	W. O'Neal	May
324.	Reactor Safety and Hazards Manual Second Draft on Reactor Design	C. Walter	May
325.	Instrumentation Summary	W. Russell	May

Memo No.	Subject	Author	Month
	(1962 contd.)		
326.	Reactor Instrumentation	L. Huntsman	May
327.	Heat Transfer Analysis of Nickel Shim No. 6	N. Balling	May
328.	Reactivity vs Asymptotic Period	C. Donaghy	May
329.	Fueled BeO Densities in Reference to MEL 573 Specification	A. Rothman	May
330.	Activation of the Aft Reactor Duct	A. Lorenz	May
331.	Thermocouple Material Content in the Reactor	W. Russell	May
332.	Bendix Liaison Meeting, May 1962, Control Actuator Development	J. Day	May
333.	Ceramic Components: Reactor Safety and Hazard Manual	A. Rothman	May
334.	Density of Beryllium Oxide	D. Smith	June
335.	Transverse Structural Stability of Reactor Tube Array	A. Miller	June
336.	Tie Rod Temperature Distribution	W. O'Neal	June
337.	Two-Dimensional Heat Transfer Codes	M. Mintz	June
338.	Chemical Analysis of Ledoux of BeO Powder	J. Collins	June
339.	Operation Manual, Cold Assembly Procedure, Test Vehicle Ducting	J. Behne	May
340.	Heat Transfer and Core Design Pre-Mortem	H. Reynolds	June
341.	Modulus of Rupture Tests of LRL Tubes at Elevated Temperatures	W. Sandholtz	June
342.	Core Temperature Rise Resulting From Shim Rod Withdrawal at Maximum Velocity	C. Donaghy	June
343.	Radiation Heating of the Aft Reactor Duct Flange	A. Lorenz	June
344.	Fission Fragment Recoil Loss	C. Donaghy	June
345.	Suggested Specifications for Livermore Crit Automatic Data System	T. Varljen	June
346.	Reactor Test Facility	W. Miller	June
347.	Use of Boron 11 in Base Block Coating	R. Werner	June
348.	Loss of Airflow Accident	C. Donaghy	June

Memo No.	Subject	Author	Month
	(1962 contd.)		
349.	Experimental Verification of the Nickel Absorption Cross-Sections	A. Cole	July
350.	Appraisal of Critical Mass Without Recourse to Digital Computer Codes	E. Goldberg	July
351.	The Effect on Thrust of a Core Length Change	J. Moyer	June
352.	Heat Transfer of Shaevitz Engineering Displacement Transducer	N. Balling	July
353.	Disassembly Considerations	C. Walter	July
354.	Side Support Gap	H. Reynolds	July
355.	Preliminary Neutronic Calculations of the Effect of Dome Modification to Tory II-C (C-RD)	A. Cole	July
356.	Temperature Overshoot Resulting from Slow Withdrawal Rate of Shim Rods	C. Donaghy	July
357.	The Effect on Thrust of a Side Reflector Change	J. Moyer	August
358.	Side Support System	E. Arbtin	July
359.	Bendix Liaison Meeting, July 1962, Control Pneumatic Actuator Development	J. Day	July
360.	Control System	E. Sheridan	July
361.	Control Rod Weights	J. Hovingh	July
362.	Radiation and BeO Hazards Resulting from High Power Operation	E. Goldberg	July
363.	Thermal Stress Characteristics in Cylinders	C. Walter	July
364.	Remarks on Loading Optimization	J. Hadley	July
365.	Final Report Dimensional Buildup Expected on Reactor	G. Patraw	July
366.	Transition and Base Plate Pressure Drop	B. Rose	July
367.	Control Rod Worth	S. Kellman	July
368.	Results of Front Reflector Core Interface Redesign	W. O'Neal	July
369.	Review of the Operating Envelopes and Limits of the Reactor Side Support System	H. Rodean	August

Memo No.	Subject	Author	Month
	(1962 contd.)		
370.	Possible Reverse Pressure Loads on Reactor Resulting from a Sudden Change to Subcritical Inlet Operations	H. Rodean	July
371.	Radiation Leakage and Radiation Levels External to the Reactor	A. Lorenz	August
372.	Base Plate Temperature Rise	J. Hovingh	August
373.	Radiation Levels within the Reactor and Radiation Damage	A. Lorenz	August
374.	Exit Nozzle	J. Behne	August
375.	Tie Rod Operating Temperatures	J. Pierce	August
376.	Summary of Radiation Effects Studies	A. Lorenz	August
377.	Exit Nozzle Influence Parameter Study for Design Point Flight Conditions	M. Mintz	August
378.	Bendix Liaison Meeting, August 1962, Control Actuator Development	J. Day	August
379.	Rejection Criteria in the Core Temperature Averaging Network	T. Varljen	August
380.	Selection of Final Coating System for Base Blocks	R. Werner	August
381.	Side Support Springs	N. Brown	September
382.	Determination of Power Delivered to the Air Stream	C. Barnett	September
383.	Neutron Streaming	S. Kellman	September
384.	Preliminary Appraisal of Critical Mass Using Machine Calculations	V. Hampel	September
385.	Test Vehicle Brake System	N. Anderson	September
386.	Subsystem Checkout of AV4 Airflow Control System	G. Boyadjieff	September
387.	A Method of Controlling a Future Flight Reactor	V. Hampel	September
388.	Subsystem Checkout of AV5 Air Temperature Control System	M. Jacques	September
389.	Cross-sections and Transfer Coefficients of Materials Used in Diffusion Code Calculations	V. Hampel	September
390.	Reactor Parts List	E. Platt	September
391.	Subsystem Checkout of AV3 Air Flow Control System	G. Boyadjieff	September

Memo No.	Subject	Author	Month
	(1962 contd.)		
392.	Final Radial and Axial Boundaries Between Fuel Classes	V. Hampel	September
393.	A Postulated Maximum Credible Accident: Sudden Cut-Off of Coolant Air	E. Goldberg	October
394.	Steady State Characteristics of the NTS Air Supply	R. Hollstien	October
395.	Fueled Tube Requirements	V. Hampel	October
396.	Fueled Tube Requirements, Rev. I	V. Hampel	October
397.	Fuel Loading Map	V. Hampel	October
398.	Emergency Use of Safety Rods During High Power Reactor Operation	H. Rodean	October
399.	Description of NTS Railroad Equipment	N. Anderson	October
400.	Placement of Tie Rods in the Reactor	V. Hampel	October
401.	Change of Thrust with Core Length (Supplement to Memo 351)	J. Moyer	October
402.	Change of Thrust With a Reflector Modification (Supplement to Memo 357)	J. Moyer	October
403.	As-Built Throat Area of the Aero-dynamic Grid	J. Pitts	October
404.	Strain Relaxation and Residual Stress	E. Robinson	October
405.	Action Based on Heat Transfer and Reactor Design Pre-Mortem Meetings	C. Walter	October
406.	Duct Pressures During Cold Blowdown	R. Hollstien	October
407.	Tory II-C Performance	M. Mintz	October
408.	Neutronic Cross-sections for Nickel, Iron,Cobalt, René 41, and Hastelloy R-235	A. Cole	October
409.	Fueled Tube Requirements (Rev. II)	V. Hampel	October
410.	Bendix Liaison Meeting, October 1962, Control Actuator Development	J. Day	October
411.	Duct Pressures During Automatic Control of the Air Supply	R. Hollstien	October
412.	Control Rod Catcher Mechanisms	J. Pierce	October
413.	Effect of Improved Moderator and Fuel Cross-sections on Neutronics Calculations	A. Cole	October
414.	Criticality vs Various Water Accident Conditions	V. Hampel	November

Memo No.	Subject	Author	Month
	(1962 contd.)		
415.	Spatial Power Profile of the Reactor at High Temperature	V. Hampel	November
416.	Summary of Reactor Transient Aerothermodynamics	H. Rodean	November
417.	Calculations of Pressure Loss Across the Wipers in the Side Support System	N. Balling	October
418.	Fuel Loading Map: Modification	H. Reynolds	November
419.	Heat Transfer Analysis of the Side Support System	N. Balling	November
420.	Cursory Investigation of Ignition of F-48	C. Walter	October
421.	Hydrostatic Test Plan of Support Grid	G. Patraw	November
422.	Appraisal of Critical Mass of Tory II-C Without Recourse to Digital Computer Codes: (Contd.)	E. Goldberg	November
423.	Thermal Stress Relaxation	C. Walter	November
424.	Median Fission Energies	V. Hampel	November
425.	Fueled Tube Requirements (Rev. III)	V. Hampel	November
426.	Notching of Guard Tubes	W. O'Neal	November
427.	Effect of the Change of Fuel in Reactor	A. Lorenz	November
428.	Chronicle of Events Leading to the Final Fuel Loading Maps	V. Hampel	November
429.	Radiation Effects Studies: Summary	A. Lorenz	November
430.	AV4 Airflow Control Valve Subsystem Test Results	G. Boyadjieff	November
431.	Curling of Tie Rod Guard Tubes and Adjacent Fueled Tubes	M. Mintz	November
432.	Nuclear Control System Performance During a Typical Full Power Run	R. Hollstien	November
433.	Log Power Control System Step Response	R. Hollstien	November
434.	Log Power Control System Response to Step Reactivity Disturbances	R. Hollstien	November
435.	Core Temperature Control System Transient Response	E. Alexander	November
436.	The Effect on Reactivity and Power Profile Due to Tie Rod Exchange	V. Hampel	December

Memo No.	Subject	Author	Month
	(1962 contd.)		
437.	Tie Rod Status Report	W. O'Neal	November
438.	Predicted Safe Operating Conditions for Programmed Control Rod Withdrawal During Reactor Startup	H. Rodean	November
439.	Reactor Duct Instrumentation	E. Jackson	December
440.	Review of Low Temperature Ignitions of Columbium Alloys in Flow Tests Conducted at Marquardt	W. Wells	December
441.	Lightning Rod Effect	S. Kellman	December
442.	AV3 Air Flow Control Valve Subsystem Test Results	G. Boyadjieff	December
443.	Test Results: Subsystem Checkout of the Tory II-C Air Flow Control System Temperature Control Valves, AV5A-5B	M. Jacques	December
444.	Air Supply Analog System Performance with Modified Capacitance Between Valves AV5A and the Heaters	R. Hollstien	December
445.	Test Vehicle Description	J. Behne	December
	1963		
446.	Neutronic Design	E. Goldberg	January
447.	Results of Matrix Model Test	G. Patraw	January
448.	Effect of Scram Logic Circuit Speed on Power Level and Core Temperature Scram Systems	E. Alexander	January
449.	Monthly Liaison Meeting with Bendix, December 1962, Pneumatic Actuator Development	J. Day	January
450.	Installation of Air Flow Control Valves AV3 and AV4 at NTS	G. Boyadjieff	January
451.	Base Plate Temperature Distribution	M. Mintz	January
452.	Preliminary Analysis of Heat Transfer in an Advanced Tory Design	S. Kellman	January
453.	Strength of Irradiated René 41	W. O'Neal	January
454.	Neutron Economy, Revised	S. Ross	January
455.	Effect of the U^{235} (γ, fission) Reaction	A. Lorenz	January
456.	Core Temperature Control System Response to Step Reactivity Disturbances	E. Alexander	January

Memo No.	Subject	Author	Month
	(1963 contd.)		
457.	Accuracy of Calculated Dependence of Reactivity on Temperature	A. Cole	January
458.	Radiation Flux Field: Lateral Leakage Contribution	A. Lorenz	January
459.	A.A.S. Piping Pressure Drop	M. Jester	January
460.	Nuclear Heating of Vehicle Components and Proposed Shielding	A. Lorenz	January
461.	Tie Rod Status	C. Walter	February
462.	Dummy Core Tension Control Tube Air Flow	M. Jester	February
463.	Blowdown Operation with the Reactor Flow Simulator	J. Pitts	February
464.	Non-uniform Air Pressure across the Core	T. Stubbs	February
465.	Suggested Test Plan for Side Support Pressure Drop Tests	D. Jordan	February
466.	Experiments at "N" Division	E. Goldberg	February
467.	Special Fuel Tubes	A. Williams	February
468.	Control Rod Attachment Test	J. Hovingh	February
469.	The Dynamic Modulus and the Coefficient of Linear Thermal Expansion of Hafnium	J. Hovingh	February
470.	Experiment to Size Side Support Wipers	N. Brown	February
471.	Some Ground Rules for the P.D.M. Data Reduction Program	T. Varljen	February
472.	Activation Experiment Proposal	A. Lorenz	March
473.	Fast Flux in the LPTR Center Facility	C. Walter	March
474.	Plating Calculations of Tie Rods	R. Doyas	March
475.	Subsystem Checkout at NTS of Temperature Control Valves (AV5)	M. Jacques	March
476.	Bendix Liaison Meeting, Control Actuator Development	J. Day	March
477.	Weighted Averaging Device for Core Temperature	R. Staker	March
478.	Control Actuator No. 1 Performance Data at Room Temperature and 1200°F under Load Simulation	G. Boyadjieff	March

Memo No.	Subject	Author	Month
	(1963 contd.)		
479.	Safety Consideration and Failure Protection of the Control System	G. Boyadjieff	March
480.	Control of the Tube Conveyor and Cutter in Bldg. 192-C	R. Hollstien	March
481.	Facility Testing and Evaluation Group	M. Smith	March
482.	Control and Safety Systems Assembly Procedure — Part I	E. Jackson	March
483.	The Effects of Xenon-135 on Axially Integrated Power in Fueled Tube Columns. Corrigenda and Addenda to Tory II-C Memos No. 415 and 446	V. Hampel	March
484.	Shear Strength of Control Rod Welds	J. Hovingh	March
485.	Qualitative and Quantitative Chemical Analyses of Materials for the Reactor	E. Lounsbury	April
486.	Vernier Actuator Serial No. 1 Room Temperature and Pressure	G. Wright	March
487.	Tie Rod Gold Coating	W. Hay	March
488.	An Assessment of the Possibility of Operating BeO Fueled Reactor Tubes at 3000°F Wall Temperature (CRD Title)	A. Rothman	March
489.	Fueled Tube Assembly Check System	A. Williams	April
490.	Power Smearing Due to Fueled Tube Stagger	G. Pierce	April
491.	Short Time Irradiation Effects on Enriched Boron Carbide	J. Hovingh	April
492.	Fuel Loss-Coors and LRL Fuel Elements	C. Hoenig	April
493.	Experiments at "N" Division No. II	E. Goldberg	April
494.	Documentation of an Improved Cross Section for Base Block Material	V. Hampel	April
495.	Revision of Nuclear Heating in Aft Reactor Regions	A. Lorenz	April
496.	Monte Carlo Analysis of Neutron Distribution in Regions Forward of the Active Core	A. Lorenz	April

Memo No.	Subject	Author	Month
	(1963 contd.)		
497.	Re-evaluation of the Disparity Between the Calculated and Measured Axial Power Profile of Tory II-A, and its Effect upon the Tory II-C Design	V. Hampel	April
498.	Heating of Solenoid No. 1225	G. Pierce	April
499.	Modulus of Rupture Testing Quality Assurance Program	J. Collins	April
500.	Reactor Parameter Variations	J. Hadley	April
501.	Reactivity Effects due to Mass Perturbations of Tory II-C Materials	V. Hampel	April
502.	Summary Report Vernier SN-1 Actuator	G. Wright	April
503.	Foil Activation Experiments on the Reactor	T. Varljen	April
504.	Bendix Liaison Meeting Control Actuator Development	M. Jacques	May
505.	Heat Transfer Analysis of Coated Base Blocks and Transition Cartridges	J. Hovingh	May
506.	Dimensional Analysis of Fueled Tubes	J. Collins	May
507.	Specially Measured Fueled Tubes	J. Collins	May
508.	The Effect of Exposure to Water Vapor on the Short Time Strength of Coors BeO	E. Robinson	May
509.	Road Test of Truck Transport of the Reactor	A. Miller	April
510.	Stability Testing of Fueled Tubes	J. Collins	May
511.	Failure of Tubes Due to Thermal Stress with Radially Inward Heat Flux	N. Brown	May
512.	Control Rod Heating in Power Transients	J. Hadley	May
513.	AV-3, PFM1-B Transfer Function	R. Staker	May
514.	Results of the Gamma Counter Inspection Phase of the Fueled Tubes Quality Assurance Program	J. Collins	May
515.	Neutronic Pre-Mortem	A. Cole	May

APPENDIX B

LIST OF KEY TORY II-C MEMORANDA BY SUBJECT

Ceramic Tubes			
Thermal stress in cylinders	363	C. Walter	7/62
BeO density	334	D. Smith	6/62
Fueled BeO density	329	A. Rothman	5/62
Additives in fueled BeO	318	J. Kane	5/62
Ceramic tube dimensions	286	J. Collins	3/62
Ceramic tube fabrication	283	C. Walter	3/62
Horseradish	268	A. Rothman	2/62
Camber	216	G. Patraw	11/61
Controls			
Nuclear control system performance	432	R. Hollstien	11/62
Control system	360	E. Sheridan	7/62
Reactor safety system	320	E. Jackson	5/62
Reactor safety system	198	C. Walter	11/61
Control actuator specification	46	R. Finnigan	12/60
Reactor			
René 41 strength	453	W. O'Neal	1/63
Matrix model test	447	G. Patraw	1/63
Tie rod status report	437	W. O'Neal	11/62
Notching of guard tubes	426	W. O'Neal	11/62
Support grid test	421	G. Patraw	11/62
Reactor parts list	390	E. Platt	9/62
Base block coating	380	R. Werner	8/62
Front reflector-core interface	368	W. O'Neal	7/62
Dimensional buildup	365	G. Patraw	7/62
Side support system	358	E. Arbtin	7/62
Tube array stability	335	A. Miller	6/62
Silicide coating	312	J. Rynders	5/62
Control rod temperature and loads	297	J. Hovingh	3/62
Side reflector tube size	292	A. Miller	3/62
Control rod buckling	279	J. Hovingh	2/62
Peripheral shim stress	264	W. O'Neal	2/62
Peripheral shim temperature	260	W. O'Neal	2/62

Reactor, continued

Barrel angle at reflected core periphery	259	W. O'Neal	2/62
Unit cell tests	248	N. Brown	1/62
Control rod thermal stress .	246	J. Hovingh	1/62
Transition tube design . .	240	W. O'Neal	1/62
Ground and flight loads . .	197	E. Arbtin	11/61
Hastelloy C properties . .	134	E. Jackson	7/61

Neutronics

Neutronic design	446	E. Goldberg	1/63
Radiation effects . . .	429, 495	A. Lorenz	11/62
Power profile	415	V. Hampel	11/62

Operation and Instrumentation

Core temperature averaging .	477	R. Staker	3/63
Duct instrumentation . .	439	E. Jackson	12/62
Safe operating conditions .	438	H. Rodean	11/62
Power	382	C. Barnett	9/62
Operating limits of side support system	369	H. Rodean	8/62
Thermocouple material content	331	W. Russell	5/62
Reactor instrumentation . .	326	L. Huntsman	5/62
Instrumentation summary .	325	W. Russell	5/62
Operations and test programs .	299	C. Barnett	3/62
Boron steel strips	266	C. Barnett	2/62
Critical experiment	228	C. Barnett	12/61

Test Vehicle and Test Facility

Test vehicle	445	J. Behne	1/63
Inlet grid throat area . .	403	J. Pitts	10/62
Reactor test facility	346	W. Miller	6/62
Test vehicle assembly procedure	339	J. Behne	5/62
Inlet grid	287	J. Pitts	3/62
Heater pressure drop . .	244	W. Wells	1/62
Bunker vehicle disconnect and alignment	223	J. Pitts	12/61

Test Vehicle and Test Facility, continued			
Duct joints	184	S. Giampapa	10/61
Test vehicle natural frequencies .	177	A. Miller	10/61
Dynamic analog of test vehicle .	167	A. Weston	9/61
Nozzle cooling	163	J. Behne	9/61
Heater balls	143	J. Kane	8/61
Thermodynamics			
Base block temperature . . .	451	M. Mintz	1/63
Transient aerothermodynamics .	416	H. Rodean	11/62
Performance	407	M. Mintz	10/62
Emergency use of safety rods .	398	H. Rodean	10/62
Transition and base block pressure drop	366	B. Rose	7/62
Heater transient behavior . .	311	M. Mintz	4/62
Heat balance equation . . .	309	H. Rodean	4/62
Time constants	295	H. Rodean	4/62
SEA LION analysis of reactor test .	238	H. Rodean	1/62

APPENDIX C

LIST OF PERTINENT UCRL REPORTS

UCRL No.	Subject	Author	Date
5019	ANGIE	S. Stone, R. Stuart	11/25/57
5019 Suppl.	Preparation of Input for the IBM 704 ANGIE Code and Operating Instructions	S. Stone	–
5082	Solution of the Time-Dependent Thermal Neutron Diffusion Equation	L. Deverall	1/14/58
5235	A Non-Destructive Method for Determination of Fuel Loss from Reactor Fuel Elements	J. Carpenter	1/7/59
5237-T	Work in Progress at UCRL on Materials for Nuclear Propulsion	O. Krikorian	6/12/58
5293	ZOOM: A One-Dimensional, Multigroup, Neutron Diffusion Theory Reactor Code for the IBM 704	Stone, et al.	11/19/58
5363	Gamma and Neutron Heating in and about a Homogeneous Reactor	Raymond Fox	9/30/58
5381	Thermal Fracture Resistance of Simulated Beryllia Fuel Elements for Pluto – Preliminary Report	R. Finke, R. Meuser	11/5/58
5397	Sea Level Nuclear Ramjet Parameter Study	R. Finke, et al.	3/16/59
5465 Summary	Control Concepts for Nuclear Ramjet Reactors	R. Finnigan	2/9/59
5515	Pluto Programmatic Report I	Propulsion Div. Staff	1/3/59
5515 Suppl. I	Appendices I-VI for Pluto, Programmatic Report I	Propulsion Div. Staff	1/3/59
5515 Suppl. II	Appendices VII-X for Pluto, Programmatic Report I	Propulsion Div. Staff	1/3/59
5625 Rev.	The Nuclear Ramjet Propulsion System	T. C. Merkle	5/15/61
5682	9-ZOOM, A One-Dimensional Multigroup Neutron Diffusion Theory Reactor Code for the IBM 709	S. Stone	8/25/59
5692	Temperatures and Thermal Stresses in Hexagonal Tubes and Pierced Plates with Internal Heat Sources	R. B. Meuser	9/22/59
5693	Thermal Fracture of Beryllia Fuel Elements	R. Meuser	19/59

UCRL No.	Subject	Author	Date
5804	An Accurate Expression for Gas Pressure Drop in High-Speed Subsonic Flow with Friction and Heating	Robert Fox	12/59
5829	Pluto Quarterly Progress Report No. 2 (October-December, 1959)	Propulsion Div. Staff	1/7/60
5925	Pluto Quarterly Progress Report No. 3 (January-March, 1960)	Propulsion Div. Staff	4/1/60
5956	SOPHIST I An IBM 709/7090 Code which Calculates Multigroup Transfer Coefficients for Gaseous Moderators	E. Canfield, et al.	10/19/61
6031	Control Concepts for Nuclear Ramjet Reactors	R. Finnigan	6/11/60
6036	Pluto Quarterly Progress Report No. 4 (April-June, 1960)	Propulsion Div. Staff	7/1/60
6076	9-ANGIE—A Two-Dimensional, Multigroup, Neutron-Diffusion-Theory Reactor Code for the IBM 709 or 7090	S. Stone	10/28/60
6076 Suppl. I	The 4K ANGIE Code	S. Stone	3/5/62
6100	The Design and Construction of the Site 401 Disassembly Facility	W. H. Moran	8/18/60
6143	Pluto Quarterly Progress Report No. 5 (July-September, 1960)	Propulsion Div. Staff	9/30/60
6148	Escape of Fission Products from UO_2-Loaded BeO Fuel Elements	H. Hicks, J. Armstrong	1/12/61
6187 Rev. I	Engineering Testing of the F-48 Columbium Alloy	J. Cox, R. Werner	8/2/61
6238	Application and Evaluation of Ceramic Materials in Tory Reactor Systems	J. H. Moyer, et al.	11/30/60
6258	Pluto Quarterly Report No. 6	Nuclear Prop. Div. Staff	1/3/61
6325	Some Experiences with Noble-Metal, Metal Sheathed Thermocouples	W. E. Bostwick	2/6/61
6329	Summary Report on a High-Temperature Beryllium-Oxide Critical Experiment	R. Finke, et al.	3/21/61
6331	Sea Lion—A-Time-Dependent Approximate Aerothermodynamic Code to Calculate Axial Temperature Distributions of Multiple Conduits	R. Var, P. Uthe	6/27/61
6349 Abstract	NOMAC – A Multichannel Aerothermodynamic Digital Computer	M. Mintz, P. Uthe	2/20/61

UCRL No.	Subject	Author	Date
6376	Pluto Quarterly Report No. 7	Nuclear Prop. Div. Staff	4/3/63
6398	The Pluto Program	H. Reynolds	4/19/61
6457	Some Properties of Beryllium Oxide	J. Lillie	5/19/61
6476	Nuclear Ramjet Reactor Test Facility Requirements	C. Walter W. C. Miller	7/24/61
6502-T	Beryllium Oxide: Its Properties and Application in Nuclear Reactors	A. Rothman	6/28/61
6516	Pluto Quarterly Report No. 8	Nuclear Prop. Div. Staff	7/3/61
6589	A Note on Platinum/Platinum-Rhodium Thermocouple Uncertainty	W. Bostwick	9/19/61
6609-T Abstract	Materials Requirements for Nuclear Ramjets	H. Reynolds	2/62
6625	Pluto Quarterly Progress Report No. 9	Nuclear Div. Staff	10/10/61
6673	A Cooled-Reflector, Hot-BeO-Core Critical Experiment	R. Finke E. Goldberg	10/27/61
6704-T	Development Work on BeO and Fuels	A. Rothman	11/30/61
6726	Pluto Quarterly Report No. 10	Nuclear Prop. Div. Staff	1/5/62
6743-T	Properties of BeO Ceramics and their Application in a Nuclear Propulsion System (Pluto)	A. Rothman	9/62
6743-T Summary	Refractory Materials for a Nuclear Ramjet Engine (Pluto)	A. Rothman	9/62
6758-T	Experiments with Nickel as a Reactor Reflector Material	A. Cole	1/19/62
6765-T	Experiments Involving Gaps in Critical Assemblies	A. Cole	1/25/62
6784-T Abstract	The Pluto Nuclear Ramjet Program	H. Reynolds	2/6/62
6829-T	Pluto Aerothermodynamic Transients	H. Rodean	3/16/62
6833-T	Neutronic Design of Tory II-C Control Rod System	E. Goldberg	3/16/62
6834-T	Nuclear Heating of Tory II-C Hafnium Control Rods	S. Kellman A. Lorenz	3/15/62
6839-T	Growth of Beryllium Oxide Single Crystals	H. Newkirk	3/15/62

UCRL No.	Subject	Author	Date
6843-T	Hot Spots in High-Power-Density Gas-Cooled Reactors	R. Finke	3/22/62
6844-T	Fuel Element Development and Fabrication	W. Sandholtz	3/62
6846-T	Determination of the Critical Mass and of Spatial Fuel Distribution of The Tory II-C Reactor	V. Hampel	3/19/62
6855	Tory II-C System	C. Walter	3/62
6871	Fuel Elements for Pluto	J. Cahoon, C. Hoenig, A. Rothman	3/30/62
6877	On the Thermal Stress Behavior of Pluto Fuel Elements	W. Myers, et al.	4/9/62
6890	Pluto Quarterly Report No. 11	Nuclear Prop. Div. Staff	4/4/62
6891	Gamma Energy Deposition in Infinite Source Media	A. Lorenz	5/15/62
6896	Observations on the Sintering of BeO	J. Kahn	4/16/62
6912	SOPHIST II, A Group Cross Section IBM 709/7090 Code	J. Pettibone E. Canfield	5/21/62
6921-T	The Crystal Structure of BeO and its Piezoelectric Properties	D. Smith	5/17/62
6923 Rev.	The Pluto Program	H. Reynolds	1/14/63
6927-T Abstract	Microstructure of BeO: Preferred Orientation of Extruded Tubes	J. Kahn	5/18/62
6941	The Pluto Program	Nuclear Prop. Div. Staff	6/8/62
6992	Pluto Quarterly Progress Report No. 12	Prop. Div. Staff	7/10/62
7073	Tory II-C Nuclear Instrumentation System	G. St. Leger-Barter	9/26/62
7079	Pluto Quarterly Report No. 13 (July-September 1962)	Nuclear Prop. Div. Staff	10/4/62
7086	Nuclear Ramjet Reactors	C. Walter	10/8/62
7187	Pluto Quarterly Report No. 14	Nuclear Prop. Div. Staff	1/14/63
7252-T Summary	Summary of BeO Research at LRL, Livermore	C. Cline	2/63

UCRL No.	Subject	Author	Date
7258-T Abstract	Mechanical Properties of Beryllium Oxide at Elevated Temperatures	W. Barmore, et al.	2/63
7266	Control of the Tory II-C Nuclear Ramjet Engine	A. Alexander, et al.	3/6/63
7272	Tory II-C Safety Analysis Report	E. Goldberg	NYP

INDEX

Acceleration s of reactor vehicle . . IV-1
Air
  Flow rate control V-5
  Heater III-105-107
  Properties VI-2
  Storage III-105-107
  Temperature control V-6
Aft adapter III-42
Aft reflector III-33-35
Areas, frontal
  Active core III-18
  Forward reflector III-19
Areas, nozzle throat I-1, 75
Auxiliary drive, test vehicle . . III-77

Base blocks III-45, 46, 47
Brake system, test vehicle III-73, 74, 75

Cell plates III-42, 43, 44
Ceramics and cermets VI-4-16
Coatings VI-18
Cobalt alloys VI-20, 22
Columbium alloys VI-23, 25
Component analysis IV-4
Component operating characteristics
  Cold inlet gas conditions, summary . I-32
  Design point, summary I-4
  Hot-wall off-design conditions,
  summary I-46
  Structural limit conditions, summary . I-18
Compression spring III-42
Control, air flow rate V-5
Control, air pipe III-78
Control, air temperature V-6
Control rod III-57, 58
  Analysis and heat transfer data . . I-74
  Flow rate I-46
  Mach number I-11, 14, 25, 28, 39, 42, 53
  Pressure drop I-4, 18, 32, 46
  Temperature I-4, 11, 14, 18, 25, 28, 32, 39, 42, 46, 53, 56
  Worth II-4, 6
Control Tie rod III-38, 39
  Analysis and heat transfer data . . I-74
  Flow rate I-4, 18, 32, 46
  Mach number I-12, 15, 26, 29, 40, 43, 54, 57
  Power distribution I-12, 15, 26, 29, 40, 43, 54, 57
  Pressure I-12, 15, 26, 29, 40, 43, 54, 57
  Pressure drop I-4, 18, 32, 46
  Temperature I-4, 12, 15, 18, 26, 29, 32, 40, 43, 54, 57

Control system, reactor III-61-67
Criticality II-1

Delayed neutron characteristics . . II-4
Design point conditions I-1
Diffuser
Grid III-78
Inlet data I-73
Operation I-1
Pressure recovery ratio . . . I-1
Duct
Access III-79
Aft inlet III-79
Aft reactor III-59, 60
Controls III-79
Forward inlet III-78
Reactor III-59, 60, 79
Shroud III-57
Support system III-78, 80
System III-78

Exhaust pressure, nozzle I-1
Exit nozzle influence parameters . I-72

Ferrous alloys VI-28-38
Flatcar III-73
Flow distribution, component . . I-3
Flow rate
Component I-3, 4, 18, 32, 46
Reactor I-3
Forward adapter III-42
Forward reflector inserts . . . III-36, 37
Forward reflector section . . . III-22
Frontal areas
Active core III-18
Forward reflector III-19
Fuel
Class description II-8
Loading, radial zones II-9
Loading map II-7
Fueled tubes III-25
Analysis and heat transfer data . . I-73
Flow rate I-3, 4, 18, 32, 46
Loading distribution III-24
Mach number I-3, 6, 20, 34, 48
Material power density I-3
Modulus of rupture VI-13
Power density I-4, 18, 32, 46
Power distribution I-6, 20, 34, 48
Pressure I-6, 20, 34, 48
Pressure drop I-4, 18, 32, 46
Quantities III-23, 24
Temperature I-3, 4, 6, 18, 20, 32, 34, 46, 48
Thermal stress I-3, 6, 20, 34, 48
Thrust coefficient vs flow passage . I-71

Furnace III-107

Gamma energy spectra II-21, 23
Gas temperature, exit I-4, 18, 32, 46
Grid, support III-48
Guard tubes II-25
  Analysis and heat transfer data . . I-74
  Flow rate I-3, 4, 18, 32, 46
  Mach number I-9, 13, 16, 23, 27, 30, 37, 41, 44, 51, 55, 58
  Power density I-4, 18, 32, 46
  Power distribution I-9, 13, 16, 23, 27, 30, 37, 41, 44, 51, 55, 58
  Pressure I-9, 13, 16, 23, 27, 30, 37, 41, 44, 51, 55, 58
  Pressure drop I-4, 18, 32, 46
  Temperature I-4, 9, 13, 16, 18, 23, 27, 30, 32, 37, 41, 44, 46, 51, 55, 58

Hafnium VI-40

Inserts, forward reflector . . . III-36, 37
Instrumentation III-83, 98
Isodose map II-43

Locomotive III-109

Mach number
  Control rod I-11, 14, 25, 28, 39, 42, 53
  Control tie rod I-12, 15, 26, 29, 40, 43, 54, 57
  Fueled tube I-3, 6, 20, 34, 48
  Guard tube I-9, 13, 16, 23, 27, 30, 37, 41, 44, 51, 55, 58
  Missile I-1, 3
  Side reflector region I-7, 21, 35, 49
  Tie rod I-8, 22, 36, 50
  Vs thrust I-2
  Vs thrust coefficient I-2
Material distribution II-5
Momentum recovery of bleed . . . I-1

Neutron economy II-3
Neutron flux II-24
Nickel alloy VI-42-55
Nickel tubes III-20, 22, 25-28
Nozzle III-79
  Analysis and heat transfer data . . I-75
  Cooling air pipe III-77
  Divergence factor I-1
  Exhaust pressure I-1
  Parameter influence I-72
  Throat area I-1
  Velocity coefficient I-1
Nuclear control modes V-3

Nuclear heating density II-25-33
Active core (summary) II-25
Aft reactor regions II-33
Control rod II-28
Forward regions II-31, 32
Guard tubes II-26, 27
Peripheral regions II-29, 30
Tie rods II-26, 27

Operating characteristics, component summary
Cold inlet gas condition I-32
Design point conditions I-4
Hot-wall off-design condition . . I-46
Structural limit condition . . . I-18
Operating limits V-7
Outrigger wheels III-75, 76

Performance maps
Flow rate I-60-68
Power I-60-68
Gas pressure I-60-68
Temperature I-60-68
Wall temperature I-60-68
Performance parameters I-3
Performance summary I-3
Peripheral shims III-17, 29-32
Analysis and heat transfer data . I-73
Flow rate I-3
Piping, bunker III-101, 102
Platinum alloys VI-56-58
Power density, fueled tube . . . I-3
Power distribution
Control rod I-11, 14, 25, 28, 39, 42, 56
Control tie rod I-12, 15, 26, 29, 40, 43, 54, 57
Fueled tube I-6, 20, 34, 48
Guard tube I-9, 13, 16, 23, 27, 30, 37, 41, 44, 51, 55, 58
Side reflector I-7, 21, 35, 49
Side support structure I-17, 31, 45, 59
Tie rod I-8, 22, 36, 50
Power profile II-16, 20
Pressure
Control rod I-11, 14, 25, 28, 39, 42, 56
Control tie rod I-12, 15, 26, 29, 40, 43, 54, 57
Drop, total I-3, 4, 18, 32, 46
Fueled tube I-6, 20, 34, 48
Guard tube I-9, 13, 16, 23, 27, 30, 37, 41, 44, 51, 55, 58
Inlet, total I-3
Recovery ratio, diffuser I-1
Side reflector I-7, 21, 35, 49
Side support structure I-17, 31, 45, 59
Tie rod I-8, 22, 36, 50

Proposed test plan V-1

Radial fuel zone boundaries . . II-9-14
Radiation dose rate II-41, 42
Radiation leakage II-34-40
  Gamma II-35, 36
  Neutron II-37-40
  Summary II-34
Railroad III-108
Reactor
  Assembly, data summary . . III-1, 2, 3
  Characteristics II-3
  Control system III-61-67
  Dimensions III-3
  Flow rate, total I-3
  Radii and tolerances III-6
Reactivity requirements II-2

Safety rod III-68-70
Safety system III-68-70
Shims, peripheral III-28-31
  Analysis and heat transfer . . I-73
  Flow rate I-4, 18, 32, 46
  Power density I-4, 18, 32, 46
  Pressure drop I-4, 18, 32, 46
  Temperature I-4, 18, 32, 46
Shim rod position vs multiplication
constant II-6
Side reflector III-17
  Flow rate I-3, 4, 18, 32, 46
  Frontal area III-18, 19
  Power density I-4, 18, 32, 46
  Power distribution I-7, 21, 35, 49
  Pressure I-7, 21, 35, 49
  Pressure drop I-4, 18, 32, 46
  Radial temperature analysis . . I-6, 19, 33, 47
  Temperature I-4, 7, 18, 21, 32, 35, 46, 49
  Tubes III-28
  Tubes, analysis and heat transfer
  data I-73
Side support system III-51-56
  Analysis and heat transfer data . I-73-74
  Flow rate I-3, 4, 18, 32, 46
  Power density I-4, 18, 32, 46
  Power distribution I-17, 31, 45, 59
  Pressure I-17, 31, 45, 59
  Pressure drop I-4, 18, 32, 46
  Temperature I-4, 17, 18, 31, 32, 45, 46, 59
Site 401 description III-99
Site 401 map III-100
Spacer sleeves III-43
Spring, compression III-42
Spring segment III-51, 54, 56
Stress, thermal, fueled tube . . I-3, 6, 20, 34, 48, IV-6

Structural limit operating conditions . I-1
Support grid III-48, 49, 50
Support rail III-52, 56

Temperature
Ambient I-1
Analysis, side reflector I-5, 7, 19, 21, 33, 35, 47, 49
Control rod . . . . See control rod, temperature
Control tie rod . . . . . . See control tie rod, temperature
Fuel elements . . . . . . See fuel element, temperature
Gas, exit I-4, 18, 32, 46
Guard tube . . . . See guard tube, temperature
Inlet, total I-3
Side reflector . . . . . . See side reflector, temperature
Side support structure . . . . See side support structure, temperature
Tie rod . . . . See tie rod, temperature
Wall peak, components I-4, 18, 32, 46
Test facility III-99
Test vehicle III-73, IV-3
Thrust I-3
Thrust coefficient I-1
Thrust coefficient vs Mach number . I-2
Thrust coefficient, net
Effect of friction factor I-70
Effect of fueled tube discharge coefficient I-70
Effect of fueled tube flow passage diameter I-70
Effect of fueled tube flow passage diameter, constant I-71
Effect of heat transfer coefficient . I-70
Effect of peak fueled tube wall temperature I-70
Effect of reactor inlet pressure . I-70
Thrust coefficient parameter influence I-69
Thrust loading total reactor, axial . I-3
Thrust losses I-69
Thrust, net I-1
Thrust vs Mach number I-2
Tie rod assembly III-38, 39
Tie rod
Analysis and heat transfer data . I-73
Flow rate I-3, 4, 18, 32, 46
Mach number I-8, 22, 36, 50
Power density I-4, 18, 32, 46
Power distribution I-8, 22, 36, 50
Pressure I-8, 22, 36, 50
Pressure drop I-4, 18, 32, 46
Temperature I-4, 8, 10, 18, 22, 24, 32, 36, 38, 46, 50, 52
Time constants and thermal capacities. I-75

Transition parts III-33, 34, 35
Truck assembly III-76, 77
Tube column numbering system . III-9-15
Tube stagger arrangement . . . III-20
Typical reactor operation sequence . V-2

Unfueled tubes III-26
  Quantities III-23
Unit cell
  Arrangement and designation . . III-8
  Frontal areas III-18, 19
  Peripheral III-17
  Standard and control, active core . III-15
  Standard and control, forward reflector III-16

Weight and surface density, component III-55
Weights and CG locations . . . IV-2
Wiper bars III-52, 56
Wipers III-52, 53, 55, 56
Wireway III-77